SOVIET PHYSICS

JETP

A translation of the Zhurnal Éksperimental'noĭ i Teoreticheskoĭ Fiziki.

Vol. 11, No. 6. pp. 1195-1403 (Russ. orig. vol. 38, No. 6, pp 1657-1950, June, 1960) Dec., 1960

ON THE MECHANISM OF EMISSION OF PROMPT FISSION NEUTRONS

V. N. NEFEDOV

Submitted to JETP editor July 29, 1959

J. Exptl. Theoret. Phys. (U.S.S.R.) 38, 1657-1662 (June, 1960)

The spectra of fission neutrons emitted at certain angles to the direction of flight of the fragments (0 and 180°, 40 and 120°, and 90°) have been measured. The spectra of neutrons emitted by light and heavy fragments separately are compared. The kinetic energy and temperature of the light and heavy U^{235} fission fragment groups at the instant of emission of fission fragments are also determined.

MODERN theory of nuclear fission presupposes that the fission neutrons are emitted from the excited moving fragments. Experiments on the investigation of the spectra of the fission neutrons confirm this assumption, but do not provide unequivocal data on the kinetic energy and temperature of the fission fragments at the instant when the neutrons are emitted. The purpose of the present investigation was to determine experimentally the kinetic energy and the temperature of the fragments.

MEASUREMENT PROCEDURE

The neutron energy was determined by measuring the time of flight. We measured the time interval between the instant of fission of the U^{235} nucleus in a scintillation fission chamber and the instant when the emitted neutrons were registered by a detector installed at a known distance L from the fission chamber. The neutron spectrum was measured with a 64-channel time analyzer.[1] The time stretching principle was used to measure short time intervals (0 to 0.25 μsec). FÉU-1V photomultipliers were used. The geometry of the experiment and a block diagram of the neutron spectrometer are shown in Fig. 1.

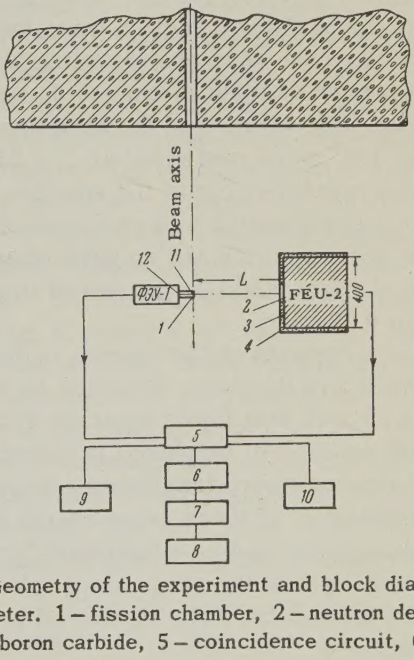

FIG. 1. Geometry of the experiment and block diagram of the spectrometer. 1 – fission chamber, 2 – neutron detector, 3 – lead, 4 – boron carbide, 5 – coincidence circuit, 6 – amplifier, 7 – pulse amplitude-to-duration converter, 8 – 64-channel time analyzer, 9 – fragment monitor, 10 – neutron monitor, 11 – layer of U^{235}, 12 – layer of ZnS(Ag).

The scintillation fission chamber was a 20 × 30 mm aluminum cup covered with a light pipe of organic glass. One milligram of U^{235} was deposited on the bottom. A layer of ZnS(Ag) was placed on the light pipe to register the fission fragments emitted from the U^{235} layer. The U^{235} and ZnS(Ag) layers of 8 mm diameter were 20 mm apart. The chamber thus registered only fragments whose trajectories made angles not greater than 15° with the chamber axis. The chamber was connected to the vacuum system to produce the necessary gas pressure. The use of a ZnS(Ag) detector was made possible by the fact that only a small part of the leading edge of the pulse was used.

The variation of the spectrometer efficiency with the neutron energy was established experimentally. This was done with a scintillation fission chamber that registered almost all the fragments moving in a solid angle 2π. In this case the measured neutron spectrum corresponds to the general spectrum, which is well known from other investigations and obeys the Watt formula[2]

$$N(E) = e^{-E}\sinh\sqrt{2E}$$

(E is in megavolts).

To produce fission of the U^{235}, the chambers were bombarded with a beam of neutrons from a reactor, at an intensity of 1×10^9 neut/cm^{2}sec.

The fission neutrons were registered with a 30×20 mm stilbene crystal. The spectra of neutrons emitted at 0 and 180°, 40 and 120°, and 90° to the fragment flight direction were measured. The spectra of the neutrons traveling at 0 and 180° were measured at flight distances L equal to 25 and 40 cm. The spectra of the neutrons traveling at 40 and 120° were measured at L = 25 cm. During the measurement of the spectra, the fission chamber was evacuated to a pressure of 0.01 mm Hg. The spectrometer had an adjustment by which the time of flight could be measured in a range from 0 to 0.13 μsec.

In measurements of the spectra of the neutrons that travelled in the same direction as the fragments, a 50×45 mm liquid detector comprising a 2-percent solution of terphenyl in toluol was used for the light and heavy fragments separately. The flight distance L in these experiments was 50 cm. The spectrometer had an adjustment for measuring the time of flight in the range from 0 to 0.25 μsec. The different spectra were measured in the following manner.

The overall spectrum of both the heavy and light fragments was measured first with the fission chamber evacuated to 0.01 mm Hg. This was followed by measurement of the spectrum of the neutrons traveling in the same direction as the heavy fragments. The fission chamber was filled for this purpose with argon at 600 mm Hg. The heavy fragments were slowed down more rapidly in the gas, so that at this pressure the chamber recorded only the light fragments. This is seen from the differential fragment-count vs. chamber pressure curve of Fig. 2, where the maximum at p = 430 mm Hg corresponds to the heavy group of fragments, while that at 700 mm corresponds to the light group. From the geometry of the experiment it is seen that only neutrons traveling in the direction of the heavy fragments were registered in our case. Check calculations have shown that the spectrum of these neutrons is due essentially to the neutrons emitted from the heavy fragments. The spectrum of the neutrons from the light fragments was found by subtracting the heavy-fragment spectrum from the overall neutron spectrum.

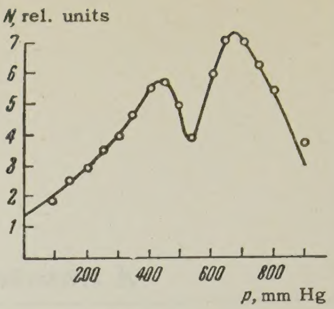

FIG. 2. Differential curve of the count of fragments in the fission chamber vs. the argon pressure.

To check the correctness of the experiments, control measurements were made, in which a paraffin scatterer 14 cm thick was placed between the fission chamber and the neutron detector. Such a paraffin layer scatters the neutrons almost completely and only the fission gammas reach the detector. If the experiments are correctly set up, then only the peak due to the gammas emitted during the instant of fission of the U^{235} remains on the curve. The results of the control measurements (see Fig. 5) confirm the correctness of the data obtained.

In reducing the measurement data, the position of the peak due to the fission gammas was taken as the time reference. The width of the gamma peak at half its height was used to determine the resolution of the spectrometer, which was found to be 5×10^{-9} sec.

EXPERIMENTAL RESULTS AND DATA REDUCTION

The experimentally obtained neutron spectra for different emission angles φ relative to the fragment trajectories are shown in Fig. 3. Reduction of these data yielded the neutron energy spectra in the laboratory frame (l.s.), shown in Fig. 4. It is seen from the curves that the number of neutrons

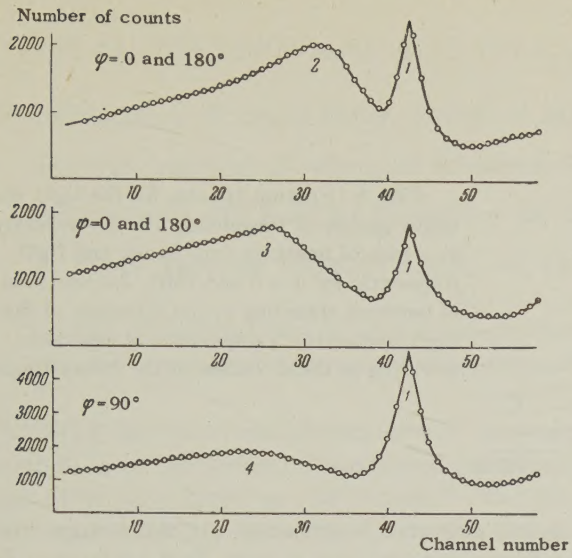

FIG. 3. Experimental spectra of fission neutrons for different angles of emission φ relative to the direction of fragment travel. 1 – peak of prompt fission gammas, 2 – spectrum for flight distance L = 25 cm, 3 – spectrum for L = 40 cm, and 4 – for 25 cm. The abscissas indicate the number of the time-analyzer channel.

and their energy distribution depend on the angle between the directions of the fragments of the neutrons. This result confirms the assumption that the fission neutrons are emitted by rapidly moving excited fragments. The ratio of the number of neutrons traveling at 90° to the fragments to the number of neutrons traveling in the same direction as the fragments, obtained experimentally by measuring the fission neutron spectra at different angles, was found to be 0.17. This quantity agrees well with the results of Wilson,[3] $N(90°)/N(0°) = 0.18$, and is somewhat smaller than the value obtained by Fraser,[4] 0.23.

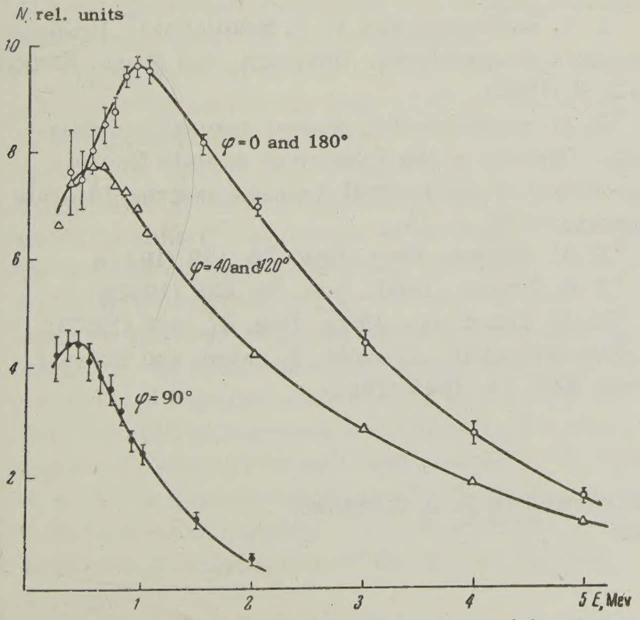

FIG. 4. Energy spectra of fission neutrons, lab. system.

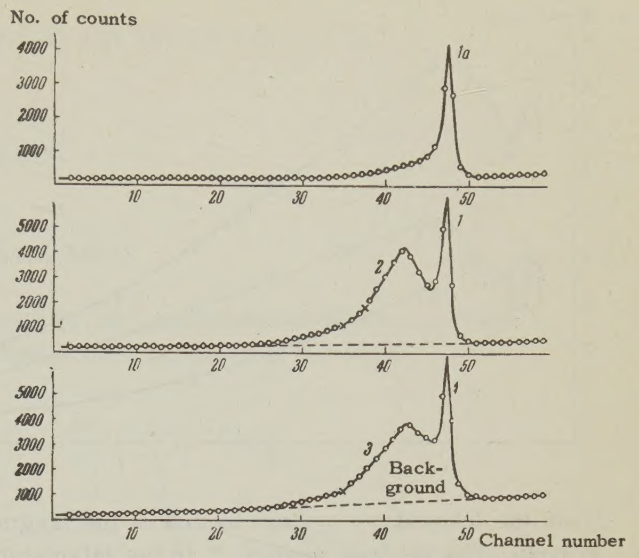

FIG. 5. Experimental curves, obtained in a liquid neutron detector. 1 – peak of prompt fission gammas, 1a – curve obtained with paraffin scatterer, 2 – summary curve for neutrons from light and heavy fragments for 0 and 180°, 3 – spectrum of neutrons traveling in the direction of the heavy fragments.

The experimental curves for the separate measurements of the spectra of the neutrons from the light and the heavy groups of fragments are shown in Fig. 5. The corresponding energy spectra of the neutrons are shown in Fig. 6. The maxima in the 0.2 – 0.3 Mev region on the curves are obviously produced by neutrons traveling in a direction opposite to the fragments that emit them at speeds smaller than the fragment speeds. The main part of the spectra is made up, on the other hand, by neutrons traveling in the same direction as the fragments. The neutron spectra are thus the sums of these two components. An analysis of the curves of Figs. 5 and 6 permits a determination of the fragment velocity at the instant when it emits the neutrons. The kinks and the experimental curves of Fig. 5, denoted by crosses and corresponding to the minima on the curves of Fig. 6, pertain to neutrons with zero energy in the reference frame of the resting fragments. In the laboratory system, consequently, these neutrons have the same velocities as the fragments from which they are emitted. The velocities of the heavy and light fragments obtained by such an analysis are:

$$V_h = (0.88 \pm 0.08) \cdot 10^9 \text{ cm/sec},$$
$$V_l = (1.1 \pm 0.12) \cdot 10^9 \text{ cm/sec}.$$

The values obtained for the fragments at the instant of neutron emission are close to values obtained by others, $V_h = 0.96 \times 10^9$ cm/sec and $V_l = 1.42 \times 10^9$ cm/sec.[5]

To determine the fragment excitation energy it is necessary to recalculate the obtained spectra

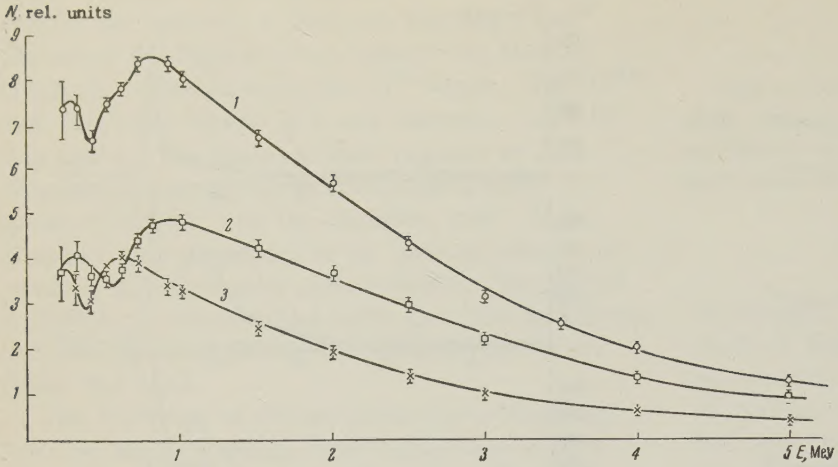

FIG. 6. Neutron spectra for the light and heavy groups of fragments, l.s. 1 – summary spectrum of neutrons from heavy and light fragments, for $\varphi = 0$ and 180°, 2 – spectrum of neutrons traveling in the direction of the light fragments, 3 – spectrum of neutrons traveling in the direction of the heavy fragments.

from the laboratory system to that of the fragments at rest. The neutron energy E in the laboratory system can be calculated from the formula[6]

$$E(\varepsilon, \varphi) = \varepsilon [1 - r^2 + 2r^2 \cos^2 \varphi + 2r \cos \varphi (1 - r^2 + r^2 \cos^2 \varphi)^{1/2}], \tag{1}$$

where φ is the angle between the fragment and neutron flight directions, r is the ratio of the fragment speed to the neutron speed in the rest frame of the fragment, and ϵ is the energy of the neutron in the same frame. The probability per unit solid angle of emission of a neutron at an angle φ is given by

$$f(\varepsilon, \varphi) = \frac{1}{4\pi} \left(\frac{E}{\varepsilon}\right)^{3/2} \left\{1 + r\left[1 - \frac{E}{\varepsilon} \sin^2 \varphi\right]^{1/2}\right\}^{-1}. \tag{2}$$

The l.s. neutron spectrum at an emission angle φ can therefore be described by

$$N(E, \varphi) = f(\varepsilon, \varphi) N(\varepsilon), \tag{3}$$

where $N(\epsilon)$ is the neutron spectrum in the rest frame of the fragment.

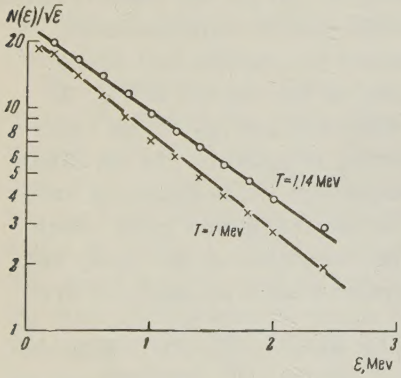

FIG. 7. Neutron spectra for the light (circles) and heavy (crosses) groups of fragments in a system where the fragments are at rest. Solid curves – calculated from Eq. (4).

Using this formula, the experimental spectra obtained in this investigation can be recalculated to the rest frame of the fragments. Figure 7 shows the neutron spectra separate for the light and for the heavy group of fragments (in the frame where these fragments are at rest), obtained by recalculating the experimental curves of Fig. 6. An analysis of the spectra has shown that they fit quite well the Maxwellian distribution

$$N(\varepsilon) \sim \sqrt{\varepsilon} \exp(-\varepsilon/kT), \tag{4}$$

where T is the neutron temperature of the fragments. The experimental spectra agree best with the theoretical ones, calculated from (4), when the fragment temperatures are T_l = 1.14 Mev and T_h = 1 Mev. In addition, analysis has shown that the light fragments emit 30 percent more fragments than the heavy ones. A similar result was obtained by Fraser.[4]

It must be noted in conclusion that the procedure employed here can be successfully applied to an investigation of the neutron-fission spectra of other elements, including the neutrons from the spontaneous fission of Cf^{252}.

---

[1] I. A. Radkevich and V. V. Sokolovskiĭ, Приборы и техника эксперимента, (Instrum. and Meas. Engg.) No 2, 3 (1956).

[2] B. G. Erozolimskiĭ, Физика деления атомных ядер, Physics of the Fission of Atomic Nuclei. Appendix 1 to the journal Атомная энергия (Atomic Energy), 1957, p. 74.

[3] R. R. Wilson, Phys. Rev. 72, 189 (1947).

[4] J. S. Fraser, Phys. Rev. 88, 536 (1952).

[5] R. B. Leachman, Phys. Rev. 87, 444 (1952).

[6] De-Benedetti, Francis, Preston, and Bonner, Phys. Rev. 74, 1645 (1948).

Translated by J. G. Adashko
323

SOVIET PHYSICS JETP VOLUME 11, NUMBER 6 DECEMBER, 1960

THE (*p, d*) REACTION AND INELASTIC SCATTERING OF PROTONS ON Be^9

O. F. NEMETS, L. S. SALTYKOV, and M. V. SOKOLOV

Physics Institute, Academy of Sciences, Ukrainian S.S.R.

Submitted to JETP editor December 13, 1959

J. Exptl. Theoret. Phys. (U.S.S.R.) 38, 1663-1664 (June, 1960)

Angular distributions of protons inelastically scattered by Be^9 nuclei and of deuterons from the $Be^9(p, d)Be^8$ reaction were measured for incident proton energies of 6.8 Mev.

DESPITE the many measurements of the angular distribution of inelastically scattered particles which have been made on Be^9 nuclei[1-7] and the other experiments to determine the spin and parity of the level in Be^9 at 2.43 Mev, these parameters are still not established uniquely. At the same time, they play a decisive role in the choice of a model for the Be^9 nucleus. We have carried out measurements in the external beam of the cyclotron of the Physics Institute of the Ukr. S.S.R. Academy of Sciences for a proton energy of 6.8 Mev and with the same geometry as in reference 8. The difference was that in place of deuterons, hydrogen molecular ions were brought to the target and the ionization chamber was replaced by a scintillation spectrometer. The thickness of the beryllium target was 1.4 mg/cm². The target was prepared by vacuum deposition.

In Fig. 1 we show the angular distribution obtained for the inelastically scattered protons (solid curve 1). It is characterized by a broad maximum in the region of angles 80 – 90° and an increase of the reaction cross section at small angles; the latter shows that the direct reaction mechanism plays an important part.

The dashed curve 2 in Fig. 1 shows the results of computations for the case of direct interaction of the incident proton with a nucleon in the nucleus[9] for $r_0 = 4 \times 10^{-13}$ cm. Calculations for the case of direct excitation of rotational levels in the alpha particle model[10] are shown in the same figure by the dashed curve 3 (assuming $r_0 = 5.6 \times 10^{-13}$ cm). In the first case the parity of the 2.43-Mev level must be positive while for the second it must be negative. In both cases the comparison of the theoretical and experimental results can hardly be considered satisfactory and consequently the parity of the state cannot be established uniquely. In addition, neither theory explains the increase in cross section at small angles. This is apparently related to electrical interaction of the proton with the nucleus.[11]

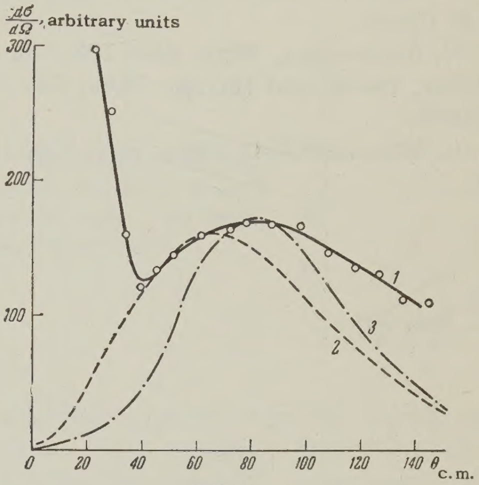

FIG. 1

The angular distribution of deuterons from the $Be^9(pd)Be^8$ reaction is shown in Fig. 2 by the solid curve 1. Here also for comparison we give the results of calculations for the case when the incident proton interacts only with the unpaired neutron[12] (dashed curve 2) and the results of computations in the Born approximation[13] (curve 3); the curves are adjusted at 20°. In both cases the orbital angular momentum of the neutron was taken equal to unity in accordance with the known values of the spins of the ground states of Be^9 and Be^8 ($3/2^-$ and 0^+).

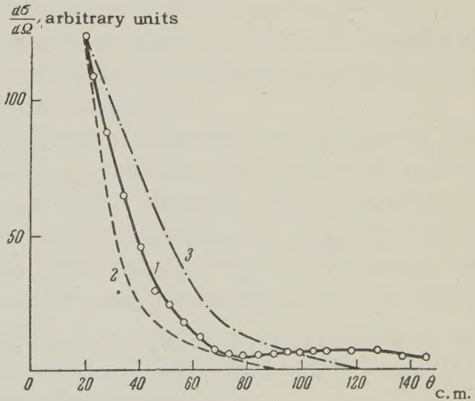

FIG. 2

The angular distribution found for the deuterons is in agreement with the results of work carried out for other proton energies.

The authors take this opportunity to express their gratitude to Professor M. V. Pasechnik for his interest in the work, to Yu. A. Bin'kovskii for preparing the target and to the personnel of the cyclotron laboratory for making possible uninterrupted operation of the apparatus.

---

[1] Benveniste, Finke, and Martinelli, Phys. Rev. **101**, 655 (1956).

[2] J. B. Reynolds and K. G. Standing, Phys. Rev. **101**, 158 (1956).

[3] S. W. Rasmussen, Phys. Rev. **103**, 186 (1956).

[4] Weber, Davis, and Marion, Phys. Rev. **104**, 1307 (1956).

[5] R. G. Summers-Gill, Phys. Rev. **109**, 1591 (1958).

[6] T. S. Green and R. Middleton, Proc. Phys. Soc. A69, 28 (1956).

[7] J. W. Haffner, Phys. Rev. **103**, 1398 (1956).

[8] N. I. Zaika and O. F. Nemets, Izv. Akad. Nauk. SSSR, Ser. Fiz. (in press).

[9] Austern, Butler, and McManus, Phys. Rev. **92**, 350 (1953).

[10] R. R. Haefner, Revs. Modern Phys. **23**, 228 (1951).

[11] C. J. Mullin and E. Guth, Phys. Rev. **82**, 141 (1951).

[12] T. I. Kopaleĭshvili, JETP **30**, 1145 (1956), Soviet Phys. JETP **3**, 973 (1957).

[13] J. Dabrowski and J. Sawicki, Nuovo cimento **12**, 293 (1954).

Translated by M. Hamermesh
324

SOVIET PHYSICS JETP VOLUME 11, NUMBER 6 DECEMBER, 1960

SKIN EFFECT AND SHOCK WAVES IN AN INDUCTION GAS DISCHARGE

S. E. GREBENSHCHIKOV and M. D. RAĬZER

Submitted to JETP editor December 14, 1950

J. Exptl. Theoret. Phys. (U.S.S.R.) 38, 1665-1667 (June, 1960)

A gas discharge induced at a frequency of 300 cps is investigated. The shock wave was found to detach itself from the current layer under the conditions of the experiment. The current distribution in the discharge chamber is determined by the nature of the skin effect for metallic conductors.

IN most experiments on induction gas discharges, the main attention was focused on phenomena occurring in the first or second half cycle of the current in the gas.[1] A study of a current that flows in the gas for a prolonged period is, however, very important. Great interest attaches here to an investigation of the influence of shock waves and of skin effect on the course of the processes in a gas discharge.

We investigated gas discharges in an axially-symmetrical magnetic field at a frequency f = 300 kcs. The magnetic field was produced by an oscillating discharge from a capacitor bank ($C = 0.36\ \mu f$, $U_C = 30$ to 50 kv) into an inductive copper turn (300 mm diameter, $L = 0.53\ \mu h$) of rectangular cross section (height h = 60 mm, thickness 3 mm). The copper turn encircled the vacuum chamber, which consisted of a glass cylinder (200 mm. dia., h = 30 mm), sealed on both sides by rubber-gasketed glass disks. The main experiments were carried out with the chamber filled with hydrogen and with air in the range $p = 5 \times 10^{-1}$ to 10^{-2} mm Hg. The maximum current in the gas was $I_g = 15$ kiloamp. From a comparison of the oscillograms of the current in the gas and in the copper turns it follows that the ratio of the plasma reactance to resistance is $\omega L/R \gg 1$.

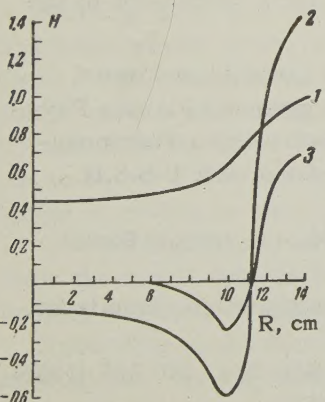

FIG. 1. Discharge in hydrogen, p = 0.05 mm Hg. Curve 1 – magnetic field in the absence of a discharge, 2 – magnetic field during the second half cycle of current, 3 – during the third half cycle.

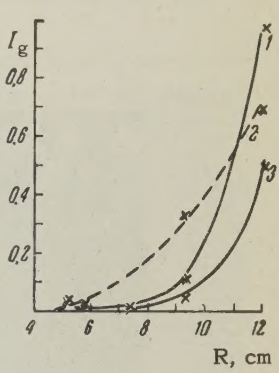

FIG. 2. Discharge in hydrogen, p = 0.05 mm Hg. Curves 1, 2, and 3 are for the first, second, and third half cycles, respectively.

The distribution of the magnetic field in the central plane of the discharge chamber is shown in Fig. 1. The field intensity in the center of the chamber is approximately 1500 oe. The current in the gas should contract towards the center of the chamber at the given magnetic field configuration under the influence of the electrodynamic forces.[1]

Figure 2 shows the distributions of the current in the gas along the radius of the chamber.* Adjacent to the side wall of the vacuum chamber is a current layer approximately 3 cm wide, in which 90 or 80 percent of I_g is concentrated. No motion of the current layer is observed during the entire discharge, nor does the character of the current distribution in the gas change. It is seen from the plots that after two half cycles of current almost the entire magnetic field is concentrated in the current layer, and there is no field in the center of the chamber.

A high-speed photograph (Fig. 3) shows that a glowing ring, approximately 3 mm wide and of the same height as the chamber, is produced at the wall of the vacuum chamber during the instant of breakdown. The ring contracts toward the center of the chamber, and its brightness at the center

---

*Figures 1 and 2 are plotted in arbitrary units, at the instants of time corresponding to the maximum current in the gas during different half cycles.

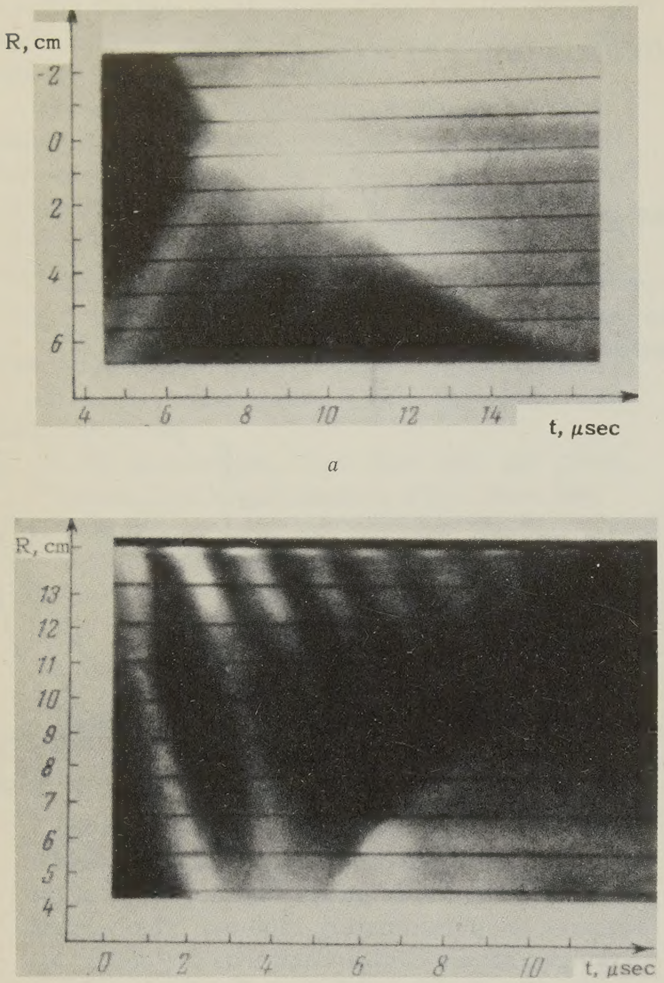

a

b

FIG. 3. High-speed photograph of a discharge in air. a – p = 0.07 mm Hg; b – p = 0.05 mm Hg.

increases greatly at the instant of contraction. The initial speed of motion of the ring, $v = 2 \times 10^6$ to 1.5×10^7 cm/sec, depends on the current in the gas, the pressure, and on the type of gas. It is in good agreement with the expression $v \sim (I_g/p)^{1/2}$ (Fig. 4). The rate of contraction of the ring decreases as the center of the chamber is approached.

Measurements made with high-speed transducers[2] have shown that the entire volume of the vacuum chamber becomes filled with ionized gas after one or at most two half cycles of current. From a comparison of the high-speed photographs and the voltage oscillograms obtained with high-frequency transducers it follows that the speed of propagation of the ionization along the radius of the vacuum chamber corresponds to the speed of the glowing ring.

The narrow glowing ring observed on the photographs, the contraction of which is accompanied by ionization of the gas, represents apparently the front of the shock wave. The character of the dependence of the speed of motion of the glowing rings on the gas pressure ($v \sim p^{-1/2}$) agrees with the results of experiments on shock waves.[3]

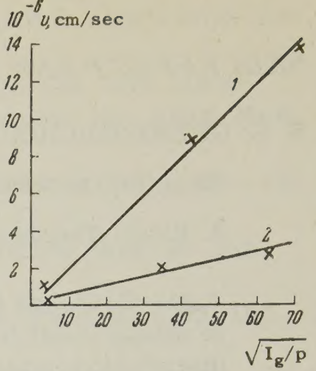

FIG. 4. Dependence of the speed of the shock wave on the ratio of the current in the gas to the pressure. 1 – for hydrogen, 2 – for air.

The character of distribution of the currents and magnetic fields in the presence of an ionized gas in the entire volume of the vacuum chamber is evidence of the existence of skin effect, which occurs in a plasma as it does in metal conductors.[4] The thickness of the skin layer, ~ 3 cm, yields an estimate for the conductivity of the plasma, namely $\sigma = 7 \times 10^{13}$ cgs esu.

In spite of the propagation of shock waves under the influence of the magnetic field, the current layer remains at the side wall of the chamber. This is probably due to the fact that during one half cycle of the field, the current layer does not have time to move away from the wall, owing to the short time of application of the force. The presence of a strong vortical electric field ($E \sim 400$ v/cm) produces a breakdown at the chamber wall during each succeeding half cycle of current. The presence of a clearly pronounced skin effect leads here to the shielding of the magnetic field in the inner regions of the chamber.

It should be noted that the glow of the plasma does not characterize the behavior of the current in the gas in this case.

The authors are grateful to R. A. Latypov and A. G. Frank for help with the experiments, and to L. M. Kovrizhnykh, M. S. Rabinovich, A. A. Rukhadze, and I. S. Shpigel' for a discussion of the results.

---

[1] S. M. Osovets, Физика плазмы и проблема управляемых термоядерных реакций, (Plasma Physics and the Problem of Controllable Thermonuclear Reactions), Vol. 2, Acad. Sci. U.S.S.R., 1958, p. 238.

[2] I. S. Shpigel', JETP **36**, 411 (1959), Soviet Phys. JETP **9**, 285 (1959).

[3] A. Kolb, Magnetohydrodynamics, Atomizdat, 1958, p. 82.

[4] R. Carruthers, Appl. Sci. Res. B5, 135 (1955).

Translated by J. G. Adashko

SOVIET PHYSICS JETP VOLUME 11, NUMBER 6 DECEMBER, 1960

ENERGY LOSSES OF FAST μ MESONS IN THICK LAYERS OF MATTER

M. I. DAĬON

P. N. Lebedev Physics Institute, Academy of Sciences, U.S.S.R.

Submitted to JETP editor December 24, 1959

J. Exptl. Theoret. Phys. (U.S.S.R.) 38, 1668-1672 (June, 1960)

If energy losses of μ mesons in the ground are taken into account [by formulas (1) and (2)], it is found that the μ-meson spectrum previously measured underground (depth ~40 m water equivalent) agrees with the results of the corresponding measurements[2,3] performed at sea level.

In the present article, we compare the μ-meson spectrum underground (at a depth of ~40 m water equivalent), measured in 1958 by the mass-spectrometer method,[1] with the μ-meson spectrum at sea level obtained recently by Pine, Davisson, and Greisen,[2] embracing the μ-meson energy region up to the value of ~200 Bev.

Since the change in the spectrum depends primarily on the μ-meson energy loss in the ground, the obtained results can be a check of the theoretical formulas for determining the energy loss.

To transform the spectrum at the ground to our depth of observation, it is necessary first to know the thickness of the ground and to take into account the energy loss by means of the known theoretical formulas.

1. In a previous work[1] we were unable to measure sufficiently accurately the thickness of the ground above the apparatus or to determine its density. We therefore employed comparative measurements of the intensity of the hard component at sea level (I_0) and at the given depth (I) by means of a separate telescope composed of three rows of counters with a lead filter. The intensity ratio was

$$I_0/I = 11.13 \pm 0.43.$$

Starting from this value and the μ-meson spectrum at sea level, according to the data of Caro et al.,[3] we determined the minimum value of the μ-meson momentum (p_0) necessary for the traversal of the given layer of ground. This turned out to be ~9.8 Bev and corresponded to a μ-meson range of ~40 m in water.

On the other hand, we determined the depth from the direct data of Ehmert[4] on the intensity of cosmic radiation at different depths under water.

According to the formulas used by Ehmert to approximate his experimental data, our depth was also equivalent to ~40 m of water.

On the basis of the above, and also from a comparison of the obtained ratio I_0/I with the data of other authors, we conclude that the amount of ground above our setup was 4700—4800 g/cm^2 and that its stopping power was equivalent to ~40 m of water.*

2. The energy loss, dE/dx, of a μ meson passing through the ground (in the energy region $> 10^9$ ev), calculated with the formula obtained by Barrett et al.,[5]† is

$$-dE/dx = 1.88 + 0.0766 \ln (E'_m/\mu c^2) + 3.5 \cdot 10^{-6} E, \qquad (1)$$

where

$$E'_m = E^2/(E + \mu^2 c^2/2\mu_e)$$

and dE/dx is expressed in Mev g^{-1} cm^2. This formula takes into account the energy losses due to ionization (with allowance for the polarization of the medium), bremsstrahlung, pair production and nuclear interaction. As for the latter, in the energy region of interest to us ($10^{10} - 10^{11}$ ev), it gives a small contribution ($2-3\%$) to the total loss. The values of the total μ-meson energy loss calculated according to formula (1) are in good agreement with the calculations of Murdoch, Ogilvie, and Rathgeber.[6] At energies $< 10^9$ ev, we took the value of the energy loss as 2.1 Mev g^{-1} cm^2.

3. A μ meson having a momentum p at sea level will have, after passing through a layer of ground of thickness h g/cm^2, a momentum $p_1 < p$, owing to its being slowed down. In the recalculation of the spectrum it should be borne in mind that there is a change in the width of the momentum interval to which the same particles

---

*It should be mentioned that the particles are slowed down in the ground less than in water. In the range region of interest to us, $R_2 \approx 1.19\, R_1$, where R_1 and R_2 are the ranges of the particles in g/cm^2 in water and in the ground, respectively.[2]

†In reference 2 the last term of this formula was taken equal to 3.0×10^{-6} E.

belong at sea level (dp) and at the given depth (dp_1), namely:[7]

$$dp_1/dp = k = [B(p_1)/B(p)]\,[f(p/\mu)/f(p_1/\mu)], \qquad (2)$$

where in the energy region $p < \mu^2/\mu_e$

$$B = \log\frac{4\mu_e^2(p/\mu)^4}{I^2(z)} - 2\frac{(p/\mu)^2}{1+(p/\mu)^2}.$$

4. The table gives all data necessary to transform the Pine-Davisson-Greisen spectrum to our depth. Additional data for the analogous transformation of the spectrum of Caro et al.[3] are also shown here.

In columns 2 and 3 of the table are shown the values of the absolute μ-meson intensity at sea level (according to references 2 and 3); column 4 shows the momentum loss Δp, calculated according to formula (1), in passing through a layer of ground of thickness 4750 g/cm^2; column 5 gives the corresponding momentum of the μ mesons at our depth ($p_1 = p - \Delta p$); column 6 gives the values of k calculated according to formula (2); and, finally, columns 7 and 8 give the values of the absolute intensities of the μ mesons at our depth.

Figure 1 duplicates the μ-meson momentum spectrum at our depth[1] and was obtained from measurements with magnetic fields $H_1 = 3300$ oe and $H_2 = 6300$ oe. On the same figure are shown the values of the intensity recalculated from sea level (see table).

DISCUSSION OF RESULTS

1. From Fig. 1 it is seen that the experimental data[1] are in good agreement with the Pine-Davisson-Greisen spectrum transformed to our depth of observation. For momenta $p \gtrsim 0.5$ Bev it is observed that the calculated values of the intensity are a little higher than the experimental values, which is probably due to not taking into account the scattering of slow particles in the ground in the recalculation of the spectra[2,3] to our depth.

Momentum p at sea level (Bev/c)	Absolute intensity at sea level, 10^{-8}cm^{-2}sec^{-1}sr^{-1} (Mev/c)$^{-1}$		Momentum loss over path of 4750 g/cm^2 underground (Bev/c)	Momentum p_1 at depth of 4750 g/cm^2 underground (Bev/c)	dp_1/dp	Absolute intensity of particles with momentum 10^{-8}cm^{-2} ×sec^{-1}sr^{-1}(Mev/c)$^{-1}$	
	from ref. 3	from ref. 2				*	†
1	2	3	4	5	6	7	8
10	10	10	~9.8	~0.2	0.79	12.7	12.7
10.4	9	9	~9.9	~0.5	0.70	12.8	12.9
10.9	8	8.05	10.0	0.9	0.74	10.7	10.8
11.94	6.7	7.2	10.14	1.8	0.79	8.45	9.05
14.9	4	4.3	10.4	4.5	0.88	4.55	4.9
20	1.72	2.1	10.77	9.14	0.93	1.85	2.26
30	0.555	0.73	11.2	18.7	~0.96	0.58	0.76
40	0.230	0.33	11.5	28.4	~1	0.23	0.33
50	0.12	0.17	11.8	38.1	~1	0.12	0.17
60		0.11	12.0	47.8	~1	—	0.11

*With spectrum of reference 3. †With spectrum of reference 2.

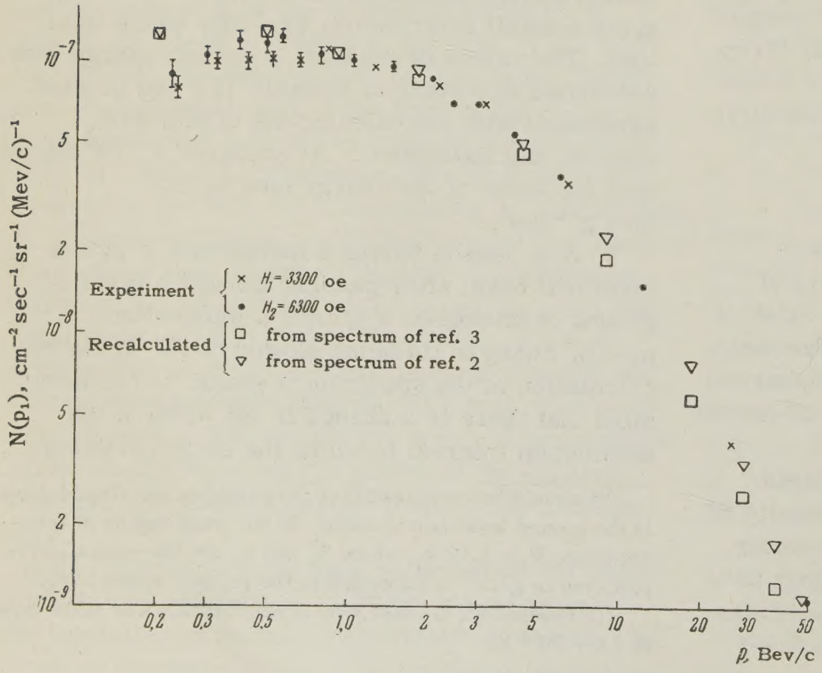

FIG. 1. Experimentally measured μ-meson momentum spectrum underground (for two values of the magnetic field) and spectra recalculated from sea level.

The spectrum of Caro et al.[3] in the energy region $\gtrsim$ 15 Bev is somewhat steeper than the spectrum in reference 2, but the difference in the spectra is within the limits of statistical accuracy of both experiments. It may be dependent on the specific character of each apparatus, for example, a different effectiveness for excluding shower events.

We note that previously,[1] in transforming the spectrum of Caro et al.,[3] we did not take into account the increase in the μ-meson energy loss with increasing energy (the increase between 10 to 60 Bev is ~20%). An account of the increase in the energy loss leads to somewhat poorer agreement between the recalculated data of Caro et al. and the experimental data in the high-energy region (see Fig. 1).

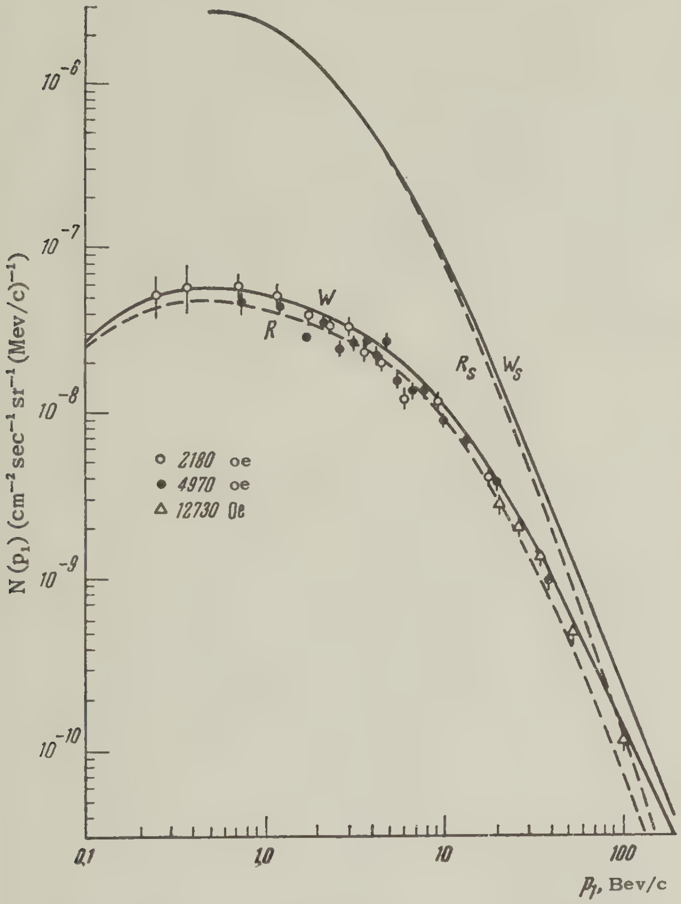

FIG. 2. μ-meson momentum spectrum[6] at depth of 7000 g/cm² and comparison with spectrum at sea level (R_s, W_s).

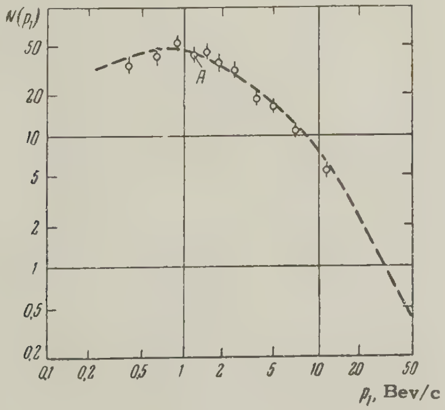

FIG. 3. μ-meson momentum spectrum[9] at depth of 3800 g/cm². Circles indicate experimental data;[1] A – point of normalization of both spectra.

2. Murdoch, Ogilvie, and Rathgeber[6] obtained the μ-meson momentum spectrum at a depth of 7000 g/cm² below the ground up to momentum values of ~100 Bev/c (Fig. 2). In comparing their spectrum with the spectrum at sea level,* the authors took into account only the values of the μ-meson energy loss and obtained agreement between the transformed spectrum and the measured one.

3. A measurement of the momentum spectrum under the ground at a depth of 3800 g/cm² was carried out in reference 9. The authors found that their spectrum was in agreement with the spectrum of Caro et al., recalculated to their depth with allowance for scattering of the particles in the ground.† However, comparing their results with the data of reference 1, they erroneously assumed that both experiments were carried out at the same depth (see Fig. 3). As a matter of fact, there is a considerable difference in the depths (3800 and 4750 g/cm²), which, first, does not allow a direct comparison of both spectra, and, second, removes the apparent discrepancy in the results as noted by the authors[9] with regard to the value of the energy loss in the ground.‡

CONCLUSIONS

Good agreement is observed between the μ-meson differential spectrum measured at a depth of

---

*The spectrum for sea level was used in two forms (see Fig. 2): 1) the directly measured[8] spectrum extrapolated above 20 Bev/c, varying as $p^{-2.75}$ and denoted $W_s(p)$; 2) the same spectrum, but corrected[5] for π–μ decay in the atmosphere, denoted R_s (the latter being in agreement with the data of reference 3).

†In the energy region considered here, the spectrum of Caro et al. is practically no different from the Pine-Davisson-Greisen spectrum.

‡This misunderstanding arose from a certain vagueness in terminology: on the one hand, the authors, in measuring the intensity of cosmic radiation under thick layers of water, expressed the thickness in meters of water; on the other hand, in a number of articles the thickness of the ground is expressed in meters of water equivalent, where layers of ground and water are considered to be equivalent if they contain equal amounts of matter in g/cm². As shown above, however, such layers are not at all equivalent as regards the slowing down of charged particles.

~4700 g/cm^2 underground in the energy region 2×10^8 to 5×10^{10} ev[1] and that calculated for the given depth on the basis of the Pine-Davisson-Greisen spectrum[2] by taking into account the μ-meson energy loss in the ground. The spectrum of Caro et al.[3] transformed to the given depth of observation gives somewhat poorer agreement with the experimental results in the high-energy region, but the accuracy of the latter is not sufficient to ascribe any great significance to this difference. The authors of the latter work[6,9] also arrive at the conclusion that the μ-meson differential spectrum obtained by them at depths of 3800 and 7000 g/cm^2 are in agreement with the μ-meson spectrum at sea level recalculated for these depths; the μ-meson spectrum at sea level used there is in close agreement with the Pine-Davisson-Greisen spectrum in the energy region under consideration.

[1] M. I. Daĭon and L. I. Potapov, JETP **36**, 697 (1959), Soviet Phys. JETP **9**, 488 (1959).

[2] Pine, Davisson, and Greisen, Proc. International Cosmic Ray Conf. **1**, M., VINITI, 1960.

[3] Caro, Parry, and Rathgeber, Australian J. Sci. Instr. **A4**, 16 (1951).

[4] A. Ehmert, Z. Physik **106**, 751 (1937).

[5] Barrett, Bollinger, Cocconi, Eisenberg, and Greisen, Revs. Modern Phys. **24**, 133 (1952).

[6] Murdoch, Ogilvie, and Rathgeber, Proc. International Cosmic Ray Conf. **1**, M, VINITI, 1960.

[7] E. P. George and G. S. Shrikantia, Nuclear Phys. **1**, 54 (1956).

[8] B. G. Owen and J. G. Wilson, Proc. Phys. Soc. (London) **A68**, 409 (1955).

[9] Ashton, Wolfendale, and Nash, Proc. International Cosmic Ray Conf. **1**, M., VINITI, 1960.

Translated by E. Marquit

326

SOVIET PHYSICS JETP VOLUME 11, NUMBER 6 DECEMBER, 1960

THE THERMAL CONDUCTIVITY OF SUPERCONDUCTORS IN THE INTERMEDIATE STATE

N. V. ZAVARITSKIĬ

Institute for Physical Problems, Academy of Sciences, U.S.S.R.

Submitted to JETP editor January 7, 1960

J. Exptl. Theoret. Phys. (U.S.S.R.) 38, 1673-1684 (June, 1960)

The thermal conductivities of lead, tin and gallium in the intermediate state were measured between 0.15 and 3.7°K. It was found that the transition to the intermediate state is, for heat transport due to phonons, accompanied by an increase in thermal resistivity ΔW_{gi} which is proportional to T^{-3} over the whole temperature range. The magnitude of ΔW_{gi} is close to that calculated on the assumption that the phonons are scattered by conduction electrons in the normal state domains. For heat transport by electrons the increase in thermal resistivity ΔW_{ei} depends weakly on the impurity content of the specimen. Only the dependence of $\Delta W_{ei}/W_{es}$ on T/T_c is similar for all metals. This ratio decreases approximately 30 times between $0.4T_c$ and $0.9T_c$. At temperatures below $\sim 0.4T_c$ the value of ΔW_{ei} is close to that calculated on the assumption that the electron mean free path is limited by the boundaries of the intermediate state domains.

IN this work we study the additional thermal resistivity which arises when heat is conducted across alternate domains of normal and superconducting phases. An investigation of this effect makes possible an understanding of the phenomena occurring when particles cross the phase boundaries. As is known, a periodic structure arises in the intermediate state, for example, in a cylindrical specimen in a magnetic field $H > \frac{1}{2}H_c$, which is perpendicular to the axis of the cylinder. As a result of the effects studied, the thermal conductivity in the intermediate state may be several times smaller than the conductivity not only in the normal, but also in the superconducting phase. Mendelssohn and Olsen[1] were the first to find a reduction in the thermal conductivity of a specimen in the intermediate state, during measurements on lead-bismuth alloys. This effect was also found in pure metals (see Abrikosov and Zavaritskiĭ[2] for references), but there has been no systematic investigation over a wide temperature range.

Heat transport in a superconductor is effected by two mechanisms: by lattice phonons and by electrons. One or the other is dominant, depending on the temperature, the impurity content, etc. The problem posed for this work was the elucidation of the nature of the heat transport for each mechanism separately in the intermediate state.* We measured several metals for this purpose: lead, tin, and gallium. The results obtained for lead were used to determine the change in phonon conductivity, those for tin the change in phonon and electron conductivity and those for gallium the heat conduction by electrons.

The heat conductivity measurements were made on single crystal specimens ~50 mm long and ~1 mm in diameter. The tin and lead specimens were cast in vacuo in thin walled glass capillaries in which crystallization took place immediately after casting. The glass was then removed by etching in hydrofluoric acid. The gallium specimens were prepared as in our previous work.[3] For the specimens, lead with $\sim 10^{-3}\%$ impurity content, tin with $2 \times 10^{-3}\%$, and gallium with between 0.2 and $\sim 5 \times 10^{-4}\%$ impurity were used. Tables I

TABLE I. Characteristics of the specimens used for studying phonon heat conductivity

Specimen	Diameter cm	Phonon mean free path at T = 0.3° K			$10^8 a_s$, cm (from (2) for $\eta = 0.5$)
		$10^8 l_{gs}$, cm [from (3)]	$10^8 l'_{gi}$, cm [from (4)]	$10^8 l_{gn}$, cm	
Sn	0.175	130	11.5	1.2	7
Pb-1	0.13	28	7	1.1	4.2
Pb-2	0.21	28	9	1.1	5.4
		at $T \sim 0.1$°K			
Ga 3G-c	0.3	~200	~70	—	—

In calculating a_s, results of the direct measurement of Δ were used for tin,[9] and the values of Δ calculated from measurements of penetration depth[10] according to the formulae given by Ginzburg[11] and Gor'kov[12] were used for lead.

---

*The results obtained in this work show the inaccuracy of the earlier suggestions[2] that it is sufficient to consider only the change in lattice conduction in order to explain the decrease of thermal conductivity in the intermediate state.

TABLE II. Characteristics of the specimens used for studying electronic heat conductivity

Ga specimen	Diameter cm	K_{T_c} *, $W \cdot cm^{-1} deg^{-1}$	$\rho_0/\rho_{293°K}$	% ** impurity	$\frac{\Delta W_{ei}}{W_{es}}$ at $T=3,5T_c$	$\frac{\Delta W_{ei}}{(\Delta W_{ei})_{spec.\ c\text{-}10}}$
3G-c	0,3	$3.5 \cdot 10^{-2}$	$1,4 \cdot 10^{-2}$	$2 \cdot 10^{-1}$	—	—
c-6	0,12	0,9	$5,4 \cdot 10^{-4}$	$7,7 \cdot 10^{-3}$	0,5	2
c-7	0,083	2,8	$1,6 \cdot 10^{-4}$	$2,3 \cdot 10^{-3}$	0,9	1.5
c-8	0.16	4	$1.2 \cdot 10^{-4}$	$1,7 \cdot 10^{-3}$	1.25	1,4
c-9	0,115	8	$6 \cdot 10^{-5}$	$8,6 \cdot 10^{-4}$	2.0	1.2
c-10	0,11	~13	$\sim 3.6 \cdot 10^{-5}$	$5 \cdot 10^{-4}$	2.7	1
a-5	0,16	16	$8 \cdot 10^{-5}$	$2 \cdot 10^{-3}$	1.25	—
b-4	0,16	34	$8 \cdot 10^{-5}$	$2 \cdot 10^{-3}$	0.5	—
b-5	0,083	~120	$2,4 \cdot 10^{-5}$	$5,5 \cdot 10^{-4}$	1.1	—
Sn specimen	0,175	48	$1,6 \cdot 10^{-4}$	$2 \cdot 10^{-3}$	1.0	—

*For a number of specimens K_{T_c} is the result of extrapolating the measured $K_s(T)$ (according to Zavaritskiĭ[3]).

**The impurity content is calculated from analysis of specimen 3G-c on the assumption that $\rho_0/\rho_{293°}$ is proportional to the impurity content of the metal.

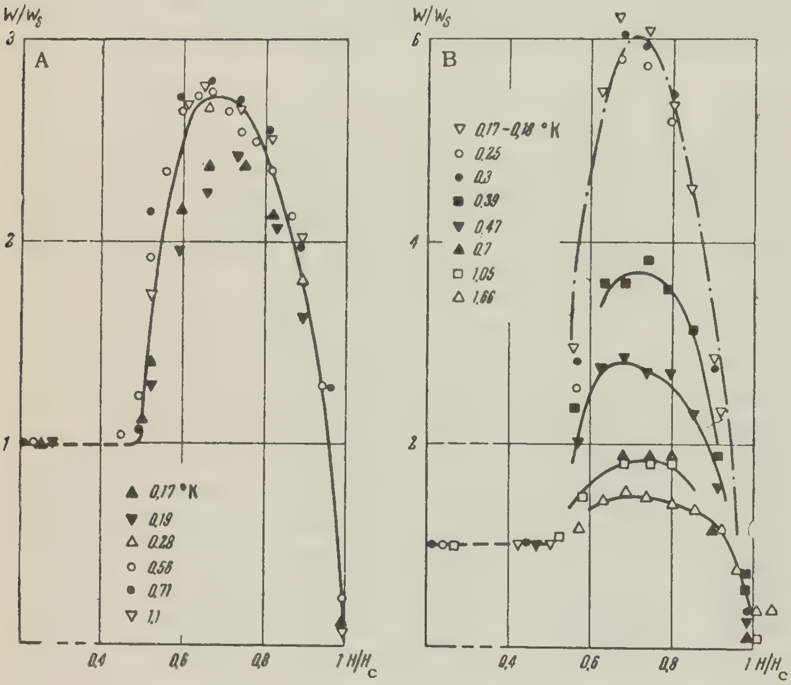

FIG. 1. The variation of thermal resistance for: A – lead (Pb-1) and B – tin in the intermediate state for various temperatures (degrees Kelvin). The dash-dot curve corresponds to $a\Delta W_{ei}$ = const.

and II show the characteristics of the specimens used.

A method similar to that used previously[4] was employed to measure thermal conductivity. The dependence of thermal resistivity on the strength of the magnetic field perpendicular to the specimen axis was measured at constant temperature. During each measuring cycle the temperature of one of the thermometers on the specimen was held constant. A correction was applied to take into account the change in mean temperature of the specimen as the temperature gradient varied during the experiment; this reached some tenths of one per cent in different cases. In the work on gallium, the specimen was heated above the critical temperature after each measuring cycle and brought back into the superconducting state in a magnetic field compensated to within ~ 0.2 oe.

RESULTS AND DISCUSSION

The results of measurements of the thermal resistivity of specimens of lead, tin, and gallium in the intermediate state are shown in Figs. 1 and 2. The conductivity of a number of specimens in the superconducting state is plotted in Fig. 3.

As can be seen from Figs. 1 and 2, the transition from the superconducting to the intermediate state (at a field $\frac{1}{2}H_c$) is generally accompanied

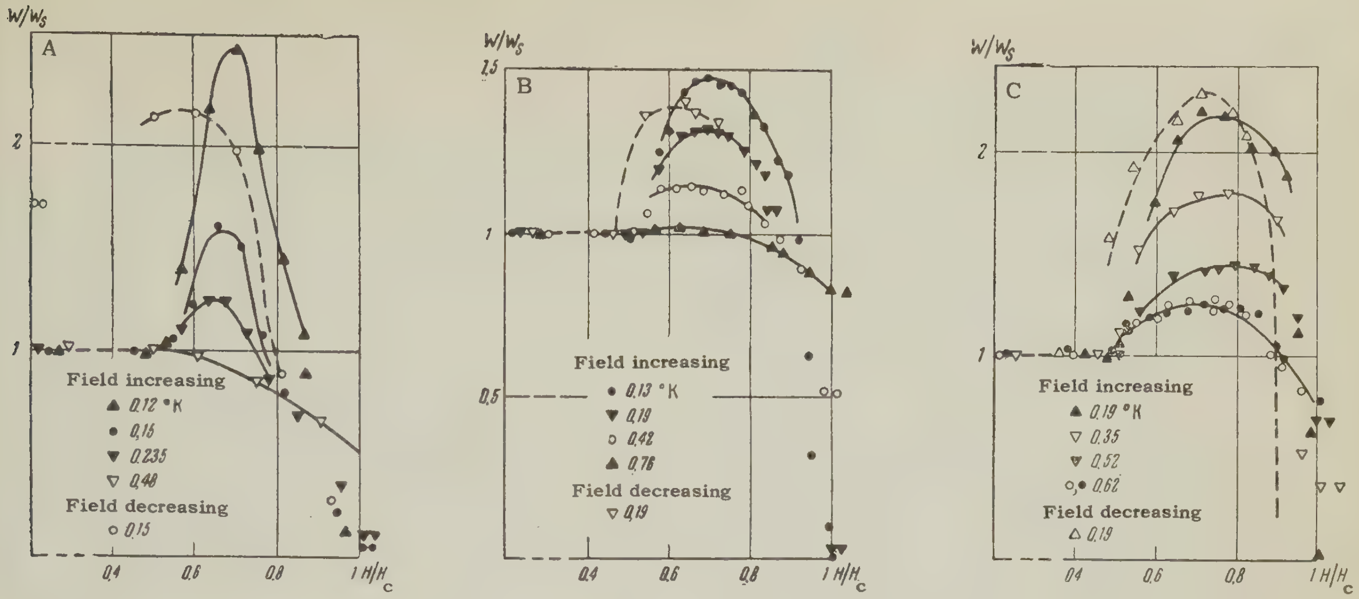

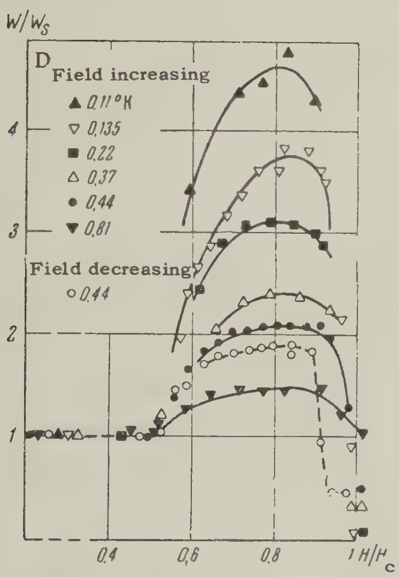

FIG. 2. The variation of thermal resistance for gallium specimens in the direction of the c axis in the intermediate state for various temperatures: A – specimen 3G-c, B – specimen c-6, C – specimen c-8, D – specimen c-9. The data of Zavaritskiĭ[3] were used to determine the value of H_c for each curve.

by an increase in thermal resistivity W.* This increase was reproduced in all the control measurements (see, for example, the data for the two series of measurements in Fig. 2C for 0.62°K). The magnitude of the increase is independent of the heat flow along the specimen, as shown by extra experiments in which the heat flow was changed by a factor of up to ten. Hysteresis effects were often found on the reverse transition from the normal to the superconducting state (by reducing the magnetic field). Some of these (see, for example, Fig. 2D) are apparently related to a supercooling of the normal phase, as a result of which the transition from the normal to the intermediate state only takes place in a field less than H_c. Others (see, for example, Fig. 2A) are connected with "frozen-in" normal phase domains, which cause the thermal resistivity to remain larger than in the superconducting phase after the field has been switched off. These effects, which are due to the existence of "frozen-in" domains, are found only in gallium specimens with $2 \times 10^{-1}\%$ impurity. In what follows we will discuss only the results obtained with the magnetic field increasing.

The behavior of the heat transfer through the successive domains of normal and superconducting phases is given, to first order, by the quantity

$$\Delta W_i = W_i - \{(1-\eta)W_s + \eta W_n\}, \tag{1}$$

where W_i, W_s and W_n are the thermal resistivities in the intermediate, superconducting, and normal states and η is the concentration of normal phase. For a cylindrical specimen in a magnetic field perpendicular to its axis, η changes from 0 to 100% as the field changes from $\frac{1}{2}H_c$ to H_c. At the same time, the period of the intermediate state structure, a, also changes; according to E. M. Lifshitz and Sharvin,[5]

$$a = \sqrt{\Delta d / \varphi(\eta)} \tag{2}$$

(Δ is the surface tension between the normal and superconducting phases, d is the specimen diameter, and $\varphi(\eta)$ is a dimensionless parameter tabulated by Lifshitz and Sharvin[5]*, and must also be taken into account.

---

*We should note that the increase in resistivity in the intermediate state makes it possible to reduce by several-fold the conductivity of a superconducting "heat switch" in the "open" position.

*Although relation (2) was obtained[5] by considering the intermediate state of an infinite sheet, it can also be used for determining the period of the structure in a cylindrical specimen, according to a calculation by Sharvin.

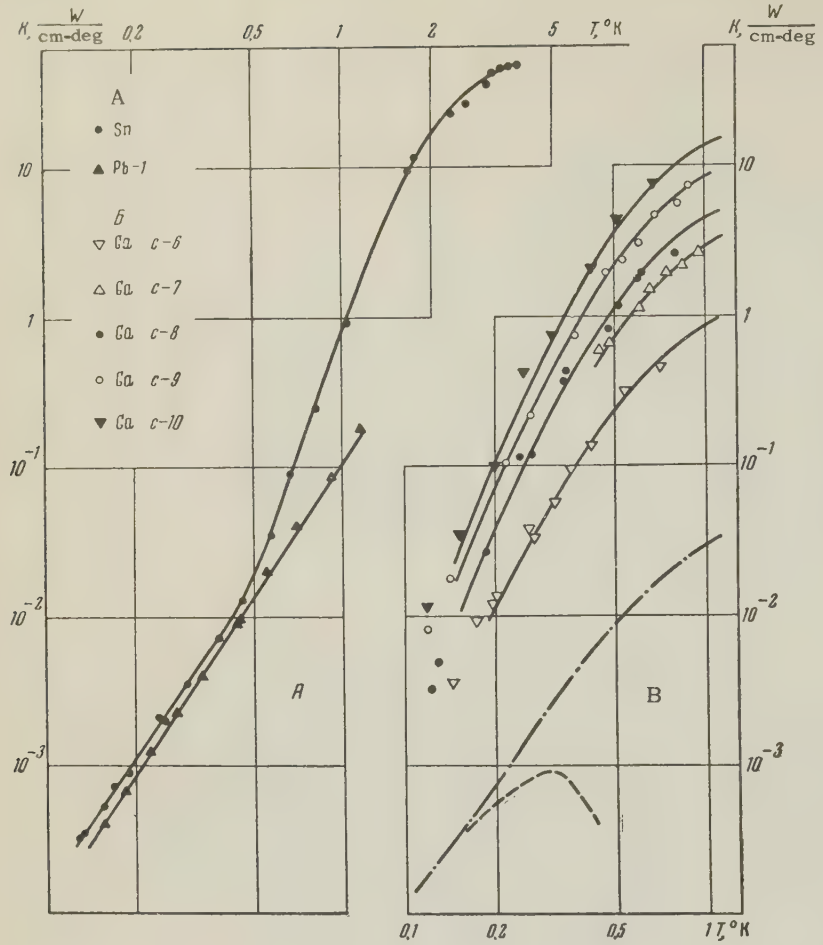

FIG. 3. The thermal conductivity of specimens in the superconducting state. The dot-dash curve is for specimens 3G-c, the dashed curve represents the lattice conductivity of specimens 3G-c according to the data of Zavaritskiĭ.[3]

1. THE LATTICE HEAT CONDUCTIVITY

In order to understand the mechanism of heat transfer by phonons, the most useful experimental results are those obtained in the temperature region where in the superconducting state the electronic heat conductivity is negligibly small compared with the phonon conductivity. According to Montgomery,[6] this occurs at temperatures lower than ~1°K for lead and lower than ~0.3°K for tin.[4]

As can be seen in Fig. 1, the transition to the intermediate state in this temperature region is accompanied by a sharp increase in thermal resistivity (6 times for tin and 2.5 times for lead). The relative increase in resistivity $\Delta W_{gi}/W_{gs}$ changes only negligibly with temperature. At constant temperature ΔW_{gi} varies in inverse proportion to the period of the intermediate state structure.* In all specimens investigated, the temperature variation of the absolute magnitude of ΔW_{gi} was close to T^{-3}. As the temperature was reduced from 1 to 0.15°K, the change in the value of $T^3 \Delta W_{gi}$ was not more than 20 or 30% (see Fig. 4).

At temperatures so much lower than T_c, the thermal resistivity of the normal domains is negligibly small compared with that of the superconducting domains.* The extra resistance ΔW_{gi} can therefore only relate to a change in conductivity of the superconducting phase, which is determined by phonon heat transport. The phonon heat conductivity K_g can be expressed in terms of the phonon mean free path l_g, the velocity u, and the lattice heat capacity per unit volume C, by the relation

$$K_g \sim \tfrac{1}{3} l_g u C \qquad (3)$$

or, on substituting numerical values,

$$K_g \sim G l_g T^3 \ \mathrm{W/cm\text{-}deg}, \qquad (3a)$$

---

*In all cases the change in phonon resistivity in the intermediate state departed from the relation $a\Delta W_{gi} = \text{const}$ by less than 10% with the proportion of normal phase varying from 20 to 80%.

*For tin at 0.3°K, W_n/W_s is $\sim 10^{-3}$; for lead at 1° and 0.3°K this ratio is $\sim 5 \times 10^{-2}$ and 5×10^{-3}.

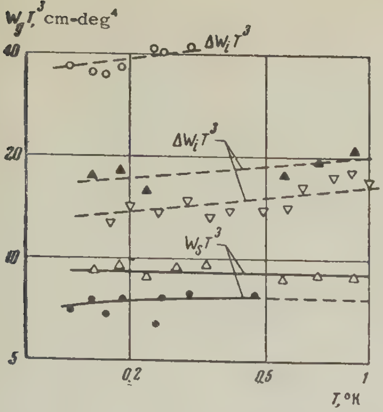

FIG. 4. The dependence of W_gT^3 on temperature: ○, ● – Sn specimens; △, ▲ – Pb-1; ▽ – Pb-2.

where $G_{Pb} = 4$,[7] $G_{Sn} = 1$,[4] and $G_{Ga} = 0.5$.[8] From expression (3a), ΔW_{gi} can be related to the change in the inverse of the phonon mean free path, produced by extra scattering in the intermediate state. We obtain

$$1/l'_{gi} = 1/l_{gi} - 1/l_{gs} \sim GT^3\,\Delta W_{gi}/(1-\eta) \qquad (4)$$

(l_{gi} and l_{gs} are the phonon mean free paths in the intermediate and superconducting states). The magnitude of l'_{gi} changes little in the temperature range studied, as can be seen from Fig. 4, but possibly increases slightly with decreasing T. Since the dimensions of the superconducting domains in the intermediate state $a_s = a(1-\eta)$, it follows from the proportionality of ΔW_{gi} and i/a and relation (4) that l'_{gi} varies in the entire intermediate range in the same way as the dimensions of the superconducting layers. A calculation of the absolute value of l'_{gi} from relation (4) indicates (cf. Table I) that l'_{gi} is close to the dimensions of the superconducting layers.

Let us compare our results with the mechanism for extra scattering of phonons, proposed independently by Abrikosov and Zavaritskiĭ[2] and by Laredo and Pippard.[13] The essentials of this mechanism are as follows: because of the presence of conduction electrons, the phonon free path in the normal domains, l_{gn}, is small* (see Table I) and therefore the transition of a phonon from a superconducting to a normal region is accompanied by its immediate scattering. If the phonon mean free path in the superconducting state is limited only by scattering at lattice defects and at the specimen boundaries, then in the intermediate state the dimensions of the superconducting domains will also limit it, leading to a considerable reduction of l_g (see Table I). The direct proportionality between l'_{gi} and a_s and their close agreement are explained in this way. Some difference between the absolute values of l'_{gi} and a_s in our specimens may be due to the approximation in Eq. (4), since the real structure of the intermediate state in a cylindrical specimen[15] must differ somewhat from the assumed structure consisting of alternating layers crossing the whole specimen. An increase in l'_{gi} can also be produced by phonons "jumping" through the normal domains without being scattered; this becomes especially probable if l_{gn} is comparable with the width of the normal domains. The slight increase in l'_{gi} with decreasing temperature may be connected with this effect.

The mechanism described above can, in this way, explain at least qualitatively the whole range of phenomena observed for phonon heat transport in the intermediate state.

2. THE ELECTRONIC HEAT CONDUCTIVITY

We used the data obtained for gallium and tin to elucidate the behavior of the electron heat transport in the intermediate state. We discuss here only the properties of gallium specimens prepared from metal with less than ~0.01% impurity, for which the lattice conductivity is negligibly small compared with the electronic heat conductivity (Fig. 3) over the whole range of measurements (0.15 to 1°K). For tin we use the results obtained between 0.7 and ~3°K, with a correction applied below 1°K for the contribution K_g of the lattice heat conductivity.*

Let us first consider the results of measurements on the thermal resistivity of gallium specimens with their length along the crystallographic c axis. The large number of specimens studied enabled us in this case to find the main features of the phenomenon of interest. The transition to the intermediate state for all specimens is accompanied by the appearance of an increase in thermal resistance. There is apparently no direct proportionality between the change in ΔW_{ei} and the inverse of the period of the structure 1/a†, as a result of which a maximum of ΔW_{ei} is usually found at $\eta \sim 0.5 - 0.7$ (see Fig. 2). In what follows we shall consider just $(\Delta W_{ei})_{max}$.

---

*The variation of lattice thermal conductivity in the normal state K_{gn} is at sufficiently low temperatures, $K_{gn} = BT^2$ where $B_{Pb} = 1.3 \times 10^{-3}$ W cm^{-1} deg^{-3}, $B_{Sn} = 3.5 \times 10^{-4}$ W cm^{-1} deg^{-3}.[6,14] It follows from this relation and Eq. (3) that the phonon mean free path in the normal state $l_{gn} = l/T$, where $l_{Pb} = 3.25 \times 10^{-4}$ cm·deg and $l_{Sn} = 3.5 \times 10^{-4}$ cm·deg.

*In calculating the lattice conductivity it is assumed that for tin between 0.7 and 1°K in the superconducting state $K_{gs} = 0.135T^3$, and in the intermediate state $K_{gi} = 0.025T^3$. The correction for the lattice conductivity is ~10% at 1°K and ~50% at 0.7°K.

†In all the curves of the change of electronic thermal resistance in the intermediate state, both for gallium and for tin specimens, a systematic increase in the value of $a\Delta W_{ei}$ is observed, reaching 300% when the fraction of normal phase varies from 20 to 80%.

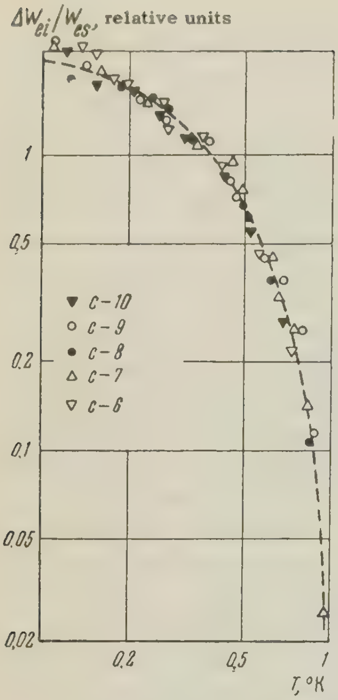

FIG. 5. The dependence of $\Delta W_{ei}/W_{es}$ on temperature in gallium along the c axis. $\Delta W_{ei}/W_{es}$ was taken as 1 at T = 0.38°K (see Table II for values of $\Delta W_{ei}/W_{es}$).

The relative value of the change in thermal resistance $\Delta W_{ei}/W_{es}$ depends on the impurity concentration. As the amount of impurity is decreased from $10^{-2}\%$ (specimen c-6) to $5 \times 10^{-4}\%$ (specimen c-10) the magnitude of $\Delta W_{ei}/W_{es}$ increases (at T ~ 0.1°K) from 0.8 to 6. In the temperature range studied $\Delta W_{ei}/W_{es}$ is not constant, but continously decreases with increasing temperatures, most sharply in the temperature region above ~ 0.4°K. This temperature dependence of the ratio $\Delta W_{ei}/W_{es}$ appears to be universal for all specimens (see Fig. 5). The temperature dependence of the absolute value of ΔW_{ei} — the change of thermal resistance in the intermediate state (Fig. 6) — likewise agrees for all specimens. The impurity content has only little influence on the value of ΔW_{ei}. As the impurity concentration is reduced almost 15-fold, ΔW_{ei} is only reduced to one half (see Fig. 2).

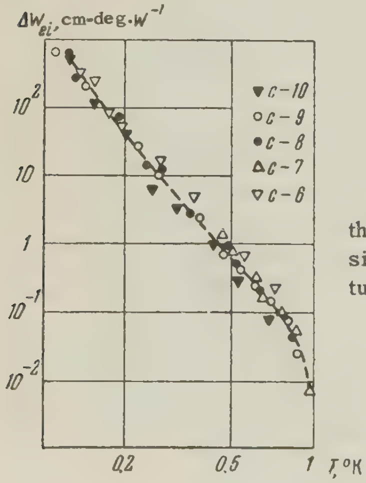

FIG. 6. The variation in the absolute value of the resistance ΔW_{ei} with temperature in gallium specimens.

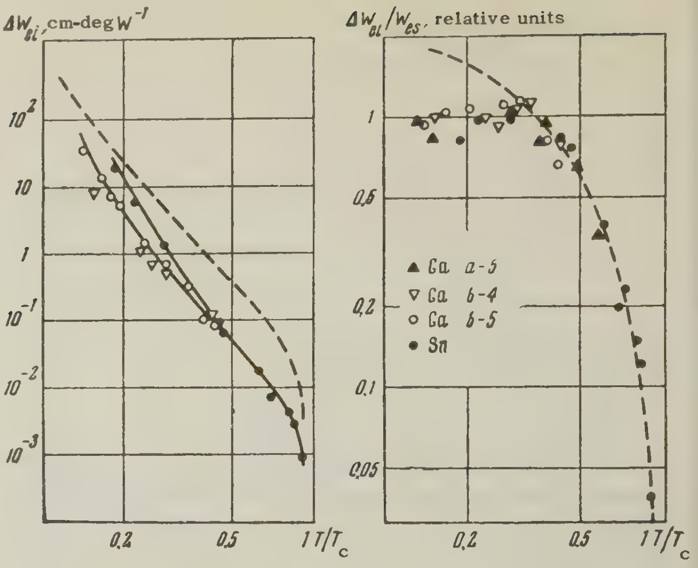

FIG. 7. The dependence of thermal resistance change in gallium and tin specimens in the intermediate state on reduced temperature. $\Delta W_{ei}/W_{es}$ was taken as 1 at $T/T_c = 0.35$. The broken curves correspond to the dependence for gallium specimens along the c axis (according to Figs. 6 and 7).

Gallium specimens of different orientation differ both in the absolute value of ΔW_{ei} and in the law of its temperature variation (see Fig. 7A). The anisotropy of ΔW_{ei} to some extent reflects the anisotropy in the thermal conductivity of gallium in the superconducting state.[3] The largest value of ΔW_{ei} is found along the c axis, corresponding to the minimum thermal conductivity K_{es} and in this direction the temperature variation of both K_{es} and ΔW_{ei} is more gradual than in the other directions. There is not, actually, a complete correspondence between the anisotropies in K_{es} and ΔW_{ei}. This is seen most clearly in the character of the temperature dependence of the relative change of thermal resistance $\Delta W_{ei}/W_{es}$. This dependence for gallium agrees over the whole temperature range studied only along the a and b axes (see Fig. 7). Along the c axis the dependence of $\Delta W_{ei}/W_{es}$ on T is considerably different at temperatures below $\sim 0.35 T_c$. We should remark that the c direction is also differentiated from the other two in the anisotropy of the energy spectrum of the superconductor excitations.[3]

The results for tin, in which there is a considerably more rapid variation of ΔW_{ei} than for gallium (Fig. 7), confirm the absence of a general relation between ΔW_{ei} and T/T_c for all superconductors. It is therefore all the more interesting that these metals display a similar dependence of the relative change in thermal resistance $\Delta W_{ei}/W_{es}$ on the reduced temperature. At temperatures $T \geq 0.35 T_c$ this dependence is the same, within the experimental accuracy, for all the specimens

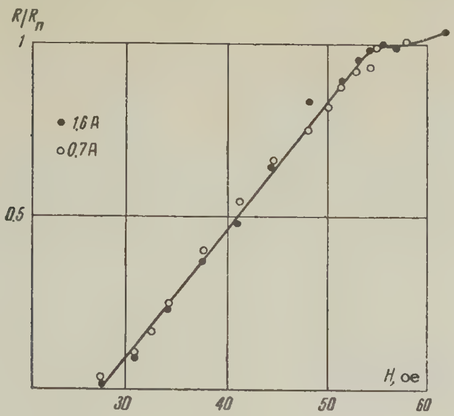

FIG. 8. The field dependence of resistance of gallium specimen c-9, with the magnetic field perpendicular to its axis, for two values of the current through the specimen.

studied, and below ~ $0.35T_c$ only gallium along the c axis shows a departure from the general relation. It appears that the variation of the relative change in thermal resistance with reduced temperature is one of the main features of heat transport by electrons across alternate regions of normal and superconducting phases.

We suggest, unlike, for example, Hulm,[16] that the increase in resistance in the intermediate state is determined mainly by the change in electronic heat transport in the superconducting domains (we are concerned here with the so-called "normal" electrons of the superconductor). Both the occurrence of an appreciable effect at temperatures much below the critical, where the resistivity of the normal phase is negligibly small compared with that of the superconducting, and the results of the following additional experiments bear out this suggestion.

a) The electrical resistivity of the specimens R was measured in the intermediate state. We found that $R = \eta R_n$, where R_n is the resistivity of the specimen and η is the concentration of normal phase. No additional increase in resistivity of the normal phase was found in the intermediate state (Fig. 8) which might be expected if there were an increase in the thermal resistivity of the normal domains.

b) The thermal resistivity W of a tin single crystal of high purity with the length along the four-fold axis was measured. Measurements were made with the directions of a magnetic field along the directions of maximum and minimum variation of thermal conductivity in the normal state (the angle between these directions is 22.5°). Although the thermal resistivity in these two directions differs by a factor of 1.5 in the normal domains, the difference in the absolute value of ΔW_{ei} did not exceed 5 – 10% (see Fig. 9).

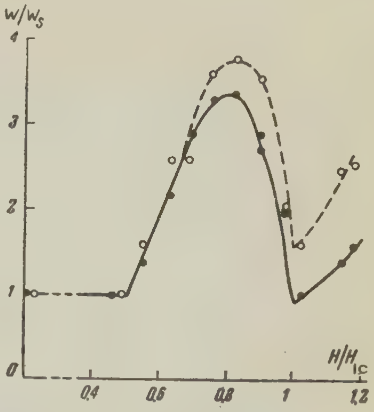

FIG. 9. The variation of thermal resistance of a high purity tin specimen (impurity ~5×10^{-5}%, $W_s \approx 9 \times 10^{-3}$ cm·deg·W^{-1}) in the intermediate state (at 2.2°K), for the field directed: ● – along the minimum of conductivity change, ○ – along the maximum.

By analogy with the case of phonon heat transport, it seems natural to connect the reduction in electronic thermal conductivity in a structure consisting of alternate layers of normal and superconducting phases, with the existence of an additional "scattering" of electrons. Since the change in the absolute value of ΔW_{ei} with impurity content is insignificant, we can assume that this mechanism and the scattering of electrons by impurities are additive to a first approximation. Assuming, in line with present theory,[17-19] that the electron mean free path in a superconductor, due to scattering by impurities, is independent of temperature,* then the reciprocal free path for the extra scattering mechanism is

$$\frac{1}{l'_{ei}} = \frac{1}{l_{ei}} - \frac{1}{l_{es}} \approx \frac{\Delta W_{ei}}{W_{es}} \frac{LT_c\sigma/l}{K_{T_c}(1-\eta)},$$

where K_{T_c} is the thermal conductivity at the critical temperature, L is the Lorenz number and σ/l is the ratio of the conductivity of the specimen to the mean free path, measured in the normal state. Using the value $\sigma/l \approx 5 \times 10^{10}$ derived from experiments on the size effect on electrical resistance,[20,21] we find that for $T \lesssim 0.4T_c$ the free path l'_{ei} is close to the dimensions of the superconducting domains.† Thus, at least qualitatively, the reduction in the electronic heat conductivity in the intermediate state is explained by the assumption that the electron mean free path is limited by the phase boundaries. We should note that this reduction in mean free path can, in fact, be produced either by an extra scattering of the electrons or by their elastic reflection at the phase boundaries. In the present case it only makes sense to talk of reflection according to classical laws since the width of the transition layer between the phases ($\sim 10^{-5}$ cm) is many times greater than the electron wavelength ($\sim 10^{-7}$ cm). A qualitative calculation of the resistance produced by reflection shows that it is sufficient to assume that $\sim 50\%$ of the electrons are elastically reflected at the phase boundaries in order to explain the results obtained on tin for $T \lesssim 0.4 T_c$.

---

*Except for the tin specimen used in the additional experiments, all the specimens were studied in the temperature region where the electron mean free path is mainly determined by impurity scattering.

†For a change in concentration of normal phase from 0.2 to 0.8 the ratio l'_{ei}/a_s in tin decreases from 1.2 to 0.5.

The mean free path l'_{ei} is only close to the dimensions of the superconducting domains a_s at the lowest temperatures. It follows from relation (5) and from the dependence $\Delta W_{ei}/W_{es}$ on T that the ratio l'_{ei}/a_s increases with increasing temperature. This may be taken as an indication that the additional scattering (or reflection) of electrons at a phase boundary disappears as the critical temperature is approached.* From the data of Fig. 7 it follows that the decrease in scattering (or reflection) of electrons is almost the same for all the superconductors.

While we could relate the reduction in mean free path for phonon heat transport to scattering of phonons by conduction electrons in the normal domains, in the case of electronic thermal conductivity the effect of scattering of electrons by electrons is too small to explain the observed effect. It is not impossible that the appearance of an extra thermal resistivity in this case is connected with the different energy spectra of electrons in the superconducting and normal phases of the metal. If, in fact, the energy-momentum relations are different for electrons in the two phases, then there will be additional scattering when the phase boundary is crossed. We should mention that we are concerned here with the so-called "normal" electrons of a superconductor, which do not show superconducting properties. This difference in the energy spectra, together with the decrease in this difference as the temperature approaches T_c, as follows from the form of the $\Delta W_{ei}/W_{es} - T/T_c$ relation, agrees qualitatively with the present theory. We can ascertain whether all the results obtained can be explained quantitatively only after making the appropriate calculations.

The authors thank P. L. Kapitza, A. I. Shal'nikov, A. A. Abrikosov and Yu. V. Sharvin for their interest in the work and for discussions.

---

*The change in the period of the intermediate state structure is small, over the temperature range studied, compared with the the change in $\Delta W_{ei}/W_{es}$. Thus, while $\Delta W_{ei}/W_{es}$ decreases nearly 30-fold between 0.5 and 0.9 T_c, the increase in the period of the structure, a, amounts to only ~40%.[9]

[1] K. Mendelssohn and J. L. Olsen, Proc. Phys. Soc. **A63**, 2 (1950), Phys. Rev. **80**, 859 (1950).

[2] A. A. Abrikosov and N. V. Zavaritskiĭ, Supplement to D. Shoenberg's Superconductivity, IIL, 1955.

[3] N. V. Zavaritskiĭ, JETP **37**, 1506 (1959), Soviet Phys. JETP **10**, 1069 (1960).

[4] N. V. Zavaritskiĭ, JETP **33**, 1085 (1957), Soviet Phys. JETP **6**, 837 (1958); Progress in Cryogenics, London, Vol. 1 p 207, 1959.

[5] E. M. Lifshitz and Yu. V. Sharvin, Dokl. Akad. Nauk SSSR **79**, 783 (1951).

[6] H. Montgomery, Proc. Roy. Soc. **A244**, 85 (1958).

[7] Horowitz, Silvidi, Malaker, and Daunt, Phys. Rev. **88**, 1182 (1952).

[8] G. Seidel and P. H. Keesom, Phys. Rev. **112**, 1083 (1959).

[9] Yu. V. Sharvin, JETP **33**, 1341 (1957), Soviet Phys. JETP **6**, 1031 (1958).

[10] J. M. Lock, Proc. Roy. Soc. **A208**, 391 (1951).

[11] V. L. Ginzburg, JETP **30**, 593 (1956), Soviet Phys. JETP **3**, 621 (1956).

[12] L. P. Gor'kov, JETP **36**, 1918 (1959), Soviet Phys. JETP **9**, 1364 (1959).

[13] S. J. Laredo and A. B. Pippard, Proc. Camb. Phil. Soc. **51**, 368 (1955).

[14] M. Garfinkel and P. Lindenfeld, Phys. Rev. **110**, 883 (1958).

[15] A. I. Shal'nikov, JETP **33**, 1071 (1957), Soviet Phys. JETP **6**, 827 (1958).

[16] J. K. Hulm, Phys. Rev. **90**, 1116 (1953).

[17] Bardeen, Cooper, and Schrieffer, Phys. Rev. **108**, 1175 (1957).

[18] Bogolyubov, Tolmachev, and Shirkov, Новый метод в теории сверхпроводимости, (A New Method in the Theory of Superconductivity), Academy of Sciences Press, 1958.

[19] A. A. Abrikosov and I. M. Khalatnikov, Usp. Fiz. Nauk **65**, 551 (1958).

[20] E. R. Andrew, Proc. Phys. Soc. **A62**, 77 (1949).

[21] J. E. Kunzler and C. A. Renton, Phys. Rev. **108**, 1397 (1957).

Translated by R. Berman
327

SOVIET PHYSICS JETP VOLUME 11, NUMBER 6 DECEMBER, 1960

INVESTIGATION OF HIGH-ENERGY PROTONS EMITTED IN THE PHOTODISINTEGRATION OF Li^6

E. B. BAZHANOV and L. A. KUL'CHITSKIĬ

Leningrad Physico-Technical Institute

Submitted to JETP editor January 8, 1960

J. Exptl. Theoret. Phys. (U.S.S.R.) 38, 1685-1687 (June, 1960)

Protons with energies of 16 Mev and above are studied. Data relating to the excitation functions, angular distributions, and n-p coincidences suggest a rather high probability for the formation of highly excited states in He^5 and Li^5 nuclei as a result of a single-particle reaction with the Li^6 nucleus.

WE have investigated photodisintegrations of the Li^6 nucleus, leading to the formation of protons with energies above 16 Mev, with the synchrotron of the U.S.S.R. Academy of Sciences Physico-Technical Institute operating at 100 Mev. A 100-mg/cm^2 target consisting of 90% Li^6 and 10% Li^7 was employed. The protons were registered with the aid of the previously described[1] scintillation-counter telescopes.

1. We obtained curves of the photoproton yield as a function of the gamma-ray energy for the energy interval E = 35 to 87 Mev, and simultaneously for five proton groups with mean energies $\overline{E}_p$ of 16, 20, 25, 30, and 35 Mev. The width of the energy interval for each group was 20 - 25% of the mean energy of the corresponding group. The excitation function for protons with a mean energy $\overline{E}_p = 20$ Mev, obtained from the experimental yield curve by the method of Penhold and Leiss,[2] is shown in Fig. 1. For the other proton groups the yield and cross-section curves have the same general outlines but are displaced on the energy scale in accordance with the change in the proton energy. The measurements were carried out for angles $\theta = 57.5$ and 102.5°, but no substantial difference in the yield curves was noted.

A characteristic feature of the cross-section curves, practically in the whole of the investigated interval, is the comparatively slow change of the cross section with the gamma-ray energy. If it is assumed that the protons are the product of the $Li^6(\gamma,p)He^5$ reaction, then on the basis of the level scheme of the He^5 nucleus[3] it is possible to say that, for instance, for $\overline{E}_p = 20$ Mev, quanta with a mean energy of 29 - 34 Mev should take part in the process if the He^5 nucleus remains in the ground or first excited state at an energy of about 3 — 6 Mev, or quanta with an energy ≥ 45 Mev if the excitation energy of the final He^5 nucleus is 16.7 Mev or higher. The excitation function would depend much more strongly on the energy of the quanta, if (as was found for C^{12}, reference 4) the probabilities for the formation of highly excited states of He^5 and (or) for the simultaneous breakup of Li^6 into three particles were not comparable with the probability for the formation of a He^5 nucleus in the ground or in a weakly excited state. The decay into three particles would explain naturally the fact that protons belonging to a narrow energy interval are produced by quanta of arbitrary energy with an insignificant change in cross section.

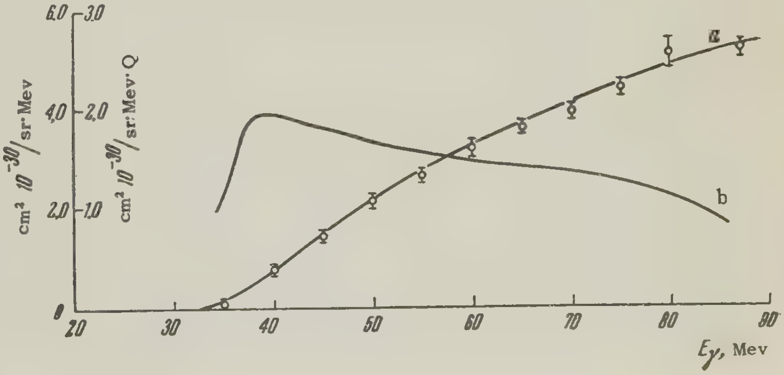

FIG. 1. Yield curve (a) and cross section curve (b) for protons with $\overline{E}_p = 20$ Mev from the Li^6 nucleus at an angle of 57.5°. The left-hand ordinate scale is for curve b, and the right-hand for curve a. The errors are statistical.

2. For the purpose of obtaining additional information, measurements of n-p coincidences were undertaken for the bremsstrahlung of gamma quanta with a maximum energy of 87 Mev. A scintillation counter with a volume of 6.3×10^3 cm^3, filled with a 5 g/l solution of p-terphenyl in xylene was employed to register the neutrons. The proton telescope was set at an angle of 78° and the neutron telescope at an angle of 90° to the direction of the gamma-ray beam. The counting efficiency of n-p coincidences, determined by the $D_2O - H_2O$ method, that is under conditions of 100-percent correlation of the emission angles of the neutron and the proton in the photodisintegration of deuterium, was 0.104 ± 0.039.

It can be shown, from the energy balance of the reaction, that the contribution of the reactions

$$\mathrm{Li}^6(\gamma p)\,\mathrm{He}^5, \quad \mathrm{He}^5 \rightarrow \mathrm{He}^4 + n;$$
$$\mathrm{Li}^6(\gamma n)\,\mathrm{Li}^5, \quad \mathrm{Li}^5 \rightarrow \mathrm{He}^4 + p$$

to the n-p coincidences should be small, on account of the quite high thresholds for proton ($E_p \geq 16$ Mev) and neutron ($E_n \geq 9$ Mev) registration; this can, however, only be shown for cases when the He^5 and Li^5 nuclei remain in the ground or first excited states. The contribution from these reactions is possible if the second ($E_{exc} = 16.7$ Mev) or even higher levels of the He^5 and Li^5 are excited; the Li^6(γpn)He^4 reaction should also make a definite contribution. If in addition the quantum interacts with quasideuteron formations in the Li^6 nucleus, then a correlation between the emission angle of the neutron and proton can be expected. Experimentally the following results were obtained:

The observed ratio of coincidences and the number of registered protons	0.0102 ± 0.0035
The same, assuming a 100-percent correlation between the emission angles of the neutron and proton	0.098 ± 0.074
The same, assuming an isotropic distribution of the emitted neutrons	0.3 - 0.4

(the calculated efficiency of the neutron counter, assuming an isotropic neutron distribution, is 2.5 - 3.5%).

Taking into account the large dimensions of the neutron counter, it seems improbable that the contribution of correlated n-p coincidences exceeded substantially 10% of the total number of registered protons. The fact that 30 - 40% of these protons can be accompanied by neutrons speaks in favor of the assumption of a considerable probability for the formation of He^5 and Li^5 nuclei in strongly excited states. A considerable contribution of these states could explain the observed shape of the cross-section curves. The possibility that strongly excited He^5 and Li^5 nuclei are produced was previously expressed by Komar and Yavor[5] in connection with the photodisintegration of Ne^{20}. At present we are making attempts to measure the angular correlation of emitted neutrons and protons.

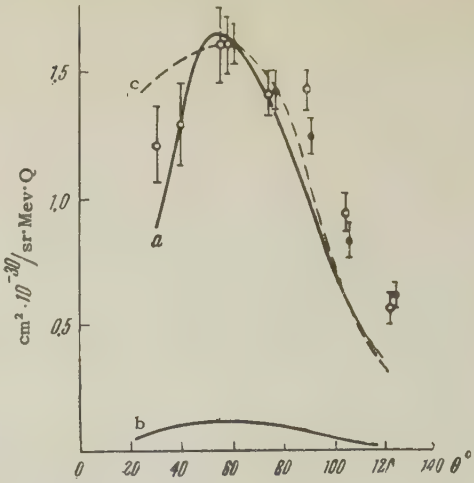

FIG. 2. Angular proton distribution for $\overline{E}_p = 25$ Mev. The ordinate scale is given for the experimental points and for curve b. The errors are statistical.

3. The investigations of the angular photoproton distributions for $E_{\gamma max} = 87$ Mev are in better qualitative agreement with the concepts of a single-nucleon interaction mechanism between the gamma quanta and the Li^6 nucleus. Figure 2 shows the angular distribution of 20- to 31-Mev protons. Curve a is calculated from Shklyarevskiĭ's formulas, obtained on the basis of the shell model for the single-nucleon interaction mechanism and normalized according to the experimental data for $\theta = 60°$. However, the quantitative agreement with theory (curve b) is unsatisfactory. Curve c is obtained from ideas about the quasideuteron interaction mechanism, as previously,[1] and is also normalized for $\theta = 60°$. It is obvious that at small angles (smaller than 60°) curve c lies considerably above the experimental points, while the shape of the angular proton distribution for a single-nucleon interaction mechanism (curve a) is in better agreement with the experimental data.

In conclusion, the authors wish to express their gratitude to Prof. A. P. Komar and the laboratory co-workers for their attention and interest in the work, and also to the synchrotron crew headed by N. N. Chernov.

Note added in proof (May 3, 1960): The results of the investigation of the correlation of the emission angles of neutrons and protons show that while a weakly expressed correlation apparently exists for the C^{12} nucleus, no such correlation for Li^6 is observed. The isotropic yield of neutrons, registered in coincidence with protons, confirms the assumption of a single-nucleon mechanism in the photodisintegration of Li^6.

---

[1] Bazhanov, Volkov, and Kul'chitskiĭ, JETP **35**, 322 (1958), Soviet Phys. JETP **8**, 224 (1959).

[2] A. S. Penhold and J. E. Leiss, Phys. Rev. **114**, 1332 (1959).

[3] F. Ajzenberg-Selove and T. Lauritsen, Nucl. Phys. **11**, 1 (1959).

[4] E. B. Bazhanov, JETP **38**, 267 (1960), Soviet Phys. JETP **11**, 193 (1960).

[5] Bazhanov, Volkov, Komar, Kul'chitskiĭ, Chizhov, and Yavor, Тр. Всесоюзной конф. по ядерным реакциям при малых и средних энергиях, Trans. of the All-Union Conference on Nuclear Reactions at Low and Medium Energies, Acad. of Sci. Press, p. 463, 1958.

[6] G. M. Shklyarevskiĭ, JETP **36**, 1492 (1959), Soviet Phys. JETP **9**, 1057 (1959).

Translated by Z. Barnea
328

SOVIET PHYSICS JETP VOLUME 11, NUMBER 6 DECEMBER, 1960

ABSORPTION OF ULTRASOUND IN ZINC AT LOW TEMPERATURES

A. A. GALKIN and A. P. KOROLYUK

Institute of Radiophysics and Electronics, Academy of Sciences, Ukrainian S.S.R.

Submitted to JETP editor January 10, 1960

J. Exptl. Theoret. Phys. (U.S.S.R.) 38, 1688-1694 (June, 1960)

Magnetic oscillations of the absorption coefficient of sound in zinc for several directions of the wave vector **k** relative to the crystallographic axes of a single crystal are studied under the conditions when $l \gg \lambda$ (l is the electron mean free path and λ is the wavelength of the sound). The magnetic field rotated in a plane perpendicular to the vector **k**. In accordance with the theory, the oscillation period (in 1/H) is found to be constant. It was found to be possible to measure the extreme diameters of Fermi surfaces for a number of crystallographic directions, on the basis of the magnitude of the period. From the anisotropy of the absorption coefficient in a strong field, it was found that the Fermi surface of zinc is open in the direction of the six-fold symmetry axis. A new method is proposed for estimating the electron mean free path. It is shown that for the metal under investigation the mean free path is anisotropic and varies between 0.2 and 0.6 mm.

1. INTRODUCTION

As was shown in a number of researches,[1-5] the ultrasonic absorption coefficient in metals α oscillates upon change of the magnetic field intensity. The theory of this phenomenon has been constructed by V. L. Gurevich[6] for different mutual orientations of the wave vector of the sound **k** and the field **H**. Calculations have been carried out under the assumption of an arbitrary dispersion law for the energy of the electrons, on the basis of a model proposed by Pippard.[7]

The chief consequence of the theory is the constancy of the period of oscillation of the absorption coefficient as a function of the reciprocal of the field intensity. The period of (ΔH^{-1}) is connected with the value of the extreme (relative to the direction of **H**) diameter D_{ext} of the Fermi surface (perpendicular to the vectors **k** and **H**) by the relation

$$D_{\text{ext}} = |p_1 - p_2|_{\text{ext}} = e\lambda / c\Delta H^{-1}. \qquad (1)$$

Thus, measurement of the oscillation period for different directions of the vectors **k** and **H** relative to the crystallographic axes in single crystals of metallic samples makes it possible to obtain valuable information on the characteristics of the Fermi surface.

Two researches on the absorption coefficient of ultrasound in zinc at low temperatures have been reported. In the work of Morse and Bohm,[5] no oscillations of the absorption coefficient were observed in this metal. Our own first measurements,[2] carried out at an ultrasonic frequency of 70 Mcs, have shown that oscillations are observed in zinc, but in a number insufficient for measurement of the period. As is well known, the number and amplitude of the oscillations depend on the ratio of the length of the mean free path of the electron to the sound wavelength, l/λ, and increase with increase of this ratio.

Since the path length is determined by the purity of the metal, it was necessary to increase the frequency of the ultrasonic vibrations for trustworthy measurements. In the present communication, experiments are described which were carried out with a variation of frequency from 60 to 220 Mcs on single crystals of zinc at temperatures 1.65 — 4.2°K in a magnetic field perpendicular to **k**, with intensities up to 7000 oe. The arrangement $\mathbf{k} \perp \mathbf{H}$ was chosen in order to simplify the interpretation of the oscillograms, inasmuch as in this case there are no periodic increases in the absorption coefficient connected with the longitudinal component of the vector **k** in the direction of **H**.[6]

In addition to the study of oscillations, great interest attaches to the investigation of the absorption coefficient of ultrasound in a strong magnetic field, when $l \gg \lambda \gg r$, where r is the radius of the Larmor orbit, $r = cp/eH$. As shown previously,[1,2] the behavior of the absorption coefficient under these conditions is connected in a definite fashion with the asymptotic conductivity tensor. The absorption coefficient in a strong field has been considered theoretically in the papers of Kaner[8] and Gurevich,[9] where it was shown that one can obtain information on the topology of the Fermi surface from a study of the anisotropy of the absorption coefficient in the magnetic field.

2. TECHNIQUE OF OBTAINING SPECIMENS AND METHOD OF MEASUREMENT

Single crystals of zinc, produced by the method of Obreimov-Shubnikov, served as specimens for measurements of the absorption coefficient. The initial metal had a purity of 99.9998 percent and was characterized by the following ratio of resistances at helium and room temperatures: $R_{4.2}/R_{300} = 2 \times 10^{-4}$.

For a more accurate determination of the orientation of the axes in the crystal, the latter was grown in the form of a sphere of diameter 15 mm. The direction of the axes was determined from the reflection of the crystallographic planes on a double-curve goniometer, after which plane parallel plates 4 — 6 mm thick were cut off by an electro-erosion method.

An X-cut quartz disc of diameter 5—6 mm with a fundamental resonant frequency of 20 Mcs was attached to each plane face of the specimen. Good acoustic contact with the specimen was obtained over a wide range of temperatures by employing as an adhesive a low-temperature vacuum putty. One of the quartz plates mentioned served as the source of ultrasonic vibration, and the second as a receiver. The direction of propagation of sound coincided with the direction normal to the plane surface of the specimen.

To obtain ultrasonic frequencies above 20 Mcs, the quartz plates were excited in the odd harmonics: third, fifth, ninth and eleventh (which correspond to frequencies of 60, 100, 180 and 200 Mcs). The generator driving the quartz worked in a pulse system with pulse length of 0.5—0.6 microsecond.

The pulse was passed through the specimen, amplified in the receiving circuit, and detected by a peak detector. A voltage proportional to the amplitude of the input signal was applied to a recorder which plotted it as a function of the magnetic field. Since the absorption coefficient is proportional to the logarithm of the intensity of the signal, one could determine the change of the coefficient in the magnetic field by this recording.

The necessity of the comparatively short-length pulses produced by the generator arose because of the fact that the time of flight of the ultrasonic signal from the generating crystal to the receiver through the specimen amounted to ~1 microsecond, while the normal operation of the receiver was possible only in the absence of the powerful initial pulse of the generator, which produced great parasitic signals.

The small thickness of the specimen was connected with the difficulty of "sounding" through it: with increase in the number of the harmonic in which the quartz generator operated, the power of the radiated sound decreased and the sensitivity of the detecting crystal also decreased. Furthermore, with increase in frequency, the coefficient of sound absorption in the metal increased. All this led to the result that, in thick specimens, the signal is lost in the noise of the detector circuit.

The construction of the low-temperature equipment allowed the possibility of rotating the specimen relative to the direction of the magnetic field while maintaining the perpendicularity of the vectors **k** and **H**. The oscillation curves were recorded for a change in the direction of the field through each 3°.

3. RESULTS OF MEASUREMENTS

The periods of the oscillation of the ultrasonic absorption coefficient were measured for different orientations of the magnetic field, which rotated in a plane perpendicular to the sound wave vector.

Figure 1 illustrates one of the oscillation curves, recorded on the recorder for a frequency of the ultrasound of 220 Mcs. The wave vector was directed along $[10\bar{1}0]$ (the axes OX, OY and OU passed through the centers of the prism faces), and the **H** vector along the $[11\bar{2}0]$ direction.

Figure 2 shows the dependence of the number of oscillations (plotted along the ordinate) on the reciprocal of the magnetic field for a number of directions of the vector **H** in the $(10\bar{1}0)$ plane. As

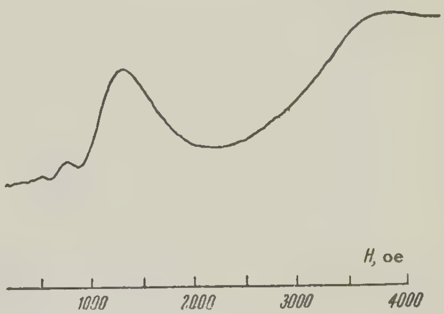

FIG. 1. Record of the amplitude of an ultrasonic pulse transmitted through the specimen as a function of the magnetic field. T = 1.65° K, ν = 220 Mcs.

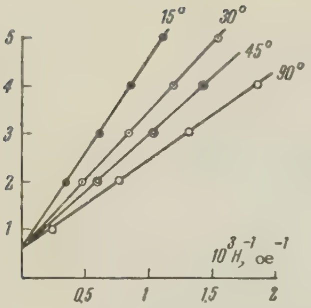

FIG. 2. Dependence of the number of oscillations (determined by the maximum of the absorption) on the inverse value of the magnetic field for a number of directions of **H** in the (10$\bar{1}$0) plane.

is seen from the drawing, the experimental points, which correspond to maximum absorption, fall on a straight line, which testifies to the constancy of the period in the reciprocal field.

In the work of Gurevich,[6] the oscillating part of the absorption coefficient is described by the equation

$$\Delta\alpha = \alpha' \sin\left[(ck/eH)\,|p_1 - p_2| \pm \pi/4\right]. \qquad (2)$$

From the extrapolation of the curves of Fig. 2 to H → ∞, one can obtain a value of the constant phase which, according to theory, is equal to $-\pi/4$; the negative sign of the phase shows that the corresponding diameter of the surface responsible for the oscillations is a maximum.[6]

The measured periods of oscillation of ΔH^{-1} were used to calculate the extreme diameters of the Fermi surface according to Eq. (1). The angular dependencies of the extreme diameter of the Fermi surface perpendicular to the vector **H** are shown in Fig. 3, a, b, c, for rotation of the magnetic field in the planes (11$\bar{2}$0), (0001), and (11$\bar{1}$0) The less reliable values obtained from oscillation curves for a small number of oscillations are indicated by dashed lines. The accuracy of the measurement of the period of oscillation in the inverse field, according to which the diameter is calculated, was within 5–10 percent.

In zinc, at liquid helium temperatures, there is a significant anisotropy of the absorption coefficient in the absence of the magnetic field, and when the wave vector **k** is directed along the [0001] axis the absorption increases so much that it has not yet been possible to investigate the crystal along this axis at 220 Mcs.

The periods of oscillation in the (0001) and (11$\bar{2}$0) planes were measured at 100 and 180 Mcs, respectively, at a temperature of 1.65°K. Simultaneously wit the measurement of the period of oscillations, the dependence of the absorption coefficient on the direction of the magnetic field was studied at a frequency of 60 Mcs. The vector **k** in these measurements was also perpendicular to the direction of the field, the value of which was 7000 oe.

The diagrams of the change of the quantities $\alpha(H) - \alpha_0$, where $\alpha(H)$ is the absorption coefficient in the field and α_0 in the absence of the field are represented in Fig. 4a, b and c for directions of the wave vector **k**: a—along [0001], b—along [10$\bar{1}$0] and c—along [11$\bar{2}$0]. The angle $\phi = 0$ corresponds to the direction of the magnetic field in planes perpendicular to the vector **k**: for the case a—along [11$\bar{2}$0], b—along [0001] and c—along [0001].

As is seen from the drawing, for the direction of the vector **k** along the [0001] axis, the value of the absorption coefficient lies entirely outside the circle $\alpha = \alpha_0$. For other directions of the line, $\alpha(H)$ is located inside the circle mentioned, having a strongly anisotropic character.

4. ESTIMATE OF THE FREE PATH OF THE ELECTRON

In accord with the theory,[6] to each oscillation of the absorption coefficient of sound in the magnetic field there corresponds a change in the diameter of the electronic orbit by a value of the

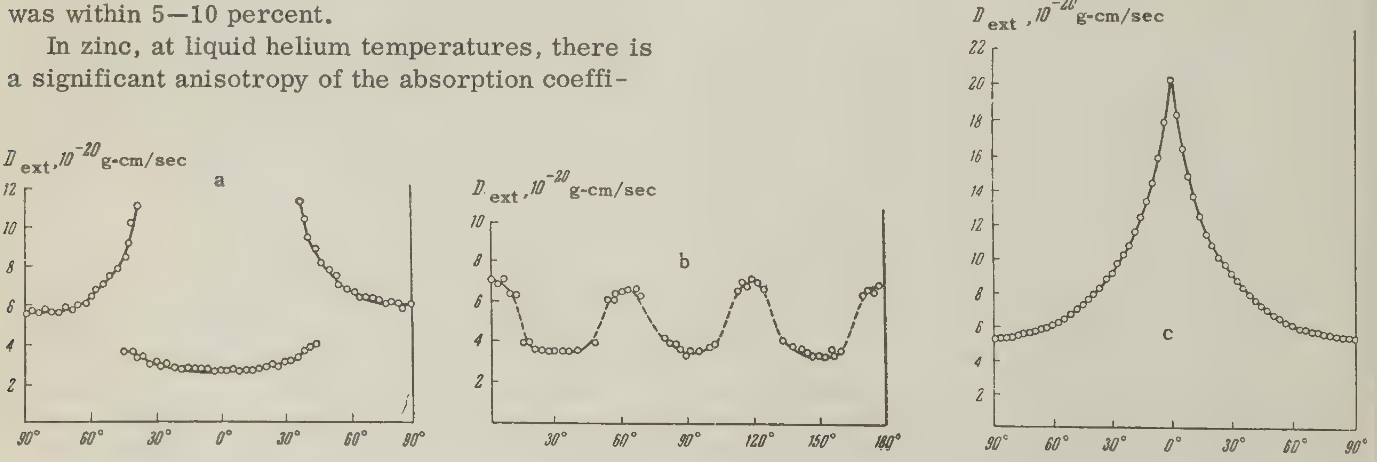

FIG. 3. Angular dependence of the extreme diameter of the Fermi surface. Diameter is perpendicular to **H** and lies in the plane: a – (11$\bar{2}$0), b – (0001), c – (10$\bar{1}$0). The angle $\varphi = 0°$ corresponds to the direction of the field for a – along [11$\bar{2}$0], for b and c – along [0001].

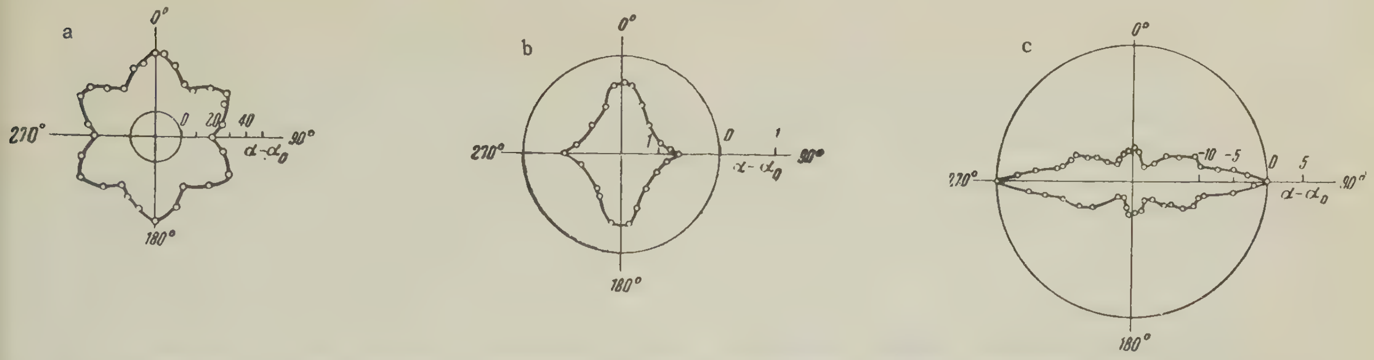

FIG. 4. Dependence of the difference of the absorption coefficients in a field of 7000 oe and without the field (in db/cm) on the direction of the magnetic field. a – k directed along [0001], b – k directed along [10$\bar{1}$0], c – k along [11$\bar{2}$0]. T = 4.2°K, $\nu = 60$ Mcs.

sound wavelength. If we assume that the form of the trajectory of the electron differs little from a circle, one can estimate the length of its free path l by taking into account the number of oscillations and determining from them the maximum diameter of orbit in a weak field:

$$l = \pi\lambda(n+1). \qquad (3)$$

The factor $n + 1$ is obtained by virtue of the fact that the oscillations from the side of the strong field can begin for a minimum diameter of the electronic orbit, equal to λ at least.

Another method of estimating the path length consists in the following. If we measure the component ($p_\perp$) of the momentum of the electron perpendicular to the vectors **k** and **H**, and also the minimum magnetic field for which oscillations cease, then we can estimate the path length from the relation

$$p_\perp / r_{max} = eH_{min}/c.$$

Since the quantity $p_\perp = D_{ext}/2$ is measured from the period of oscillations of ΔH^{-1}, it becomes possible to use this relation for determination of l.

The path lengths determined by the two methods for different directions of k in the crystal are shown in the table.

Direction of **k**	Path l, mm		Temperature, °K
	From no. of oscillations	From $p_\perp$	
[0001]	0.5	0.6	1.65
[10$\bar{1}$0]	0.22	0.2	4.2
[11$\bar{2}$0]	0.27	0.24	1.65

5. DISCUSSION OF RESULTS

The values obtained for the extreme diameters of the Fermi surface testify to the sharp departure of the law of energy dispersion of the electrons from the quadratic.

It is not yet possible to establish the complete form of the Fermi surface from the momentum values obtained. The difficulties are connected with the fact that it is not known to what value of p_z correponds the particular value of p_y obtained in the experiment (the z axis is directed along the field, the x axis along the wave vector). If we assume that the oscillations are connected with the central cross section of the surface, then the values of the diameters for certain directions do not "join" one another. This points to the result that the oscillations are possibly connected not only with the central but with other cross sections, that is, the Fermi surface for zinc has a complicated configuration. On the other hand, investigation of the oscillations of the absorption along the six-fold axis was carried out at comparatively low frequency, but this did not permit a sufficiently accurate measurement of the extreme value of the momentum. It is possible that carrying out investigations at much higher frequencies would permit the construction of the Fermi surface.

Analysis of the diagrams of rotation of the absorption coefficient, carried out on the basis of theory,[8,9] shows that there are directions in zinc of open trajectories of the electrons. The experiments are best explained if one assumes that the Fermi surface for zinc contains a "corrugated cylinder" in it, with axis in the direction [0001]. In fact, since the fundamental contribution to the coefficient α is made by electrons moving perpendicular to the wave vector of the sound over a range of the wavelength λ, while the quantity of such electrons in the case in which **k** is directed along the axis of the corrugated cylinder increases in a strong field (for $\mathbf{k} \perp \mathbf{H}$), then the absorption coefficient in the field must increase, and for an arbitrary direction of **H** must be larger than α_0.

The same situation occurs if the vector **k** is directed along the axis [0001]. Small maxima along the binary axes indicate the presence of closed electronic trajectories in the case of direction of the field along these axes. Rotation diagrams for **k** along the axes $[10\bar{1}0]$ and $[11\bar{2}0]$ show that the Fermi surface is closed along these directions.

It is interesting to note that the position of the maxima of the sound absorption coefficient on the rotation diagram in planes $(10\bar{1}0)$ and $(11\bar{2}0)$ coincides with the position of the minima of the resistance $\Delta R/R$ on similar diagrams in galvanomagnetic measurements.[10,11]

An estimate of the density of electrons made from the mean value of the momentum shows that the fundamental groups of current carriers are responsible for the oscillations of the absorption coefficient. Thus, the mean value of the momentum in the plane (1010), $\bar{p} = 6 \times 10^{-20}$ g-cm/sec, which gives an estimate of 0.6×10^{22} electrons per cm^3 for the density.

Thus measurements of the diameters in the principal crystallographic directions are not sufficient for construction of the complete Fermi surface in zinc: it is also necessary to obtain a more detailed diagram of rotation, to increase the purity of the metal in this case, and to carry out investigation at higher frequencies.

In conclusion, we consider it our pleasant duty to thank É. A. Kaner and M. I. Kaganov for discussion of the results and valuable advice, and also V. I. Bogatov for the steady supply of liquid helium.

---

[1] A. A. Galkin and A. P. Korolyuk, JETP **37**, 310 (1959), Soviet Phys. JETP **10**, 219 (1960).

[2] A. A. Galkin and A. P. Korolyuk, JETP **34**, 1025 (1958), Soviet Phys. JETP **7**, 708 (1958).

[3] Morse, Bohm, and Gavenda, Phys. Rev. **109**, 1394 (1958).

[4] H. E. Bömmel, Proc. 5th Int. Conf. on Low Temp. Physics and Chemistry, Wisconsin, 1958, p. 272.

[5] R. W. Morse and H. V. Bohm, ibid., p. 509.

[6] V. L. Gurevich, JETP **37**, 71 (1959), Soviet Phys. JETP **10**, 51 (1960).

[7] A. B. Pippard, Phil. Trans. Proc. Soc. (London) **A250**, 325 (1957).

[8] É. A. Kaner, JETP **38**, 212 (1960), Soviet Phys. JETP **11**, 154 (1960).

Translated by R. T. Beyer
329

SOVIET PHYSICS JETP VOLUME 11, NUMBER 6 DECEMBER, 1960

ELASTIC γP SCATTERING AT 40 – 70 MEV AND THE POLARIZABILITY OF THE PROTON

V. I. GOL'DANSKIĬ, O. A. KARPUKHIN, A. V. KUTSENKO, and V. V. PAVLOVSKAYA

P. N. Lebedev Physics Institute, Academy of Sciences, U.S.S.R.

Submitted to JETP editor January 12, 1960

J. Exptl. Theoret. Phys. (U.S.S.R.) 38, 1695-1707 (June, 1960)

Elastic γp scattering at 40 to 70 Mev is investigated and the differential cross sections at 45, 75, 90, 120, 135, and 150° are determined. The results obtained are compared with the theory that takes into account the anomalous proton magnetic moment as well as the effect of mesic cloud polarization. The cross section of γp scattering at 90° corresponds to a proton electric polarizability $\alpha_E = (11 \pm 4) \times 10^{-43}$ cm^3. In addition to the experimental results, we use the dispersion relations with which the value of the sum of the electric (α_E) and magnetic (α_M) polarizabilities can be obtained from the π-photoproduction data: $\alpha_E + \alpha_M = 11 \times 10^{-43}$ cm^3. With account of this value, the obtained experimental data correspond to the following values of the proton polarizabilities:

$$\alpha_E = (9 \pm 2) \cdot 10^{-43}\,\mathrm{cm}^3, \quad \alpha_M = (2 \mp 2) \cdot 10^{-43}\,\mathrm{cm}^3$$

Corresponding to the value obtained for the electric polarizability is an rms fluctuation of the proton electric dipole length $(\overline{r^2})^{1/2} = (3.5 \text{ to } 5) \times 10^{-14}$ cm.

1. INTRODUCTION

THE elastic scattering of γ quanta by protons differs radically from the well-known Compton effect on electrons. The difference is due primarily to the anomalous magnetic moment of the proton. The scattering of γ quanta by spin-½ particles was considered in its general form by Pauli. The theory of such scattering was subsequently developed by Powell,[1] Gell-Mann and Goldberger,[2] Low,[3] Klein,[4] and Capps.[5] The scattering amplitude obtained in references 2 to 5 includes, along with the Thomson term, also additional terms linear in the frequency of the γ quantum.

The γp scattering cross section in the laboratory system (l. s.), accurate to terms of order γ^2 (where $\gamma = h\nu/Mc^2$ and M is the proton mass) is given by a formula similar to that of Powell:

$$\frac{d\sigma}{d\Omega}(\theta) = \frac{1}{2} r_0^2 \{[1 - 2\gamma(1 - \cos\theta) + 3\gamma^2(1 - \cos\theta)^2](1 + \cos^2\theta) + \gamma^2[(1 - \cos\theta)^2 + f(\theta)]\}, \tag{1}$$

where $r_0 = e^2/Mc^2$, and the role of the anomalous magnetic moment is characterized by the term

$$f(\theta) = a_0 + a_1 \cos\theta + a_2 \cos^2\theta. \tag{2}$$

The coefficients a_0, a_1 and a_2 are power functions of the anomalous part of the proton anomalous magnetic moment $\lambda_a = 1.7896$. Their values are

$$a_0 = 2\lambda_a + \tfrac{9}{2}\lambda_a^2 + 3\lambda_a^3 + \tfrac{3}{4}\lambda_a^4 = 42.88, \tag{3}$$

$$a_1 = -4\lambda_a - 5\lambda_a^2 - 2\lambda_a^3 = -34.63, \tag{4}$$

$$a_2 = 2\lambda_a + \tfrac{1}{2}\lambda_a^2 - \lambda_a^3 - \tfrac{1}{4}\lambda_a^4 = -3{,}12. \tag{5}$$

It is obvious that the presence of the anomalous magnetic moment leads not only to an overall increase in the scattering cross section, but also to definite change in the type of angular distribution, viz: to an increase in the fraction scattered in the backward hemisphere.

Effects due to the anomaly of the magnetic moment are by far not the only feature of scattering of γ quanta by protons. The presence of the meson cloud makes possible a direct interaction between the γ quanta and this cloud. This manifests itself not only in the photoproduction of pions, but also in scattering. The Thomson cross section of $\gamma\pi^+$ scattering is 45 times greater than that of γp scattering, and the meson effects should greatly influence the γp scattering picture not only near the photoproduction threshold, but even at much lower energies.

The absorption of γ quanta leads to polarization of the meson cloud and induces in the proton electric and magnetic dipoles which give rise to secondary radiation. This, for example, is the cause of Rayleigh scattering, well known from optics, the role of which in the Compton effect on protons was noted by Capps[5] and considered in detail by A. M. Baldin,[5] who investigated the influence of proton polarizability on the γp scattering.

The amplitude of the Rayleigh scattering is proportional to the square of the γ-quantum frequency, the proportionality constants for the electric and magnetic dipole transitions being the electric and magnetic polarizability constants of the protons. These characterize both the ability of the meson clouds to become deformed under the influence of the external electric and magnetic fields, and the static distribution of the electric charge and the magnetic moment. The question of a possible delineation of the roles of these different phenomena will not be considered here. The term 'polarizability' used here is therefore not equivalent to the one normally employed for neutral particles, a fact that must be kept in mind throughout.

Although the scattering-amplitude terms due to the proton polarizability are proportional to the square of the frequency, they interfere only with the constant Thomson term, and lead therefore to terms quadratic in the frequency in the formula for the scattering cross section. Confining ourselves to similar quadratic terms in the cross section for γp scattering, we arrive at the following expression for the differential cross section of the Rayleigh-Powell γp scattering, in the l.s.,

$$d\sigma / d\Omega = \tfrac{1}{2} r_0^2 \{[1 - 2\gamma(1 - \cos\theta) + 3\gamma^2(1 - \cos\theta)^2 - 2A_E\gamma^2](1 + \cos^2\theta) - 4A_M\gamma^2\cos\theta + \gamma^2[(1 - \cos\theta)^2 + f(\theta)]\}, \qquad (6)$$

where $f(\theta)$ is defined by (2), and the dimensionless factors A_E and A_M represent the polarizabilities α_E and α_M, expressed in units $(e^2/\hbar c)(\hbar/Mc)^3 = 6.8 \times 10^{-44}\,\mathrm{cm}^3$.

As shown by V. A. Petrun'kin (private communication), Eq. (6) can be rigorously derived from the dispersion relations at low frequencies. In the interpretation of γp scattering experiments at energies much lower than the photomesic threshold (when $\gamma \ll 1$), use can be made of Eq. (6), in which two parameters, the electric and magnetic polarizabilities of the proton, must be determined experimentally. It is clear that at low energies the proton polarization causes only a slight difference between (6) and (1), if the latter is limited to terms proportional to γ^2. Therefore, in spite of the relative simplicity of the theoretical interpretation of the results, the accuracy requirements imposed on the experiment will be more stringent than in investigations of harder γ quanta.

The purpose of the present investigation was to ensure as high an experimental accuracy as possible, so that experiments on scattering of γ quanta of energy 40 – 70 Mev by protons could yield data on the polarizability of protons.

2. EXPERIMENTAL PROCEDURE

The experiments were carried out with the 265-Mev synchrotron of the Physics Institute of the Academy of Sciences, at a maximum bremsstrahlung spectrum energy of 75 Mev, i.e., at energies much below the threshold of photoproduction of π^0 mesons. Since only the scattered γ quanta need be recorded at these energies (without coincidence with the recoil protons), we used a target large enough to ensure a γp-scattering counting rate on the order of 0.5 or 1 pulse/minute.

Target. A diagram of the setup is shown in Fig. 1. The bremsstrahlung beam from the synchrotron was collimated and made to strike a liquid-hydrogen target. The working part of the target was a cylindrical vessel, elongated in the direction of the beam axis (12 cm dia., 30 cm long), approximately 3.5 l in capacity, filled with liquid hydrogen. Double walls of foamed polystyrene (PS-4) of approximate density 40 mg/cm^3 made up a cavity 1 cm deep in the unexposed part of the target. This cavity was filled with liquid nitrogen. The total capacity of the target vessel (~ 8.5 l of liquid hydrogen) ensured, at an average rate of evaporation of ~ 0.6 l/hr, continuous operation for approximately eight hours without refilling. The chosen working length of the target kept its exposed walls from entering the "field of view" of the detecting telescopes (except in the experiments at 150°), thus reducing considerably the background due to the unfilled target.

Detector. The high-threshold (~ 35 Mev) γ-quantum detectors used were two telescopes, consisting of three scintillation counters (terphenyl in toluol, 3 g/l), with a lead converter past the first counter and an aluminum absorber ahead of the last one (Fig. 1). Each counter was provided with a FÉU-33 photomultiplier. The photomultipliers operated in a specially selected mode ($E_{\text{FÉU}}$ = 3 to 4 kv), producing output pulses of 30 – 40 v amplitude from a Co^{60} source when operating directly into an RK-50 cable. It was thus possible to dispense with further amplification of the pulses from the photomultipliers.

Paraffin absorbers 5 or 7 cm thick were placed at the inputs of the telescope channels, to reduce the loading of the first counter, A, by soft electrons and γ quanta.

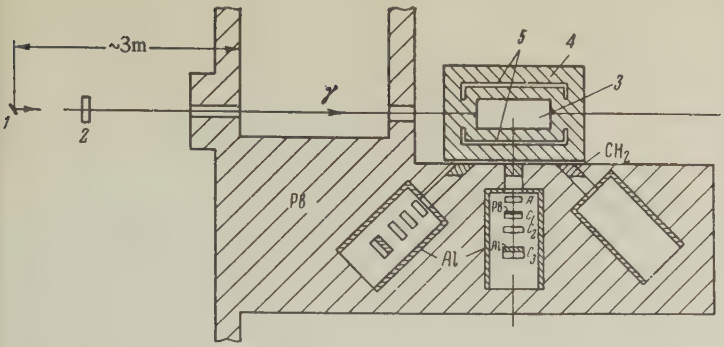

FIG. 1. Diagram of experimental setup: 1 – synchrotron target, 2 – monitor, 3 – liquid-hydrogen target, 4 – polystyrol walls, 5 – liquid nitrogen, C_1, C_2, C_3 – scintillation counters connected for coincidence, A – anticoincidence counter.

Electronic Circuitry. A block diagram of the electronic apparatus used in the experiment is shown in Fig. 2. A few additional explanations are in order. Two fast coincidence circuits of the parallel type with D2V germanium diodes were used. The first discriminator (D_1), used to reduce the load of the slow circuits, was temperature-compensated for threshold drift. The second discriminator (D_2) is the one developed by Park[7], so that a low-gain amplifier can be used. The shaped pulses from both coincidence circuits were fed to a slow anticoincidence circuit, which excluded the count due to charged particles. The possibility of simultaneous registration of the readings in all three channels made for convenient monitoring of the individual circuit elements.

The outputs of the two coincidence circuits and of the anticoincidence circuit were fed to transmission circuits controlled by the accelerator. The readings were registered only during a time interval somewhat longer than the duration of the intensity pulse from the synchrotron, thereby reducing the cosmic-ray background (by about 50). It was also possible to apply a signal to prevent registration of the readings whenever the character of the synchrotron pulses changed.

Monitors. The intermediate monitor used was a thin-wall ionization chamber, placed ahead of the first collimator. All the measurements were reduced to a definite number of counts in this chamber. The absolute value of the energy flux passing through the collimator for a given number of monitor counts was regularly determined from the activity of standardized carbon detectors in the reaction $C^{12}(\gamma, n)C^{11}$, the cross section of which is known.[8,9] The detectors were placed at the center of the target. To make the absolute calibration of the monitor more precise, data on the activation of the carbon were periodically compared with the readings of a thick-walled graphite chamber with a known absolute sensitivity (so-called Lax chamber). The values of the γ-quantum flux obtained by the two methods coincided within approximately 3%.

Experimental Conditions. The electron pulses from the synchrotron were stretched to approximately 300 μsec, corresponding to a change in maximum energy of the bremsstrahlung spectrum from 62 to 75 Mev. The shape of the pulse (approximately rectangular) was monitored visually with the aid of an IO-4 oscillograph synchronized with the accelerator.

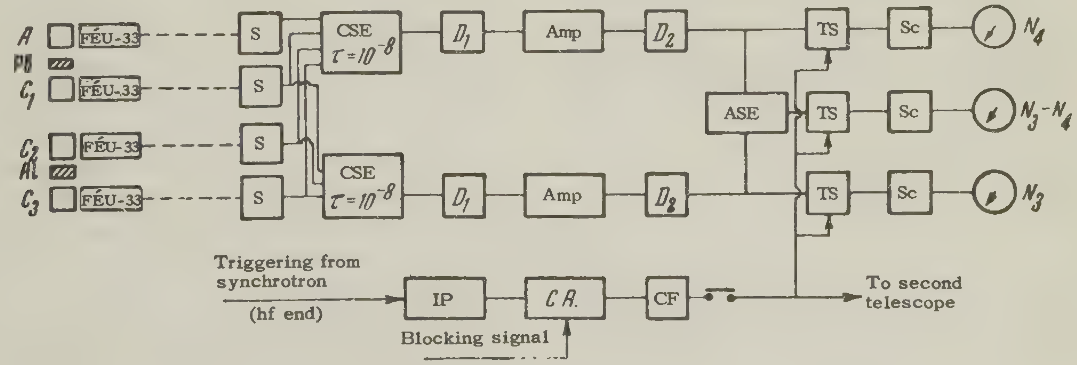

FIG. 2. Block diagram of the electronic apparatus: C_1, C_2, C_3, A – scintillation counters, S – pulse shaping, CSE – coincidence selection element, D_1, D_2 – discriminators, Amp – amplifier, ASE – anticoincidence selection element, TS – transmission system, Sc – scalar, N – corresponding mechanical counters, IP – transmission pulses, CA – anticoincidence circuit, CF – cathode follower.

The detecting telescopes were placed at 45, 75, 90, 120, 135, and 150° to the direction of the bremsstrahlung beam, and measurements were made simultaneously at two angles. Since the efficiencies of the two telescopes differed somewhat, the positions of the telescopes were interchanged at fixed time intervals, and the average readings of the two telescopes were used for each angle.

Cycles of measurements with hydrogen were alternated with measurements of the background. In experiments with the target empty, the average background for all angles was approximately 40% of the counting rate in the main experiments.

To check the stability of the operation of the entire setup, daily control measurements were made of the counting rate from a thick carbon target, both under the operating conditions and at the maximum bremsstrahlung energy, 265 Mev.

3. DETERMINATION OF THE TELESCOPE EFFICIENCY

To determine the differential cross sections from the measured yields of γp scattering, it is necessary to know the energy dependence of the efficiency of the telescopes employed for counting scattered γ quanta. We used in this investigation a method which we developed especially[10] to determine this dependence in the energy range from 35 to 150 Mev. This method is based on registration of the Compton scattering of the bremsstrahlung beam by electrons at a small angle (3°), for different maximum bremsstrahlung energies. The results of such a calibration are shown in Fig. 3.

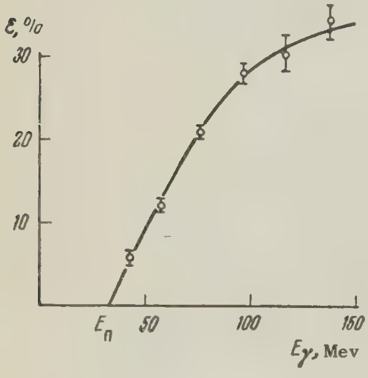

FIG. 3. Energy dependence of the efficiency of registration of γ quanta by the coincidence telescope (the errors are statistical).

The energy threshold of the telescope, $E_{thr} \approx 35$ Mev, calculated from the totality of the mean energy losses of the electrons leaving the converter, agreed with the experimentally obtained value.

An important factor was that in the calibration experiments, as in the main experiments, the entire working surface of the telescope was irradiated at once, since the telescope was located in these calibration experiments sufficiently far (11 m) from the carbon target (1.5 cm thick). In addition, the absolute bremsstrahlung flux was determined by the same methods as in the main experiments. The different errors in the determination of the absolute results of the main and calibration experiments were thus eliminated and our experiments yielded essentially a direct comparison of the differential angular cross sections for Compton scattering, known for the electrons and unknown for the protons.

4. REDUCTION OF THE EXPERIMENTAL DATA

The number of counts produced by a telescope located at an angle θ to the direction of the incident photon beam, referred to a definite number of counts of the monitor chamber, can be represented in the form

$$B = \iiint a\eta(E, E_{max})\,\varepsilon(E'(E,\theta))\,\frac{d\sigma}{d\Omega}(E,\theta)\,n_0 dV d\Omega\, dE, \qquad (7)$$

where

$$a = E_{\text{tot}} \Big/ \int \eta(E, E_{max})\, E dE$$

is the γ-quantum flux (per unit area) averaged over the irradiated area; $\eta(E, E_{max})$ is the bremsstrahlung spectrum, $\epsilon(E')$ is the efficiency for registration of γ quanta of energy E' (which corresponds to the initial energy E) scattered at an angle θ, n_0 is the number of hydrogen nuclei per unit volume, dV is the element of working volume in the target; and $d\Omega$ is the solid angle "seen" by the telescope, corresponding to this volume.

The integral $J_\theta = \iint n_0 dV d\Omega$ is practically independent of the energy of a primary γ quanta.* This integral was calculated for each angle in accordance with the specific geometry of the experiment. To test the calculations, the ratio $J_\theta / J_{90°}$ was compared with the data obtained in an auxiliary experiment, in which the number of counts from a "point target" of PS-4 foamed polystyrol (a small cube 2 cm on each side) was compared with the number of counts from a cylinder of the same material, simulating the working volume of the liquid-hydrogen target.

Taking the cross section $\overline{d\sigma/d\Omega}$, averaged over the angles and energies, outside the integral sign, we obtain

$$\overline{d\sigma / d\Omega} = B / aJ_E J_\theta, \qquad (8)$$

---

*The calculation of the absorption of γ quanta in the target will be discussed later on.

where

$$J_E = \int_{\mathrm{thr}}^{E_{max}} \eta(E,\, E_{max})\, \varepsilon(E'(E,\, \theta))\, dE.$$

The bremsstrahlung spectrum of the synchrotron is given for a thick target by the Eyges formula, and a plot of $\epsilon(E')$ is shown in Fig. 3, where it is obvious that the integral J_E varies with the scattering angle θ because of the change in the energy of the scattered quantum. Figure 4 shows the products of the efficiency ϵ of registration of the scattered γ quanta and the distribution function η in the spectrum of the primary bremsstrahlung, for different scattering angles, as a function of the energy of the incident γ quanta. It is seen that the curves are approximately symmetrical and have a maximum near 56 Mev with an average half-width of approximately 25 Mev. The absolute value of J_E for 90° was computed graphically. The corrections for the change in the registration efficiency at different angles were also calculated graphically, from the ratio of the areas under the corresponding curves. They range from + 5% for 75° to - 15.4% for 150°.

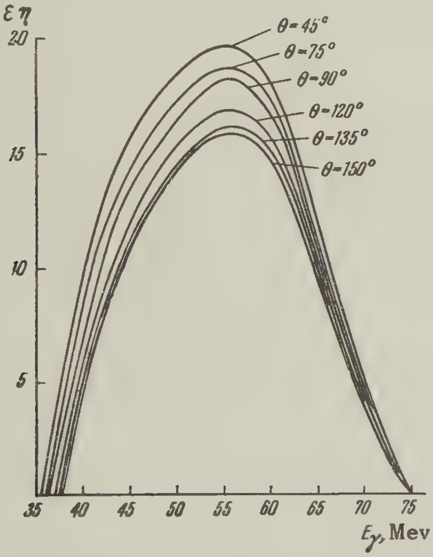

FIG. 4. The product of the registration efficiency of the scattered γ quantum and the distribution function in the spectrum of the primary bremsstrahlung (for different scattering angles).

The experimentally obtained differential cross sections for γp scattering at 45, 75, 90, 120, 135, and 150° are listed in the table (column 2). These results must be corrected for absorption in the target and for the contribution of the background processes.

Corrections for Absorption in the Target. Under the working conditions, some of the incident bremsstrahlung is absorbed in the walls and in the hydrogen of the target (~ 1.5%). The scattered radiation is also absorbed in amounts that vary with the angle, from 2.2% at 90° to 4.7% at 150°. The calculated corrections for the absorption of incident, scattered, and background γ quanta in the target are listed in column 3 of the table. Corrections for absorption in the paraffin filter and in the walls of the telescope were obviated by the fact that $\epsilon(E)$ was also measured in the presence of these absorbers.

Calculation of the Background. Since we did not separate the Compton γp scattering by registering the coincidence of the scattered γ quanta with the recoil protons, it was very important to allow for all possible background sources capable of making a noticeable contribution to the registration of γ quanta by a telescope with an approximate threshold of 35 Mev.

When a high registration threshold is obtained for both the telescope as a whole and for each individual counter (several Mev), it becomes impossible to register the Compton scattering of the γ quanta by the target electrons at large angles.

The single processes that produce high-energy quanta at the angles of interest to us are Delbruck scattering and radiative pair production. The cross section of Delbruck scattering[12] on hydrogen is small ($\sigma_{\mathrm{tot}} \sim 10^{-34}\,\mathrm{cm}^2$), and this scattering has a strong forward orientation ($\sim 1/\theta^4$), so that it can be neglected completely even at 45°. According to estimates made by Feinman and Gomez,[13]

Angle θ, deg.	$10^{32}\,\frac{d\sigma}{d\Omega}(\theta)$, cm^2/sr (without correction)	Correction for absorption of primary and registered γ quanta, $\Delta\sigma/\sigma$, %	Correction for extraneous processes (in units of 10^{-34} cm^2/sr)				$10^{32}\,\frac{d\sigma}{d\Omega}(\theta)$, cm^2/sr (final values)
			Rutherford scattering of electrons with subsequent radiation	Pair production at large angles with subsequent radiation	Emission of bremsstrahlung radiation at large angles	Total Correction	
45	4.66 ± 0.28	+6.5	—127	—14.1	—5.4	—146	3.40 ± 0.28
75	1.21 ± 0.08	+3.5	—10.7	—1.4	—0.47	—12.6	1.12 ± 0.08
90	1.14 ± 0.05	+3.5	—6.7	—0.7	—0.3	—7.7	1.10 ± 0.05
120	1.30 ± 0.08	+4.5	—1.4	—0.18	—0.06	—1.6	1.34 ± 0.08
135	1.48 ± 0.08	+6.5	—0.89	—0.09	—0.04	—1.0	1.56 ± 0.08
150	1.82 ± 0.07	+6.5	—0.36	—0.04	—0.01	—0.4	1.93 ± 0.07

the cross section for radiative pair production (production of a pair in the field of the nucleus with subsequent bremsstrahlung of one of the electrons in the same field) is approximately equal to the cross section $\sigma_{\gamma p}$ of the Compton γp scattering at a laboratory angle of 50° and $E_\gamma = 40$ Mev, but amounts to only ($1/4$) $\sigma_{\gamma p}$ at $E_\gamma = 50$ Mev. In view of the strong energy and angular ($\sim 1/\theta^4$) variations of the cross sections of this process, its total contribution at $E_\gamma \approx 56$ Mev and 75° is merely ~ 3% of the γp scattering. Since only a small part of the γ quanta emitted in radiative pair production has an energy greater than 35 Mev (threshold of our telescope), this process can be neglected at all angles except 45°. No corrections were therefore introduced for 75 — 150°, while the data for 45° were not used at all for further calculations of the polarizability of the proton, in view of the uncertainty in the value of the correction.

A background was produced also by multiple processes in the matter ahead of the target, in the target itself, and finally between the target and the first counter of the telescope, causing γ quanta of energies greater than 35 Mev to enter the telescope. To estimate the contribution of such processes, we calculated the number of high-energy electrons generated at small angles by Compton scattering and by pair production in the target and in the matter ahead of the target. We then considered a) the bremsstrahlung of these electrons at large angles in the direction of the counting channels (using Hough's data[14]), and b) their Rutherford scattering (using Mott's formula) in the direction of the counter channels with subsequent forward emission of bremsstrahlung in the matter ahead of the telescope. In addition, pair production at large angles in the hydrogen of the target[15] and the subsequent bremsstrahlung were considered. The results of the calculations are also listed in the table (columns 4 — 7).

The last column of the table gives the final values of the differential cross sections of γp scattering after making the corrections for the background processes and for absorption in the target. These final values are shown in Fig. 5 together with the data of other experimental investigations[16–18] for γ quanta of like energies (~ 60 Mev).

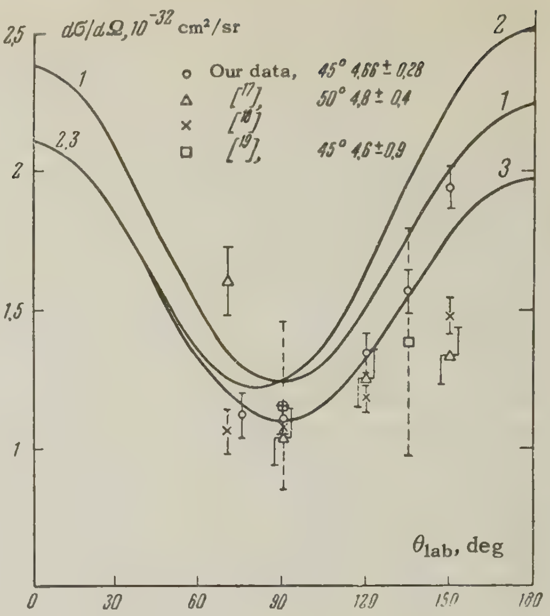

FIG. 5. Experimental data on γp scattering with ~60-Mev γ quanta. Curves — calculated: 1 — for $A_E = A_M = 0$; 2 — for $A_E = 0$, $A_M = 16$; 3 — for $A_E = 16$ and $A_M = 0$. The γp scattering cross sections compatible with the value $A_E + A_M = 16$ ($A_E, A_M > 0$) lies between curves 2 and 3 (θ — angle in the laboratory system).

Systematic Errors. The tabulated errors in the determination of the γp scattering cross sections are due only to statistical errors of the main measurements. The principal possible source of systematic errors, namely the inaccuracy in the determination of the flux of the bremsstrahlung quanta, is excluded because a direct comparison is used between the cross section of Compton scattering by protons and by electrons. Nevertheless, an error due to two inaccuracies in the determination of the product of the effective working volume of the target by the solid angle "seen" by the telescope, in the calibration and in the main (integral J_θ) experiments, does remain. We estimate this error to be ± 4%. In comparing the results of the calculation and the main experiments, additional errors of statistical origin arise, connected with the determination of the flux of γ quanta from the monitor counts in the two types of experiments and the summation of the dispersions of many points on the curve of the efficiency of registration of the γ quanta by the telescopes. The systematic errors due to the possible inaccuracy in the shape of the bremsstrahlung spectrum used in the calculations are of opposite signs in the calibration and in the main experiments, and are almost completely cancelled. The total value of the possible systematic error in the determination of the γp-scattering cross sections at angles from 75 to 150° is estimated at ±6%.

Returning now to the statistical errors listed in the table, we note that the errors for five experimental points range from +3.6 to + 7.2%. The square root of the sum of dispersions for all five points equals 11.7%. Thus, when using the experimental points for comparison with the calculated curves (see

Fig. 5 curves 1-3), the mean statistical error calculated for an individual point is approximately 2.4%, while the total mean error (statistical plus systematic) is approximately 8%.

5. DETERMINATION OF PROTON POLARIZABILITY

To determine the electric and magnetic polarizability of the proton, we compare the results of Eq. (6) with those in the table and in Fig. 5. Even if we disregard the obviously excessive value of the γp-scattering cross section at 45°, we have five experimental values for the two parameters A_E and A_M of Eq. (6). It must be borne in mind, however that by far not all measurements of the angular distribution are equally sensitive to the values of A_E and A_M. As can be seen from (6), the forward-scattering (0°) cross section is a function of the sum of A_E and A_M, but not of each of these quantities individually:

$$\frac{d\sigma}{d\Omega}(0^\circ) = \frac{1}{2} r_0^2 \{2[1 - 2(A_E + A_M)\gamma^2] + 5.13\gamma^2\}. \quad (9)$$

On the other hand, the backward scattering, at 180°, depends only on the difference

$$\frac{d\sigma}{d\Omega}(180^\circ) = \frac{1}{2} r_0^2 \{2[1 - 4\gamma + 12\gamma^2 - 2(A_E - A_M)\gamma^2] + 78.39\gamma^2\}. \quad (10)$$

Our experiment yielded a γp-scattering pattern essentially only in the rear hemisphere, at laboratory angles from 75 to 150°. Using these experimental values only, we can obtain only A_E with a sufficient degree of determinacy, since γp-scattering cross sections at angles close to 90° are very insensitive to A_M. Using only the value

$$\frac{d\sigma}{d\Omega}(90^\circ) = (1.10 \pm 0.05) \cdot 10^{-32}\ \text{cm}^2/\text{sr}$$

we obtain

$$A_E = 16 \pm 5.8 \quad \text{or} \quad \alpha_E = (11 \pm 4) \cdot 10^{-43}\ \text{cm}^3$$

We can make use of the dispersion relation as an additional source of information to account for the forward γp scattering, which was not measured experimentally, and thus obtain a better value of α_E and and estimate of the magnetic polarizability α_M.

Cini and Stroffolini[19] have shown that the cross sections of forward γp scattering $(d\sigma/d\Omega)$ (0°) are completely determined at energies below the photomeson threshold by the total cross sections, obtained directly by experiment, of the photoproduction of pions induced by unpolarized γ quanta, and that separate meson photoproduction cross sections for γ quanta polarized parallel and antiparallel to the proton spin need be known for the calculation of $(d\sigma/d\Omega)$ (0°) only at higher energies. Using the relations given by Bernardini[20] we obtain

$$\frac{d\sigma}{d\Omega}(0^\circ) = \left[\frac{e^2}{Mc^2} - \frac{\gamma^2}{4\pi^2}\left(\frac{\hbar}{Mc}\right)^{-1} \int_0^\infty \frac{\sigma_p(\gamma') + \sigma_a(\gamma')}{\gamma'^2 - \gamma^2} d\gamma'\right]^2$$
$$+ \gamma^2 \left[\frac{\lambda_a^2}{2} \frac{e^2}{Mc^2} - \frac{\gamma^2}{4\pi^2}\left(\frac{\hbar}{Mc}\right)^{-1} \int_0^\infty \frac{\sigma_p(\gamma') - \sigma_a(\gamma')}{\gamma'(\gamma'^2 - \gamma^2)} d\gamma'\right]^2$$
$$+ \gamma^2 \frac{1}{32\pi^2}\left(\frac{\hbar}{Mc}\right)^{-2} [\sigma_p^2(\gamma) + \sigma_a^2(\gamma)], \quad (11)$$

where $\sigma_p(\gamma)$ and $\sigma_a(\gamma)$ are the total cross sections for the photoproduction of pions on protons for γ quanta of energy γMc^2 (laboratory system), polarized parallel and antiparallel to the proton spin, respectively. The sum $\sigma_p(\gamma) + \sigma_a(\gamma) = \sigma_t(\gamma)$ is the total photoproduction cross section for an unpolarized beam of γ quanta.

The last term vanishes below the photoproduction threshold and we have, accurate to terms of order γ^2,

$$\frac{d\sigma}{d\Omega}(0^\circ) = r_0^2 \left\{1 - \left[\frac{1}{2\pi^2}\left(\frac{e^2}{\hbar c}\frac{\hbar}{Mc}\right)^{-1} \int_0^\infty \frac{\sigma_\pi(\gamma') + \sigma_a(\gamma')}{\gamma'^2 - \gamma^2} d\gamma' - \frac{\lambda_a^4}{4}\right]\gamma^2\right\}. \quad (12)$$

Comparing (12) and (9) (bearing in mind that the very definition of polarizability applies to quanta of zero energy) and going from A_M and A_E to α_M and α_E, we obtain

$$\alpha_E + \alpha_M = \frac{1}{4\pi^2}\frac{\hbar}{Mc}\int_0^\infty \frac{\sigma_t(\gamma)}{\gamma^2} d\gamma. \quad (13)$$

It is obvious that as long as α_E and α_M are positive, (13) characterizes the upper limit of the values of each of the two proton polarizabilities.

Using the latest data on the photoproduction of $\pi^\pm$ mesons[20] and π^0 mesons[21,22] (see Fig. 6), we obtain $\alpha_E + \alpha_M = 11 \times 10^{-43}\ \text{cm}^3$, i.e., $A_E + A_M = 16$.

Inasmuch as (13) is obtained from the most general properties of the scattering matrix, there are no reasons to cast any doubts on it at all. Therefore, provided (6) is correct, i.e., provided the scattering theory used here is valid with sufficient accuracy there is no need for taking into account higher powers of the γ-quantum frequency, we can readily establish the limits of the γp-scattering cross sections for all angles. If A_E and A_M are positive, and if $A_E + A_M = 16$, these limits are the curves obtained from (6) at $A_E = 0$, $A_M = 16$ and $A_E = 16$, $A_M = 0$. It is seen from Fig. 5, where the values of $(d\sigma/d\Omega)$ (θ) compatible with $A_E + A_M = 16$ lie in the region between curves 2 and 3, that all our experimental data for

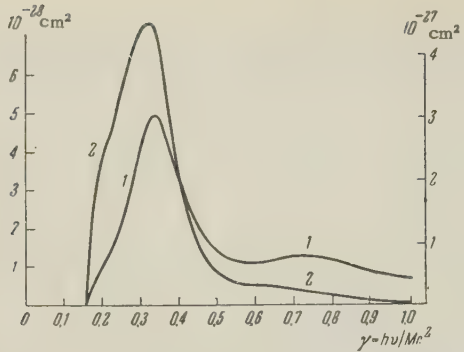

FIG. 6. Data on the total production cross sections of π^+ and π^0 mesons on protons, employed in determining the sum of electric and magnetic polarizability of the proton. Curve 1 – the value of $\sigma_{\pi^0} + \sigma_{\pi^+}$ (left-hand scale); curve 2 – the value of $(\sigma_{\pi^0} + \sigma_{\pi^+})\gamma^2$ (right-hand scale).

75 – 150° fall in this region, while the values obtained in references 16 – 18 for the γp-scattering cross sections in the backward hemisphere are somewhat too low.

Using $A_E + A_M = 16$ and calculating the value of A_E by the method of least squares to give best agreement with our results, we obtain $A_E = 13 \pm 3$ and $A_M = 3 \pm 3$, while the sum of the weighted squares of the errors is $D = 1.8 \times 10^{-66}\,\text{cm}^4\cdot\text{sr}^{-2}$.

We thus conclude that

$$\alpha_E = (9 \pm 2)\cdot 10^{-43}\,\text{cm}^3, \qquad \alpha_M = (2 \mp 2)\cdot 10^{-43}\,\text{cm}^3.$$

6. DISCUSSION OF THE RESULTS

The magnetic polarizability of the proton, as already indicated by Baldin,[6b] is thus much less than the electric polarizability. A determination of the magnetic polarizability of the proton is more sensitive to a possible contribution to the γp-scattering cross section from terms proportional to higher powers of the γ-quantum frequency (greater than γ^2), and therefore a detailed analysis of the role of these terms is of interest if a more refined value of A_M is desired. As regards the electric polarizability, we see not only that the sum $A_E + A_M$ agrees with our experimental data, but the optimal value $A_E = 13 \pm 3$ agrees within the limits of errors with the value obtained above from the cross section for scattering at 90° ($A_E = 16 \pm 5.8$).

A direct comparison of the experimental results with the curve obtained from (1) (without allowance of the polarizability of the proton) gives a much larger sum of weighted squares of errors, $D = 10.3 \times 10^{-66}\,\text{cm}^4\text{sr}^{-2}$, than obtained with (6). The best agreement with (1) is obtained by increasing all the experimental cross sections by 8%; this, however, is at the border of possible systematic errors.

The question of electric polarizability of nucleons has been extensively discussed in the literature of late in connection with the development of theoretical ideas[23,24] on the role of polarizability of neutrons electrically scattered by small angles in the Coulomb field of heavy nuclei. The electrical polarizability of the neutron $(\alpha_E)_n = (8 \pm 3.5) \times 10^{-41}\,\text{cm}^3$, calculated by Aleksandrov[25] from an analysis of the data on neutron scattering, certainly contradicts the totality of data on the scattering of γ quanta and photoproduction of π mesons, a fact noted in the theoretical papers[7,26-30] and now again confirmed in our experiments.

The last analysis of the new experiments on neutron scattering[28] has led, to be sure, to a reduction in the limiting value of α_E, namely $0 < (\alpha_E)_n < 2 \times 10^{-41}\,\text{cm}^3$, but does not give any more definite results. As long as $\alpha_E \sim 10^{-42}\,\text{cm}^3$, neutron experiments can hardly establish quantitatively the contribution of the electric polarizability. The main path towards determining the electric and magnetic polarizability of the nucleon – properties due to the change in the structure of the meson cloud in the nucleon – lies therefore in a study of the meson processes and primarily the photoproduction of pions and the nucleon Compton effect.

Rough estimates of the electric polarizability of the neutron based on meson theories, yield a quantity on the order of[26,28]

$$(e^2/\hbar c)\,(f^2/\hbar c)\,(\hbar/\mu c)^3 = 1.6\cdot 10^{-42}\,\text{cm}^3,$$

where $(f^2/\hbar c) = 0.08$. A result close to this estimate $(\alpha_E)_n = (1.6 \text{ to } 1.8) \times 10^{-42}\,\text{cm}^3$ was obtained[26] by calculating the polarizability of the meson cloud in a nucleon, with the aid of the Chew theory for functions with Gaussian and exponential forms, with a cutoff parameter 5.6 $\mu c/\hbar$.

In analyzing the data on pion photoproduction and γp scattering, Baldin[6] obtained for the lower limit of nucleon polarizability (assuming single-meson exchange only) a value $(\alpha_E)_p = 4 \times 10^{-43}\,\text{cm}^3$. The upper limit of $(\alpha_E)_p$, derived by him by assuming nearly equal values for the γp-scattering cross section at 90° and the Thompson cross section $(r_0^2/2)$, is estimated at $1.4 \times 10^{-42}\,\text{cm}^3$. From the data on pion photoproduction, Breit and Rustgi[29] obtained a similar estimate, $(\alpha_E)_n \lesssim 2 \times 10^{-42}\,\text{cm}^3$.

It must be borne in mind that, because the cross section σ^- of the process $\gamma + n \rightarrow \pi^- + p$ exceeds near the threshold the cross section σ^+ of the process $\gamma + p \rightarrow \pi^+ + n$, and because of the considerable contribution of the threshold region to the dispersion integral (13), the electric polarizability of the neutron should be 20 or 30% greater than the corresponding value for the proton.[6b,29] As is clear from our calculations with Eq. (13), the upper limit for the electric polarizability of the proton can be reduced to $(\alpha_E)_p = 1.1 \times 10^{-42}\,\text{cm}^3$.

To arrive at our final conclusions regarding the value of $(\alpha_E)_p$, we used also the calculated limiting value of the sum $(\alpha_E + \alpha_M)_p = 1.1 \times 10^{-42}\,\text{cm}^3$; however, even the direct results of the experiments confirm in general our various theoretical estimates of $(\alpha_E)_p$.

In conclusion, let us consider the problem of the mean-square fluctuation $(\overline{r^2})^{1/2}$ of the displacement of the center of distribution of the electric charge in the polarized proton about its center of gravity, associated with α_E.

According to references 6 and 29, this value is connected with the electric polarizability of the proton by the usual relation

$$(\overline{r^2})^{1/2} = \left[\tfrac{3}{2}\,\alpha_E\,(e^2/\hbar c)^{-1}\,\Delta E/\hbar c\right]^{1/2}, \tag{14}$$

where ΔE is the energy difference between the ground and the polarized states of the proton. Since the polarization is due to the excitation of the meson cloud or to the occurrence of a resonant isobar state, a suitable choice of ΔE lies between μc^2 and $2\mu c^2$.

For $\alpha_E = 9 \times 10^{-43}\,\text{cm}^3$ we obtain from (14), for the proton, the mean-squared fluctuation of the length of the induced electric dipole

$$(\overline{r^2})^{1/2} = 3.5 \text{ to } 5\cdot 10^{-14}\,\text{cm}.$$

It is undoubtedly desirable to develop a more detailed theory of magnetic polarizability of the proton, so as to relate the values of α_E and α_M with the contributions from different mechanisms of pion photoproduction, to obtain theoretical limits for α_M, and to compare them with experiment, and also to compare the fluctuations of the lengths of electric and magnetic nucleon dipoles.

The authors express warm gratitude to S. P. Balat'ev, R. G. Vasil'kov, E. V. Minarik, and A. Samiullin for help with the experiments, and to G. Ivanov for active participation in the reduction of the results. It is also our pleasure to thank the entire synchrotron crew for help in many hours of experiments and express sincere gratitude to A. M. Baldin and V. N. Gribov for participating in discussion of the results of the work.

Note added in proof (May 20, 1960). V. N. Gribov has advised us that the roles of the different factors in the quadratic (in the frequency) terms of the amplitude of Rayleigh (E1) scattering (see Introduction) are made clear by the following expression for this amplitude (in units e^2/Mc^2):

$$R = (1 - A_E\gamma^2)(\mathbf{e}\mathbf{e}') = \left\{1 - \left[\frac{1}{3}r_e^2\left(\frac{Mc}{\hbar}\right)^2 + \frac{1}{4} + \frac{\gamma_a}{2} + A_E^*\right]\gamma^2\right\}(\mathbf{e}\mathbf{e}'),$$

where $\mathbf{e}$ and $\mathbf{e}'$ are unit vectors in the direction of polarization of the incident and scattered protons, r_e is the electric radius of the proton, A_E^* is a measure of polarizability analogous to our A_E but now in its usual sense.

---

[1] J. L. Powell, Phys. Rev. 75, 32 (1949).

[2] M. Gell-Mann and M. Goldberger, Phys. Rev. 96, 1433 (1954).

[3] F. E. Low, Phys. Rev. 96, 1428 (1954).

[4] A. Klein, Phys. Rev. 99, 998 (1955).

[5] R. Capps, Phys. Rev. 106, 1031 (1957).

[6] A. M. Baldin, a) Paper at Conference on Elementary Particles, Padua-Venice, 1957 b) Nucl. Phys. in press.

[7] E. C. Park, J. Sci. Instr. 33, 257 (1956).

[8] Barber, George, and Reagan, Phys. Rev. 98, 73 (1955).

[9] P. S. Baranov, Dissertation, Phys. Inst. Acad. Sci. 1955.

[10] Gol'danskiĭ, Karpukhin, and Pavlovskaya, Приборы и техника эксперимента (Instrum. and Meas. Techniques), No 3, 1960.

[11] L. Eyges, Phys. Rev. 81, 982 (1951).

[12] A. I. Akhiezer and V. B. Berestetskiĭ, Квантовая злектродинамика (Quantum Electrodynamics), Fizmatizdat, 1959.

[13] L. G. Hyman, Mass. Inst. Tech. PhD Thesis, 1959.

[14] P. V. C. Hough, Phys. Rev. 74, 80 (1948).

[15] R. C. Miller, Phys. Rev. 95, 796 (1954).

[16] C. Oxley and V. L. Telegdi, Phys. Rev. 100, 435 (1955).

[17] C. Oxley, Phys. Rev. 110, 733 (1958).

[18] Pugh, Gomez, Frisch, and Janes, Phys. Rev. 105, 982 (1957).

[19] M. Cini and R. Stroffolini, Nucl. Phys. 5, 684 (1958).

[20] G. Bernardini, Paper at Ninth International Conference on High-Energy Physics, Kiev, 1959.

[21] Vasil'kov, Govorkov, and Gol'danskiĭ, JETP 37, 11 (1959), Soviet Phys. JETP 10, 7 (1960); Nucl. Phys. 12, 337 (1959).

[22] K. Berkelman and J. Waggoner, Phys. Rev. in press.

[23] Yu. A. Aleksandrov and I. I. Bondarenko, JETP 31, 726 (1956), Soviet Phys. JETP 4, 612 (1957).

[24] Barashenkov, Stakhanov, and Aleksandrov, JETP 32, 154 (1957), Soviet Phys. JETP 5, 144 (1957).

[25] Yu. A. Aleksandrov, **33**, 294 (1957), Soviet Phys. **6**, 228 (1958).

[26] W. S. Barashenkov and B. M. Barbashov, Nucl. Phys. **9**, 426 (1958).

[27] Blokhintsev, Barashenkov, and Barbashov, Usp. Fiz. Nauk **68**, 417 (1959), Soviet Phys. Uspekhi **2**, 505 (1960).

[28] R. M. Thaler, Phys. Rev. **114**, 827 (1959).

[29] G. Breit and M. L. Rustgi, Phys. Rev. **114**, 830 (1959).

[30] L. L. Foldy, Phys. Rev. Lett. **3**, 105, 1959.

Translated by J. G. Adashko
330

A SEARCH FOR THE ρ^0 *MESON AND A CHECK OF THE DISPERSION RELATIONS IN* π-N *SCATTERING*

V. G. ZINOV, A. D. KONIN, S. M. KORENCHENKO, and B. PONTECORVO

Joint Institute for Nuclear Research

Submitted to JETP editor January 13, 1960

J. Exptl. Theoret. Phys. (U.S.S.R.) 38, 1708-1714 (June, 1960)

The total π^--p interaction cross sections (σ_t^-) were measured with an accuracy of 1.5 – 2% for about 50 pion energies between 140 and 360 Mev. The pion energy was known to within ±1%. No anomalies in the energy dependence of σ_t^- were found which could indicate the existence of a ρ^0 meson with a mass in the range of 270 to 410 Mev/c^2.

The data are inconsistent with the energy value $E_2 = 650$ Mev for the second maximum of σ_t^- found by Frisch et al.[7] but agree with the conclusion drawn by Brisson et al.[8] that it should be located at a lower energy ($E_2 \approx 610$ Mev). The data are in agreement with the dispersion relations for π^--p scattering. It is thus demonstrated that the Puppi-Stanghellini problem as such no longer exists and that it arose only as a result of an inaccurate knowledge of the total π^--p interaction cross section.

INTRODUCTION

THE energy dependence of the total cross section of the π^--p interaction σ_t^- has already been investigated in a wide energy interval several years ago. For energies up to 360 Mev, where the most precise data were obtained, the cross section was measured with a precision not exceeding ~5%, while the energy for which the cross section was being determined was known only within ±6 Mev. At the same time the precise measurement of this cross section with good energy resolution is of undoubted interest for several reasons.

First, as was already communicated earlier,[1] by determining the energy dependence of the total cross section σ_t^- very precisely it is possible in principle to observe a definite type of "threshold anomalies" which could furnish information on π-π interaction, or would indicate the existence of the still unknown ρ^0 particle.

Secondly, it is of definite interest to express the energy dependence of the total π-N cross section in the state with an isotopic spin $T = 1/2\,[\sigma(1/2)]$ with the aid of a small number of Breit-Wigner type of "resonance" curves. This requires experimental data of great precision.

Thirdly, some authors[2] doubt the validity of the dispersion relations for π-N scattering. From this point of view a more careful measurement of the σ_t^- than has been carried out to date in a sufficiently wide energy interval is essential for the precise calculation of the real part of the π^--p scattering amplitude.

In the present work we present the experimental investigations which we have undertaken in connection with the above.

Preliminary results were communicated at the Conference on the Physics of High-Energy Particles in Kiev in 1959.

THE EXPERIMENTS

a) The geometry of the experiment. The total interaction cross sections of negative pions with hydrogen were measured by the weakening of the meson beam passing through a hydrogen scatterer. The general setup for the experiment is shown in Fig. 1. The meson beam incident on the hydrogen target was formed by a rectangular collimator 3 cm wide (in the yoke of the synchrocyclotron magnet), by the deflecting magnet, and by counters 1 and 2 connected in coincidence. The mesons after passing through the scatterer were registered by counter 3, connected in coincidence with counters 1 and 2. The counters were made of scintillating plastic and were of the following dimensions: counter 1 – 0.8 × 3 × 6 cm; counter 2 – 0.5 × 3 × 6 cm; counter 3 – 1 × 10 × 10 cm (the last value for each counter gives the vertical dimension). The mean angle of registration by counter 3 was 10.5°. Liquid hydrogen in a foamed polysterol container (wall thickness 0.8 g/cm^2)

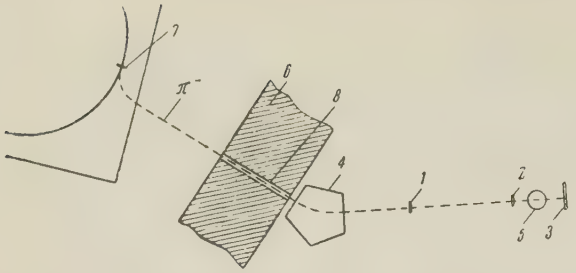

FIG. 1. Experimental setup (schematic): 1, 2, 3 – scintillation counters, 4 – deflecting magnet, 5 – hydrogen scatterer, 6 – yoke of the synchrocyclotron magnet, 7 – beryllium target inside the synchrocyclotron chamber, 8 – pion collimator.

served as the target.[3] The density of the hydrogen was taken as 0.0708 g/cm²; the mean number of hydrogen nuclei in the path of the beam corresponding to this density amounted to $(0.4607 \pm 0.0023) \times 10^{24}$ nuclei/cm².

b) Electronic apparatus. The apparatus used in this experiment was essentially the same as in reference 3. FÉU-33 photomultipliers were used for the scintillation counters. To increase the counting efficiency and to decrease the role of the apparatus "drift," the resolving time of the coincidence circuits used was increased to 2×10^{-8} sec. Two scaling devices of the "Kalina" type, each preceded by an additional scale-of-4 scaler with a dead time of 0.1 μsec, were used for counting the transmitted mesons.

For the precision required of the total cross sections (2%) it was essential that the operating stability of the apparatus amount to about several hundredths of a percent. It was, therefore, desirable to have an objective criterion for the satisfactory quality of the operation of the apparatus. Such a criterion can be the reproducibility of the results over long periods of time (tens of hours). If we take, for example, the coincidence count of counters 1, 2, and 3 (the count of 1 and 2 is the monitor) and measure it a sufficient number of times then, in the absence of errors due to the apparatus "drift," the deviations of each measurement from the mean will obey a Gaussian distribution with a calculable dispersion. However, such a control consumes almost as much time as all the measurements. The information already accumulated in the course of measuring the total cross section was, therefore, employed for the control. The measurements were repeated 5 — 6 times for each energy. The deviations of the coincidence count N_{123} from its mean value with the hydrogen were summed for various energies. The result of this summation (Fig. 2) shows that the distribution of the deviations is in very good agreement with the Gaussian distribution (solid curve in Fig. 2) with a dispersion calculated on the assumption of the absence of apparatus "drift" and other errors, except for the statistical fluctuations in the number of pion-interaction events after their registration by counters 1 and 2.

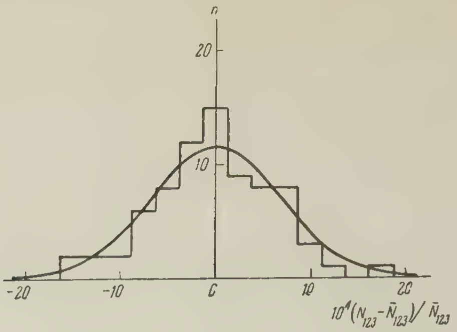

FIG. 2. The spread of the deviations of the normalized coincidence count N_{123} (with hydrogen) from the mean value; n is the number of measurements having a given deviation; the solid curve is the distribution function calculated on the assumption that the deviations are due only to statistical fluctuations.

c) Determination of the negative-pion momentum. In the investigated range where the cross section depends rather strongly on the energy, the determination of the cross section with the above-mentioned precision makes sense only if the negative-pion momentum is measured with a precision of about 1%. Such a precision in the momentum determination is also essential for the possible observation of a ρ^0 meson, since the expected width of the anomalous region is small, and consequently cross-section measurements for pion energies differing by less than 5 Mev are required. For this purpose, the field of the deflecting magnet was stabilized during measurements at a given energy with a precision of 0.1% (by utilizing the Hall effect in a germanium disc), and at times even more precisely (by making use of the nuclear-resonance effect). The value of the field was determined from the current appearing in the germanium crystal owing to the Hall effect. The Hall current was measured with an instrument of the 0.5 class graduated with a precision of 0.5% directly in values of the negative-pion momentum by the method of the current-carrying filament. The required pion energy was obtained as follows. First the necessary field of the deflecting magnet was established, and then the beryllium target was positioned within the synchrocyclotron by remote control for maximum intensity of the pion beam.

Owing to the certain lack of precision entailed in the setting up of the meson target, the final precision of the mean value of the negative-pion momentum amounted to ~ 1%.

The energy spread of the beam depended on the collimator width in the yoke of the synchrocyclotron magnet, and according to graphically obtained estimates amounted to ±0.5 Mev/cm, i.e., ±1.5 Mev for a collimator 3 cm wide. The energy loss in the hydrogen was ~3 Mev.

THE ENERGY VARIATION OF THE CROSS SECTIONS IN THE REGION OF MESON-PRODUCTION THRESHOLDS (150 — 180 Mev)

At an incident negative-pion energy of 150 Mev, three meson-production reactions by mesons are possible:

1. $\pi^- + p \rightarrow \pi^- + \pi^+ + n$ threshold 172 Mev,
2. $\pi^- + p \rightarrow \pi^- + \pi^0 + p$ threshold 165 Mev,
3. $\pi^- + p \rightarrow \pi^0 + \pi^0 + n$ threshold 160 Mev.

In principle, anomalies due to π-π interaction can be expected in the threshold regions. In so narrow an energy interval (~10 Mev), attention was chiefly paid only to the relative cross-section variation.

The energy of the primary beam of negative pions was held constant, and mesons of required energy were obtained by lowering the primary-meson energy in a graphite absorber. The relative cross-section variation was measured in steps of ~2 Mev. Figure 3 shows the results of two measurement series obtained on different days. It is seen that, within the precision of the experiment (~1.5%), no anomalies in the dependence of the cross sections on the energy were observed. It should be noted that the values of the "hydrogen difference" given are not proportional to the cross sections, since this method of energy "reduction" by means of a graphite absorber requires the introduction of strongly energy-dependent corrections.

It must be emphasized that the interaction in reactions 1, 2, and 3 can only lead to anomalies when two negative pions form a bound system.

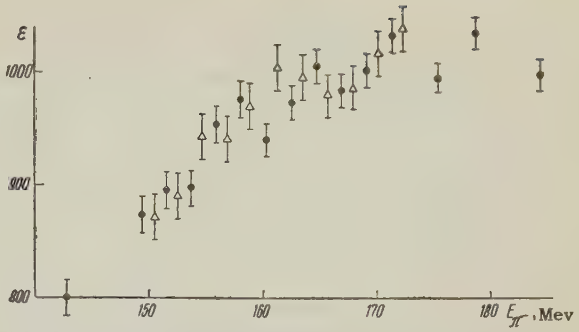

FIG. 3. The energy dependence of the effect of the hydrogen (ε) in relative units in the region of the thresholds of meson production (the results of two series of measurements made on different days).

Phenomenologically such a system is in itself a new particle. Therefore it is clear that the investigations must be conducted in a wider energy region, since the neutral boson, differing from the π^0 meson, can in principle have an arbitrary mass.

THE ENERGY VARIATION OF CROSS SECTIONS IN THE 160 — 360 Mev REGION

In this section we give not only experimental relative cross-section variations, but also the absolute values of the cross sections. The final results of the absolute measurements of the total cross sections are listed in Table I. It is not essential that we list the corrections made for all the energies. We merely state their nature:

1. A correction for the μ-meson admixture in the negative-pion beam, determined as usual from the negative-pion absorption curve in copper.

2. Account of the number of scattered negative pions and recoil protons incident on counter 3, on the basis of the known angular distributions.

3. The contribution of the Coulomb- and nuclear-scattering interference of negative pions, calculated from the formulas of Solmitz[4] and from the known phase shifts of π^--p scattering.

TABLE I. Total π^--p-interaction cross sections for different energies*

E_{π^-}, Mev	σ_t^-, 10^{-27} cm^2	E_{π^-}, Mev	σ_t^-, 10^{-27} cm^2	E_{π^-}, Mev	σ_t^-, 10^{-27} cm^2	E_{π^-}, Mev	σ_t^-, 10^{-27} cm^2
158.2	56.4±2.0	220.2	52.2±1.0	254.7	39.8±0.8	302.5	28.9±0.8
171.7	67.2±1.1	225.0	50.2±0.9	258.0	38.8±0.8	307.7	28.1±0.8
178.4	67.2±1.1	228.3	48.2±0.9	261.4	36.8±0.8	313.0	28.7±0.7
185.2	67.7±1.0	231.6	49.0±0.9	266.5	35.6±0.8	318.2	27.0±0.6
189.9	67.8±0.8	234.9	44.5±0.9	271.6	33.4±0.8	323.5	26.2±0.6
196.2	64.0±1.1	238.2	44.9±0.9	276.7	31.1±0.8	328.2	26.4±0.6
201.0	63.8±1.0	241.5	42.7±0.9	281.8	32.4±0.8	334.2	26.0±0.6
205.8	59.3±1.0	244.8	43.1±0.9	286.9	31.6±0.8	345.0	24.9±1.0
210.6	58.7±1.1	248.1	41.0±0.9	292.0	30.5±0.8	361.0	25.2±1.0
215.4	55.6±1.0	251.4	39.3±0.9	297.2	29.3±0.8		

*The indicated errors do not include those connected with the imprecise determination of the mean number of hydrogen nuclei in the path of the beam (±0.5%), and with the admixture of muons in the beam (±1.5%). These errors are statistical.

4. Account of the multiple Coulomb scattering of the pions in the hydrogen (its contribution is considerable when the beam diverges, which it always does, if only on account of the scattering in counter 2).

5. Control measurements of the difference between the target and the dummy, due to the fact that the experiments with the hydrogen and without it were conducted with different containers.

In Table II we have listed only the corrections corresponding to two energy values, in order to give some idea of their magnitude.

DISCUSSION OF RESULTS

a) Search for the ρ^0 meson. Here the ρ^0 is defined as a pseudoscalar meson with zero charge and isotopic spin. In the experiment whose results were cited in the preceding section we proposed to search for a relatively narrow anomaly in the energy dependence of the total cross section σ_t^-, inasmuch as such an anomaly can in principle indicate the existence of a ρ^0 meson. The idea[2] consists of the fact that in one or both of the $\pi^-+p \to \pi^0+n$ and $\pi^-+p \to \pi^-+p$ reactions an anomaly can appear near the threshold of the hypothetical $\pi^-+p \to \rho^0+n$ reaction. The width of this anomaly can be obtained from the condition $kR \ll 1$, where k is the momentum of the emitted ρ^0 meson in the c.m.s., and R is the interaction radius. If it is assumed that $R \sim \hbar/m_\pi c$, then the maximum peak width in the energy dependence turns out to be about 40 Mev in the laboratory system $m_{\rho^0} \sim 400$ Mev/c^2. Actually the width can be considerably smaller than this, and therefore a good energy resolution was employed in the experiments. The amplitude of the anomaly $\sigma(\pi^-p \to \rho^0 n)_{k=1/R}/\sigma_t(\pi^-p)$ can, in principle, approach several percent.

The obtained data indicate that in the 140- to 360-Mev energy region there exist no cross-section anomalies with an amplitude of, say, 3 — 4%. This means that we have not found a ρ^0 meson with a mass in the interval of 270 — 410 Mev/c^2. Of course this does not mean that such a meson does not exist. At the Kiev Conference on the Physics of High-Energy Particles in 1959 investigations[5] were reported in which different methods of searching for the ρ^0 meson also did not offer indications of its existence.

b) The total cross section in the state with $T = \frac{1}{2}$. Klepikov, Meshcheryakov, and Sokolov[6] analyzed in 1959 the body of information on the total cross sections of the π-N interaction on the basis of all the published data, and also on the basis of the data of this work. The "total" cross sections in states with an isotopic spin of $T = \frac{3}{2}$ $[\sigma(\frac{3}{2})]$ and $T = \frac{1}{2}$ $[\sigma(\frac{1}{2})]$ were approximated by resonance formulas of the Breit-Wigner type; the method of maximum likelihood was used. Thus all the curve parameters and the corresponding error ranges were found. It should be noted that in the energy region of 250 — 1500 Mev it was impossible to describe the energy dependence of $\sigma(\frac{1}{2})$ in terms of Breit-Wigner curves, if simultaneous use was made of the data of this work and of the data of reference 7, where two maxima in the energy dependence of the cross section σ_t^- had been observed at $E_2 \sim 650$ Mev and $E_3 \sim 950$ Mev. Apparently this difficulty was connected with an error in the determination of the pion energy in the experiments of the American authors and confirms the conclusion of the French group[8] that the maxima are at $E_2 \approx 610$ Mev and $E_3 \approx 880$ Mev.

c) Pion-nucleon scattering and the dispersion relations. At the Conference on the Physics of High-Energy particles in 1958 the position concerning the application of the dispersion relations to the π^+-p and π^--p processes was summed up as follows:

1. The body of information on the π^+-p and π^--p scattering processes is fully compatible with the dispersion relations and makes it possible to determine the coupling constant of meson-nucleon interaction f^2, which turns out to be 0.08, within a precision of 10%.

2. Data relating only to π^+-p scattering allow a sufficiently precise determination of f^2.

3. The information relating only to π^--p scattering was less satisfactory in the sense that it turned out difficult to reconcile with the value of f^2 obtained from π^+-p-scattering experiments (the so-called Puppi-Stanghelli problem).

One can say that it had always been natural to

TABLE II. Corrections introduced in the determination of the total cross sections (in percent)

Energy of π^- mesons, Mev	Admixture of μ^- mesons	Forward-scattered π^- mesons and protons	Interference of the Coulomb and nuclear scattering	Coulomb multiple scattering in the hydrogen	Difference between the dummy and the target
201.0 ± 2	6.5 ± 1.5	3.1 ± 0.4	-0.3	-1.2 ± 0.3	-0.3 ± 1.0
297.2 ± 3	3.5 ± 1.5	3.5 ± 0.4	$+0.3$	-0.8 ± 0.2	-0.2 ± 1.3

regard with caution the possibility of the "revolutionary" inference of Puppi and Stanghellini (which has been particularly emphasized by a number of other authors) not only in view of its far-reaching theoretical consequences, but particularly in view of certain logical contradictions inherent in it. These contradictions consisted of the following: experimentally nothing was known about the interaction of states with $T = 1/2$, and it is therefore incomprehensible how in the absence of such information a real contradiction of the dispersion relations could arise.

In 1959 there appeared some theoretical work which indicated the lack of serious difficulties in the application of the dispersion relations to π-N scattering.[10] The most convincing results were cited in reference 6, where the data of the present work together with other published data had been used. On the basis of the total cross-section curves, obtained as indicated in the preceding section, the authors of reference 6 calculated the real part of the π^--p forward-scattering amplitude and obtained the corresponding range of errors. Figure 4 shows the calculated curve of the real part of the forward-scattering amplitude, obtained from the "dispersion integral," and its particular values obtained for certain energies from the angular distribution of the π^--p scattering and from the total cross sections. It must be emphasized that in plotting the points given in Fig. 4, values of the total cross sections obtained from "calculated curves" (reference 6) were employed. The use of a calculated $\sigma_t^-(E)$ curve leads to a smaller error than the use of a separate total cross-section measurement, since the width of the error region of $\sigma_t^-(E)$ is small.

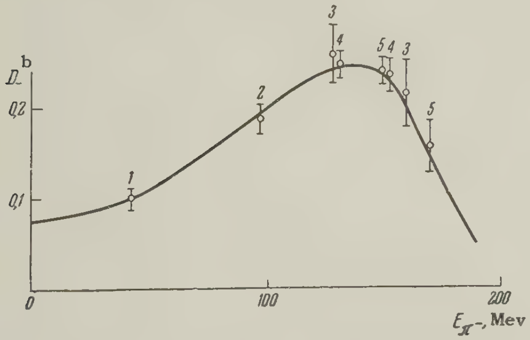

FIG. 4. The real part of the π^--p forward-scattering amplitude D_-^b in $\hbar/m_\pi c$ units. The solid curve was calculated by Klepikov et al.[6] on the basis of all the total cross-section measurements: 1 – Barnes et al. (Rochester),[11] 2 – Edwards et al. (Liverpool),[12] 3 – Budagov et al. (Dubna),[13] 4 – Kruse and Arnold (Chicago),[14] 5 – Ashkin et al. (Carnegie).[15] All points in the figure are plotted with account of the latest data on total cross sections.

As can be seen, it is difficult to expect better agreement of the calculated D_-^b curve and the values obtained from angular distributions and total cross sections. Inasmuch as the Puppi-Stanghellini problem has been widely discussed, albeit, in our opinion, not quite thoroughly, it is appropriate to pose the question why it arose. It is at present perfectly clear that the Puppi-Stanghellini "discrepancy" was simply due to an inexact knowledge of the total π^--p cross sections which entered both in the "dispersion integral," and also in the "experimental" values of the real part of the forward-scattering amplitude. More precise measurements of σ_t^- and better methods of processing the experimental data for the calculation of the dispersion integral remove this discrepancy. This is obvious if only from the fact that the π^--p interaction data of Ashkin et al.[15] for energies of 150 and 170 Mev, which were in 1956 the main source of the discrepancy, fit the present D_-^b curves excellently (cf. Fig. 4) if use is made of the latest data on total cross sections.

The authors are indebted to S. N. Sokolov, A. I. Mukhin, V. A. Meshcheryakov, and N. P. Klepikov for very useful and numerous discussions, and also to Yu. N. Denisov for considerable help in stabilizing and measuring the magnetic field.

---

[1] Zinov, Konin, Korenchenko, and Pontecorvo, JETP **36**, 1948 (1959), Soviet Phys. JETP **9**, 1386 (1959); V. I. Gol'danskiĭ and Ya. A. Smorodinskiĭ, JETP **36**, 1950 (1959), Soviet Phys. JETP **9**, 1387 (1959).

[2] G. Puppi and A. Stanghellini, Nuovo cimento **5**, 1305 (1957).

[3] V. G. Zinov and S. M. Korenchenko, JETP **34**, 301 (1958), Soviet Phys. JETP **7**, 210 (1958).

[4] F. T. Solmitz, Phys. Rev. **94**, 1799 (1954).

[5] Bernardini, Querzoli, Salvini, Silverman, and Stoppini, Conference on the Physics of High-Energy Particles (Report by G. Bernardini), Kiev, 1959.

[6] Klepikov, Sokolov, and Meshcheryakov, Conference on the Physics of High-Energy Particles (Report by B. Pontecorvo), Kiev, 1959.

[7] H. C. Burrowes et al., Phys. Rev. Lett. **2**, 119 (1959).

[8] Brisson, Detoef, Falk-Vairant, Van Rossum, Valladas, and Yuan, Phys. Rev. Lett. (preprint).

[9] G. Puppi, Annual International Conference on High-Energy Physics, Geneva, 1958.

[10] cf., for example, H. J. Schnitzer and G. Salzman, Phys. Rev. **113**, 1153 (1959).

[11] Barnes, Rose, Giacomelli, Ring, and Miyake, Phys. Rev. (preprint).

[12] Edwards, Frank, and Holt, Proc. Phys. Soc. **73**, 856 (1959).

[13] Budagov, Viktor, Dzhelepov, Ermolov, and Moskalev, JETP **38**, 1047 (1960), Soviet Phys. JETP **11**, 755 (1960).

[14] U. E. Kruse and R. C. Arnold, Phys. Rev. **116**, 1008 (1959).

[15] Ashkin, Blaser, Feiner, and Stern, Phys. Rev. **101**, 1149 (1956).

Translated by Z. Barnea
331

SOVIET PHYSICS JETP VOLUME 11, NUMBER 6 DECEMBER, 1960

NONRADIATIVE TRANSITIONS IN HEAVY μ-MESIC ATOMS

M. YA. BALATZ, L. N. KONDRAT'EV, L. G. LANDSBERG, P. I. LEBEDEV, YU. V. OBUKHOV, and B. PONTECORVO

Submitted to JETP editor January 19, 1960

J. Exptl. Theoret. Phys. (U.S.S.R.) 38, 1715-1719 (June, 1960)

The spectra of mesic x-ray photons emitted by μ-mesic atoms of uranium and lead are studied with the aid of a scintillation spectrometer. It is shown that the 2P → 1S radiative transition rate per stopped muon is appreciably smaller in mesic uranium than in lead. Thus it is experimentally demonstrated that there exists a hitherto unobserved nonradiative transition mechanism in which the transition energy is transferred directly to the nucleus.

1. INTRODUCTION

TWO mechanisms for the fission of heavy nuclei by μ^- mesons were predicted by Wheeler[1]: "internal" fission, in which the energy necessary for fission is released when the nucleus captures a muon from a lower level of a mesic atom, and "external" fission, in which the muon does not disappear and the energy necessary for fission is released in a nonradiative mesic-atom transition to the 1S level.

Zaretskiĭ[2] calculated the nonradiative transition probability in mesic atoms of heavy nuclei, or more precisely the probability that the energy of the 2P → 1S transition is not released in the form of x rays, but is transferred directly to the nucleus.

In the work of Belovitskiĭ et al.[3] carried out with the aid of photographic film the conclusion was reached that the μ^--meson stoppages in U^{238} lead only to "internal" fission with a probability of 0.07 (nonradiative fission was not observed by these authors and has a probability of less than 1%). In the work of Diaz et al.[4]* carried out by means of electronic particle-counting methods, the conclusion is also reached that nonradiative fission, if it takes place, only amounts to a small fraction of the number of fission events.

Except for these experiments, which gave negative results the 1P → 1S nonradiative transition mechanism for mesic atoms proposed by Zaretskiĭ was not studied experimentally. Thus, until recently, only two 2P → 1S transition mechanisms were known in a mesic atom: (1) the emission of a mesic x-ray quantum, and (2) the Auger effect, which does not play a substantial part in heavy nuclei.

This paper is devoted to the study of nonradiative transitions.* The study of this phenomenon is not only of independent interest but could also provide valuable information on the properties of heavy nuclei.

2. EXPERIMENTAL SETUP

As was shown by Zaretskiĭ,[2] the probability of nonradiative transitions in the μ-mesic atom of uranium, in which the nuclear-level density is large, should be considerable. In the μ-mesic atom of lead, in which the nuclear-level density is small, this probability is practically zero. The fraction of nonradiative 2P → 1S transitions in mesic uranium was, therefore, determined by measuring the yield differences of the corresponding radiative x-ray transitions in uranium and lead. The fact that the transition energies of mesic uranium and mesic lead are similar (~6 Mev) facilitated the comparison of the photon yields, inasmuch as practically no corrections of the experimental spectra were required.

A beam of negative pions with a momentum of 270 Mev/c from the cyclotron of the Joint Institute for Nuclear Research was employed in our work. The schematic setup of the experiment is shown on Fig. 1. The muons which were stopped in the target were separated by a "telescope" consisting of three scintillation counters, connected according to a 1 + 2 − 3 scheme (coincidences of counters 1 and 2, in anticoincidence with counter 3).

The range curve obtained with a thin (4g/cm^2 Pb) target is shown in Fig. 2. The measurements of the mesic x-ray photon emission spectra were carried out with thicker targets; the uranium (100 × 100 mm

---

*We are grateful to Dr. Moyer who acquainted us with these results during the Kiev Conference.

*Preliminary results were published at the 9th International Conference on the Physics of High-Energy Particles in Kiev, 1959 (cf. paper by A. I. Alikhanov).

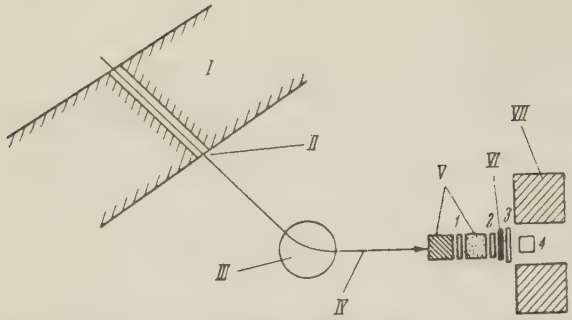

FIG. 1. Experimental setup (schematic): I – concrete shield, II – collimator (100 mm diameter), III – deflecting magnet, IV – negative-pion beam, V – absorber (75 g/cm² Cu + 32 g/cm² B_4C), VI – target, VII – shielding of counter 4 (20 cm Pb); 1, 2 – plastic scintillators, 100 mm diameter and 10 mm thickness; 3 – the same, 125 mm diameter and 12 mm thickness; 4 – NaI(Tl) crystal, 30 mm diameter and 10 mm thickness.

× 10.7 g/cm²) and lead (100 × 100 mm × 10.3 g/cm²) targets were equivalent with regard to the ionization losses.

A scintillation counter 4, consisting of an NaI(Tl) crystal of 30 mm diameter and 35 mm high, and of a FÉU-33 photomultiplier, was used to detect the gamma rays. The gamma-counter pulse was fed to a 64-channel pulse-height analyzer which was monitored by the signal of the coincidence scheme (1 + 2 − 3) + (2 + 4). The background of accidental coincidences amounted to about 1/20 of the total count.

A Na^{24} source with γ-ray energies of 1.38 and 2.76 Mev was employed for energy calibration and to check the linearity of the whole system.

During the measurements the uranium and lead targets were periodically exchanged. All the obtained spectra had the same shape and were shifted relative to each other.

3. MEASUREMENT RESULTS AND THEIR DISCUSSION

Figure 3 shows the photon spectra for mesic uranium and lead in the 3- to 8-Mev energy region. The spectra are normalized for equal numbers of μ^- mesons stopped in the target. In the lead spectrum we see clearly the peak with an energy of ~5.3 Mev. In view of the small dimensions of the NaI(Tl) crystal this peak is due to three values of energy lost by the photons in the crystal: (1) E_γ, (2) $E_\gamma - 0.51$ Mev, and (3) $E_\gamma - 1.02$ Mev, where $E_\gamma = 6.02$ Mev (reference 5) is the photon energy of the 2P → 1S transition in mesic lead. Uranium gives fewer counts in the 5- to 5.5-Mev energy region, and practically the same number as lead in regions sufficiently far from 5.5 Mev. The mean energy of the peak, corresponding to the 2P → 1S transition is larger in uranium than in lead by about 200 kev.

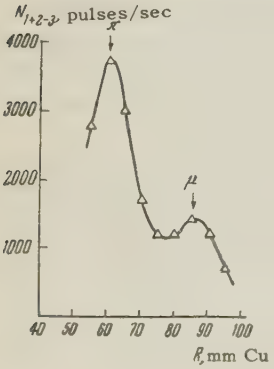

FIG. 2. Range curve (R is the absorber thickness, N – the number of coincidences in arbitrary units).

The difference in the intensity of the photons with an energy of ~6 Mev in mesic uranium and mesic lead for identical geometries and close emission energies indicates that here the effect of the nonradiative μ^-meson transition to the 1S level of mesic uranium has indeed been observed. A quantitative estimate of the probability of this process seems to us to be difficult. In order to determine the ratio of intensities of the radiative 2P → 1S transitions in mesic uranium and mesic lead, it is necessary to know the number of counts in each analyzer channel which are really due to photons from the 2P → 1S transition. In other words, it is necessary to know the contribution of "background" counts, that is of counts which are not connected with the 2P → 1S transition. The "background" counts are due to other transitions in the mesic atom, and also to the presence of electrons in the primary beam.

The determination of the background is a rather complex problem, and new studies will be devoted to its solution. At present, we can only indicate rather rough limits for this background. We know, from measurements with a Cerenkov gas counter, that the "background" counts in the photon energy region $E_\gamma > 4$ Mev are both for uranium and for lead mainly due to the electron background. This background depends weakly on the target material and on the channel number of the analyzer. Clearly, the counting rates in uranium and lead at ~8 Mev are the lower limits of the background levels in uranium and lead in the energy region ~5 Mev of interest to us (Fig. 3). The upper limit of the background will obviously be the curve obtained by smooth interpolation of the uranium and lead spectra for energy ranges with $E_\gamma < 5$ Mev and $E_\gamma > 5$ Mev (Fig. 3).

Assuming that the probability for nonradiative transition in lead W_n is negligibly small by comparison with the probability of photon emission

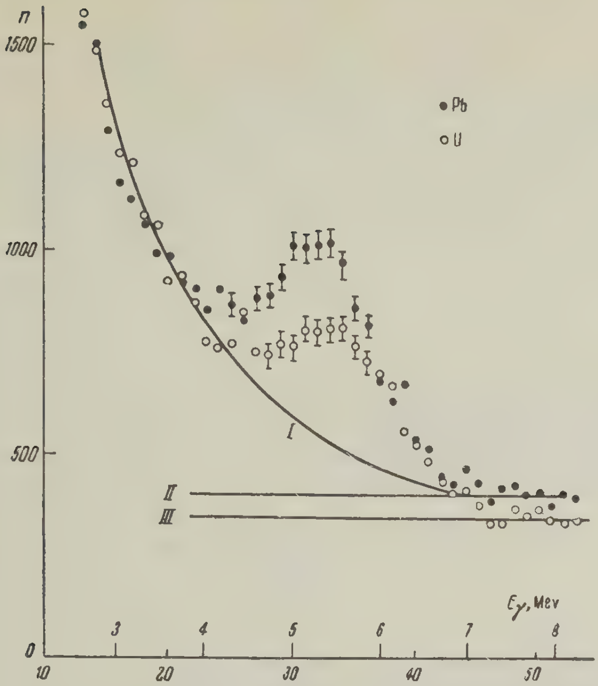

FIG. 3. Photon spectra from mesic lead and mesic uranium: I – the upper limit of the background, II – the lower limit of the background in lead, III – the lower limit of the background in uranium (n is the number of counts per analyzer channel).

W_γ, and taking into consideration the above-mentioned background limits, we obtain

$$0.1 < (W_n / W_\gamma)_{U^{238}} < 1. \qquad (1)$$

Another, also rough, estimate of the background can be obtained from the condition that the width of the uranium and lead peaks must be equal. From this estimate we obtain $(W_n/W_\gamma)_{U^{238}} \sim 0.2$, that is a value close to the lower limit of inequality (1).

On the above grounds it is possible to conclude that the probabilities of radiative and nonradiative transitions in U^{238} are comparable,* while radiative transitions apparently predominate.

Preliminary experiments indicate that nonradiative transitions take place in Th^{232}.

A value of ~5 to 20 was predicted in Zaretskiĭ's work for the ratio $(W_n/W_{h\nu})_{U^{238}}$. This result contradicts inequality (1). However, in Zaretskiĭ's estimate it was assumed that in the uranium nucleus $\rho\Gamma_{nuc} \gg 1$, where ρ is the mean density of uranium levels excited by $2P \to 1S$ transitions and Γ_{nuc} is their mean nuclear width. In this case it is possible to neglect processes in which the excited nucleus with the muon in the 1S state returns to the ground state with the muon in the 2P state. As was noted by Zaretskiĭ during the discussion of our results, the hypothesis that $\rho\Gamma_{nuc} \gg 1$ is actually unfounded. If $\rho\Gamma_{nuc} \ll 1$, then the oscillation processes of the muon between the 2P and 1S state with the simultaneous oscillation of the nucleus between the excited and ground level cannot be neglected, and therefore the ratio W_n/W_γ decreases considerably.[6]

At present, more precise measurements of the W_n/W_γ ratio for various mesic atoms are being carried out.

The authors sincerely thank A. I. Alikhanov for his continuous interest in their work, and D. F. Zaretskiĭ who acquainted them with his work before its publication.

---

*Our preliminary communication at the Kiev Conference (in 1959) that the radiative and nonradiative $2P \to 1S$ transition probabilities in U^{238} are "approximately equal" was not sufficiently grounded.

[1] J. A. Wheeler, Revs. Modern Phys. **21**, 133 (1949).

[2] D. F. Zaretskiĭ, Papers by Soviet Scientists at the Second International Conference on the Peaceful Uses of Atomic Energy, Acad. of Sci. Press, 1958.

[3] Belovitskiĭ, Kashukeev, Mikhul, Petrascu, Romanova, and Tikhomirov, The Fission Mechanism of Uranium Nuclei under the Action of Slow μ^-mesons, Joint Institute for Nuclear Research, Preprint, 1959.

[4] Diaz, Kaplan, MacDonald, and Pyle, Phys. Rev. Lett. **3**, 234 (1959).

[5] V. L. Fitch and J. Rainwater, Phys. Rev. **92**, 789 (1953).

[6] D. F. Zaretsky and V. M. Novikov, Nucl. Phys. (in press).

Translated by Z. Barnea
332

SOVIET PHYSICS JETP VOLUME 11, NUMBER 6 DECEMBER, 1960

ANISOTROPY OF THE ELECTRICAL RESISTANCE OF Mg *AND* Pt *SINGLE CRYSTALS IN A MAGNETIC FIELD AT 4.2°K*

N. E. ALEKSEEVSKIĬ and YU. P. GAĬDUKOV

Institute for Physical Problems, Academy of Sciences, U.S.S.R.

Submitted to JETP editor January 29, 1960

J. Exptl. Theoret. Phys. (U.S.S.R.) **38**, 1720-1722 (June, 1960)

The anisotropy of the electrical resistance of Mg and Pt single crystals located in a magnetic field is investigated. The dependences found are characteristic of metals with open Fermi surfaces.

It has been reported previously[1,2] that the galvanomagnetic properties of single crystals of a number of metals are extremely anisotropic. As is well known,[3,4] strong anisotropy of the galvanomagnetic properties should be observed in metals with open Fermi surfaces.

In connection with the fact that the electric resistance of polycrystalline specimens of Mg and Pt located in a magnetic field increases without limit,[5,6] it could be assumed that the Fermi surfaces of these metals were either closed with $n_1 = n_2$ (n_1 and n_2 are the number of electrons and holes, respectively) or open. The resistance in large magnetic fields should be practically isotropic in the first case, and strongly anisotropic in the second.

Inasmuch as the galvanomagnetic properties of Mg and Pt were investigated only in polycrystalline specimens, there was interest in carrying out measurements on single crystals of these metals also. For this purpose we grew single crystals of Mg and Pt with different orientations. The ratio of resistance at room temperature and temperature of 4.2°K ranged from 230 to 610 for the Mg samples and from 1900 to 2400 for Pt.

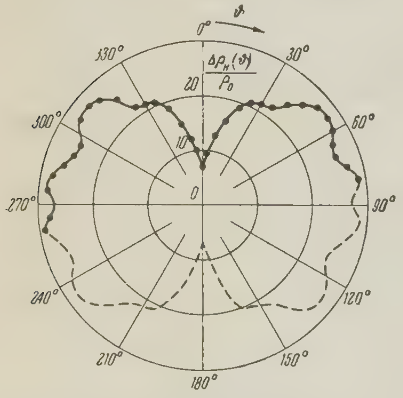

FIG. 1. Polar plot of the resistance of an Mg sample; $\rho_{300^\circ K}/\rho_{4.2^\circ K} = 230$, H = 23500 oe.

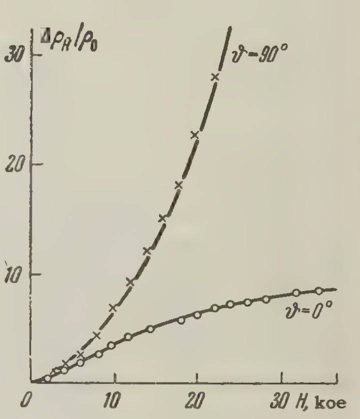

FIG. 2. Dependence of the resistance on the magnetic field for an Mg specimen (see Fig. 1).

A polar plot is shown in Fig. 1 of the change of the transverse resistance in a magnetic field $\Delta\rho_H(\vartheta)/\rho_0 = \rho_H(\vartheta)/\rho_{H=0} - 1$ for a single crystal of Mg, the axis of which formed an angle of 65° with the [0001] axis. For this specimen, as for the other specimens, the minimum resistance in the diagram is observed for a magnetic field direction coinciding with the direction of the projection of the [0001] axis on the plane of rotation of the magnetic field.

For investigation of the dependence of the resistance on the magnetic field in the direction of the maxima of the polar diagrams, an unlimited increase was observed, according to a law that was nearly quadratic. (Fig. 2).

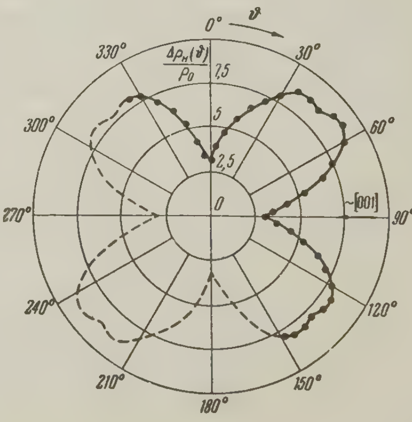

FIG. 3. Polar plot of the resistance of of a Pt specimen; $\rho_{300^\circ K}/\rho_{4.2^\circ K} = 1900$. H = 23500 oe.

For specimens whose axis was parallel to the [0001] direction, the anisotropy of the resistance is practically nonexistent; in this case, the resistance increases without limit for an arbitrary direction of the magnetic direction of the magnetic field according to a square law. It is known that the other metals of hexagonal structure (Zn and Cd) behave in similar fashion.[7]

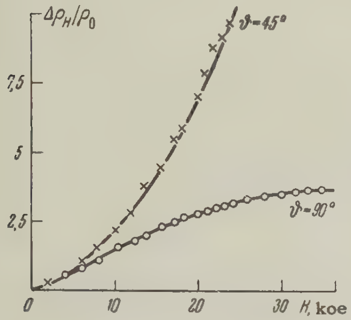

FIG. 4. Dependence of the resistance on the magnetic field for a Pt specimen (see Fig. 3).

Investigation of single crystals of Pt has shown that the latter also posesses a strong anisotropy of electrical resistance in a magnetic field. The results of measurements for one of the Pt samples are shown in Figs. 3 and 4. The axis of the sample departs from the [001] axis by about 10°. It is seen from the drawings that the behavior of the resistance of Pt in a magnetic field is similar to the behavior of the other metals previously studied with a strong anisotropy in the resistance.[1,2] Measurements carried out on some specimens showed that the minimum in the polar diagrams in the direction of a fourth order axis is observed for any orientation of the current relative to the axes of the crystal.

Saturation and unlimited growth of resistance, observed for different crystalline directions, give grounds for assuming that magnesium and platinum have Fermi surfaces of the open type.

If we attempt to represent the form of the Fermi surface, then, just as we noted for Tl,[1] such a surface could be a "corrugated plane." However, for such a type of Fermi surface, for a specimen of Mg with axis parallel to the direction [0001], one should have expected saturation of the resistance in the magnetic field, and not a quadratic increase observed experimentally. The results we obtained for platinum are very similar to the results for the non-transition metals (for example, for Pb[1]). Borovik and Volotskaya, carrying out measurements on polycrystalline platinum,[6] came to very similar conclusions.

At best, the experimental results for platinum describe a Fermi surface of the "spatial grid of cylinders" type, with cylinder directed along the fourfold axes order of the platinum reciprocal lattice.

In conclusion, we consider it our pleasant duty to thank Academician P. L. Kapitza for his great attention to the present work. We also thank G. É. Karstens for help in the determination of the orientation of the specimens.

---

[1] N. E. Alekseevskiĭ and Yu. P. Gaĭdukov, JETP 36, 447 (1959), Soviet Phys. JETP 9, 311 (1959).

[2] N. E. Alekseevskiĭ and Yu. P. Gaĭdukov, JETP 37, 672 (1959), Soviet Phys. JETP 10, 481 (1960).

[3] Lifshitz, Azbel', and Kaganov, JETP 31, 63 (1956), Soviet Phys. JETP 4, 41 (1957).

[4] I. M. Lifshitz and V. G. Peschanskiĭ, JETP 35, 1251 (1958), Soviet Phys. JETP 8, 875 (1959).

[5] E. S. Borovik, Doctoral dissertation, Physico-Technical Institute, Academy of Sciences, Ukrainian SSR, Kharkov, 1954.

[6] E. S. Borovik and V. G. Volotskaya, Физика металлов и металловедение (Phys. Met. and Metallurgy) 6, 60 (1958).

[7] Lazarev, Nakhimovich, and Parfenova, JETP 9, 1169 (1939).

Translated by R. T. Beyer
333

SOVIET PHYSICS JETP VOLUME 11, NUMBER 6 DECEMBER, 1960

RANGE AND ENERGY DISPERSION OF U^{233} *FISSION FRAGMENTS*

K. A. PETRZHAK, YU. G. PETROV, and É. A. SHLYAMIN

Radium Institute, Academy of Sciences, U.S.S.R.

Submitted to JETP editor January 28, 1960

J. Exptl. Theoret. Phys. (U.S.S.R.) 38, 1723-1728 (June, 1960)

The range distribution of U^{233} fission fragments (Sr^{91-92}, Y^{92-93}, Zr^{97}, Ba^{140}, and Ce^{143}) in various gases is studied. The dependence of the range dispersion on the nature of the gas is established. From the range dispersion the kinetic energy due exclusively to fission processes is determined. The results are compared with available experimental data and Fong's statistical theory.

INTRODUCTION

FROM the data on the distributions of the fragment energies and velocities, obtained with the aid of ionization chambers and by the time-of-flight method, it is only possible to determine the dispersion of the total kinetic energy for a given mass ratio of the fragments indirectly.

A direct determination of the kinetic energy dispersion of fragments of given mass and charge in the fission of U^{233} and U^{235} was carried out by Good and Wollan.[1] From the range distribution of fragments which emitted delayed neutrons the authors obtained the value $\Delta E/E = 5\%$ for I^{137} and 8% for Br^{87}. In reference 2 the energy distribution of Zr^{97} in the fission of U^{235} by thermal neutrons was obtained with the aid of a magnetic spectrometer. The half-width of the distribution was 11.4%.

In connection with the fact that no exhaustive data on the kinetic-energy dispersion of U^{233} fission fragments is available, it is of interest to determine its value for a series of fragments of different masses.

It is known that the measurement of the dispersion of fission-fragment ranges makes it possible to determine the kinetic-energy dispersion of the fragments with given M and Z. To determine the kinetic-energy dispersion of U^{233} fission fragments, we therefore used in this paper fission-fragment ranges in various gases obtained by collecting the fragments on thin films and subsequently analyzing these radiochemically.

EXPERIMENTAL METHOD

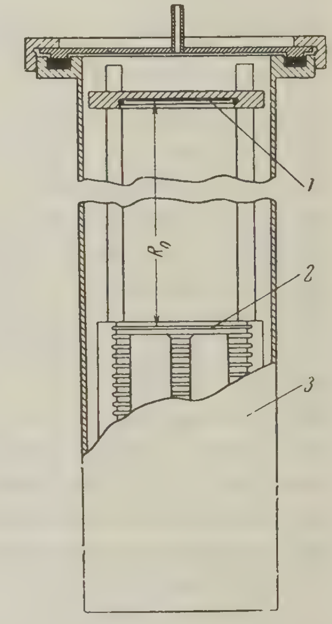

FIG. 1. Section of the container in which the irradiation was carried out. 1 — U^{233} target, 2 — holder for rings with films, 3 — aluminum airtight container, R_0 — the distance between the target and the first film.

The apparatus (Fig. 1) consisted of an airtight aluminum container, in which a holder for rings with collodion films and a uranium target were placed. The films were inserted behind each other within a space of 2.5 mm: the distance R_0 between the first film and the target was 136 mm. In all there were thirty films, each ~ 6 $\mu g/cm^2$ thick. The container was filled with various gases: hydrogen, helium, nitrogen, air, neon, and argon. The gas pressure was chosen such that the range of the heaviest fragment group should retain the same value in all the gases and that it should be within the first ten films. U^{233} targets of 76, 110, 145, 228, 284 $\mu g/cm^2$ with a spot diameter of 22 mm, obtained by plating platinum in an alcohol solution of uranyl nitrate, were employed in the experiments. The container was irradiated in the reactor of the U.S.S.R. Academy of Sciences during 1 — 2 hours at a constant temperature with a neutron flux of 10^{12} neutrons/cm^2-sec. The activity of each film was then measured with a torsion β counter. In order to get rid of the activity

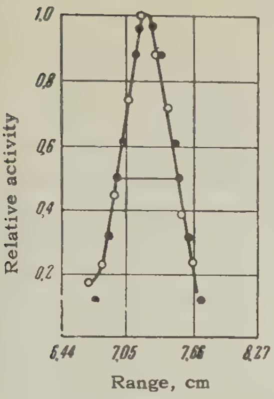

FIG. 2. Range distribution of Ba^{140} nuclei in hydrogen. ○ – experimental points, ● – Gaussian distribution.

induced in the aluminum rings by the irradiation, the films were transferred into new rings. The two-hump curve of the activity distribution as the function of the film position obtained from these measurements made it possible to ascertain the reproducability of the experimental results, and to choose the necessary group of films for subsequent radiochemical analysis for this or that element. The chemical analysis was carried out by the usual methods,[3] except for such simplifications as the preliminary separation of the fragments with the aid of films[4] permits. The elements Sr, Y, Zr, Ba, and Ce were separated, and the identification of the isotopes by mass number was carried out by measuring their half-lives.

As a result of the radiochemical analysis of the films, range-distribution curves were obtained for the U^{233} fission fragments Sr^{91-92}, Y^{91-93}, Zr^{97}, Ba^{140}, and Ce^{143} in hydrogen, helium, nitrogen, air, neon, and argon. From these data we determined the mean ranges and the range dispersion.

EXPERIMENTAL RESULTS

Figure 2 shows the experimental range-distribution curve of Ba^{140} nuclei in hydrogen. The Ba^{140} activity of different films, reduced to the solid angle of the first film relative to the target, is plotted in relative units along the ordinate axis; the fragment range in centimeters for a hydrogen pressure of 760 mm Hg and t = 15°C is plotted on the abscissa. For comparison, points corresponding to a Gaussian distribution with a half-width equal to the experimental one are plotted in the figure. As is evident from the figure, good agreement between the experimental and Gaussian curve is observed. Such agreement was also obtained for different fragments in other gases.

These results differ from those of reference 5, where the differential curves are steeper on the far side from the source. The authors of reference 5 assume that the deviation of these curves from the Gaussian curves can be explained either by the nonuniform thickness of the uranium layer, or by the imperfect collimation of the fragments.

The observed range spread of fragments of a given mass can be due to a number of reasons: 1) the kinetic-energy fluctuation of the fragment, caused by the diversity of the nuclear deformation at the instant of fragment separation; 2) the change in the kinetic energy resulting from the nuclear-charge fluctuation during the formation of a fragment of given mass; 3) the statistical fluctuation of the number of collisions with electrons and nuclei during the slowing down of the fragments in the gas; 4) the change in the kinetic energy when a neutron is emitted by the fragment; 5) the slowing down in the target material; 6) the geometry of the apparatus.

To determine the effect of the target, we recorded the dependence of the magnitude of the range dispersion of Ba^{140} in helium on the source thickness. Extrapolation of the curve to zero thickness made it possible to exclude the dispersion ΔS_{source} due to the slowing down of the fragments in the uranium layer. The contribution of the source to the dispersion for fragments of different mass was determined from the relation

$$[\Delta S_{\mathbf{source}}]_M = [\Delta S_{\mathbf{source}}]_{Ba} R_{Ba}/S_M. \qquad (1)$$

The correction for the geometry, ΔS_{geom}, due to the fact that the beam is not parallel, amounted according to calculations to 1.3% for the group of light fragments, and 1.6% for the group of heavy fragments. The magnitudes of the range dispersions with account of the effect of the source thick-

TABLE I. The ranges and the range dispersion of U^{233} fission fragments

Gas	Sr^{91-92}		Y^{92-93}		Zr^{97}		Ba^{140}		Ce^{143}	
	R. cm	S, %	R, cm	S, %	R, cm	S, %	R, cm	S, %	R, cm	S, %
Hydrogen	10.05	7.37	10.05	6.66	9.61	7.92	7.58	6.13	7.68	5.12
Helium	15.75	7.09	15.68	6.84	15.61	6.99	11.93	7.03	12.02	5.86
Nitrogen	2.58	9.51	2.52	9.41	2.50	10.27	—	—	1.86	9.26
Air	2.54	8.04	2.51	7.61	2.44	8.20	1.85	9.87	1.84	8,71
Neon	4.80	9.86	4.84	8.69	4.66	9.60	—	—	—	—
Argon	2,60	10.59	2.58	9.88	2.49	9.38	1.85	11.38	1.81	10,31

ness and corrected for the geometry, i.e., the values

$$S = [(S_{\text{exp}} - \Delta S_{\text{source}})^2 - \Delta S^2_{\text{geom}}]^{1/2},$$

are listed in Table I (R is the mean fragment range in centimeters in the investigated gas for p = 760 mm Hg and t = 15°C, S is the relative range dispersion in percents).

The experimental range values listed in the table are corrected for absorption in the collodion films and in the target material.

After correcting for the source thickness and the geometry of the apparatus, the range dispersion can be represented by the sum:

$$S^2 = S^2_{\text{fiss}} + S^2_{\text{braking}}, \qquad (2)$$

where the first term is determined only by processes connected with the fission and does not depend on the subsequent interaction of the fragment with the material, while the second term is a function of the mass and charge of the stopping gas. This was indeed the basis for the division of these quantities.

The fragment-range spread of fragments passing through a substance is due to the statistical fluctuation of the number of collisions with electrons and nuclei. The relative spread due to electron collisions is 0.1%, which is negligibly small by comparison with the fraction of the spread due to nuclear collisions.

The dispersion due to nuclear collisions can be calculated from the formula:[6]

$$S^2_\nu = \text{const}\,(R_\nu/R)^2\, M_1M_2\,/\,(M_1 + M_2)^2,$$

where R_ν is the end part of the range where braking is exclusively due to nuclear collisions, R is the total fragment range, M_1 and M_2 are the nuclear masses of the fragment and of the stopping gas. The ratio R_ν/R was calculated after Bohr.[7] It turned out that it is approximately equal for heavy and light fragments and varies within 10%, depending on the nature of the gas. Owing to this, by substituting (3) in (2), the latter can be written in the form

$$S^2 = S^2_{\text{fiss}} + \text{const}\cdot M_1M_2/(M_1 + M_2)^2. \qquad (4)$$

From this it is evident that S^2 is a linear function of the parameter $M_1M_2/(M_1 + M_2)^2$.

The dependence of S^2 on $M_1M_2/(M_1 + M_2)^2$ was plotted from the experimental data for all investigated fragments. As an example, Fig. 3 shows the results for Sr^{91-92} and Ba^{140}. The intersection of the straight lines with the ordinate axis determines the value of S^2_{fiss} for each fragment.

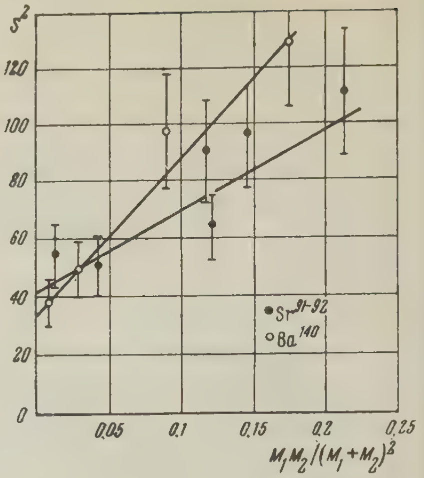

FIG. 3. The graph of the $S^2[M_1M_2/(M_1 + M_2)^2]$ function for Sr^{91-92} and Ba^{140}.

According to Bohr,[6] the fragment range varies as $\sqrt{E}$. The range dispersion is, therefore, connected with the dispersion of the kinetic energy by the relation

$$2\Delta R/R = \Delta E/E.$$

Consequently, in Fig. 3 the intercepts with the ordinate axis characterize the kinetic-energy dispersion of fragments with a given mass.

To obtain the dispersion of the kinetic energy connected with the diversity of the deformations at the instant of fragment separation, it is necessary to exclude the dispersion caused by the recoil during the emission of a prompt neutron, and the fluctuation of the kinetic energy of the fragments due to the charge distribution during the fission into fragments of a given mass.

Assuming that the neutrons are emitted by the moving fragment isotropically in the c.m.s., we obtain a value of 3% for $(\Delta E/E)_n$ for the groups of heavy and light fragments. Account of the charge distribution during the formation of fragments of a given mass add to the dispersion a contribution $(\Delta E/E)_Z$ amounting to between 1 and 2% for all fragments. The final values of $(\Delta E/E)_0$, listed in Table II, are found from the relation

$$[\Delta E/E]^2 = [\Delta E/E]^2_0 + [\Delta E/E]^2_n + [\Delta E/E]^2_Z.$$

From the equality of the fragment momenta at the instant of fission, it is possible to assume that the kinetic energy of the complementary fragment and the total kinetic energy of the two fragments will have the same relative dispersion, i.e.

$$[\Delta E/E]_l = [\Delta E/E]_h = [\Delta E/E]_t$$

for a given M_h/M_l ratio.

In Fig. 4 the dependence of $\Delta E_t(M_h/M_l)$ has been plotted from the data of Table II; the values of the total kinetic energy were taken from the work of

TABLE II. Dispersion of the kinetic energy of U^{233} fission fragments

Fragment	Sr^{91-92}	Y^{92-93}	Zr^{97}	Ba^{140}	Ce^{143}
$\Delta E/E$, %	12.9	12.4	13,2	11.6	9.4
$[\Delta E/E]_0$, %	12.3	11.8	12.8	11.2	8.7
ΔE_t, Mev	19.7	19,0	21,3	17,7	13.6
M_h/M_l	1.51	1,48	1,37	1,55	1.64

Fraser and Milton.[8] For comparison, we have given the dependence of the total kinetic-energy dispersion of the two particles on the mode of fission, obtained from the topological plots of that work. We note that these topological plots do not take into account the recoil due to prompt-neutron emission.

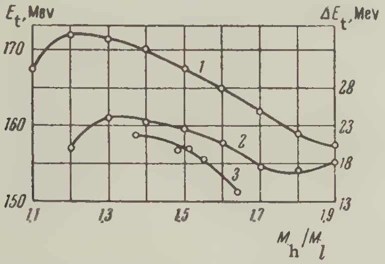

FIG. 4. The dependence of the total kinetic energy and of the dispersion of the kinetic energy on the mode of fission: 1 – total kinetic energy, 2 – dispersion of the total kinetic energy, calculated according to the contour diagrams of Fraser and Milton,[8] 3 – dispersion of the total kinetic energy according to the data of this paper.

DISCUSSION OF RESULTS

The precision of the range determination is 2%. The main part of this error is connected with the unequal thickness of the collodion films. The film thickness was determined by allowing a collodion drop of constant weight to spread over a surface of known area. Thus the equal thickness of the films depended on the uniform spreading out of the collodion and on the constancy of the weight of the drop.

The indeterminacy in fixing the end of the range, due to the sagging of the films during irradiation, was 0.5%. The fragment range was determined from a curve plotted on the average with ten points, each of which was the result of a separate radiochemical analysis. In this connection, the contribution of the radiochemical-analysis error to the precision estimates of the range determination did not exceed 0.5%. The small temperature variations during the irradiation did not affect the value of the mean range but caused an increase in the dispersion of the ranges.

The error in the determination of the range dispersion with account of all the enumerated factors amounted to 10%.

The values of the kinetic-energy dispersion obtained in the present paper are in good agreement with the data of reference 2 and with the results obtained from the contour diagrams of reference 8. As is evident from Fig. 4, the calculated dependence of the total kinetic-energy dispersion on the mode of fission has a maximum for $M_h/M_l = 1.3$, that is in the region of the twice closed shell with $Z = 50$ and $N = 82$ for the heavy fragment. The obtained results do not confirm Fong's theory,[10] according to which the dispersion of the total kinetic energy has a maximum for the most probable mode of fission, and is about 10 Mev.

In conclusion, the authors express their gratitude to E. B. Nikol'skaya for her help in carrying out the radiochamical analysis.

---

[1] W. M. Good and E. O. Wollan, Phys. Rev. **101**, 249 (1956).

[2] Cohen, Cohen, and Coley, Phys. Rev. **104**, 1046 (1956).

[3] Nat. Nucl. Energy Ser. Div. IV, Plutonium Project Record 9, Radiochemical Studies of the Fission Products, Book 3, ed. by C. D. Corryell and N. Sugarman.

[4] Petrzhak, Nikol'skaya, Petrov, and Shlyamin, Радиохимия, (Radiochemistry) **1**, 227 (1959).

[5] Katcoff, Miskel, and Stanley, Phys. Rev. **74**, 631 (1948).

[6] N. Bohr, Phys. Rev. **59**, 270 (1941).

[7] N. Bohr, Kgl. Danske Videnskab. Selskab, Mat.-fys. Medd. **18**, No. 8 (1948).

[8] J. S. Fraser and J. C. D. Milton, Phys Rev. **93**, 818 (1954).

[9] Protopopov, Baranov, Selitskiĭ, and Eĭsmont, JETP **36**, 1932 (1959), Soviet Phys. JETP **9**, 1374 (1959).

[10] P. Fong, Phys. Rev. **102**, 434 (1956).

Translated by Z. Barnea
334

THE DENSITY OF LIQUID OXYGEN ON THE SATURATION CURVE

D. L. TIMROT and V. P. BORISOGLEBSKIĬ

Moscow Power Institute

Submitted to JETP editor February 6, 1960

J. Exptl. Theoret. Phys. (U.S.S.R.) **38**, 1729-1732 (June, 1960)

The results of density measurements of liquid oxygen on the saturation curve are presented and compared with data in the literature.

THE density of liquid oxygen on the saturation curve at different temperatures has been insufficiently studied. In the existing literature[1-6] the maximum discrepancies among the values of density amount to 5% (at −210°C). The discrepancy between the results of the most reliable studies[5,6] is 1.2%.

We have studied the temperature and pressure dependence of the density of liquid oxygen along the isochores, in a constant-volume piezometer. What one obtains directly from an experiment are quasi-isochores, because of the presence of the stray volume involved in the communication system. A correction for the stray volume was applied by the "sealed capillary" method[7] and did not exceed 0.2%.

When changing from one isochore to another, some oxygen was liberated from the piezometer. The quantity of oxygen liberated was measured (in the gaseous state) in a dry gasometer. The saturation curve was determined in p − t coordinates from the kink in the quasi-isochores. (The pressure p is given below in kg/cm^2 throughout, and the temperature t in degrees C.)

The density on an isochore was calculated from the formula $\rho = G_i/V_p$, where G_i is the quantity of oxygen in the piezometer, determined by inverse summation of the amounts liberated, corrected for the stray volume of the piezometer, and V_p is the piezometer volume.

The heavy-walled piezometer and gasometer (Fig. 1) were placed in a cryostat and a thermostatic bath, respectively. The basic elements of the apparatus were made of stainless steel. The piezometer volume (in cm^3) was determined from the formula

$$V_p = V_0 [1 + 3\bar{\alpha}_t t + \beta (p - 1)], \qquad (1)$$

where $V_0 = 541.65$ cm^3 and $\beta = 7.29 \times 10^{-6}$ cm^2/kg. The mean coefficient of linear expansion $\bar{\alpha}_t$ for the material of the piezometer, which we obtained experimentally over the temperature interval t = 0° to −200°C, is given by the formula

$$10^6 \cdot 3\bar{\alpha}_t = 51{,}03 + 0.66 \left(\frac{t}{100}\right) - 3{,}18 \left(\frac{t}{100}\right)^2. \qquad (2)$$

The coefficient of isothermal compressibility β in (1) was obtained numerically from the geometric dimensions of the piezometer, using the theory of thick-walled shells.[9]

The oxygen pressure in the piezometer was measured with a piston manometer. The gasometer pressure was measured with a precision open mercury manometer with a mirror indicator. The temperature of the oxygen in the cryostat and thermostatic bath were measured with standard resistance thermometers made of spectrally pure platinum. Liquid nitrogen and Freon-12 were used in turn as thermostatic liquids in the cryostat. The temperature field within the cryostat was monitored with copper-constantan thermocouples — three in the upper portion and a movable one inside the volume.

A total of 184 experimental points were obtained, spaced uniformly on 10 quasi-isochores and the saturation curve, and 57 liberations of oxygen were made into the gasometer.

The density of the gaseous oxygen within the gasometer, at room temperature and a pressure not exceeding 3.5 kg/cm^2, was determined from Meyer's tables.[8] In this region of the parameters of state, oxygen differs little from a perfect gas

t,° C	p, kg/cm^2	ρ, g/cm^3
−194.03	0.27	1.1879
−153.50	10,20	0,9712
−151.73	11,28	0,9589
−147.03	14.66	0.9272
−141.50	19.44	0.8847
−132.04	29,44	0,7972
−129.48	33,31	0,7673
−125.21	39,72	0.7086
−121.06	46.72	0.6227
−119.70	49,14	0.5795

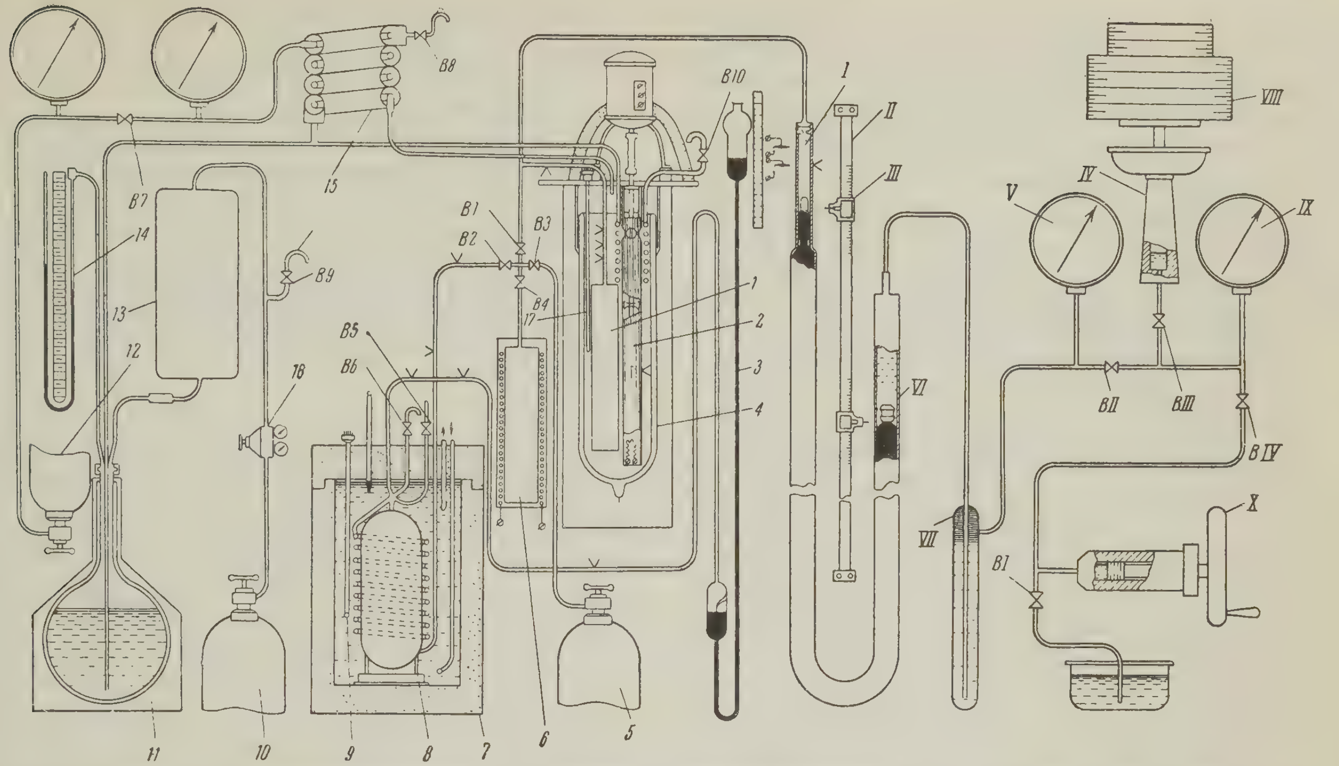

FIG. 1. Diagram of experimental arrangement. 1 – piezometer with attached capillary; 2 – stirrer with cooling element and heater; 3 – open mercury manometer with flexible tube; 4 – glass Dewar vessel; 5 – oxygen cylinder; 6 – thermomultiplier; 7 – thermostat; 8 – gasometer; 9 – standard platinum resistance thermometer; 10 – nitrogen cylinder; 11 – metal Dewar flask containing liquid nitrogen; 12 – cylinder of Freon-12; 13 – intermediate volume; 14 – open mercury manometer; 15 – nitrogen-Freon heat exchanger; 16 – reducing valve; 17 – standard platinum resistance thermometer; I – left leg of differential mercury manometer, with small magnet; II – measuring scale of differential manometer; III – measuring follower-indicator; IV – right leg of differential mercury manometer, with large magnet; V – standard Bourdon spring manometer; VI – piston manometer; VII – oil-water separator; VIII – weights for the piston manometer; IX – technical Bourdon spring manometer; X – oil screw-press; Bl – main throttle valve; B2 – safety shut-off valve for gasometer; B3 – oxygen filling valve; B4 – thermo-multiplier valve; B5 – valve from gasometer to vacuum pump; B6 – oxygen vent to atmosphere; B7 – Freon supply valve; B8 – heat exchanger valve; B9 – pressure relief valve; B10 – cooling element valve; BI – oil supply valve; BII – piezometer system valve; BIII – piston manometer valve; BIV – oil press valve; v – locations of sealed-in thermocouples.

and has been quite well studied experimentally. The error in the determination of its density is therefore negligibly small.

Of the experimental values of oxygen density which we obtained, the ones which refer to the saturation line are given in the table. An analysis of the inaccuracies of the experiment showed that the maximum relative error of our measurements amounts to ±0.15%.

Figure 2 gives a comparison of our data with the results of other workers. Of all these, the values obtained by Biltz et al.[6] by the pycnometer

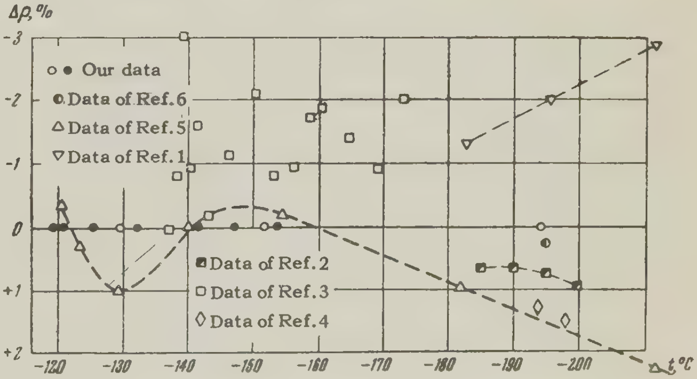

FIG. 2. Discrepancies between experimental data of various authors and the results of the present work: ○ – first series of experiments; ● – second series of experiments.

method agree the best with our data. The discrepancy in this case does not exceed 0.25%. The results of Mathias and Kamerlingh-Onnes are sometimes lower and sometimes higher than our density values. The greatest discrepancy occurs at low pressures and at pressures ~30 kg/cm^2, amounting to 1.7% at t ~ −200°C. The discrepancies with the data of other investigators[1–4] appear to be quite chaotic over the entire extent of the saturation curve, and vary between +2 and −3%.

---

[1] J. Dewar, Proc. Roy. Soc. **73**, 251 (1904).

[2] E. C. C. Baly and F. G. Donnan, J. Chem. Soc. **81**, 911 (1902).

[3] F. E. Germann, Physik. Z. **14**, 857 (1913).

[4] J. Inglis and J. Coates, J. Chem. Soc. **89**, 886 (1906).

[5] E. Mathias and H. Kamerlingh-Onnes, Comm. Phys. Lab. Leiden **117** (1911).

[6] Biltz, Fischer, and Wünnenberg, Z. anorg. allg. Chem. **193**, 351 (1930).

[7] D. L. Timrot, Изв. Всес. теплотехн. ин-та, (News, All-Union Heat-Eng. Inst.) No. 1 (1949).

[8] C. H. Meyers, J. Res. N.B.S. **40**, 457 (1948).

[9] Ponomarev, Biderman, Likharev, Makushin, Malinin, and Fedos'ev, Основы современных методов расчета на прочность, (Fundamentals of Modern Methods of Stress Analysis) Mashgiz, M. (1950).

Translated by D. C. West
335

SOVIET PHYSICS JETP VOLUME 11, NUMBER 6 DECEMBER, 1960

NEUTRON SPECTRA FROM THE $d + p$ REACTION

N. A. VLASOV, S. P. KALININ, B. V. RYBAKOV, and V. A. SIDOROV

Submitted to JETP editor February 15, 1960

J. Exptl. Theoret. Phys. (U.S.S.R.) 38, 1733-1737 (June, 1960)

Neutron spectra from the reactions H (d, n) 2p with $E_d = 18.6$ Mev and D (p, n) 2p with $E_p = 8.6$ Mev have been measured at an angle of 0° by the time-of-flight method. The spectrum shapes can be satisfactorily explained by pair interaction between the nucleons in the final state.

In fast-deuteron collisions with light nuclei there is a large probability for the breakup of the deuterons with emission of nucleons which have a continuous spectrum.[1,2] The spectra have a complex shape which depends considerably on the form of the target nucleus. This indicates the large role played by the interaction of the reaction products in their final state. A simpler case is the breakup of a deuteron by a proton. In this reaction only free nucleons are produced, whose pair interaction can be taken into account on the basis of data on nucleon-nucleon scattering.

In this paper the neutron spectra from the reactions H (d, n) 2p with 18.6-Mev deuterons and D (p, n) 2p with 8.6-Mev protons are investigated by the time-of-flight method (the total c.m.s. energy of the three nucleons is 4 and 3.5 Mev, respectively), and it is shown that the spectrum shape is basically determined by the pair interaction of the nucleons in the singlet S state, produced in the reaction.

The first results of the study of neutron spectra from the D (p, n) 2p reaction, obtained in our laboratory, were reported at the Paris Conference in the summer of 1958. Analogous results for this reaction were obtained by other authors.[3-5]

MEASUREMENT METHOD

The work was carried out on the 1.5-m cyclotron of the Atomic Energy Institute of the U.S.S.R. Academy of Sciences. Gas targets 3.5 cm thick with a window of thin nickel or platinum foil were filled with hydrogen up to a pressure of 5 atm, and with deuterium up to a pressure of 2 atm. The bottom of the target was made of lead. The neutron spectra were measured at 0° to the cyclotron beam. The neutrons were registered by a scintillation counter with a stilbene crystal (3 cm in diameter and 2 cm high) for flight distances up to 3 m, and with a tolane crystal (8 cm in diameter and 3 cm high) for larger distances. The counter was connected to the circuit of a multi-channel neutron time-of-flight spectrometer.[6,7]

The spectrometer operates by utilizing the natural modulation of the cyclotron beam. The time analyzer operates on the "vernier" principle. The time resolution of the spectrometer is 2.5 mμsec. The channel width of the time analyzer is about 0.8 mμsec. The recording system has 256 channels with a capacity of 2^{16} pulses per channel, and a digital printing device for data extraction.

The time distribution of the scintillation-counter pulses is measured within an interval equal to two cyclotron periods. The presence of two analogous peaks (two γ-ray peaks, for instance) in this spectrum makes it possible to monitor the time scale.

As an illustration of the experimental conditions, Fig. 1 shows the time-of-flight distribution of neutrons emitted at 0° in bombarding hydrogen with deuterons. The measurements were conducted in turn in a gas-filled and in an empty target. The figure shows the difference between the results of these measurements (filled circles) and the background from the empty target. For the case of bombarding deuterium with protons the background was considerably smaller.

MEASUREMENT RESULTS

Figures 2 and 3 show the obtained energy spectra of the neutrons. The apparatus "width" (defined as the γ-peak width at half the height) corresponds to three intervals between the points. The statistical precision of the measurements is fully characterized by the observed spread of the points.

The cross section for neutron production (the area under the experimental points) at an angle of 0° is (150 ± 15) mb/sr for the H (d, n) 2p, and (47 ± 5) mb/sr for the d (p, n) 2p reaction.

In the center-of-mass system of the three nu-

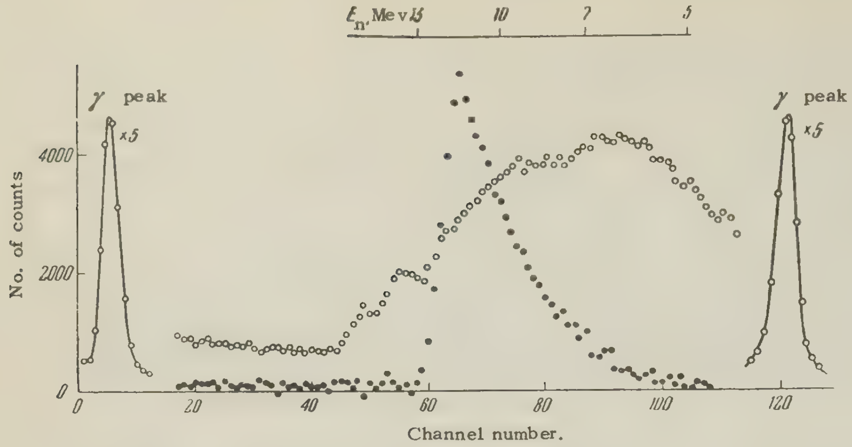

FIG. 1. Time-of-flight distribution of neutrons from the H(d, n)2p reaction at 0° to the directions of 18.6-Mev deuterons. The distance between the target and the counter was 2.8 m. The channel width of the time analyzer was 0.836 mμsec. The counter threshold was 3.2 Mev.

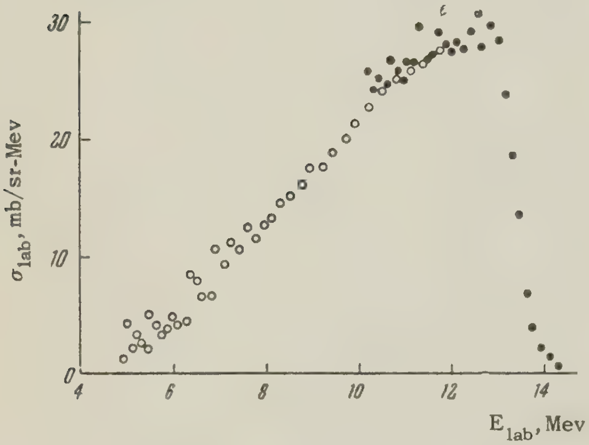

FIG. 2. The spectrum of neutrons produced at 0° by bombarding hydrogen with 18.6-Mev deuterons. The filled circles correspond to a flight distance of 7 m, and the open ones to a flight distance of 1.58 m.

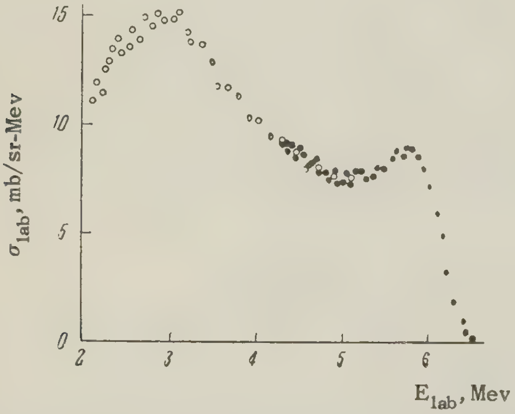

FIG. 3. The spectrum of neutrons produced at 0° by bombarding deuterium with 8.6-Mev protons. The filled circles correspond to a flight distance of 5.15 m, and the open ones to a flight distance of 1.58 m.

cleons, the cross sections for neutron production are (20 ± 2) mb/sr, and (11 ± 1) mb/sr at 0° and 180° to the incident deuterons, respectively.

DISCUSSION OF RESULTS

Figures 4 and 5 show the obtained neutron spectra in the c.m.s. In the spectrum observed at 0° to the direction of the incident deuterons only the maximum at the upper bound is distinct; this maximum corresponds to the production of two protons with a small relative velocity. In the spectrum observed at 180°, in addition to the peak at the bound, there is also a maximum for a neutron energy of 0.6 Mev, which by its position corresponds to a velocity of the neutron relative to one of the protons in its final state.

Thus, it is evident from the obtained spectra that as a result of the $d + p \rightarrow 2p + n$ reaction there is a large probability for the production of nucleon pairs with a small energy of relative motion; this can be explained by their attractive interaction in the final state.

In reference 8 it was shown that in the collision of a fast deuteron with a nucleon the probability of obtaining in the final state two nucleons with a small relative momentum $\overline{P}$, within an interval $d\overline{P}$, is proportional to $|\varphi(r)|^2 d\overline{P}$, where $\varphi(r)$ is the wave function of the relative motion of two nucleons in the S state (outside the range of nuclear forces) known from the data on nucleon-nucleon scattering. If we consider only a small range of relative-energy values of the two nucleons ($E \ll E_0$, where E_0 is the total energy of the three nucleons produced in the reaction) then we can neglect the dependence of the remaining factors which determine this probability on the relative nucleon energy. Watson[9] obtained an analogous result.

The relative-energy distribution of a proton and a neutron is given by the expression

$$d\sigma = \text{const}\cdot\sqrt{E}\,dE/(E+\varepsilon),$$

where $\epsilon = 2.23$ for the triplet, and $\epsilon = 0.07$ Mev

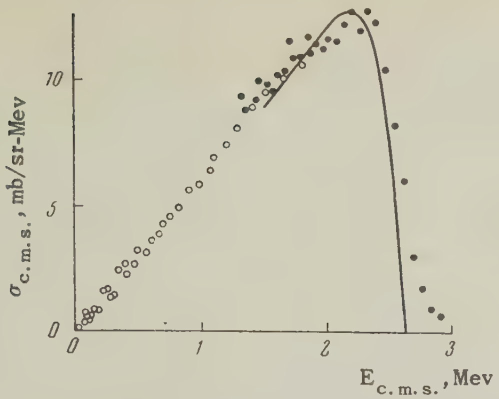

FIG. 4. Neutron spectrum from the $d + p \rightarrow 2p + n$ reaction in the c.m.s., observed at an angle of 0° to the direction of the deuterons ($E_0 = 4.0$ Mev).

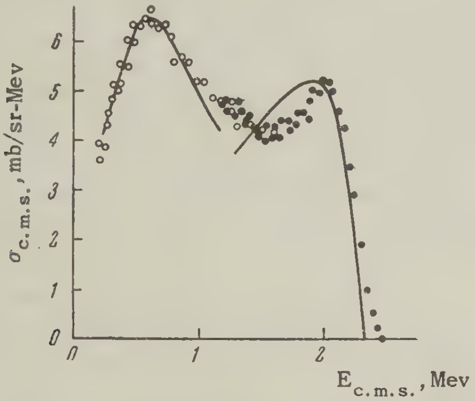

FIG. 5. Neutron spectrum from the $d + p \rightarrow 2p + n$ reaction in the c.m.s., observed at 180° to the direction of the deuterons ($E_0 = 3.5$ Mev).

for the singlet state. The distribution has a maximum when E is on the order of ϵ. For our energies ($E_0 = 4$ and 3.5 Mev) the condition $E \ll E_0$ is satisfactorily fulfilled for the singlet state in the region of the maximum.

The neutron-spectrum curve for $\epsilon = 0.07$ Mev thus obtained is plotted in Fig. 5 in the neutron-energy region of about 0.6 Mev. The apparent larger width of the maximum in the c.m.s. of the three nucleons is due to the superposition of the c.m.s. velocities of the two nucleons on their relative velocity. The theoretical curve is in excellent agreement with the experimental points. Curves with ϵ from 0.03 to 0.15 Mev fit within the experimental errors. The proton-neutron interaction in the triplet state ($\epsilon = 2.23$ Mev) would have yielded a considerably broader maximum.

In the case of two protons with small relative energies only the interaction in the singlet S state need be taken into account. The relative-energy distribution has in this case a more complicated form[8] on account of the Coulomb interaction. The theoretical neutron spectra corresponding to the interaction of protons in the final state are shown in Figs. 4 and 5 (near the upper bound of the spectra). They are in qualitative agreement with the experimental curves but have a somewhat larger "width" of the maximum (especially for $\theta_{n,d} = 180°$ where the precision of the measurements is higher and E_0 is smaller). No better agreement is to be expected, apparently, for the Coulomb repulsion makes the width of the two-proton relative-energy distribution considerably larger than for a neutron and proton in the singlet state, and the condition that the relative energy be small in the region of the maximum is fulfilled to a considerably lesser extent.

Komarov and Popova[10] carried out a detailed neutron-spectrum calculation for the $d + p \rightarrow 2p + n$ interaction with account of nucleon pair interaction on the basis of data on nucleon-nucleon scattering. The Born approximation was employed to account for the interaction of the pair with a third nucleon. The obtained curves are in good agreement with the experimental results in the entire neutron-energy region. The calculations also explain the variation of the relative height of the maxima with angle. The calculated ratio of the cross section for neutron production at 0° and 180° is in good agreement with the experimental value.

The authors are grateful to the staff of the Cyclotron Laboratory of the Atomic Energy Institute of the U.S.S.R. Academy of Sciences who assisted in the work, and also to A. M. Popova who took part in discussing the results.

---

[1] Bogdanov, Vlasov, Kalinin, Rybakov, and Sidorov, JETP **30**, 185 (1956), Soviet Phys. JETP **3**, 113 (1956).

[2] Bogdanov, Vlasov, Kalinin, Rybakov, and Sidorov, JETP **30**, 981 (1956), Soviet Phys. JETP **3**, 793 (1956).

[3] Nakada, Anderson, Gardner, McClure, and Wong, Phys. Rev. **110**, 594 (1958).

[4] Wong, Anderson, Gardner, McClure, and Nakada, Phys. Rev. **116**, 164 (1959).

[5] L. Cranberg and R. K. Smith, Phys. Rev. **113**, 587 (1959).

[6] Kurashov, Linev, Rybakov, and Sidorov, Атомная энергия, (Atomic Energy) **5**, 135 (1958).

[7] Kurashov, Linev, Rybakov, and Sidorov, Приборы и техника эксперимента, (Instrum. and Meas. Engg.) No. 5 (1960).

[8] A. B. Migdal, JETP **28**, 3 (1955), Soviet Phys. JETP **1**, 2 (1955).

[9] K. M. Watson, Phys. Rev. **88**, 1163 (1952).

[10] V. V. Komarov and A. M. Popova, JETP **38**, 1559 (1960), Soviet Phys. JETP **11**, 1123 (1960).

Translated by Z. Barnea
336

SOVIET PHYSICS JETP VOLUME 11, NUMBER 6 DECEMBER, 196

CERENKOV RADIATION OF DIPOLES IN A MEDIUM WITH SPATIAL DISPERSION

G. A. BEGIASHVILI and É. V. GEDALIN

Tbilisi State University, Institute of Physics, Academy of Sciences, Georgian S.S.R.

Submitted to JETP editor July 13, 1959; resubmitted February 17, 1960

J. Exptl. Theoret. Phys. (U.S.S.R.) 38, 1738-1739 (June, 1960)

An analysis is made of the Cerenkov radiation of electric dipoles and magnetic dipoles in an isotropic non-gyrotropic medium with spatial dispersion. The Cerenkov radiation of a current loop in such a medium is also considered.

THE Cerenkov radiation of a charged particle in a medium with spatial dispersion has been considered by a number of authors.[1,2] In the present paper we consider the Cerenkov energy losses of particle bunches for particles with dipole moments (electric and magnetic) in an isotropic non-gyrotropic medium with spatial dispersion. It is assumed that the bunch radiates as a point particle with dipole moment corresponding to the entire bunch. We also consider the Cerenkov radiation of a closed current ring in a medium of this kind. These analyses are desirable for investigating the possibility of excitation of new kinds of waves (which arise when spatial dispersion is considered) by means of the Cerenkov effect.[1]

1. In frequency regions which lie close to one of the natural resonant frequencies of the medium, we can use the well-known reciprocal dispersion expansion*

$$\mathbf{E} = (1/\varepsilon_0 + \beta n^2)\,\mathbf{D}. \qquad (1)$$

Then, the Cerenkov radiation loss for an electric dipole with arbitrary orientation is given by

$$dF = \frac{\omega^3\,d\omega}{c^2 v}\sum_i \left\{p_z^2 + \frac{p_r^2}{2}\left(\frac{v^2}{c^2}n_i^2 - 1\right)\right\}\left(1 - \frac{c^2}{v^2 n_i^2}\right)|1 + \beta n_i^4|^{-1}, \qquad (2)$$

$$n_{1,2}^2 = -1/\varepsilon_0\beta \pm \sqrt{(1/\varepsilon_0\beta)^2 + 1/\beta}. \qquad (3)$$

Cerenkov radiation is excited at a frequency ω only when

$$v > c/n_i(\omega) \qquad (4)$$

and is distributed over two cones which are defined by the condition

$$\cos\vartheta_i = c/vn_i(\omega) \qquad (5)$$

(ϑ_i is the angle between the direction of motion of the dipole† and the radiation direction).

Ginzburg has shown[1] that when $\beta > 0$ one of the roots of Eq. (3) is always smaller than unity and the radiation condition (4) is not satisfied for it. In this case the Cerenkov radiation is distributed over the surface of one (ordinary) cone. When $\beta < 0$ the radiation condition (4) is satisfied for both roots and the radiation is distributed over the surfaces of two cones.

It is of interest to consider the intensity distribution of the Cerenkov radiation over these cones. Let I_1 be the intensity of the radiation for the "ordinary" cone and I_2 the intensity for the "new" cone; then we have

$$\frac{I_2}{I_1} = \frac{(1 - c^2/v^2n_2^2)\,\{p_z^2 + {}^1/_2 p_r^2\,(v^2n_2^2/c^2 - 1)\}\,|1 + \beta n_1^4|}{(1 - c^2/v^2n_1^2)\,\{p_z^2 + {}^1/_2 p_r^2\,(v^2n_1^2/c^2 - 1)\}\,|1 + \beta n_2^4|}. \qquad (6)$$

When $\epsilon_0^2|\beta| \ll 1$ and $n_2^2 \gg n_1^2$, for a dipole which is oriented along the direction of motion we find $I_2/I_1 \ll 1$, that is, the Cerenkov radiation is almost completely concentrated in the "ordinary" cone. For a dipole which is perpendicular to the direction of motion we have $I_2/I_1 \sim 1$.

2. In considering the Cerenkov radiation of magnetic dipoles we will distinguish between current dipoles and "true" dipoles;[4] "true" magnetic dipoles are dipoles formed from magnetic poles.

For the frequency region in which the expansion in (1) applies, we have for a current magnetic dipoles

$$dF = \frac{\omega^3 d\omega}{c^2 v}\sum_i n_i^2\left\{\mu_r^2\left[\left(1 - \frac{1}{n_i^2}\right)^2 - \frac{1}{2}\left(1 - \frac{c^2}{v^2n_i^2}\right)\right.\right.$$
$$\left.\left.\times\left(1 - \frac{v^2}{c^2n_i^2}\right)\right] + \mu_z^2\left(1 - \frac{c^2}{v^2n_i^2}\right)\right\}|1 + n_i^4\beta|^{-1}, \qquad (7)$$

while for a true magnetic dipole

$$dF = \frac{\omega^3 d\omega}{c^2 v}\sum_i\left(1 - \frac{c^2}{v^2n_i^2}\right)$$
$$\times\; n_i^2\left[\mu_z^2 + \frac{\mu_r^2}{2}\left(n_i^2\frac{v^2}{c^2} - 1\right)\right]|1 + n_i^4\beta^{-1}. \qquad (8)$$

---

*In the present paper we use the notation of references 1 and 3.

†The direction of motion is taken along the z axis.

The intensity distribution of the Cerenkov radiation over the cones is different for the current and true dipoles. If $\epsilon_0^2|\beta| \ll 1$ we have $I_2/I_1 \sim 1$ for any orientation of a current dipole. For true magnetic dipoles $I_2/I_1 \sim 1$ for a moment oriented along the direction of motion and $I_2/I_1 \gg 1$ for a moment oriented perpendicularly to the direction of motion. This difference in the radiation distribution over the cones for current and true magnetic dipoles is due to the fact that moving true dipoles are not equivalent to moving current magnetic moments if $\epsilon \neq 1$.[4]

We now give the expression for the Cerenkov radiation loss of a current loop which moves through a medium of this kind where it is assumed that the plane of the current loop is perpendicular to the direction of motion. If (1) applies we have

$$dF = \frac{8\pi^2 a^2 I_0^2 \omega d\omega}{c^2 v} \sum_i I_1^2 \left(a \frac{n_i \omega}{c} \sqrt{1 - \frac{c^2}{v^2 n_i^2}} \right) |1 + n_i^4 \beta|^{-1}, \tag{9}$$

where a is the radius of the loop, I_0 is the current strength in the loop, and I_1 is a Bessel function. It is apparent that for a point current loop ($a \rightarrow 0$) Eq. (9) becomes the formula for the Cerenkov radiation of a magnetic dipole.

In frequency regions of the Cerenkov radiation which are remote from resonance frequencies of the medium it is not necessary to take spatial dispersion into account.

The authors are indebted to N. M. Polievktova-Nikoladze for her interest in this work.

---

[1] V. L. Ginzburg, JETP **34**, 1593 (1958), Soviet Phys. JETP **7**, 1096 (1958).

[2] Agranovich, Pafomov, and Rukhadze, JETP **36**, 238 (1959), Soviet Phys. JETP **9**, 160 (1959).

[3] B. M. Bolotovskiĭ, Usp. Fiz. Nauk **62**, 201 (1957).

[4] V. L. Ginzburg and V. Ya. Éĭdman, JETP **35**, 1508 (1958), Soviet Phys. JETP **8**, 1055 (1959).

Translated by H. Lashinsky
337

SOVIET PHYSICS JETP VOLUME 11, NUMBER 6 DECEMBER, 1960

RECURRENT CONSTRUCTION OF ANGULAR OPERATORS

J. FISCHER* and S. CIULLI†

Submitted to JETP editor August 28, 1959

J. Exptl. Theoret. Phys. (U.S.S.R.) **38**, 1740-1750 (June, 1960)

The purpose of the authors was to give a practical recursion method for constructing the angular operators characterizing the angular and spin dependence of the S matrix. Only differential operations are used in the method, and the use of Racah transformations and calculations with Clebsch-Gordan coefficients can be avoided. Using this method, the angular operators for a given process can be found if the angular operators for a simpler process are known. In the present paper we solve the problem of how the system of angular operators changes when one initial and one final scalar particle are replaced by particles with spin ½. Practical formulas and example are given.

INTRODUCTION

THE purpose of S-matrix theory is to obtain the cross sections for elementary processes as a function of the energies, charges, angles and spins in the reaction. This can be done either directly, by starting from some theory (perturbation theory, Tamm-Dancoff method, Chew-Low theory, or the theory of dispersion relations), or phenomenologically, by using some semiempirical postulates concerning the dynamical character of the process, such as, for example, the assumption of the existence of resonant (isobar) states.

However, in both cases, irrespective of the particular dynamical features of the process, it is advantageous to expand the S matrix in series in the eigenfunctions of the angular momentum and isotopic spin operators for the initial and final states of the process. The form of this expansion can be found using only general conservation laws which follow from the symmetry of the process with respect to well-known transformation groups.

Using this expansion, one can extract the angular, spin and isotopic spin dependence by substituting the expressions in the dynamical equations. In general this gives a system of equations for the expansion coefficients which depend only on the energy. In the case of phenomenological theories, one can write the amplitude for the resonant state as a function of the angle and isotopic spin variables. Finally, the expansion in such an orthonormal set can be used for the phase analysis of experimental data.

The S matrix for any reaction can be written in the form

$$S = \sum a\,(JM\,(f);\ J^0M^0\,(i))\,|\,JM\,(f)\rangle\,\langle J^0M^0\,(i)\,|,$$

where $|\,J^0M^0(i)\rangle$ and $|\,JM\,(f)\rangle$ are the state vectors of the initial and final states; $|\,a\,|^2$ is the intensity of the corresponding transition; J^0, M^0 and J, M are the quantum numbers of the total angular momentum and its z component in the initial and final states, respectively; (i) and (f) are quantum numbers which, together with J^0, M^0, or J, M, respectively, form a complete set for the initial and final state; the summation is extended over all quantum numbers. We shall be interested only in the angular parts of (i) and (f) and will not write the other indices explicitly, so that the dependence on other variables, such as the energy, isotopic spin, parity, etc. must be included in the coefficients a. The invariance of the S matrix under space transformations requires, in addition to conservation of total angular momentum $J = J^0$, $M = M^0$, that the coefficients a be independent of M. Thus,

$$S = \sum_{J(f)(i)} a\,(\text{energies}, \ldots J(f)(i))\,\mathcal{Y}\,(\text{angles and spins}, J(f)(i)), \tag{1}$$

where the "angular operators" $\mathcal{Y}$ are defined by

$$\mathcal{Y}\,(J\,(f)\,(i)) = \sum_{M=-J}^{J} |\,JM\,(f)\rangle\,\langle JM\,(i)\,| \tag{2}$$

and are normalized to 2J + 1 (cf. references 1 and 2).

The angular operators are completely defined by (2) and can, in principle, be found for any process. However, practical computations are simple for processes of the type a + b → a′ + b′ (cf. reference 1). Each new particle seriously complicates the computations, introducing one or two summations over Clebsch-Gordan coefficients, and thus, with increasing number of particles, the number of terms to be summed increases very rapidly.

---

*Associate of the Physics Institute of the Czechoslovak Academy of Sciences, Prague.

†Associate of the Institute for Atomic Physics, Bucharest, Rumania.

Our purpose is to give a recursion method for constructing the angular operators for reactions involving many particles, which enables one to express them in terms of the angular operators describing simpler reactions. (Unlike the method of Biedenharn, Blatt and Rose,[3] our method avoids the complicated summations associated with repeated Racah transformations.) This method is especially simple for practical computations, since it uses only differential operations (cf. also reference 4).

In the present paper we shall consider the method for constructing the angular operators for reactions of the type $f + a \rightarrow f' + a'_1 + \ldots + a'_n$, where f and f′ are fermions and a, a'_i are any particles, from the angular operators of the reaction

$$s + a \rightarrow s' + a'_1 + \ldots + a'_n,$$

where s, s′ are bosons with spin 0. In other words, we shall find the operator Ξ, which transforms $\mathcal{F}(s + a \rightarrow s' + a'_1 + \ldots + a'_n)$ into $\mathcal{F}(f + a \rightarrow f' + a'_1 + \ldots + a'_n)$:

$$\Xi\mathcal{F}(s + a \rightarrow s' + a'_1 + \ldots + a'_n) = \mathcal{F}(f + a \rightarrow f' + a'_1 + \ldots + a'_n). \tag{3}$$

In later papers we shall develop the method for constructing the operator Ω defined by the relation

$$\Omega\mathcal{F}(a_1 + a_2 \rightarrow a'_1 + \ldots + a'_n) = \mathcal{F}(a_1 + a_2 \rightarrow a'_1 + \ldots + a'_n + s'_{n+1}), \tag{3′}$$

and the operator Ξ' which enables one to obtain the angular operators for the reaction $f_1 + f_2 \rightarrow a'_1 + \ldots + a'_n$ or $a_1 + a_2 \rightarrow f'_1 + f'_2 + \ldots a'_n$ from the angular operators of the reactions $s_1 + s_2 \rightarrow a'_1 + \ldots + a'_n$ or $a_1 + a_2 \rightarrow s'_1 + s'_2 + \ldots a'_n$.

In addition to Ξ, Ω and Ξ', the operators Ω_V, which transform a particle with spin 0 into a particle with spin 1, are of great practical importance:

$$\Omega_V\mathcal{F}(a_1 + a_2 \rightarrow s' + a'_2 + \ldots + a'_n) = \mathcal{F}(a_1 + a_2 \rightarrow v' + a'_2 + \ldots + a'_n).$$

It is known (cf. for example, references 1, 2, and 4) that the operators Ω_V have the following form:

$$\sqrt{\frac{l}{2l+1}}\,\mathbf{q} + \frac{1}{\sqrt{l(2l+1)}}\,Q\frac{\partial}{\partial\mathbf{Q}}, \qquad -\frac{i}{\sqrt{l(l+1)}}\left[\mathbf{Q}\times\frac{\partial}{\partial\mathbf{Q}}\right],$$

$$-\sqrt{\frac{l+1}{2l+1}}\,\mathbf{q} + \frac{1}{\sqrt{(l+1)(2l+1)}}\,Q\frac{\partial}{\partial\mathbf{Q}}, \tag{4}$$

where $\mathbf{Q}$ is the momentum vector of the particle and $\mathbf{q} = \mathbf{Q}/Q$.

Knowing the explicit form of the operators Ξ, Ω, Ξ' and Ω_V, and applying them the necessary number of times (and in definite succession) to the complete set of the simplest angular operators

$$\mathcal{F}(s_1 + s_2 \rightarrow s'_1 + s'_2) = \frac{2l+1}{4\pi}P_l(\cos\vartheta)$$

[where $P_l(\cos\vartheta)$ is the Legendre polynomial of degree l], one can obtain the angular operators for a reaction with an arbitrary number of particles having any spin values.

1. NOTATION

Our problem is to find the operator Ξ, which, according to (3), adds a spin ½ to the initial and final states. Let us use $\mathcal{L}$ and $\mathcal{F}$ to denote the angular operators before and after this introduction. We call the corresponding processes the $\mathcal{L}$ process and the $\mathcal{F}$ process. For example, if $\pi_1 + \pi_2 \rightarrow \pi'_1 + \pi'_2$ is an $\mathcal{L}$ process, then the $\mathcal{F}$ process will be $\pi + N \rightarrow \pi' + N'$. On the other hand, if $\pi + N \rightarrow \pi' + N'$ is the $\mathcal{L}$ process, the $\mathcal{F}$ process will be $N_1 + N_2 \rightarrow N'_1 + N'_2$.

Let us assume that the final state of the $\mathcal{L}$ process is characterized by a set of quantum numbers J, (f) for the angular momenta. Then among the quantum numbers describing the final state of the $\mathcal{F}$ process there will appear an additional quantum number ½, corresponding to the spin, which must be combined with the angular momenta in the set J, (f). This latter angular momentum may be an orbital angular momentum, or a spin, or, finally, a sum of several orbital angular momenta and several spins. In the following we shall denote it, irrespective of its nature, by the symbol $\mathbf{l}_1$; we denote the total angular momentum $\mathbf{l}_1 + \frac{1}{2}\boldsymbol{\sigma}$ by $\mathbf{j}_1$. By $\mathbf{l}_2$ we denote, again independent of its nature, the angular momentum which is added to $\mathbf{l}_1$. We denote the sum $\mathbf{l}_1 + \mathbf{l}_2$ by $\mathbf{l}_{12}$, and the corresponding quantum number by l_{12}. Similarly, $\mathbf{l}_{13} = \mathbf{l}_{12} + \mathbf{l}_3$ and $\mathbf{l}_{1,i+1} = \mathbf{l}_{1i} + \mathbf{l}_{i+1}$. After combining the angular momenta $\frac{1}{2}\boldsymbol{\sigma}$ and $\mathbf{l}_1$, the values of the angular momenta $l_{12}, l_{13}, \ldots l_{1n}$, unlike $l_1, l_2, \ldots l_n$, are no longer good quantum numbers. In place of $l_{12}, l_{13}, \ldots l_{1n}$, there appear numbers $j_{12}, j_{13}, \ldots j_{1n}$, corresponding to the angular momenta

$$\mathbf{j}_{12} = \mathbf{l}_{12} + {}^1\!/_2\,\boldsymbol{\sigma}, \ \ldots, \ \mathbf{j}_{1i} = \mathbf{l}_{1i} + {}^1\!/_2\,\boldsymbol{\sigma}, \ \ldots,$$

$$\mathbf{j}_{1n} = \mathbf{l}_{1n} + {}^1\!/_2\,\boldsymbol{\sigma}.$$

Thus the final state of the $\mathcal{L}$ process will be characterized by the set of quantum numbers l_1, l_2,

$\ldots \boldsymbol{l}_n$, $\boldsymbol{l}_{12}, \ldots \boldsymbol{l}_{1n}$ (together with numbers characterizing the angular momenta which make up $\boldsymbol{l}_1, \ldots \boldsymbol{l}_n$), and the final state of the $\mathscr{F}$ process by the set $l_1, l_2, \ldots l_n, \frac{1}{2}, j_1, j_{12} \cdots j_{1n}$ (again, of course, together with numbers characterizing the angular momenta which make up $\boldsymbol{l}_1, \ldots \boldsymbol{l}_n$). The angular momenta of the initial states of the $\mathscr{L}$ process and $\mathscr{F}$ process will be denoted by the same symbols with an additional null superscript (for example, $\boldsymbol{l}_1^0$, l_1^0, etc),

2. PROJECTION OPERATORS

Our problem is to find the complete set of operators $\mathscr{F}$ if we know the complete set of operators $\mathscr{L}$. The operators $\mathscr{F}$ differ from $\mathscr{L}$ in having one additional spinor in both the initial and final state. Consequently, if we multiply any $\mathscr{L}$ by the direct product of two spinors, we obtain a quantity which can be expanded in the complete set $\mathscr{F}_k$:

$$\mathscr{L}\begin{pmatrix}1 & 0\\ 0 & 1\end{pmatrix} = \sum_{k'} c_{k'}\mathscr{F}_{k'}, \tag{5}$$

where the index k′ denotes a complete set of angular momentum quantum numbers.* The unit matrix was chosen because it is a scalar combination of the new spinors; then the $c_{k'}$ are also scalars.

In the relation (5), $\mathscr{L}$ is assumed to be known and $\mathscr{F}$ unknown. If we now find a projection operator P_k, which, acting on $\Sigma c_{k'}\mathscr{F}_{k'}$, leaves only the term $c_k\mathscr{F}_k$ and annihilates all the others, we will be able to use (5) for finding any $\mathscr{F}_k$ for which $c_k \neq 0$. Let us write P_k as a product of the following projection operators:

$$P_{l_1} \ldots P_{l_n} P_{j_1} P_{j_{12}} \ldots P_{j_{1m}} \text{ and } P_{l_1^0} \ldots P_{l_m^0} P_{j_1^0} \ldots P_{j_{1m}^0},$$

where the first acts from the left on $\mathscr{L}$ or $\mathscr{F}$ (final state operators), while the second operates from the right (initial state operators). Then*

$$c_{l_1 \ldots j_{1m}^0}\mathscr{F}_{l_1 \ldots j_{1m}^0} = P_{j_1} P_{j_{12}} \ldots P_{j_{1m}} \mathscr{L}\begin{pmatrix}1 & 0\\ 0 & 1\end{pmatrix} P_{j_1^0} P_{j_{12}^0} \ldots P_{j_{1m}^0}. \tag{6}$$

Here we have used the relation

$$P_{l_{1i}}\mathscr{L}_{l_1 \ldots l_{1n};\, l_1^0 \ldots l_{1m}^0} = \mathscr{L}_{l_1 \ldots l_{1n};\, l_1^0 \ldots l_{1m}^0}. \tag{7}$$

The operators P have the following property:

$$P_{j_{1h}} P_{l_{1i}} = P_{l_{1i}} P_{j_{1h}}, \quad \text{if} \quad h \geqslant i.$$

In fact, since $\mathbf{j}_{1h} = \boldsymbol{l}_{1i} + \sum_{k=i+1}^{h} \boldsymbol{l}_k + \frac{1}{2}\boldsymbol{\sigma}$,

$$[l_{si}^r,\, j_{1h}^s] = [l_{1i}^r,\, l_{1i}^s] = i\sum_t \varepsilon^{rst} l_{1i}^t, \tag{9}$$

where the indices r, s, and t label the Cartesian components of the vectors, and ϵ^{rst} is the completely antisymmetric unit tensor. Because of (9), $\boldsymbol{l}_{1i}^2$ and $\mathbf{j}_{1h}^2$ commute (cf. reference 6, Chap. III) (i.e., they can be brought simultaneously to diagonal form), from which (8) follows directly.

Using (8), we can write the right side of (6) in the form

$$P_{j_1} P_{l_1} P_{j_{12}} P_{l_{12}} \ldots P_{j_{1n}} P_{l_{1n}} \mathscr{L}\begin{pmatrix}1 & 0\\ 0 & 1\end{pmatrix} P_{l_{1m}^0} P_{j_{1m}^0} \ldots P_{l_1^0} P_{j_1^0}. \tag{10}$$

Here we have also made use of (7). Now we prove the relation*

$$P_{j_{1i}} P_{l_{1i}} = R_{j_{1i}}^{\pm} P_{l_{1i}}, \qquad j_{1i} = l_{1i} \pm {}^1\!/_2, \tag{11}$$

$$R_{j_{1i}}^{\pm} = (2l_{1i}+1)^{-1}(j_{1i} + {}^1\!/_2 \pm \boldsymbol{\sigma}\mathbf{l}_{1i}). \tag{12}$$

In fact, $P_{l_{1i}}$ can be expressed as a sum of two terms

$$P_{l_{1i}} = P_{l_{1i}+{}^1\!/_2} P_{l_{1i}} + P_{l_i-{}^1\!/_2} P_{l_{1i}}. \tag{11'}$$

The operator $\boldsymbol{\sigma}\cdot\boldsymbol{l}_{1i} = \mathbf{j}_{1i}^2 - \boldsymbol{l}_{1i}^2 - {}^3\!/_4$, acting on the first term on the right, gives $j_{1i}(j_{1i}+1) - l_{1i}(l_{1i}+1) - {}^3\!/_4 = l_{1i}$, and on the second term gives $-(l_{1i}+1)$. Therefore applying (11′) on the left to $R_{j_1i}^{+}$ or $R_{j_1i}^{-}$, we get (11) with the upper and lower signs, respectively. By using (11), the operator $\mathscr{F}$ can be represented in the form†

$$\mathscr{F} = c^{-1} R_{j_1} \ldots R_{j_{1n}} \mathscr{L}\begin{pmatrix}1 & 0\\ 0 & 1\end{pmatrix} R_{j_{1m}^0} \ldots R_{j_1^0}, \tag{13}$$

if $c \neq 0$.

We emphasize that the operators $R_{j_1} \ldots R_{j_1n}$ do not commute with one another, but that the corresponding operators $P_{j_1} \ldots P_{j_1n}$ do. Nevertheless the order $P_{j_1} \ldots P_{j_1n}$ chosen in formula (6) (and similarly the order $P_{j_1^0n} \ldots P_{j_1^0}$) is necessary for the derivation of (13), since only in this case, by using relation (7), can we form groups of the type $P_{j_1 i} P_{l_1 i}$ (and similarly $P_{l^0_1 i} P_{j^0_1 i}$) and use formula (11).

---

*The proof of relation (5) is given in reference 5.

†The method given in Sec. 2 and 3 can be used to calculate only those $\mathscr{F}$ operators for which there exist $\mathscr{L}$ operators characterized by the same values of $l_1 \ldots l_n, l_1^0, \ldots l_m^0$. As we shall see later, there are comparatively few $\mathscr{F}$ operators for which this condition is not fulfilled. These cases are treated in Sec. 4.

*The operators $R^{\pm}$ were used by Lepore[7] in studying the polarization of nucleons after scattering.

†Because of the hermiticity of $\boldsymbol{l}_{1i}$ and $\frac{1}{2}\boldsymbol{\sigma}$, the initial R operators have the same form as the final operators (cf. Appendix 1). However, the only cases which have physical meaning in practical computations are those with m = 1 or 2, since no more than two particles collide in elementary processes, i.e., in the initial state, after adding the spin, there can be no more than one orbital angular momentum and two spins. In addition, it can be shown (cf. Appendix 1) that the first operation on the right is superfluous, so that in the majority of cases one can proceed without the initial R operators.

3. CALCULATION OF THE COEFFICIENT c

We use the normalization condition for the angular operators:

$$|c|^2 (2j_{1n} + 1) = (c)^2 \operatorname{Sp} \int \mathscr{J}^+ \mathscr{J}$$
$$= \operatorname{Sp} \int P_{J^0} P_{L^0} \mathscr{L}^+ \begin{pmatrix} 1 & 0 \\ 0 & 1 \end{pmatrix} P_L P_J P_J P_L \mathscr{L} \begin{pmatrix} 1 & 0 \\ 0 & 1 \end{pmatrix} P_{L^0} P_{J^0},$$

where Sp is the trace over only the new spin variable, and $\int$ contains, in addition to an integral, the trace over the variables for the old spins. P_L is the product of all the final projection operators for the $\mathscr{L}$ process, while P_{L^0}, P_J and P_{J^0} are constructed similarly. Using the property of the trace of a product of operators and the relation $P_J^2 = P_J$, we have

$$|c|^2 (2j_{1n} + 1) = \operatorname{Sp} \int \mathscr{L}^+ \begin{pmatrix} 1 & 0 \\ 0 & 1 \end{pmatrix} P_L P_J P_L \mathscr{L} \begin{pmatrix} 1 & 0 \\ 0 & 1 \end{pmatrix} P_{L^0} P_{J^0} P_{L^0}. \tag{14}$$

By using (12), $P_L P_J P_L$ can be written as

$$P_L P_J P_L = P_{l_1} \ldots P_{l_n} P_{l_{12}} \ldots P_{l_{1n}} R_{j_1} \ldots R_{j_{in}} P_{l_1}$$
$$\ldots P_{l_n} P_{l_{12}} \ldots R_{l_{1n}}.$$

This product can be calculated by applying the relation

$$P_{l_{1i+1}} R_{j_{1i}} P_{l_{1i+1}} R_{j_{1i+1}} = \varkappa_i P_{l_{1i+1}} R_{j_{1i+1}}$$

(the proof of which is given in Appendix 2) successively for $i = 1, 2, 3 \ldots n-1$. Here we make use of the fact that $P_{l_1 i}$ commutes with all the $P_{l_1 h}$ for $h \geq i$, and, consequently, with all the $R_{j_1 h}$ with $h \geq i$ [cf. Eq. (12)]. The numerical coefficients κ_i have the following values:

$$j_{1i} = l_{1i} + \tfrac{1}{2}, \qquad j_{1i+1} = l_{1i+1} + \tfrac{1}{2}:$$
$${}^+\varkappa_i^+ = [(l_{1i+1} + l_{1i} + 2)(l_{1i+1} + l_{1i} + 1)$$
$$- l_{i+1}(l_{i+1} + 1)] / 2(l_{1i+1} + 1)(2l_{1i} + 1);$$
$$j_{1i} = l_{1i} + \tfrac{1}{2}, \qquad j_{1i+1} = l_{1i+1} - \tfrac{1}{2}:$$
$${}^+\varkappa_i^- = -[(l_{1i+1} - l_{1i})(l_{1i+1} - l_{1i} - 1)$$
$$+ l_{i+1}(l_{i+1} + 1)] / 2l_{1i+1}(2l_{1i} + 1);$$
$$j_{1i} = l_{1i} - \tfrac{1}{2}, \qquad j_{1i+1} = l_{1i+1} + \tfrac{1}{2}:$$
$${}^-\varkappa_i^+ = -[(l_{1i+1} - l_{1i})(l_{1i+1} - l_{1i} + 1)$$
$$+ l_{i+1}(l_{i+1} + 1)] / 2(l_{1i+1} + 1)(2l_{1i} + 1);$$
$$j_{1i} = l_{1i} - \tfrac{1}{2}, \qquad j_{1i+1} = l_{1i+1} - \tfrac{1}{2}:$$
$${}^-\varkappa_i^- = [(l_{1i+1} + l_{1i})(l_{1i+1} + l_{1i} + 1)$$
$$- l_{i+1}(l_{i+1} + 1)] / 2l_{1i+1}(2l_{1i} + 1). \tag{15}$$

We have thus eliminated from the final state all the R operators except for the last, $R_{j_1 n}$, and from the initial state all the R operators except for $R_{j^0_1 m}$. Of these two operators, one of them, say $R_{j^0_1 m}$, is irrelevant (cf. Appendix 1), so that we have in place of (14),

$$|c|^2 (2j_{1n} + 1)$$
$$= \varkappa_1 \ldots \varkappa_{n-1} \varkappa^0_1 \ldots \varkappa^0_{m-1} \operatorname{Sp} \int P_{L^0} \mathscr{L}^+ P_L R_{j_{1m}} P_{L^0} \mathscr{L} P_{L^0}.$$

The term in R which is proportional to $\boldsymbol{\sigma} \cdot \boldsymbol{l}_{1n}$ [cf. Eq. (12)] vanishes when we take the trace, and only $(2j_{1n} + 1)/(2l_{1n} + 1)$ remains. Thus, remembering that

$$\int P_{L^0} \mathscr{L}^+ P_L P_L \mathscr{L} P_{L^0} = \int \mathscr{L}^+ \mathscr{L} = 2l_{1n} + 1,$$

we get the final result

$$|c| = \sqrt{\varkappa_1 \ldots \varkappa_{n-1} \varkappa^0 \ldots \varkappa^0_{m-1}}.$$

The phase of the coefficient c remains undetermined, but it is unimportant for the finding of the complete set of $\mathscr{J}$ operators. Equation (13) now becomes

$$\mathscr{J}_{l_1, \ldots, l_n j_1 j_{12}, \ldots, j_{1n}\; l^0_1, \ldots, l^0_m\; j^0_1, \ldots, j^0_{1m}}$$
$$= R_{j_1} R_{j_{12}} \ldots R_{j_{1n-1}} R_{j_{1n}} \mathscr{L}_{l_1, \ldots, l_n l_{12}, \ldots, l_{1n};\; l^0_1, \ldots, l^0_m\, l^0_{12}, \ldots, l^0_{1m}}$$
$$\times R_{j^0_{1m-1}} \ldots R_{j^0_{12}} R_{j^0_1} (\varkappa_1 \varkappa_2, \ldots, \varkappa_{n-1} \varkappa^0_1 \varkappa^0_2, \ldots, \varkappa^0_{m-1})^{-1/2}. \tag{16}$$

4. ANALYSIS OF THE RESULTS

Formula (16) enables us to find the explicit form of the $\mathscr{J}$ operators if a complete set of $\mathscr{L}$ operators is known, under the condition, of course, that none of the coefficients κ_i or κ^0_i are equal to zero. We note, however, that the case where any one of these numbers is zero is possible only when conditions are imposed on the angular momentum quantum numbers of the $\mathscr{J}$ process which cannot be fulfilled (cf. reference 5).

There remains for us to treat the cases where the assumption made in deriving formula (6) is not satisfied (cf. footnote 3). The occurrence of such cases is related to the fact that the $\mathscr{L}$ operators from which the $\mathscr{J}$ operators are constructed, are subject to the condition of conservation of the total angular momentum $l_{1n} = l^0_{1m}$, which is not necessary for the $\mathscr{J}$ operators. When the spin ½ is added, frequently one or both of the numbers l_{1n}, l^0_{1m} lose their meaning, but then the conservation law may manifest itself as a limitation on the possible values of $l_1, l_2, \ldots l_n, l^0_1, l^0_2, \ldots l^0_m$, which do not lose their meaning. The result is that not all the $\mathscr{J}$ operators can be constructed from the $\mathscr{L}$ operators by the procedure described in the preceding sections.

Let us choose the case $n = m = 1$, in which all the $\mathscr{L}$ operators are related by the condition $l_1 = l^0_1$. There are four possibilities for the $\mathscr{J}$ operators:

$$j_1 = l_1 \pm \tfrac{1}{2} = j_1^0 = l_1^0 \pm \tfrac{1}{2}, \qquad j_1 = l_1 \pm \tfrac{1}{2} = j_1^0 = l_1^0 \mp \tfrac{1}{2}.$$

The first two cases satisfy the condition $l_1 = l_1^0$, so that we can use formula (16), but in the other two cases formula (16) is not applicable since there is no $\mathcal{L}$ operator for which $l_1 = l_1^0 \mp 1$. We proceed as follows (assuming, for example, $j_1 = l_1 + 1/2 = j_1^0 = l_1^0 - 1/2$): if l_1^0 is an orbital angular momentum, we multiply the $\mathcal{J}$ operator for $j_1 = l_1 + 1/2 = j_1^0 = l_1^0 + 1/2$ on the right by $\boldsymbol{\sigma}\cdot\mathbf{p}$, where $\mathbf{p}$ is the momentum corresponding to the angular momentum l_1^0. The operator $\boldsymbol{\sigma}\cdot\mathbf{p}$ will not change j_1^0 (since it is a scalar), but it will change the parity with respect to $\mathbf{p}$, i.e., it will change l_1^0 by unity, so that $j_1^0 = l_1^0 - 1/2$. Similarly we obtain the $\mathcal{J}$ operator for $j_1 = l_1 - 1/2 = l_1^0 + 1/2$ from $j_1 = l_1 - 1/2 = j_1^0 = l_1^0 - 1/2$ by multiplying by $\boldsymbol{\sigma}\cdot\mathbf{p}$ on the right. If l_1 is also an orbital angular momentum, we can achieve the same result by multiplying by $\boldsymbol{\sigma}\cdot\mathbf{q}$ on the left. Cases where both l_1 and l_1^0 are total angular momenta must be treated separately. Since every elementary reaction has no more than two particles in the initial state ($m \leq 2$), l_1^0 can occur only as the combination of a simple orbital angular momentum with some spin of $1/2$, 1 or greater. In such a case we can increase or decrease l_1^0 by unity by applying the operator $\boldsymbol{\sigma}\cdot\mathbf{V}^{\pm}$, where

$$N\mathbf{V}^{\pm} = \mathbf{l}_\alpha^0 \left(l_1^0(l_1^0+1) - l_\alpha^0(l_\alpha^0+1) + l_\beta^0(l_\beta^0+1)\right) - \mathbf{l}_\beta^0 \left(l_1^0(l_1^0+1) + l_\alpha^0(l_\alpha^0+1) - l_\beta^0(l_\beta^0+1)\right) \mp 2i\left(l_1^0 \pm \tfrac{1}{2} + \tfrac{1}{2}\right)[\mathbf{l}_\alpha^0 \times \mathbf{l}_\beta^0],$$

$$\mathbf{l}_1^0 = \mathbf{l}_\alpha^0 + \mathbf{l}_\beta^0 \tag{17}$$

and $\bar{N}$ is a normalization constant.

The method described here can also be used when $n \neq 1$ or $m \neq 1$. The only difference is that, for $n = m = 1$, there are comparatively many operators (two out of four) for which formula (16) is not suitable, whereas for $n, m \neq 1$ they occur quite rarely (cf. the detailed analysis in reference 5).

5. EXAMPLES

1. From the angular operators for the reaction $\pi_1 + \pi_2 \rightarrow \pi_1' + \pi_2'$, which are equal to

$$\mathcal{L} = (4\pi)^{-1}(2l+1)P_l(\mathrm{pq}), \tag{18}$$

we can by this method construct the angular operators for the reaction $\pi + N \rightarrow \pi' + N'$. In this case, $n = m = 1$, and formula (16) assumes the form

$$\mathcal{J}_{l,\,j;\,l^0,\,j^0} = R_j^{\pm}\,\mathcal{L}_{l;\,l^0}.$$

According to (11), we get for the upper sign,

$$\mathcal{J} = (4\pi)^{-1}(l + 1 + \sigma\mathrm{l})\,P_l(\mathrm{pq}).$$

This gives

$$\mathcal{J} = (4\pi)^{-1}\{(l+1)P_l + i\sigma[\mathrm{p}\times\mathrm{q}]P_l'\}. \tag{19a}$$

Similarly, for the lower sign on R, the calculation gives

$$\mathcal{J} = \frac{1}{(4\pi)}\{lP_l - i\sigma[\mathrm{p}\times\mathrm{q}]P_l'\}. \tag{19b}$$

In addition, the conservation law for the total angular momentum, $j = j^0$, allows the angular operators with $j = l \pm 1/2 = l^0 \mp 1/2$ (we shall not take account of conservation of internal parity of the mesons), which can be found (according to the method described in the preceding Section) by multiplying (19a, b) by $\boldsymbol{\sigma}\cdot\mathbf{p}$ on the right or (equivalently) by $\boldsymbol{\sigma}\cdot\mathbf{q}$ on the left. The resulting expressions agree, except for sign, with the operators given by Ritus[1] [formulas (8) and (8′)].

2. The angular operators for the process $\pi_1 + \pi_2 \rightarrow \pi_1' + \pi_2' + \pi_3'$ have the form*

$$\mathcal{L} = \sum_{M,\,\mu} C_{LM}^{l_\beta,\,M-\mu,\,l_\alpha\mu}\,Y_{l_\beta M-\mu}(\mathrm{r})\,Y_{l_\alpha\mu}(\mathrm{q})\,Y_{l^0M}^{*}(\mathrm{p}), \tag{20}$$

where $L = l_\alpha + l_\beta,\ l_\alpha + l_\beta - 1, \ldots |l_\alpha - l_\beta|$. By using the methods of Sections 2 – 4, we can obtain from them the angular operators for the process

$$\pi + N \rightarrow \pi_1' + \pi_2' + N'.$$

If, in particular, $l_\alpha = 0$ or 1, we should get the operators given in Tables I, II and III of reference 2. For example, for $l_\alpha = 1$, $L = l_\beta$, Eq. (20) takes the form

$$\mathcal{L} = i\sqrt{3}(4\pi)^{-3/2}(2l^0+1)[l^0(l^0+1)]^{-1/2}\,\mathrm{q}[\mathrm{p}\times\mathrm{r}]\,P_{l_\beta}(\mathrm{pr}). \tag{21}$$

We now show how we can obtain from $\mathcal{L}$ the angular operator (II.8), which is defined by the quantum numbers $J = L - 1/2 = l^0 - 1/2$, $l_\alpha = 1$, $L = l_\beta$, $l^0 = l_\beta$. According to formula (16), (II.8) must be equal to the expression $R_J^-\mathcal{L}$. In this case the spin of $1/2$ is combined in the final state with the total orbital angular momentum $\mathbf{L}$, i.e., $n = 1$, while $\mathbf{L} = \mathbf{l}_\alpha + \mathbf{l}_\beta$ and $\mathbf{J} = \mathbf{L} + 1/2\,\boldsymbol{\sigma}$ play the roles of the angular momenta $\mathbf{l}_1$ and $\mathbf{j}$, respectively (cf. Sec. 1). Therefore,

$$R_J^- = (2L+1)^{-1}(L - \sigma\mathrm{L}) = (2l^0+1)^{-1}(l^0 - \sigma\mathrm{L}),$$

---

*We use the notation introduced in reference 2: $\mathbf{p}$, $\mathbf{q}$, and $\mathbf{r}$ are unit vectors parallel, respectively, to the initial and to the two final relative momenta. Unlike reference 2, we denote the corresponding angular momenta by $\boldsymbol{l}^0$, $\boldsymbol{l}_\alpha$ and $\boldsymbol{l}_\beta$ respectively. The following abbreviations are also used: $\tilde{\mathbf{P}} = \mathbf{p}\times\mathbf{r}$, $\mathbf{P}_x = \mathbf{r} - \mathbf{p}(\mathbf{p}\cdot\mathbf{r})$. The angular operators of reference 2 will be denoted by Roman numerals I, II or III (the numbers of the tables) and the number giving the location of the operator in the table. For example, $(\mathrm{I}.4) = (4\pi)^{-3/2}\{l_\beta P_{l_\beta} - i\boldsymbol{\sigma}\cdot\mathbf{P}_y P_{l_\beta}'\}$, where P_{l_β} depends on $\mathbf{p}\cdot\mathbf{r}$.

since in our case $L = l_\beta = l^0$. Furthermore,

$$\mathbf{L} = -i\left[\mathbf{q}\times\frac{\partial}{\partial\mathbf{q}}\right] - i\left[\mathbf{r}\times\frac{\partial}{\partial\mathbf{r}}\right]$$

and consequently,

$$R_J^- \mathscr{L} = \sqrt{3}\,(4\pi)^{-3/2}\,[l_\beta(l_\beta+1)]^{-1/2}\{il_\beta\,\mathbf{P}_y\mathbf{q}\,P_{l_\beta} + ((\sigma\mathbf{r})(\mathbf{pq}) - (\sigma\mathbf{q})(\mathbf{pr}))\,P'_{l_\beta} + (\sigma\mathbf{P}_y)(\mathbf{P}_y\mathbf{q})\,P''_{l_\beta}\}. \tag{22}$$

which coincides with (II.8).

3. In this example we consider the case where the final angular momenta are coupled differently, so that j_α (where $j_\alpha = l_\alpha + \frac{1}{2}\sigma$) and not L is defined. In this case the quantities l_α, l_β, j_α and J play the role of the angular momenta l_1, l_2, j_1 and j_{12}. For example, according to formula (16), the operator (III.10), which is defined by the quantum numbers $J = l_\beta - \frac{1}{2} = l^0 - \frac{1}{2}$, $l_\alpha = 1$, $j_\alpha = \frac{3}{2}$, $l^0 = l_\beta$, should be equal to $({}^+\kappa^-)^{-1/2} R^+_{j_\alpha} \times R_J \mathscr{L}$, where

$${}^+\varkappa^-_\alpha = \frac{-(1-L+1)(1-L) + l_\beta(l_\beta+1)}{2L(2l_\alpha+1)} = \frac{2l_\beta - 1}{3l_\beta}.$$

We note that the projection operator R_J^- coincides with the operator R_J^- of the preceding example, so that to calculate (III.10) we need only apply the operator $({}^+\kappa^-)^{-1/2} R^+_{j_\alpha}$ to (II.8). We have

$$R^+_{j\alpha}\,(\mathrm{II.\,8}) = 1/\sqrt{3}\,(4\pi)^{-3/2}[l_\beta(l_\beta+1)]^{-1/2} \times \{(i(2l_\beta-1)\mathbf{P}_y\mathbf{q} - (l_\beta-2)(\sigma\mathbf{r})(\mathbf{pq}) - (\sigma\mathbf{q})(\mathbf{pr}) + l_\beta(\sigma\mathbf{p})(\mathbf{qr}))\,P'_{l_\beta} + 3((\sigma\mathbf{P}_y)(\mathbf{P}_y\mathbf{q}) - \sigma\mathbf{q}(1-(\mathbf{pr})^2)\,P''_{l_\beta}\}. \tag{23}$$

Multiplying this expression by $({}^+\kappa^-)^{-1/2}$, we get the required angular operator in quite simple form. It is clear that these calculations are not very difficult and can be carried out almost automatically. By using the properties of Legendre polynomials (cf. reference 8), one can verify that the result agrees with (III.10) within a sign.

In conclusion, the authors express their thanks to S. M. Bilen'kiĭ, V. I. Ritus and R. M. Ryndin for valuable comments.

APPENDIX 1

We prove that the operator $R_{j_1^0 m}$ in (13) is irrelevant, i.e., we prove the relation

$$R_{j_{1m}}\mathscr{L}\begin{pmatrix}1 & 0\\ 0 & 1\end{pmatrix}R_{j^0_{1m}} = R_{j_{1n}}\mathscr{L}\begin{pmatrix}1 & 0\\ 0 & 1\end{pmatrix}. \tag{A1.1}$$

First of all we must show that the projection operators for the initial state have the same form as those for the final state. Since the final operators act from the left on vectors $|\rangle$, while the initial ones act from the right on vectors $\langle|$, the initial operators are obtained from the final ones by Hermitian conjugation. Since the operators σ and l are Hermitian, we have, for example,

$$R^-_{j_0} = \frac{(l^0 - \sigma \mathbf{l}^0)}{(2l^0+1)}. \tag{A1.2}$$

We note that, in practical calculations, when l^0 is expressed in terms of differential operators, it is necessary to express l in terms of $\overleftarrow{\partial}/\partial x$ and not in terms of $\overrightarrow{\partial}/\partial x$. From the well-known identity

$$\overleftarrow{\partial}/\partial x = -\overrightarrow{\partial}/\partial x$$

we have

$$\mathbf{l}^0 = -i\left[\mathbf{r}\times\frac{\overrightarrow{\partial}}{\partial\mathbf{r}}\right] = -i\left[\frac{\overleftarrow{\partial}}{\partial\mathbf{r}}\times\mathbf{r}\right].$$

We may therefore also write

$$R^-_{j^0} = \frac{l^0 + i\,[(\overleftarrow{\partial}/\partial\mathbf{r})\,\mathbf{r}]}{(2l^0+1)}.$$

The same result applies for $R^+_{j^0}$.

To prove (A1.1) independently of the specific form of $\mathscr{L}$, it is convenient to shift the operator $R_{j_1^0 m}$ in (A1.1) to the left side of $\mathscr{L}$ and to compute the product $R_{j_1 n} R_{j_1^0 m}$. To do this we transform the initial state of the angular operator as follows:[*]

$$|\tilde{a}\rangle = (\langle a|U^+)^T, \tag{A1.3}$$

where, in the l, m representation, the matrix U has the form

$$U_{m,m'} = (-1)^{l-m}\delta_{m,-m'},$$
$$U = U^*, \qquad U^{-1} = U^T = U^+. \tag{A1.4}$$

After the transformation (A1.3), the angular operator

$$\mathscr{L} = \sum_{m=-l}^{l} |l, m\rangle\langle l, m|$$

assumes the form

$$\mathscr{L}^\sim = \sum_m (-1)^{l-m}|l, m\rangle|\widetilde{l, -m}\rangle = \sqrt{2l+1}\sum_m C_{00}^{lml-m}|lm\rangle|\widetilde{l, -m}\rangle. \tag{A1.5}$$

In the space of the functions $|\widetilde{l, m}\rangle$, the orbital angular momentum operator is $-\widetilde{l^0}$, where[†]

---

[*] The properties of the transformation (A1.3) are investigated, for example, in references 9 and 10.

[†] In the general case, $\tilde{A} = UA^{+T}U^T$. In fact, from $|a\rangle = A|b\rangle$, we get $|\tilde{a}\rangle = UA^{+T}U^T|\tilde{b}\rangle$. Thus, because of the Hermitian conjugation, the operation ~ is nonlinear: $\widetilde{aA+bB} = a^*\tilde{A} + b^*\tilde{B}$ (σ_x, σ_y, and σ_z are to be treated as complex coefficients). However, in the case of $R_{j^0_{1m}}$, the nonlinear part of the transformation has already been carried out, since $R_{j_{1m}}$ acts on the vector $\langle a| = \langle b|R$. From this and from (A1.5) it follows that $|\tilde{a}\rangle = UR^{0T}U^T|\tilde{b}\rangle$. For this reason we can treat the complex combinations l_+, l_-, l_0 in (A1.7).

$$\widetilde{\mathbf{l}}^0 = U\mathbf{l}^{0T} U^x. \qquad (A1.6)$$

In fact,

$$(\widetilde{l}^0_z)_{mm'} = U_{mr}(l_z^{0T})_{rs}(U^T)_{sm'} = (-1)^{l-m}\delta_{m,-r}(l_z^{0T})_{rs}$$
$$\times\,\delta_{m,-s}(-1)^{l-m'} = (-1)^{2l+m+m'}(-m\delta_{mm'}) = -(l_z^0)_{mm'},$$
$$(\widetilde{l}^0_x \pm i\widetilde{l}^0_y)_{m\,1,m} = -(l_x^0 \pm il_y^0)_{m\pm 1,m}. \qquad (A1.7)$$

We can therefore write (A1.1) in the form

$$R_{j_{1n}}\begin{pmatrix}1 & 0\\ 0 & 1\end{pmatrix}\widetilde{R}_{j^0_{1m}}\mathscr{L}^{\sim} = R_{j_{1n}}\mathscr{L}^{\sim}, \qquad (A1.8)$$

where

$$\widetilde{R}^{\pm}_{j^0_{1n}} = \frac{(j^0_{1m} + {}^1/_2 \pm \sigma\widetilde{\mathbf{l}}^0_{1m})}{(2l^0_{1m}+1)} = \frac{(j^0_{1m} + {}^1/_2 \mp \sigma\mathbf{l}^0_{1m})}{(2l^0_{1m}+1)}.$$

It is important to note that the operator $-\sigma\cdot l^0_{1m}$ acts on $\mathscr{L}^{\sim}$ in the same way as $\sigma\cdot l_{1n}$. In fact $\mathscr{L}^{\sim}$ is an eigenfunction of the operator $\mathbf{L}^2 = (l_{1n} + l^0_{1m})^2$ with eigenvalue $L(L+1)$ equal to zero. Using the formula

$$L_i\psi^m_L = (-1)\sqrt{L(L+1)}\,C^{Lm+i1-i}_{Lm}\,\psi^{m+i}_L,$$

we have $\mathbf{L}\mathscr{L}^{\sim} = 0$, and consequently,

$$\sigma\mathbf{l}_{1n}\mathscr{L}^{\sim} = -\sigma\mathbf{l}^0_{1m}\mathscr{L}^{\sim}.$$

Therefore

$$R_{j_{1m}}\widetilde{R}_{j^0_{1m}}\mathscr{L}^{\sim} = R^2_{j_{1n}}\mathscr{L}^{\sim} = R_{j_{1n}}\mathscr{L}^{\sim}, \qquad (A1.9)$$

which was required. The last equality follows directly from the definition of a projection operator.

APPENDIX 2

Let us prove the relation

$$P_{l_{1i+1}}R_{j_{1i}}P_{l_{1i+1}}R_{j_{1i+1}} = \varkappa_i P_{l_{1i+1}}R_{j_{1i+1}} \qquad (A2.1)$$

and find the explicit form of κ. Using formulas (7) and (12), and the fundamental property of projection operators,

$$P^2_{j_{1i+1}} = P_{j_{1i+1}},$$

we can bring the left side of (A2.1) step by step to the form

$$P_{j_{1i+1}}P_{l_{1i+1}}R_{j_{1i}}P_{l_{1i+1}}P_{j_{1i+1}}.$$

For the proof of (A2.1) we must consider the expression

$$P_{j_{1i+1}}P_{l_{1i+1}}\sigma\mathbf{l}_{1n}P_{l_{1i+1}}R_{j_{1i+1}}$$

and determine how it acts on an arbitrary wave function. The projection operators $P_{j_{1\,i+1}}$ and $P_{l_{1,i+1}}$ preserve only that part of any wave function which is an eigenfunction of the operators $j^2_{1,i+1}$, $l^2_{1,i+1}$ and $\frac{1}{4}\sigma^2$, with eigenvalues equal to $j_{1,i+1}(j_{1,i+1}+1)$, $l_{1,i+1}(l_{1,i+1}+1)$ and $\frac{3}{4}$, respectively. Thus our problem reduces to the calculation of the matrix element

$$\langle l_{1i}\,l_{i+1}\,l_{1i+1}\,\tfrac{1}{2}\,j_{1i+1}|\,\sigma\mathbf{l}_{1i}\,|\,l_{1i}\,l_{i+1}\,l_{1i+1}\,\tfrac{1}{2}\,j_{1i+1}\rangle.$$

The explicit form of this matrix element is given in reference 6, formula (3.101):

$$\langle l_{1i}\,l_{i+1}\,l_{1i+1}\,\tfrac{1}{2}\,j_{1i+1}|\,\sigma\mathbf{l}_{1i}\,|\,l_{1i}\,l_{i+1}\,l_{1i+1}\,\tfrac{1}{2}\,j_{1i+1}\rangle$$
$$= \frac{l_{1i}(l_{1i}+1) - l_{i+1}(l_{i+1}+1) + l_{1i+1}(l_{1i+1}+1)}{2l_{1i+1}(l_{1i+1}+1)}$$
$$\times\{j_{1i+1}(j_{1i+1}+1) - l_{1i+1}(l_{1i+1}+1) - \tfrac{3}{4}\}.$$

Now, starting from formula (12), we can write the left side of (A2.1) as

$$\Big[\frac{j_{1i}+{}^1/_2}{2l_{12}+1} \pm \frac{l_{1i}(l_{1i}+1) - l_{i+1}(l_{i+1}+1) + l_{1i+1}(l_{1i+1}+1)}{(2l_{1i}+1)\,2l_{1i+1}(l_{1i+1}+1)}$$
$$\times\{j_{1i+1}(j_{1i+1}+1) - l_{1i+1}(l_{1i+1}+1) - \tfrac{3}{4}\}\Big]P_{l_{1i+1}}R_{j_{1i+1}}.$$

It is clear that, depending on the choice of $j_{1i} = l_{1i} \pm \frac{1}{2}$ and $j_{1,i+1} = l_{1,i+1} \pm \frac{1}{2}$ we get the four values ${}^{\pm}\kappa^{\pm}_{l}$ given in the text.

---

[1] V. I. Ritus, JETP **32**, 1536 (1957), Soviet Phys. JETP **5**, 1249 (1957).

[2] S. Ciulli and J. Fischer, Nuovo cimento **12**, 264 (1959).

[3] Biedenharn, Blatt, and Rose, Revs. Modern Phys. **24**, 249 (1952); J. M. Blatt and L. C. Biedenharn, Revs. Modern Phys. **24**, 258 (1952).

[4] S. Ciulli and J. Fischer, Compt. rend. **249**, 1090 (1959).

[5] J. Fischer and S. Ciulli, Recurrent Construction of Angular Operators, preprint, Joint Institute for Nuclear Research, 1959.

[6] B. Condon and G. Shortley, Theory of Atomic Spectra, Cambridge, 1935.

[7] J. V. Lepore, Phys. Rev. **79**, 137 (1950).

[8] P. M. Morse and H. Feshbach, Methods of Theoretical Physics, McGraw-Hill, New York, 1953, p. 1325; E. Madelung, Die mathematischen Hilfsmittel des Physikers, Berlin, 1950, p. 104.

[9] U. Fano and G. Racah, Irreducible Tensorial Sets, Academic Press, New York, 1959.

[10] A. R. Edmonds, Angular Momentum in Quantum Mechanics, Princeton, New Jersey, 1957.

Translated by M. Hamermesh
338

SOVIET PHYSICS JETP VOLUME 11, NUMBER 6 DECEMBER, 1960

CRITICAL VELOCITY FOR RADIATION OF LIGHT IN OPTICALLY ANISOTROPIC MEDIA

I. M. FRANK

P. N. Lebedev Physics Institute, Academy of Sciences, U.S.S.R.

Submitted to JETP editor December 21, 1959

J. Exptl. Theoret. Phys. (U.S.S.R.) 38, 1751-1757 (June, 1960)

The radiation of an optical source characterized by an arbitrary frequency which moves uniformly in an optically anisotropic transparent medium is considered. The phase velocity, the velocity along the ray, and the group velocity of the radiation produced by such a source are investigated.

THE theory of the Cerenkov effect in crystals was developed as far back as 1940.[1] A number of interesting features of this radiation in optically anisotropic media (which have still not been investigated experimentally) have been pointed out in theoretical papers.[2,3] In recent years the Doppler effect in optically anisotropic media has also been analyzed theoretically.[4] The general features of radiation produced by various kinds of optical sources moving uniformly in refractory media have also been treated.[5] The critical velocity required by such sources for the production of various forms of radiation (Cerenkov radiation, complex Doppler effect, etc.) has been studied in detail only for an isotropic medium;[6] the case of an anisotropic medium has received only brief treatment.[5] In the present paper this problem is considered in greater detail.

In an optically isotropic medium, Cerenkov radiation is produced at a frequency ω when the velocity of the charge reaches the phase velocity of light $u(\omega) = c/n(\omega)$ for this frequency. This familiar condition comes directly from the relation between the frequency of the Cerenkov radiation and the direction of the wave vector:

$$(vn(\omega)/c)\cos\theta = 1. \tag{1}$$

The minimum value of the angle θ between the wave vector and the velocity is zero; consequently the minimum velocity is given by $v = u(\omega)$.

The phase velocity $u(\omega)$ is just as important for the radiation of an arbitrary source moving in an optically isotropic medium. The radiation spectrum of a uniformly moving system characterized by a frequency $\omega_0 = \omega_0'\sqrt{1-\beta^2}$ is given by[6]

$$k(\omega)\cos\theta = (\omega \pm \omega_0)/v, \quad k(\omega) = \omega n(\omega)/c = \omega/u. \tag{2}$$

Here $k(\omega)$ is the magnitude of the wave vector for frequency ω. In Eq. (2) the plus sign is taken for the so-called anomalous "superluminal" Doppler frequencies, if they are possible; the minus sign corresponds to the usual case of radiation in the medium. The Cerenkov radiation spectrum is obtained from Eq. (2) if we take $\omega_0 = 0$. If both sides of Eq. (2) are divided by ω, it becomes identical with Eq. (1) when $\omega_0 = 0$.

Equation (2) contains the phase velocity only, and is thus independent of the group velocity. This is natural, since the propagation of spectrally decomposed light, i.e., light at a given frequency ω, is determined completely by its phase velocity in an isotropic medium. Thus, the presence of a given frequency component in a spectrum (i.e., the conditions that must be satisfied for its production) depends on the phase velocity and not the group velocity. However, it is reasonable that the appearance of the radiation itself, not a given frequency component in the radiation, is to be associated with the group velocity.[5,6] It is reasonable to expect that the group velocity will play the same role for radiation in an optically anisotropic medium. However, the propagation of light in anisotropic media has a number of special features. For this reason the critical velocity of a radiator moving in an anisotropic medium requires special analysis.

An important factor in anisotropic media is that the phase velocity depends on the polarization of the wave as well as the direction of the vector $\mathbf{k}(\omega)$. We consider monochromatic waves of a given polarization, which propagate from some point. If we select waves for which the vector $\mathbf{k}(\omega)$ lies in a small solid angle (i.e., a narrow cone of normals to the wave surface), we find that the directional dependence of $k(\omega)$ is important as well as its magnitude. Because of this dependence, the direction of propagation of the waves, i.e., the direction of the ray, is not the same as the direction of the vector $\mathbf{k}(\omega)$. Hence the velocity $u'(\omega)$ is important; this is the velocity with which the phase of the wave is displaced in the direction of wave propagation, i.e., in the direction of the ray. Obviously, this velocity is given by

$$u'(\omega) = u(\omega)/\cos\alpha = c/n(\omega)\cos\alpha, \qquad (3)$$

where α is the angle between the ray and the normal to the wave (cf. Fig. 1).

If we lay off the velocity u' in the direction of wave propagation, i.e., in the direction of each ray, we obtain the so-called ray surface, which is the surface of constant phase for waves that emanate from a given center. In applying the Huygens principle to an anisotropic medium, the surface of the waves propagating from each point is actually obtained by plotting the ray surface to some appropriate scale. Thus, in problems involving the propagation of light in anisotropic media, the velocity u' plays the same role as the phase velocity in isotropic media. In particular, as is well known, the wave surface for Cerenkov radiation can also be obtained by means of the Huygens principle. It is not difficult to extend this procedure to an anisotropic medium and to verify in this case that the threshold for the appearance of a given frequency component ω is given by the relation $v = u'$.[5]

The analogy between u' and the phase velocity in an isotropic medium extends to the relation between u' and the group velocity w. If, from u' we form $k' = w/u'$, which is analogous to the wave vector, then

$$\partial k'/\partial\omega = 1/w, \quad k' = \omega/u' = k\cos\alpha. \qquad (4)$$

Actually u' is the velocity of propagation of phase in the direction of the ray; the group velocity is in the same direction, so that $\partial k'/\partial\omega$ must have the same significance as $dk/d\omega$ in an isotropic medium. In this case, as in an isotropic medium, the notion of a group velocity is meaningful only in the frequency region in which the optical absorption is small. We shall assume that this condition is satisfied in the case at hand.

Because of its properties, u' might be called the second phase velocity. We shall call it the ray velocity.

The velocity u' also has an independent meaning, since we do not actually deal with a plane wave with a precisely defined direction, because true monochromatic waves do not exist. Just as a wave packet in some small frequency range propagates with a group velocity w, a packet of monochromatic waves in some angular range defines a ray velocity u'. In order to obtain plane waves, each of which is characterized by a vector $\mathbf{k}$, it is necessary to perform a double expansion, i.e., in frequency and in direction. Each of these partial waves is then characterized by the vector $\mathbf{k}$, (i.e., by the frequency) and by the phase-velocity vector. Hence, Eqs. (1) and (2), which contain the phase velocity, can be generalized to the case of optically anisotropic media if by k we understand the magnitude of this vector for a frequency ω and for a given direction of the normal to the plane of waves with a given polarization.

It should be noted, however, that the magnitude of k depends on the angle θ. Hence, in determining the value of v necessary for the production of a frequency component ω, we cannot proceed as in the case of an isotropic medium, i.e., we cannot simply take $\theta = 0$. The point is that when θ changes the quantity $n(\omega)$ also changes; consequently the maximum value of $n(\omega)\cos\theta$, which determines the minimum value of v in Eq. (1), is not necessarily obtained when $\theta = 0$. Actually, the maximum value of this quantity occurs when $\theta = \alpha$, where α is the angle between the direction of the ray and the vector $\mathbf{k}$. Comparing Eqs. (1) and (3) we see now that $v = u'$.

The critical-velocity problem for radiation in optically anisotropic media can be understood by an analysis of Figs. 1 and 2.

In Fig. 1 we show the surface for the vectors $\mathbf{k}(\omega)$ for an optically inhomogeneous medium, for example for the extraordinary ray in a uniaxial crystal. If the $\mathbf{k}$ surface is given, it is easy to find the $\mathbf{k}'$ surface. To find the $\mathbf{k}'$ corresponding to a given $\mathbf{k} = \mathbf{k}_1 = \overrightarrow{OB}$, we lay off the plane tangent to the surface at the point B. Then the normal OB′ to this surface determines the

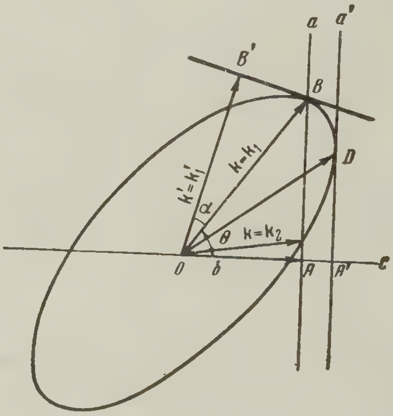

FIG. 1

magnitude and direction of the vector k'_1.*

It is easy to determine the directions of the vectors $\mathbf{k}(\omega)$ which satisfy Eq. (2) for a velocity v if we use the graphical construction proposed by Pafomov.[3,5] We assume that the velocity of the radiator with respect to the $\mathbf{k}$ surface is given by OC. In the direction OC we lay off a segment OA of length

$$b = (\omega \pm \omega_0)/v. \tag{5}$$

We assume here, as in Eq. (2), that the sign and magnitude of ω_0 are chosen in accordance with the conditions of the problem. For example, for ordinary Doppler frequencies we take ω_0 negative. If, in addition, $\omega < \omega_0$, the quantity b is negative and the segment OA must be laid off in the direction opposite to OC.

In order to find $\mathbf{k}$, we lay off the plane a, which passes through the point A and is perpendicular to the segment OA. This plane intersects the surface along some curve, which, as can be shown easily, represents the geometric locus of the ends of the $\mathbf{k}$ vectors which satisfy Eq. (2). For these vectors $k \cos\theta = b$, where θ is the angle between the given directions of $\mathbf{k}$ and $\mathbf{v}$ (cf. Fig. 1). Keeping in mind the value of b, we obtain Eq. (2) from Eq. (5) identically.

For fixed values of ω_0 and ω, b is inversely proportional to v. It is apparent that the plane a does not intersect the wave-vector surface for every value of b, that is, the frequency ω is not generated for every velocity. The critical velocity is obtained when plane a touches the surface. From Fig. 1 this condition corresponds to $b = OA'$, with plane a coinciding with a′. Under these conditions the $\mathbf{k}$ cone contracts about the direction OD. Since the plane a′ touches the surfaces at the point D, the normal to the plane, i.e., $b = OA'$, coincides with the direction of the ray conjugate to $k = OD$. In this case $b = k'$. Thus, from Eq. (5) we have

$$k'(\omega) = \frac{\omega}{u'^2}\mathbf{u}' = \frac{\omega \pm \omega_0}{v^2}\mathbf{v}. \tag{6}$$

In the particular case of Cerenkov radiation, i.e., for $\omega_0 = 0$, we immediately obtain from Eq. (5) the condition $\mathbf{v} = \mathbf{u}'$ for the critical velocity. Obviously Eq. (6) is a general condition which determines the velocity necessary for the appearance of a frequency component ω.[5] If b [right side of Eq. (6)] is positive, $\mathbf{u}'$ is in the same direction as $\mathbf{v}$. For negative values of b, these two vectors are in opposite directions. From Fig. (1), this condition corresponds to the case in which the plane a′ (tangent to the $\mathbf{k}$ surface) is to the left of the origin.

In the case shown in Fig. 1 the $\mathbf{k}$ surface is an ellipsoid. In order for a frequency component ω to appear in the spectrum the magnitude of b must be smaller than the corresponding radius vector of the ellipsoid, that is to say, v must be greater than some critical value. If the $\mathbf{k}$ surface were hyperbolic the reverse would hold. The quantity b would have to be greater than the corresponding radius vector and this means that the frequency component ω could be radiated only at a velocity smaller than the critical velocity.

In Fig. 1 we show the $\mathbf{k}$ surface for the extraordinary ray in a uniaxial crystal. In order to find the complete radiation pattern, a similar plot must also be made for the ordinary ray. In this case the $\mathbf{k}$ surface is a sphere, so that the cone of $\mathbf{k}$ vectors that satisfy Eq. (2) for the frequency ω is circular. As the velocity is reduced, this cone contracts about the direction of motion (or in the opposite direction for negative v). The critical velocity $v = u = u'$ for the ordinary rays differs from that for the extraordinary rays. The only exception is the case in which the radiator moves along the optical axis of the crystal.*

The radiation in a biaxial crystal exhibits a special feature. As is well known, the $\mathbf{k}$ surface cannot be represented by two independent surfaces in this case. The surface is more complicated in a biaxial crystal. However, a construction similar to that shown in Fig. 1 results in two $\mathbf{k}$ cones. The threshold velocities necessary for the production of each of these radiation cones are different, and when the velocity approaches the critical velocity the corresponding cone contracts about the direction of the $\mathbf{k}$ vector conjugate to the ray directed along the velocity (or opposite to it). Just as in a uniaxial crystal, each direction of the **k** vector for waves of a given polarization is associated in this case with one direction of the ray, and vice versa.

---

*It is easy to verify this construction. For small deviations of the vector $\mathbf{k}$ from $\mathbf{k}_1$, the end of the former slides along a plane which is tangent at point B. Hence the projection of vector $\mathbf{k}$ on OB′ is not sensitive to small changes in the wave vector. Whence it follows that the phases of a packet of plane waves characterized by vectors $\mathbf{k}$ which are almost in the direction of $\mathbf{k}_1$ are the same along the axis OB′. Thus interference effects cause addition of these waves in the direction OB′, i.e., $k'_1 = \overrightarrow{OB'}$ is a ray which corresponds to the normal to the plane of the wave in the direction of $\mathbf{k}_1$.

*It should be recalled that Eq. (2) only gives possible directions for the vector $\mathbf{k}$ for radiation at a given frequency. For an actual radiation source the wave amplitudes for certain directions of $\mathbf{k}$ or even for the entire $\mathbf{k}$ cone can be zero. For example, in Cerenkov radiation, dipole radiation, or radiation from a linear multipole oriented in the direction of motion, there is no cone due to ordinary rays when the motion is parallel to the axis of the crystal, because waves of the appropriate polarization cannot be generated.

The above considerations apply in all cases, except for cases in which the direction of the ray or the **k** vector is close to one of the optical axes of the crystal. In these cases, features analogous to internal and external refraction appear. These are as follows. It is well known that a ray which coincides with the optical axis of a biaxial crystal is to be associated with a **k**-vector cone rather than a single **k**. Hence, if a radiator moves along the axis of the crystal and its velocity approaches the critical velocity, the **k** cone does not contract about one direction, in contrast with the usual case. The threshold in this case is the **k**-vector cone associated with the ray directed along the axis (this cone is common for both forms of radiation in the crystal).

There is also an analog for internal refraction. In a biaxial crystal there is a direction for the **k** vector close to the direction of the axis which contains a whole cone of rays rather than one ray. Hence, if this direction satisfies Eq. (2), propagation takes place in the direction of the generatrices of the cone which is associated with this **k**. It is apparent that in this case the light emanates from the crystal in the form of a parallel beam of finite thickness. This feature, which is a consequence of internal refraction, has been pointed out by Ginzburg.[1]

Up to this point we have discussed radiation at a definite frequency ω. From what has been said it follows that the ray in whose direction a given frequency ω first appears (or disappears) as v changes is in the direction of **v** (or is in the opposite direction if b is negative). Actually a spectrum of frequencies is always radiated. For each of the frequencies there is a characteristic radiation cone, and the frequency spectrum associated with a given form of radiation (for example the spectrum of ordinary or "superluminal" Doppler frequencies, or any component of the complex Doppler effect) occupies some finite solid angle.

We now consider the conditions under which a given form of radiation is produced and the frequency is not given. We first consider the case of radiation in the direction of a ray that coincides with the direction of motion. In Fig. 2 we show the dependence of k' on frequency ω for waves of a given polarization in a medium. The direction of the ray for which $k'(\omega) = k'_V(\omega)$ is taken to coincide with the direction of the velocity. In this same figure we draw lines corresponding to three possible values of b:

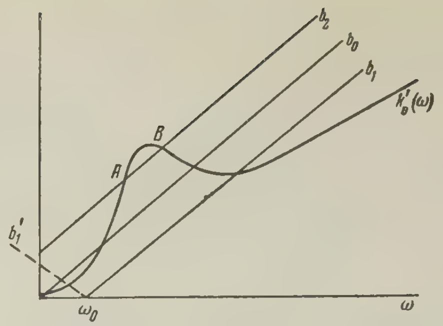

FIG. 2

$$b_0 = \omega/v, \; b_1 = (\omega - \omega_0)/v, \; b_2 = (\omega + \omega_0)/v. \qquad (7)$$

It is apparent that the intersections of these lines with the $k'_V(\omega)$ curve yields the frequencies that satisfy Eq. (6), i.e., the frequency components radiated along the ray in the direction of the velocity; these are the threshold frequencies for a given velocity. The intersections with the line b_0 gives the Cerenkov radiation frequencies; intersections with b_1 give the ordinary Doppler frequencies, with b_2 the "superluminal" Doppler frequencies.

Figure 2, as can easily be shown, is completely analogous to Fig. 1 of reference 6, which shows the features of radiation in an optically isotropic medium. The only difference is the fact that there the angle θ is arbitrary while here it is fixed in such a way as to give the direction of the ray (i.e., $\theta = \alpha$). The conclusions that can be obtained from an analysis of the curves will obviously be the same in both cases. They are the following. The slope of $k'_V(\omega)$ is, in accordance with Eq. (4), $dk'_V/d\omega = 1/w$. Here w is the group velocity for frequency ω for a ray in the direction of the velocity. The slope of the line b is 1/v. When v changes the slope of the line changes and the point at which it intersects the curve is displaced, that is to say, the threshold frequency is changed. The intersection vanishes or appears for those values of v for which the line b is tangent to the $k'_V(\omega)$ curve. In order for the line b to be tangent it is necessary that at the point of tangency the slope of $k'_V(\omega)$, i.e., $dk'_V(\omega)/d\omega$, be equal to 1/v. Thus, the production of radiation or new components requires that

$$v = w(\omega_{\lim}), \qquad (8)$$

where $\omega_{\lim}$ is the frequency which first appears in the radiation spectrum [this frequency must satisfy Eq. (6)].

The quantity b_1 can be negative if $\omega < \omega_0$. In this case, in Eq. (6) we must substitute $k'(\omega)$ for a ray directed in the direction opposite to the velocity and make $k'(\omega)$ negative. Changing the signs on both sides of Eq. (6), we then obtain

$$k'_{-v}(\omega) = (\omega_0 - \omega)/v. \tag{6a}$$

Here $\mathbf{k}'_{-\mathrm{v}}(\omega)$ is the vector $\mathbf{k}'$ for the ray directed opposite to the velocity vector. If a reversal of direction of the ray does not change the magnitude of $\mathbf{k}'$, as is the case in a usual medium, the solution of Eq. (6a) can again be found by means of Fig. 2. The sought Doppler frequency is obtained as the intersection of the line $b'_1 = (\omega_0 - \omega)/v$ (dashed line in Fig. 2) with the $k'_V(\omega)$ curve. As is apparent from the figure, an intersection of this kind always exists, corresponding to the obvious fact that in the ordinary Doppler spectrum there is a frequency component which can be radiated in the direction opposite to the direction of motion. In principle, more than one intersection is possible (complex Doppler effect). Just as for positive b, the threshold for the complex Doppler effect requires (beside intersection) that the line b_1 be tangent to the $k_{-V}(\omega)$ curve. Repeating the analysis given above we find that in this case the group velocity must be negative and equal to v. The negative sign means that the group velocity is opposite to the vector $\mathbf{k}'_{-\mathrm{V}}(\omega)$, i.e., the velocity. Thus, the condition for the appearance of a new radiation component is again given by Eq. (8).

All of these results are completely analogous to those obtained earlier for an isotropic medium (cf. references 5 or 6). If we consider the possible intersections of the lines b with the $k'_V(\omega)$ curve it is apparent (as in an isotropic medium) that the presence of a frequency ω' for which $w(\omega') < v$ means that there must also be a frequency ω'' for which $w(\omega'') > v$, that is to say, the composition of the radiation is necessarily complex. Let us assume that at the point of intersection of the line b with the $k'_V(\omega)$ curve the curve rises more sharply than the line, i.e., $dk'_V/d\omega = 1/w > 1/v$ (cf. for example point A on the line b_2). This means that at the point of intersection the line moves from the region above the $k'_V(\omega)$ curve into the region of the plane under the $k'_V(\omega)$ curve. Then, at higher frequencies there must be at least one intersection for which $dk'_V/d\omega = 1/w < 1/v$ (point B in Fig. 2). At this intersection, the line moves from the region under the curve to the region above the curve. That this is true follows from the fact that for sufficiently high ω the tangent to the $k'_V(\omega)$ curve approaches 1/c (in the limit $n = 1$ and $\alpha = 0$) and, since $1/c < 1/v$, all lines b for high ω must be above the $k'_V(\omega)$ curve.

We may note that the meaning of the provisional term "complex radiation" for an anisotropic medium is somewhat different than the meaning of this term for an optically isotropic medium. In an isotropic medium complex radiation means that there are several frequency components for a set of values of v, ω_0, and θ. In the anisotropic medium there are two radiation cones for the two polarization directions. In addition, there are two other possibilities: waves at different frequencies may have the same directions for $\mathbf{k}$, i.e., coincident wave normals, or waves at different frequencies may have the same ray directions. As is apparent from the above, here we have considered the case in which the several frequencies for a given form of radiation are characterized by the same ray direction.

In this paper we have considered only the particular case in which the direction of the ray coincides with the direction of the velocity (or is opposite to it). Complex radiation effects are obviously also possible for other ray directions.

---

[1] V. L. Ginzburg, JETP **10**, 608 (1940).

[2] B. M. Bolotovskiĭ, Usp. Fiz. Nauk **62**, 201 (1957).

[3] V. E. Pafomov, Dissertation, Inst. Phys. Acad. Sci., 1957.

[4] K. A. Barsukov and A. A. Kolomenskiĭ, J. Tech. Phys. (U.S.S.R.) **29**, 954 (1959), Soviet Phys.-Tech. Phys. **4**, 868 (1960). K. A. Barsukov, JETP **36**, 1485 (1959), Soviet Phys. JETP **9**, 1052 (1959).

[5] I. M. Frank, Usp. Fiz. Nauk **68**, 397 (1959).

[6] I. M. Frank, JETP **36**, 823 (1959), Soviet Phys. JETP **9**, 580 (1959).

Translated by H. Lashinsky
339

SOVIET PHYSICS JETP VOLUME 11, NUMBER 6 DECEMBER, 1960

ALPHA-DEUTERON MODEL OF THE LI^6 NUCLEUS

T. I. KOPALEĬSHVILI, I. Sh. VASHAKIDZE, V. I. MAMASAKHLISOV, and G. A. CHILASHVILI

Institute of Physics, Academy of Sciences, Georgian S.S.R.

Submitted to JETP editor December 19, 1959

J. Exptl. Theoret. Phys. (U.S.S.R.) **38**, 1758-1764 (June, 1960)

On the assumption that the nucleons in the Li^6 nucleus are predominantly grouped in subsystems in the form of an alpha particle and a deuteron, the energy of the relative motion of these subsystems is calculated and it is shown that it has a minimum in the region of negative values. The energy of the O^+, $T = 1$ excited state of the Li^6 nucleus is also determined.

1. It is known that each nucleon in a nucleus can be regarded in first approximation as moving in a certain average field of the other nucleons. Recently it has become clear, however, that for a better description of the properties of nuclear matter one should take account more carefully of the interaction of the nucleons. In the uniform theory of the nucleus which was developed as a result of this consideration, this interaction is taken into account by considering the collective motions of the whole nucleus, while in the many-body theory which was developed for the case of the nucleus system by Brueckner and Bethe, the approximation which gives the average field consists in the introduction of the so-called correlated pairs. However, for the validity of either theory it is necessary that the number of nucleons in the nucleus be sufficiently large.

In the case of the lightest nuclei, containing only a few nucleons, the collective description is not applicable, and it is not excluded that the effect of the interaction may with good probability result in the formation within the nucleus of individual internally-bound subsystems. In other words, in the case of the lightest nuclei one of the possible ways for taking account of the interaction of the nucleons, more rigorously than is done by introducing an overall average field with a single center of symmetry, may consist in the assumption that the nucleons within such a nucleus are bound into separate groups with a center of symmetry in each of these groups. In addition, it is known that temporary agglomerations of nucleons occur preferentially in the surface layer of the nucleus. Since, as we go toward light nuclei, the relative importance of surface effects increases, it should be expected that in them these agglomerations of nucleons forming substructures will have relatively higher stability.

Recently many investigators[1-6] have called attention to the idea of the existence of substructures within atomic nuclei in the form, for example, of deuterons, tritons, and alpha particles. Of course, the original assumption that there exist in the nucleus alpha particles in the form of stable and unchangeable structural units is not applicable. However, it is entirely possible that the nucleons in light nuclei preferentially group themselves into alpha particles where the composition of each of these particles, because of the exchange of nucleons, is subjected to a continual change.

On the basis of this assumption, Biel[7] made a calculation of the binding energy of Be^8 and C^{12} and found satisfactory agreement with experiment for an appropriate choice of the mixture of Serber and symmetric forces. It should, however, be noted that all the work in this direction refers to light nuclei of the type 4n, containing 2, 3, or 4 alpha particles.

But, one asks, what can one say about a nucleus in which in addition to alpha particles there are two or three nucleons? Can one, for example, treat the Li^6 nucleus in some approximation as a system of an alpha particle and a deuteron, assuming consequently that the two extra nucleons beyond the alpha particle form a bound system in the form of a deuteron?

Before attempting to answer this question, we point out that from the non-existence of the nuclei He^5 and Li^5, it follows that one nucleon is not bound with the first closed shell consisting of two protons and two neutrons constituting an alpha particle. On the other hand, there exists the stable nucleus Li^6 containing two nucleons outside a closed shell.

In order to make these two results consistent one can adopt two assumptions: 1) the simultaneous joining of a proton and a neutron to the alpha particle results in the break-up of the latter and in the formation of a complicated system of six nucleons with new couplings; 2) in the formation of the Li^6 nucleus, the alpha particle is not broken up, but is effectively bound, not with each of the nucleons individually, but with the system of proton and neutron together.

The adoption of the second assumption enables one to make the natural conclusion that the proton and neutron outside the closed shell in the Li^6 nucleus should form a bound system. In fact, if these nucleons were independent of one another, then from the fact that each of them is not bound to the closed shell, it would follow that both nucleons simultaneously are not bound to this shell, which would imply the impossibility of formation of the Li^6 nucleus. The existence of the Li^6 nucleus means consequently that the proton and neutron in this nucleus are not independent of one another, but are in some bound state.

Later it will be shown that when there is a coupling between the two nucleons which are outside the closed shell in the Li^6 nucleus, the Schrödinger equation for the whole nucleus actually has a solution corresponding to a negative total energy. In connection with this, we investigate in the present paper the conditions of stability of a system of three protons and three neutrons forming subsystems with four and two nucleons respectively; in other words, we solve the problem of whether the energy of the relative motion of these subsystems has a minimum in the region of negative values of the energy and, if it does have such a minimum, whether the energy at the minimum corresponds to the binding energy of the two subsystems to one another as determined from data on the mass defect of the Li^6 nucleus.

2. Following Biel, we assume that both the forces between the two nucleons and their wave functions have a Gaussian shape, and we try to find the conditions under which the energy of the system of six nucleons in the Li^6 nucleus, which is divided into two subsystems which are individually bound in the form of an alpha particle and a deuteron and are continually interchanging nucleons, is a minimum. We also determine the parameters which characterize the Li^6 nucleus in its ground and excited states.

Each state of the nucleon will be expressed as a vector $\mathbf{i}(i_1, i_2, i_3)$, where i_1 denotes the spin of the nucleon and can take on two values: 1 or 2; i_2 is the isotopic spin of the nucleon also taking on values 1 and 2, and i_3 is equal to 1 or 2 indicating to which of the subsystems, alpha particle or deuteron, the given nucleon belongs.

It is obvious that there are altogether eight states: (111), (121), (211), (221), (112), (122), (212) and (222). We denote them respectively by the numbers 1, 2, 3 . . . 8. The six nucleons are to be distributed over these states. Without loss of generality we can assume that, for example, the first four nucleons fill the states 1, 2, 3, and 4 forming an alpha particle. The remaining two nucleons are distributed over the other four states: 5, 6, 7, and 8. The number of such distributions is obviously equal to six. These six distributions correspond to different states of the deuteron in the nucleus. These states will also correspond to states of the Li^6 nucleus as a whole since, by our assumption, for not too large excitations the alpha particle in the nucleus will always be in its ground state with a total spin and isospin equal to 0.

If we denote the total spin and isospin of the Li^6 nucleus by S and T and their projections, respectively, by M_S and M_T, these six distributions will correspond to states with $S = 1$, $T = 0$, $M_S = 0, \pm 1$ and $S = 0$, $T = 1$, $M_T = 0, \pm 1$. The first three of these states correspond to the normal state of the deuteron and determine the ground level of the Li^6 nucleus, while the other three correspond to a singlet state of the pair of nucleons. We assume that the singlet state of the nucleon pair forming the deuteron ($S = 0$, $T = 1$, $M_T = 0$), determines one of the excited states of the Li^6 nucleus. As for the remaining two states ($S = 0$, $T = 1$, $M_T = \pm 1$), they characterize the energies of the isobaric nuclei Be^6 and He^6. Ascribing the total angular momentum of the Li^6 nucleus to the spin of the deuteron, we assume that the orbital angular momentum of the relative motion of the deuteron and alpha particle in both the ground state and in the excited state which we are considering are equal to zero.

We write the antisymmetrized wave functions $\Psi = \Psi^{ST}_{M_S M_T}$, corresponding to given values of S, T, M_S and M_T in the form

$$\Psi^{10}_{10} = \sum_p \pm p\alpha^1_{11}\alpha^2_{12}\alpha^3_{21}\alpha^4_{22}\alpha^5_{11}\alpha^6_{12}\psi(1234; 56), \tag{1}$$

$$\Psi^{01}_{01} = \sum_p \pm p\alpha^1_{11}\alpha^2_{12}\alpha^3_{21}\alpha^4_{22}\alpha^5_{11}\alpha^6_{21}\psi(1234; 56), \tag{2}$$

where $\alpha^f_{i_1 i_2}$ are products of the spin and isospin wave functions of the nucleon f with given values of i_1 and i_2; $\psi(1234; 56)$ is the spatial part of the wave function of the Li^6 nucleus in which the first four indices correspond to nucleons in the alpha particle and the last two to the nucleons forming the deuteron; the summation extends over all permutations p of the superscripts, where the sign is determined by the parity of the corresponding permutation. We note that we have not introduced expressions for the other four functions $\Psi^{ST}_{M_S M_T}$ since they are not used in calculating the energy of the system.

Neglecting the Coulomb interaction of the protons, we have for the total Hamiltonian of the system

$$\hat{H} = -\frac{\hbar^2}{4}\left(\frac{1}{M_n} + \frac{1}{M_p}\right)\sum_i \nabla_i^2 + \sum_{i>j} V(i, j), \tag{3}$$

where M_n and M_p are the masses of the neutron and proton,

$$V(i, j) = (W + BP^{\sigma}_{ij} - \mathcal{H}P^{\tau}_{ij} - MP^{\sigma}_{ij}P^{\tau}_{ij})\,F(i, j), \tag{4}$$

where P^{σ}_{ij} and P^{τ}_{ij} are the Bartlett and Heisenberg exchange operators; W, B, $\mathcal{H}$ and M give the fractions corresponding to interactions of the Wigner, Bartlett, Heisenberg, and Majorana type; F(i, j) is the radial part of the nucleon-nucleon interaction.

Our problem consists in calculating the mean value of the energy

$$E = \int \Psi^* \hat{H} \Psi d\tau \Big/ \int \Psi^* \Psi d\tau, \tag{5}$$

and minimizing it with respect to the parameter appearing in Ψ. To obtain the energy in the ground state we must set $\Psi = \Psi^{01}_{01}$, while $\Psi = \Psi^{10}_{10}$ will determine the energy of one of the excited states of the Li^6 nucleus with angular momentum 0^+, close in energy to the isobaric nuclei He^6 and Be^6.

As mentioned earlier, we choose both the potential energy of the two nucleons and the spatial wave function of the system to have a Gaussian shape, i.e.,

$$\psi(1234; 56) = \exp\left\{-\tfrac{1}{2}\lambda s_{12}^2 - \tfrac{1}{2}\mu \sum_{i>j=1}^{4} r_{ij}^2 - \tfrac{1}{2}\nu r_{56}^2\right\}, \tag{6}$$

$$F(i, j) = V_0 \exp(-\beta r_{ij}^2), \tag{7}$$

where $\mathbf{r}_{ij} = \mathbf{r}_i - \mathbf{r}_j$, $\mathbf{s}_{12}$ is the radius-vector between the centers of the alpha particle and the deuteron. V_0 and β are taken from data on the scattering of nucleons by alpha particles and are equal[8] to $V_0 = -45$ Mev, $\beta = 0.266 \times 10^{26}\ \text{cm}^{-2}$; μ is determined from the binding energy of the alpha particle and is equal to $0.316 \times 10^{26}\ \text{cm}^{-2}$; λ is a variational parameter determining the equilibrium distance between the centers of the alpha particle and the deuteron. The coefficient ν which is a parameter in the trial function for the system of the two nucleons 5 and 6, forming a deuteron in the triplet state, is determined from the condition that the energy of this system for the given values of V_0 and β have a minimum. From this condition we find that $\nu = 0.150 \times 10^{26}\ \text{cm}^{-2}$.

We mention that with this value of ν the binding energy of the system consisting of the two nucleons 5 and 6 turns out to be negative and numerically equal to 0.41 Mev. Thus, the values of the parameters μ, ν, V_0 and β chosen by us lead to bound stable states of He^4 and H^2 with a binding energy of 27 Mev for the alpha particle and 0.41 Mev for the deuteron, instead of the experimental values of 28.1 and 2.2 Mev for the free alpha particle and deuteron.

One might get better agreement with experiment with regard to the binding energy of the deuteron and the nucleus at the expense of a slight change in the binding energy of the alpha particle, but this would require us to choose a somewhat different value for μ, different from that used by us and taken from reference 8. However, since we are interested not in the total energy of the Li^6 nucleus, but only in the difference $\epsilon(Li^6) = \epsilon(\alpha) - \epsilon(d)$, which gives the relative energy of alpha particle and deuteron, the use of an exact value of $\epsilon(d)$ is not significant. Besides, it can be shown that changing the binding energy of the deuteron within the limits considered has no essential effect upon the position of the minimum in the energy of the relative motion of the alpha particle and deuteron.

3. It is not possible to find the energy minimum analytically because of the complicated nature of the expressions. We therefore went over to a numerical method. In Fig. 1 we show the energy curves for the ground state of Li^6. Curve 1 corresponds to a Serber force and curve 2 to a symmetric force, where the ordinate is the difference $E(\lambda) - E(0)$, where $E(0)$ is the energy of the system when the alpha particle and the deuteron are at infinity. We see that the curves actually do have a minimum, which shows that the nucleon configuration in the Li^6 nucleus which we are considering is stable. Also, in both cases the minimum in the energy occurs at the same value, $\lambda = 0.0316 \times 10^{26}\ \text{cm}^{-2}$. For the corresponding val-

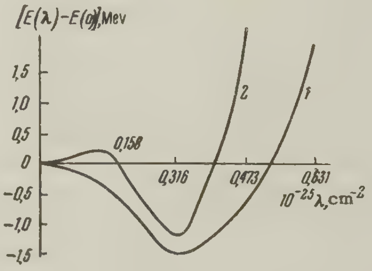

FIG. 1

ues of the energy in the case of the Serber forces we have -1.58 Mev, and for the case of the symmetric forces -1.42 Mev.

In treating the problem of Be^8 and C^{12}, Biel[7] obtained better agreement with experiment by assuming that the total nucleon-nucleon interaction consists of a mixture of Serber and symmetric forces with relative weights of 0.7 and 0.3. If we choose this same mixture for our case, the relation between the energy and the parameter λ has the form shown in Fig. 2. In this case the value obtained for the energy at the minimum is -1.52 Mev, which is in good agreement with the experimental value of the binding energy of the deuteron to the alpha particle in the Li^6 nucleus, as found from data on the mass defect and equal to -1.48 Mev. The value $\lambda = 0.0316 \times 10^{26}$ cm^{-2} corresponds to an equilibrium distance between the centers of the alpha particle and deuteron equal to 2.52×10^{-13} cm. Thus we see that the centers of gravity of the subsystems in the Li^6 nucleus are moved with respect to one another, while the distance between them exceeds their individual radii.

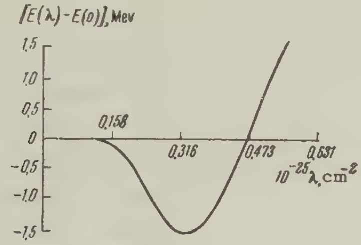

FIG. 2

Now let us consider the excited state of the Li^6 nucleus. Such a state, according to our model, can arise as a result of excitation in general of the alpha particle and of the deuteron and from their relative motion. But we know that the alpha particle has no bound states with excitation energy below 20 Mev, so that the observed levels of the Li^6 nucleus lying below 20 Mev cannot be the result of excitation of the alpha particle.

The wave function $\Psi^{01}_{0M_T}$ corresponds to a state of the Li^6 nucleus with $S = 0$ and $T = 1$. In the spectrum of the Li^6 nucleus the level with $T = 1$ which is a component of the isotopic triplet ($M_T = 0$) has an energy of 3.57 Mev.[9] The remaining components of the isotopic triplet ($M_T = \pm 1$) correspond to the ground states of the He^6 and Be^6 nuclei. Since this level corresponds to spin 0^+, in our model the transition from the ground state with angular momentum 1^+ to this excited state can occur only via a transition of the deuteron in the nucleus from a triplet state to a singlet state. In such a transition we must also consider the possibility of a change in the average energy of relative motion. Therefore the total change in energy will consist of two parts, one of which is caused by a change in the binding energy of the deuteron and the other by a change in the energy of relative motion.

In Fig. 3 we show the dependence of the difference in energy of relative motion $E^*(\lambda) - E^*(0)$ on the parameter λ for the case of a mixture of Serber and symmetric forces. This curve also has a minimum, where the energy at the minimum is 0.66 Mev. Using the fact that the energy of relative motion at the minimum in the ground state is equal to -1.52 Mev, we have 0.86 Mev for the change in this energy in the transition considered.

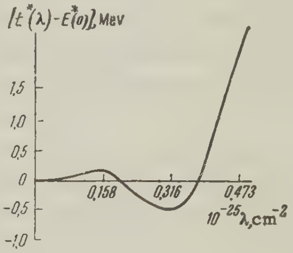

FIG. 3

As for the change in energy occurring as a result of a change in the spin state of the deuteron, our calculation shows that it is equal to 3.91 Mev. Thus, we obtain a value of 4.77 Mev for the total excitation energy of the Li^6 nucleus for the transition to the state $S = 0$, $T = 1$. This value differs somewhat from the experimental value of the energy of the corresponding level, which is 3.57 Mev.

We point out that if we chose for the change in energy of the deuteron when only the spin state changes the experimental value of 2.23 Mev, the total excitation energy would be 3.1 Mev, which would allow us to conclude that there is more or less satisfactory agreement with experiment. Consequently, the actual disagreement with experiment, though not insignificant if we consider the approximate nature of our calculations, leads to a discrepancy with experiment for the value of the change in internal energy of the deuteron in a transition to the singlet state.

This discrepancy is apparently caused by the fact that in both the ground and excited states we have used the same value of β, changing only the depth of the nucleon-nucleon interaction for the singlet state by 0.6. Actually the values of β for the singlet and triplet state differ markedly from one another. We were forced to proceed in this way because the variation of β in the transition from the triplet state to the singlet state could not be accounted for consistently in our calculations because of the presence of exchange integrals in the expressions for the potential energy. We therefore assigned an average value to the coefficient β throughout our calculations, this value being obtained from experimental data on the scattering of nucleons by alpha particles. As we see from this paper, this value of β together with $V_0 = -45$ Mev assures the stability of the He^4 nucleus and gives the correct value for its binding energy.

The average value of the coefficient β which we used differs little from its correct value in the triplet state of the deuteron, so that the shift to the average value should not essentially affect our calculations for the ground state of the Li^6 nucleus. For the excited state such a change may lead to a fundamental error since the value of the coefficient β in the singlet state is considerably different from its value in the triplet state. This error in our opinion also would lead to the result that we obtain 4.77 Mev for the excitation energy instead of the experimentally observed 3.57 Mev. It is possible also that the slight rise in the curves of Figs. 1 — 3 near the origin is due to an error in the choice of the value of the coefficient β.

In connection with the results obtained above, we should mention the following. In references 10 and 11 it is stated that the wave function of a nucleus of type 4n built up on the alpha particle model is identical, after antisymmetrization in all the nucleons, to the wave function in the single particle approximation. However, it is easy to see that such an identity is obtained only if, in the individual wave functions referring both to the internal state of the alpha particle and to the relative motion, the corresponding parameters of the oscillator functions coincide and are equal to the parameter appearing in the wave function of the single particle approximation. In the cited paper of Biel, the parameter in the wave function describing the relative motion of the alpha particles in the Be^8 nucleus is treated as a variational parameter, and by applying the condition for minimum energy it is shown that it is not equal to the parameter characterizing the internal state of the alpha particles. In the same way, as we see from (6), for the case of the Li^6 nucleus, the parameters appearing in the wave functions for the internal states of the alpha particle and deuteron and the wave function of their relative motion differ from one another. One can therefore conclude that our treatment preserves a definite individuality of the alpha particle and deuteron in the Li^6 nucleus and is not identical to a description of this nucleus in the single particle approximation.

In conclusion it is our duty to express our gratitude to the computing center of the Academy of Sciences of the Georgian S.S.R. in the persons of D. A. Kveselav and E. N. Dekanosidze, on the one hand, and to the computing center of the Academy of Sciences of the Armenian S.S.R. in the persons of of R. A. Aleksandryan and F. M. Ter-Mikaélyan on the other, for carrying out our requests for tabulation of functions and computation of a large number of fifth-order determinants.

---

[1] V. I. Mamasakhlisov, JETP **24**, 190 (1953); Trudy, Institute of Physics, Academy of Sciences, Georgian S.S.R. **3**, 31 (1955).

[2] P. Cüer and J. Combe, Compt. rend. **239**, 351 (1954).

[3] A. Herzenberg, Nuovo cimento **1**, 986, 1008 (1955); Nucl. Phys. **3**, 1 (1957).

[4] L. I. Schiff, Phys. Rev. **98**, 1281 (1955).

[5] V. I. Ostroumov and R. A. Filov, JETP **37**, 643 (1959), Soviet Phys. JETP **10**, 459 (1960).

[6] I. Sh. Vashakidze and G. A. Chilashvili, JETP **29**, 157 (1955).

[7] S. J. Biel, Proc. Phys. Soc. **A70**, 866 (1957).

[8] Hochberg, Massey, and Underhill, Proc. Phys. Soc. **A67**, 957 (1954).

[9] F. Ajzenberg and T. Lauritsen, Revs. Modern Phys. **27**, 77 (1955).

[10] J. K. Perring and T. H. R. Skyrme, Proc. Phys. Soc. **A69**, 600 (1956).

[11] K. Wildermuth and Th. Kanellopoulos, Nucl. Phys. **7**, 150 (1958); Nucl. Phys. **9**, 499 (1959).

Translated by M. Hamermesh
340

SOVIET PHYSICS JETP VOLUME 11, NUMBER 6 DECEMBER, 1960

MOTION OF NUCLEONS IN AN ANISOTROPIC OSCILLATOR POTENTIAL WITH ACCOUNT OF SPIN-ORBIT INTERACTION

D. V. VOLKOV and E. V. INOPIN

Physico-Technical Institute, Academy of Sciences, Ukr. S.S.R.

Submitted to JETP editor December 21, 1959

J. Exptl. Theoret. Phys. (U.S.S.R.) **38**, 1765-1770 (June, 1960)

A method is proposed for the calculation of the wave function and energy levels of nucleons moving in an oscillator potential. The general case of a potential which does not possess axial symmetry but in which account is made of spin-orbit interaction is considered. An essential feature of the calculations is that use is made of smallness of the spin-orbit coupling constant. In the limiting case of a strongly deformed nucleus the solution can be obtained in a simple analytical form. Investigation of this solution indicates that the spin-orbit interaction significantly affects the axial symmetry of the nucleus. Thus the axially symmetric shape of the nucleus becomes more stable and is the cause of the discontinuous nature of the transition from axial nuclei to nonaxial ones.

1. INTRODUCTION

THE question of the motion of a particle in an anisotropic oscillator potential with account of the spin-orbit coupling (s.o.c.) plays an important role in the treatment of bound states of individual nucleons by means of a generalized model. This problem was solved by Nilsson,[1] who calculated the wave functions and the eigenvalues of the nucleon energy for the axially-symmetrical case (two of the three oscillator frequencies coincide).

In connection with the theory of nonaxial nuclei, developed by Davydov and his co-workers, considerable interest attaches to an investigation of motion in an oscillator field in the general, nonaxial case (all three frequencies different).

Geĭlikman[3] calculated the equilibrium deformations of the nuclei, using the anisotropic oscillator model, and showed that the equilibrium form of the nucleus has no axial symmetry if the number of nucleons in excess of the filled shell (or holes in the shell) is more than two. No account of the s.o.c. was taken in these calculations. This raises the question of the extent to which the results of Geĭlikman are modified by allowance for the s.o.c. It is also clear that the s.o.c. should exert a significant influence on the wave functions of the nucleons, and must therefore be taken into account in the calculation of the magnetic and quadrupole moments of the nuclei, the β-decay half lives, and other quantities that characterize the nucleus.

In the present paper we propose a method of calculating the wave functions and eigenvalues of the energies of nucleons moving in an oscillator field for the general case of absence of axial symmetry and presence of s.o.c.

It must be noted that the method proposed here differs substantially from that of Nilsson. Nilsson employs the isotropic-oscillator representation and diagonalizes both the s.o.c. and the terms due to nonsphericity. In this connection, the matrix elements which are not diagonal in N (the principal quantum number of the shell for the isotropic oscillator) are discarded. Nilsson proposes an approximate method of allowing for these discarded elements. The inaccuracy connected with this approximation is of order ϵ_κ (ϵ is the nonsphericity parameter and κ is the parameter of the s.o.c.) and is comparable with the value of s.o.c. at not too small deformations. In addition, this method of allowing for the discarded terms is difficult to employ in many cases of practical importance (for example, to correct the wave functions).

The method we propose is based essentially on the smallness of the s.o.c. ($\kappa \approx 0.05$), which is diagonalized in the anisotropic-oscillator representation, and only terms of order κ^2 are discarded.

2. THE HAMILTONIAN

The Hamiltonian describing the motion of nucleons in a nuclear field with allowance for the s.o.c. has the form

$$H = H_0 + \lambda \mathrm{s}\,[\operatorname{grad} V(\mathbf{r}) \times \mathbf{p}], \qquad H_0 = \mathbf{p}^2/2 + V(\mathbf{r}), \tag{1}$$

where λ is the s.o.c. constant (we use a system of units in which $M = \hbar = 1$, M is the nucleon mass).

In the case of an anisotropic oscillator potential

$$V(\mathbf{r}) = \tfrac{1}{2} \sum_i \omega_i^2 x_i^2, \tag{2}$$

where in the general case all three parameters (frequencies) ω_1 are different and satisfy the supplementary condition $\omega_x \omega_y \omega_z = \omega_0^3 = \text{const}$. Substituting (2) in (1) we obtain

$$H = \tfrac{1}{2} \sum_i (p_i^2 + \omega_i^2 x_i^2) + \tfrac{1}{2} \lambda \sum_{ikl} \varepsilon_{ikl} \sigma_i \omega_k^2 x_k p_l, \tag{3}$$

where σ_i are the Pauli matrices.

The Hamiltonian (3) is conveniently rewritten in terms of the following representation for the operators x_k and p_k:

$$x_k = \frac{1}{\sqrt{2\omega_k}} (a_k^+ + a_k), \qquad p_k = i \sqrt{\frac{\omega_k}{2}} (a_k^+ - a_k), \tag{4}$$

where a_k and a_k^+ are known operators with commutation relations

$$[a\ , a_l^+] = \delta_{kl}, \qquad [a_k, a_l] = [a_k^+, a_l^+] = 0. \tag{5}$$

In the representation considered here the operator H has to form

$$H = \frac{1}{2} \sum_i \omega_i (a_i a_i^+ + a_i^+ a_i) + i\varkappa \sum_{ikl} \varepsilon_{ikl} \sigma_i f_{kl} a_k^+ a_l$$
$$+ \frac{i\varkappa}{2} \sum_{ikl} \varepsilon_{ikl} \sigma_i g_{kl} (a_k a_l - a_k^+ a_l^+), \tag{6}$$

where $\kappa = -\lambda\omega_0/2$ is the dimensionless s.o.c. parameter

$$f_{kl} = \frac{\omega_k + \omega_l}{2\omega_0} \sqrt{\omega_k \omega_l}, \qquad g_{kl} = \frac{\omega_k - \omega_l}{2\omega_0} \sqrt{\omega_k \omega_l}.$$

We see from (6) that the s.o.c. operator breaks up into two terms, containing the operators a_i^+ and a_k, respectively, in the combinations $a_k^+ a_l$ and $a_k a_l - a_k^+ a_l^+$.

We can use perturbation theory to estimate the role of these terms. In the second approximation of perturbation theory, terms of the type $a_l^+ a_k$ lead to energy denominators of the form $\omega_l + \omega_k$, which can vanish only in the limiting case as ω_k and $\omega_l \rightarrow 0$; but in this case, as is readily seen from (6), the numerator will also tend to 0, and much faster than the denominator at that. This difference in the behavior of the energy denominators, together with the smallness of the s.o.c. constant ($\kappa \sim 0.05$), makes it possible to neglect, with sufficiently good degree of accuracy (up to quantities of order κ^2) the terms containing $a_l a_k - a_l^+ a_k^+$ in the s.o.c. operator. In this approximation, the Hamiltonian has the form

$$H = \tfrac{1}{2} \sum_i \omega_i (a_i a_i^+ + a_i^+ a_i) + i\varkappa \sum_{ikl} \varepsilon_{ikl} \sigma_i f_{kl} a_k^+ a_l. \tag{7}$$

Because all the operators a_i and a_k^+ enter into the Hamiltonian only in pairs of the form $a_i^+ a_k$, the matrix elements for states with different values of N (the principal quantum number of the shell) vanish, and the determination of the eigenvalues of the Hamiltonian (7) reduces to diagonalization of matrices with a finite number of dimensions for each specific value of N.

In the diagonalization of the Hamiltonian in the representation of the anisotropic oscillator without the s.o.c., the basis vectors will be denoted by $|n_x n_y n_z \pm\rangle$ (the signs ± correspond to spin projections $\pm 1/2$). The matrix elements of the operators a_k are determined here by the relations

$$a_x | n_x n_y n_z \pm\rangle = \sqrt{n_x}\, | n_x - 1 n_y n_z \pm\rangle,$$
$$a_x^+ | n_x n_y n_z \pm\rangle = \sqrt{n_x + 1}\, | n_x + 1 n_y n_z \pm\rangle$$

and analogously for a_y, a_y^+, a_z, and a_z^+. The solution of the Schrödinger equation with fixed N can be written in the form

$$\Psi_N = \sum_{n_x + n_y + n_z = N} C_{n_x n_y n_z \pm} | n_x n_y n_z \pm\rangle. \tag{8}$$

If we take into account the invariance of the Hamiltonian under rotation through an angle π about the principal axes of the ellipsoid (symmetry group D_2) and under the transformation $x_i \rightarrow x_i$, $p_i \rightarrow -p_i$, $\sigma_i \rightarrow -\sigma_i$, connected with time inversion, we find that each energy level corresponds to two solutions $\Psi_N^{(+)}$ and $\Psi_N^{(-)}$. Here the functions $\Psi_N^{(+)}$ contain only the basis vectors corresponding to the eigenvaluesof the operator $U_z = \sigma_z (-1)^{n_x + n_y}$ of rotation through an angle π about the z axis, equal to +1, while the function $\Psi_N^{(-)}$ contains vectors corresponding to the eigenvalue −1. In addition, it is found that the coefficients C, which determine these functions, are connected by the relation

$$C^{(+)}_{n_x n_y n_z \pm} = \pm (-1)^{N - n_y} C^{(-)}_{n_x n_y n_z \mp} \tag{9}$$

and have the form

$$C^{(+)}_{n_x n_y n_z \pm} = i^{n_y} A_{n_x n_y n_z \pm}, \tag{10}$$

where $A_{n_x n_y n_z}$ are real numbers.

Thus, each solution is characterized by a definite number N (N = 0, 1, 2, . . .). For a given N, there are (N + 1)(N + 2) basis vectors $|n_x n_y n_z \pm\rangle$. The diagonalization of the Hamiltonian in this representation makes it possible to construct the same number of solutions. Since the solutions of type $\Psi_N^{(+)}$ and $\Psi_N^{(-)}$ correspond to different eigenvalues of the operator U_z, which commutes with the Hamiltonian, these functions can be obtained independently, and the corresponding secular equation will be of degree not $(N+1)(N+2)$, but $(\frac{1}{2})(N+1)(N+2)$. In addition, it is clear that there is no need for solving the equation for both $\Psi_N^{(+)}$ and $\Psi_N^{(-)}$. By obtaining $\Psi_N^{(+)}$ we can directly construct $\Psi_N^{(-)}$ from (9). Finally, relation (10) shows that each coefficient $C^{(+)}$ is expressed through only one real number.

3. LIMITING CASES

We assume that $\omega_x \geq \omega_y \geq \omega_z$ (which obviously does not limit the generality) and consider several limiting cases.

a) Case of a strongly nonspherical with large degree of nonaxiality: $\omega_x - \omega_z \gg \kappa$, $\omega_y \gg \kappa$, $\omega_x - \omega_y \gg \kappa$. In this case the s.o.c. makes a contribution of order κ^2 and can be disregarded.

b) Case of strongly nonspherical nucleus with arbitrary nonaxiality: $\omega_x - \omega_z \gg \kappa$, $\omega_y - \omega_z \gg \kappa$, $\omega_x - \omega_z$ arbitrary.

In this case, which is of great practical interest, we can discard in the s.o.c. the terms which are not diagonal in n_z, since they give corrections of order κ^2. We then obtain

$$H = A(N, n_z) + \tfrac{1}{2}(\omega_x - \omega_y)(\overset{+}{a}_x a_x - \overset{+}{a}_y a_y) + i\varkappa f_{xy}(\overset{+}{a}_x a_y - \overset{+}{a}_y a_x)\sigma_z,$$

$$A(N, n_z) = \tfrac{1}{2}(\omega_x + \omega_y)(N - n_z) + n_z\omega_z + \tfrac{1}{2}(\omega_x + \omega_y + \omega_z). \tag{11}$$

By means of the canonical transformation

$$a_x^{+\prime} = \cos\varphi a_x^+ - i\sin\varphi a_y^+, \quad a_x' = \cos\varphi a_x + i\sin\varphi a_y,$$
$$a_y^{+\prime} = -i\sin\varphi a_x^+ + \cos\varphi a_y^+, \quad a_y' = i\sin\varphi a_x + \cos\varphi a_y; \tag{12}$$

$$\sin\varphi = \sigma_z\sqrt{(1-\cos 2\varphi)/2}, \qquad \cos\varphi = \sqrt{(1+\cos 2\varphi)/2},$$
$$\cos 2\varphi = \Delta/\sqrt{\Delta^2 + (2\varkappa')^2}, \qquad \Delta = (\omega_x - \omega_y)/\omega_0, \quad \varkappa' = \varkappa f_{xy}/\omega_0 \tag{13}$$

the Hamiltonian (11) assumes the form

$$H = A(N, n_z) + \tfrac{1}{2}\omega_0\sqrt{\Delta^2 + (2\varkappa')^2}(a_x^{+\prime}a_x' - a_y^{+\prime}a_y'). \tag{14}$$

Since the transformation (12) is canonical, the spectrum of eigenvalues of the operators $a_x^{+\prime}a_x'$ and $a_y^{+\prime}a_y'$ will be the same as for the operators $a_x^+a_x$ and $a_y^+a_y$ (their eigenvalues and n_x' and n_y' are integers, including zero). Comparing (14) and (11) we reach the conclusion that an account of the s.o.c. reduces in this case the problem of the energy levels to the problem of the oscillator without s.o.c. but with other frequencies: ω_x and ω_i are replaced by frequencies ω_x' and ω_y' such that

$$\Delta' \equiv (\omega_x' - \omega_y')/\omega_0 = \sqrt{\Delta^2 + (2\varkappa')^2}. \tag{15}$$

It follows therefore that if the solution of the problem of minimum energy of the nucleus without account of the s.o.c. leads to an equilibrium value of the parameter $\Delta' = \Delta_0'$, then allowance for the s.o.c. leads to a reduction of Δ, i.e., to an increase in the nonaxiality, in accordance with the relations

$$\Delta_0 = \sqrt{\Delta_0'^2 - (2\varkappa')^2}, \qquad \Delta_0' \geqslant 2\varkappa',$$
$$\Delta_0 = 0, \qquad \Delta_0' \leqslant 2\varkappa', \tag{16}$$

which follow from (15) and from the fact that Δ' is defined only in the region $\Delta' \geq 2\kappa'$. If Δ_0' is found to be in the region $0 \leq \Delta_0' \leq 2\kappa'$, this means, as shown in Fig. 1, that we must disregard this "nonphysical" region. The minimum energy will correspond here to the value $\Delta_0' = 2\kappa'$ or, according to (16), $\Delta_0 = 0$.

It is seen from Fig. 1 that if a small perturbation of the nucleus changes the position of the energy minimum (dotted curve), but does not take it out of the nonspherical region, then $\Delta_0 = 0$ as before. We conclude thus that the s.o.c. stabilizes the axial form of the nucleus, making it stable with respect to small perturbations.

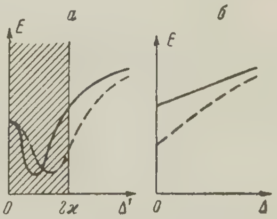

FIG. 1. Dependence of the energy of the nucleus on the nonaxiality; a – effective oscillator without s.o.c., b – real oscillator. The shaded (nonphysical) region on Fig. a corresponds to the point $\Delta = 0$ on Fig. b. The solid curve on Fig. a and the corresponding solid curve on Fig. b show the dependence of the nuclear energy on the nonaxiality; the dotted line represents the same dependence in the presence of a small perturbation.

Figure 2 shows, by way of illustration of the influence of the s.o.c. on the axiality, the dependence of nonaxiality parameter γ on the number of nucleons in the shell $N = 3$, obtained by Geĭlikman without accounting for the s.o.c., and the dependence calculated from (16) with $\kappa' = \kappa = 0.05$ and $\beta = 0.4$. The parameters β and γ are

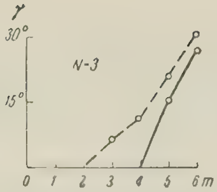

FIG. 2. Dependence of the parameter of nonaxiality of the nucleus γ on the number of nucleons m in the unfilled shell (N = 3). The dotted line shows the same dependence in the absence of s.o.c., while the solid one corresponds to the presence of s.o.c.

related with the frequencies ω_x, ω_y, ω_z by equations that correspond to the usual definition of β and γ:

$$\omega_x = (1 + s_0 + s_1)\,\omega(s_0, s_1), \quad \omega_y = (1 + s_0 - s_1)\,\omega(s_0, s_1),$$
$$\omega_z = (1 - 2s_0)\,\omega(s_0, s_1),$$
$$s_0 = \frac{1}{2}\sqrt{5/4\pi}\,\beta\cos\gamma, \quad s_1 = \sqrt{15/4\pi}\,\beta\sin\gamma, \tag{17}$$

$\omega(s_0, s_1)$ is determined from the requirement $\omega_x\omega_y\omega_z = \omega_0^3$.

It is seen from Fig. 2 that the s.o.c. leads to greater stability of the axial form of the nucleus (in this case the nucleus becomes nonaxial with five external nucleons, and not with three as in the absence of s.o.c.). In addition, the transition from the axial to the nonaxial form becomes sharper — the minimum and nonaxiality amounts to $\gamma = 15°$ and not 6.5°.

In conclusion, we determine the wave functions for this limiting case. The wave function of the state characterized by the quantum numbers n'_x, n'_y, n_z, and Σ ($\Sigma = \pm 1/2$ is the spin projection) can obviously be written in the form

$$\Psi^{\pm}_{x'_x n'_y n_z} = (n'_x!\; n'_y!\; n_z!)^{-1/2} (a_x^{+\prime})^{n'_x} (a_y^{+\prime})^{n'_y} (a_z^{+})^{n_z} \,|\, 000 \pm\rangle. \tag{18}$$

Substituting in (18) the expressions $a_x^{+\prime}$ and $a_y^{+\prime}$, according to (12), we obtain finally

$$\Psi^{\pm}_{n'_x n'_y n_z} = (n'_x!\; n'_y!\; n_z!)^{-1/2} (\cos\varphi a_x^{+} - i\sin\varphi a_y^{+})^{n'_x}$$
$$\times(-i\sin\varphi a_x^{+} + \cos\varphi a_y^{+})^{n'_y} (a_z^{+})^{n_z} \,|\, 000 \pm\rangle. \tag{19}$$

The authors express deep gratitude to G. Ya. Lyubarskiĭ for valuable discussions.

---

[1] S. G. Nilsson, Kgl. Danske Videnskab. Selsk., Mat.-Fys. Medd., 29, No. 16 (1955).

[2] A. S. Davydov and G. F. Filippov, JETP 35, 440 (1958) and 36, 1497 (1959), Soviet Phys. JETP 8, 303 (1959) and 9, 1061 (1959). A. S. Davydov and V. S. Rostovskiĭ, JETP 36, 1788 (1959), Soviet Phys. JETP 9, 1275 (1959).

[3] B. T. Geĭlikman, JETP 35, 989 (1958), Soviet Phys. JETP 8, 690 (1959).

Translated by J. G. Adashko
341

SOVIET PHYSICS JETP VOLUME 11, NUMBER 6 DECEMBER, 1960

KINETIC EQUATION FOR RAPIDLY VARYING PROCESSES

V. P. SILIN

P. N. Lebedev Physics Institute, Academy of Sciences, U.S.S.R.

Submitted to JETP editor December 24, 1959

J. Exptl. Theoret. Phys. (U.S.S.R.) 38, 1771-1777 (June, 1960)

A kinetic equation is considered for processes characterized by times which are small or comparable with collision times. In the most interesting case of a gas of charged particles in the absence of a magnetic field, and for frequencies which greatly exceed the Langmuir frequency ω_0, it is found that not the Debye screening range but the distance traversed by the particle during the period of the field is the maximal impact parameter in the Coulomb logarithm. The effective frequency of collisions between electrons and ions, which determines the dissipative part of the complex dielectric permittivity tensor for a plasma located in a strong, constant magnetic field is computed for the same case of high frequencies. If, moreover, the electron Larmor frequency is much greater than the Langmuir frequency, then there is a resonance character to the dependence of the maximal impact parameter in the Coulomb logarithm on the frequency of the variable field.

1. The Boltzmann kinetic equation is unsuitable under conditions in which the characteristic dimensions of the inhomogeneities are comparable with the characteristic impact parameters of the particles participating in the collisions, or when an initiated collision is not completed within the characteristic time of change in the distribution of the particles. A generalization of the Boltzmann equation to the case of extremely inhomogeneous problems was given by Chapman and Cowling[1] for the case of a gas of rigid spheres, and by Bogolyubov[2] in obtaining generalized Boltzmann equations for an arbitrary law of interaction of the gas particles.

The account below is devoted to obtaining the kinetic equation for gas particles with weak interaction, which is suitable for describing rapidly varying processes. An example of such a gas is a plasma in which the particles interact according to Coulomb's law, while an appreciable contribution to the scattering of the particles is made by long-range collisions for which the interaction can be regarded as weak. Because of the slowness in fall off of the Coulomb forces, the time during which long-range collisions take place lies in a wide range from $\tau_{\min} \sim e^2 m^{1/2} (\kappa T)^{-3/2} \sim 10^{-8} T^{-3/2}$ to $\tau_{\max} \sim \sqrt{m/4\pi e^2 n_0} = \omega_0^{-1} \sim 10^{-5} n_0^{-1/2}$. Here, T is the temperature, and n_0 is the density of electrons per unit volume; ω_0 is the Langmuir frequency. Under conditions in which the characteristic time of the process τ_{pr} satisfies the inequality

$$\tau_{min} \ll \tau_{\text{pr}} \ll \tau_{max},$$

there is a wide region ($\tau_{\min} \ll \tau_{\max}$) in which not only can the interaction be regarded as weak, but we can also consider the collisions without regarding the time variation of the distribution. Also, there is a wide region ($\tau_{\text{pr}} \ll \tau_{\max}$) in which the collisions are changed appreciably. Actually, in this latter region, the collisions are suppressed because of the rapid change in the particle distribution, and τ_{pr} plays the role of a maximum collision time.

The situation is somewhat more complicated in the case of a high-frequency process taking place in a plasma placed in a strong magnetic field. Here, under the condition that the variable frequency ω is close to the Larmor frequency of the electrons Ω and is much greater than the Langmuir frequency, the effective maximal collision time is equal to $(\omega\omega_0)^{-1/2}$ in order of magnitude, as shown below. If $|\omega \pm \Omega| \gg \omega_0$, then the effective maximal collision time is $\sim |\Omega^2 - \omega^2|^{-1/2}$.

2. We consider the interaction between gas particles to be weak. The kinetic equation for such a gas in the case of a slowly changing process was found by Landau.[3] To obtain the corresponding kinetic equation that describes rapidly changing processes, we make use of perturbation theory. It was shown by Bogolyubov[2] that, in the construction of such an equation for the distribution function $f(\mathbf{p}, \mathbf{r})$, it is necessary to determine the correlation function $g(\mathbf{p}, \mathbf{r}, \mathbf{p}', \mathbf{r}')$. For a known correlation function, the equation for the distribution function can be written in the form

$$\frac{\partial f}{\partial t} + \mathbf{v}\frac{\partial f}{\partial \mathbf{r}} - n\frac{\partial f}{\partial \mathbf{p}}\frac{\partial}{\partial \mathbf{r}}\int d\mathbf{r}'\, d\mathbf{p}' f(\mathbf{p}', \mathbf{r}')\, U(|\mathbf{r} - \mathbf{r}'|)$$
$$- n\frac{\partial}{\partial \mathbf{p}}\int d\mathbf{r}'\, d\mathbf{p}'\, g(\mathbf{p}, \mathbf{r}, \mathbf{p}', \mathbf{r}')\frac{\partial U(|\mathbf{r} - \mathbf{r}'|)}{\partial \mathbf{r}} = 0. \qquad (1)$$

Here $f(\mathbf{p}, \mathbf{r}, t)$ is the particle distribution function normalized to unity, n is the number of particles per unit volume, U is the potential of pair forces, which we shall assume to be central, $\mathbf{v}$ is the velocity of the particles.

Because of the small interaction of the particles, the correlation function can be described by the following approximate equation:

$$\frac{\partial g}{\partial t} + \mathbf{v}\frac{\partial g}{\partial \mathbf{r}} + \mathbf{v}'\frac{\partial g}{\partial \mathbf{r}'}$$
$$= \left[f(\mathbf{p}', \mathbf{r}')\frac{\partial f(\mathbf{p}, \mathbf{r})}{\partial \mathbf{p}} - f(\mathbf{p}, \mathbf{r})\frac{\partial f(\mathbf{p}', \mathbf{r}')}{\partial \mathbf{p}'}\right]\frac{\partial U(|\mathbf{r} - \mathbf{r}'|)}{\partial \mathbf{r}}. \qquad (2)$$

Under the assumption of an adiabatic turning on of the interaction in the infinitely distant past, Eq. (2) can easily be written in the form

$$g(\mathbf{p}, \mathbf{r}, \mathbf{p}', \mathbf{r}', t) = \int_{-\infty}^{0} d\tau \left\{\frac{\partial}{\partial r_i} U(|\mathbf{r} - \mathbf{r}' - (\mathbf{v} - \mathbf{v}')\tau|)\right\}$$
$$\times \left\{\frac{\partial}{\partial p_i} + \frac{\partial v_j}{\partial p_i}\tau\frac{\partial}{\partial r_j} - \frac{\partial}{\partial p_i'} - \frac{\partial v_j'}{\partial p_j'}\tau\frac{\partial}{\partial r_j'}\right\} f(\mathbf{p}, \mathbf{r} - \mathbf{v}\tau, t + \tau)$$
$$\times f(\mathbf{p}', \mathbf{r}' - \mathbf{v}'\tau, t + \tau). \qquad (3)$$

Equation (3), along with Eq. (1), gives the generalized kinetic equation which is suitable for describing rapidly changing processes.

3. We consider in detail the case of a spatially homogeneous distribution. In this case the kinetic equation takes on the following form:

$$\frac{\partial f(\mathbf{p}, t)}{\partial t} = n\frac{\partial}{\partial p_i}\int d\mathbf{p}' \int_{-\infty}^{0} d\tau\, \mathscr{E}_{ij}((\mathbf{v} - \mathbf{v}')\tau)$$
$$\times \left\{f(\mathbf{p}', t + \tau)\frac{\partial f(\mathbf{p}, t + \tau)}{\partial p_j} - f(\mathbf{p}, t + \tau)\frac{\partial f(\mathbf{p}', t + \tau)}{\partial p_j'}\right\}. \qquad (4)$$

Here

$$\mathscr{E}_{ij}(\mathbf{v}\tau) = \int d\mathbf{r}\, \frac{\partial U(r)}{\partial r_i}\frac{\partial U(|\mathbf{r} - \mathbf{v}\tau|)}{\partial r_j} = \frac{1}{(2\pi)^3}\int d\mathbf{k}\nu^2(k)\, k_i k_j e^{i\mathbf{k}\mathbf{v}\tau},$$
$$\nu(k) = \int U(r)\, e^{i\mathbf{k}\mathbf{r}}\, d\mathbf{r}.$$

If the time dependence is weak, then one can neglect the difference between $t + \tau$ and t in the arguments of the distribution function on the right side of Eq. (4). Then Eq. (4) transforms into the Landau equation:

$$\frac{\partial f}{\partial t} = \frac{\partial}{\partial p_i}\int d\mathbf{p}'\, I_{ij}(\mathbf{v} - \mathbf{v}', 0)\left\{f(\mathbf{p}')\frac{\partial f(\mathbf{p})}{\partial p_j} - f(\mathbf{p})\frac{\partial f(\mathbf{p}')}{\partial p_j'}\right\},$$
$$I_{ij}(\mathbf{v}, 0) = n\int_{-\infty}^{0} d\tau\, \mathscr{E}_{ij}(\mathbf{v}\tau) = \frac{v^2\delta_{ij} - v_i v_j}{v^3} A(0),$$
$$A(0) = \frac{n}{4\pi}\int_{0}^{\infty} q^3\nu^2(q)\, dq. \qquad (5)$$

In order to make clear the difference between Eq. (4) and the usual equation of Landau (5), we consider a linearized Eq. (4), assuming that the nonequilibrium increment δf is small in comparison with the equilibrium distribution function f_0. Moreover, owing to the linearization, we can put the time dependence in the form $\exp(-i\omega t)$. Then the right-hand side of Eq. (4) takes the form

$$\frac{\partial}{\partial p_i}\int d\mathbf{p}'\, I_{ij}(\mathbf{v} - \mathbf{v}', \omega)\left\{f_0(\mathbf{p}')\frac{\partial}{\partial p_j}\delta f(\mathbf{p}) + \delta f(\mathbf{p}')\frac{\partial}{\partial p_j} f_0(\mathbf{p})\right.$$
$$\left. - f_0(\mathbf{p})\frac{\partial}{\partial p_j'}\delta f(\mathbf{p}') - \delta f(\mathbf{p})\frac{\partial}{\partial p_j'} f_0(\mathbf{p}')\right\}.$$

The resultant equation differs from the corresponding right-hand side obtained in the linearization of the Landau equation in the frequency dependence of the kernel $I_{if}(\mathbf{v}, \omega)$, which is determined by the following formula:

$$I_{ij}(\mathbf{v}, \omega) = \frac{n}{(2\pi)^3}\int d\mathbf{k}\nu^2(k)\, k_i k_j\left\{i\mathrm{P}\frac{1}{\mathbf{k}\mathbf{v} - \omega} + \pi\delta(\mathbf{k}\mathbf{v} - \omega)\right\}. \qquad (6)$$

Here P denotes the principal value.

On the basis of Eq. (6), it is easy to conclude that the frequency dependence can become important only under conditions in which v/ω — the distance traversed by the particle during the period of oscillation — is small in comparison with the characteristic impact parameter $\rho \sim 1/k$.

The kernel of the collision integral (6) can be written in the form

$$I_{ij}(\mathbf{v}, \omega) = v^{-3}(v^2\delta_{ij} - v_i v_j)[A'(\omega, v) + iA''(\omega, v)]$$
$$+ v^{-3} v_i v_j [B'(\omega, v) + iB''(\omega, v)]. \qquad (7)$$

It is easy to see that, by (6), the quantities A' and A'' (and, correspondingly, B' and B'') are connected by a dispersion relation of the usual type:

$$A''(\omega) = \frac{1}{\pi}\int d\omega \mathrm{P}\frac{A'(\omega')}{\omega' - \omega}. \qquad (8)$$

4. To determine the dissipation it is necessary first to know A' and B'. We find these quantities for the case of Coulomb interaction, when $\nu(k) = 4\pi e^2/k^2$. In the consideration of the Coulomb case, it is necessary to cut off the integration over the impact parameter both above ($\rho_{\max}$) and below ($\rho_{\min}$). We have

$$A'(\omega, v) = \pi e^4 n\left[\ln\frac{\rho_{min}^{-2} + \omega^2/v^2}{\rho_{max}^{-2} + \omega^2/v^2} - \frac{1}{v^2/\omega^2\rho_{min}^2 + 1}\right.$$
$$\left. + \frac{1}{v^2/\omega^2\rho_{max}^2 + 1}\right],$$
$$B'(\omega, v) = 2\pi e^4 n\,[(v^2/\omega^2\rho_{min}^2 + 1)^{-1} - (v^2/\omega^2\rho_{max}^2 + 1)^{-1}]. \qquad (9)$$

In the low frequency region, where $\omega \ll v/\rho_{\max}$, the quantity A' goes over into $A(0) \equiv A(0, v)$.

while B' falls off as ω^2. By virtue of the fact that $\rho_{\max}$ is equal to the Debye radius in order of magnitude, the low-frequency region is obtained for $\omega \ll \omega_0 = \sqrt{4\pi e^2 n/m}$. In the opposite case, in which $\omega \gg \omega_0$, (but, at the same time, $\omega \ll v/\rho_{\min}$, where $\rho_{\min} \sim e^2/\kappa T$), we have

$$A'(\omega, v) \approx \pi e^4 n\,[\ln(\omega^2/v^2\rho_{min}^2) + 1],$$
$$B'(\omega, v) \approx -2\pi e^4 n. \tag{10}$$

In this expression for A', it is v/ω, rather than $\rho_{\max}$, that appears as the argument of the logarithm. This physically clear result was essentially obtained earlier, for example, in the calculation of the high frequency absorption in an interstellar electron gas (with the aid of the Einstein relations).[4]

It must be remarked that the approximate equation (2) which we have used is not suitable for the description of long-range correlation of particles interacting according to Coulomb's law for the case of frequencies which are small in comparison with the Langmuir frequency ω_0. Therefore, in consideration of the Coulomb case, one is obliged to cut off the integration at the Debye radius of screening. As was shown by Bogolyubov,[2] one can improve the accuracy of Eq. (2) so that it correctly describes the effects of screening. However, in this case, the kinetic equation is actually not obtained, inasmuch as it is not possible to solve the resulting equation for the correlation function. Such a situation occurs both in the case of consideration of slow processes and also in our case of rapidly changing processes.

5. We shall apply the above to the case of a gas in which there are charged particles located in a constant and homogeneous magnetic field, and also in a homogeneous but time dependent electric field. The distribution function of an alpha type of particles of such a gas then obeys the kinetic equation

$$\frac{\partial f_\alpha}{\partial t} + \mathbf{v}\frac{\partial f_\alpha}{\partial \mathbf{r}} + e_\alpha\left(\mathbf{E} + \frac{1}{c}[\mathbf{v}\times\mathbf{H}]\right)\frac{\partial f_\alpha}{\partial \mathbf{p}}$$
$$-\frac{\partial f_\alpha}{\partial \mathbf{p}}\frac{\partial}{\partial \mathbf{r}}\int d\mathbf{p}'\,d\mathbf{r}'\sum_{\alpha'} n_{\alpha'}U_{\alpha\alpha'}(|\mathbf{r}-\mathbf{r}'|)\,f_{\alpha'}(\mathbf{p}',\mathbf{r}')$$
$$= J_\alpha \equiv \int d\mathbf{r}'\,d\mathbf{p}'\sum_{\alpha'} n_{\alpha'}\frac{\partial U_{\alpha\alpha'}(|\mathbf{r}-\mathbf{r}'|)}{\partial \mathbf{r}}\frac{\partial}{\partial \mathbf{p}}g_{\alpha\alpha'}(\mathbf{p},\mathbf{r},\mathbf{p}',\mathbf{r}',t), \tag{11}$$

while the correlation function g has the form

$$g_{\alpha\alpha'}(\mathbf{p},\mathbf{r},\mathbf{p}',\mathbf{r}',t) = \int_{-\infty}^{0} d\tau\left\{\frac{\partial}{\partial \mathbf{r}}U_{\alpha\alpha'}(|\mathbf{r}-\mathbf{r}'+\mathbf{a}(\tau,\mathbf{v},\mathbf{v}',\alpha,\alpha',t)|)\right\}\times\left\{\frac{\mathbf{H}}{H^2}\left[\mathbf{H}.\left(\frac{\partial}{\partial \mathbf{p}}-\frac{\partial}{\partial \mathbf{p}'}\right)\right]+\frac{1}{H^2}\mathbf{H}\times\left[\left(\cos\Omega_\alpha\tau\frac{\partial}{\partial \mathbf{p}}\right.\right.\right.$$
$$\left.-\cos\Omega_{\alpha'}\tau\frac{\partial}{\partial \mathbf{p}'}\right)\times\mathbf{H}\Big]-\frac{1}{H}\mathbf{H}\times\left[\sin\Omega_\alpha\tau\frac{\partial}{\partial \mathbf{p}}-\sin\Omega_{\alpha'}\tau\frac{\partial}{\partial \mathbf{p}'}\right]+\frac{1}{H}\mathbf{H}\times\left[\frac{1-\cos\Omega_\alpha\tau}{m_\alpha\Omega_\alpha}\frac{\partial}{\partial \mathbf{r}}-\frac{1-\cos\Omega_{\alpha'}\tau}{m_{\alpha'}\Omega_{\alpha'}}\frac{\partial}{\partial \mathbf{r}'}\right]$$
$$-\frac{1}{H^2}\mathbf{H}\times\left[\frac{\sin\Omega_\alpha\tau}{m_\alpha\Omega_\alpha}\frac{\partial}{\partial \mathbf{r}}-\frac{\sin\Omega_{\alpha'}\tau}{m_{\alpha'}\Omega_{\alpha'}}\frac{\partial}{\partial \mathbf{r}'}\right]\times\mathbf{H}-\tau\frac{\mathbf{H}}{H}\mathbf{H}\times\left(\frac{1}{m_\alpha}\frac{\partial}{\partial \mathbf{r}}-\frac{1}{m_{\alpha'}}\frac{\partial}{\partial \mathbf{r}'}\right)\Big\}f_{\alpha'}(\mathbf{P}',\mathbf{R}',t+\tau)\,f_\alpha(\mathbf{P},\mathbf{R},t+\tau), \tag{12}$$

where $(\Omega_\alpha = e_\alpha H/m_\alpha c)$

$$\mathbf{P} = \frac{\mathbf{H}}{H}(\mathbf{pH}) + \frac{\mathbf{H}\times[\mathbf{p}\times\mathbf{H}]}{H^2}\cos\Omega_\alpha\tau$$
$$+\frac{[\mathbf{p}\times\mathbf{H}]}{H}\sin\Omega_\alpha\tau + e_\alpha\int_t^{t+\tau}dt'\left\{\frac{\mathbf{H}}{H}(\mathbf{HE}(t'))\right.$$
$$+\frac{\mathbf{H}\times[\mathbf{E}(t')\times\mathbf{H}]}{H^2}\cos\Omega_\alpha(\tau+t-t')$$
$$\left.+\frac{[\mathbf{E}(t')\times\mathbf{H}]}{H}\sin\Omega_\alpha(\tau+t-t')\right\},$$

$$\mathbf{R} = \mathbf{r} + \frac{1}{m_\alpha}\int_t^{t+\tau}dt'\,\mathbf{P}(t'), \qquad \mathbf{a} = \int_t^{t+\tau}dt'\left[\frac{\mathbf{P}(t')}{m_\alpha}-\frac{\mathbf{P}'(t')}{m_{\alpha'}}\right].$$

In the case of a spatially homogeneous distribution, the right side of the kinetic equation (11) takes the form

$$J_\alpha(p,t) = \sum_{\alpha'} n_{\alpha'}\frac{\partial}{\partial p_i}\int d\mathbf{p}'\int_{-\infty}^{0}d\tau\left\{\mathscr{E}_{ij}^{\alpha\alpha'}(\mathbf{v},\mathbf{v}',\tau,t)\frac{\partial}{\partial p_j}\right.$$
$$\left.-\mathscr{E}_{ij}^{\alpha'\alpha}(\mathbf{v}',\mathbf{v},\tau,t)\frac{\partial}{\partial p_j'}\right\}f_{\alpha'}(\mathbf{P}',t+\tau)\,f_\alpha(\mathbf{P},t+\tau), \tag{13}$$

$$\mathscr{E}_{ij}^{\alpha\alpha'}(\mathbf{v},\mathbf{v}',\tau,t) = \int d\mathbf{r}\,\frac{\partial U_{\alpha\alpha'}(r)}{\partial r_i}\frac{\partial U_{\alpha\alpha'}(|\mathbf{r}+\mathbf{a}|)}{\partial r_l}$$
$$\times\left\{\frac{H_l H_j}{H^2}+\left(\delta_{lj}-\frac{H_l H_j}{H^2}\right)\cos\Omega_\alpha\tau - e_{lmj}\frac{H_m}{H}\sin\Omega_\alpha\tau\right\}$$
$$= \frac{1}{(2\pi)^3}\int d\mathbf{k}\nu_{\alpha\alpha'}^2(k)\,e^{i\mathbf{ka}}\times\left\{\frac{H_l H_j}{H^2}+\left(\delta_{lj}-\frac{H_l H_j}{H^2}\right)\cos\Omega_\alpha\tau\right.$$
$$\left.-e_{lmj}\frac{H_m}{H}\sin\Omega_\alpha\tau\right\}. \tag{14}$$

For the case of Coulomb interaction, $\nu_{\alpha\alpha'}(k) = 4\pi e_\alpha e_{\alpha'}k^{-2}$, and therefore

$$\mathscr{E}_{ij}^{\alpha\alpha'}(\mathbf{v},\mathbf{v}',\tau,t) = \frac{2\pi e_\alpha^2 e_{\alpha'}^2}{a}\left(\delta_{il}-\frac{a_i a_l}{a^2}\right)$$
$$\times\left\{\frac{H_l H_j}{H^2}+\left(\delta_{lj}-\frac{H_l H_j}{H^2}\right)\cos\Omega_\alpha\tau - e_{lmj}\frac{H_m}{H}\sin\Omega_\alpha\tau\right\}, \tag{15}$$

$$\mathbf{a}(\tau,\mathbf{v},\mathbf{v}',\alpha,\alpha',t) = \frac{\mathbf{H}}{H}(\mathbf{v}-\mathbf{v}',\mathbf{H})\tau + \mathbf{H}\times\left[\left(\frac{\mathbf{v}\sin\Omega_\alpha\tau}{H^2\Omega_\alpha}\right.\right.$$
$$\left.\left.-\frac{\mathbf{v}'\sin\Omega_{\alpha'}\tau}{H^2\Omega_{\alpha'}}\right)\times\mathbf{H}\right]+\left[\mathbf{v}\frac{1-\cos\Omega_\alpha\tau}{H\Omega_\alpha}-\mathbf{v}'\frac{1-\cos\Omega_{\alpha'}\tau}{H\Omega_{\alpha'}}\right]\times\mathbf{H}$$
$$+\int_t^{t+\tau}dt'\int_{t'}^{t'+\tau}dt''\left\{\frac{\mathbf{H}}{H}(\mathbf{HE}(t''))\left(\frac{e_\alpha}{m_\alpha}-\frac{e_{\alpha'}}{m_\alpha'}\right)\right.$$
$$+\left(\frac{e_\alpha\cos\Omega_\alpha(\tau+t'-t'')}{m_\alpha H^2}-\frac{e_{\alpha'}\cos\Omega_{\alpha'}(\tau+t'-t)}{m_{\alpha'}H^2}\right)$$
$$\times[\mathbf{H}\times[\mathbf{E}(t'')\times\mathbf{H}]]+[\mathbf{E}(t'')\times\mathbf{H}]\left(\frac{e_\alpha}{m_\alpha H}\sin\Omega_\alpha(\tau+t'-t'')\right.$$
$$\left.\left.-\frac{e_{\alpha'}}{m_{\alpha'}H}\sin\Omega_{\alpha'}(\tau+t'-t'')\right)\right\}. \tag{16}$$

It should be noted that the integration over τ in the case of Coulomb interaction must be carried out from $\tau_{\max}$ to $\tau_{\min}$, which corresponds to the cutting off of the impact parameter integral at both high and low values.

6. We use the kinetic equation obtained in Sec. 5 for determining the dissipation of electromagnetic waves brought about by collisions of electrons with ions. In this case it is expedient to carry out the calculation with logarithmic accuracy, keeping in mind the occurrence of a large Coulomb logarithm. In such an approximation,

$$\mathscr{E}_{ij}^{\alpha\alpha'}(\mathbf{v}, \mathbf{v}', \tau) = 2\pi e_\alpha^2 e_{\alpha'}^2 [\delta_{ij}(\mathbf{v}-\mathbf{v}')^2 - (v_i - v_i')(v_j - v_j')] \, |\tau|^{-1} \, |\mathbf{v}-\mathbf{v}'|^{-3} \cos \Omega_\alpha \tau. \tag{17}$$

Comparatively simple calculations, carried out in detail in the determination of the dielectric permittivity tensor for frequencies below the Langmuir frequency ω_0, show that we can use in our case for the complex dielectric permittivity tensor the usual expression,[5] in which the dissipation processes are characterized by an effective collision frequency ($\nu_{\text{eff}\,i}$). The only difference is that in the expression for the effective collision frequency between electrons and ions

$$\nu_{\text{eff}\,i} = \tfrac{4}{3} \sqrt{2\pi}\, e^2 e_i^2 n_i m^{-1/2} (\varkappa T)^{-3/2} L' \tag{18}$$

we have, in place of the usual Coulomb logarithm $L = \ln(\kappa T e^{-2} \rho_{\max})$ (here, $\rho_{\max} = \sqrt{\kappa T/m}\, \tau_{\max}$ is the maximal impact parameter, equal in order of magnitude, to the Debye radius) the following expression:

$$L' = \int\limits_{\tau_{min}}^{\tau_{max}} \frac{d\tau}{\tau} \cos \Omega\tau \cos \omega\tau \qquad \left(\Omega = \frac{eH}{mc}\right). \tag{19}$$

In particular, for $|\omega \pm \Omega| \gg \omega_0$,

$$L' \approx \ln\left(\frac{\varkappa T}{e^2} \sqrt{\frac{\varkappa T}{m\,|\Omega^2 - \omega^2|}}\right). \tag{20}$$

If the frequency of the electromagnetic field is close to the gyroscopic frequency $|\Omega - \omega| \ll \omega_0$, but is at the same time larger than the Langmuir frequency, the Coulomb logarithm is shown to be equal to

$$L' \approx \ln\left(\frac{\varkappa T}{e^2} \sqrt{\frac{\varkappa T}{m 2\omega\omega_0}}\right). \tag{21}$$

Under the conditions in which $\omega \ll \omega_0$ and $\Omega \ll \omega_0$, Eq. (19) evidently yields the usual Coulomb logarithm.

I take this opportunity to express my thanks to V. L. Ginzburg for his interest in the present research and for useful discussions.

APPENDIX

THE COLLISION INTEGRAL IN A STRONG ELECTRIC FIELD

In a constant electric field, the collision integral (13) takes the form

$$J_\alpha(\mathbf{p}, t) = \sum_{\alpha'} n_{\alpha'} \frac{\partial}{\partial p_i} \int d\mathbf{p}' \int\limits_{-\infty}^{0} d\tau \mathscr{E}_{ij}^{\alpha\alpha'}(\mathbf{v}-\mathbf{v}', \tau) \times \left\{\frac{\partial}{\partial p_j} - \frac{\partial}{\partial p_j'}\right\} f_{\alpha'}(\mathbf{p}' + e_{\alpha'}\mathbf{E}\tau, t+\tau) f_\alpha(\mathbf{p} + e_\alpha \mathbf{E}\tau, t+\tau), \tag{A.1}$$

where, for the case of Coulomb interaction,

$$\mathscr{E}_{ij}^{\alpha\alpha'}(\mathbf{v}, \tau) = 2\pi e_\alpha^2 e_{\alpha'}^2 |\tau|^{-1} (\delta_{ij} V^2 - V_i V_j) V^{-3}, \qquad \mathbf{V} = \mathbf{v} - (e_\alpha / m_\alpha - e_{\alpha'} / m_{\alpha'}) \mathbf{E}\tau. \tag{A.2}$$

For slowly changing processes, taking the weakness of the interaction into account, we can transform in (A.1) in the distribution functions f from $t + \tau$ to t (which is completely analogous to what was done in reference 2). Then the collision integral takes the form

$$J_\alpha(p, t) = \sum_{\alpha'} \frac{\partial}{\partial p_i} \int d\mathbf{p}' \left\{ f_{\alpha'}(\mathbf{p}', t) \frac{\partial f_\alpha(\mathbf{p}, t)}{\partial p_j} - f_\alpha(\mathbf{p}, t) \frac{\partial f_{\alpha'}(\mathbf{p}', t)}{\partial p_j'} \right\} \times I_{ij}^{\alpha\alpha'}(\mathbf{v}-\mathbf{v}'), \tag{A.3}$$

$$I_{ij}^{\alpha\alpha'}(\mathbf{v}) = n_{\alpha'} \int\limits_{-\tau_{max}}^{-\tau_{min}} d\tau \, \mathscr{E}_{ij}^{\alpha\alpha'}(\mathbf{v}, \tau). \tag{A.4}$$

---

[1] S. Chapman and T. Cowling, The Mathematical Theory of Non-Uniform Gases (Cambridge, 1939).

[2] N. N. Bogolyubov, Проблемы динамической теории в статистической физике, (Problems of Dynamical Theory in Statistical Physics) Gostekhizdat, 1946.

[3] L. D. Landau, Phys. Z. Sowjetunion **10**, 154 (1936).

[4] Al'pert, Ginzburg, and Feĭnberg, Распространение радиоволн, (Propagation of Radiowaves) Gostekhizdat, 1953, Sec. 82.

[5] A. V. Gurevich, JETP **35**, 392 (1958), Soviet Phys. JETP **8**, 271 (1959).

Translated by R. T. Beyer
342

SOVIET PHYSICS JETP VOLUME 11, NUMBER 6 DECEMBER, 1960

ON THE SCATTERING OF TRANSVERSELY POLARIZED FERMIONS

A. A. SOKOLOV and M. M. KOLESNIKOVA

Moscow State University

Submitted to JETP editor December 28, 1959

J. Exptl. Theoret. Phys. (U.S.S.R.) **38**, 1778-1785 (June, 1960)

The elastic scattering of transversely polarized fermions is considered. It is shown that in the ultrarelativistic case scattering of the longitudinally polarized fermions is characterized by the four dimensional intrinsic angular momentum tensor. In the latter case the scattered fermions remain transversely polarized in interactions proportional to the matrices ρ_1 and ρ_2; on the contrary, in interactions proportional to the matrices ρ_3 and ρ_4, the longitudinal component may appear after scattering (if the particle has a non-zero rest mass).

1. INTRODUCTION

IN the motion of a free fermion, described by the Dirac equation

$$\psi = L^{-3/2}\sum_{s} C_s b_s \exp\{-i\varepsilon cKt + i\mathbf{kr}\}, \qquad (1)$$

where $K = \sqrt{k^2 + k_0^2}$ is the positive $(\epsilon = 1)$ energy of the particle, $\mathbf{k}$ is its momentum, k_0 is the rest mass; we shall characterize the polarization property by the unit three dimensional vector $\mathbf{s}^0$.

For the longitudinal (s_3^0 parallel to the vector $\mathbf{k}$) and transverse ($s_{1,2}^0$ perpendicular to the vector $\mathbf{k}$) components we have

$$s_1^0 = (C_1^+C_{-1} + C_{-1}^+C_1)\, s_0^{-1}, \qquad s_2^0 = i\,(C_{-1}^+C_1 - C_1^+C_{-1})\, s_0^{-1},$$
$$s_3^0 = (C_1^+C_1 - C_{-1}^+C_{-1})\, s_0^{-1}, \qquad (2)$$

respectively, where

$$s_0 = C_1^+C_1 + C_{-1}^+C_{-1}. \qquad (3)$$

As is well known, either the four dimensional spin pseudovector $(\hat{\xi}_\mu = \sigma,\ i\rho_1)$:

$$\zeta_3 = Ks_3^0, \qquad \zeta_{1,2} = k_0 s_{1,2}^0 \qquad \zeta_t = -i\zeta_4 = ks_3^0, \qquad (5)$$

or the intrinsic angular momentum tensor of the electron $(\zeta_{23} = \rho_3\sigma_1;\ -i\hat{\xi}_{14} = \rho_2\sigma_1,$ etc$)$

$$\mu_3 = \zeta_{12} = k_0 s_3^0, \qquad \mu_{1,2} = Ks_{1,2}^0,\ \ \varepsilon_1 = -i\zeta_{14} = ks_2^0,$$
$$\varepsilon_2 = -ks_1^0,\ \varepsilon_3 = 0 \qquad (5a)$$

can be formed from the unit three dimensional vector $\mathbf{s}^0$ by averaging of the type

$$\zeta = \int \psi^+ K\hat{\zeta}\psi\, d^3x \qquad (4)$$

with corresponding matrices $\hat{\xi}$.

Equation (4) can be generalized to the case of the presence of states of both positive and negative energies by using the relation

$$K\hat{\zeta} \rightarrow \tfrac{1}{2}(\alpha\mathbf{k} + \rho_3 k_0)\,\hat{\zeta} + \tfrac{1}{2}\,\hat{\zeta}\,(\alpha\mathbf{k} + \rho_3 k_0). \qquad (6)$$

In the case of the free motion, the generalized matrices will, in similar fashion, commute with the Hamiltonian, and will lead to the result (4) in averaging for states with positive energy.

For matrices of the spin pseudovector (see references 1 – 3) and for the intrinsic momentum tensor, we shall have here

$$K\sigma \rightarrow k_0\rho_3\sigma + \rho_1\mathbf{k}, \qquad K\rho_1 \rightarrow \sigma\mathbf{k},$$
$$K\rho_3\sigma \rightarrow k_0\sigma - \rho_2\,[\mathbf{k}\times\sigma], \qquad -iK\rho_2\sigma \rightarrow \rho_3\,[\sigma\times\mathbf{k}] \qquad (6a)$$

respectively. From the latter matrices we can form the matrix

$$\sigma^0 = \mathbf{k}^0\,(\sigma\mathbf{k}^0) + \rho_3\,(\sigma - \mathbf{k}^0\,(\sigma\mathbf{k}^0)) \qquad (\mathbf{k}^0 = \mathbf{k}/k), \quad (6b)$$

which also commutes with the Hamiltonian. The eigenvalues of the components of this matrix will be equal to the components of the unit three dimensional spin vector $\mathbf{s}^0$. The transformation laws in the Lorentz rotations for the three dimensional $\mathbf{s}^0$ can be found from the corresponding transformation rules for the four dimensional ζ_μ or $\zeta_{\mu\nu}$ (see references 4 and 5). They have a somewhat peculiar form:

$$s_3^{\prime 0} = s_3^0\cos\gamma + s_1^0\sin\gamma, \qquad s_1^{\prime 0} = s_1^0\cos\gamma - s_3^0\sin\gamma,$$
$$s_2^{\prime 0} = s_2^0, \qquad (7)$$

where

$$\cos\gamma = (\beta_1 - \beta\cos\theta)\,[(\beta_1 - \beta\cos\theta)^2 + \beta^2(1 - \beta_1^2)\sin^2\theta]^{-1/2},$$
$$\sin\gamma = (\beta\sqrt{1 - \beta_1^2}\sin\theta)\,[(\beta_1 - \beta\cos\theta)^2 + \beta^2(1 - \beta_1^2)\sin^2\theta]^{-1/2},$$

β is the velocity of motion of the primed system of coordinates relative to the unprimed, which we direct along the z axis. The x axis is chosen in such a fashion that the velocity of motion of the particle $\beta_1 = k/K$ relative to the unprimed system lies in the zx plane.

It follows from these equations that interchanges of the longitudinal and transverse components of the polarization will take place for particles with nonzero rest mass $(k_0 \neq 0)$ in the transition from one inertial frame to another. Only in the case $\theta = 0$, i.e., when the direction of the velocity of motion β_1 of the particle coincides with the velocity of motion β of the primed system will the longitudinal components remain longitudinal and the transverse components transverse. Conversely, for $\beta = \beta_1/\cos\theta$, the longitudinal components as a whole transform into the transverse and vice versa, as a result of the Lorentz transformations, if $s_2^0 = 0$.

For $k_0 \neq 0$, one can characterize the polarization both by a four dimensional spin pseudovector ζ_μ and by the intrinsic momentum tensor $\zeta_{\mu\nu}$, or by the unit three dimensional vector $\mathbf{s}^0$. All these quantities will be mutually connected by the relations (4) and (5). If the mass of the fermion is equal to zero $(k_0 = 0)$ then $\beta_1 = 1$ in all systems of coordinates, and the angle $\gamma = 0$. Hence both the longitudinal and the transverse components of the polarization preserve their invariance separately $(s_3'^0 = s_3^0;\ s_{1,2}'^0 = s_{1,2}^0)$.

For $k_0 = 0$, the longitudinally polarized fermions (for example, the neutrino) must be described by a spin pseudovector $(\zeta_3 = ks_3^0,\ \zeta_{1,2} = 0)$, while the transversely polarized, by an intrinsic magnetic moment tensor $(\mu_{1,2} = ks_{1,2}^0,\ \mu_3 = 0)$.

2. FUNDAMENTAL FORMULAS FOR SPIN REVERSAL IN ELASTIC SCATTERING

In the investigation of the behavior of the polarization of a fermion in elastic scattering $(K' = K$, and the primes denote quantities referring to the scattered state), it is first necessary to compute the values of the coefficients $C'_{s'}$ which will be connected with the initial coefficients C_s by the relation

$$C'_{s'} = \frac{1}{2}\sum_s \bar{\rho}_\mu(s', s)\,\bar{\sigma}_\nu(s', s)\,C_s, \tag{8}$$

where the values for $\bar{\rho}_\mu(s', s)$, $\bar{\sigma}_\nu(s', s)$ are given by Eqs. (12) — (14) of reference 6, in which the scattering of longitudinally polarized fermions $(C_1 = 1,\ C_{-1} = 0)$ was considered. Here it is best to characterize the polarization by a spin pseudovector.

In the present work, we want to investigate the scattering of transversely polarized fermions; we shall therefore describe the polarization properties by an intrinsic magnetic-moment tensor.

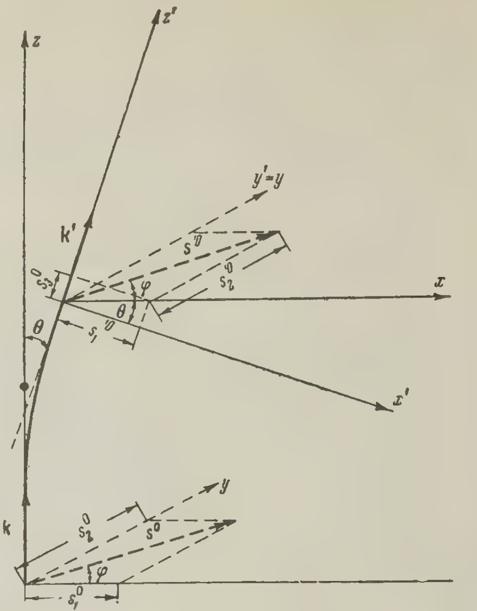

Scattering of transversely polarized fermions by a center of force.

Let the fermion move along the z axis before scattering, and let its spin be characterized by the vector $\boldsymbol{\mu}$ directed perpendicularly to the motion, making angle φ with the x axis. In this case, we must set $C_1 = 1/\sqrt{2}$, $C_{-1} = e^{i\varphi}/\sqrt{2}$ inasmuch as we have here

$$s_0 = 1, \qquad s_1^0 = \cos\varphi, \qquad s_2^0 = \sin\varphi, \qquad s_3^0 = 0,$$

as is seen from Eqs (2) and (3). Without affecting the generality of the discussion, we can choose the zx plane so that the momentum of the scattered fermion lies in this plane (see drawing).

We shall find general formulas that characterize the polarization after scattering as a function of the character of the interaction.

a) First we consider the case of interactions proportional to the matrices ρ_1 and ρ_2 (see reference 6), i.e., $A^t = \rho_1\sigma_4$ (temporal component of the pseudovector interaction), $P = \rho_2\sigma_4$ (pseudoscalar interaction), $V^s = \rho_1\boldsymbol{\sigma}\cdot\mathbf{n}$ (spatial component of the vector interaction) and $T^t = \rho_2\boldsymbol{\sigma}\cdot\mathbf{n}$ (space-time component of the tensor interaction). The three dimensional vector $\mathbf{n}$ defines some direction which is connected with the scattering center and which is specified by the directions of the magnetic moment and the momenta of the motion.

In all these cases it is easy to prove that the longitudinal component of the polarization (i.e., the projection of the spin of the scattered fermion on the z′ axis, which we direct along the momentum $\mathbf{k}$) vanishes $(s_3'^0 = 0)$. In other words, in these interactions, the longitudinally polarized fermion remains longitudinal, as was shown in reference 6, while the transversely polarized fermion remains transverse.

To determine the rotation of the vector of the transverse polarization of the scattered fermion, we have the following expressions from (2) and (8):

$$s_1'^0 = R_1 \cos\varphi + Q_1 \sin\varphi, \qquad s_2'^0 = R_2 \sin\varphi + Q_2 \cos\varphi, \quad (9)$$

$$Q_{1,2}^{A,P} = 0, \qquad R_1^{A,P} = \mp 1, \qquad R_2^{A,P} = -1. \quad (10)$$

In Eq. (10), the minus sign refers to R_1^A and the plus to R_1^P, and so forth. The corresponding value for the quantity s_0', which characterizes the total (for finite spin s') effective cross section, will be equal to

$$s_0'^{A,P} = (k^2/2K^2)(1 \pm \cos\theta). \quad (11)$$

In a similar way we find

$$s_0'^V = \frac{k^2}{K^2}(a^2 + b^2), \qquad R_{1,2}^V = \frac{a^2 - b^2}{a^2 + b^2}, \qquad Q_{1,2}^V = \pm \frac{2ab}{a^2 + b^2},$$

$$s_0'^T = \frac{k^2}{K^2}(a'^2 + b'^2), \qquad R_{1,2}^T = \mp \frac{a'^2 - b'^2}{a'^2 + b'^2},$$

$$Q_{1,2}^T = \frac{2a'b'}{a'^2 + b'^2}; \quad (12)$$

$$\left.\begin{matrix} a \\ a' \end{matrix}\right\} = n_1 \sqrt{\frac{1 \mp \cos\theta}{2}} \pm n_3 \sqrt{\frac{1 \pm \cos\theta}{2}},$$

$$\left.\begin{matrix} b \\ b' \end{matrix}\right\} = \pm n_2 \sqrt{\frac{1 \mp \cos\theta}{2}}, \quad (13)$$

where θ is the scattering angle.

b) In the case of interactions proportional to the matrices ρ_4 and ρ_3:

$$V^{\mathrm{sp}} = \rho_4\sigma_4, \qquad S = \rho_3\sigma_4, \qquad T^{\mathrm{sp}} = \rho_3(\sigma\mathbf{n}), \qquad A^{\mathrm{sp}} = \rho_4(\sigma\mathbf{n}) \quad (14)$$

we find that as a result of the scattering, in addition to the rotation of the transverse component of the polarization vector, an additional longitudinal component must appear (if the mass of the fermion $k_0 \neq 0$). In this case we have

$$s_0'^{V,S} = \tfrac{1}{2}(1 + k_0^2/K^2) \pm \tfrac{1}{2}(1 - k_0^2/K^2)\cos\theta,$$

$$Q_{1,2}^{V,S} = 0, \quad R^{V,S} = 1, \quad R_1^{V,S} = \frac{(K^2 + k_0^2)\cos\theta \pm (K^2 - k_0^2)}{(K^2 + k_0^2) \pm (K^2 - k_0^2)\cos\theta}, \quad (15)$$

$$s_0'^{A,T} = \bar{a}'^2 + \bar{b}'^2 + \bar{a}^2 + \bar{b}^2,$$

$$R_{1,2}^{A,T} = \frac{(\bar{b}^2 - \bar{a}^2) \mp (\bar{b}'^2 - \bar{a}'^2)}{\bar{a}^2 + \bar{b}^2 + \bar{b}'^2 + \bar{a}'^2}, \quad Q_{1,2}^{A,T} = -\frac{2\bar{a}'\bar{b}' \mp 2\bar{a}\bar{b}}{\bar{a}^2 + \bar{b}^2 + \bar{a}'^2 + \bar{b}'^2}. \quad (15a)^*$$

In Eqs. (15) and (15a), one must set $\bar{a}' = k_0 a'/K$, $\bar{b}' = k_0 b'/K$, $\bar{a} = a$, $\bar{b} = b$ in the case of the A interaction, and $\bar{a}' = a$, $\bar{b}' = b$, $\bar{a} = k_0 a/K$, $\bar{b} = k_0 b/K$ for the T interaction.

As we have already noted for the interactions (14), longitudinal polarization can appear as a result of the scattering; this polarization should be characterized by the components

$$s_3'^0 = R_3 \cos\varphi + Q_3 \sin\varphi; \quad (16)$$

$$R_3^{V,S} = \frac{2k_0 K \sin\theta}{(K^2 + k_0^2) \pm (K^2 - k_0^2)\cos\theta},$$

$$R_3^{A,T} = \frac{2(\bar{a}\bar{a}' + \bar{b}\bar{b}')}{\bar{a}'^2 + \bar{b}'^2 + \bar{a}^2 + \bar{b}^2},$$

$$Q_3^{V,S} = 0, \qquad Q_3^{A,T} = \frac{2(\bar{a}'\bar{b} - \bar{a}\bar{b}')}{\bar{a}'^2 + \bar{b}'^2 + \bar{a}^2 + \bar{b}^2}; \quad (17)$$

the values of the coefficients $\bar{a}$, $\bar{b}$, etc are the same as in Eqs. (15) and (15a).

It is seen from (16) and (17) that the longitudinal polarization for fermions with zero rest mass ($k_0 = 0$) should not appear in the scattering of transversely polarized fermions.

3. POLARIZATION EFFECTS IN SCALAR AND VECTOR INTERACTIONS

We shall investigate in more detail the polarization properties in certain special cases. First we note that these polarization properties in elastic scattering (in the first Born approximation) depend only on the initial polarization, the scattering angle and the character of the interaction, inasmuch as the quantities s_0' and s'^0 do not depend on the matrix element of the energy of interaction

$$u_{\mathbf{k}'\mathbf{k}} = \int e^{i\kappa\mathbf{r}} u(r)\, d^3x, \quad (18)$$

(see reference 6), where $\kappa = \mathbf{k} - \mathbf{k}'$, and $u(r)$ is the spatial part of the interaction energy.

For example, as is seen from Eq. (15), the component of the unit vector $\mathbf{s}'^0$ along the axis $y' = y$ for V^t or S interactions remains unchanged ($s_2'^0 = s_2^0$), while the spin vector in the $(x'z')$ plane, located in a system of coordinates associated with the motion of the fermion,* is turned through some angle. As a result, a longitudinal component appears, as is seen from Eq. (17).

In the nonrelativistic case ($k_0 = K$), it follows from Eqs. (15) and (17) that, both for V^t and for S interactions, the same result holds:

$$s_3'^0 = \sin\theta\cos\varphi,$$

$$s_1'^0 = \cos\theta\cos\varphi, \qquad s_2'^0 = \sin\varphi, \quad (19)$$

---

*The different signs on the right side of Eq. (15a) refer to the indices 1 and 2, respectively.

*We shall denote by x′y′z′ the auxiliary set of coordinates connected with the motion of the fermion. Before scattering of the fermion, the x′y′z′ system coincides with the xyz system. After scattering, only the y′ axis coincides with the y axis. The x′, z′ axes are rotated, relative to the x, z axes, respectively, through the scattering angle θ (see drawing).

i.e., just as in the scattering of longitudinally polarized particles (see reference 6), the spin vector of the scattered fermion maintains the direction of the original spin: $\mathbf{s}'^0 = \mathbf{s}^0$. This specific case is also shown in the drawing.

On the other hand, in the ultrarelativistic case ($k_0 \ll K$), the longitudinal component of the polarization will gradually vanish with increase in energy, and the fermion will again become transversely polarized. In this case the spin in V^t interaction maintains its orientation relative to the x′ axis ($s_1'^0 = s_1^0 = \cos\varphi$). In the case of S interaction, it changes this orientation to the opposite ($s_1'^0 = -s_1^0 = -\cos\varphi$).

We note that in the general case, in connection with the appearance of longitudinal polarization as the result of the scattering, the intrinsic magnetic moment is rotated in the z′x′ plane through an angle

$$\tan\alpha' = \mu_3'/\mu_1' = 2k_0^2\sin\theta\,/\,[(K^2 + k_0^2)\cos\theta \pm (K^2 - k_0^2)]. \tag{20}$$

The plus sign here refers to V^t interaction, and the minus to S interaction.

It is interesting to note that for these same interactions an analogous formula was obtained in reference 6 for the angle of rotation in the system connected with the motion of the particle. This was done for the case of longitudinally polarized fermions. However, this rotation did not refer to the intrinsic magnetic moment, directed in our case perpendicular to the momentum, but to the spin pseudovector of the fermion, which was directed parallel to the momentum.

As another example, we consider the scattering of a charged fermion by a fixed magnetic moment $\boldsymbol{\mu}'$. In this case, we can represent the interaction energy in the form

$$U = -ie\rho_1(\boldsymbol{\sigma}\mathbf{A}),$$

where $\mathbf{A}$ is the vector potential created by the magnetic moment. The matrix element will be proportional to the following expression (see reference 6):

$$V^t = -ie\rho_1\boldsymbol{\sigma}\mathbf{n}, \quad \text{and} \quad \mathbf{n} = [\boldsymbol{\varkappa}\cdot\boldsymbol{\mu}'], \quad \boldsymbol{\varkappa} = \mathbf{k} - \mathbf{k}'. \tag{21}$$

As a result of scattering, the transversely polarized fermion should remain transversely polarized (inasmuch as this interaction is proportional to the matrix ρ_1). However, in the plane perpendicular to the direction of the momentum of the scattered fermion (i.e., in the x′y′ plane), the intrinsic magnetic moment ought to rotate through some angle which depends on the direction of the magnetic moment $\boldsymbol{\mu}'$.

If the magnetic moment $\boldsymbol{\mu}'$ is directed along the momentum $\mathbf{k}$ of the incident fermion ($\mu_y' = \mu_x' = 0$), we shall have, in the system connected with the motion of the fermion:

$$s_1'^0 = -\cos\varphi, \qquad s_2'^0 = -\sin\varphi, \qquad s_3'^0 = 0. \tag{22}$$

If the magnetic moment $\boldsymbol{\mu}'$ is perpendicular to the direction $\mathbf{k}$ ($\mu_z' = 0$), we get

$$s_{1,2}'^0 = \frac{\mu_y'^2 - \mu_x'^2\sin^4(\theta/2)}{\mu_y'^2 + \mu_x'^2\sin^4(\theta/2)}\begin{pmatrix}\cos\varphi\\ \sin\varphi\end{pmatrix} + \frac{2\mu_x'\mu_y'\sin^2(\theta/2)}{\mu_y'^2 + \mu_x'^2\sin^4(\theta/2)}\begin{pmatrix}-\sin\varphi\\ \cos\varphi\end{pmatrix}, \tag{23}$$

i.e., if $\mu_y' = 0$ and $\mu_x' \neq 0$, we again obtain the expressions (22) for the unit vector, and for $\mu_x' = 0$ and $\mu_y' \neq 0$ we have

$$s_1'^0 = \cos\varphi, \qquad s_2'^0 = \sin\varphi, \qquad s_3'^0 = 0. \tag{24}$$

Hence it is seen that if the magnetic moment $\boldsymbol{\mu}'$ is perpendicular to the momentum of the incident and scattered mesons (i.e., perpendicular to the plane $\mathbf{k}'\cdot\mathbf{k}$), then $\mu_x' = \mu_z' = 0$ and, therefore, in accord with (24), the polarization vector maintains its direction in the system of coordinates connected with the motion of the particle. Now, if $\boldsymbol{\mu}'$ lies in the plane $\mathbf{k}'\cdot\mathbf{k}$, then the polarization vector changes its direction to the opposite. We recall that before scattering the components of the spin were equal to $s_1^0 = \cos\varphi$, $s_2^0 = \sin\varphi$, $s_3^0 = 0$.

4. AZIMUTHAL ASYMMETRY IN THE SCATTERING OF POLARIZED FERMIONS

In our previous work,[6] we considered the scattering of longitudinally polarized fermions, and found that the differential effective cross section was the same as in the scattering of unpolarized fermions. This result is completely understandable, since no asymmetry should be noted for longitudinal fermions relative to the azimuthal scattering angle φ, and therefore, neither in the case of a linear combination of different interactions, nor in the case of a more exact solution of this problem (for example, by the damping method) should an azimuthal asymmetry connected with longitudinal polarization be obtained.

It should be emphasized that in the scattering of longitudinal fermions by the magnetic moment $\boldsymbol{\mu}'$ directed perpendicularly to the momentum $\mathbf{k}$ ($\mu_x' \neq 0$, $\mu_y' \neq 0$), azimuthal asymmetry can be observed. However, this asymmetry characterizes only the azimuthal asymmetry connected with the presence of a transverse component of the scattering magnetic moment $\boldsymbol{\mu}'$, and is completely independent of the initial degree of longitudinal polarization of the scattered fermions.

In the scattering of transversely polarized fermions, we can expect the phenomenon of azimuthal asymmetry. It is true that in carrying out calculations in the Born approximation only for the presence of one form of interaction, we found that the quantity s_0' does not depend on the angle φ (see Sec. 2). However, this dependence can appear a) in the case of scattering in the presence of a linear combination of separate interactions, or b) in the presence of a single form of interaction but for a more exact solution of the problem, for example, by the method of damping.

We shall consider each of these cases in more detail.

a) Combination of separate interactions can take place, for example, in the investigation of the scattering of a particle possessing an electric charge e and a magnetic moment $\mu = \mu\sigma$ by a fixed center which has an electric charge e′ and a magnetic moment μ'.

In this case the matrix element characterizing the spin part of the interaction takes the form

$$C'_{s'} = \frac{1}{2} \sum_{s=-1,1} (ee'\bar{\rho}_4(s',s)\bar{\sigma}_4(s',s) - ie'\mu\bar{\rho}_2(s',s)\bar{\boldsymbol{\sigma}}(s',s)\boldsymbol{\varkappa}$$
$$+ ie\bar{\rho}_1(s',s)\bar{\boldsymbol{\sigma}}(s',s)[\boldsymbol{\varkappa}\times\boldsymbol{\mu}'] + \mu\bar{\rho}_3(s',s)\bar{\boldsymbol{\sigma}}(s',s)[\boldsymbol{\varkappa}\times[\boldsymbol{\varkappa}\times\boldsymbol{\mu}']])\,C_s,$$

where $\kappa = \mathbf{k} - \mathbf{k}'$.

In order to avoid the effects of azimuthal asymmetry connected with the presence of a transverse component of the magnetic moment μ' of the scattering center, we direct this moment along the z axis ($\mu_z' = \mu'$, $\mu_x' = \mu_y' = 0$). Here we find for the coefficients $C_{s'}'$ [by means of Eq. (8)]:

$$C'_{s'} = \sum_s \left\{\frac{1}{2}(1 + ss')(p - sq) - \frac{1}{2}s(1 - ss')\,m\right\} C_s; \quad (25)$$

$$p = ee'\cos\frac{\theta}{2}, \qquad q = 2\mu'(e + 2\mu k_0)\frac{k^2}{K^2}\sin^2\frac{\theta}{2}\cos\frac{\theta}{2},$$
$$m = e'(ek_0 - 2\mu k^2)\frac{1}{K}\sin\frac{\theta}{2}. \quad (26)$$

If we assume for transversely polarized fermions $C_1 = 1/\sqrt{2}$, $C_{-1} = e^{i\varphi}/\sqrt{2}$, we obtain the following expression for the quantity s_0' which characterizes the effective cross section:*

$$s_0' = (p^2 + q^2 + m^2)(1 - \delta\cos\varphi), \quad (27)$$

where the asymmetry coefficient δ is equal to

$$\delta = 2qm / (p^2 + q^2 + m^2). \quad (28)$$

It is evident from the latter formula that the azimuthal asymmetry must hold in the case in which the scattering center also possesses an electric charge ($e' \neq 0$) and a magnetic moment ($\mu' \neq 0$) (see also reference 7, where the azimuthal asymmetry was investigated for double scattering).

b) Exactly the same azimuthal asymmetry can be obtained in the scattering of transverse fermions in the presence of one form of interaction but with allowance for damping. For example, in the simplest case of the scattering of a fermion of charge e by a fixed charge e′ (V^t interaction) with account of damping, we find (see references 8 and 9):

$$s_0'' = \frac{1}{2}K^{-2}[(K^2 + k_0^2) + \cos\theta\,(K^2 - k_0^2)](1 + \delta\sin\varphi), \quad (29)$$

where the asymmetry coefficient is

$$\delta = 2\alpha'\sin\theta\,Kk_0 / [(K^2 + k_0^2) + \cos\theta'(K^2 - k_0^2)],$$
$$\alpha' = \frac{k^3}{16\pi^2 c\hbar\,KU_{\mathbf{k}'\mathbf{k}}} \oint d\Omega'' u_{\mathbf{k}'\mathbf{k}''} u_{\mathbf{k}''\mathbf{k}} \frac{(\mathbf{k} - \mathbf{k}'')(\mathbf{k} + \mathbf{k}')}{\mathbf{k}(\mathbf{k} + \mathbf{k}')}.$$

Here $d\Omega''$ is the solid angle of the vector $\mathbf{k}''$.

In a similar way one can easily determine the azimuthal asymmetry in the presence of other interactions, solving the problem by the method of damping.

---

[1] H. A. Tolhoek, Revs. Modern Phys. **28**, 277 (1956) (translation in Usp. Fiz. Nauk **63**, 761 (1957).

[2] Yu. M. Shirokov, JETP **21**, 748 (1951); **35**, 1005 (1958), Soviet Phys. JETP **8**, 703 (1959).

[3] P. Stichel, Z. Physik **157**, 89 (1959).

[4] Sokolov, Ternov, and Loskutov, JETP **36**, 930 (1959), Soviet Phys. JETP **9**, 657 (1959).

[5] G. Ascoli, Z. Physik **150**, 407 (1958).

[6] A. A. Sokolov and M. M. Kolesnikova, JETP **38**, 165 (1956), Soviet Phys. JETP **11**, 120 (1960).

[7] A. A. Sokolov, J. Phys. U.S.S.R. **9**, 363 (1945).

[8] Sokolov, Guseĭnov, and Kerimov, JETP **34**, 110 (1958), Soviet Phys. JETP **7**, 76 (1958). Nucl. Phys. **5**, 390 (1958).

[9] A. A. Sokolov, Введение в квантовую электродинамику, (Introduction to Quantum Electrodynamics) (Fizmatgiz, Moscow, 1958), Sec. 36.

Translated by R. T. Beyer
343

---

*We recall that the connection of s_0' with the differential effective cross section is determined by Eq. (15) of reference 6.

SOVIET PHYSICS JETP VOLUME 11, NUMBER 6 DECEMBER, 1960

IDENTIFICATION OF EXCITONS WITH LIGHT WAVES IN A CRYSTAL AND THE MACROSCOPIC THEORY OF EXCITONS WITH AND WITHOUT ACCOUNT OF RETARDATION

S. I. PEKAR

Institute of Physics, Academy of Sciences, Ukrainian S.S.R.

Submitted to JETP editor January 2, 1960

J. Exptl. Theoret. Phys. (U.S.S.R.) 38, 1786-1797 (June, 1960)

Excitons are identified with light waves in a crystal. The theory of excitons is reduced to the macroscopic theory of light waves. The energy bands, limiting energies for $\mathbf{k} \to 0$, effective masses etc. of excitons are expressed in terms of the dielectric constant tensor $\epsilon(\omega, \mathbf{k})$. In the limit $c \to \infty$, we obtain the results of the conventional exciton theory, based on the Schrödinger equation and neglecting retardation of interactions between particles. The results show that retardation can be neglected when the electromagnetic wave that accompanies an exciton is longitudinal. If, however, the wave possesses a rotational field, retardation considerably affects the results in regions where the refractive index is not very large. Exciton energies and effective masses then differ from those derived by means of the Schrödinger equation. Crystals of different symmetries are considered.

EXCITONS and light waves in crystals are physical concepts of entirely different origins and have been described mathematically in entirely different ways. Light waves are described by Maxwell's equations, with the mechanical motions of electrons and nuclei in a crystal taken into account entirely by the tensor form of the dielectric constant $\epsilon(\omega)$ (ω is the wave frequency). Beginning with Frenkel's first paper,[1] excitons have been described by the Schrödinger equation without allowing for retardation in the interactions between particles of a crystal.

Exciton absorption of light in a crystal has so far been treated as a quantum transition in which a photon is absorbed and an exciton is created. This procedure would be justified if light and molecules were two weakly interacting subsystems, as in the case of a gas. In a crystal, however, only the effect of the electromagnetic field on molecules can be regarded as a small perturbation, whereas the effect of the molecules on the field is not a small perturbation. There is a great difference between light waves in a crystal and in a vacuum; for the same frequency we find different wavelengths, different dispersion laws, etc. An exception occurs when the refractive index n in a crystal is very close to unity, but this is not usually the case in the absorption region.

The mechanical energy of crystal electrons and nuclei makes an important contribution to the energy of a light wave. We thus have a mixed "electromagnetic-mechanical" wave. However, the same can be said of an exciton wave, since it follows from references 2–6 that an exciton wave generates an accompanying electromagnetic wave that contributes greatly to the energy of the exciton. Excitons must therefore be identified with light waves in a crystal; both are small oscillations (excitations) of a system consisting of two strongly interacting parts — a crystal and an electromagnetic field.

As an illustration let us consider the optical vibration of an ionic lattice.[6] This vibration, when regarded as a mechanical phenomenon, is a typical exciton, but it is accompanied by the appearance in the crystal of fictitious charges and polarization currents that vary periodically in space and in time. The currents establish an electromagnetic field oscillating with the same frequency and wavelength. The amplitude of field oscillations is uniquely determined by the amplitude of normal ionic vibration, which can thus obviously be identified with an infrared light wave in the crystal.

As in our earlier papers,[2,4] we shall in general define an exciton as any excited state of the system that is characterized by a single wave vector $\mathbf{k}$ (with otherwise discrete quantum numbers). Regarding a crystal together with an electromagnetic field as a conservative system performing small quantized harmonic oscillations, we can identify the photon energy $\hbar\omega(\mathbf{k})$ with the exciton energy. The scattering of an exciton on lattice vibrations, accompanied by phonon creation or absorption, should be identified with the Raman scattering of a light quantum on the lattice vibrations.

Our earlier conclusion[3,4] that when the exciton lifetime is infinite no light is absorbed in a crystal, regardless of the magnitude of the phototransition oscillator strength per unit cell, now becomes trivial. Absorption becomes possible only as a result of exciton decay accompanied by a thermal transition of the system to excited states of another type.

For a quantitative study of excitons it is obviously just as necessary to consider the retardation of electromagnetic interactions as in the case of light waves. The Schrödinger equation is therefore, generally speaking, inadequate for excitons since it accounts only for instantaneous interactions between charges at all distances. There are two ways in which excitons can be studied while accounting for retardation in long-range interactions.

1) The Schrödinger Hamiltonian of the crystal should be supplemented by the energy of the rotational part of the field and by its interaction with particles. The latter is introduced into the Schrödinger problem of particle motion as a small external (classical) time-dependent perturbation. The rotational part of the field is determined self-consistently from the Maxwell equations, into the right-hand members of which we substitute the charges and currents that are derived from a solution of the Schrödinger problem.

The solution of the self-consistent problem as a whole enables us to determine the dispersion law for small vibrations of the entire conservative system, i.e., the dependence of ω on **k**. When these vibrations are quantized the energy of an exciton is given by

$$u_{\mathbf{k}} = \hbar\omega(\mathbf{k}). \tag{1}$$

We followed this first procedure in references 2, 4 and 7, where the above-mentioned dispersion law was derived.

The solution of the unperturbed Schrödinger problem neglecting retardation is thus an auxiliary intermediate step. At this stage we can use the results given in numerous publications where excitons were considered on the basis of the Schrödinger equation. It must be emphasized, however, that the corresponding Schrödinger excited crystal states are not in general real excitons, and that the corresponding eigenenergies differ considerably from the energies of real excitons when retardation is taken into account, as we shall see below.

We shall avoid conflict with conventional terminology by applying the term "exciton" to states of the auxiliary Schrödinger problem which neglects retardation. For real states of the entire conservative system (crystal plus electromagnetic field) we now introduce the term "light-exciton." (The word "photon" would not adequately express the large contribution from the mechanical energy of the particles.)

2) A second method for studying light-excitons will be used in this paper. The macroscopic electromagnetic field accompanying a light-exciton wave is defined by Maxwell's equations and is treated as a light wave. When we confine ourselves to cases in which the wavelength is considerably greater than the lattice constant, this field can be calculated by conventional macroscopic crystal optics, retardation in long-range interactions now being taken into account immediately. The energy of this light wave as calculated from the equations of electrodynamics will, as we know, include the mechanical energy of motion of the particles (electrons and nuclei). The dispersion law $\omega = \omega(\mathbf{k})$ that is determined for the wave will then be identified with that for small harmonic vibrations of the entire conservative system mentioned above, whereupon (1) will give the energy of the light-exciton.

The advantage of this second procedure lies in the fact that it is now entirely unnecessary to formulate and solve an auxiliary Schrödinger problem. On the other hand, it is necessary to specify (borrow from some source) the dependence of the dielectric constant ϵ on frequency ω and on the wave vector **k**. The dependence of ϵ on **k** is called the spatial dispersion. The dependence of ϵ on ω and **k** reflects the specific character of mechanical particle motion in the crystal, and its theoretical derivation would, of course, require solving the Schrödinger problem for the crystal.

Thus, identifying light-excitons with light waves in the crystal and assuming the electric field **E**, induction **D**, and magnetic field **H** to be proportional to

$$\exp\{i(\mathbf{kr} - \omega t)\} \quad (\mathbf{k} = \omega n \mathbf{s}/c, \quad |\mathbf{s}| = 1), \tag{2}$$

we obtain for the amplitude of the electric field the well-known vector equation

$$\mathbf{D} = \varepsilon(\omega, \mathbf{k})\,\mathbf{E} = n^2[\mathbf{E} - \mathbf{s}(\mathbf{sE})], \tag{3}$$

which is equivalent to a system of three homogeneous scalar equations. When the determinant of this system is set equal to zero we obtain the familiar equation for n:

$$\bar{\varepsilon} n^4 + [\bar{\varepsilon}^2 - \bar{\varepsilon}\,\mathrm{Sp}\,\varepsilon]\, n^2 + \varepsilon_1\varepsilon_2\varepsilon_3 = 0. \tag{4}$$

It is assumed here that the Cartesian coordinates are taken along the principal axes of the tensor $\epsilon(\omega, 0)$. Then the determinant for ϵ equals $\epsilon_1\epsilon_2\epsilon_3$, to terms of order $\mathbf{k}^2$. In (4) we have

$$\bar{\varepsilon} = (s, \varepsilon s), \quad \overline{\varepsilon^2} = (s, \varepsilon^2 s), \quad \mathrm{Sp}\,\varepsilon = \sum_{j=1}^{3} \varepsilon_j, \tag{5}$$

where ϵ_j ($j = 1, 2, 3$) are the principal values of the tensor ϵ.

If the dependence of ϵ on ω and $\mathbf{k}$ is given, (4) is used to determine $n(\omega)$ for a given direction of $\mathbf{s}$, thus determining $\omega(\mathbf{k})$ and the light-exciton energy (1). The existence of spatial dispersion raises (4) to higher than the fourth power in n, and more than two branches of the dispersion $n(\omega)$ are therefore obtained. These branches for different special cases are considered in references 2 and 6–9.

We can speak of light-exciton energy bands u_k, in a rigorous sense, only when the light-exciton possesses a very long lifetime, i.e., when light absorption in the crystal is negligibly small, as will be assumed below. In an infinite crystal the allowed bands comprise the values of u_k that correspond to real values of n. The values of u_k [and, correspondingly, of $\omega(\mathbf{k})$] that correspond to complex values of n are forbidden. In addition to spatial energy bands, a finite crystal may have allowed surface bands representing waves for which only the projection of $\mathbf{k}$ perpendicular to the crystal surface is complex. In the present work we do not consider surface bands or finite crystals.

In order to consider extremely long light-exciton waves we must assume $n \to 0$ in the preceding equations. It then follows from (3) that at least one of the principal values of ϵ must equal zero and that the corresponding projection of $\mathbf{E}$ may differ from zero:

$$\varepsilon_j(\omega', 0) = 0, \qquad \mathbf{E}_j \neq 0. \tag{6}$$

Here ω' [the roots of (6)] are the frequencies of the limiting waves, which do not depend on the direction of wave propagation ($\mathbf{s}$). It will be shown below that for "purely mechanical" excitons the limiting frequencies and energies generally depend on $\mathbf{s}$. When crystal symmetry causes two or three principal values of ϵ to vanish at the same frequency ω', two or three projections of the electric vector may correspondingly differ from zero for the limiting wave. The trivial case of an extremely long radio wave with $\omega = 0$ will not be considered.

Equations (1)–(6) provide the basis for a macroscopic theory of real light-excitons in a crystal. It is interesting to determine the relationships between the properties of light-excitons and excitons. The latter are understood to be the corresponding excited crystal states calculated by means of the Schrödinger equation, neglecting retardation and the rotational part of the field accompanying the electromagnetic wave. Such calculations are very common in the literature. The exciton theory is obviously a limiting case of the light-exciton theory with retardation neglected (i.e., $c \to \infty$). At the same time, for a wave with given values of ω and $\mathbf{k}$, $\mathbf{k}$ could remain finite in (2) only with n also approaching infinity. Passing to this limit in (4), the dependence of ω on $\mathbf{k}$ becomes possible only through spatial dispersion. We thus find that the neglect of spatial dispersion in electrodynamics is equivalent to the assumption of an infinitely narrow exciton energy band.

For extremely long exciton waves we must assume $k \to 0$ in (1)–(5) in addition to the limit $n \to \infty$ discussed above. The frequencies ω_0 of limiting exciton waves will then differ greatly from the frequencies ω' of limiting light-exciton waves, as will be evident from the examples discussed below.

We shall consider different possible types of light-excitons and some of their properties. When it is necessary to assign a specific dependence of ϵ_j on ω and $\mathbf{k}$, this dependence will be assumed to have the form

$$\varepsilon_j(\omega, \mathbf{k}) = \varepsilon_{0j} + G_j / (\mathscr{E}_{0j} + F_j(\mathbf{k}) - \hbar\omega), \tag{7}$$

where ϵ_{0j}, G_j and $\mathscr{E}_{0j}$ are constants. We may assume $F_j(0) = 0$ for a suitable value of $\mathscr{E}_{0j}$. It has been shown in reference 4 that ϵ_j actually has the form (7) if ω is in the vicinity of an isolated exciton light-absorption band. In this frequency region we shall assume that the two other principal values of ϵ are constants: $\epsilon_{j'} = \epsilon_{0j'}$, $j' \neq j$.

Exceptions occur when different principal values of $\epsilon(\omega, 0)$ coincide because of crystal symmetry, as in the case of cubic crystals. In such instances two exciton energy levels which coincide for $\mathbf{k} = 0$ are separated when $\mathbf{k} \neq 0$,[9] giving rise to two close absorption bands, neither of which can be regarded as isolated. The expression for $\epsilon_j(\omega, \mathbf{k})$ then contains two fractions of the type seen in the right member of (7), with identical values of $\mathscr{E}_{0j}$ but different $F_j(\mathbf{k})$. Thus (7) represents ϵ_j only when $\mathbf{k} = 0$.

We shall hereinafter confine ourselves to crystals possessing an inversion center and not lower than rhombic symmetry. In such crystals $\epsilon(\omega, \mathbf{k})$ is an even function of $\mathbf{k}$; the principal axes of $\epsilon(\omega, 0)$ coincide with 2-fold or 4-fold crystallographic axes and are therefore independent of ω. It will also be of importance that in such crystals the principal axis of the $\epsilon(\omega, 0)$ tensor is also the principal axis of the $\epsilon(\omega, \mathbf{k})$ tensor when $\mathbf{k}$ is parallel or perpendicular to this axis.

Light-excitons of the following three types are possible in a crystal.

1. Longitudinal light-excitons, $\mathbf{E} \parallel \mathbf{s}$. The right member of (3) vanishes, so that $\epsilon \mathbf{E} = 0$, i.e., $\mathbf{E}$ and $\mathbf{k}$ can be oriented only in one of the principal polarization directions j and the corresponding principal value ϵ_j vanishes:

$$\mathbf{E} = \mathbf{E}_j, \qquad \varepsilon_j(\omega, \mathbf{k}) = 0. \tag{8}$$

The second of these equations determines the dependence of ω on $\mathbf{k}$, which is possible only because of spatial dispersion.

For this wave the induction $\mathbf{D}$, the magnetic field strength, and the rotational part of the electric field all vanish. Since n does not appear in (3) the limiting transition $n \rightarrow \infty$ is without effect. A longitudinal light-exciton is consequently identical with the corresponding exciton and can be calculated by means of the Schrödinger equation, neglecting retardation, as has usually been done.

When ϵ_j is represented by (7), we obtain from (1) and (8)

$$u_{\mathbf{k}}^{\parallel} = \hbar\omega(\mathbf{k}) = \mathscr{E}_{0j} + G_j / \varepsilon_{0j} + F_j(\mathbf{k}). \tag{9}$$

Here the dependence of G_j and ϵ_{0j} on $\mathbf{k}$ must also be taken into account.

2. Tranverse light-excitons, $\mathbf{E} \perp \mathbf{s}$. According to (3) $\mathbf{E}$ can only have one of the principal polarization directions ($\mathbf{E} = \mathbf{E}_j$), while the dependence of ω on $\mathbf{k}$ is given by*

$$n^2 \equiv (ck/\omega)^2 = \varepsilon_j(\omega, \mathbf{k}). \tag{10}$$

The frequencies ω' of long light-exciton waves are in the limit the same as for longitudinal light-excitons, and are determined by (6). It follows from (10) that in those frequency regions where spatial dispersion can be neglected, ω must be a monotonic function of $|\mathbf{k}|$ since $\epsilon_j(\omega)$ is a single-valued increasing function of ω. Thus the limiting long wave ($\mathbf{k} = 0$) corresponds to the lower boundary of the light-exciton energy band. Moreover, ω does not depend on the direction of $\mathbf{k}$ so long as this remains perpendicular to $\mathbf{E}$.

It should not be concluded from the monotonic dependence of ω on $|\mathbf{k}|$ that the second boundary of the allowed light-exciton energy band corresponds to extremely short waves. With decreasing wavelength the existing macroscopic theory becomes invalid, but not before spatial dispersion becomes important, thus complicating (10) and, in general, destroying the monotonic dependence of ω on $|\mathbf{k}|$. Thus in the second quadrant of Fig. 2 in reference 7 the abscissa of the extreme right-hand point of the dispersion curve corresponds to the upper boundary of the allowed frequency band. At the same time the refractive index of the wave is approximately 15, so that the wave is neither extremely long nor extremely short.

In the present case of a transverse light-exciton, we shall now pass to the limit of a "purely mechanical" exciton. For this purpose we let $c \rightarrow \infty$ in (10), thus obtaining

$$\varepsilon_j(\omega, \mathbf{k}) = \infty. \tag{11}$$

This determines the dependence of ω on $\mathbf{k}$ for a transverse exciton and is quite different from (10), which determines $\omega(\mathbf{k})$ for a light-exciton. (10) leads to the essential dependence of ω on $\mathbf{k}$ even in the case of negligible spatial dispersion, whereas in (11) such dependence is possible only as a result of spatial dispersion. When, for example, ϵ_j is given by (7), Eq. (11) leads to

$$u_{\mathbf{k}}^{\perp}(\mathrm{exc}) = \hbar\omega(\mathbf{k}) = \mathscr{E}_{0j} + F_j(\mathbf{k}). \tag{12}$$

A comparison with (9) shows that for $\mathbf{k} = 0$ the energy of a transverse exciton is diminished relative to that of a longitudinal exciton by the amount G_j/ϵ_{0j}:

$$u_0^{\parallel} - u_0^{\perp}(\mathrm{exc}) = G_j / \varepsilon_{0j}. \tag{13}$$

It was shown above that $\mathbf{E}$ for longitudinal and transverse light-excitons must have one of the principal directions of polarization. The converse is easily derived from (3): If $\mathbf{E}$ has one of the principal polarization directions, the light-exciton must be either longitudinal or transverse. It can also be shown that if $\mathbf{s}$ is parallel to a principal polarization direction, $\mathbf{E}$ must be either parallel to $\mathbf{s}$ or parallel to one of the principal polarization axes that are perpendicular to $\mathbf{s}$. Consequently, only longitudinal or transverse light-excitons are possible.

In order to exhaust the possible types of light-excitons we need only to consider those for which $\mathbf{E}$ and $\mathbf{s}$ are neither parallel nor perpendicular.

3. Light-excitons with $\mathbf{E}$ and $\mathbf{s}$ neither parallel nor perpendicular. It follows from the foregoing discussion that now neither $\mathbf{E}$ nor $\mathbf{s}$ is parallel to one of the principal polarization axes. We shall first consider the case in which $\mathbf{s}$ is perpendicular to one of the principal polarization directions (j). (3) and (4) now have two solutions, one of which is for transverse light-excitons:

$$n^2 = (ck/\omega)^2 = \varepsilon_j(\omega, \mathbf{k}), \ \mathbf{E} = \mathbf{E}_j. \tag{14}$$

This type has already been considered.

---

*Since $\mathbf{k}$ will be perpendicular to the principal polarization direction j, the latter will be a principal axis of the two tensors $\varepsilon(\omega, \mathbf{k})$ and $\varepsilon(\omega, 0)$, thus coinciding with one of the Cartesian coordinate axes.

The other solution is

$$n^2 = \left(\frac{ck}{\omega}\right)^2 = \frac{\varepsilon_i\varepsilon_l - \varepsilon_{il}\varepsilon_{li}}{s_i^2\varepsilon_i + s_l^2\varepsilon_l + s_i s_l(\varepsilon_{il} + \varepsilon_{li})},$$
$$i \neq l \neq j, \tag{15}$$

with **E** lying in a plane perpendicular to the j axis, while its direction is determined by $(\mathbf{s}, \mathbf{D}) = 0$, i.e.,

$$E_i(s_i\varepsilon_i + s_l\varepsilon_{li}) + E_l(s_i\varepsilon_{il} + s_l\varepsilon_l) = 0. \tag{16}$$

Here the subscripts i and *l* denote the two principal axes of $\epsilon(\omega, 0)$ perpendicular to j.

In the frequency region where spatial dispersion may be neglected $|\mathbf{k}|$ is a single-valued function of ω. Consequently, ω is a monotonic function of $|\mathbf{k}|$ for the given direction of **s**, and limiting long waves correspond to the boundaries of the energy band. This does not apply to the case in which spatial dispersion is taken into account, since **k** then appears in the right member of (15); this equation then is not of the first degree in $\mathbf{k}^2$ and has several roots of $\mathbf{k}^2$ for a given frequency. We shall now pass to the limit of a "purely mechanical" exciton in (15) and (16). Setting $c \to \infty$ in (15), we obtain (since $\epsilon_i \neq \epsilon_l$)

$$s_i^2\varepsilon_i(\omega, \mathbf{k}) + s_l^2\varepsilon_l(\omega, \mathbf{k}) + s_i s_l[\varepsilon_{il}(\omega, \mathbf{k}) + \varepsilon_{li}(\omega, \mathbf{k})] = 0. \tag{17}$$

This equation determines the dependence of ω on **k** for the exciton.

In the final case **s** is perpendicular to none of the principal polarization directions. (4) now splits into the two equations

$$n_\alpha^2 \equiv \left(\frac{ck_\alpha}{\omega}\right)^2 = \frac{1}{2}\left\{\frac{\Omega}{\bar{\varepsilon}} - \left[\left(\frac{\Omega}{\bar{\varepsilon}}\right)^2 - 4\frac{\varepsilon_1\varepsilon_2\varepsilon_3}{\bar{\varepsilon}}\right]^{1/2}\right\}, \tag{18}$$

$$n_\beta^2 \equiv \left(\frac{ck_\beta}{\omega}\right)^2 = \frac{1}{2}\left\{\frac{\Omega}{\bar{\varepsilon}} + \left[\left(\frac{\Omega}{\bar{\varepsilon}}\right)^2 - 4\frac{\varepsilon_1\varepsilon_2\varepsilon_3}{\bar{\varepsilon}}\right]^{1/2}\right\}. \tag{19}$$

Here $\Omega = \bar{\epsilon}\,\mathrm{Sp}\,\epsilon - \bar{\epsilon}^2$.

The direction of **E** is determined from (3) and is not perpendicular to that of **s**. When spatial dispersion exists each of these equations determines more than one dispersion branch of $\omega(\mathbf{k})$, which could be investigated only for a definite dependence of ϵ on **k**.

The frequency region in which spatial dispersion may be neglected can be investigated qualitatively. In this case

$$\Omega = \varepsilon_1\varepsilon_2(1 - s_3^2) + \varepsilon_1\varepsilon_3(1 - s_2^2) + \varepsilon_2\varepsilon_3(1 - s_1^2),$$
$$\varepsilon_{il} = 0, \quad i \neq l. \tag{19a}$$

For $\mathbf{k}_\beta^2 \geq \mathbf{k}_\alpha^2$ the solutions (18) and (19) will be called long-wave and short-wave light-excitons, respectively. Allowed frequency and energy bands for these light-excitons are determined from the condition that the radicands and the right members of (18) and (19) be positive. The same qualitative statements can be made concerning the dependence of ω on **k** for each of these light-excitons as in the case of a transverse light-exciton, with the following addition. For all ω for which n_α is real, n_β is also real. But it is also possible to have ω for which only n_β is real, but not n_α. This means that every allowed energy band of light-exciton (18) must be inside the band of light-exciton (19). The latter band is therefore wider than the former.

If for some frequency $\bar{\omega}$ we have $\Omega^2 = 4\bar{\epsilon}\epsilon_1\epsilon_2\epsilon_3$ and $\Omega/\bar{\epsilon} > 0$, then $\bar{\omega}$ is the common boundary of α and β (the sign of the radicand reverses when $\omega = \bar{\omega}$). When $\omega = \bar{\omega}$, $(d\omega/d|\mathbf{k}|)_{\bar{\omega}} = 0$ for both light-excitons. These relationships are shown approximately in the figure. For ω' determined from (6) the limiting long wave will be either the α wave (if $(\Omega/\bar{\epsilon})_{\omega'} > 0$) or the β wave (if $(\Omega/\bar{\epsilon})_{\omega'} < 0$). ω' is the boundary of the allowed band and, unlike $\bar{\omega}$, does not depend on the direction of **s**. The figure shows that the allowed bands may be entirely within the region of such long waves that macroscopic considerations and the neglect of spatial dispersion are possible for the entire band.

In (18) and (19) we now make the limiting transition from light-excitons to excitons, for which purpose we set $c \to \infty$. In (18) only directions of **s** perpendicular to one of the principal polarization directions are then possible, resulting in a transverse exciton which is represented by (11) and (12).

In (19) the same limiting transition leads to

$$\bar{\varepsilon} \equiv \sum_{i=1}^{3} s_i^2\varepsilon_i(\omega, \mathbf{k}) = 0, \tag{20}$$

which extends (17) to the case in which all three projections of **s** differ from zero. (20) is fulfilled when all three principal values ϵ_i are finite. Consequently, putting $n \to \infty$ in (3), we obtain $\mathbf{E} \parallel \mathbf{s}$. The exciton is thus longitudinal although the original light-exciton (19) was not longitudinal. This result as well as the freedom for the direction of **s** distinguishes the present case from the previously considered longitudinal light-exciton. According to (20) the dependence of ω on k_1, k_2, k_3 is discontinuous at $\mathbf{k} = 0$. Assuming $\mathbf{k} \to 0$ in (20), we obtain

$$\sum_{i=1}^{3} s_i^2\varepsilon_i(\omega, 0) = 0, \tag{21}$$

which determines the frequencies of long exciton waves in the limit. These frequencies, i.e., the roots of (21), depend on **s**. The limiting value of the exciton energy therefore depends on the direction of **k** when its modulus approaches zero.

If, for example, in the given frequency region the principal contribution to the dielectric constant ϵ_j comes from the term associated with a virtual transition of the system to a single exciton state, while transitions to other states make negligibly small contributions, we have

$$\varepsilon_j = 1 + G_j / [\mathscr{E}_{0j} + F_j(\mathbf{k}) - \hbar\omega], \quad \varepsilon_l = \varepsilon_i = 1; \quad l, i \neq j. \tag{22}$$

In this case (20) leads to

$$u_{\mathbf{k}}(\text{exc}) = \hbar\omega(\mathbf{k}) = \mathscr{E}_{0j} + G_j s_j^2 + F_j(\mathbf{k}). \tag{23}$$

In a crystal for which $\epsilon_1 = \epsilon_2 \neq \epsilon_3$ the aforementioned principal contribution is received by both ϵ_1 and ϵ_2, so that

$$\varepsilon_1 = \varepsilon_2 = 1 + G / [\mathscr{E}_0 + F(\mathbf{k}) - \hbar\omega], \qquad \varepsilon_3 = 1. \tag{24}$$

In this case (20) leads to

$$u_{\mathbf{k}}(\text{exc}) = \hbar\,\omega(\mathbf{k}) = \mathscr{E}_0 + G(s_1^2 + s_2^2) + F(\mathbf{k}). \tag{25}$$

(13), (23) and (25) for limiting small values of $|\mathbf{k}|$ agree with the direct calculation of exciton energy by means of the Schrödinger equation.[3] (13) also agrees with calculations of particular exciton modes—polarized lattice vibrations.[6,10-13]

EXCITON EFFECTIVE MASSES

For the purpose of determining the effective mass of a light-exciton, $u_{\mathbf{k}}$ is expanded in powers of $\mathbf{k}$ near $\mathbf{k} = 0$. In the case of a strictly longitudinal light-exciton retardation may be neglected, as has been shown above, and the dependence of $u_{\mathbf{k}}$ on $\mathbf{k}$ can be calculated by means of the Schrödinger equation, as is customary in the literature. The macroscopic theory discussed above then yields no new results, particularly for the effective mass. We shall consider a non-longitudinal light-exciton, for which, when retardation is taken into account, very different results are obtained.

The dependence of ω on $\mathbf{k}$ is determined by (4), in which spatial dispersion may be disregarded since we are now considering the region of limiting long light-exciton waves.

There is no special reason why $d\epsilon_j/d\omega$ should vanish at the same frequency ω' at which ϵ_j vanishes. Therefore, excluding unlikely chance coincidences, we shall assume that in the region $\omega \approx \omega'$ we have

$$\varepsilon_j = g_j \hbar(\omega - \omega') + \ldots, \quad \hbar g_j \equiv (d\varepsilon_j/d\omega)_{\omega'}. \tag{26}$$

When ϵ_j in (4) is expanded in powers of $\omega - \omega'$ and only first-degree terms are retained, we obtain the following expressions for the effective mass: in crystals where $\epsilon_1 = \epsilon_2 = \epsilon_3$,

$$u_{\mathbf{k}} = \hbar\omega(\mathbf{k}) = \hbar\omega' + \hbar^2\mathbf{k}^2/2\mathfrak{m} + \ldots, \quad \mathfrak{m} = g(\hbar\omega')^2/2c^2; \tag{27}$$

in crystals where $\epsilon_1 = \epsilon_2 \neq \epsilon_3$, for an ordinary ray which is a transverse light-exciton of the type represented by (14) at frequencies where $\epsilon_h \equiv \epsilon_1 = \epsilon_2 \approx 0$, $\epsilon_3 \neq 0$,

$$u_{\mathbf{k}} = \hbar\omega(\mathbf{k}) = \hbar\omega' + \hbar^2\mathbf{k}^2/2\mathfrak{m}_h + \ldots, \quad \mathfrak{m}_h = g\ (\hbar\omega')^2/2c^2. \tag{28}$$

For an extraordinary ray which is a light-exciton of the type represented by (15) at frequencies where $\epsilon_3 \approx 0$, $\epsilon_h \equiv \epsilon_1 = \epsilon_2 \neq 0$,

$$u_{\mathbf{k}} = \hbar\omega(\mathbf{k}) = \hbar\omega' + \hbar^2(k_1^2 + k_2^2)/2\mathfrak{m} + \ldots,$$

$$\mathfrak{m} = g_3(\hbar\omega')^2/2c^2. \tag{29}$$

This equation shows that the light-exciton effective mass becomes infinite in direction 3. With spatial dispersion taken into account it would be finite but relatively very large. This means that for an extraordinary long-wave ray the projection of the group velocity is very much smaller in direction 3 than in other directions for the same values of the wave-vector projections.

At frequencies where $\epsilon_h \equiv \epsilon_1 = \epsilon_2 \approx 0$, $\epsilon_3 \neq 0$, for an extraordinary ray we obtain

$$u_{\mathbf{k}} = \hbar\omega(\mathbf{k}) = \hbar\omega' + \hbar^2 k_3^2 / 2\mathfrak{m} + \ldots, \quad \mathfrak{m} = g_h(\hbar\omega')^2 / 2c^2. \tag{30}$$

Here the light-exciton effective mass is infinite in directions 1 and 2, while the group velocity is very small.

For crystals with all three ϵ_j different, at frequencies for which one of the principal values of ϵ, such as ϵ_3, vanishes, (29) is obtained.

The effective mass of a light-exciton can be very much smaller than the mass m of a free electron. For example, if the frequency dependence of ϵ_j is represented by (7), we have

$$g_j = \varepsilon_{0j}^2 / G_j. \tag{31}$$

In order to estimate the parameter G_j we assume that dispersion results from electron polarization and that the electron state of the crystal can be considered on the basis of the Heitler-London-Heisenberg approximation (which assumes weak interactions between electrons belonging to different unit cells). Then

$$G_j = \frac{2\pi e^2 N\hbar^2 f_j}{m\mathscr{E}_{0j}} = \frac{2\pi I^2 f_j}{\mathscr{E}_{0j}} \left(\frac{a_0}{d}\right)^3, \tag{32}$$

where $a_0 = \hbar^2/me^2 = 0.529$ A, $I = e^2/a_0 = 27.1$ ev, f_j is the oscillator strength per unit cell for a phototransition from the ground state to the exciton state in question, $N = 1/d^3$ is the number of cells per unit volume, and d is the cubic-lattice constant. Let us, for example, consider a crystal with $d = 10a_0$, $\epsilon_{0j} = 2$, $\mathscr{E}_{0j} = 2$ ev. Assuming $f_j = 0.1$, we obtain $G_j = 0.23$ ev, $g_j = 17.4\ \text{ev}^{-1}$, $\mathfrak{m}/m = 7.5 \times 10^{-5}$.

So small a value of the light-exciton effective mass corresponds, for the given kinetic energy, to a large value of its group velocity, which can considerably exceed the velocity of mechanical electron motion. It is thus shown that in the long-wave region a light-exciton is much more an electromagnetic than a mechanical phenomenon. According to (31) and (32), when the oscillator strength f_j is reduced $\mathfrak{m}$ increases but remains considerably smaller than m even for very small f_j. Thus in the crystal considered above $\mathfrak{m} = m$ only for $f_j = 7.5 \times 10^{-6}$. The light-exciton retains its predominantly electromagnetic character down to such small oscillator strengths. The foregoing numerical example shows that the properties of an exciton, particularly its effective mass, are strongly modified when retardation is taken into account.

It is important to estimate how far from the boundary of the allowed energy band the quadratic approximation for the dependence of u_k on **k** and the above-discussed effective masses still remain valid. The error of the approximation arises from the neglect of higher powers of $\omega - \omega'$ in (26). With (7) used for $\epsilon_j(\omega)$, (26) can be written as

$$\varepsilon_j(\omega) = \frac{\varepsilon_{0j}^2}{G_j}\hbar(\omega - \omega') - \frac{\varepsilon_{0j}^3}{G_j^2}\hbar^2(\omega - \omega')^2 + \ldots \tag{33}$$

It thus appears that the quadratic term may be dropped if

$$|\hbar\omega - \hbar\omega'| = |u_{\mathbf{k}} - u_0| \ll G_j/\varepsilon_{0j}. \tag{34}$$

In our numerical example above this means that $|u_k - u_0| \ll 0.115$ ev. Therefore at room temperature light-excitons possessing moderate quasi-kinetic thermal energy $u_k - u_0$ are still characterized by the aforementioned effective masses. In the study of such phenomena as light-exciton scattering by lattice vibrations and by impurities, light-exciton diffusion, collisions of light-excitons with current carriers etc., one should use the energies, effective masses and other light-exciton properties that really exist in crystals, rather than those of "purely mechanical" excitons.

We have considered the effective masses of light-excitons at the boundaries of the allowed energy bands corresponding to limiting long waves. Effective masses can also be introduced at other band boundaries corresponding in **k** space to the point $\mathbf{k} = \mathbf{k}^0 \neq 0$. The energy u_k is then expanded in powers of the differences $k_i - k_i^0$. For instance, it has been noted above that the frequency $\bar{\omega}$ (see the figure) is not the absolute band boundary but is the boundary only for waves having a given direction of $\mathbf{s}$. But when $\mathbf{s}$ is chosen so that $\bar{\omega}$ as a function of $\mathbf{s}$ is an extremum (a maximum or a minimum when ω is the upper or lower band boundary, respectively) this frequency is the absolute boundary of bands α and β. Effective masses can be introduced at the corresponding point $\mathbf{k}^0$ since the expansion of $\omega - \bar{\omega}$ in powers of $k_i - k_i^0$ begins with quadratic terms. The results, which are easily obtained from (18) and (19), will not be given here.

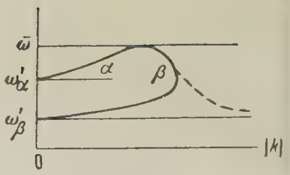

Energy bands of light-excitons in biaxial crystals for a given direction of k. $\overline{\omega}$, but not ω'_α or ω'_β, depends on the direction of k.

A frequency region where spatial dispersion is important may also contain band boundaries near which effective masses can be introduced. For example, in Fig. 2 of our reference 7, corresponding to negative exciton effective mass M, the extreme right-hand point of the dispersion branch in the second quadrant is the upper boundary of the allowed band (as already mentioned above). At this point the expansion of the light-exciton energy is

$$u_{\mathbf{k}} = \mathscr{E}_0 + \hbar^2 q^2/M + \hbar^2(|\mathbf{k}| - q)^2/2\mathfrak{m} + \ldots,$$

$$\mathfrak{m} = {}^1\!/_4\, M,\ q^2 = \mathscr{E}_0\sqrt{2MG}/c\hbar^2. \tag{35}$$

Here $\mathscr{E}_0$ and G are the parameters of (7). (35) was derived for an isotropically polarized crystal where the effective mass M of a "purely mechanical" exciton is also isotropic; it is also assumed that at the boundary in question we have $n^2 \gg \epsilon_0$. The boundary of the light-exciton energy band in **k** space is the sphere $|\mathbf{k}| = q$, along the radii of which the light-exciton effective mass $\mathfrak{m}$ is one-fourth the exciton effective mass. The light-exciton mass becomes infinite along tangents to the sphere.

When the same dispersion branch, represented in Fig. 2 of reference 7, enters the region of very large n, where $|\mathbf{k}| \gg q$ and where the dispersion curve merges with its rectilinear asymptote, we obtain for this region

$$u_{\mathbf{k}} = \mathscr{E}_0 + \hbar^2 \mathbf{k}^2/2M + \ldots, \tag{36}$$

i.e., the light-exciton acquires the properties of a mechanical exciton and is characterized by the effective mass of the latter. This follows naturally, since for $n \gg 1$ we should obtain results close to those for the limiting case $n \to \infty$. (36) is valid for values of $|\mathbf{k}|$ that are fairly large but still considerably smaller than π/d. The exciton band boundary $\mathscr{E}_0$ is not the boundary of the light-exciton band.

Equation (36) is also obtained for very large n in the case of M > 0, which is represented in Fig. 1 of reference 7. The lower boundary of the allowed light-exciton band will be the closest root ω' of (6) on the lower-frequency side of $\omega_0 = \mathscr{E}_0/\hbar$. When this band lies lowest so that the root does not exist, the lower boundary will be $\omega = 0$, at which

$$n = \sqrt{\varepsilon_{\text{stat}}} \neq 0, \quad \omega(\mathbf{k}) = c|\mathbf{k}|/\sqrt{\varepsilon_{\text{stat}}} + \ldots, \qquad (36a)$$

i.e., an effective mass cannot be introduced.

It must be remembered that a crystal in thermal equilibrium contains mainly low-energy light excitons such as phonons, which have an allowed band width of the order kT. In this case the great majority of light-excitons will be associated with very large refractive indices n since there will be very many more large values than small values of $|\mathbf{k}|$ in $\mathbf{k}$ space. These light-excitons can therefore be regarded as mechanical excitons. For this reason retardation may be neglected in connection with such properties as exciton specific heat and thermal conductivity.

The idea for the present paper originated in a conversation with L. D. Landau, whom the author wishes to thank. É. I. Rashba and M. A. Krivoglaz participated in a discussion of the results.

---

[1] Ya. I. Frenkel', Phys. Rev. **37**, 17, 1276 (1931).

[2] S. I. Pekar, JETP **33**, 1022 (1957), Soviet Phys. JETP **6**, 785 (1958).

[3] S. I. Pekar, JETP **35**, 522 (1958), Soviet Phys. JETP **8**, 360 (1959).

[4] S. I. Pekar, JETP **36**, 451 (1959), Soviet Phys. JETP **9**, 314 (1959).

[5] J. J. Hopfield, Phys. Rev. **112**, 1555 (1958).

[6] M. Born and K. Huang, Dynamical Theory of Crystal Lattices, Oxford Univ. Press, 1954 (Russ. Transl. IIL, 1958) § 8); K. Huang, Proc. Roy. Soc. (London) **A208**, 352 (1951); Nature **167**, 779 (1951).

[7] S. I. Pekar, JETP **34**, 1176 (1958), Soviet Phys. JETP **7**, 813 (1958).

[8] V. L. Ginzburg, JETP **34**, 1593 (1958), Soviet Phys. JETP **7**, 1096 (1958).

[9] S. I. Pekar and B. E. Tsekvava, Физика твердого тела, (Solid State Physics) **2**, 261 (1960), Soviet Phys.—Solid State **2**, 242 (1960).

[10] Lyddane, Sachs, and Teller, Phys. Rev. **59**, 673 (1941).

[11] H. B. Callen, Phys. Rev. **76**, 1394 (1949).

[12] K. B. Tolpygo, JETP **20**, 497 (1950).

[13] M. A. Krivoglaz and S. I. Pekar, JETP **31**, 343 (1956), Soviet Phys. JETP **4**, 286 (1957).

Translated by I. Emin
344

SOVIET PHYSICS JETP VOLUME 11, NUMBER 6 DECEMBER, 1960

POLARIZATION OF ELECTRONS IN ELASTIC SCATTERING WITH ACCOUNT OF THE FINITE SIZE OF THE NUCLEUS

B. K. KERIMOV and V. M. ARUTYUNYAN

Moscow State University

Submitted to JETP editor January 3, 1960

J. Exptl. Theoret. Phys. (U.S.S.R.) **38**, 1798-1802 (June, 1960)

The scattering phase shifts and polarization of elastically scattered electrons are computed with account of the finite size of the scattering center. An expression for azimuthal asymmetry in double scattering has been obtained, as well as a correction to the usual Mott formula due to the second and fourth charge-density moments.

1. INTRODUCTION

THE distinguishing feature of the scattering of a partially polarized beam of electrons on nuclei is the so-called azimuthal asymmetry in the angular distribution of the scattering. As Mott has shown,[1] an effect of such a type can be observed in the double scattering of electrons on a point force center. This effect has frequently been confirmed experimentally.[2] However, the experiments have been carried out[2-4] in the region of low energies (several hundred kev), when the wavelength of the electrons is large in comparison with the nuclear dimensions and, naturally, the nucleus can be regarded as a point scatterer. As in the case of single scattering, it can be expected that for high energies of the incident electrons the effect of the structual features of an extended nucleus on the azimuthal asymmetry will be considerable.

The azimuthal asymmetry for double scattering of a beam of Dirac particles on a potential was computed from damping theory in refs. 5–7. In the present work we calculated the polarization that arises in the elastic scattering of an incident beam of electrons with account of the extended character of the heavy center.

As is known, the azimuthal asymmetry in double scattering at the angles θ_1 and θ_2, φ_2 is characterized by the quantity

$$\delta(\theta_1, \theta_2) = 2\Delta(\theta_1)\Delta(\theta_2), \quad \Delta(\theta) = i(fg^* - f^*g)/(ff^* + gg^*), \tag{1}$$

f and g are the Dirac amplitudes of scattering. Inasmuch as there is no azimuthal asymmetry in first approximation, it is necessary to solve the problem in the second approximation in $(Z/137)^2$ to obtain a finite value of δ.

2. SCATTERING PHASES AND AMPLITUDES WITH ACCOUNT OF THE NUCLEAR DIMENSIONS

In accounting for the effect of the finite dimensions of the nucleus on electron scattering, it is more advantageous to work not with the potential but with the density charge distribution inside the nucleus, which gives valuable information on the electromagnetic structure of the nucleus. Initially, it is easy to take account of the effects brought about by the finiteness of the nucleus in the expressions for the phase shifts obtained in references 7 and 8. However, it is not difficult to show that for the determination of Im f and Im g it suffices to limit oneself to phases computed in the first approximation in the interaction potential, since the subsequent approximation gives the effects of polarization for double scattering of the order of $(Z/137)^2$, which is insignificant for light nuclei. In this approximation, the phase shifts of elastic scattering $\delta_l^{(1)}$ and $\delta_l^{(2)}$ of Dirac particles have the form[7,8]

$$\tan\delta_l^{(1,2)} = -\frac{kK}{c\hbar}\left(\alpha\int_0^\infty j_l^2(kr)V(r)r^2\,dr + \beta\int^\infty j_{l\pm1}^2(kr)V(r)r^2\,dr\right), \tag{2}$$

where V(r) is the interaction potential with the scattering center, $j_l(kr)$ are the spherical Bessel functions, $\hbar k$ is the momentum, $c\hbar K = c\hbar(k_0^2 + k^2)^{1/2}$ is the energy, $\hbar k_0/c$ is the electronic mass, $\alpha = 1 + k_0/K$ and $\beta = 1 - k_0/K$. Here the plus sign relates to $\delta_l^{(1)}$ and the minus to $\delta_l^{(2)}$. Equations (2) possess the interesting feature that the amplitudes of f and g obtained with their help contain in themselves the imaginary parts of f and g computed by the usual diagram techniques in the second approximation,[9] thus greatly simplifying the calculations.

The transformation

$$j_l^2(kr) = \frac{1}{2kr}\int_0^{\pi} \sin\left(2kr\sin\frac{\varphi}{2}\right)\cos\frac{\varphi}{2}\,P_l(\cos\varphi)\,d\varphi, \tag{3}$$

where $P_l(\cos\varphi)$ are the Legendre polynomials, together with account of the equation for the potential $\Delta V = -4\pi Ze^2\rho(r)$, permits us to reduce (2) to a form suitable for computation:

$$\tan\delta_l^{(1,2)} = -\frac{1}{8k^2}\left(\frac{Ze^2kK}{c\hbar}\right)\int_0^{\pi}\frac{\sin\varphi}{\sin^2(\varphi/2)}\,[\alpha P_l(\cos\varphi) + \beta P_{l\pm1}(\cos\varphi)]\,F(k,\varphi)\,d\varphi. \tag{4}$$

Here we have introduced the universal notation for the form factor of the nuclear charge:

$$F(k,\varphi) = \frac{4\pi}{2k\sin(\varphi/2)}\int_0^{\infty} r\rho(r)\sin\left(2kr\sin\frac{\varphi}{2}\right)dr. \tag{5}$$

Equation (4) makes it possible to consider the effects brought about by the finite dimensions of the nucleus in both single and double scattering on nuclei for an arbitrary, spherically symmetric charge distribution, since the form factors of all models of the charge density which agree well with experiment are well known (see ref. 10). Summation of the corresponding Mott series for the amplitudes of f and g can be developed by the method advanced by Arutyunyan and Muradyan.[11] However, certain general results can be obtained even without taking a concrete form for the finite charge distribution ρ of the nucleus. In the case of not very large energies, all the form factors reduce to a rather simple expansion:

$$F(k,\varphi) = 1 - \frac{2}{3}k^2\langle r^2\rangle\sin^2\frac{\varphi}{2} + \frac{2}{15}k^4\langle r^4\rangle\sin^4\frac{\varphi}{2} + \ldots, \tag{6}$$

where $\langle r^2\rangle$ is the mean square radius of the nuclear charge distribution, $\langle r^4\rangle$ is the so-called fourth nuclear charge density moment. For very high energies, it is necessary to consider higher moments. However, as the experiments of Hofstadter have shown,[10] the first term of the expansion in F is sufficient up to 200 Mev. In the given case, integration in (4) can be carried out and the phase shifts [with account of the first three terms in (6)] finally take the following form:

$$\tan\delta_l^{(1,2)} = -c_l^{(1,2)} + (Ze^2kK/6c\hbar)\langle r^2\rangle(\alpha\delta_{l,0} + \beta\delta_{l\pm1,0}) - (Ze^2k^3K/60c\hbar)\langle r^4\rangle[\alpha(\delta_{l,0} - \tfrac{1}{3}\delta_{l,1}) + \beta(\delta_{l\pm1,0} - \tfrac{1}{3}\delta_{l\pm1,1})]. \tag{7}$$

Here $c_l^{(1,2)}$ are the phase shifts of scattering on a point Coulomb center. Although the integral values of $c_l^{(1,2)}$ diverge, finite results can be obtained in the determination of f and g, by means of a limiting transition (see references 8 and 11). Account of the higher moments can be carried out in similar fashion, i.e., one can obtain the expression for $\tan\delta_l^{(1,2)}$ in the form of an expansion over all the moments. For the determination of f and g in the approximation $(Z/137)^2$, one must carry out a summation of the series:

$$f(\theta) = \frac{1}{2ik}\sum_{l=0}^{\infty}[(l+1)(e^{2i\delta_l^{(1)}} - 1) + l(e^{2i\delta_l^{(2)}} - 1)]\,P_l(\cos\theta),$$

$$g(\theta) = \frac{1}{2ik}\sum_{l=1}^{\infty}(-e^{2i\delta_l^{(1)}} + e^{2i\delta_l^{(2)}})\,P_l^{(1)}(\cos\theta), \tag{8}$$

which is not difficult to obtain, inasmuch as the indices $\delta_{l,l'}$ in the expression (7) automatically take in summation over l, and the Coulomb amplitudes are known (see references 1 and 8). Omitting the calculations, we give the expressions for f and g in the given approximation:

$$\begin{aligned}
f(\theta) = &-\frac{1}{2k^3}\left(\frac{Ze^2kK}{c\hbar}\right)(\alpha + \beta\cos\theta)\left(\frac{1}{2\sin^2(\theta/2)} + \frac{1}{3}k^2\langle r^2\rangle\right.\\
&\left.-\frac{1}{15}k^4\langle r^4\rangle\sin^2\frac{\theta}{2}\right) + \frac{i}{2k^5}\left(\frac{Ze^2kK}{c\hbar}\right)^2\left[\frac{\alpha^2 + 2\alpha\beta + \beta^2\cos\theta}{2\sin^2(\theta/2)}\ln\right.\\
&\times\sin\frac{\theta}{2} + \frac{\alpha\beta}{3}k^2\langle r^2\rangle(1 + \cos\theta) + \frac{\alpha^2 + \beta^2\cos\theta}{18}k^4\langle r^2\rangle^2\\
&\left.+\frac{1}{30}k^4\langle r^4\rangle\left(\alpha^2\cos\theta + 2\beta\cos^2\theta + \frac{\alpha\beta}{2}\cos^2\theta - \frac{3}{2}\alpha\beta\right)\right],
\end{aligned}$$

$$\begin{aligned}
g(\theta) = &\frac{1}{2k^3}\left(\frac{Ze^2kK}{c\hbar}\right)\beta\left(\cot\frac{\theta}{2} - \frac{1}{3}k^2\langle r^2\rangle\sin\theta\right.\\
&\left.+\frac{1}{15}k^4\langle r^4\rangle\sin\theta\sin^2\frac{\theta}{2}\right)\\
&-\frac{i}{2k^5}\left(\frac{Ze^2kK}{c\hbar}\right)^2\left[\frac{2\alpha\beta\sin(\theta/2) + \beta^2\sin\theta\cos(\theta/2)}{2\sin^2(\theta/2)\cos(\theta/2)}\ln\sin\frac{\theta}{2}\right.\\
&+\frac{\alpha\beta}{3}k^2\langle r^2\rangle\sin\theta + \frac{\beta^2\sin\theta}{18}k^4\langle r^2\rangle^2\\
&\left.+\frac{1}{30}k^4\langle r^4\rangle\left(\beta\sin2\theta + \frac{\alpha\beta}{4}\sin2\theta - \frac{3}{2}\alpha\beta\sin\theta\right)\right].
\end{aligned} \tag{9}$$

Here we have discarded the infinite imaginary amplitudes of the point field, since they make no contribution to the scattering cross section and mutually cancel in the determination of $\delta(\theta_1, \theta_2)$.

3. AZIMUTHAL ASYMMETRY

As expected, it follows directly from (1) and (9) that $\Delta(\theta) = 0$ in first approximation, and there is no asymmetry in φ for double scattering. Only terms of second order contribute to this effect, and we get the following expression from (1) and (9) for the degree of polarization experienced by the initially unpolarized beam of electrons in double scattering:

$$\Delta(\theta) = \Delta^{\mathrm{p}}(\theta)\Big[1 + \frac{2}{3}\sin^2\frac{\theta}{2}\Big(k^2\langle r^2\rangle + \frac{2}{3}k^4\langle r^2\rangle^2\sin^2\frac{\theta}{2} - \frac{1}{5}k^4\langle r^4\rangle\sin^2\frac{\theta}{2}\Big) + \frac{1}{3}\frac{\cos^2(\theta/2)}{\ln\sin(\theta/2)}\Big(2k^2\langle r^2\rangle + \frac{4}{3}k^4\langle r^2\rangle^2\sin^2\frac{\theta}{2} - \frac{1}{3}k^4\langle r^2\rangle^2 - \frac{1}{5}k^4\langle r^4\rangle - \frac{1}{5}k^4\langle r^4\rangle\sin^2\frac{\theta}{2}\Big)\Big]. \tag{10}$$

$$\Delta^{\mathrm{p}}(\theta) = \frac{2Z}{137}\frac{vc^{-1}(1 - v^2/c^2)^{1/2}}{1 - v^2c^{-2}\sin^2(\theta/2)}\frac{\sin^3(\theta/2)}{\cos(\theta/2)}\ln\sin\frac{\theta}{2} \tag{11}$$

represents the usual Mott formula for a point center. For the differential double-scattering cross section of electrons, with account of the nuclear dimensions, we have the expression

$$\sigma(\theta_1, \theta_2, \varphi_2) = \sigma_0(\theta_1)\sigma_0(\theta_2)[1 + \delta(\theta_1, \theta_2)\cos\varphi_2], \tag{12}$$

where

$$\sigma_0(\theta) = \sigma^{\mathrm{p}}\Big[1 - \frac{4}{3}k^2\langle r^2\rangle\sin^2\frac{\theta}{2} + \frac{4}{9}k^4\langle r^2\rangle^2\sin^4\frac{\theta}{2} + \frac{4k^4}{15}\langle r^4\rangle\sin^4\frac{\theta}{2}\Big],$$

$$\sigma^{\mathrm{p}} = \frac{1}{4k^6}\Big(\frac{Ze^2kK}{c\hbar}\Big)^2\frac{(1 - v^2c^{-2}\sin^2(\theta/2))}{\sin^4(\theta/2)} \tag{13}$$

is the scattering cross section of a beam of electrons on a finite nucleus in the approximation employed.

As is seen, Eq. (10), for high energies, will determine the effect of the nuclear dimensions on the polarization properties of the electron beam. For energies of the order of 50—100 Mev, we can simplify (10) and limit ourselves to the terms $k^2\langle r^2\rangle$:

$$\Delta(\theta) = \Delta^{\mathrm{p}}(\theta)\Big[1 + \frac{2}{3}k^2\langle r^2\rangle\Big(\sin^2\frac{\theta}{2} + \frac{\cos^2(\theta/2)}{\ln\sin(\theta/2)}\Big)\Big]. \tag{14}$$

As an illustration of the results obtained, we estimate the effects produced by the finiteness of the nuclear dimensions for C^{12}. The nucleus C^{12} is relatively simple and has been well studied in experiments of electron scattering. Frego and Hofstadter[10] studied in detail the charge distribution in the ground state of C^{12}. The most reasonable value of the mean square radius — 2.40 f — was determined. In particular, the model with charge distribution density

$$\rho = \rho_0(1 + \alpha r^2/a_0^2)\exp(-r^2/a_0^2),$$

gave the best agreement with experiment with $\alpha = 4/3$. Here a_0 is a parameter proportional to the mean square radius, and is chosen in agreement with experiment. We select one of the possible values, $a_0 = 1.635 \times 10^{-13}$ cm. The normalization factor can be determined from the condition

$$\int_0^\infty 4\pi r^2\rho(r)\,dr = 1.$$

The moments computed on the basis of this model are

$$\langle r^2\rangle = 5.790 \cdot 10^{-26}\ \mathrm{cm}^2, \qquad \langle r^4\rangle = 5.061 \cdot 10^{-51}\ \mathrm{cm}^4.$$

The ratio $\Delta/\Delta^{\mathrm{P}}$ is shown in the drawing as a function of the scattering angle for different values of the energy of the incident electrons. As is seen, even for $E = 100\ m_0c^2$, the deviations of Δ from the case corresponding to a pure point distribution amount to 20—30% (for mean angles). For $E = 200\ m_0c^2$, the effect of the extension of the nucleus on the polarization is already appreciable. For high energies of the electrons ($\gtrsim 150$ Mev), along with elastic scattering, the process of meson formation is also possible, which is not considered in the present work.

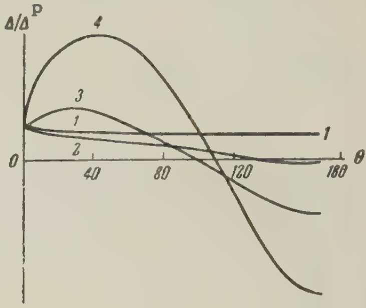

Dependence of $\Delta/\Delta^{\mathrm{P}}$ on the scattering angle for the electronic energy values: curve 1 — 100, 2 — 200, 3 — 300, 4 — 400 m_0c^2.

On the basis of the results obtained, it is possible to draw the following conclusions. In polarization phenomena for the double scattering of high energy electrons, the finite dimensions of the nucleus play an important role. For small angles and low energies, this effect is insignificant; however, at large angles, it predominates over point scattering. Unfortunately, the absence at the present time of experiments on double scattering of electrons at high energies still does not permit us to estimate the accuracy of Eq. (10). It can be expected that comparison with experiment will make it possible to find some additional information on nuclear dimensions, and to make precise the choice of one model or another.

I express my thanks to Prof. A. A. Sokolov for discussion of the results.

---

[1] N. F. Mott, Proc. Roy. Soc. (London) **A124**, 425 (1929); **A135**, 429 (1952).

[2] N. Mott and H. Massey, Theory of Atomic Collisions, Oxford, 1933.

[3] N. Ryu, J. Phys. Soc. Jap. **7**, 125, 130 (1952); **8**, 575, 804 (1953).

[4] W. G. Pettus, Phys. Rev. **109**, 1458 (1958).

[5] A. Sokolov, J. Phys. U.S.S.R. **9**, 363 (1945).

[6] A. A. Sokolov and B. K. Kerimov, JETP **33**, 827 (1957), Soviet Phys. JETP **6**, 639 (1958).

[7] Sokolov, Kerimov, and Guseĭnov, Nucl. Phys. **5**, 390 (1958).

[8] Sokolov, Arutyunyan, and Muradyan, JETP **36**, 594 (1959), Soviet Phys. JETP **9**, 412 (1959).

[9] R. H. Dalitz, Proc. Roy. Soc. (London) **A206**, 509 (1951).

[10] R. Hofstadter, Revs. Modern Phys. **28**, 214 (1956).

[11] V. M. Arutyunyan and R. M. Muradyan, JETP **36**, 1542 (1959), Soviet Phys. JETP **9**, 1094 (1959).

Translated by R. T. Beyer
345

SOVIET PHYSICS JETP VOLUME 11, NUMBER 6 DECEMBER, 1960

APPLICATION OF DISPERSION RELATION TECHNIQUES TO A STUDY OF THE SIMPLEST GREEN'S FUNCTIONS IN MESODYNAMICS

V. V. MALAKHOV, E. P. RASHEVSKAYA, and V. Ya. FAĬNBERG

Submitted to JETP editor January 3, 1960

J. Exptl. Theoret. Phys. (U.S.S.R.) 38, 1803-1813 (June, 1960)

An approximate system of dispersion equations for the meson and nucleon Green's functions and the vertex function is studied in pseudoscalar charge-symmetric mesodynamics. The asymptotic behavior of these functions, corresponding to infinite values of Z_2^{-1} and Z_3^{-1}, is determined in the weak-coupling case.

1. INTRODUCTION

IN this paper we present certain results of a study within the framework of the dispersion relation approach, of the single-particle Green's functions and the vertex function in pseudoscalar charge-symmetric mesodynamics. The analogous problems as they appear in electrodynamics have been discussed previously.[1,2]* The main purpose of this type of investigation is a clarification of the asymptotic behavior of the Green's functions. This would make it possible to decide on the renormalizability properties of the theory and on the connection between the dispersion relation and Lagrangian formulations of quantum field theory. However, the analysis of the simplest approximate set of dispersion equations shows that in all probability there exists no effective expansion parameter (even in the weak coupling case) in the asymptotic region which would make it possible to estimate the contributions from many-particle Green's functions. For the strong coupling case the problem of boundary conditions which would determine a unique solution (see Sec. 3) remains unsolved.

It should also be mentioned that, in contrast to the approximate dispersion equations for scattering problems (obtained on the basis of the Mandelstam representation[6]) where one studies matrix elements on the energy shell with free external lines ($p_i^2 = m_i^2$), for a study of contributions to the asymptotic region of single particle Green's functions and the vertex function due to higher order approximations it is necessary to know the analytic structure of matrix elements with virtual ($p_i^2 \neq m_i^2$) external lines.

In Sec. 2 the approximate equations are derived for the meson Green's function $\Delta(q^2)$, nucleon Green's function $G(p)$, and the vertex Green's function $F_i(p, p')$. The derivation is based on the analytic structure of these functions and the unitarity condition. Dispersion relations are proven for $F_i(p, p')$ as a function of p^2 in the physical region ($p'^2 = m^2$, $q^2 = (p-p')^2 = \mu^2$). In Sec. 3 is discussed the approximate set of equations which reduces to the solution of the Hilbert problem.[7] A unique solution is obtained by making use of the boundary condition (13c) and the requirement that the solution, if it can be expanded in a power series in the coupling constant (weak coupling), should coincide with the corresponding perturbation theory series. The asymptotic behavior of $F_i(p, p')$ in p^2 and q^2 is found in the weak coupling case. The results obtained are discussed briefly in Sec. 4. Section 5 consists of a mathematical appendix.

2. DERIVATION OF THE EQUATIONS

1. The dispersion relations for the meson Green's function $\Delta(x-x')\delta_{ij} = i\langle 0 | T\varphi_i(x) \times \varphi_j(x') | 0\rangle$ and the nucleon Green's function $G_{\alpha\beta}(x-x') = i\langle 0 | T\psi_\alpha(x)\bar{\psi}_\beta(x') | 0\rangle$ can be derived without particular use of the causality principle (see, e.g., reference 8) and have the form*

$$\Delta(q^2) = \frac{1}{(2\pi)^4}\int e^{iqx}\Delta(x)\,dx = \frac{1}{\mu^2 - q^2 - i\varepsilon} + \int\limits_{(3\mu)^2}^{\infty} \frac{\rho(q'^2)\,dq'^2}{q'^2 - q^2 - i\varepsilon}, \tag{1}$$

$$G(p) = \frac{1}{(2\pi)^4}\int e^{ipx}G(x)\,dx = \frac{1}{m - \hat{p} - i\varepsilon} + \int\limits_{(m+\mu)^2}^{\infty} \frac{\rho_1(p'^2) + \hat{p}\rho_2(p'^2)}{p'^2 - p^2 - i\varepsilon}\,dp'^2. \tag{2}$$

---

*In a similar vein are the papers by Redmond and Uretsky[3] and by Bogolyubov, Logunov, and Shirkov[4] (see also reference 5).

*We assume here that $\Delta(q^2)$ and $G(p)$ fall off as their arguments increase; $x^2 = x_0^2 - \mathbf{x}^2$; i, j = 1, 2, 3 are the isotopic indices of the meson; α, β (= 1, ... 8) are the spinor and isotopic indices of the nucleon.

Here $\varphi(x)$ and $\psi(x)$ are meson and nucleon field operators in the Heisenberg representation; m and μ are the nucleon and meson masses; ρ and ρ_λ are real spectral functions with the properties: $\rho \geq 0$, $\rho_2\sqrt{p^2} \pm \rho_1 > 0$, $\rho_2 > 0$; all quantities are renormalized quantities.

Making use of the equations of motion

$$(\Box_x - \mu^2)\,\varphi_i(x) = j_i(x), \qquad (i\hat{\nabla}_x - m)\,\psi(x) = \eta(x)$$

(where

$$j(x) = i\frac{\delta S}{\delta\varphi_{in}(x)}S^*, \qquad \eta(x) = i\frac{\delta S}{\delta\bar{\psi}_{in}(x)}S^*,$$

S being the S-matrix operator: $|n^{\text{out}}> = s\,|n^{\text{in}}>$, where the states $|n^{\text{in}}>$ correspond to incoming and the states $|n^{\text{out}}>$ to outgoing waves) as well as of the expansion in terms of a complete set of states $|n^{\text{in}}>$ (or $|n^{\text{out}}>$) we find

$$\rho(q^2) = \tfrac{1}{3}\,(2\pi)^3\,\mathrm{Sp}\sum_n (\mu^2 - q^2)^{-2}\,\langle 0\,|\,j_i(0)\,|n^{in}\rangle\langle n^{in}|\,j_i(0)\,|\,n\rangle$$
$$\times\,\delta(p_n - q), \tag{3}$$

$$\rho_1(p^2) + \hat{p}\rho_2(p^2) = (2\pi)^3\sum_n (m - \hat{p})^{-2}\,\langle 0\,|\,\eta(0)\,|\,n^{in}\rangle$$
$$\times\,\langle n^{in}\,|\,\bar{\eta}(0)\,|\,n\rangle\,\delta(p_n - p). \tag{4}$$

Thus, in order to find ρ and ρ_λ for all values of the arguments, one would have to know all the matrix elements $<0\,|\,j\,|\,n>$ and $<0\,|\,\eta\,|\,n>$; in practice this is an insoluble problem. The following expressions are found from covariance considerations for the simplest matrix elements $<0\,|\,j_i\,|\,p_1,p_2>$ and $<0\,|\,\eta\,|\,p_1,q_1>$, where $|\,p_1,p_2>$ is a state of a nucleon (p_1) and antinucleon (p_2), and $|\,p_1,q_1>$ is a state of a nucleon (p_1) and a meson (q_1):

$$\langle 0\,|\,j_i\,|\,p_1,\,p_2\rangle = \bar{U}_+(\mathbf{p}_1)\,\gamma_5\tau_i F(q^2)\,U_-(\mathbf{p}_2), \qquad q = p_1 + p_2; \tag{5}$$

$$(2q_{10})^{1/2}\,\langle 0\,|\,\eta\,|\,p_1 q_1\rangle = \gamma_5\tau_i\,(F_1(p^2) + \hat{p}F_2(p^2))\,U_-(\mathbf{p}_1),$$
$$p = p_1 + q_1; \tag{6}$$

where $U_\mp$ are solutions of the Dirac equation for a particle and antiparticle, and F and F_λ $(\lambda = 1, 2)$ are invariant functions.*

Introducing Eqs. (5) and (6) into (3) and (4) we obtain

$$\rho(q^2) = (\mu^2 - q^2)^{-2}\,q^2(16\pi^2)^{-1}$$
$$(1 - 4m^2/q^2)^{1/2}\,|\,F(q^2)\,|^2\,\theta(q^2 - 4m^2) + \sum_n{}'\langle\ldots\rangle, \tag{7}$$

$$\rho_1(p^2) + \hat{p}\,\rho_2(p^2) = \frac{3}{16\pi^2 p^2}\,(p^2 - (m+\mu)^2)^{1/2}(p^2 - (m-\mu)^2)^{1/2}$$
$$\times\Big\{\frac{\mu^2 m}{(m^2 - p^2)^2}\,(|F_1|^2 + p^2|\,F_2|^2) + \frac{1}{2}\Big(1 - \frac{\mu^2\,(p^2 + m^2)}{(p^2 - m^2)^2}\Big)$$
$$\times(F_1^*F_2 + F_2^*F_1) + \hat{p}\Big[\frac{1}{2p^2}\Big(1 - \frac{\mu^2(p^2 + m^2)}{(p^2 - m^2)^2}\Big)(|\,F_1\,|^2 + p^2\,|\,F_2\,|^2)$$
$$+ \frac{m\mu^2}{(p^2 - m^2)^2}\,(F_1^*F_2 + F_2^*F_1)\Big]\Big\} + \sum_n{}''\langle\ldots\rangle. \tag{8}$$

The $\Sigma'<\ldots>$ in Eq. (7) and the $\Sigma''<\ldots>$ in Eq. (8) denote the contributions of all remaining terms to ρ and ρ_λ respectively. Since each term in Σ' and Σ'' gives a positive contribution to ρ and ρ_2, the study of the asymptotic behavior of the first terms on the right side of Eqs. (7) and (8) gives important information on the renormalizability character of the theory[9] (see also subsection 4).* Consequently, as a first approximation, one may start the study of the properties of ρ and ρ_λ from an analysis of $F(q^2)$ and $F_\lambda(p^2)$.

2. The analytic properties of F and F_λ follow from the analytic properties of the vertex Green's function†

$$F_i^c(p,\,p') = i\int e^{ipx - iqy}(\Box_y - \mu^2)(i\hat{\nabla}_x - m)$$
$$\times\langle 0\,|\,T\,\psi(x)\,\varphi_i(y)\,|\,p'\rangle\,dx\,dy = (2\pi)^4\delta(p - q - p')\,i\int e^{ipx}$$
$$\times(i\hat{\nabla}_x - m)\,\langle 0\,|\,T\,\psi(x)\,j_i(0)\,|\,p'\rangle\,dx = (2\pi)^4\,\delta(p - q - p')$$
$$\times\,i\int e^{-iqx}(\Box_y - \mu^2)\langle 0\,|\,T\,\eta(0)\,\varphi_i(y)\,|\,p'\rangle\,dy. \tag{9}$$

It is not difficult to see that [in the following we omit the factor $(2\pi)^4\,\delta(p - p' - q)$ from $F^C(p,\,p')$]

$$\bar{U}(\mathbf{p})\,F_i^c(p,p') \to \langle p\,|\,j_i(0)\,|\,p'\rangle$$
$$= \bar{U}(\mathbf{p})\,\gamma_5\tau_i F(q^2)\,U(\mathbf{p}'),\quad p^2 \to m^2,\quad p_0 > 0; \tag{10}$$

$$F_i^c(p,\,p') \to (2q_0)^{1/2}\langle 0\,|\,\eta(0)\,|\,p',\,q_i\rangle$$
$$= \gamma_5\tau_i\,(F_1(p^2) + \hat{p}\,F_2(p^2))\,U(\mathbf{p}'),$$
$$q^2 \to \mu^2,\ q_0 > 0. \tag{11}$$

In the general case

$$F_i^c(p,\,p') = \gamma_5\tau_i\,(F_1(p^2,\,q^2) + \hat{p}\,F_2(p^2,\,q^2))\,U(\mathbf{p}'), \tag{12}$$

---

*The function $F(q^2)$ may be called the mesonic form factor of the nucleon.

*We observe that the nucleon + antinucleon state is not the lowest energy state in $\sum_n$ in Eq. (3); therefore a study of this state does not lead to any quantitative results whatever about the behavior of $\Delta(q^2)$ in the region $q^2 \ll m^2$. Apparently states $|n>$ in Eq. (3) with 3, 5 ... (up to $n = 2m/\mu$) mesons play a dominant role in this region. However an analysis of these states is beset by great mathematical difficulties. The meson + nucleon state in Eq. (4) is the lowest energy state [since $p_n^2 > (m + \mu)^2$] and so the contribution of this state may be decisive in determining the behavior of $G(p)$ in the region $|p^2| < (m + 2\mu)^2$.

†The vertex Green's function should be distinguished from the vertex part [see below, Eq. (14)].

and it follows from a comparison of Eqs. (10), (11), and (12) that

$$F(q^2) = F_1(m^2, q^2) + mF_2(m^2, q^2), \tag{13a}$$

$$F_\lambda(p^2) = F_\lambda(p^2, \mu^2), \tag{13b}$$

$$F(\mu^2) = F_1(m^2, \mu^2) + mF_2(m^2, \mu^2) = g, \tag{13c}$$

with g the renormalized coupling constant.

The vertex Green's function $F_i^c(p, p')$ and the vertex part $\Gamma_i^5(p, p')$ are related by

$$F_i^c(p, p') = (\mu^2 - q^2)\,\Delta(q^2)\,(m - \hat{p})\,G(p)\,\Gamma_5^i(p, p')\,U(\mathbf{p}'). \tag{14}$$

Let us begin by studying the analytic properties of $F_i^c(p, p')$ as a function of q^2. For $p^2 < 0$

$$F_i^c(p, p') = F_i^+(p, p') = i\int e^{-iqx}(\Box_x - \mu^2)\langle 0|\theta(x)[\varphi_i(x), \eta(0)]_-|p'\rangle\,dx, \tag{15a}$$

i.e., F_i^c coincides with the retarded Green's function. Let us also introduce the advanced Green's function

$$F_i^-(p, p') = -i\int e^{-iqx}(\Box - \mu^2)\langle 0|\theta(-x)[\varphi_i(x), \eta(0)]_-|p'\rangle\,dx. \tag{15b}$$

In the system $\mathbf{p}' = 0$, as a consequence of the identities

$$q_0 = \frac{p^2 - q^2 - m^2}{2m}, \qquad p_0 = \frac{p^2 + m^2 - q^2}{2m},$$
$$|\mathbf{p}| = |\mathbf{q}| = \left(\frac{(q^2 - m^2 - p^2)^2 - 4p^2m^2}{4m^2}\right)^{1/2}, \tag{16}$$

the functions F_i^+ and F_i^- can be directly analytically continued into the upper and lower half planes respectively of the complex variable $z = q^2$. Since on the real axis we have $F_i^+(p, q^2) = F_i^-(p, q^2)$ for $q^2 < (3\mu)^2$, a single analytic function $F_i(p, z)$ exists, regular in the entire complex plane cut along $(3\mu)^2 \le q^2 < \infty$* with

$$\lim_{z \to q^2 \pm i\varepsilon} F_i(p^2, z) = F_i^\pm(p^2, z). \tag{17}$$

In an entirely analogous manner one proves that for $q^2 < 0$ there exists a single analytic function $F_i(z', q^2)$ regular in the entire complex $z' = p^2$ plane except for the cut $(m + \mu)^2 \le p^2 < \infty$ on the real axis. Here

$$\lim_{z' \to p^2 \pm i\varepsilon} F_i(z', q^2) = F_i^\pm(z', q^2) = \pm i\int e^{ipx}(i\hat{\nabla}_x - m) \times \langle 0|\theta(\pm x)[\psi(x), j_i(0)]_-|p'\rangle\,dx,$$

$$F_i^+(p^2, q^2) = F_i^c(p, p'), \quad q^2 < 0 \quad (\operatorname{Im} z = \operatorname{Im} z' = 0). \tag{18}$$

Since for $\operatorname{Re} z < (3\mu)^2$ and $\operatorname{Re} z' < (m + \mu)^2$ the functions $F_i(p^2, z)$ and $F_i(z', q^2)$ coincide it follows that they represent a single analytic function $F_i(z', z)$ of two complex variables z' and z.

For real values of z and z' the expression

$$-\tfrac{1}{2} i\tau_i\gamma_5 [F_1^+(p^2, q^2) - F_1^-(p^2, q^2) + \hat{p}(F_2^+(p^2, q^2) - F_2^-(p^2, q^2))]$$

is equal, for $p^2 < 0$, to

$$\tfrac{1}{2}(2\pi)^4 \sum_n \langle 0|j(0)|n\rangle\langle n|\eta(0)|p'\rangle\,\delta(p_n - q). \tag{19}$$

and, for $q^2 < 0$, to

$$\tfrac{1}{2}(2\pi)^4 \sum_n \langle 0|\eta(0)|n\rangle\langle n|j(0)|p'\rangle\,\delta(p_n - p) \tag{20}$$

The expression (20), which is the absorptive part of $F(p^2, q^2)$ for $q^2 < 0$, can be analytically continued to the physical point $q^2 = \mu^2$ provided that $p^2 \ge (m + \mu)^2$. Indeed, the matrix element

$$(2\pi)^4 \langle n|j(0)|p'\rangle\,\delta(p_n - p) = \int e^{-iqx}\langle n|j(x)|p'\rangle\,dx$$

goes over as $q^2 \to \mu^2$, $q_0 > 0$ [since, as a consequence of conservation of nucleon number, $p_n^2 = p^2 = (p' + q)^2 \ge (m + \mu)^2$]* into the matrix element for the scattering of a meson by a nucleon into a final state n in the physical region of total energy $p_0 = (p_0' + q_0)$. Thus it is rigorously proved that the functions $F_\lambda^+(p^2)$ [see Eqs. (6) and (13b)] are boundary values of analytic functions $F_\lambda(z) = F_\lambda(z, q^2)(q^2 \to \mu^2)$ regular in the entire complex plane except for the cut $(m + \mu)^2 \le \operatorname{Re} z < \infty$ $(\operatorname{Im} z = 0)$.

As regards the absorptive part (19), it is not possible in the general case to prove the validity of analytic continuation to the point $p^2 = m^2$ for an arbitrary ratio of m to μ starting from only the covariance, causality and spectrum properties of the theory,[11] although such proof is possible in any order of perturbation theory.[12] In what follows we shall neglect the terms in Eq. (20) with $p_n^2 < 4m^2$ so that in our approximation $F(q^2)$ [see Eqs. (5) and (13a)] is the boundary value of an analytic function regular in the entire complex plane except for the cut $4m^2 \le \operatorname{Re} z < \infty$. We do not explicitly write out the dispersion relations for $F(q^2)$ and $F_\lambda(p^2)$ since this requires a knowledge of the asymptotic behavior of $F(z)$ and $F_\lambda(z)$ as $|z| \to \infty$. This question is clarified in Sec. 3.

3. In essence, Eqs. (19) and (20) express the unitarity conditions for the vertex Green's function $F_i(p, p')$, which make it possible to relate $F_i(p, p')$ to other matrix elements. It is much more difficult to decide now what is a reasonable

---

*Strictly speaking it is the invariant functions $F_1(p^2, z)$ and $F_2(p^2, z)$ of Eq. (12) that have these analyticity properties.

*Electromagnetic and weak interactions are ignored.

approximation than in the case of ρ and ρ_λ, since the contributions of the various terms to the summation over n in Eqs. (19) and (20) have different signs. At this time we can suggest nothing better than a restriction to the simplest terms in Eqs. (19) and (20), i.e., keeping the term corresponding to the nucleon-antinucleon pair (in the intermediate state) in Eq. (19), and the term corresponding to a nucleon and meson in Eq. (20).[*] We then obtain, in place of Eqs. (19) and (20), the approximate equations (see Sec. 5, item 1)

$$F^+(q^2) - F^-(q^2) = iA(q^2)(F^+(q^2) + F^-(q^2)), \tag{21}$$

$$\begin{aligned} F_1^+(p^2) - F_1^-(p^2) + \hat{p}(F_2^+(p^2) - F_2^-(p^2)) = i\,(A_1(p^2) \\ + \hat{p}A_2(p^2))[F_1^+(p^2) + F_1^-(p^2) + \hat{p}(F_2^+(p^2) + F_2^-(p^2))], \end{aligned}$$

$$A(q^2) = \mathrm{Re}\,A_0(q^2)/(1 - \mathrm{Im}\,A_0(q^2)), \tag{22}$$

where $A_0(q^2)$ is the partial amplitude for elastic nucleon-antinucleon scattering in the singlet spin and triplet isotopic spin S-state in the barycentric frame ($\mathbf{q} = 0$);

$$A_1(p^2) = {}^1\!/_2\,(a_s + a_p), \quad \sqrt{p^2}A_2(p^2) = {}^1\!/_2\,(a_s - a_p),$$

$$a_{s,p}(p^2) = \mathrm{Re}\,A_{s,p}(p^2)/(1 - \mathrm{Im}\,A_{s,p}(p^2)),$$

with $A_{s,p}(p^2)$ the partial amplitude for elastic meson-nucleon scattering in their barycentric frame ($\mathbf{p} = 0$) in the S- and P-state respectively with total spin and isospin $1/2$.

It is easy to see on the basis of conservation laws precisely why these states entered into Eqs. (21) and (22). We leave out the details of the calculations. Let us only note that in the derivation of Eqs. (21) and (22) we took into account the fact that $F^+(q^2) = (F^-(q^2))^*$ and $F_\lambda^+(p^2) = (F_\lambda^-(p^2))^*$. This reality condition on the absorptive parts, Eqs. (19) and (20), can be satisfied in the approximation under discussion by taking half of the sum over $|n^{in}\rangle$ and $|n^{out}\rangle$ states on the right side of Eqs. (19) and (20).

If the contributions from inelastic processes are ignored, then

$$A(q^2) = \tan\delta_0(q^2), \qquad a_{s,p}(p^2) = \tan\delta_{s,p}(p^2),$$

where $\delta_0(q^2)$ and $\delta_{s,p}(p^2)$ are the phase shifts in the above-indicated states.

In Born approximation[†]

$$A(q^2) = A^b(q^2) = -\frac{3g^2}{16\pi}(1 - \zeta^{-1})^{1/2}, \tag{23}$$

$$A_1^b(p^2) = -\frac{g^2}{16\pi}\left(\frac{3\xi - 1}{2\xi} + \frac{\ln\xi}{(1-\xi)}\right), \tag{24}$$

$$A_2^b(p^2) = \frac{g^2}{16\pi m}\left(\frac{\xi + 1}{2\xi^2} + \frac{\ln\xi}{(1-\xi)}\right). \tag{25}$$

Here we have for simplicity put $\mu = 0$ and introduced the dimensionless variables $\zeta = q^2/4m^2$ and $\xi = p^2/m^2$; for ξ and $\zeta \gg 1$

$$A^b \to -3g^2/16\pi,$$

$$A_1^b \to -3g^2/32\pi, \qquad A_2^b \to -g^2\ln\xi/16\pi m\xi.$$

3. STUDY OF THE APPROXIMATE SYSTEM

1. Let us assume $A(q^2)$ and $A_\lambda(p^2)$ to be known functions, independent of the unknown functions Δ, G and F_i^c. Then the approximate system of equations (1), (2), (7), (8), (21), and (22)[*] separates and in fact reduces to a study of the last two relations, i.e., to the solution of the homogeneous Hilbert problem:[7] to find an analytic function $F(z)$ (analogously for F_λ) regular in the entire plane except for the cut and of finite order at infinity, given the boundary condition on the cut $F^+(q^2) = K(q^2)F^-(q^2)$ where $K(q^2)(1 + iA(q^2))/(1 - iA(q^2))$ is a known function which vanishes nowhere.

As is well known, the solution of such a problem is not unique. To obtain a unique solution additional boundary conditions must be imposed on $F(z)$. In our case one such additional boundary condition consists of the relation (13c). However in the approximation under consideration this is not sufficient. If the validity of perturbation theory for $g \to 0$ (weak coupling) is assumed then one can demand that the solution that was found should coincide with the corresponding perturbation theory expression. If on the other hand (as is quite permissible) perturbation theory has no region of applicability (i.e., the solution cannot be expanded in a series near $g = 0$) then the question of additional boundary conditions becomes much more complex and has not been solved so far.[†] Nevertheless the absence of additional constants and unphysical singularities may be taken as additional criteria for determining a unique solution.

2. The solution of Eq. (21), satisfying the stated conditions has the form

$$F(z) = g\exp\left[\frac{(z-\mu^2)}{\pi}\int_{4m^2}^{\infty}\frac{\tan^{-1}A(z')\,dz'}{(z'-z)(z'-\mu^2)}\right]. \tag{26}$$

---

[*] The asymptotic vanishing of $F(q^2)$ and $F_\lambda(p^2)$ with increasing q^2 and p^2 would provide some justification for the legitimacy of this approximation. However, (see Sec. 3), in the weak coupling approximation, when the asymptotic behavior can be determined explicitly, the functions do not vanish. On the other hand, for small $p^2 < (m + 2\mu)^2$, the indicated approximation may turn out to be not bad for $F_\lambda(p^2)$.

[†] The expression $A^b(q^2)$ is given in reference 13.

[*] We assume that the terms Σ' and Σ'' are omitted from Eqs. (7) and (8).

[†] This question is of general importance for the theory of dispersion equations.[14]

It is easy to see that the asymptotic behavior of $F(z)$ as $|z| \to \infty$ is determined by the properties of the integral

$$J = \frac{1}{\pi} \int_{4m^2}^{\infty} \frac{\tan^{-1} A(z')}{z' - \mu^2}\, dz'.$$

If the integral J converges then $F(z) \to \text{const}$ as $|z| \to \infty$. If the integral diverges* then there are two possibilities:

a) $\tan^{-1} A(z) \to \text{const} = \alpha > 0$. In this case $F(z)$ falls off asymptotically. In particular for $\text{Re}\, z \to -\infty$ ($\text{Im}\, z = 0$), $F(z) \to g|z|^{-\alpha}$,

b) $\tan^{-1} A(z) \to \text{const} = \beta < 0$. Then $F(z)$ increases asymptotically: $F(z) \to g|z|^{-\beta}$ for $\text{Re}\, z \to -\infty$ ($\text{Im}\, z = 0$).

It is interesting that for $A(z) \to \pm\infty$ as $z \to \infty$ the asymptotic behavior of $F(z)$ is independent of $A(z)$: $F(z) \to g|z|^{\mp 1/2}$.

If it is assumed that perturbation theory is valid for $F(z)$ in the weak coupling case ($g \to 0$) then, taking into account that $A^b(z') \ll 1$, we obtain by replacing $\tan^{-1} A^b(z')$ by $A^b(z')$ and expanding the exponent in Eq. (26) in a series, the following

$$F(z) \approx g\left[1 + \frac{(z - \mu^2)}{\pi} \int_{4m^2}^{\infty} \frac{A^b(z')\, dz'}{(z' - z)(z' - \mu^2)}\right]. \qquad (27)$$

Expression (27) [with $A^b(q^2)$ given by (23)] coincides with the renormalized vertex Green's function calculated to terms of order $\sim g^3$. The asymptotic behavior of $F(z)$ in the weak coupling case not using perturbation theory is found by substituting expression (23a) into Eq. (26):

$$F(z) \to g\left(\frac{|z|}{4m^2}\right)^{3g^2/16\pi^2}, \qquad \text{Re}\, z \to -\infty, \qquad \text{Im}\, z = 0. \quad (28)$$

Thus, in the weak coupling case, $F(q^2)$ increases asymptotically.

3. Equation (20), equivalent to the Hilbert problem for two analytic functions $F_1(z)$ and $F_2(z)$, cannot be solved in closed form. It can be reduced to the solution of two Fredholm equations † with singular kernels.[7] An exact solution of this system may turn out to be not a bad approximation to reality in the region $|p^2| < (m + 2\mu)^2$ and would express the dependence of the vertex function on the values of the meson-nucleon scattering phase shifts in the $S_{1/2}$ and $P_{1/2}$ states. We do not discuss this question, but consider instead the asymptotic solution of Eq. (22) for $p^2 > m^2$. In this case, if we let $\mu^2 = 0$ (and discard terms of order μ^2/p^2 and higher) we can find an exact solution for the system (22) satisfying the boundary conditions formulated above. As is shown in Sec. 5 (item 2) the solution has the form

$$F_1^{\pm}(p^2) + \hat{p} F_2^{\pm}(p^2) = \sum_{r=1}^{2} C_r \exp\left\{\frac{1}{\pi} \int_{(m+\mu)^2}^{\infty} \frac{\varphi_1^r(z') + \hat{p}\varphi_2^r(z')}{z' - p^2 \mp i\varepsilon}\, dz'\right\}, \qquad (29)$$

$$\varphi_1^{1,2}(p^2) = \tan^{-1}\left(-\frac{1 + A_2'^2 - A_1^2}{2A_1} \pm \frac{[(1 + A_2'^2 + A_1^2)^2 - 4A_1^2 A_2'^2]^{1/2}}{2|A_1|}\right), \qquad (29a)$$

$$\sqrt{p^2}\, \varphi_2^{1,2}(p^2) = \tan^{-1}\left(-\frac{1 + A_1^2 - A_2'^2}{2A_2'} \pm \frac{[(1 + A_1^2 + A_2'^2)^2 - 4A_1^2 A_2'^2]^{1/2}}{2|A_2'|}\right), \qquad (29b)$$

$$A_2'(p^2) = \sqrt{p^2}\, A_2(p^2).$$

The constants C_1 and C_2 are related by

$$\sum_{r=1}^{2} C_r \exp\left\{\frac{1}{\pi} \int_{(m+\mu)^2}^{\infty} \frac{\varphi_1^r(z) + m\varphi_2^r(z)}{z - m^2}\, dz\right\} = g, \qquad (30)$$

which leaves the ratio C_1/C_2 arbitrary. This arbitrariness can be removed by requiring agreement with renormalized perturbation theory for $g \to 0$. Otherwise the arbitrariness in the choice of a solution remains. It is important to emphasize that in the weak coupling case (A_1 and $A_2' \ll 1$) only the term $\sim C_1$ enters into the corresponding expressions for $F_1(p^2)$ and $F_2(p^2)$ calculated by perturbation theory. Setting $C_2 \equiv 0$ in Eqs. (29) and (30) and expanding in powers of A_1^b and $A_2'^b$ we find (for $g \to 0$) the expression

$$F_1(p^2) + \hat{p} F_2(p^2) \approx g\left(1 + \frac{p^2 - m^2}{\pi} \int_{(m+\mu)^2}^{\infty} \frac{A_1^b(z)\, dz}{(z - p^2)(z - m^2)} + \frac{\hat{p}}{\pi} \int_{(m+\mu)^2}^{\infty} \frac{A_2^b(z)\, dz}{z - p^2} - \frac{m}{\pi} \int_{(m+\mu)^2}^{\infty} \frac{A_2^b(z)\, dz}{z - m^2}\right), \qquad (31)$$

which coincides with the result of renormalized perturbation theory accurate to terms of order g^3. The asymptotic behavior for weak coupling not by perturbation theory is given by

$$p^2 \to -\infty \begin{cases} F_1(p^2) \sim \left(\dfrac{|p^2|}{m^2}\right)^{3g^2/32\pi^2}, & (32a) \\ F_2(p^2) \sim \left(\ln\left|\dfrac{p^2}{m^2}\right|\right)^2 \left(\left|\dfrac{p^2}{m^2}\right|\right)^{3g^2/32\pi^2 - 1}. & (32b) \end{cases}$$

Thus, in the weak coupling approximation, $F_1(p^2)$ increases asymptotically and $F_2(p^2)$ decreases. If Eqs. (29) and (30) with $C_1 \equiv 0$ are taken as the solution, then F_1 and F_2 fall off asymptotically ($\text{Re}\, z \to -\infty$, $\text{Im}\, z = 0$) in the weak coupling approximation:

---

*We assume that $\int_{4m^2}^{\infty} \frac{\tan^{-1} A(z')dz'}{z'^2}$ converges.

†These equations follow from the dispersion relations for $F_\lambda(z)$ obtained under the assumption of a definite asymptotic behavior for these functions.

$$F_1(z) \sim |z|^{-\pi^{-1}\tan^{-1}(32\pi/3g^2)}, \qquad (33a)$$

$$F_2(z) \sim |z|^{-\pi^{-1}\tan^{-1}(32\pi/3g^2)-1/2}, \qquad (33b)$$

in disagreement with perturbation theory.

4. To conclude this section we discuss briefly the role of inelastic processes in the determination of the asymptotic behavior of $F(q^2)$. If the omitted terms in Eq. (21) are denoted by $\Psi(q^2)$ then we are led to the inhomogeneous Hilbert problem:[7]

$$F^+(q^2) = \frac{1+iA(q^2)}{1-iA(q^2)} F^-(q^2) + \frac{\Psi(q^2)}{1-iA(q^2)}. \qquad (34)$$

A solution of Eq. (34), satisfying condition (13c) and not involving additional constants, is given by

$$F^{\pm}(q^2) = F_0^{\pm}(q^2)\left(\frac{q^2-\mu^2}{\pi}\int\limits_{(3\mu)^2}^{\infty} \frac{\widetilde{\Psi}(z)\,dz}{(z-\mu^2)(z-q^2\mp i\varepsilon)} + 1\right),$$

$$\widetilde{\Psi}(z) = \Psi(z)(1+A^2(z))^{-1/2}|F_0^{\pm}(z)|^{-1}, \qquad (35)$$

with $F_0^{\pm}(z)$ the solution of the corresponding homogeneous problem [Eq. (26)].

From a physical point of view it seems most natural to assume that $A(q^2) \rightarrow 0$ as $q^2 \rightarrow \infty$. In that case $F_0(q^2)$ approaches a constant and only one possibility exists for making $F(q^2)$ in Eq. (35) fall off asymptotically:

$$\widetilde{J} \equiv \frac{1}{\pi}\int\limits_{(3\mu)^2}^{\infty} \frac{\widetilde{\Psi}(z)\,dz}{z-\mu^2} = 1, \qquad (36)$$

i.e., $\Psi(q^2)$ must vanish for $q^2 \rightarrow \infty$.* In an analogous manner the necessary conditions are found for $F(q^2)$ to decrease asymptotically for a different possible behavior of $A(q^2)$. The contribution of inelastic processes to $F_\lambda(p^2)$ may be similarly considered and a condition of the type (36) is easily obtained by introducing an inhomogeneous term $\Psi_1(p^2) + \hat{p}\Psi_2(p^2)$ into Eq. (22); however, all this is not necessary since at the present time nothing is known about the asymptotic behavior of partial waves, nor about the other matrix elements that contribute to $\Psi(q^2)$ and $\Psi_\lambda(p^2)$.

4. DISCUSSION

1. The renormalization constants Z_2 and Z_3 are expressed in terms of the spectral functions $\rho(q^2)$ and $\rho_2(p^2)$ by [see Eqs. (7) and (8)]:

$$Z_3^{-1} = 1 + \int\limits_{(3\mu)^2}^{\infty} \rho(q^2)\,dq^2, \qquad (37)$$

$$Z_2^{-1} = 1 + \int\limits_{(m+\mu)^2}^{\infty} \rho_2(p^2)\,dp^2. \qquad (38)$$

In the approximation considered here the convergence of the above integrals is determined, according to Eqs. (7) and (8), by the asymptotic behavior of $F(q^2)$ and $F_\lambda(p^2)$: if these functions vanish at infinity sufficiently fast so that the integrals in Eqs. (37) and (38) converge then Z_2 and Z_3 will be finite; otherwise Z_2^{-1} and Z_3^{-1} are divergent constants. It is important to note here that the latter result cannot be improved upon by taking into account higher approximations for ρ and ρ_2 so that the falling off of $F(q^2)$ and $F_\lambda(p^2)$ is a necessary (but not sufficient) condition for finiteness of the renormalization constants Z_2 and Z_3. As has been seen in the previous section the asymptotic behavior of $F(q^2)$ and $F_\lambda(p^2)$ can be determined only very crudely, since in the strong coupling case ($g \sim 1$) it is not clear what serves as an expansion parameter, and in the weak coupling case in the lowest approximation an increasing asymptotic behavior is obtained for $F(q^2)$ [see Eq. (28)] and $F_\lambda(p^2)$ [see Eqs. (32a, b)]. We are thus led to the conclusion that in the first approximation for weak coupling the constants Z_2^{-1} and Z_3^{-1} diverge. It follows from the dispersion relations for $\Delta(q^2)$ and $G(p)$ that in this approximation these functions decrease at infinity slower than the corresponding free particle Green's functions Δ_0 and G_0 [the explicit asymptotic behavior is easy to derive starting from Eqs. (1), (2), (7) and (8), (28), (32a) and (32b)].

2. It is important to note the following: independent of whether $F(q^2)$ and $F_\lambda(p^2)$ increase or decrease asymptotically it is impossible in the approximation under consideration to run into an internal inconsistency of the "zero-charge" type,[15] characteristic of certain approximate solutions of the Schwinger-Dyson equations. This is related to the fact that the vertex part $\Gamma_5^i(p, p')$, determined by the relation (14) for given Δ, G and $F_\lambda^c(p, p')$, decreases for increasing values of its arguments as is easy to deduce from Eqs. (1), (2), (7), (8) and (14).*

3. It seems to us that as a consequence of the great mathematical difficulties that arise when one attempts to estimate the importance of higher order approximations in the dispersion relation approach, as well as due to the absence of an effective expan-

---

*At the same time, condition (36) may impose limitations on possible values of the constant g.

*It follows from the work of Lehmann, Symanzik, and Zimmerman[9] that in the approximation in which inelastic processes are ignored the falling off of $\Gamma_5(p, p')$ as a function of q^2 (for $p^2 = p'^2 \neq m^2$) and $p^2(p'^2 = m^2, q^2 = \mu^2)$ is a necessary and sufficient condition for the absence of unphysical singularities ("ghost states") in $\Delta(q^2)$ and $G(p)$.

sion parameter in the asymptotic region, progress on the question of internal consistency of such an approach and its relation to the Lagrangian formulation of quantum field theory will have to await the application of new, in particular statistical, methods of calculation of the many-particle matrix elements which play an important role at high energies.

5. MATHEMATICAL APPENDIX

1. In order to obtain Eqs. (21) and (22) we made use of the partial wave expansion for the nucleon-antinucleon and meson-nucleon elastic scattering amplitudes, $<p_1, l; p_1', l' \,|\, \overline{U}{}^{r}_{+}(\mathbf{p})\, \eta(0)\,|\, p'r'>$ and $<q_1^j, p_1 \,|\, j\,(0)\,|\, p'>$. If terms that do not contribute to $F^+(q^2) - F^-(q^2)$ and $F_\lambda^+(p^2) - F_\lambda^-(p^2)$ are omitted this expansion looks as follows (in the barycentric frame for the corresponding process):

$$(q^2/2)^{1/2}(4\pi)^{-1}\langle p_1, l; p_1', l' \,|\, \overline{U}{}^{r}_{+}(\overline{\mathbf{p}})\, \eta(0)\,|\, p', r'\rangle$$

$$= |\mathbf{p}|^{-1}\delta_{rr'}\delta_{ll'}\sum_l (2l+1)\, A_l(q^2)\, P_l(\cos\theta)$$

$$+ \text{ isotopic triplet terms} \tag{39}$$

$$\tau_j(2\omega)^{1/2} E\,(E+\omega)^{-1}\langle p_1, r_1; q', j \,|\, j_i(0)\,|\, p', r\rangle$$

$$= |\mathbf{q}|^{-1}\tau_i \sum_l ((l+1)\, A_{l+}(p^2)\, P_{l+}^{r_1, r}(\cos\theta')$$

$$+ l A_{l-}(p^2)\, P_{l-}^{r_1, r}(\cos\theta')). \tag{40}$$

The notation in Eq. (39) is as follows: $q = p + p' = p_1 + p_1'$, $\mathbf{q} = 0$, θ is the angle between $\mathbf{p}$ and $\mathbf{p}_1$; $A_l(q^2)$ is the partial wave amplitude for nucleon-antinucleon scattering in the singlet state with orbital angular momentum l and total isospin 1; $(r, l)(r', l') = 1, 2$ are the indices denoting the antinucleon and nucleon states; $P_l(\cos\theta)$ are Legendre polynomials. If the inelastic processes are small then $A_l(q^2) \approx \exp(-i\delta_l(q^2)) \sin\delta_l(q^2)$ with $\delta_l(q^2)$ the phase shift in the corresponding state.

The notation in Eq. (40) is as follows: $p = p' + q = p_1 + q_1$, $\mathbf{p} = 0$; $p_0' = p_{10} = E$ is the nucleon energy; $q_0 = q_{10} = \omega$ is the meson energy; θ' is the angle between $\mathbf{p}'$ and $\mathbf{p}_1$; $A_{l\pm}(p^2)$ are the partial wave meson-nucleon scattering amplitudes in states of total angular momentum $I = l \pm \frac{1}{2}$ and isospin $\frac{1}{2}$ with $A_{0+}(p^2) \equiv A_s(p^2)$, $A_{1-}(p^2) \equiv A_p(p^2)$; $P_{l\pm}^{r, r'}(\cos\theta')$ are the angular polynomials introduced in reference 16.

$$A_{l\pm}(p^2) = \exp\{-i\delta_{l\pm}(p^2)\}\sin\delta_{l\pm}(p^2)$$

in the energy region $(m+\mu)^2 \leq p^2 = (E+\omega)^2 \leq (m+2\mu)^2$, where $\delta_{l\pm}(p^2)$ is the phase shift in the corresponding state.

2. We now prove that Eq. (29), together with Eqs. (29a) and (29b), constitutes a solution of Eq. (22) for $\mu^2 = 0$. For $\mu^2 \neq 0$ we obtain from Eq. (29), making use of Eq. (16) with $q^2 = \mu^2$

$$F^+(\hat{p}) - F^-(\hat{p}) = i\Big\{\tan[(\varphi_1(p^2) + \hat{p}\varphi_2(p^2))\,\theta(p^2 - (m+\mu)^2)]$$

$$+ \tan\Big[\mathbf{e}\gamma\,((m+\mu)^2 - p^2)^{1/2}(p^2 - (m-\mu)^2)^{1/2}$$

$$\times \frac{1}{\pi}\int\limits_{(m+\mu)^2}^{\infty}\frac{\varphi_2(z)\,dz}{z^2 - p^2}\,\theta((m+\mu)^2 - p^2)\,\theta(p^2 - (m-\mu)^2)\Big]\Big\}$$

$$\times (F^+(\hat{p}) + F^-(\hat{p})),$$

$$F^\pm(\hat{p}) = F_1^\pm(p^2) + \hat{p}F_2^\pm(p^2), \qquad \theta(x) = \begin{cases} 1 & x > 0 \\ 0 & x < 0 \end{cases}; \tag{41}$$

where $\mathbf{e}$ is a unit vector in the direction of $\mathbf{p}$. It is seen that for $\mu \to 0$ the second term on the right side of Eq. (41) vanishes and we obtain Eq. (22) under the condition

$$\tan[\varphi_1(p^2) + \hat{p}\varphi_2(p^2)] = A_1(p^2) + \hat{p}A_2(p^2),$$

from which one obtains Eqs. (29a) and (29b). It is elementary to prove that at infinity the solution (29) is of finite order if it is taken into account that $\varphi_2(z)$ falls off not slower than $1/\sqrt{z}$ as $z \to \infty$ [see Eq. (29b)].

---

[1] V. Ya. Faĭnberg, JETP **37**, 1361 (1959), Soviet Phys. JETP **10**, 968 (1960).

[2] V. D. Mur and V. D. Skarzhinskiĭ, JETP **38**, 1817 (1960), this issue p. 1309.

[3] P. J. Redmond, Phys. Rev. **112**, 1404 (1958). P. J. Redmond and J. L. Uretsky, Phys. Rev. Lett. **1**, 147 (1958).

[4] Bogolyubov, Logunov, and Shirkov, Метод дисперсионных соотношений и теория возмущений, (The Dispersion Relations Method and Perturbation Theory) preprint, Dubna (1959).

[5] Kirzhnits, Faĭnberg, and Fradkin, JETP **38**, 239 (1960), Soviet Phys. JETP **11**, 174 (1960).

[6] S. Mandelstam, Phys. Rev. **112**, 1344 (1958).

[7] N. I. Muskhelishvili, Сингулярные интегральные уравнения (Singular Integral Equations) Gostekhizdat, 1946.

[8] H. Lehmann, Nuovo cimento **11**, 342 (1954).

[9] Lehmann, Symanzik, and Zimmermann, Nuovo cimento **2**, 425 (1955).

[10] N. N. Bogolyubov and D. V. Shirkov, Введение в теорию квантованных полеи, (Introduction to Quantum Field Theory) M., 1957 [Engl. Transl., Interscience, 1959].

[11] R. Oehme, Phys. Rev. **111**, 1430 (1958).

[12] Y. Nambu, Nuovo cimento **6**, 1064 (1957); **9**, 610 (1958). K. Symanzik, Progr. Theor. Phys. **20**, 690 (1958).

[13] Federbush, Goldberger, and Treiman, Phys. Rev. **112**, 642 (1958).

[14] Castellejo, Dalitz, and Dyson, Phys. Rev. **101**, 453 (1956).

[15] L. D. Landau and I. Ya. Pomeranchuk, Dokl. Akad. Nauk SSSR **102**, 489 (1955). E. S. Fradkin, JETP **29**, 258 (1955), Soviet Phys. JETP **2**, 361 (1956).

[16] Tamm, Gol'fand, and Faĭnberg, JETP **26**, 649 (1954).

Translated by A. M. Bincer
346

SOVIET PHYSICS JETP VOLUME 11, NUMBER 6 DECEMBER, 1960

TRANSITION RADIATION FOR A CHARGED PARTICLE AT OBLIQUE INCIDENCE

G. M. GARIBYAN

Physics Institute, Academy of Sciences, Armenian S.S.R.

Submitted to JETP editor January 6, 1960

J. Exptl. Theoret. Phys. (U.S.S.R.) 38, 1814-1816 (June, 1960)

The transition radiation emitted in the forward direction by a charge in oblique incidence at the boundary between two media is considered. It is shown that the intensity of the radiation is essentially independent of the angle of incidence of the particles so long as this angle is far from 90°.

THE total intensity of the transition radiation emitted by a relativistic particle in the forward direction in passing through a boundary between two media is proportional to the particle energy.[1] It is of interest to investigate the intensity of the transition radiation as a function of the entrance angle of the particle into the medium. The problem of a charge moving into a medium at oblique incidence has been solved earlier in general form[2] (cf. also reference 3). In the present note the energy losses due to the forward radiation of an extreme relativistic particle which moves into a medium at oblique incidence are calculated by the Landau method[4] and by a direct calculation of the energy flux.

Let the plane z = 0 be the boundary separating two media characterized by dielectric constants ϵ_1 and ϵ_2. The particle moves with velocity **v** in the yz plane. As has been shown in reference 2, the Fourier component of the electric vector of the radiation field in the second medium is given by the formula

$$\mathbf{E}_2'(\mathbf{k}) = \boldsymbol{\varkappa} e_{2\varkappa} + \mathbf{j} e_{2y} - \mathbf{n}(\varkappa^2 e_{2\varkappa} + k_y e_{2y})/\lambda_2,$$

$$e_{2\varkappa} = \frac{ei}{2\pi^2}\frac{\lambda_1\lambda_2}{\varepsilon_1\lambda_2+\varepsilon_2\lambda_1}\left\{\frac{-1/\lambda_1 - v_z/\omega}{k^2-\omega^2\varepsilon_1/c^2} + \frac{\varepsilon_1/\varepsilon_2\lambda_1 + v_z/\omega}{k^2-\omega^2\varepsilon_2/c^2}\right. \quad (1)$$

$$\left. - \frac{k_y v_y (k_z - \lambda_2 + \lambda_1)}{\omega\lambda_1\lambda_2}\left(\frac{1}{k^2-\omega^2\varepsilon_1/c^2} - \frac{1}{k^2-\omega^2\varepsilon_2/c^2}\right)\right\},$$

$$e_{2y} = \frac{ei}{2\pi^2}\frac{v_y}{\lambda_1+\lambda_2}\frac{\omega(\lambda_1+k_z)}{c^2}\left(\frac{1}{k^2-\omega^2\varepsilon_1/c^2} - \frac{1}{k^2-\omega^2\varepsilon_2/c^2}\right). \quad (2)$$

Here $\omega = \mathbf{k}\cdot\mathbf{v} = k_y v_y + k_z v_z$; **i**, **j** and **n** are unit vectors along the x, y and z axes; κ is the component of the wave vector **k** in the xy plane; $\lambda_{1,2}^2 = \omega^2\epsilon_{1,2}/c^2 - \kappa^2$, where the real and imaginary parts of λ_1 and λ_2 are taken as positive. We also introduce the angle of incidence of the particle at the boundary between the media φ; $v_z = v\cos\varphi$ and $v_y = v\sin\varphi$.

In carrying out the calculation it is convenient to rotate the coordinate axes about the x direction through an angle φ such that the new z′ axis coincides with the particle trajectory. Then, denoting all quantities in the new coordinate system by primes we have

$$E_{2z'}'(\mathbf{k}') = [k_y\sin\varphi - (\varkappa^2/\lambda_2)\cos\varphi]\, e_{2\varkappa}$$

$$+ [\sin\varphi - (k_y/\lambda_2)\cos\varphi]\, e_{2y},$$

$$\mathbf{E}_{2t'}'(\mathbf{k}') = \mathbf{i}' k_x' e_{2\varkappa} + \mathbf{j}'\{[k_y\cos\varphi + (\varkappa^2/\lambda_2)\sin\varphi]\, e_{2\varkappa}$$

$$+ [\cos\varphi + (k_y/\lambda_2)\sin\varphi]\, e_{2y}\},$$

$$\mathbf{H}_2'(\mathbf{k}') = c\omega^{-1}[\boldsymbol{\varkappa} + (\mathbf{n}'\cos\varphi - \mathbf{j}'\sin\varphi)\lambda_2]\times \mathbf{E}_2'(\mathbf{k}')] \quad (3)$$

where $\mathbf{E}_{2t'}'(\mathbf{k}')$ is the projection of the Fourier component of the radiation field on the plane perpendicular to the direction of motion of the particle. We must keep in mind the fact that

$$\omega = k_z' v, \qquad k_y = \omega v^{-1}\sin\varphi + k_y'\cos\varphi,$$

$$k_z = \omega v^{-1}\cos\varphi - k_y'\sin\varphi, \quad \boldsymbol{\varkappa} = \mathbf{i}' k_x' + (\mathbf{j}'\cos\varphi + \mathbf{n}'\sin\varphi)\, k_y.$$

Using Eq. (3) we can compute the force due to the radiation field which acts on the particle (cf. reference 4)

$$F_2(\varphi) = ev\int_0^\infty dt\int E_{2z'}'(\mathbf{k}')$$

$$\times \exp\left\{ivt\left(\lambda_2 + k_y'\sin\varphi - \frac{\omega}{v}\cos\varphi\right)\cos\varphi\right\} d\mathbf{k}', \quad (4)$$

as well as the Poynting vector in the second medium at a plane z′ = const (cf. reference 1):

$$S_{2z'}(\varphi) = \frac{c}{4\pi}\int_{-\infty}^{+\infty} [\mathbf{E}_2'\times\mathbf{H}_2']_{z'}\, dt\, dx'\, dy'. \quad (5)$$

We now sketch the calculation for the second case. Since $k^2 - \omega^2\epsilon_{1,2}/c^2 = k'^2 - \omega^2\epsilon_{1,2}/c^2$, the denominators of the total-radiation expressions contain factors characteristic of normal incidence of the particle on the separation boundary; for an extreme relativistic particle these factors lead to the emission of transition radiation at very small angles to the direction of motion of the particle.

Furthermore, since

$$\lambda_{1,2} = \Big[\frac{\omega^2}{v^2}\Big(\cos^2\varphi - (1-\beta^2) - \frac{\sigma_{1,2}}{\omega^2}\Big) - 2\frac{\omega}{v}k_y'\sin\varphi\cos\varphi - \varkappa'^2 + k_y'^2\sin^2\varphi\Big]^{1/2},$$

if

$$\cos\varphi > \sqrt{\sigma_{1,2}/\omega^2}, \qquad \cos\varphi > \sqrt{1-\beta^2} \tag{6}$$

(σ_1 and σ_2 are the plasma frequencies of the media) we find that

$$\mathbf{E}_{2t'}'(\mathbf{k}') = \frac{ei}{2\pi^2}\varkappa'\Big(\frac{1}{k'^2 - \varepsilon_2\omega^2/c^2} - \frac{1}{k'^2 - \varepsilon_1\omega^2/c^2}\Big). \tag{7}$$

In the present case the magnetic field is

$$\mathbf{H}_2'(\mathbf{k}') = \beta^{-1}[\mathbf{n}' \times \mathbf{E}_{2t'}(\mathbf{k}')],$$

so that the further calculations are very simple and for $\omega > \sqrt{\sigma_{1,2}}$ we obtain formulas which coincide with the formulas for the case of perpendicular incidence.

If the condition in (6) is not satisfied the quantities $\lambda_{1,2}$ become purely imaginary and since the expressions for the radiation fields contain the factor $\exp(i\lambda_2 z)$ these fields fall off exponentially with z.

The condition in (6) can be understood on the basis of the following qualitative considerations. As is well known, transition radiation is formed in some region of space around the trajectory of the particle in the first and second media. For oblique incidence of the particle it is evident that the transition radiation will be generated (just as in the case of perpendicular incidence) if the formation zone satisfies the same conditions. For example, in the second medium the formation zone for radiation of frequency ω is a cone with opening angle (relative to the particle trajectory) given approximately by $\sqrt{\sigma_2}/\omega$ (for frequencies $\omega < \sqrt{\sigma_2}/\sqrt{1-\beta^2}$). Hence it is clear that it is only when $\cos\varphi < \sqrt{\sigma_2}/\omega$ that the formation zone in the second medium is affected, because part of it extends into the first medium.

Thus, as the angle of incidence of the particle increases the softer photons tend to be suppressed: with further increases in φ the suppression extends to harder and harder photons. This effect can be used for generating transition radiation in a narrow frequency range since the long-wave portion of the radiation spectrum can be suppressed by rotation of the medium. The total number of emitted photons remains almost the same because the lower frequency limit appears in the formula logarithmically [cf. reference 1, Eq. (14)].

Results similar to these have been obtained by Korkhmazyan,[5] who used the method of images.

---

[1] G. M. Garibyan, JETP **37**, 527 (1959), Soviet Phys. JETP **10**, 372 (1960).

[2] G. M. Garibyan, Izv. AN Arm. S.S.R., Ser Fiz.-Mat. Nauk, **11**, No. 4 (1958).

[3] N. A. Korkhmazyan, ibid., **11**, No. 6 (1958).

[4] L. D. Landau and E. M. Lifshitz, Электродинамика сплошных сред, (Electrodynamics of Continuous Media) Gostekhizdat, 1957.

[5] N. A. Korkhmazyan, Izv. AN Arm. S.S.R., Ser. Fiz.-Mat. Nauk (in press).

Translated by H. Lashinsky
347

SOVIET PHYSICS JETP VOLUME 11, NUMBER 6 DECEMBER, 1960

APPLICATION OF THE DISPERSION METHOD FOR INVESTIGATION OF THE SIMPLEST GREEN'S FUNCTIONS IN QUANTUM ELECTRODYNAMICS

V. D. MUR and V. D. SKARZHINSKIĬ

P. N. Lebedev Physics Institute, Academy of Sciences, U.S.S.R.

Submitted to JETP editor January 9, 1960

J. Exptl. Theoret. Phys. (U.S.S.R.) **38**, 1817-1823 (June, 1960)

The dispersion relation technique is used to study the electron propagation function $G(\hat{p})$ and the current matrix element $\langle 0|\eta(0)|p', k\rangle$ as functions of $p^2 = (p' + k)^2$. It is shown that in the two-particle approximation (no more than two particles in the intermediate state) the analytical properties of the matrix element under study (with respect to the variable p^2) lead to a Hilbert boundary problem, which is then solved. Explicit expressions for the electron spectral propagation functions are derived in the given approximation, and the asymptotic behavior of $G(\hat{p})$ and $\Gamma_\mu(p, p'; k)$ is determined for $-p^2 \to \infty$, $p'^2 = -m^2$ and $k^2 = 0$.

1. INTRODUCTION

AT the present time it is possible to develop a new approach to the study of the problems of quantum field theory. This method is connected with the use of the dispersion relations for different Green's functions (or matrix elements) of the interacting fields. In such an approach, an infinite set of interlocking integral equations is generated; these connect all possible matrix elements on the energy surface, and definite boundary conditions are necessary for the solution of this set.

In quantum electrodynamics, and especially in quantum field theory, the dispersion technique has already furnished a number of interesting results; in these cases, correspondence with perturbation theory is chosen as a reasonable boundary condition. Thus, for example, in the work of Faĭnberg,[1] the behavior of the photon propagation function $D_{\mu\nu}(k)$ and the matrix element of the current $\langle 0|j_\mu(0)|p, p'\rangle$ were studied as functions of the square of the photon momentum $k^2 = (p + p')^2$ for $p^2 = p'^2 = -m^2$. In addition, a number of other problems was also considered. In this connection, the study of similar quantities as functions of the square of the electron momentum p^2 is of interest. This is the object of the present research.*

By definition,

$$G_{\alpha\beta}(x-y) = \langle 0|T\psi_\alpha(x)\bar{\psi}_\beta(y)|0\rangle = \frac{1}{(2\pi)^4}\int G_{\alpha\beta}(p)\, e^{ip(x-y)}\, dp, \tag{1.1}$$

where $\psi(x)$ is the renormalized Heisenberg operator which satisfies the equation

$$(\hat{\nabla}_x + m)\psi(x) = \eta(x), \qquad \hat{\nabla}_x = \gamma_\mu \partial/\partial x_\mu,$$
$$\gamma_\mu = \gamma_\mu^+, \qquad xy = \mathbf{xy} + x_4 y_4, \qquad x_4 = ix_0. \tag{1.2}$$

It is known that the Fourier transform of the electron propagation function has the spectral representation

$$G(\hat{p}) = \frac{1}{i}\left\{\frac{-i\hat{p}+m}{p^2+m^2-i\varepsilon} + \int_{-\infty}^{-m^2} \frac{-i\hat{p}\rho_1(p'^2)+\rho_2(p'^2)}{p^2-p'^2-i\varepsilon}\, dp'^2\right\}; \tag{1.3}$$

$$\rho_1(p^2) = \frac{(2\pi)^3}{4(p^2+m^2)^2}\,\mathrm{Sp}\left\{\left(2m + \frac{p^2-m^2}{i\hat{p}}\right)\right.$$
$$\left.\times \sum_n \langle 0|\eta(0)|n\rangle\langle n|\bar{\eta}(0)|0\rangle\,\delta(p-p_n)\right\},$$

$$\rho_2(p^2) = \frac{(2\pi)^3}{4(p^2+m^2)^2}\,\mathrm{Sp}\left\{\left(m^2 - p^2 + \frac{2mp^2}{i\hat{p}}\right)\right.$$
$$\left.\times \sum_n \langle 0|\eta(0)|n\rangle\langle n|\bar{\eta}(0)|0\rangle\,\delta(p-p_n)\right\}. \tag{1.4}$$

Thus the spectral functions ρ_1 and ρ_2 are expressed bilinearly by the current matrix elements $\langle 0|\eta(0)|n\rangle$. In the present research, the behavior of the first non-vanishing matrix element* $\langle 0|\eta(0)|p', r; k, \lambda\rangle$ is studied by the dispersion relation technique as a function of $p^2 = (p' + k)^2$.

2. ANALYTICAL PROPERTIES OF THE FORM FACTOR

We consider the electron form factor

$$\tilde{e}_\mu^\lambda (2\omega)^{-1/2} F_\mu^{in}(p)\, u_-(p') = i\langle 0|\eta(0)|p', r; k, \lambda; in\rangle, \tag{2.1}$$

---

*A similar investigation into the application to mesodynamics has been made in the research of Malakhov, Rashevskaya, and Faĭnberg.[2]

*For brevity, we call the matrix element $i\langle 0|\eta(0)|p', k\rangle$ the form factor of the electron.

where $p + p' + k = 0$; $\tilde{e}^{\lambda}_{\mu} = e^{\lambda}_{\mu} - k_{\mu}k^{-2}(e^{\lambda}k)(1 - \sqrt{d_l})$ are the four photon polarization vectors in arbitrary scale; $u_-(p')$ satisfies the equation $(i\hat{p}' + m)u_-(p') = 0$.

It is easy to prove that for $p'^2 = -m^2$ and $k^2 = 0$,

$$F^{in}_{\mu}(p) = ie(-i\hat{p} + m)\,G(-\hat{p})\,\Gamma_{\mu}(-p,\ p';\ k) \qquad (2.2)$$

The requirements of relativistic and gauge invariance lead to a general expression for the form factor:

$$F^{in}_{\mu}(p) = \left(\gamma_{\mu} - \frac{p'_{\mu}\hat{k}}{p'k}\right) F_1(p^2) + i\sigma_{\mu\nu}k_{\nu}\,F_2(p^2)$$
$$+ ik_{\mu}\,F_3(p^2) + k_{\mu}\,\hat{k}F_4(p^2) + e\,\frac{p'_{\mu}\hat{k}}{p'k}, \qquad (2.3)$$

where $\sigma_{\mu\nu} = \frac{1}{2}(\gamma_{\mu}\gamma_{\nu} - \gamma_{\nu}\gamma_{\mu})$. In accord with (2.2),*

$$k_{\mu}F^{in}_{\mu}(p)\,u_-(p') = e\hat{k}u_-(p'). \qquad (2.4)$$

We now investigate the analytical properties of $<0\,|\,\eta(0)\,|\,p', k>$ in the variable p^2. Making use of the reducing formula of reference 4, we transform to the relation

$$\tilde{e}^{\lambda}_{\mu}(2\omega)^{-1/2}F^{in}_{\mu}(p)\,u_-(p') = \int dx e^{-ipx} f^{in}_{\lambda}(x,\ k)\,u_-(p'), \quad (2.5)$$

where

$$f^{in}_{\lambda}(x,\ k) = -e^{-ikx}\{\theta(-x_0)$$
$$\times\langle 0\,|\,[\eta(0),\ \bar{\psi}(x)]_+\,|\,k,\ \lambda\rangle\}(-\hat{\nabla}_x + m) = 0$$

for $x_0 > 0$, $x^2 > 0$.

By virtue of the fact that $k^2 = 0$ in the system of coordinates $\mathbf{p}' = 0$, we have $|\,\mathbf{p}\,| = -p_0 - m$. Therefore, for $p_0 \rightarrow p_0 + i\Gamma$, the factor $\exp\{\Gamma\,|\,x_0 + \mathbf{e}\cdot\mathbf{x}\,|\}$ appears under the integral in (2.5), thus guaranteeing the regularity of the desired function in the lower half plane of the complex variable p_0 or, what is the same thing, the regularity of p^2. (The indeterminacy at the cone $x^2 = 0$ is removed as usual by the addition of the factor $\exp\{-\epsilon\mathbf{x}^2\}$ $\epsilon \rightarrow +0$).

Similar to the above, the quantity

$$\tilde{e}^{\lambda}_{\mu}(2\omega)^{-1/2}F^{out}_{\mu}(p)\,u_-(p') = i\langle 0\,|\,\eta(0)\,|\,p',\ r;\ k,\ \lambda;\ out\rangle$$
$$= \tilde{e}^{\lambda}_{\mu}(2\omega)^{-1/2}\left\{\left(\gamma_{\mu} - \frac{p'_{\mu}\hat{k}}{p'k}\right)F^{*}_1(p^2) + i\sigma_{\mu\nu}k_{\nu}\,F^{*}_2(p^2)\right.$$
$$\left. + ik_{\mu}F^{*}_3(p^2) + k_{\mu}\hat{k}F^{*}_4(p^2) + e\,\frac{p'_{\mu}\hat{k}}{p'k}\right\}u_-(p') \qquad (2.6)$$

can be put in the form

$$\tilde{e}^{\lambda}_{\mu}(2\omega)^{-1/2}F^{out}_{\mu}(p)\,u_-(p') = \int dx e^{-ipx} f^{out}_{\lambda}(x,\ k)\,u_-(p'),$$
$$f^{out}_{\lambda}(x,\ k) = e^{-ikx}\{\theta(x_0)$$
$$\langle 0\,|\,[\eta(0),\ \bar{\psi}(x)]_+\,|\,k,\ \lambda\rangle\}(-\hat{\nabla}_x + m) = 0 \qquad (2.5')$$

for $x_0 < 0$, $x^2 > 0$, and is therefore regular in the upper half plane of p^2.

In addition,

$$\tilde{e}^{\lambda}_{\mu}(2\omega)^{-1/2}[F^{in}_{\mu}(p) - F^{out}_{\mu}(p)]\,u_-(p')$$
$$= -(2\pi)^4\sum_n \langle 0\,|\,\eta(0)\,|\,n\rangle\langle n\,|\,\bar{\eta}(0)\,|\,k,\ \lambda\rangle\,\delta(p + p_n) = 0 \qquad (2.7)$$

for $p^2 > -m^2$.

Consequently, there exists a single analytical function $\tilde{e}^{\lambda}_{\mu}(2\omega)^{-1/2}F_{\mu}(z)\,u_-(p')$ which is regular through the complex z plane, with the exception of the cut along the real axis from the point $-m^2$ to $-\infty$, so that

$$\lim_{z\rightarrow p^2 - i\varepsilon} \tilde{e}^{\lambda}_{\mu}(2\omega)^{-1/2}F_{\mu}(z)\,u_-(p') = \tilde{e}^{\lambda}_{\mu}(2\omega)^{-1/2}F^{in}_{\mu}(p)\,u_-(p'),$$
$$\lim_{z\rightarrow p^2 + i\varepsilon} \tilde{e}^{\lambda}_{\mu}(2\omega)^{-1/2}F_{\mu}(z)\,u_-(p') = \tilde{e}^{\lambda}_{\mu}(2\omega)^{-1/2}F^{out}_{\mu}(p)\,u_-(p'). \qquad (2.8)$$

3. THE HILBERT PROBLEM FOR THE FORM FACTOR

We have thus established the analytical properties of the form factor as a function of p^2. For the determination of this function, however, it is necessary to have some sort of condition on the line of the cut. Such a condition is usually obtained in the expansion of $\tilde{e}^{\lambda}_{\mu}(2\omega)^{-1/2}[F^{in}_{\mu}(p) - F^{out}_{\mu}(p)]\,u_-(p')$ over the complete set of states $|\,n>$, if we break off the resultant infinite series at some term. We note that for such a cut off it is necessary to sum over the intermediate states of $|\,n>$ in the following fashion in order to preserve the Hermitian character of $i[F_k(p^2) - F^{*}_k(p^2)]$:

$$\sum_n |\,n\rangle\langle n\,| = \tfrac{1}{2}\sum_n\{|\,n,\ in\rangle\langle n,\ in\,| + |\,n,\ out\rangle\langle n,\ out\,|\}.$$

Taking into account the vanishing of the current matrix elements over the vacuum and the single-particle state, and limiting ourselves to the first term in the sum over $|\,n>$ (the two-particle approximation), we obtain

$$\tilde{e}^{\lambda}_{\mu}(2\omega)^{-1/2}[F^{in}_{\mu}(p) - F^{out}_{\mu}(p)]\,u_-(p') = \frac{1}{2(2\pi)^6}$$
$$\times\int d\mathbf{p}'_1\,d\mathbf{k}_1\sum_{r_1,\lambda_1}\tilde{e}^{\lambda_1}_{\mu_1}\frac{1}{\sqrt{2\omega_1}}[F^{out}_{\mu_1}(p_1)\,u_-(p'_1)\,f_{p'_1,\,k_1,\,p',\,k}$$
$$- F^{in}_{\mu_1}(p_1)\,u_-(p'_1)\,f^{*}_{p'_1,\,k_1,\,p',\,k}], \qquad (3.1)$$

where $f_{p'_1,k_1,p',k}$ is the Compton effect amplitude. This relation makes it possible to express the desired form factor in terms of the phase of the Compton scattering, but we shall limit ourselves, for simplicity, to the solution of the problem for the case in which the amplitude $f_{p'_1,k_1,p',k}$ is computed by perturbation theory in the Born ap-

---

*Here we have used the relation:[3]

$$G^{-1}(-\hat{p}) - G^{-1}(\hat{p}') = -k_{\mu}\Gamma_{\mu}(-p, p'; k).$$

proximation:

$$f_{p_1', k_1, p', k} = -ie^2(2\pi)^4\delta(p_1' + k_1 + p' + k)(4\omega\omega_1)^{-1/2}$$

$$\times \bar{u}_-(p_1')\left[\hat{e}^{\lambda_1}\frac{-i(\hat{p}' + \hat{k}) + m}{(p' + k)^2 + m^2}\hat{e}^{\lambda}\right.$$

$$\left. + \hat{e}^{\lambda}\frac{-i(\hat{p}' - \hat{k}_1) + m}{(p' - k_1)^2 + m^2}\hat{e}^{\lambda_1}\right]u_-(p'). \tag{3.2}$$

Then, after a number of calculations, we obtain

$$F_l(p^2) - F_l^*(p^2) = \sum_{k=1}^{2} ig_{lk}(p^2)[F_k(p^2) + F_k^*(p^2)] + ig_{l0}(p^2)e;$$

$$g_{11}(p^2) = -\frac{e^2}{8\pi}\theta(-p^2 - m^2)\left[1 + \frac{m^2(p^4 - 4p^2m^2 - m^4)}{2p^4(p^2 + m^2)}\right.$$

$$\left. + \frac{m^2(p^2 + 3m^2)}{(p^2 + m^2)^2}\ln\frac{-p^2}{m^2}\right],$$

$$g_{12}(p^2) = -\frac{e^2}{8\pi}\theta(-p^2 - m^2)m^3\left[-\frac{3p^2 + m^2}{2p^4}\right.$$

$$\left. + \frac{1}{p^2 + m^2}\ln\frac{-p^2}{m^2}\right],$$

$$g_{10}(p^2) = -\frac{e^2}{8\pi}\theta(-p^2 - m^2)$$

$$\times\frac{2m^2}{p^2 + m^2}\left[\frac{-p^2 + m^2}{p^2} - \frac{2m^2}{p^2 + m^2}\ln\frac{-p^2}{m^2}\right],$$

$$g_{21}(p^2) = -\frac{e^2}{8\pi}\theta(-p^2 - m^2)$$

$$\times\frac{m^3}{p^2 + m^2}\left[\frac{3p^2 + m^2}{2p^4} - \frac{1}{p^2 + m^2}\ln\frac{-p^2}{m^2}\right],$$

$$g_{22}(p^2) = -\frac{e^2}{8\pi}\theta(-p^2 - m^2)$$

$$\times\left[1 + \frac{m^2(p^2 + m^2)}{2p^4} + \frac{m^2}{p^2 + m^2}\ln\frac{-p^2}{m^2}\right],$$

$$g_{20}(p^2) = -\frac{e^2}{8\pi}\theta(-p^2 - m^2)$$

$$\times\frac{m}{p^2 + m^2}\left[\frac{p^2 - m^2}{p^2} + \frac{2m^2}{p^2 + m^2}1\ \frac{-p^2}{m^2}\right]. \tag{3.3}$$

The g_{lk} for $l = 3, 4$ are certain functions (for brevity, we shall not write them out) having the following asymptotic values for $-p^2 \to \infty$:

$$g_{31}(p^2) \to \frac{e^2 m}{8\pi p^2}, \quad g_{32}(p^2) \to \frac{e^2}{8\pi}, \quad g_{30}(p^2) \to -\frac{e^2 m}{2\pi p^2}\ln\frac{-p^2}{m^2},$$

$$g_{41}(p^2) \to -\frac{3e^2m^4}{4\pi p^6}\ln\frac{-p^2}{m^2}, \qquad g_{42}(p^2) \to -\frac{e^2 m}{8\pi p^2},$$

$$g_{40}(p^2) \to -\frac{e^2}{4\pi p^2}.$$

We note that, since $g_{lk}(-m^2) = 0$, $l = 1, \ldots, 4$, we have $F_l(-m^2) - F_l^*(-m^2) = 0$ and, consequently, in contrast with the work of Faĭnberg,[1] no difficulties arise here connected with the infrared divergence.

The relations (3.3) represent the inhomogeneous Hilbert boundary problem for two unknown functions $F_1(p^2)$ and $F_2(p^2)$, which are analytic in the region described above. An exact solution of this problem meets with considerable difficulty and we shall therefore solve it by the iteration method. Assuming that $F_2(p^2)$ falls off at infinity not more slowly than a finite power of p^2, and neglecting the asymptotically small term $ig_{12}(F_2 + F_2^*)$ in (3.3), we get

$$F_1(p^2) - F_1^*(p^2) = ig_{11}(p^2)[F_1(p^2) + F_1^*(p^2)] + ig_{10}(p^2)e,$$

$$F_2(p^2) - F_2^*(p^2) = ig_{21}(p^2)[F_1(p^2) + F_1^*(p^2)]$$

$$+ ig_{22}(p^2)[F_2(p^2) + F_2^*(p^2)] + ig_{20}(p^2)e. \tag{3.3'}$$

The general solution of the Hilbert problem with the boundary condition (3.3′) has the following form:[5]

$$F_l(z) = \exp[\Gamma_l(z)]\left\{\mathscr{P}_l(z) - \frac{1}{2\pi}\int_{-\infty}^{-m^2}\frac{g_l(t)\,dt}{(t - z)\exp[\Gamma_l^+(t)]}\right\}, \tag{3.4}$$

where the notation

$$\Gamma_l(z) = -\frac{z + m^2}{\pi}\int_{-\infty}^{-m^2}\frac{\operatorname{arc\,tg} g_{ll}(t)\,dt}{(t + m^2)(t - z)}, \quad g_1 = \frac{eg_{10}}{1 + ig_{11}},$$

$$g_2 = \frac{g_{21}(F_1 + F_1^*) + g_{20}e}{1 + ig_{22}}$$

is used.

The solution (3.4) of the Hilbert problem was determined with accuracy up to an arbitrary polynomial $\mathscr{P}_l(z)$. Here as always in the dispersion approach, there is the problem of the boundary conditions that set off the solution uniquely. As such a condition, we require that the expansion of the imaginary part of the resultant solution in a series in the coupling constant coincide with the corresponding series of perturbation theory, which in this case does not contain any divergences. Furthermore, we get still another condition from (2.2), $F_1(-m^2) = e$.

The solution satisfying this boundary condition is

$$F_1(p^2) = e\exp[\Gamma_1^-(p^2)]\left\{1 - \frac{p^2 + m^2}{2\pi}\right.$$

$$\left.\times\int_{-\infty}^{-m^2}\frac{g_{10}(t)\,dt}{(t + m^2)[1 + ig_{11}(t)]\exp[\Gamma_1^+(t)](t - p^2 + i\varepsilon)}\right\},$$

$$F_2(p^2) = -\frac{\exp[\Gamma_2^-(p^2)]}{2\pi}$$

$$\times\int_{-\infty}^{-m^2}\frac{g_{21}(t)[F_1(t) + F_1^*(t)] + g_{20}(t)e}{[1 + ig_{22}(t)]\exp[\Gamma_2^+(t)](t - p^2 + i\varepsilon)}dt,$$

$$\Gamma_l^{\mp}(p^2) = \lim_{z \to p^2 \mp i\varepsilon}\Gamma_l(z). \tag{3.5}$$

As $-p^2 \to \infty$,

$$F_1(p^2) \to \text{const}\cdot\left(\frac{-p^2}{m^2}\right)^{e^2/8\pi^2}, \quad F_2(p^2) \to \frac{\text{const}}{m}\left(\frac{-p^2}{m^2}\right)^{-1}. \tag{3.6}$$

It is not difficult to note that further iteration does not change the asymptotic value of $F_1(p^2)$, and of $F_2(p^2)$ either. Thus, for $-p^2 \to \infty$, we get

$$F_\mu^{in,\,out}(p) \to \text{const}\cdot\gamma_\mu\left(\frac{-p^2}{m^2}\right)^{e^2/8\pi^2},$$

which differs significantly from the known result $-p = p'$, when $(i\hat{p} + m)G(\hat{p})\Gamma_\mu(p, p; 0) \xrightarrow[-p^2\to\infty]{} \text{const}\cdot\gamma_\mu$ (Ward's theorem).

The solution (3.5) found for the Hilbert problem is the asymptotic solution of the set of dispersion equations

$$F_1(p^2) = e + \frac{p^2+m^2}{2\pi i}\int_{-\infty}^{-m^2}\frac{F_1(t) - F_1^*(t)}{(t+m^2)(p^2-t-i\varepsilon)}dt,$$

$$F_2(p^2) = \frac{1}{2\pi i}\int_{-\infty}^{-m^2}\frac{F_2(t) - F_2^*(t)}{p^2-t-i\varepsilon}dt \tag{3.7}$$

with $F_l - F_l^*$ determined from (3.3).

4. THE ELECTRON PROPAGATION FUNCTION IN THE TWO-PARTICLE APPROXIMATION

The results we have obtained make it possible to compute the spectral functions ρ_1 and ρ_2 in the two-particle approximation in the following fashion:

$$\begin{aligned}\rho_1(p^2) = \frac{1}{16\pi^2}\Big\{&-\frac{p^2+m^2}{p^4}|F_1|^2 - m\frac{p^2+m^2}{p^4}(F_1F_2^* + F_1^*F_2)\\ &+\frac{p^4-m^4}{p^4}|F_2|^2 - \frac{m^2}{p^4}e(F_1+F_1^*)\\ &-\frac{m(p^2+m^2)}{2p^4}e(F_2+F_2^*) - \frac{m(3p^2-m^2)}{2p^4}ed_l(F_3+F_3^*)\\ &+\frac{p^4-m^4}{2p^4}ed_l(F_4+F_4^*) + \frac{e^2}{p^2+m^2}\Big[\frac{2m^2(m^2-p^2)}{p^4}\\ &+(1-d_l)\frac{3p^4-p^2m^2+2m^4}{2p^4}\Big]\Big\},\end{aligned}$$

$$\begin{aligned}\rho_2(p^2) = \frac{1}{16\pi^2}\Big\{&\frac{p^2+m^2}{p^2}(F_1F_2^* + F_1^*F_2) + 2m\frac{p^2+m^2}{p^2}|F_2|^2\\ &+\frac{m}{p^2}e(F_1+F_1^*) + \frac{p^2+m^2}{2p^2}e(F_2+F_2^*)\\ &+\frac{p^2-3m^2}{2p^2}ed_l(F_3+F_3^*) + m\frac{p^2+m^2}{p^2}ed_l(F_4+F_4^*)\\ &+\frac{me^2}{p^2+m^2}\Big[+\frac{4m^2}{p^2} + (1-d_l)\frac{2p^2-m^2}{p^2}\Big]\Big\}.\end{aligned} \tag{4.1}$$

It is natural that the functions $F_3(p^2)$ and $F_4(p^2)$, which are connected in elementary fashion with $F_1(p^2)$ and $F_2(p^2)$, drop out of the expressions for ρ_1 and ρ_2 in the case $d_l = 0$, since, in such a case, as is seen from (2.1) and (2.3), they do not enter into the current matrix element. In calibration with $d_l = 1$, in the e^2 approximation, the relations (4.1) coincide with the results of Gell-Mann and Low.[6]

It is seen from (4.1) that $\rho_1(p^2)$ and $\rho_2(p^2)$ have a simple pole at the point $p^2 = -m^2$, as was to be expected. This corresponds to the infrared divergence in $G(p)$, but it is not important for the asymptotic case of interest to us. Asymptotically, we have for $-p^2 \to \infty$:

$$\rho_1(p^2) \sim \left(\frac{-p^2}{m^2}\right)^{-1+e^2/4\pi^2}, \qquad \rho_2(p^2) \sim m\left(\frac{-p^2}{m^2}\right)^{-1+e^2/8\pi^2}, \tag{4.2}$$

whence we find that the renormalization constant

$$Z_2^{-1} = 1 + \int_{-\infty}^{-m^2}\rho_1(p^2)\,dp^2 \tag{4.3}$$

is infinite. Nevertheless, it is not possible to confirm that this result is preserved upon consideration of higher approximations, because it can be shown* that the exact spectral functions vanish more rapidly than in the two-particle approximation.

In the given approximation, we get from (2.2), (3.6), and (4.2),

$$G(\hat{p}) \sim \frac{\hat{p}}{p^2}\left(\frac{-p^2}{m^2}\right)^{e^2/4\pi^2}, \qquad \Gamma_\mu(p, p') \sim \gamma_\mu\left(\frac{-p^2}{m^2}\right)^{-e^2/8\pi^2}. \tag{4.4}$$

Thus, in the two-particle approximation, in spite of the infinity of the renormalization constant Z_2^{-1}, a false pole does not arise in $G(\hat{p})$, by virtue of the vanishing of $\Gamma_\mu(p, p')$ as $-p^2 \to \infty$.[7] However, complete investigation of this problem in the dispersion method, as also of a number of other similar problems, requires consideration of higher approximations, which entail great difficulties.

In conclusion, the authors wish to express their sincere thanks to V. Ya. Faĭnberg for his constant attention to the research and for numerous discussions.

---

[1] V. Ya. Faĭnberg, JETP **37**, 1361 (1959), Soviet Phys. JETP **10**, 968 (1960).

[2] Malakhov, Rashevskaya, and Faĭnberg, JETP (in press).

[3] E. S. Fradkin, JETP **29**, 258 (1955), Soviet Phys. JETP **2**, 361 (1956).

[4] Lehmann, Symanzik, and Zimmermann, Nuovo cimento **1**, 205 (1955).

[5] N. I. Muskhelishvili, Сингулярные интегральные уравнения (Singular Integral Equations) (OGIZ, 1946).

[6] M. Gell-Mann and F. Low, Phys. Rev. **95**, 1300 (1954).

[7] Lehmann, Symanzik, and Zimmermann, Nuovo cimento **2**, 425 (1955).

Translated by R. T. Beyer
348

---

*The complete set of states in quantum electrodynamics includes states with a negative norm. Furthermore, it must be remembered that the result (4.2) coincides with the Born approximation for $f_{p_1', k_1, p', k}$.

SOVIET PHYSICS JETP VOLUME 11, NUMBER 6 DECEMBER, 1960

POSSIBILITY OF APPLICATION OF THE (n, 2n) REACTION IN NUCLEAR SPECTROSCOPY

V. V. KOMAROV, A. B. KUREPIN, and A. M. POPOVA

Institute of Nuclear Physics, Moscow State University

Submitted to JETP editor January 11, 1960

J. Exptl. Theoret. Phys. (U.S.S.R.) **38**, 1824-1828 (June, 1960)

The (n, 2n) reaction is treated as a stripping reaction. The angular distribution of the center of mass of two neutrons simultaneously emitted as a result of direct interaction is computed. It is found that it is important to take into account the interaction between the emitted neutrons in the final state. As an example, the angular distributions are calculated for the reactions $Be^9(n, 2n)Be^8$ and $Pb^{208}(n, 2n)Pb^{207}$ corresponding to the 2.9- and 1.63-Mev levels of the final nuclei. It is shown that it should be possible to elucidate the mechanism of the (n, 2n) reaction and determine the characteristics of the nuclear energy levels by investigating the angular dependences in the spectra of neutrons emitted from targets irradiated with neutrons.

1. INTRODUCTION

EVER since Butler[1] showed the possibility of using reactions of the stripping and pick-up type to obtain data on the spectroscopy of the nucleus, there have appeared a large number of papers containing valuable data on the characteristics of nuclear states. The angular distributions of these types of reactions differ in their sharply pronounced structure, which allows one to obtain information on the relation between the spins and parities of the initial and final states of the nuclei that take part in the reaction. Data which are identical from the viewpoint of different formalisms have been obtained for the angular distributions of the products of these reactions.[2] Thus, the stripping and pick-up reactions have occupied an important place in the methods of nuclear spectroscopy.

At the same time, it has been shown that the Coulomb scattering of the products of these reactions lead to appreciable disparities with the results based on theories that do not take into account the effect of the charge of the particles. The Coulomb scattering of the deuteron and proton waves in the (p, d) and (d, p) reactions lead, in the case of light and medium nuclei, to a shift of the angular distribution maximum towards the larger angles, to a broadening and lowering of these maxima, and, in the case of heavy nuclei, to a complete distortion of the shape of Butler's angular distributions. These effects are especially strong at comparatively low incident particle energies.

In the present work, the (n, 2n) reactions are considered as reactions of the pick-up type. It has been shown previously that the energy distribution of the products of reactions in which several particles are emitted, among which are two neutrons, has a narrow peak, which is caused by the interaction of these neutrons in the final singlet state.[3-5] If the strong interaction of neutrons of small relative energy is taken into account, one can speak of the possibility of a pick-up mechanism, i.e., the simultaneous emission, almost in the same direction, of the two interacting neutrons as a result of a direct interaction between the incident neutron and the nucleus. An analogy with the (n, d) and (p, d) reactions occurs in the case of the (n, 2n) reaction, also because the direct interaction in reactions in which two nucleons are emitted is essentially of a surface character.[6]

It is possible that in the distribution of the total momentum of the two emitted neutrons there appear peaks corresponding to the energy levels of the nucleus A − 1 in the reaction A (n, 2n) A − 1. As shown later on, for specific examples, the dependence of the area of these peaks on the direction of motion of the center of mass of the two neutrons has the same character both in the stripping and in the pick-up reactions (see also reference 7).

Thus, taking the (n, 2n) reactions, instead of the (n, d) and (p, d) reactions, one may expect to obtain the characteristics of the energy levels of medium and heavy nuclei from the shape of the angular distributions, since the Coulomb effects in the ordinary pick-up reactions have a large value for such nuclei. Neudachin drew the attention of the authors to this fact.

2. CALCULATION OF THE ANGULAR DISTRIBUTIONS

The effective differential cross section of the (n, 2n) reaction, under the assumption of the simultaneous emission of both neutrons with relative energies in the interval between E_{nn} and $E_{nn} + dE_{nn}$ as the result of the direct interaction calculated in the Born approximation, has the same form as in ordinary stripping theory:[8]

$$\frac{d\sigma}{dE_{nn}d\Omega_1 d\Omega_2} = \frac{\mu_{n0}M_n\mu_{2n}}{16\pi^2\hbar^2\mu_n^2}\frac{k_{2n}k_{nn}}{k_{n0}}[B(Q)]^2$$
$$\times V_0^2 A^2\left(|E_b| + \frac{\hbar^2}{2\mu_n}z^2\right)^{-2} z^{-2}[j'(za) - g_l(\varkappa a)\,j(za)]^2\,\frac{3\theta^2}{a}, \tag{1}$$

where

$$\mu_{n0} = M_n M_i/(M_i + M_n), \qquad \mu_n = M_n M_f/(M_f + M_n),$$

$$\mu_{2n} = 2M_n M_f/(M_f + 2M_n), \qquad \frac{\hbar^2 k_{nn}^2}{M_n} = E - \frac{\hbar^2 k_{2n}^2}{2\mu_{2n}},$$

$$\mathbf{z} = \mathbf{k}_{2n} - \left(\frac{M_f}{M_f + M_n}\right)\mathbf{k}_{n0}, \qquad \mathbf{Q} = \frac{\mathbf{k}_{2n}}{2} - \mathbf{k}_{n0};$$

M_i and M_f are the masses of the initial and final nuclei; $\mathbf{k}_{n0}$, $\mathbf{k}_{2n}$, and $\mathbf{k}_{nn}$ are the wave vectors of the incident neutron, of the center of mass of the two emitted neutrons, and of their relative motion; E and E_b are the energy in the c.m. system after collision and the binding energy of a neutron in the initial nucleus; $d\Omega_1$ and $d\Omega_2$ are elements of the solid angle for the vectors $\mathbf{k}_{2n}$ and $\mathbf{k}_{nn}$; θ^2 is a dimensionless normalized width; l is the orbital angular momentum of the picked-up neutron; a is the radius of interaction;

$$g_l(\varkappa a) = \frac{1}{rh_l^{(1)}(i\varkappa r)}\frac{d}{dr}\left(rh_l^{(1)}(i\varkappa r)\right)\Big|_{r=a}$$

is the logarithmic derivative at the boundary of the nucleus expressed in terms of spherical Hankel functions of the first kind; $\varkappa = 2\mu_n|E_b|)^{1/2}/\hbar$; the function $j_l(za)$ is the same as in reference 9. The interaction in the final state of the two neutrons emitted as a result of the reaction is included in the matrix element in the integral

$$\int V_{nn}e^{i\mathbf{Q}\boldsymbol{\rho}}\varphi_{2n}(\boldsymbol{\rho})\,d\boldsymbol{\rho}.$$

Here ρ is the vector between the neutrons and the final state, V_{nn} is the interaction potential of the neutrons in the final state expressed in the form of a potential well of depth V_0 and radius $\rho_0 = 2.65$ fermi. The radial part of the wave function of the two neutrons has the form[7]

$$\varphi_{2n}^{(1)} = A\sin k\rho/\rho \qquad (\rho < \rho_0),$$
$$\varphi_{2n}^{(2)} = \frac{i\sqrt{\pi}}{k_{nn}\rho}\left[e^{-ik_{nn}\rho} - e^{ik_{nn}\rho}\right] + \frac{\sqrt{\pi}}{\alpha_s - ik_{nn}}\frac{e^{ik_{nn}\rho}}{\rho} \quad (\rho > \rho_0). \tag{2}$$

The coefficient A and the modulus of the wave vector k are found by matching the logarithmic derivatives of the functions $\varphi_{2n}^{(1)}$ and $\varphi_{2n}^{(2)}$ at $\rho = \rho_0$. These values depend only on the choice of the form of the interaction between the neutrons, the scattering length, and the magnitude of the relative energy of the two neutrons; α_s is the generalized scattering length;

$$1/\alpha_s = 1/\alpha_{s0} - k_{nn}^2\rho_0/2, \qquad \alpha_{s0} = \sqrt{\mu_n\varepsilon}/\hbar;$$

$\epsilon = 70$ kev is the interaction energy of the neutrons.

In formula (1) the integral given above takes the form

$$B = \int_0^{\rho_0}\frac{\sin Q\rho}{Q}\sin k\rho\,d\rho.$$

The energy distribution described by expression (1) has a narrow maximum caused by the interaction of the two neutrons in the final singlet state in the region $E_{nn} = 0$ to 160 kev. The magnitude of k weakly depends on the relative energy of the two neutrons and is equal to 11.04×10^{12} cm^{-1}.

We list the values of A^2 for different values of relative energy of the two neutrons E_{nn}:

E_{nn}, Mev	0.02	0.04	0.06	0.08	0.10	0.12	0.14	0.16
$A^2 \times 10^{22}$, cm²	298	237	159	139	114	97	84	60

The angular distribution relative to the motion of the center of mass of the two interacting neutrons for the angle ϑ in the c.m. system of the two neutrons and the final nucleus is obtained by integrating the energy distribution over the narrow region E_{nn} from 0 to 160 kev for each ϑ. By comparing the absolute values of the cross sections for transition to different levels of the final nucleus, we can determine the relative values of the normalized widths.

3. REACTION $Be^9(n, 2n)Be^8$. EXAMPLE OF CALCULATION

As an example of the use of this method of calculation, the angular distributions have been plotted for the center of mass of the two emitted neutrons from the (n, 2n) reaction on Be^9, at an incident neutron energy of 14 Mev, for the 2.9-Mev excited state of the Be^8 nucleus.

In Fig. 1a are shown the angular distributions for an orbital angular momentum of the picked-up

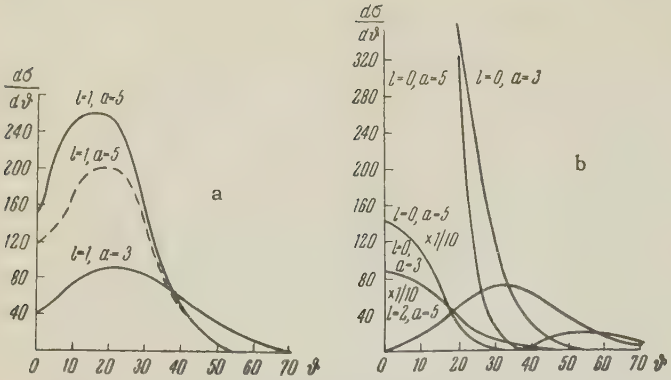

FIG. 1. Angular distribution of the center of mass of two interacting neutrons from the reaction $Be^9(n, 2n)Be^8$ for the 2.9 Be^8 level at an incident neutron energy of 14 Mev. a) $l = 1$, dotted curve was calculated according to Butler's theory; b) $l = 0$ and 2.

neutron equal to unity. This case agrees with experiment, since the neutron is probably picked up from the p shell of Be^9. It is seen from the figure that the angular distributions have a marked dependence on the radius of interaction a. Since the final state of the two neutrons is unbound, the maximum of the angular distribution is somewhat different from the maximum on Butler's curve (dotted curve in Fig. 1a) for the emission of a bound state (dineutron). The angular distributions for $l = 0$ and $l = 2$ (curve in Fig. 1b) are considerably different from those shown in Fig. 1a. Comparison of the curves of Figs. 1a and 1b shows that the angular momentum of the picked-up neutron can be determined from the experimental angular distributions by comparison with their calculated angular distributions, just as is done when the usual Butler curves are used.

4. REACTION $Pb^{208}(n, 2n)Pb^{207}$. EXAMPLE OF CALCULATION

The interaction of two neutrons in the final state distorts somewhat the shape of the usual Butler curve (Fig. 1a), especially at large angles. Therefore the angular dependence for the reaction $Pb^{208}(n, 2n)Pb^{207}$, with an excitation energy of 1.63 Mev for the Pb^{207}, was calculated with only those terms of our formula similar to Butler's formula taken into account. The radius of interaction was obtained from the formula $1.4 \times 10^{-13} A^{1/3}$ cm. In this case the orbital angular momentum $l = 6$ is uniquely determined, since the levels of Pb^{208} and Pb^{207} have been studied in detail, and their spins are equal to 0^+ and $13/2^+$. The levels neighboring on the investigated level of Pb^{207}, namely, 0.89 and 2.34 Mev, are sufficiently far apart, and the angular distribution for them is determined by orbital angular momenta of different parity. The calculated curve is shown in Fig. 2.

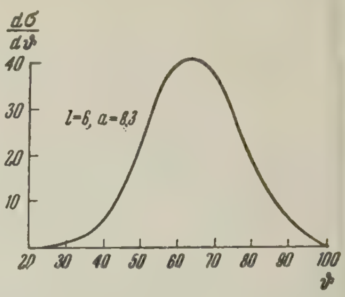

FIG. 2. Angular distribution of the center of mass of two interacting neutrons from the reaction $Pb^{208}(n, 2n)Pb^{207}$ for the 1.63-Mev level at an incident neutron energy of 14 Mev (in arbitrary units).

The maximum of the distribution lies at an angle large enough for experimental measurements to be conveniently carried out. The value of the effective cross section at the maximum is approximately one order lower than the value of the cross section at the maximum of the angular distribution for $l = 1$.

5. POSSIBILITY OF EXPERIMENTAL VERIFICATION AND CONCLUSIONS

Special investigations to reveal the marked peculiarities in the angular distributions of neutrons from the (n, 2n) reaction were not carried out. It is almost impossible to obtain directly by experiment the distributions of the total momentum vector of the two neutrons, except for individual cases, for example, the reaction $Be^9(n, 2n)Be^8$. However, the energy distributions of the emitted neutrons can be investigated.

The peak of these distributions, which is due to the interaction of the two neutrons at small relative energies, should occur when E_n is equal to half the maximum energy of a neutron from the (n, 2n) reaction for an infinitely heavy nucleus, and, when the energy is $M_f/2M_i$ times the maximum for a finite nucleus. It should be mentioned that there is a possibility of erroneously determining the energy states of the nuclei from the peaks in the energy distributions of inelastically scattered neutrons, since these peaks may be caused by the (n, 2n) process with simultaneous emission of two neutrons in the same direction, and not by the (n, n′) process.

The spectra of inelastically scattered neutrons, taken at different angles with respect to the direction of the incident neutrons, contain neutrons produced as a result of the investigated process in the (n, 2n) reaction, statistical processes in the (n, 2n) reaction, the cascade process in the (n, 2n) reaction, the (n, n′) process, and, finally, the accompanying reactions, for example, (n, pn). It is possible that the great majority of neutrons in the spectra owe their origin to the enumerated competitive mechanisms. Independently of this, one can determine the effect of the simultaneous emission of two neutrons in the same direction, since in this case the neutrons will be concentrated in a narrow region (of the order of hundreds of kev) of the spectrum corresponding to a definite state of the final nucleus.

The experimental problem consists of investigating the angular dependence for the narrow energy region of the neutron spectrum corresponding to the investigated state of the nucleus $A-1$ for the reaction $A(n, 2n)A-1$. In this case, one may expect a typical angular dependence similar to that shown in the figures, which allows one to determine the characteristics of the investigated levels or groups of neighboring levels, if the experimental method employed does not have the required resolving power.

The investigation of the spectra of inelastically scattered neutrons was not sufficiently complete to find any experimental confirmation of the above discussion. Rosen and Stewart[10] have shown that the probability of direct interactions in the (n, 2n) reaction on some medium and heavy nuclei at an incident neutron energy of 14 Mev was 10 — 15%. The angular distributions of the emitted neutrons in the energy interval 4 — 12 Mev, as shown in that work, resemble the angular distributions in the (n, d) and (p, d) reactions. In the work of O'Neill[11] the spectrum of neutrons inelastically scattered on lead was measured for an incident neutron energy of 14.8 Mev. The maximum obtained at an energy of $E_n = 2$ Mev may be due to the interaction of neutrons from the (n, 2n) reaction.

The experimental difficulties of the problem we are treating are offset by the possibility of elucidating the mechanism of the (n, 2n) reaction and determining the characteristics of the states of medium and heavy nuclei, and also of determining more accurately the states of the light nuclei. Of special interest is the determination of the characteristics of active nuclei which cannot be investigated by other methods, and also the investigation of secondary excited levels of even-even nuclei in order to consider the question of the splitting of these levels into a number of states with different angular momenta.

The authors thank S. S. Vasil'ev for discussion of this work.

---

[1] S. T. Butler, Proc. Roy. Soc. (London) **A208**, 559 (1951).

[2] A. G. Sitenko, Usp. Fiz. Nauk **67**, 377 (1959), Soviet Phys.-Uspekhi **2**, 195 (1959).

[3] A. B. Migdal, JETP **28**, 3 (1955), Soviet Phys. JETP **1**, 2 (1955).

[4] V. V. Komarov and A. M. Popova, JETP **38**, 253 (1960), Soviet Phys. JETP **11**, 184 (1960).

[5] V. V. Komarov and A. M. Popova, JETP **38**, 1559 (1960), Soviet Phys. JETP **11**, 1123 (1960).

[6] McCarthy, Jezak, and Kromminga, Nuclear Phys. **12**, 274 (1959).

[7] V. V. Komarov and A. M. Popova, JETP **36**, 1574 (1959), Soviet Phys. JETP **9**, 1118 (1959).

[8] E. Gerjuoy, Phys. Rev. **91**, 645 (1953).

[9] A. B. Kurepin and V. G. Neudachin, JETP **36**, 1725 (1959), Soviet Phys. JETP **9**, 1229 (1959).

[10] L. Rosen and L. Stewart, Phys. Rev. **107**, 824 (1957).

[11] G. K. O'Neill, Phys. Rev. **95**, 1235 (1954).

Translated by E. Marquit
349

SOVIET PHYSICS JETP VOLUME 11, NUMBER 6 DECEMBER, 196

USE OF THE METHODS OF QUANTUM FIELD THEORY FOR THE INVESTIGATION OF THE THERMODYNAMICAL PROPERTIES OF A GAS OF ELECTRONS AND PHOTONS

I. A. AKHIEZER and S. V. PELETMINSKIĬ

Physico-Technical Institute, Academy of Sciences, Ukrainian S.S.R.

Submitted to JETP editor January 12, 1960

J. Exptl. Theoret. Phys. (U.S.S.R.) **38**, 1829-1839 (June, 1960)

The thermodynamic potential of a gas of electrons, positrons, and photons is determined by the methods of field theory, taking account of the interaction between these particles with an accuracy up to terms proportional to $e^4 \ln e^2$. Divergences which appear in the high momentum region of the virtual particles are removed by renormalizing the charge and mass of the electron and redefinition of the vacuum level. General expressions including relativistic effects are derived, and asymptotic formulas for the exchange and correlation energies are obtained. Corrections to the black body radiation energy due to the interaction between the photons and electron-positron pairs are obtained.

1. It is shown in a number of recent papers that the methods of quantum field theory can be used for the investigation of the thermodynamic properties of various systems of mutually interacting particles. The idea of using these methods goes back to Matsubara,[1] who proposed a thermodynamic perturbation theory which is the analog of the perturbation theory of field theory. In the later work of Abrikosov, Gor'kov, and Dzyaloshinskiĭ[2] and of Fradkin[3,4] a considerable simplification was achieved by going over to momentum space and using Green's function methods. It then became possible to set up rules similar to the Feynman rules in quantum electrodynamics for the solution of problems in quantum statistics. Fradkin[3,4] extended the method of Matsubara to relativistic systems and undertook the renormalization of the thermodynamic Green's functions. However, the divergences appearing in the calculation of the thermodynamic potential are not discussed in this work, and the thermodynamic potential including the relativistic effects is not computed explicitly.*

In the present paper we determine the thermodynamic potential of a system of electrons, positrons, and photons with account of the interaction between these particles with an accuracy up to terms proportional to $e^4 \ln e^2$, where e is the charge of the electron.

We shall first consider the idealized problem of the thermodynamic potential of a gas of electrons and photons in the presence of a uniform background of positive charge which compensates for the electron charge and makes possible the existence of thermodynamic equilibrium states of the system; later we shall investigate the role of the ions which are present in real physical systems in the region of moderately low temperatures, and we shall also discuss the problem of the energy of black body radiation with account of the interaction between the photons and electron-positron pairs.

2. We give first the fundamental relations of the thermodynamic perturbation theory, which is based on the methods of quantum field theory.[2,3]

If the system is characterized by the Hamiltonian $\hat{H} = \hat{H}_0 + \hat{H}_1$, where $\hat{H}_0$ is the free field Hamiltonian and $\hat{H}_1$ describes the interaction between the elementary excitations (the operators are defined in the Schrödinger representation), the equilibrium density matrix is given by the expression

$$\rho(\beta) = \exp\{-\beta(\hat{H} - \mu\hat{N})\},$$

where β is the inverse temperature, μ is the chemical potential, and $\hat{N}$ is the operator of the number of particles. In the case of a system consisting of electrons and photons, which we shall consider later on, $\hat{N}$ is to be regarded as the difference of the number of electrons, $\hat{N}^-$, and positrons, $\hat{N}^+$.

The thermodynamic potential Ω is connected with ρ by the relation

$$\Omega = -\beta^{-1} \ln \operatorname{Sp} \rho(\beta).$$

---

*The thermodynamic potential of a nonrelativistic Boltzmann gas including only the Coulomb interaction between the particles was found by Vedenov and Larkin[5]

Assuming

$$\rho(\beta) = \rho_0(\beta) S(\beta),$$

where $\rho_0(\beta) = \exp\{-\beta(\hat{H}_0 - \mu\hat{N})\}$ is the density matrix of the free system, we obtain for $S(x_4)$ the equation

$$dS(x_4)/dx_4 = -H_1(x_4) S(x_4), \quad S(0) = 1,$$

where $H_1(x_4) = \rho_0^{-1}(x_4)\hat{H}_1\rho_0(x_4)$. This operator may be called the interaction Hamiltonian in the "interaction representation." In general, an operator F in the "interaction representation" is defined by

$$F(x_4) = \rho_0^{-1}(x_4)\hat{F}\rho_0(x_4),$$

where $\hat{F}$ is the corresponding operator in the Schrödinger representation. The solution of the equation for $S(x_4)$ obviously has the form

$$S(x_4) = T\exp\left\{-\int_0^{x_4} H_1(x_4')\,dx_4'\right\},$$

where T designates the chronological operator acting on the variable x_4.

In the case of a system of electrons and photons the interaction Hamiltonian has the form

$$H_1(x_4) = -\int j_\nu(x) A_\nu(x)\,dx,$$

where $j_\nu(x)$ is the operator of the electron-positron current density, which is proportional to the unrenormalized charge of the electron e_0, and $A_\nu(x)$ is the electromagnetic field operator. It is easily seen that

$$\frac{d\Omega}{de_0} = -\frac{V}{e_0}\frac{\langle T\{j_\nu(x) A_\nu(x) S(\beta)\}\rangle}{\langle S(\beta)\rangle},$$

where $\langle f\rangle = \mathrm{Sp}\,\rho_0(\beta) f$ and V is the volume of the system.

Let us introduce the thermodynamic Green's functions for the electrons and photons:

$$\overline{G}^e(x, x') = \langle T\{\psi(x)\overline{\psi}(x') S(\beta)\}\rangle / \langle S(\beta)\rangle,$$
$$\overline{G}^\gamma_{\lambda\nu}(x, x') = \langle T\{A_\lambda(x) A_\nu(x') S(\beta)\}\rangle / \langle S(\beta)\rangle,$$

where ψ and $\overline{\psi}$ are the operators of the electron-positron field. The thermodynamic Green's function for the electron satisfies the equation*

$$\left(\gamma_\nu\frac{\partial}{\partial x_\nu} - \gamma_4\mu + m_0\right)\overline{G}^e(x, x') - \int\overline{\Sigma}(x, x'')\overline{G}^e(x'', x')\,dx'' = \delta(x - x'),$$

where the mass operator $\overline{\Sigma}$ is defined by the relation

$$\int\overline{\Sigma}(x, x'')\overline{G}^e(x'', x')\,dx'' = ie_0\frac{\langle T\{A_\nu(x)\gamma_\nu\psi(x)\overline{\psi}(x') S(\beta)\}\rangle}{\langle S(\beta)\rangle}.$$

It follows immediately from this formula that

$$\frac{d\Omega}{de_0} = -\frac{V}{e_0}\int \mathrm{Sp}\,\overline{\Sigma}(x, x')\overline{G}^e(x', x)\,dx'$$

or, in momentum space,

$$\frac{d\Omega}{de_0} = -\frac{V}{e_0\beta(2\pi)^3}\mathrm{Sp}\sum_{p_4}\int d\mathbf{p}\,\overline{\Sigma}(p)\overline{G}^e(p),$$

where $p \equiv (\mathbf{p}, p_4)$, $p_4 = (2n+1)\pi/\beta + i\mu$, and the summation goes over all integer n.

In a similar fashion it can be shown that

$$\frac{d\Omega}{de_0} = -\frac{V}{e_0\beta(2\pi)^3}\sum_{k_4}\int d\mathbf{k}\,\overline{\Pi}_{\lambda\nu}(k)\overline{G}^\gamma_{\nu\lambda}(k). \tag{1}$$

where $k \equiv (\mathbf{k}, k_4)$, $k_4 = 2\pi n/\beta$; $G^\gamma(k)$ is thermodynamic Green's function for the photon, which satisfies Dyson's equation

$$\overline{G}^\gamma(k) = \overline{D}(k) + \overline{D}(k)\overline{\Pi}(k)\overline{G}^\gamma(k), \quad \overline{D}(k) = 1/k^2 \tag{2}$$

and $\overline{\Pi}(k)$ is the polarization operator. In first approximation the polarization operator is given by the expression

$$\overline{\Pi}^{(2)}_{\lambda\nu}(k) = \frac{e_0^2}{\beta(2\pi)^3}\sum_{p_4}\int d\mathbf{p}\,\mathrm{Sp}\,\gamma_\lambda\overline{S}(p)\gamma_\nu\overline{S}(p-k), \tag{3}$$

where $\overline{S}(p) = (i\gamma_\nu p_\nu + m_0)^{-1}$ is the thermodynamic Green's function for the electron in zeroth approximation and m_0 is the unrenormalized mass of the electron.

It follows from (2) that $\overline{\Pi}\overline{G}^\gamma = k^{-2}\overline{\Pi}(1 - k^{-2}\overline{\Pi})^{-1}$. This expression cannot be expanded in powers of $k^{-2}\overline{\Pi}$, since the integration over $\mathbf{k}$ in formula (1) leads to an infrared divergence. The quantity $\overline{\Pi}\overline{G}^\gamma$ in formula (1) must therefore, in first approximation in e_0^2, be understood as representing the expression $k^{-2}\overline{\Pi}^{(2)}(1 - k^{-2}\overline{\Pi}^{(2)})^{-1}$. The family of diagrams represented in the figure corresponds to a formal expansion of this expression in powers of e_0^2. This family is generated from the first diagram by inserting various numbers of simple electron loops. Together with the term proportional to e_0^2 this infinite family of diagrams leads to a quantity of higher order than e_0^2, but smaller than e_0^4, on account of the infrared divergence. The omitted higher order diagrams give a contribution which does not exceed the order e_0^4. Replacing $\overline{\Pi}\overline{G}^\gamma$ by the quantity $k^{-2}\overline{\Pi}^{(2)}(1 - k^{-2}\overline{\Pi}^{(2)})^{-1}$

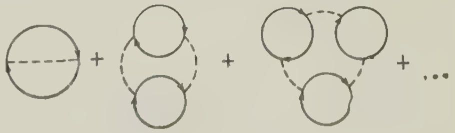

---

*Here and in the following we set $\hbar = c = 1$.

we therefore account for terms proportional to e_0^2 and terms of the form $e_0^4 f(e_0^2)$, where $f(0) = \infty$.

Integrating (1) over e_0, we obtain

$$\Omega = \Omega_0 + \Delta\Omega, \tag{4}$$

where Ω_0 is the value of Ω for $e_0 = 0$, and the quantity $\Delta\Omega$ is in this approximation given by

$$\Delta\Omega = -\frac{V}{\beta(2\pi)^3}\sum_{k_4}\int d\mathbf{k}\int_0^{e_0}\frac{de_0}{e_0}\frac{1}{k^2}\overline{\Pi}^{(2)}_{\lambda\nu}(k)\left[\left(1-\frac{1}{k^2}\overline{\Pi}^{(2)}(k)\right)^{-1}\right]_{\nu\lambda}$$

$$= \frac{V}{2\beta(2\pi)^3}\sum_{k_4}\int d\mathbf{k}\ln\det\left[\delta_{\lambda\nu}-\frac{1}{k^2}\overline{\Pi}^{(2)}_{\lambda\nu}(k)\right]. \tag{5}$$

The superscript (2) in $\overline{\Pi}^{(2)}_{\lambda\nu}$ will be omitted from now on.

3. The polarization operator $\overline{\Pi}_{\lambda\nu}(k)$ must satisfy the condition of gauge invariance:

$$\overline{\Pi}_{\lambda\nu}(k)k_\nu = 0.$$

However, the quantity $\overline{\Pi}_{\lambda\nu}$ calculated according to formula (3) does not satisfy this requirement. To make the operator $\overline{\Pi}_{\lambda\nu}$ gauge invariant we introduce the polarization operator $\overline{\Pi}_{\lambda\nu}(\mathbf{k}, ik_0)$ of quantum electrodynamics, which can be obtained from $\overline{\Pi}_{\lambda\nu}(\mathbf{k}, k_4)$ by setting $\mu = \beta^{-1} = 0$ and changing k_4 to ik_0 (k_0 is real).

Writing $\overline{\Pi}_{\lambda\nu}$ in the form

$$\overline{\Pi}_{\lambda\nu}(\mathbf{k}, k_4) = \{\overline{\Pi}_{\lambda\nu}(\mathbf{k}, k_4) - \Pi_{\lambda\nu}(\mathbf{k}, k_4)\} + \Pi_{\lambda\nu}(\mathbf{k}, k_4),$$

we see easily that the first term $\{\overline{\Pi}_{\lambda\nu} - \Pi_{\lambda\nu}\}$ does not contain any divergences and satisfies the requirement of gauge invariance; replacing the second term $\Pi_{\lambda\nu}(\mathbf{k}, k_4)$ by the gauge invariant expression

$$\Pi_{\lambda\nu}(\mathbf{k}, k_4) - \tfrac{1}{4}\delta_{\lambda\nu}\Pi_{\sigma\sigma}(\mathbf{k}, i|\mathbf{k}|),$$

we then obtain a gauge invariant expression for $\overline{\Pi}_{\lambda\nu}$.

As is known, the gauge invariant polarization operator $\Pi_{\lambda\nu}(k)$ of quantum electrodynamics has the form

$$\Pi_{\lambda\nu}(k) = (k_\lambda k_\nu - \delta_{\lambda\nu}k^2)C(k^2) \quad (\lambda, \nu = 1, 2, 3, 4),$$

where $C(k^2) \equiv C_0 + C_R(k^2)$ is a certain function of k^2 which is related to $\Pi_{\lambda\nu}$: $C(k^2) = \frac{1}{3}k^{-2} \times \Pi_{\nu\nu}(k^2)$; C_0 is a logarithmically divergent constant, and $C_R(k^2)$ the regularized value of $C(k^2)$. The gauge invarient expression for $\overline{\Pi}_{\lambda\nu}$ therefore has the form

$$\overline{\Pi}_{\lambda\nu}(\mathbf{k}, k_4) - \tfrac{1}{4}\delta_{\lambda\nu}\Pi_{\sigma\sigma}(\mathbf{k}, i|\mathbf{k}|) = \{\overline{\Pi}_{\lambda\nu}(\mathbf{k}, k_4) - \Pi_{\lambda\nu}(\mathbf{k}, k_4)\}$$

$$+ (k_\lambda k_\nu - \delta_{\lambda\nu}k^2)C(k^2), \tag{6}$$

In the following $\overline{\Pi}_{\lambda\nu}(\mathbf{k}, k_4)$ will be understood to stand for this gauge invariant expression.

The polarization operator $\overline{\Pi}_{\lambda\nu}(k)$ must be invariant under spatial rotations of the vector $\mathbf{k}$. $\overline{\Pi}_{\lambda\nu}(k)$ can therefore be written in the form

$$-\frac{1}{k^2}\overline{\Pi}_{ij}(k) = \left(\delta_{ij}-\frac{1}{\mathbf{k}^2}k_ik_j\right)A(\mathbf{k}^2, k_4)$$

$$+\delta_{ij}\frac{k_4^2}{\mathbf{k}^2}B(\mathbf{k}^2, k_4) \quad (i, j = 1, 2, 3),$$

$$-\frac{1}{k^2}\overline{\Pi}_{4i}(k) = -\frac{1}{k^2}\overline{\Pi}_{i4}(k) = -\frac{1}{\mathbf{k}^2}k_ik_4B(\mathbf{k}^2, k_4),$$

$$-\frac{1}{k^2}\overline{\Pi}_{44}(k) = B(\mathbf{k}^2, k_4),$$

where A and B are certain functions of $\mathbf{k}^2$ and k_4 related to $\overline{\Pi}_{\lambda\nu}$:

$$B = -\frac{1}{k^2}\overline{\Pi}_{44}, \quad A + \frac{k_4^2}{\mathbf{k}^2}B = -\frac{1}{2k^2}\overline{\Pi}_{\nu\nu} + \frac{1}{2\mathbf{k}^2}\overline{\Pi}_{44}.$$

It is easy to see that

$$\det\left(\delta_{\lambda\nu}-\frac{1}{k^2}\overline{\Pi}_{\lambda\nu}\right) = \left(1+\frac{k^2}{\mathbf{k}^2}B\right)\left(1+A+\frac{k_4^2}{\mathbf{k}^2}B\right)^2$$

$$= \left(1 + C - \frac{\overline{\Pi}_{44}-\Pi_{44}}{\mathbf{k}^2}\right)$$

$$\times\left(1 + C - \frac{\overline{\Pi}_{\nu\nu}-\Pi_{\nu\nu}}{2k^2} + \frac{\overline{\Pi}_{44}-\Pi_{44}}{2\mathbf{k}^2}\right)^2.$$

Formula (5) then takes the form

$$\Delta\Omega = \frac{V}{2\beta(2\pi)^3}\sum_{k_4}\int d\mathbf{k}\left\{\ln\left[1-\frac{\overline{\Pi}_{44}(k)-\Pi_{44}(k)}{[1+C(k)]\mathbf{k}^2}\right]\right.$$

$$\left.+2\ln\left[1-\frac{\overline{\Pi}_{\nu\nu}(k)-\Pi_{\nu\nu}(k)}{[1+C(k)]2k^2}+\frac{\overline{\Pi}_{44}(k)-\Pi_{44}(k)}{[1+C(k)]2\mathbf{k}^2}\right]\right\}$$

$$+\frac{3V}{2\beta(2\pi)^3}\sum_{k_4}\int d\mathbf{k}\ln[1+C(k)]. \tag{7}$$

4. The charge and the mass of the electron in the expression for the thermodynamic potential $\Omega = \Omega_0 + \Delta\Omega$ must be renormalized. As is known, the physical charge of the electron, e, is connected with the "bare" electron charge, e_0, by the relation $e^2 = e_0^2(1 + C_0)^{-1}$, whereas the physical mass, m, of the electron is related to "bare" electron mass, m_0, by $m = m_0 + \delta m$, where δm is the electromagnetic mass of the electron. For the renormalization of the mass and charge of the electron in $\Delta\Omega$ in our approximation it is clearly sufficient to neglect the quantity $C(k)$ in the first two terms of (7) in comparison with unity, and to make the expansion $3\ln[1 + C(k)] \approx 3C(k) = -k^{-2}\Pi_{\nu\nu}(k)$ in the last term, replacing everywhere e_0 by e and m_0 by m. As a result we obtain the following expression for Ω:

$$\Omega = \Omega_0 + \Delta\Omega_s + \Delta\Omega_c, \tag{8}$$

$$\Delta\Omega_s = -\frac{V}{2\beta(2\pi)^3}\sum_{k_4}\int d\mathbf{k}\frac{1}{k^2}\overline{\Pi}_{\nu\nu}(k), \tag{9}$$

$$\Delta\Omega_c = \frac{V}{2\beta(2\pi)^3}\sum_{k_4}\int d\mathbf{k}\left\{\ln\left[1+\frac{e^2\Lambda_1(k)}{k^2}\right]\right.$$

$$\left. + 2\ln\left[1+\frac{e^2\Lambda(k)-e^2\Lambda_1(k)}{2k^2}\right] - \frac{e^2\Lambda(k)}{k^2}\right\}, \qquad (10)$$

where

$$\frac{e^2}{k^2}\Lambda = -\frac{1}{k^2}(\overline{\Pi}_{\nu\nu}-\Pi_{\nu\nu}), \qquad \frac{e^2}{k^2}\Lambda_1 = -\frac{1}{\mathbf{k}^2}(\overline{\Pi}_{44}-\Pi_{44}).$$

The quantity $\Delta\Omega_S$, which is proportional to e^2, is called the exchange part of the thermodynamic potential, and the quantity $\Delta\Omega_C$, which contains the charge in higher powers than the second, is called the correlation part of the thermodynamic potential.

For the calculation of the quantities $\Lambda(k)$ and $\Lambda_1(k)$ we use expression (3) for $\overline{\Pi}_{\lambda\nu}(k)$ and the relation

$$\frac{2\varepsilon_p}{\beta}\sum_{p_4}\frac{1}{\varepsilon_p^2+p_4^2} = 1 - n_p^- - n_p^+ \equiv 1 - n_p,$$

$$n_p^- = [e^{\beta(\varepsilon_p-\mu)}+1]^{-1}, \qquad n_p^+ = [e^{\beta(\varepsilon_p+\mu)}+1]^{-1},$$

$$p_4 = (2n+1)\pi/\beta + i\mu. \qquad (11)$$

Then we obtain

$$\Lambda(k) = -\frac{1}{\pi^3}\,\mathrm{Re}\int\frac{d\mathbf{p}}{\varepsilon_p}\,n_p\,\frac{p(p+k)}{k^2-2pk}\Big|_{p_4=i\varepsilon_p},$$

$$\Lambda_1(k) = -\frac{k^2}{2\pi^3\mathbf{k}^2}\,\mathrm{Re}\int\frac{d\mathbf{p}}{\varepsilon_p}\,n_p\,\frac{pk-2p_4(k_4-p_4)}{k^2-2pk}\Big|_{p_4=i\varepsilon_p}. \qquad (12)$$

After integration over the angles we find

$$\Lambda(\omega, k_4) = \frac{2}{\pi^2}\int_0^\infty\frac{p^2dp}{\varepsilon_p}\,n_p\left\{1+\frac{2m^2-k^2}{8p\omega}\ln\frac{(k^2+2p\omega)^2+4\varepsilon_p^2k_4^2}{(k^2-2p\omega)^2+4\varepsilon_p^2k_4^2}\right\},$$

$$\Lambda_1(\omega, k_4)$$

$$= \frac{k^2}{\pi^2\omega^2}\int_0^\infty\frac{p^2dp}{\varepsilon_p}\,n_p\left\{1+\frac{4\varepsilon_p^2-k^2}{8p\omega}\ln\frac{(k^2+2p\omega)^2+4\varepsilon_p^2k_4^2}{(k^2-2p\omega)^2+4\varepsilon_p^2k_4^2}\right.$$

$$\left. - \frac{\varepsilon_pk_4}{p\omega}\tan^{-1}\frac{8p\omega\varepsilon_pk_4}{4\varepsilon_p^2k_4^2-4p^2\omega^2+k^4}\right\}. \qquad (13)$$

(Here and in the following we use the notation $\omega = |\mathbf{k}|$, $\mathbf{k}^2 = \omega^2 + \mathbf{k}_4^2$, $\epsilon_p = \sqrt{\mathbf{p}^2+\mathbf{m}^2}$.)

In the nonrelativistic approximation, when $|\mu - \mathrm{m}| \ll \mathrm{m}$, $\beta^{-1} \ll \mathrm{m}$, the expressions for Λ and Λ_1 become much simpler:

$$\frac{1}{k^2}\Lambda(\omega, k_4) = \frac{1}{k^2}\Lambda_1(\omega, k_4)$$

$$= \frac{1}{2\pi^3\omega^2}\int\frac{(\omega^2-2\mathbf{pk})/2m}{[(\omega^2-2\mathbf{pk})/2m]^2+k_4^2}\,n_pd\mathbf{p}$$

$$= \frac{m}{2\pi^2\omega^3}\int_0^\infty pdpn_p\ln\frac{(\omega^2+2p\omega)^2+4m^2k_4^2}{(\omega^2-2p\omega)^2+4m^2k_4^2}, \qquad (14)$$

where $n_p = [1+\exp\beta(p^2/2m-\mu')]^{-1}$ and $\mu' = \mu - m$. The correlation part of the thermodynamic potential takes the form*

$$\Delta\Omega_c = \frac{V}{2\beta(2\pi)^3}\sum_{k_4}\int d\mathbf{k}\left\{\ln\left[1+\frac{e^2}{k^2}\Lambda(k)\right]-\frac{e^2}{k^2}\Lambda(k)\right\}. \qquad (15)$$

5. Let us now calculate the exchange part of the thermodynamic potential, $\Delta\Omega_S$. For this purpose we write (9) in the form

$$\Delta\Omega_s = \Delta\Omega_s^R + \Delta\Omega^m + \Delta\Omega^0, \qquad (16)$$

where $\Delta\Omega^0$ is the value of $\Delta\Omega_S$ for $\mu = \beta^{-1} = 0$ and

$$\Delta\Omega^m = \frac{4Ve^2}{(2\pi)^7}\int\frac{d\mathbf{p}}{\varepsilon_p}\,n_p\int\frac{dk}{k^2}\,\frac{p(p+k)}{k^2-2pk}\Big|_{p_4=i\varepsilon_p},$$

$$dk = d\mathbf{k}\,dk_4, \quad k_4 = ik_0; \qquad (17)$$

$$\Delta\Omega_s^R = -\frac{V}{2\beta(2\pi)^3}\sum_{k_4}\int d\mathbf{k}\,\frac{1}{k^2}\,\overline{\Pi}_{\nu\nu}(\mathbf{k}, k_4) - \Delta\Omega^0 - \Delta\Omega^m. \qquad (18)$$

It will be shown below that only the first term of (16) is finite, whereas the other two terms contain divergences in the region of large momenta; we shall therefore restrict the integration in these terms to a finite relativistically invariant region in the form of a four-dimensional sphere of radius L.

The quantity $\Delta\Omega^0$ coincides with the value of Ω for $\mu = \beta^{-1} = 0$; this quantity represents a displacement of the vacuum level due to the interaction of the fields, and should be discarded.

We now show that the quantity $\Delta\Omega^m$ is connected with the renormalization of the electron mass. To this end we consider the expression for the thermodynamic potential of an ideal gas of electrons, positrons, and photons:

$$\Omega_{\mathbf{id}} = -\frac{2V}{(2\pi)^3\beta}\left\{\int d\mathbf{p}\,[\ln(1+e^{-(\varepsilon_p-\mu)\beta})\right.$$

$$\left. + \ln(1+e^{-(\varepsilon_p+\mu)\beta})] - \int d\mathbf{k}\ln(1-e^{-\omega\beta})\right\}. \qquad (19)$$

Here the first and second terms define the thermodynamic potentials of the electron and positron gases, and the third term gives the thermodynamic potential of the photon gas (the chemical potentials of the electrons and positrons are equal in magnitude but of opposite sign, since there is equilibrium between the formation and annihilation of the electron-positron pairs[6]).

The above-mentioned quantity Ω_0 can evidently be obtained from Ω_{id} by replacing in the latter the mass of the real electron m by the mass of the "bare" electron $\mathrm{m}_0 = \mathrm{m} - \delta\mathrm{m}$. Therefore

$$\Omega_{\mathbf{id}} = \Omega_0 + \delta m\frac{\partial\Omega_{\text{ид}}}{\partial m} = \Omega_0 + \frac{2Vm\delta m}{(2\pi)^3}\int\frac{d\mathbf{p}}{\varepsilon_p}\,n_p. \qquad (20)$$

---

*This formula for $\Delta\Omega_c$ was obtained by Fradkin.[3]

Let us now compute the quantity $\Delta\Omega^{\mathrm{m}}$. Performing the integration in (17) and recalling that in the approximation under consideration the electromagnetic mass of the electron is given by the expression[7]

$$\delta m = \frac{3me^2}{(4\pi)^2}\left(\ln\frac{L^2}{m^2} + \frac{1}{2}\right),$$

$\Delta\Omega^{\mathrm{m}}$ can be easily brought into the form

$$\Delta\Omega^m = \frac{3Ve^2m^2}{2\,(2\pi)^5}\left(\ln\frac{L^2}{m^2} + \frac{1}{2}\right)\int\frac{d\mathbf{p}}{\varepsilon_p}\,n_p = \frac{2Vm\delta m}{(2\pi)^3}\int\frac{d\mathbf{p}}{\varepsilon_p}\,n_p.$$

Comparing this expression for $\Delta\Omega^{\mathrm{m}}$ with the expression (20) for the thermodynamic potential of the ideal gas, we see that

$$\Omega_0 + \Delta\Omega^m = \Omega_{\text{ид}}. \tag{21}$$

To calculate $\Delta\Omega_{\mathrm{s}}^{\mathrm{R}}$ we make use of the gauge invariant expression (6) for $\overline{\Pi}_{\lambda\nu}$. Noting that

$$\Pi_{\nu\nu}(\mathbf{k},\ i\omega) = -\frac{8e^2}{(2\pi)^4}\int_{-i\infty}^{i\infty} dp_4\int d\mathbf{p}\,\frac{2m^2 + p\,(p-k)}{(m^2+p^2)\,[m^2+(p-k)^2]}\bigg|_{k_4=i\omega},$$

and using formula (17) for $\Delta\Omega^{\mathrm{m}}$, we write $\Delta\Omega_{\mathrm{s}}^{\mathrm{R}}$ in the form

$$\Delta\Omega_s^R = -\frac{4Ve^2}{(2\pi)^6}\int d\mathbf{p}\,d\mathbf{k}\left\{\frac{1}{\beta}\sum_{k_4}\frac{1}{k^2}\left[\frac{1}{\beta}\sum_{p_4}\frac{2m^2 + p\,(p-k)}{(m^2+p^2)\,[m^2+(p-k)^2]}\right.\right.$$
$$\left.+\frac{1}{2\pi}\int_{-i\infty}^{i\infty} dp_4\,\frac{2m^2 + p\,(p-k)}{(m^2+p^2)\,[m^2+(p-k)^2]}\bigg|_{k_4=i\omega}\right]$$
$$\left.+\frac{n_p}{2\pi\varepsilon_p}\int_{-i\infty}^{i\infty}\frac{dk_4}{k^2}\,\frac{p\,(p+k)}{k^2-2pk}\bigg|_{p_4=i\varepsilon_p}\right\} - \Delta\Omega^0.$$

Performing the summation over p_4 and k_4 with the help of relation (11) and the formula

$$\frac{\omega}{\beta}\sum_{k_4}\frac{1}{\omega^2+k_4^2} = N_k + {}^1/_2,$$
$$N_k = (e^{\beta\omega}-1)^{-1} \qquad \left(k_4 = \frac{2\pi n}{\beta}\right), \tag{22}$$

we obtain after some simple transformations

$$\Delta\Omega_s^R = -\frac{2Ve^2}{(2\pi)^7}\int d\mathbf{p}\,d\mathbf{k}\,U_0(\mathbf{p},\ \mathbf{k})\,n_pN_k$$
$$-\frac{Ve^2}{2\,(2\pi)^7}\int d\mathbf{p}\,d\mathbf{q}\,\{U_-(\mathbf{p},\ \mathbf{q})\,[n_p^+n_q^- + n_p^-n_q^+]$$
$$+U_+(\mathbf{p},\ \mathbf{q})\,[n_-n_- + n_p^+n_q^+]\}, \tag{23}$$

where the functions $U_\pm(\mathbf{p},\mathbf{q})$ and $U_0(\mathbf{p},\mathbf{k})$ are defined by

$$U_\pm(\mathbf{p},\ \mathbf{q}) = \frac{2\pi}{\varepsilon_p\varepsilon_q}\left[m^2\,\frac{m^2 - \mathbf{pq} \pm \varepsilon_p\varepsilon_q}{m^2(\mathbf{p}+\mathbf{q})^2 + p^2q^2 - (\mathbf{pq})^2} - 1\right],$$
$$U_0(\mathbf{p},\ \mathbf{k}) = -\frac{2\pi}{\varepsilon_p\omega}. \tag{24}$$

The superscript R in $\Delta\Omega_{\mathrm{s}}^{\mathrm{R}}$ will be omitted in the following.

In the nonrelativistic case ($|\mu - m| \ll m$, $\beta^{-1} \ll m$) the quantity $U_+(\mathbf{p},\mathbf{q})$ goes over into the Fourier transform of the Coulomb potential: $U_+(\mathbf{p},\mathbf{q}) = 4\pi/(\mathbf{p}+\mathbf{q})^2$ and the quantities $U_-(\mathbf{p},\mathbf{q})$ and $U_0(\mathbf{p},\mathbf{k})$ vanish. In the nonrelativistic case the exchange part of the thermodynamic potential is therefore given by the formula

$$\Delta\Omega_s = -\frac{Ve^2}{(2\pi)^6}\int\frac{d\mathbf{p}\,d\mathbf{q}}{(\mathbf{p}+\mathbf{q})^2}\,n_pn_q. \tag{25}$$

In the extreme relativistic limit ($\mu \gg m$ or $\beta^{-1} \gg m$) we have $U_+(\mathbf{p},\mathbf{q}) = -2\pi/pq$, $U_0(\mathbf{p},\mathbf{k}) = -2\pi/p\omega$ and the quantity $\Delta\Omega_{\mathrm{s}}$ takes the form

$$\Delta\Omega_s = \tfrac{1}{32}\,Ve^2\,\{(\partial n/\partial\mu)^2 + (4/3\beta^2)\,\partial n/\partial\mu\}, \tag{26}$$

where

$$n = 2\,(2\pi)^{-3}\int(n_p^- - n_p^+)\,d\mathbf{p}. \tag{27}$$

6. Using (8), (16), and (21), we finally write the thermodynamic potential of a gas of electrons, positrons, and photons in the form

$$\Omega = \Omega_{\mathrm{id}} + \Delta\Omega, \quad \Delta\Omega = \Delta\Omega_s + \Delta\Omega_c, \tag{28}$$

where Ω_{id}, $\Delta\Omega_{\mathrm{s}}$, and $\Delta\Omega_{\mathrm{c}}$ are given by formulas (19), (23), and (10). Eliminating the chemical potential μ from the expression for $\Delta\Omega$ by expressing it through the number of particles n with the help of (27), we obtain the correction to the energy of the system under consideration:

$$\Delta E \equiv \Delta E_s + \Delta E_c.$$

The exchange energy ΔE_{s} contains the correction to the energy of the ideal gas E_{id} which is proportional to the square of the charge; it consists of a sum of momentum integrals of products of the equilibrium numbers of the particles and certain functions of their momenta which play the role of "potential energies" for the interaction in momentum space. The "potentials" $U_0(\mathbf{p},\mathbf{k})$ and $U_-(\mathbf{p},\mathbf{k})$ are always negative; the "potential" $U_+(\mathbf{p},\mathbf{q})$ can have either sign. Taking this into account, it can be shown that for small values of the average momentum of the particles, $\Delta E_{\mathrm{s}} < 0$. For a certain value of the average momentum, which is of the order of magnitude of the mass of the electron, ΔE_{s} goes to zero; for larger values of the average momentum of the particles, $\Delta E_{\mathrm{s}} > 0$.

The correlation energy ΔE_{c} contains corrections of higher than second order in the charge; it will be shown below that this quantity is proportional to e^3 for finite temperatures, and to

$e^4 \ln e^2$ for zero temperature. It is easily seen that ΔE_C is always negative.

7. At low temperatures $(\beta^{-1} \ll \mu - m)$ the correlation part of the thermodynamic potential has, according to (10), the form

$$\Delta\Omega_c = \frac{V}{(2\pi)^3} \int_{-\infty}^{\infty} dk_4 \int_0^{\infty} \omega^2 d\omega \left\{ \ln\left[1 + \frac{e^2\Lambda_1(k)}{k^2}\right] + 2\ln\left[1 + \frac{e^2\Lambda(k) - e^2\Lambda_1(k)}{2k^2}\right] - \frac{e^2\Lambda(k)}{k^2} \right\}. \tag{29}$$

As was emphasized in Sec. 2, the region of small ω and k_4 plays the main role in this integral due to the smallness of e^2. Introducing, in the place of ω and k_4, the new variables k and φ according to the formulas $\omega = k \sin\varphi$ and $k_4 = k\cos\varphi$ and assuming, wherever possible, that k is zero, we rewrite formula (29) in the following form

$$\Delta\Omega_c = \frac{V}{(2\pi)^3} \int_0^{\pi} d\varphi \sin^2\varphi \int_0^{\infty} k^3 dk \left\{ \ln\left[1 + \frac{e^2\Lambda_1(0,\varphi)}{k^2}\right] + 2\ln\left[1 + \frac{e^2\Lambda(0,\varphi) - e^2\Lambda_1(0,\varphi)}{2k^2}\right] - \frac{e^2\Lambda(0,\varphi)}{k^2} \right\}, \tag{29$'$}$$

where Λ and Λ_1 are, according to (13), given by the formulas

$$\Lambda(0,\varphi) = \frac{1}{\pi^2}\left\{\frac{\mu\sqrt{\mu^2 - m^2}}{m^2} - \tan\varphi \tan^{-1}\left(\frac{\sqrt{\mu^2 - m^2}}{\mu}\tan\varphi\right)\right\},$$

$$\Lambda_1(0,\varphi) = \frac{1}{\pi^2\sin^2\varphi}\left\{\frac{\mu\sqrt{\mu^2 - m^2}}{m^2} - \frac{\mu^2}{m^2}\cot\varphi\tan^{-1}\left(\frac{\sqrt{\mu^2 - m^2}}{\mu}\tan\varphi\right)\right\}.$$

Integrating over k in formula (29′) and neglecting terms of order e^4, we obtain $\Delta\Omega_C$ for $\beta^{-1} \ll \mu - m$ in the following form

$$\Delta\Omega_c = \frac{Ve^4 m^4 \ln e^2}{(4\pi)^3} \int_0^{\pi} \{2[\Lambda_1(0,\varphi)]^2 + [\Lambda(0,\varphi) - \Lambda_1(0,\varphi)]^2\} \sin^2\varphi d\varphi. \tag{30}$$

The quantities $\Lambda(0,\varphi)$ and $\Lambda_1(0,\varphi)$ take the following form in the nonrelativistic $(\mu - m \equiv \mu' \ll m)$ and extreme relativistic $(\mu \gg m)$ cases:

$$\Lambda(0,\varphi) = \Lambda_1(0,\varphi) = \pi^{-2}\{\sqrt{2\mu'/m} - \cot\varphi\tan^{-1}(\sqrt{2\mu'/m}\tan\varphi)\}, \quad \mu' \ll m;$$

$$\Lambda(0,\varphi) = \mu^2/\pi^2 m^2,$$

$$\Lambda_1(0,\varphi) = \mu^2(1 - \varphi\cot\varphi)/\pi^2 m^2 \sin^2\varphi, \qquad \mu \gg m.$$

Substituting these expressions in (30) and using (27), we obtain the following formulas for the correlation energy in the nonrelativistic and extreme relativistic cases at low temperatures:

$$\Delta E_c = (2\pi)^{-4}(1 - \ln 2) V m n e^4 \ln(e^2 m n^{-1/3}),$$

$$\beta^{-1} \ll n^{2/3}/m \ll m; \tag{31}$$

$$\Delta E_c = \tfrac{1}{2}(2\pi)^{-6}(3\pi^2)^{4/3} V n^{4/3} e^4 \ln e^2,$$

$$n^{1/3} \gg \beta^{-1}, \quad n^{1/3} \gg m. \tag{32}$$

Formula (31) was obtained by Gell-Mann and Brueckner.[8]

The integration over the momenta **p** and **q** in the expression (23) for $\Delta\Omega_S$ is easily carried out for $\beta^{-1} \ll \mu - m$:

$$\Delta\Omega_s = \frac{Ve^2}{(2\pi)^4}\left\{\frac{3}{2}\left[\mu\sqrt{\mu^2 - m^2} - m^2 \ln\frac{\mu + \sqrt{\mu^2 - m^2}}{m}\right]^2 - (\mu^2 - m^2)^2\right\}. \tag{33}$$

The exchange energy in the nonrelativistic and extreme relativistic cases at low temperatures has, according to (27) and (33), the form

$$\Delta E_s = -(2\pi)^{-4}(3\pi^2)^{4/3} V n^{4/3} e^2, \quad \beta^{-1} \ll n^{2/3}/m \ll m; \tag{34}$$

$$\Delta E_s = \tfrac{1}{2}(2\pi)^{-4}(3\pi^2)^{4/3} V n^{4/3} e^2, \quad n^{1/3} \gg \beta^{-1}, \quad n^{1/3} \gg m. \tag{35}$$

8. Let us now turn to the consideration of the role of the ions. For this purpose we must assume that the temperature is sufficiently high to allow us to neglect the possibility of the formation of bound electron-ion pairs.

The thermodynamic potential of a system of electrons, photons, and ions is given by the general formula (1), in which $\overline{\Pi}_{\lambda\nu}(k)$ must be understood to represent the total polarization operator; this operator corresponds to the set of diagrams containing closed electron and ion loops. In first approximation in the charge $\overline{\Pi}_{\lambda\nu} = \overline{\Pi}^e_{\lambda\nu} + \overline{\Pi}^i_{\lambda\nu}$, where $\overline{\Pi}^e_{\lambda\nu}$ is given by formula (3) and $\overline{\Pi}^i_{\lambda\nu}$ is obtained from $\overline{\Pi}^e_{\lambda\nu}$ by replacing the chemical potential μ and the mass of the electrons m by the chemical potential μ_1 and the mass of the ions M (here and in the following the index e refers to the electrons and the index i to the ions). The chemical potentials of the electrons and ions are connected through the neutrality condition for the gas:

$$n^e = n^i, \qquad n^e = \frac{2}{(2\pi)^3}\int (n_p^- - n_p^+)\, d\mathbf{p},$$

$$n^i = \frac{2}{(2\pi)^3}\int n_p^i\, d\mathbf{p}. \tag{36}$$

For definiteness we assume that the ions have spin ½ and charge $-e$ (protons). The ions can be considered nonrelativistic in view of their large mass.

The thermodynamic potential of the system of electrons, photons, and ions is given by the formula

$$\Omega = \Omega_{\text{id}} + \Delta\Omega_s^e + \Delta\Omega_s^i + \Delta\Omega_c, \tag{37}$$

where Ω_{id} is the thermodynamic potential of an ideal gas of electrons, photons, and ions; $\Delta\Omega_s^e$ is given by formula (23), and the quantity $\Delta\Omega_s^i$ is obtained from $\Delta\Omega_s^e$ by replacing μ, m by μ_1, M. The correlation part of the thermodynamic potential $\Delta\Omega_c$ is given by formula (10), where $\Lambda = \Lambda^e + \Lambda^i$ and $\Lambda_1 = \Lambda_1^e + \Lambda_1^i$; the quantities Λ^e and Λ_1^e are given by (12) and (13), and Λ^i and Λ_1^i are obtained from Λ^e and Λ_1^e by replacing μ, m by μ_1, M.

9. The thermodynamic potential Ω can be easily determined for temperatures higher than or of the order of the temperature of degeneracy of the electrons ($\beta^{-1} \gtrsim |\mu - m|$). Here the largest term in the sum over k_4 in formula (10) for $\Delta\Omega_c$ is the term with $k_4 = 0$; the remaining terms give a contribution to $\Delta\Omega_c$ which does not exceed e^4, and can be neglected. As a result we obtain

$$\Delta\Omega_c = \frac{V}{\beta(2\pi)^2}\int_0^\infty \omega^2 d\omega \left\{\ln\left[1 + \frac{e^2\Lambda_1(\omega, 0)}{\omega^2}\right] + 2\ln\left[1 + \frac{e^2\Lambda(\omega, 0) - e^2\Lambda_1(\omega, 0)}{2\omega^2}\right] - \frac{e^2\Lambda(\omega, 0)}{\omega^2}\right\}. \quad (38)$$

Since e^2 is small, the small values of ω play the most important role in this integral; therefore, assuming, wherever possible, that ω is zero, we rewrite (38) in the form

$$\Delta\Omega_c = \frac{V}{\beta(2\pi)^2}\int_0^\infty \omega^2 d\omega \left\{\ln\left(1 + \frac{e^2\Lambda(0, 0)}{\omega^2}\right) - \frac{e^2\Lambda(0, 0)}{\omega^2}\right\}. \quad (38')$$

Here we made use of the equality of the quantities $\Lambda(0, 0)$ and $\Lambda_1(0, 0)$, which, according to (13), are given by the formula

$$\Lambda(0, 0) = \Lambda_1(0, 0) = \Lambda^e(0, 0) + \Lambda^i(0, 0) = \frac{1}{\pi^2}\int_0^\infty \frac{p^2 dp}{\varepsilon_p} n_p \left(1 + \frac{\varepsilon_p^2}{p^2}\right) + \frac{M}{\pi^2}\int_0^\infty n_p^i dp.$$

With the help of (36) it can be easily shown that $\Lambda^e(0, 0) = \partial n^e/\partial\mu$ and $\Lambda^i(0, 0) = \partial n^i/\partial\mu_1$. Integrating over ω in formula (38′), we obtain the following expression for the correlation part of the thermodynamic potential* for $\beta^{-1} \gtrsim |\mu - m|$:

$$\Delta\Omega_c = -(Ve^3/12\pi\beta)(\partial n^e/\partial\mu + \partial n^i/\partial\mu_1)^{3/2}. \quad (39)$$

It can be easily shown with the help of the neutrality condition for the gas that in the considered region of temperatures $\Delta\Omega_s^i$ is in order of magnitude M/m times smaller than $\Delta\Omega_s^e$; the contribution of the ions to the exchange energy at $\beta^{-1} \gtrsim |\mu - m|$ is therefore negligibly small.

We note that the correction to the pressure due to the interaction between the particles, $\Delta p = -\Delta\Omega/V$, is positive for $|\mu - m| \lesssim \beta^{-1} \ll m$ and negative in the region $\beta^{-1} \gtrsim |\mu - m|$, $\beta^{-1} \gg m$.

10. From formulas (23) and (39) we can obtain the correction to the energy of the system of electrons, positrons, and photons for $\mu = 0$, i.e., to the energy of black radiation:

$$\Delta E_c = -\frac{2Ve^3m^3}{3\pi^4\beta}\left[\int_1^\infty \frac{x^2 - 1/2}{(x^2 - 1)^{1/2}} \frac{dx}{e^{\beta mx} + 1}\right]^{3/2},$$

$$\Delta E_s = \frac{Ve^2m^4}{2\pi^4}\left\{\frac{\pi^2}{3(\beta m)^2}\int_1^\infty \sqrt{x^2 - 1}\frac{dx}{e^{\beta mx} + 1} + \int_1^\infty \frac{dx}{e^{\beta mx} + 1}\int_1^\infty \frac{dy}{e^{\beta my} + 1}\Big(\sqrt{x^2 - 1}\sqrt{y^2 - 1} - \frac{1}{4}\ln[(\sqrt{x^2 - 1} + \sqrt{y^2 - 1})^2/(\sqrt{x^2 - 1} - \sqrt{y^2 - 1})^2]\Big)\right\} \quad (40)$$

The formulas (40) become much simpler for $\beta^{-1} \gg m$; recalling that for $\beta^{-1} \gg m$ the energy of an ideal gas of electrons, positrons, and photons is equal to $E_{id} = 33\pi^2V/180\beta^4$, we find the following expression for the corrections to the energy of black body radiation:

$$\Delta E = \frac{5Ve^2}{288\beta^4} - \frac{Ve^3}{36\pi\sqrt{3}\beta^4} = \frac{25}{264\pi^2}E_{id}\left(e^2 - \frac{8e^3}{5\sqrt{3}\pi}\right) \quad (\beta^{-1} \gg m). \quad (41)$$

The authors express their deep gratitude to A. I. Akhiezer for valuable advice and discussions.

---

*The analogous expression for the correlation part of the thermodynamic potential in the nonrelativistic case with $m \gg \beta^{-1} \gtrsim |\mu - m|$ was obtained by Vedenov.[9]

[1] T. Matsubara, Progr. Theor. Phys. **14**, 351 (1955).

[2] Abrikosov, Gor'kov, and Dzyaloshinskiĭ, JETP **36**, 900 (1959), Soviet Phys. JETP **9**, 636 (1959).

[3] E. S. Fradkin, JETP **36**, 1286 (1959), Soviet Phys. JETP **9**, 912 (1959).

[4] E. S. Fradkin, Nucl. Phys. **12**, 465 (1959).

[5] A. A. Vedenov and A. I. Larkin, JETP **36**, 1133 (1959), Soviet Phys. JETP **9**, 806 (1959).

[6] L. D. Landau and E. M. Lifshitz, Статистическая физика, (Statistical Physics) GITTL, M.-L., 1951; Engl. Transl. Statistical Physics, Addison-Wesley, Cambridge, Mass., 1958.

[7] A. I. Akhiezer and V. B. Berestetskiĭ, Квантовая электродинамика, (Quantum Electrodynamics) GITTL, M. 1951 [AEC Transl. 2876, 1957].

[8] M. Gell-Mann and K. A. Brueckner, Phys. Rev. **106**, 364 (1957).

[9] A. A. Vedenov, JETP **36**, 641 (1959), Soviet Phys. JETP **9**, 446 (1959).

Translated by R. Lipperheide
350

SOVIET PHYSICS JETP VOLUME 11, NUMBER 6 DECEMBER, 1960

INSTABILITY OF PLASMA WITH ANISOTROPIC DISTRIBUTION OF ION AND ELECTRON VELOCITIES

A. B. KUTSENKO and K. N. STEPANOV

Physico-Technical Institute, Academy of Sciences, Ukrainian S.S.R.

Submitted to JETP editor January 12, 1960

J. Exptl. Theoret. Phys. (U.S.S.R.) 38, 1840-1846 (June, 1960)

A study is made of the propagation of magnetohydrodynamic waves in an infinite rarefied plasma with an anisotropic distribution of charged particle velocities. The conditions are derived under which instability appears as a result of the anisotropy of the distribution function. It is shown that the kinetic treatment leads to an enlargement of the instability region compared with that obtained in the quasihydrodynamic approximation.

1. It was shown by Rudakov and Sagdeev[1] that the anisotropy of the pressure in a rarefied plasma can lead to instability. Their results were generalized by Polovin and Tsintsadze[2] to the case in which the Alfven velocity is of the order of the speed of light. The considerations given in the works mentioned were based on the quasihydrodynamic approximation of Chew, Goldberger, and Low.[3] However, the quasihydrodynamical approximation correctly describes only such plasma motions in which there is no transfer of pressure along the force lines of the magnetic field. In the present research, the low frequency vibrations of an infinite plasma are considered for the case of an anisotropic distribution of ion and electron velocities; these considerations are made on the basis of the kinetic equation. Such an analysis for certain special cases was carried out previously by Vedenov and Sagdeev,[4] and also by Chandrasekhar, Kaufman, and Watson.[5]

2. The kinetic equation for small deviations of the distribution function $f_\alpha(\mathbf{r}, \mathbf{v}, t)$ of particles of type α from the equilibrium distribution has the form

$$\frac{\partial f_\alpha}{\partial t} + \mathbf{v}\frac{\partial f_\alpha}{\partial \mathbf{r}} + \frac{e_\alpha}{m_\alpha}\mathbf{E}\frac{\partial f_{0\alpha}}{\partial \mathbf{v}} + \frac{e_\alpha}{m_\alpha c}[\mathbf{v}\times\mathbf{H}]\frac{\partial f_{0\alpha}}{\partial \mathbf{v}} + \frac{e_\alpha}{m_\alpha c}[\mathbf{v}\times\mathbf{H}_0]\frac{\partial f_\alpha}{\partial \mathbf{v}} = 0, \quad (1)$$

where **E** and **H** are the intensities of the electric and magnetic fields which are produced as a result of the departure of the plasma from the state of equilibrium; $\mathbf{H}_0$ is the intensity of the external magnetic field; $f_{0\alpha}$ is the equlbrium distribution function, the index $\alpha = e$ or i for electrons and ions, respectively; $m_e = m$, and $m_i = M$.

The equilibrium distribution function evidently depends only on $v_\perp$ and $v_\parallel$ ($v_\parallel$ and $v_\perp$ are the components of the velocity **v** parallel and perpendicular to $\mathbf{H}_0$). We shall assume no fluxes of charged particles along $\mathbf{H}_0$ in the equilibrium state, so that $f_{0\alpha} = f_{0\alpha}(v_\perp^2, v_\parallel^2)$. We shall also assume that the functions $f_{0\alpha}$ fall off monotonically for increase in $\mathbf{v}_\parallel^2$. In references 4 and 5, the function $f_{0\alpha}$ was chosen in the form

$$f_{0\alpha} = \frac{n_{0\alpha} m_\alpha^{3/2}}{(2\pi)^{3/2} T_{\perp\alpha} T_{\parallel\alpha}^{1/2}} \exp\left(-\frac{m_\alpha v_\parallel^2}{2T_{\parallel\alpha}} - \frac{m_\alpha v_\perp^2}{2T_{\perp\alpha}}\right), \quad (2)$$

where $T_{\parallel\alpha}$ and $T_{\perp\alpha}$ are the "longitudinal" and "transverse" temperatures, and $n_{0\alpha}$ is the number of particles of type α per unit volume.

Solving Eq. (1) and the Maxwell equations by the Fourier-Laplace method, we can show that after a sufficient time the Fourier components of the quantities **E** and **H** will be proportional to $\exp(-i\omega' t)$, where the complex frequency $\omega' = \omega - i\gamma$ is determined from the dispersion equation. If the dispersion equation has the solution with $\gamma < 0$, then the equilibrium state is unstable. To obtain the dispersion equation, we substitute the values of f_α, **E** and **H** in the form of plane waves in Eq. (1) and in the Maxwell equations. We consider perturbations corresponding to magnetohydrodynamic waves for which the following relations hold:

$$|\omega'| \ll \omega_{Hi}, \qquad k^2\overline{v_i^2} \ll \omega_{Hi}^2, \quad (3)$$

where **k** is the wave vector, $\omega_{H\alpha} = e_\alpha H_0/m_\alpha c$, and the bar over a quantity indicates averaging over the equilibrium distribution. We shall also assume that the Alfven velocity $V_A = H_0(4\pi n_0 M)^{-1/2}$ is small in comparison with the speed of light c ($n_0 = n_{0e} = n_{0i}$). In the approximations of (3), the dispersion equation for electromagnetic waves in plasma divides into two equations:

$$n^2\cos^2\theta - \varepsilon_{11} = 0, \tag{4}$$

$$n^2 - \varepsilon_{22} - \varepsilon_{23}^2/\varepsilon_{33} = 0, \tag{5}$$

where ϵ_{ij} is the dielectric permittivity tensor, $n = kc/\omega'$, and θ is the angle between **k** and $\mathbf{H}_0$. The quantities ϵ_{ij} have the form

$$\varepsilon_{11} = \sum_\alpha \frac{\Omega_\alpha^2}{\omega_{H\alpha}^2}\left[1 + n^2\cos^2\theta\,\left(\overline{v_{\parallel\alpha}^2}/c^2 - \overline{v_{\perp\alpha}^2}/2c^2\right)\right],$$

$$\varepsilon_{22} - \varepsilon_{11} = -\sum_\alpha \frac{\Omega_\alpha^2}{\omega_{H\alpha}^2} n^2\sin^2\theta\,\left(\overline{v_{\perp\alpha}^2}/c^2\right)$$

$$\times\left[1 - \int\limits_C \frac{k_\parallel v_\parallel \Phi_\alpha(v_\parallel^2)}{k_\parallel v_\parallel - \omega'}\,dv_\parallel\right],$$

$$\varepsilon_{33} = \sum_\alpha \frac{\Omega_\alpha^2}{\omega'^2}\int\limits_C \frac{v_\parallel^2 F_\alpha(v_\parallel^2)}{1 - k_\parallel v_\parallel/\omega'}\,dv_\parallel,$$

$$\varepsilon_{23} = i\sum \frac{\Omega_\alpha^2}{\omega'\omega_{H\alpha}}\frac{\sin\theta}{\cos\theta}\int\limits_C \frac{k_\parallel v_\parallel \Psi_\alpha(v_\parallel^2)}{k_\parallel v_\parallel - \omega'}\,dv_\parallel, \tag{6}$$

where

$$\Omega_\alpha^2 = 4\pi e^2 n_0/m_\alpha, \qquad k_\parallel = k\cos\theta,$$

$$n_0\Phi_\alpha(v_\parallel^2) = -\pi\left(\overline{v_{\perp\alpha}^2}\right)^{-1}\frac{\partial}{\partial v_\parallel^2}\int\limits_0^\infty v_\perp^5 f_{0\alpha}(v_\perp^2, v_\parallel^2)\,dv_\perp,$$

$$n_0\Psi_\alpha(v_\parallel^2) = -2\pi\frac{\partial}{\partial v_\parallel^2}\int\limits_0^\infty v_\perp^3 f_{0\alpha}(v_\perp^2, v_\parallel^2)\,dv_\perp.$$

$$n_0 F_\alpha(v_\parallel^2) = 4\pi\frac{\partial}{\partial v_\parallel^2}\int\limits_0^\infty v_\perp f_{0\alpha}(v_\perp^2, v_\parallel^2)\,dv_\perp.$$

The integration over $v_\parallel$ in (6) is carried out along the contour C, which runs along the real axis from $-\infty$ to $+\infty$ for $\gamma < 0$; if $\gamma > 0$, then the contour C bypasses the singularity $v_\parallel = \omega'/k_\parallel$ below for $k_\parallel > 0$ and above for $k_\parallel < 0$.

We write out the asymptotic forms of the integrals appearing in (6):

$$\int\limits_C \frac{k_\parallel v_\parallel \Phi_\alpha(v_\parallel^2)}{k_\parallel v_\parallel - \omega'}\,dv_\parallel = \begin{cases} -k_\parallel^2\overline{v_{\perp\alpha}^4}/4\omega'^2\overline{v_{\perp\alpha}^2}, & x_\alpha \ll 1, \\ q_\alpha + i\pi\omega'|k_\parallel|^{-1}\Phi_\alpha(0), & x_\alpha \gg 1; \end{cases}$$

$$\int\limits_C \frac{v_\parallel^2 F_\alpha(v_\parallel^2)}{1 - k_\parallel v_\parallel/\omega'}\,dv_\parallel = \begin{cases} -1 - 3k_\parallel^2\overline{v_{\parallel\alpha}^2}(\omega')^{-2}, & x_\alpha \ll 1, \\ \omega'^2 k_\parallel^{-2}\left(1/u_\alpha^2 - i\pi\omega'|k_\parallel|^{-1}F_\alpha(0)\right), & x_\alpha \gg 1; \end{cases}$$

$$\int\limits_C \frac{k_\parallel v_\parallel \Psi_\alpha(v_\parallel^2)}{k_\parallel v_\parallel - \omega'}\,dv_\parallel = \begin{cases} -k_\parallel^2\overline{v_{\perp\alpha}^2}/2\omega'^2, & x_\alpha \ll 1, \\ \eta_\alpha + i\pi\omega'|k_\parallel|^{-1}\Psi_\alpha(0), & x_\alpha \gg 1, \end{cases}$$

where

$$x_\alpha = k_\parallel^2\overline{v_{\parallel\alpha}^2}/\omega'^2; \quad q_\alpha = \int\limits_{-\infty}^{\infty}\Phi_\alpha(v_\parallel^2)\,dv_\parallel,$$

$$\eta_\alpha = \int\limits_{-\infty}^{\infty}\Psi_\alpha(v_\parallel^2)\,dv_\parallel, \quad \frac{1}{u_\alpha^2} = -\int\limits_{-\infty}^{\infty}F_\alpha(v_\parallel^2)\,dv_\parallel.$$

In order of magnitude, $\eta_\alpha \sim q_\alpha \sim \overline{v_{\perp\alpha}^2}/\overline{v_{\parallel\alpha}^2}$, $u_\alpha^2 \sim \overline{v_{\parallel\alpha}^2}$.

3. Equation (4) determines the frequency of the ordinary magnetohydrodynamic wave, which is the analogue of the Alfven wave in magnetohydrodynamics. From (4) we find, with the aid of (6),

$$\omega'^2 = k^2V_A^2\cos^2\theta\left(1 + \left(\overline{v_{\perp i}^2} + \mu\overline{v_{\perp e}^2}\right)/2V_A^2 - \left(\overline{v_{\parallel i}^2} + \mu\overline{v_{\parallel e}^2}\right)/V_A^2\right), \tag{7}$$

where $\mu = m/M$. This result can be obtained in the quasihydrodynamic approximation also. Equation (7) was obtained for $\theta = 0$ previously.[1,4] It follows from (7) that the plasma is unstable if

$$\overline{v_{\parallel i}^2} + \mu\overline{v_{\parallel e}^2} > V_A^2 + \tfrac{1}{2}\left(\overline{v_{\perp i}^2} + \mu\overline{v_{\perp e}^2}\right). \tag{8}$$

Equation (5) determines the frequencies of the extraordinary magnetohydrodynamic and "sound" waves, which are the analogues of the fast and slow magnetoacoustic waves in magnetohydrodynamics. We note that the component $\epsilon_{23}^2/\epsilon_{33}$ in (5) appears as the result of consideration of the component of the electric field **E** parallel to $\mathbf{H}_0$. This component is essential in the consideration of waves with small phase velocities when $|\omega'/k_\parallel| \lesssim |\overline{v}_{\parallel i}|$.

The study of the dispersion equation (5) is materially simplified in a number of limiting cases.

a) In the case of a strong magnetic field, when $V_A^2 \gg \overline{v_i^2}$ and $V_A^2 \gg \mu\overline{v_e^2}$, we get from (5) the following expressions for the frequency and damping coefficient of the extraordinary magnetohydrodynamic wave:

$$\omega = kV_A, \tag{9}$$

$$\gamma/\omega = \frac{1}{2}V_A^{-2}\mu\sin^2\theta\left\{\pi\omega\overline{v_{\perp e}^2}|k_\parallel|^{-1}\Phi_e(V_A^2/\cos^2\theta) - u_e^2\right.$$

$$\left.\times\operatorname{Im}\frac{\left[\eta_e + \mathrm{P}\int\limits_{-\infty}^{\infty}\omega\Psi_e(v_\parallel^2)(k_\parallel v_\parallel - \omega)^{-1}dv_\parallel + i\pi\omega|k_\parallel|^{-1}\Psi_e(V_A^2/\cos^2\theta)\right]^2}{1 - u_e^2\omega|k_\parallel|^{-1}\mathrm{P}\int\limits_{-\infty}^{\infty}F_e(v_\parallel^2)(v_\parallel - \omega/k_\parallel)^{-1}dv_\parallel - i\pi\omega u_e^2|k_\parallel|^{-1}F_e(V_A^2/\cos^2\theta)}\right\}. \tag{9'}$$

For the anisotropic Maxwell distribution (2), Eq. (9′) is simplified:

$$\frac{\gamma}{\omega} = \sqrt{\frac{\pi m}{8M}}\,\frac{\sin^2\theta\sqrt{T_{\parallel e}/M}}{|\cos\theta|V_A}\left(\frac{T_{\perp e}}{T_{\parallel e}}\right)^2\exp\left\{-\frac{mV_A^2}{2T_{\parallel e}\cos^2\theta}\right\}.$$

The frequency of the "sound" wave in the case of a strong magnetic field ($V_A^2 \gg \overline{v_i^2}, \mu\overline{v_e^2}$) is determined from the equation

$$\varepsilon_{33}(\omega') = 0. \tag{10}$$

If $\overline{v_{\parallel i}^2} \gtrsim \mu\overline{v_{\parallel e}^2}$, then the "sound" wave is strongly damped as the result of Cerenkov absorption in the ionized gas: $\gamma \sim \omega \sim |k_\parallel\overline{v}_{\parallel i}|$. If $\overline{v_{\parallel i}^2} \ll \mu\overline{v_{\parallel e}^2}$, then

$$\omega = k_\parallel \sqrt{\mu u_e^2}. \tag{11}$$

The damping coefficient for θ not too close to $\pi/2$ is

$$\gamma = -(\pi u_e^2/2\,|k_\parallel|)\,F_e(0)\,\omega^2. \tag{11'}$$

In order of magnitude, $\gamma/\omega \sim \sqrt{\mu} \ll 1$. The damping in this case is brought about by Cerenkov absorption in the electron gas. If the equilibrium distribution has the form (2), then we get for the frequency and the damping coefficient of the "sound" wave

$$\omega = k_\parallel \sqrt{T_{\parallel e}/M}, \quad \gamma = |\omega| \sqrt{\pi m/8M}.$$

The analysis just given shows that a plasma with an anisotropic distribution of electron and ion velocities in a strong magnetic field is stable.

b) For a strongly non-isothermal plasma, in which the electrons are heated more strongly than the ions ($\mu\overline{v^2_{\parallel e}} \gg \overline{v^2_{\parallel i}}, \overline{v^2_{\perp i}}$ or $\mu\overline{v^2_{\perp e}} \gg \overline{v^2_{\parallel i}}, \overline{v^2_{\perp i}}$), we get a solution of the dispersion equation (5) in the form

$$\omega'^2 = \tfrac{1}{2} k^2 \left(a \pm \sqrt{a^2 - 4b}\right),$$

$$a = V_A^2 + \mu \cos^2\theta \left(\overline{v^2_{\perp e}}/2 - \overline{v^2_{\parallel e}}\right) + \mu \sin^2\theta\,(1 - q_e)\,\overline{v^2_{\perp e}} + \mu u_e^2 \cos^2\theta + \mu u_e^2 \eta_e^2 \sin^2\theta,$$

$$b = \mu u_e^2 \cos^2\theta \left[V_A^2 + \mu \cos^2\theta \left(\overline{v^2_{\perp e}}/2 - \overline{v^2_{\parallel e}}\right) + \mu \sin^2\theta\,(1 - q_e)\,\overline{v^2_{\perp e}}\right]. \tag{12}$$

In the derivation of Eq. (12), it was assumed that $|\omega'|^2 \gg k_\parallel^2 \overline{v^2_{\parallel i}}$ and $|\omega'|^2 \ll k^2 \overline{v^2_{\parallel e}}$.

The condition for instability $b < 0$ becomes especially simply for an anisotropic Maxwellian distribution (2). The regions of instability in this case are shown as shaded areas in the drawing. The dashed line in the drawing corresponds to the boundary of the region of instability, according to Rudakov and Sagdeev.[1] As is seen from the drawing, kinetic consideration leads to an increase in the region of instability in comparison with the region of instability obtained in the quasihydrodynamic approximation.

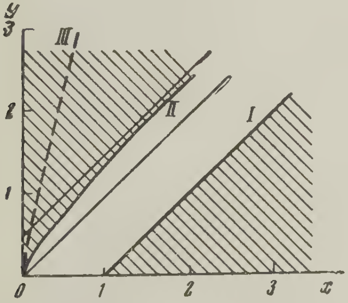

Region of instability is shaded. The curves correspond to the equations I: $y = x - 1$, II: $y = \frac{1}{2}(x + \sqrt{x^2 + 2x})$, III: $y = 3x + \sqrt{9x^2 + 3x}$, where $x = T_{\parallel e}/MV_A^2$, $y = T_{\perp e}/MV_A^2$.

If $\omega'^2 > 0$ in (12), then the damping of magnetoacoustic waves in an electron gas is determined by the expression

$$\gamma = \tfrac{1}{2}\pi k \sin^2\theta\,\omega^2\,|\cos\theta|^{-1}\left\{\Phi_e(0)\,\mu\overline{v^2_{\perp e}}\left(1 - k_\parallel^2 \mu u_e^2/\omega^2\right) - 2\Psi_e(0)\,\mu u_e^2 \eta_e - \eta_e^2 F_e(0)\,\mu u_e^4 \left(1 - k_\parallel^2 \mu u_e^2/\omega^2\right)^{-1}\right\} \times \left\{2\omega^2 - k^2\left[V_A^2 + \mu\cos^2\theta\left(\tfrac{1}{2}\overline{v^2_{\perp e}} - \overline{v^2_{\parallel e}}\right) + \mu\sin^2\theta\,(1 - q_e)\,\overline{v^2_{\perp e}} + \mu u_e^2\left(\cos^2\theta + \eta_e^2 \sin^2\theta\right)\right]\right\}^{-1}. \tag{13}$$

In the case of an anisotropic Maxwellian distribution (2), Eq. (13) takes the form

$$\gamma = \sqrt{\pi m/8M}\,\sin^2\theta\,\sqrt{T_{\parallel e}/M}\,|\cos\theta|^{-1}\,(T_{\perp e}/T_{\parallel e})^2 \times \left[\omega^2\left(1 - k_\parallel^2 T_{\parallel e}/M\omega^2\right)^{-1} - 2k_\parallel^2 T_{\parallel e}/M\right]\left\{2\omega^2 - k^2\left[V_A^2 + T_{\perp e}/M + \sin^2\theta\,T_{\perp e}\left(1 - T_{\perp e}/T_{\parallel e}\right)/M\right]\right\}^{-1}. \tag{13'}$$

For $T_{\perp e} = T_{\parallel e} = T_e$, Eqs. (12) and (13) for the frequency and the damping of the magnetoacoustic waves transform to the equations obtained in reference 6.

c) We now consider the case in which the energy of thermal motion of the particles in a direction parallel to $\mathbf{H}_0$ significantly exceeds the energy of thermal motion in the direction perpendicular to $\mathbf{H}_0$, i.e., $\overline{v^2_{\parallel\alpha}} \gg \overline{v^2_{\perp\alpha}}$. In this case, one can neglect the quantity $\epsilon_{23}^2/\epsilon_{33}$ in (5) in comparison with $\epsilon_{22} \approx \epsilon_{11}$. As a result, we get the following expression for the frequency of the extraordinary magnetohydrodynamic wave

$$\omega'^2 = k^2\left[V_A^2 - \cos^2\theta\left(\overline{v^2_{\parallel i}} + \mu\overline{v^2_{\parallel e}}\right)\right]. \tag{14}$$

This formula also follows from the expressions obtained in references 1 and 2.

If $\omega'^2 > 0$ in (13), then we have for the damping coefficient

$$\gamma = -\omega V_A^2\,\mathrm{Im}\left(\varepsilon_{22} - \varepsilon_{11} + \varepsilon_{23}^2/\varepsilon_{33}\right)/2c^2. \tag{14'}$$

Here $\epsilon_{22} - \epsilon_{11}$, ϵ_{23} and ϵ_{33} are determined by Eqs. (6) for $\omega' = \omega$. If $\omega^2 \sim k_\parallel^2 \overline{v^2_{\parallel i}}$ then, in order of magnitude, $\gamma/\omega \sim (\overline{v^2_{\perp i}}/\overline{v^2_{\parallel i}})^2 \ll 1$.

d) Let the energy of the thermal motion of the particles in the direction perpendicular to $\mathbf{H}_0$ significantly exceed the thermal energy of motion of the particles in the direction parallel to $\mathbf{H}_0$, i.e., $\overline{v^2_{\perp i}} \gg \overline{v^2_{\parallel i}}, \mu\overline{v^2_{\parallel e}}$ or $\mu\overline{v^2_{\perp e}}q_e \gg \mu\overline{v^2_{\parallel e}}, \overline{v^2_{\parallel i}}$. Assuming that $|\omega'|^2 \gg k_\parallel^2 \overline{v^2_{\parallel i}}$ and $|\omega'|^2 \ll k_\parallel^2 \overline{v^2_{\parallel e}}$, we obtain the expression for the frequency of the "magnetoacoustic" waves:

$$\omega'^2 = \tfrac{1}{2} k^2 \left(c \pm \sqrt{c^2 - 4d}\right),$$

$$c = V_A^2 + \left(1 - \tfrac{1}{2}\cos^2\theta\right)\left(\overline{v^2_{\perp i}} + \mu\overline{v^2_{\perp e}}\right) + \sin^2\theta\left(\mu u_e^2 \eta_e^2 - \mu\overline{v^2_{\perp e}}q_e\right),$$

$$d = -\sin^2\theta\cos^2\theta\left[\tfrac{1}{4}\overline{v^4_{\perp i}} + \mu u_e^2 \eta_e \overline{v^2_{\perp i}} + \mu\overline{v^2_{\perp e}}\,\mu u_e^2 q_e\right]. \tag{15}$$

It is evident that instability always takes place in the case under consideration.

If now $\overline{v_{\perp e}^2} \gg \overline{v_{\parallel e}^2}$ and $\mu\overline{v_{\perp e}^2}q_e \gg \overline{v_{\perp i}^2}$, $\overline{v_{\parallel i}^2}$, which corresponds to a sufficiently large value of the energy of thermal motion of the electrons in the direction perpendicular to $\mathbf{H}_0$, then

$$\omega'^2 = k^2 [V_A^2 + \mu \sin^2\theta (u_e^2\eta_e^2 - \overline{v_{\perp e}^2} q_e)]. \tag{16}$$

In the quasihydrodynamic approximation for $\mu\overline{v_{\perp e}^2} \gg \mu\overline{v_{\parallel e}^2}$, $\overline{v_{\perp i}^2}$, $\overline{v_{\parallel i}^2}$, we have $\omega'^2 \sim k^2\mu\overline{v_{\perp e}^2}$, in contrast to (16), where $\omega'^2 \sim k^2\mu\overline{v_{\perp e}^2}q_e (q_e \gg 1)$. If $\omega'^2 > 0$ in (16), then we get for the coefficient of damping of this wave

$$\gamma = \frac{\pi m\, k \sin^2\theta}{2M\,|\cos\theta|} [\eta_e^2 u_e^4 F_e(0) + 2\eta_e^2 u_e^2 \Psi_e'(0) - \overline{v_{\perp e}^2}\Phi_e(0)]. \tag{17}$$

We write out the expressions (16) and (17) in the case in which the equilibrium distribution has the form (2):

$$\omega'^2 = k^2 (V_A^2 - \sin^2\theta T_{\perp e}^2 / T_{\parallel e} M), \tag{16$'$}$$

$$\gamma = \sqrt{\pi m / 8M}\, k \sin^2\theta\, |\cos\theta|^{-1} \sqrt{T_{\parallel e}/M}\, (T_{\perp e}/T_{\parallel e})^2. \tag{17$'$}$$

e) Above we considered the magnetohydrodynamic waves with high frequencies, in which $|\omega'|^2 \gg k_\parallel^2\overline{v_{\parallel i}^2}$. We now find the solution of Eq. (5) for frequencies satisfying the condition $|\omega'| \ll |k_\parallel \overline{v_{\parallel i}}|$. Making use of the expressions (6), we get for θ not close to zero and $\pi/2$.

$$\gamma = |k_\parallel|\, A/\pi B,$$

$$\begin{aligned} A = \{&V_A^2 + \cos^2\theta \left[\tfrac{1}{2}(\overline{v_{\perp i}^2} + \mu\overline{v_{\perp e}^2}) - \overline{v_{\parallel i}^2} - \mu\overline{v_{\parallel e}^2}\right] \\ &+ \sin^2\theta [\overline{v_{\perp i}^2}(1 - q_i) + \mu\overline{v_{\perp e}^2}(1 - q_e)]\}\, \mu u_e^2 u_i^2 / (\mu u_e^2 + u_i^2) \\ &+ (\eta_i - \eta_e)^2 \sin^2\theta, \end{aligned}$$

$$\begin{aligned} B = {}&\sin^2\theta [\Phi_i(0)\, \overline{v_{\perp i}^2}\mu u_e^2 u_i^2/(\mu u_e^2 + u_i^2) + 2(\eta_e - \eta_i)\Psi_i'(0)] \\ &+ F_i(0) \Big\{V_A^2 + \cos^2\theta \left[\tfrac{1}{2}(\overline{v_{\perp i}^2} + \mu\overline{v_{\perp e}^2}) - \overline{v_{\parallel i}^2} - \mu\overline{v_{\parallel e}^2}\right] \\ &+ \sin^2\theta [\overline{v_{\perp i}^2}(1 - q_i) + \mu\overline{v_{\perp e}^2}(1 - q_e)]\Big\}. \end{aligned} \tag{18}$$

For $\theta = 0$, the frequency ω' is determined from the relation (7).

It follows from (18) that even for weak anisotropy, when $|1 - \eta_\alpha| \ll 1$, $|1 - q_\alpha| \ll 1$ and $|1 - 2\overline{v_{\parallel\alpha}^2}/\overline{v_{\perp\alpha}^2}| \ll 1$, it is possible to produce instabilities, if the intensity of the magnetic field is sufficiently small ($V_A^2 \ll \overline{v_{\perp i}^2}$, $\mu\overline{v_{\perp e}^2}$). However, the intensity of the magnetic field in this case cannot be so arbitrarily small because of conditions (3).

Expression (18) is valid not only in the case of weak anisotropy. It can also be used when the angle θ is close to θ_0 determined from the condition $A = 0$:

$$\sin^2\theta_0 = \frac{\overline{v_{\parallel i}^2} + \mu\overline{v_{\parallel e}^2} - {}^1\!/_2(\overline{v_{\perp i}^2} + \mu\overline{v_{\perp e}^2}) - V_A^2}{\overline{v_{\parallel i}^2} + \mu\overline{v_{\parallel e}^2} + \overline{v_{\perp i}^2}({}^1\!/_2 - q_i) + \mu\overline{v_{\perp e}^2}({}^1\!/_2 - q_e) + (\eta_i - \eta_e)^2 \mu u^2 u_i^2/(\mu u_i^2 + u_{i}^{2}} \tag{19}$$

As θ varies, γ changes sign at the point $\theta = \theta_0$.

It was shown above that the plasma is unstable if the inequality (8) holds. Let the condition (8) not be observed. Then it follows from (18) and (19) that the equilibrium state is unstable if the inequality

$$V_A^2 + \overline{v_{\perp i}^2}(1 - q_i) + \mu\overline{v_{\perp e}^2}(1 - q_e) + \mu u_e^2 u_i^2 (\eta_i - \eta_e)^2 / (\mu u_e^2 + u_i^2) < 0 \tag{20}$$

is satisfied. In the case of an anisotropic Maxwellian distribution (2) for $T_{\perp e} = T_{\perp i} = T_\perp$ and $T_{\parallel e} = T_{\parallel i} = T_\parallel$, the inequality (20) takes the form

$$V_A^2 + 4T_\perp (1 - T_\perp/T_\parallel)/M < 0 \tag{20$'$}$$

The regions of instability for $T_{\perp e} = T_{\perp i} = T_\perp$ and $T_{\parallel e} = T_{\parallel i} = T_\parallel$ are shown in the drawing (here the quantity $x = 2T_\parallel/MV_A^2$ is plotted along the abscissa and $y = 2T_\perp/MV_A^2$ along the ordinate).

We note here that the condition analogous to (20′) is written incorrectly in the work of Vedenov and Sagdeev[4] (the coefficient 2 appears instead of the coefficient 4.)

The authors express their thanks to A. I. Akhiezer, V. F. Aleksin, R. V. Polovin, and V. I. Yashin for valuable advice and discussions of the research.

---

[1] L. I. Rudakov and R. Z. Sagdeev, Физика плазмы и проблема управляемых термоядерных реакций, (Plasma Physics and the Problem of Controlled Thermonuclear Reactions) Vol 3. Acad. Sci. U.S.S.R. 1958, p. 628.

[2] R. V. Polovin and N. D. Tsintsadze, Ukr. fiz. zh. **4**, 31 (1959).

[3] G. F. Chew, M. L. Goldberger and F. S. Low, Proc. Roy. Soc. (London) **A236**, 112 (1956).

[4] A. A. Vedenov and R. Z. Sagdeev, loc. cit. ref 1 p. 278.

[5] Chandrasekhar, Kaufman, and Watson, Proc. Roy. Soc. (London) **A245**, 435 (1958).

[6] K. N. Stepanov, Ukr. fiz. zh. **4**, 678 (1959).

Translated by R. T. Beyer

SOVIET PHYSICS JETP VOLUME 11, NUMBER 6 DECEMBER, 1960

TEMPERATURE DEPENDENCE OF MAGNETOSTRICTION

E. A. TUROV and A. I. MITSEK

Institute of Metal Physics, Academy of Sciences, U.S.S.R.

Submitted to JETP editor January 9, 1960

J. Exptl. Theoret. Phys. (U.S.S.R.) 38, 1847-1851 (June, 1960)

The temperature dependence of linear (anisotropic) and volume (isotropic) magnetostriction in the low-temperature region is studied on the basis of the phenomenological method of the theory of spin waves.

1. In a recent work of the authors,[1] the temperature dependence of the ferromagnetic anisotropy constants was studied on the basis of the phenomenological theory of spin waves. The results obtained in that work can also be used for discussion of the problem of the temperature dependence of the constants of anisotropic magnetostriction; this will be done in the present article. In addition, the temperature dependence of the volume (isotropic) magnetostriction will also be considered here.

The magnetoelastic energy density of a ferromagnetic can be expressed in the general case, through terms linear in the components of the elastic stress tensor σ_{ls}, in the form

$$\mathcal{H}_{\mathrm{me}} = -\lambda_{ls;\, n_1 n_2 n_3} \sigma_{ls} m_x^{n_1} m_y^{n_2} m_z^{n_3} - G_{ijls} \sigma_{ls} \frac{\partial m_t}{\partial r_i} \frac{\partial m_t}{\partial r_j}. \qquad (1)$$

Here $m_t(r) = M_t(r)/M_0$ are the components of the unit vector of the local magnetization; M_0 is the absolute saturation; $i, j, l, s, t \equiv x, y, z$; n_1, n_2, n_3 are integers such that $n_1 + n_2 + n_3 = 2N$ is an even number; in (1), and generally in what follows, summation over twice occurring indices is understood.

The first term in (1) gives the anisotropic part of the magnetoelastic energy, expressed in the form of a series of ascending powers of the components of the magnetization. The second term represents the change of exchange energy produced by the stresses, so that

$$G_{ijls} = -\partial A_{ij} / \partial \sigma_{ls}, \qquad (2)$$

where A_{ij} are the exchange-interaction parameters. The specific form of the tensors λ and G is determined by the crystal symmetry.

We now note that the components of the elastic stress tensor σ_{ls}, in the problem under consideration, may be treated as parameters related through the elastic moduli to the equilibrium deformations of the crystal lattice, without allowance for thermal vibrations of the latter. For harmonic elastic vibrations of the lattice do not change the equilibrium deformations of the crystal and consequently do not affect the mean magnetoelastic energy of the ferromagnetic; and allowance for the anharmonicity of these vibrations leads to a thermal expansion, which in the first approximation combines additively with the temperature change of the magnetostrictive deformations. Thus the temperature dependence of the magnetostrictive deformations will be basically determined solely by the thermal oscillations of the magnetization, i.e., by the spin waves. Therefore our problem reduces to the calculation of the energy spectrum of the spin waves with, as compared with the previous work,[1] additional allowance for the magnetoelastic energy (1).

It is easy to see that addition to the Hamiltonian[1] of the magnetoelastic part (1) leads to the following expression for the energy of a spin wave:

$$\varepsilon_k = (\mu/M_0)\{2(A_{ij} - G_{ijls}\sigma_{ls}) k_i k_j + M_0 H - \frac{1}{2}\sum_N [2N(2N+1) - \Delta_\alpha][f_N(0) - \sigma_{ls}\varphi_{ls;\, N}(0)]\}, \qquad (3)$$

where

$$\varphi_{ls,\, N} = \sum_{n_1+n_2+n_3=2N} \lambda_{ls,\, n_1 n_2 n_3} \alpha_x^{n_1} \alpha_y^{n_2} \alpha_z^{n_3} \qquad (4)$$

is a homogeneous polynomial of degree 2N in the direction cosines α_i of the equilibrium magnetization.* At the same time it is necessary to add to the energy $\mathcal{H}_0$ of the ground state a term of the form

$$-\sum_N \sigma_{ls}\varphi_{ls;\, N}(0). \qquad (5)$$

---

*For the remaining symbols, see our previous paper.[1] In the expression (3) for ε_k, as compared with the corresponding formula of the other paper, the magnetostatic energy has been dropped as nonessential, and saturation ($\boldsymbol{\alpha}\mathbf{H} = \mathbf{H}$) has been assumed (see correction of a misprint, JETP 38, 667 (1960), this issue, Soviet Phys. JETP 11, 1326 (1960).

If we now calculate the thermodynamic potential Ω of the system according to the appropriate formula from reference 1 with allowance for (3) and (5), we can then find from it the components of the magnetostrictive strain tensor:

$$u_{ls} = -\frac{\partial\Omega}{\partial\sigma_{ls}} = \sum_N \left\{1 - \frac{M(0) - M(T, H)}{2M(0)}\left[2N(2N+1) - \Delta_\alpha\right]\right\}$$

$$\times\, \varphi_{ls;\,N}(0) + 2\frac{\mu}{M_0}\sum_{\mathrm{k}} G_{ijls}k_i k_j\left(e^{-\varepsilon_{\mathrm{k}}/\varkappa T} - 1\right)^{-1}, \qquad (6)$$

here M(T, H) is the mean magnetization of the crystal in field H at temperature T, and M(0) $\equiv M_0$ is the magnetization at T = 0° K. The first sum in (6) represents the anisotropic magnetostriction, which causes a dependence of the linear dimensions and shape of the ferromagnetic specimen on the direction of the magnetization. The second sum in (6) gives the isotropic magnetostriction, which leads to an additional temperature dependence of the volume of the ferromagnetic specimen as compared with a nonferromagnetic (spontaneous volume magnetostriction or thermostriction), and also to a dependence of the volume on the value of the magnetizing field in the paraprocess region (paraprocess magnetostriction).

2. We consider first the anisotropic magnetostriction. If for the polynomials $\varphi_{ls;N}$ we use harmonic polynomials, for which $\Delta\varphi_{ls;N} = 0$, then after substitution of (4) in (6) we can express the anisotropic part of the magnetostrictive strains in the form

$$u_{ls} = \sum_{n_1 n_2 n_3} \lambda_{ls;\, n_1 n_2 n_3}(T)\, \alpha_x^{n_1}\alpha_y^{n_2}\alpha_z^{n_3},$$

where the coefficients λ have the meaning of magnetostrictive constants at temperature T; here, independently of the symmetry class of the crystal, any magnetostriction constant of order $N = \frac{1}{2}(n_1 + n_2 + n_3)$ satisfies the general relation

$$[\lambda_N(0) - \lambda_N(T)]/\lambda_N(0)$$

$$= N(2N+1)[M(0) - M(T, H)]/M(0), \qquad (7)$$

which exactly coincides in form with the corresponding relation for the magnetocrystalline-anisotropy constants.*

As an example, we write the harmonic expansion of the magnetoelastic energy through terms of fourth degree in the direction cosines α_i of the magnetization (i.e., through N = 2) for crystals of cubic symmetry:

$$F_{\mathrm{me}} = \tfrac{1}{2}\lambda_1^{(1)}[\sigma_{xx}(2\alpha_x^2 - \alpha_y^2 - \alpha_z^2) + \sigma_{yy}(2\alpha_y^2 - \alpha_x^2 - \alpha_z^2)$$
$$+ \sigma_{zz}(2\alpha_z^2 - \alpha_x^2 - \alpha_y^2)] + 2\lambda_1^{(2)}[\sigma_{xy}\alpha_x\alpha_y + \sigma_{xz}\alpha_x\alpha_z + \sigma_{yz}\alpha_y\alpha_z]$$
$$+ \lambda_2^{(1)}(\sigma_{xx} + \sigma_{yy} + \sigma_{zz})[\alpha_x^4 + \alpha_y^4 + \alpha_z^4$$
$$- 3(\alpha_x^2\alpha_y^2 + \alpha_x^2\alpha_z^2 + \alpha_y^2\alpha_z^2)] + \lambda_2^{(2)}\{\sigma_{xx}[\alpha_x^4 - 3(\alpha_x^2\alpha_y^2$$
$$+ \alpha_x^2\alpha_z^2 - \alpha_y^2\alpha_z^2)] + \sigma_{yy}[\alpha_y^4 - 3(\alpha_x^2\alpha_y^2 + \alpha_y^2\alpha_z^2 - \alpha_x^2\alpha_z^2)]$$
$$+ \sigma_{zz}[\alpha_z^4 - 3(\alpha_x^2\alpha_z^2 + \alpha_y^2\alpha_z^2 - \alpha_x^2\alpha_y^2)]\}$$
$$+ 2\lambda_2^{(3)}\Big\{\sigma_{xy}\alpha_x\alpha_y\left[\alpha_z^2 - \tfrac{1}{6}(\alpha_x^2 + \alpha_y^2)\right]$$
$$+ \sigma_{xz}\alpha_x\alpha_z\left[\alpha_y^2 - \tfrac{1}{6}(\alpha_x^2 + \alpha_z^2)\right]$$
$$+ \sigma_{yz}\alpha_y\alpha_z\left[\alpha_x^2 - \tfrac{1}{6}(\alpha_y^2 + \alpha_z^2)\right]\Big\}. \qquad (8)$$

Here the lower index on λ corresponds to the order N of the constant, and the upper index enumerates the different constants of a single order. Since the generally used form of expression for F_{me} for cubic crystals differs from (8) and is nonharmonic, the relation (7) need not be satisfied by the magnetostriction constants that enter into that expression. Instead of (7) there are obtained more complicated formulas, in which "entanglement" of the magnetostriction constants of different orders occurs. For example, for the first constants $\lambda_1^{(1,2)}$ we should have

$$\Delta\lambda_1^{(1,2)}(T)/\lambda_1^{(1,2)}(0) = P_1^{(1,2)}\Delta M(T, H)/M(0), \qquad (9)$$

where $P_1^{(1)} = 3[1 - 2\lambda_2^{(2)}(0)/\lambda_1^{(1)}(0)]$ and $P_1^{(2)} = 3[1 - \lambda_2^{(3)}(0)/3\lambda_1^{(2)}(0)]$; whereas for the harmonic form of expression (8), according to (7), when N = 1 there is obtained the universal value of the coefficients $P_1^{(1)} = P_1^{(2)} = 3$.

Experiment shows that the constants λ_2 often have the same orders of magnitude as the constants λ_1. Therefore in the nonharmonic analysis of experimental data, it is hardly possible to obtain any general law for the temperature dependence of the "nonharmonic" constants λ_1: from formula (9) it is evident that, depending on the relation between $\lambda_1(0)$ and $\lambda_2(0)$, different ferromagnetics may differ not only in the magnitude but even in the sign of the temperature rate of change of the constants $\lambda_1(T)$. The advantage of the harmonic form

---

*As is known, magnetostrictive strains lead to a certain change of the magnetic anisotropy constants: to the purely crystallographic anistropy constants K_N of order N there are added magnetostrictive corrections $\delta K_N = C\lambda_{N_1}\lambda_{N_2}$, where the C's are definite linear combinations of the elastic moduli and where $N_1 + N_2 = N$.[2] By virtue of the relation (7), the temperature dependence of the magnetostrictive part of the anisotropy constants is determined by the formula

$$[\delta K_N(0) - \delta K_N(T)]/\delta K_N(0) = P_N[M(0) - M(T, H)]/M(0),$$

where $P_N = N(2N+1) - 4N_1N_2$, whereas for the crystallographic constants K_N the same formula holds but with $P_N = N(2N+1)$. For example, for a cubic crystal, to the first crystallographic anisotropy constant K_2, for which $P_2 = 10$, there is added a magnetostrictive part δK_2 with $P_2 = 6$. Since δK_N increases with decreasing temperature more slowly than does K_N, the relative contribution of the magnetostrictive strains to the anisotropy is smaller, the lower the temperature.

of expression for the magnetoelastic energy consists precisely in the fact that because it eliminates this random factor, it permits exhibition of the true law for the temperature dependence of magnetistriction.

It should be remarked that, just as for the anisotropy constants,[3] the applicability of the relation (7) is apparently limited to a narrower range of low temperatures than the range of applicability of the "$T^{3/2}$ law" for the temperature dependence of the spontaneous magnetization. Unfortunately, at the present time there exist almost no experimental investigations of the temperature dependence of the magnetostriction in the region of sufficiently low temperatures.

A theoretical calculation of the temperature dependence of the magnetostriction constants on the basis of spin-wave theory was first achieved by Gusev,[4] who showed that in the low-temperature range, always, $\Delta\lambda(T) \sim T^{3/2}$; but he did not investigate the relation between the temperature dependences of the magnetostriction and of the magnetization. A number of earlier works,[5] based on the molecular-filed approximation, led to the following relation between the first constants of magnetostriction and of spontaneous magnetization:

$$\lambda_1(T)/\lambda_1(0) = [M(T)/M(0)]^{P_1}, \tag{10}$$

where $P_1 = 2$. We remark that formula (7) for $N = 1$ in the low-temperature region, where it has its only applicability, can also be expressed approximately in the form (10), but with the difference that $P_1 = 3$.

Among the early researches it is necessary to mention also the work of Vonsovskiĭ,[6] who, within the framework of a special microscopic model, calculated the spin-orbit interaction of the electrons responsible for ferromagnetism; this enabied him to give an explanation in principle of the nonmonotonic temperature dependence of the magnetostriction constants that is sometimes observed experimentally. In this theory, however, there enter a number of undetermined parameters, so that comparison of it with experiment is difficult. In all the works enumerated, no attention was directed to the role of the form of expression for the magnetoelastic energy.

The present theory, being based on the most general modern ideas about the nature of ferromagnetic and magnetoelastic phenomena, will presumably, after its detailed verification, make possible a number of definite conclusions regarding the limits of applicability of the existing spin-wave description of these phenomena.

3. In conclusion, we give a few relations for the isotropic volume magnetostriction. From the second sum in formula (6) the relative change of volume of the ferromagnetic can be found by calculating the value of $w = \delta V/V_0 = \Sigma u_{ll}$ corresponding to this sum. For temperatures $\kappa T \gg \mu H$ we have approximately

$$w = w_0 + H\partial w/\partial H,$$

where

$$w_0 = \frac{3\zeta(5/2)\,\Gamma(5/2)\,\mu G}{2\pi^2 M_0}\left(\frac{M_0 \varkappa T}{2\mu A}\right)^{5/2} \tag{11}$$

is the spontaneous magnetostriction (thermostriction), and

$$\frac{\partial w}{\partial H} = -\frac{3\zeta(5/2)\,\Gamma(5/2)\,\mu^2 G}{2\pi^2 M_0 \varkappa T}\left(\frac{M_0 \varkappa T}{2\mu A}\right)^{5/2} \tag{12}$$

is the coefficient of paraprocess magnetostriction. Here we have for simplicity taken $A_{ij} = A\delta_{ij}$ and $G_{ijll} = G\delta_{ij}$ (cubic crystal); ζ and Γ are, respectively, the Riemann zeta function and the gamma function. We remark furthermore that according to (2) the parameter G can be defined as $G = \partial A/\partial p$, where p is hydrostatic pressure.

By comparing expressions (11) and (12) with each other and also with the corresponding expressions for the spin heat-capacity C_S and for the temperature change of spontaneous magnetization ΔM,* it is not difficult to establish the following simple relations among all these quantities:

$$\frac{1}{3}\frac{\partial w_0}{\partial T} = -\frac{5}{6}\frac{\varkappa}{\mu}\frac{\partial w}{\partial H} = \frac{1}{\Theta_c}\frac{\partial \Theta_c}{\partial p} C_S \approx 2\frac{\varkappa}{\mu}\frac{1}{\Theta_c}\frac{\partial \Theta_c}{\partial p}\Delta M. \tag{13}$$

Instead of the exchange-coupling parameter A, we have introduced here the Curie temperature Θ_c, assuming a direct proportionality between them.

The quantity $\frac{1}{3}\partial w_0/\partial T = \Delta\alpha_M$ represents an additional linear coefficient of thermal expansion, connected with thermostriction. As was to be expected in accordance with Grüneisen's law,[8] it is proportional to the spin part of the heat capacity. A quantitative estimate of $\Delta\alpha_M$ can be made by using experimental data on the paraprocess magnetostriction.[9] For the majority of magnetic materials in the room-temperature range, $\partial w/\partial H = 10^{-10}$ to 10^{-9} oe^{-1}. Hence, according to (13), $\Delta\alpha_M = 10^{-6}$ to 10^{-5}. Experimental investigations

---

*See, for example, the work of Kaganov and Tsukernik.[7] In our notation, we have

$$C_S = \frac{5\zeta(5/2)\,\Gamma(5/2)\,\varkappa}{2\zeta(3/2)\,\Gamma(3/2)\,\mu}\Delta M = \frac{5\Gamma(5/2)\,\zeta(5/2)}{8\pi^2}\varkappa\left(\frac{M_0 \varkappa T}{2\mu A}\right)^{3/2}.$$

of the volume magnetostriction at lower temperatures are unfortunately lacking.

The authors are deeply grateful to S. V. Vonsovskiĭ for valuable discussion and advice.

---

[1] E. A. Turov and A. I. Mitsek, JETP **37**, 1127 (1959), Soviet Phys. JETP **10**, 801 (1960).

[2] S. V. Vonsovskiĭ and Ya. S. Shur, Ферромагнетизм, (Ferromagnetism), Gostekhizdat (1948), p. 266.

[3] N. A. Potapkov, Dokl. Akad. Nauk SSSR **118**, 269 (1958), Soviet Phys.-Doklady **3**, 89 (1958).

[4] A. A. Gusev, Dokl. Akad. Nauk SSSR **98**, 749 (1954).

[5] N. S. Akulov, Z. Physik **52**, 389 (1928); R. Becker, Z. Physik **62**, 253 (1930).

[6] S. V. Vonsovskiĭ, JETP **10**, 762 (1940).

[7] M. I. Kaganov and V. M. Tsukernik, Физика металлов и металловедение, (Phys. of Metals and Metallurgy) **5**, 561 (1957).

[8] R. Peierls, Quantum Theory of Solids, (Oxford, Clarendon Press, 1955), Chap. 2.

[9] K. P. Belov, Упругие, электрические и галваномагнитные явления в ферромагнетиках, (Elastic, Thermal, and Electric Phenomena in Ferromagnetics), Gostekhizdat (1957), Chap. 2.

Translated by W. F. Brown, Jr.
352

SOVIET PHYSICS JETP VOLUME 11, NUMBER 6 DECEMBER, 1960

EFFECT OF SUPERFLUIDITY OF HEAVY NUCLEI ON SINGLE-PARTICLE ELECTROMAGNETIC TRANSITIONS AND β DECAY

M. G. URIN

Moscow Engineering-Physics Institute

Submitted to JETP editor February 5, 1960

J. Exptl. Theoret. Phys. (U.S.S.R.) **38**, 1852-1853 (June, 1960)

Formulas are deduced for the probabilities of single-particle electromagnetic transitions and of β decay, account being made for pair correlation of the nucleons in heavy nuclei.

It is well known that single-particle electromagnetic transitions in nuclei are determined at low excitations by the transition of the nucleon with the weakest bond. We shall show how realignment of the Fermi surface due to formation of correlated nucleon pairs,[1,4] influences these transitions.

To describe the superfluid state of heavy nuclei, we can use the canonical transformation of Bogolyubov,[3] which takes into account the correlation of nucleons whose states differ only in the sign of the projection of the total momentum on the symmetry axis of the nucleus:[1,4]

$$a_{\nu+} = u_\nu \alpha_\nu + v_\nu \beta_\nu^+, \qquad a_{\nu-} = u_\nu \beta_\nu - v_\nu \alpha_\nu^+, \qquad u_\nu^2 + v_\nu^2 = 1,$$

$\alpha_{\nu\sigma}$ is the operator of nucleon annihilation in the state characterized by the totality of quantum numbers ν, σ (σ denotes the sign of the projection of the momentum with modulus equal to Ω). The wave functions $\psi_{\nu\sigma}$ are chosen such that the transition from $\psi_{\nu+}$ to $\psi_{\nu-}$ corresponds to time reflection.

The ground state of an even nucleus is a vacuum Φ_0 for quasi particles: $\alpha_\nu \Phi_0 = \beta_\nu \Phi_0 = 0$. The ground and excited (with energy less than 2Δ) states of an odd nucleus can be considered as the ground state of the corresponding even nucleus plus one quasi particle:

$$\alpha_\nu^+ \Phi_0; \; \beta_\nu^+ \Phi_0. \tag{1}$$

The excited states of the even nucleus are characterized by the presence of at least two (in general, an even number) quasi particles

$$\alpha_{\nu_1}^+ \beta_{\nu_2}^+ \Phi_0; \; \alpha_{\nu_1}^+ \alpha_{\nu_2}^+ \Phi_0; \; \beta_{\nu_1}^+ \beta_{\nu_2}^+ \Phi_0. \tag{2}$$

The probability of single-particle electromagnetic transitions is determined by the matrix elements of the operators of multipole moments of the system

$$\mathfrak{M}_{\lambda\mu\alpha} = \sum_{\nu\sigma,\, \nu'\sigma'} \langle \nu, \sigma \,|\, \mathfrak{M}_{\lambda\mu\alpha}^{(1)} \,|\, \nu', \sigma' \rangle \, a_{\nu\sigma}^+ a_{\nu'\sigma'},$$

where $\mathfrak{M}_{\lambda\mu\alpha}^{(1)}$ is the single-particle operator of the electric ($\alpha = 0$) or magnetic ($\alpha = 1$) multipole moment of order λ.

For a deformed odd nucleus we readily obtain the probability of multipole transition, $w_{12}(\lambda)$:

$$w_{12}(\lambda) = |\langle \nu_2 + | \mathfrak{M}_{\lambda\mu\alpha}^{(1)} | \nu_1 + \rangle|^2 (u_{\nu_1} u_{\nu_2} + (-)^{\alpha+1} v_{\nu_1} v_{\nu_2})^2 + |\langle \nu_2 + | \mathfrak{M}_{\lambda\mu\alpha}^{(1)} | \nu_1 - \rangle|^2 (u_{\nu_1} u_{\nu_2} + (-)^{\alpha} v_{\nu_1} v_{\nu_2})^2. \tag{3}$$

[The probability of transition is defined as $(\frac{1}{2}) \Sigma |(\mathfrak{M}_{\lambda\mu\alpha})_{12}|^2$, where the averaging and summation are over the states of form (1).] The factor $(-)^\alpha$ is due to the relations

$$\langle \nu + | \mathfrak{M}_{\lambda\mu\alpha}^{(1)} | \nu' + \rangle = (-)^\alpha \langle \nu' - | \mathfrak{M}_{\lambda\mu\alpha}^{(1)} | \nu - \rangle,$$
$$\langle \nu + | \mathfrak{M}_{\lambda\mu\alpha}^{(1)} | \nu' - \rangle = (-)^\alpha \langle \nu' + | \mathfrak{M}_{\lambda\mu\alpha}^{(1)} | \nu - \rangle,$$

in accordance with the behavior of the operator $\mathfrak{M}_{\lambda\mu\alpha}^{(1)}$ under time reversal.

For a deformed even nucleus, the probability of transition from a state such as (2) to the ground state is given by the expression

$$w_{12}(\lambda) = |\langle \nu_2 + | \mathfrak{M}_{\lambda\mu\alpha}^{(1)} | \nu_1 + \rangle|^2 (u_{\nu_1} v_{\nu_2} + (-)^{\alpha} v_{\nu_1} u_{\nu_2})^2 + |\langle \nu_2 + | \mathfrak{M}_{\lambda\mu\alpha}^{(1)} | \nu_1 - \rangle|^2 (u_{\nu_1} v_{\nu_2} + (-)^{\alpha+1} v_{\nu_1} u_{\nu_2})^2. \tag{4}$$

The probability of transition between the excited states such as (2) is given by a formula analogous to (3).

The selection rules yield $\lambda \geq |\Omega_1 - \Omega_2|$ for the first term in (3) and (4) and $\lambda \geq \Omega_1 + \Omega_2$ for the second. In heavy nuclei, transitions with $\lambda < \Omega_1 + \Omega_2$ are realized as a rule. In this case the influence of superfluidity of the nuclei on the probability of single-particle electromagnetic transitions is expressed by the factors $(u_{\nu_1} u_{\nu_2} + (-)^{\alpha+1} v_{\nu_1} v_{\nu_2})^2$ and $(u_{\nu_1} v_{\nu_2} + (-)^{\alpha} v_{\nu_1} u_{\nu_2})^2$, which can reduce the transition probability by one order of magnitude. (Near the Fermi surface, the factors $(u_{\nu_1} u_{\nu_2} - v_{\nu_1} v_{\nu_2})^2$ and $(u_{\nu_1} v_{\nu_2} - v_{\nu_1} u_{\nu_2})^2$

are of the order $(\rho_0\Delta)^{-2}$, where ρ_0 is the energy density of the levels at the Fermi surface).

A realignment of the Fermi surface changes also the probability of β decay. For β^- decay of an odd deformed nucleus without excitation of the collective-motion levels, we readily obtain, in analogy with (3),

$$W_{12} = w_{12}\,(u^n_{\nu_1}u^p_{\nu_2})^2. \tag{5}$$

Here w_{12} is the probability of decay without allowance for "pairing"; n and p denote respectively the neutron and proton fluids; ν_1 and ν_2 characterize initial and final states of form (1).

The probability of β^- decay of an even-even (odd-odd) deformed nucleus from the ground states (to the ground states) is given by the expressions

$$W_{12} = w^{ee}_{12}\,(v^n_{\nu_1}u^p_{\nu_2})^2, \quad W_{12} = w^{oo}\,(u^n_{\nu_1}v^p_{\nu_2})^2. \tag{6}$$

The transition to β^+ decay is made by the substitution $n \rightleftarrows p$. For a decay from a ground state to a ground state, the factors occuring when superfluidity is taken into account are approximately $^1/_4$.

Formulas (3) — (6) can also be obtained in a different manner, by expressing W_{12} in terms of a single-particle Green's function and $w_{12}(\lambda)$ in terms of a two-particle Green's function. The latter is expressed, in turn, in terms of the single-particle Green's function and the correlation functions. The equations for these functions have been solved for the case of superfluidity in references 5 and 2.

The author expresses his deep gratitude to A. B. Migdal for attention to the work.

---

[1] S. T. Belyaev, Kgl. Dan. Vid. Selsk. Mat-fys Medd. **31**, 11 (1959).

[2] A. V. Migdal, JETP **37**, 249 (1959), Soviet Phys. JETP **10**, (1960).

[3] N. N. Bogolyubov, V. V. Tolmachev, and D. V. Shirkov Новый метод в теории сверхпроводимости (New Method in the Theory of Superconductivity) Acad. Sci. Press, 1958.

[4] V. G. Solov'ev, JETP **36**, 1869 (1959), Soviet Phys. JETP **9**, 1331 (1959).

[5] L. P. Gor'kov, JETP **34**, 735 (1958), Soviet Phys. JETP **7**, 505 (1958).

Translated by J. G. Adashko
353

SOVIET PHYSICS JETP VOLUME 11, NUMBER 6 DECEMBER, 1960

CYCLOTRON RESONANCE IN GERMANIUM AND SILICON AND THE EFFECT OF NEGATIVE EFFECTIVE MASSES

YU. KAGAN

Submitted to JETP editor January 15, 1960

J. Exptl. Theoret. Phys. (U.S.S.R.) **38**, 1854-1865 (June, 1960)

We consider cyclotron resonance in semiconductors with degenerate valence bands. We have determined the frequency spectrum (effective mass spectrum) for the case where the magnetic field is along the [001] axis. We have shown that there is a branch of negative cyclotron-resonance frequencies in germanium and silicon. By solving the transport equation we have obtained an expression for the absorbed power and we have considered the problem of negative absorption.

1. INTRODUCTION

DOUSMANIS and co-workers[1] have given in a recently published paper experimental data on negative effective masses as obtained by cyclotron resonance in germanium. Using a circularly polarized high-frequency field, these authors observed, with the sign of the magnetic field negative (corresponding to resonance on electrons), a new resonance localized in a frequency interval which was appreciably different from the known values of electron-resonance frequencies. (The magnetic field was in these experiments along the [001] axis; since the electronic energy spectrum in germanium is described by a set of ellipsoids of revolution situated along the [111] axes, only one frequency value can occur in these experiments.)

The new resonance occurs not as an absorption but as an emission resonance, in strong contradistinction from those observed earlier. Strictly speaking it is observed as a gap in the absorption background which occurs when $H = 0$.

Krömer[2] has somewhat earlier drawn attention to the fact that the energy spectrum of the "heavy" holes in germanium and silicon allows a change in sign of the second derivatives of the energy with respect to the quasi-momentum, so that the components of the inverse-effective-mass tensor m_{ik}^{-1} can become negative in some region of phase space. He expressed the hypothesis that negative values of the components of m_{ik}^{-1} should manifest themselves in the occurrence of a negative resistivity under well defined circumstances. Guided by Krömer's arguments, Dousmanis and co-workers, concluded that they observed resonance on negative effective masses, in the sense of the inverse-effective-mass tensor. From our further exposition it will become clear that this point of view is, strictly speaking, incorrect.

One must note, among the other effects observed in reference 1, a new clearly resolved resonance, which corresponds to a positive effective mass smaller than the ones usually ascribed to the "light" holes.

The notes by Kaus[3] and Mattis and Stevenson[4] appeared in connection with reference 1. The former considered the problem of a negative resistance and its connection with negative effective masses. The whole consideration neglected the magnetic field, and the problem of the cyclotron resonance was not considered at all. In the second note the authors superficially analyzed the problem of negative absorption during cyclotron resonance, introducing purely formally two kinds of particles, with positive and negative effective mass.

The new results obtained by Dousmanis and coworkers force us to give a careful analysis of the whole problem connected with hole cyclotron resonance in semiconductors with degenerate bands, such as germanium and silicon. This is the more necessary as all results mentioned here are essentially not included in the analysis given up to now (see, for instance, references 5 to 8). For the sake of simplicity, all considerations in this paper will be for the case where the magnetic field H is parallel to the [001] axis. It is easy in principle to generalize this to the case of an arbitrary direction of the magnetic field.

2. QUASI-PARTICLE HODOGRAPHS: FREQUENCY (EFFECTIVE-MASS) SPECTRUM

Under the conditions which are usually realized for cyclotron resonance experiments, the inequality $kT/\hbar\omega_0 \gg 1$ is satisfied, where ω_0 is the frequency of the electric field. Since most carriers are due to the external energy source, the average energy of the particles is as a rule larger than kT. The conditions for the quasi-classical approximation are thus known to be well satisfied. We shall take this into account and analyze the hodographs—the trajectories of the quasi-particles in a magnetic field in quasi-momentum space—for degenerate valence bands in germanium and silicon. The dispersion law can in this case, if referred to the cubic axes, be written in the form[5-8]

$$\varepsilon = \frac{1}{2m_0}\{Ap^2 \pm [B^2p^4 + C^2(p_x^2p_y^2 + p_y^2p_z^2 + p_x^2p_z^2)]^{1/2}\}, \quad (2.1)$$

where **p** is the quasi-momentum of the particles, m_0 the free electron mass, and A, B, and C constants (the plus sign refers to the "light" hole band; the minus sign to the "heavy" hole band).

Let the magnetic field be along the z axis. We change to a cylindrical system of coordinates and introduce the notation

$$x = \varepsilon[p_z^2/2m_0]^{-1}, \quad y^2 = p_\perp^2/p_z^2. \quad (2.2)$$

We have then instead of (2.1)

$$x = A(y^2+1) \pm [B^2(y^2+1)^2 + C^2(^1/_8 y^2(1-\cos 4\varphi) + y^2)]^{1/2}. \quad (2.1')$$

The quantities ϵ and p_z, and therefore also x, are clearly conserved in a magnetic field. It follows from (2.1′) that similarly shaped trajectories will correspond to a fixed value of x in the planes perpendicular to p_z. To find the explicit form of the hodographs, we solve (2.1′) for y^2. After some simple transformations we find

$$y^2 = \tfrac{1}{2}\gamma_1^{-1}(-\gamma_2 \pm \sqrt{\gamma_2^2 - 4\gamma_1\gamma_3}); \quad (2.3)$$

$$\gamma_1 = A^2 - B^2 - \tfrac{1}{8}C^2 + \tfrac{1}{8}C^2\cos 4\varphi, \quad (2.4)$$

$$\gamma_2 = 2(A^2 - B^2) - C^2 - 2Ax,$$

$$\gamma_3 = A^2 - B^2 + x^2 - 2Ax.$$

We shall analyze these solutions by using the experimental values of A, B, and C for Ge and Si. There are clearly no trajectories for small x. They begin at x_1, which is the solution of the equation $\gamma_2^2 = 4\gamma_3\gamma_1$ ($\varphi = \pi/4$), in the form of four symmetric points on the bisectors. When x increases further, the area of each of the four hodographs increases up to the point x_2, when the hodographs touch the p_x and p_y axes. The value of x_2 can be found from the equation $\gamma_2^2 = 4\gamma 3\gamma_1$ ($\varphi = 0$). In the range between x_1 and x_2 there are thus four hodographs which possess mirror symmetry, with respect to the planes through the bisector (type I hodographs); the cubic symmetry is realized only by the four together (see Fig. 1).

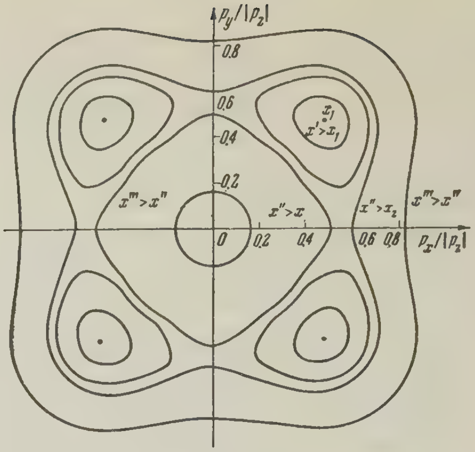

FIG. 1

When $x > x_2$ Eq. (2.3) has two solutions. We are led to two kinds of hodographs with cubic symmetry (see Fig. 1), where the area of one kind increases steadily with increasing x (type II hodographs) while the area of the second kind contracts to a point when $x = x_3$ (type III) for $x_3 = A - B$. When $x > x_3$, the double-valuedness ceases but appears again at $x = x_4 = A + B$, corresponding to hodographs of a new kind (type IV). These begin in the point y = 0 and increase steadily with increasing x. One can show that the first three hodographs refer to the "heavy" hole band and the last one to the "light" hole band. We note here a result, which is important for what follows, that when the dispersion law (2.1) holds along with hodographs which are the boundaries of an area that increases with increasing x (or ϵ for fixed p_z), there exist also hodographs with the opposite x dependence (type III).

We study now the frequency spectrum corresponding to all types of hodographs. If we consider the motion of quasi-particles in p-space for closed energy surfaces, we find easily the following expression for the frequency (see, for instance, reference 9 and also reference 10)

$$\frac{1}{\omega(\varepsilon, p_z)} = -\frac{1}{2\pi}\frac{c}{eH}\frac{\partial S(\varepsilon, p_z)}{\partial \varepsilon}, \quad (2.5)$$

where S is the area enclosed in p-space by a hodograph with a given value of ϵ and p_z. Using the notation (2.2), we get for the case under consideration

$$\frac{1}{\omega(x)} = -\frac{1}{2\pi}\frac{cm_0}{eH}\frac{\partial S'}{\partial x} \quad \text{or} \quad \frac{\omega_c}{\omega(x)} = \frac{1}{2\pi}\frac{\partial S'}{\partial x}, \quad (2.6)$$

where ω_c is the cyclotron frequency corresponding to a free positron, and

$$S' = \oint y^2 d\varphi. \quad (2.7)$$

We can write for the effective mass defined by the cyclotron resonance

$$m^*(x)/m_0 = (1/2\pi)\,\partial S'/\partial x. \tag{2.8}$$

We must draw attention to the fact that both the frequency and the effective mass are functions of x only. In other words, we shall have in p-space conical surfaces with their vertices at the point $p = 0$, corresponding to fixed values of m^* or ω/ω_c.

We consider type I hodographs corresponding to the range $x_1 < x < x_2$. We change variables: $\varphi = \pi/4 + \varphi'$. The expression for S' is then of the form

$$S' = \int_{-\varphi_1'}^{\varphi_1'} \frac{1}{\gamma_1}\sqrt{\gamma_2^2 - 4\gamma_1\gamma_3}\, d\varphi',$$

where φ_1' is determined from the condition that the expression under the radical sign vanishes

$$\varphi_1' = \tfrac{1}{2}\arcsin\sqrt{\gamma_4/\gamma_3C^2},$$

$$\gamma_4 = \gamma_2^2 - 4\gamma_3(A^2 - B^2) + \gamma_3C^2. \tag{2.9}$$

We introduce instead of φ' a variable ψ through the relation

$$\sqrt{\gamma_3C^2/\gamma_4}\,\sin 2\varphi' = \sin 2\psi.$$

The limits of integration are then equal to $\pm\pi/4$. Differentiating with respect to x under the integral sign we get after a transformation

$$\frac{\partial S'}{\partial x} = \frac{2A(-\gamma_2)}{\sqrt{\gamma_3C^2}\,(A^2 - B^2 - C^2/4)}\,\Pi_1(\vartheta, k) + \frac{4(A - x)}{\sqrt{\gamma_3C^2}}\,K(k). \tag{2.10}$$

Here K and Π_1 are respectively the complete elliptic integrals of first and third kind. The arguments ϑ and k are determined by the expressions

$$\vartheta = C^2k^2/(4A^2 - 4B^2 - C^2), \qquad k = \sqrt{\gamma_4/\gamma_3C^2}. \tag{2.11}$$

We can use one of the Legendre transformations[11] to change the complete elliptic integral of the third kind to incomplete elliptic integrals of the first and second kind. As a result, only tabulated functions will enter in the right hand side of (2.10) (see, for instance, reference 12).

An analysis of the expression obtained shows that the frequency ω decreases monotonically in the interval x_1 to x_2 tending to zero as $x \to x_2$. Let us find the limiting value of the frequency corresponding to x_1. As $x \to x_1$, we have $k \to 0$ and $\Pi_1(\vartheta, k) \to \pi/2$, $K(k) \to \pi/2$. The result is

$$\frac{\omega_c}{\omega_1} = \frac{1}{2\sqrt{\gamma_3(x_1)C^2}}\left[2(A - x_1) - \frac{A\gamma_2(x_1)}{A^2 - B^2 - C^2/4}\right].$$

We use the values of A, B, and C for germanium and silicon, which are given in the most recent papers[6,8]

	A	B	C
Ge:	13.1	8.3	12,5
Si:	4,0	1,1	4,1

(2.12)

We find then for ω_1

$$\text{Ge:}\quad \omega_1/\omega_c \approx 3{,}0, \qquad m_1^*/m_0 \approx 0.33;$$

$$\text{Si:}\quad \omega_1/\omega_c \approx 1{,}56, \qquad m_1^*/m_0 \approx 0.64. \tag{2.13}$$

One can show that (2.10) tends logarithmically to infinity as $x \to x_2$. This occurs because the condition $\partial\epsilon/\partial p_\perp = 0$ for $\varphi = 0, \pi/2, \pi, 3\pi/2$ is realized for $x = x_2$ in a saddle point. In that sense we have a situation similar to the one that occurs in metals when one changes over from closed to open surfaces (see, for instance, reference 9).

We consider now type II hodographs. We write the expression for the frequency as

$$\omega_c/\omega = (2\pi)^{-1}\int_0^{2\pi} (\partial y^2/\partial x)_\varphi\, d\varphi. \tag{2.14}$$

Using (2.3) we obtain after a number of transformations the expression ($x_2 < x < x_3$ and $x_4 < x < \infty$)

$$\frac{\omega_c}{\omega} = \frac{A}{\sqrt{(A^2 - B^2 - C^2/8)^2 - (C^2/8)^2}} + \frac{4(A - x)}{\pi\sqrt{\gamma_4}}\,K(k) - \frac{2A\gamma_2}{\pi\sqrt{\gamma_4}}\,\frac{1}{A^2 - B^2 - C^2/4}\,\Pi_1(\vartheta, k), \tag{2.15}$$

$$\vartheta = C^2/(4A^2 - 4B^2 - C^2), \quad k = \sqrt{\gamma_3C^2/\gamma_4}. \tag{2.16}$$

For $x_3 < x < x_4$ we have

$$\frac{\omega_c}{\omega} = \frac{A}{\sqrt{(A^2 - B^2 - C^2/8)^2 - (C^2/8)^2}} + \frac{4}{\pi}\,\frac{(A - x)}{\sqrt{\gamma_4 + |\gamma_3|C^2}}\,K(k) - \frac{2A\gamma_2}{\pi(A^2 - B^2)\sqrt{\gamma_4 + |\gamma_3|C^2}}\,\Pi_1(\vartheta, k),$$

$$k = \sqrt{|\gamma_3|C^2/(\gamma_4 + |\gamma_3|C^2)}, \qquad \vartheta = -C^2/4(A^2 - B^2). \tag{2.17}$$

A study of Eqs. (2.15) and (2.17) shows that the frequency increases monotonically from zero at $x = x_2$ to a value ω_∞ as $x \to \infty$. As $x \to x_2 + 0$, the period tends logarithmically to infinity.

Let us determine the value ω_∞. As $x \to \infty$ [see (2.16)]

$$k \to \sqrt{C^2/(C^2 + 4B^2)}, \tag{2.18}$$

and the frequencies and effective masses of Ge and Si are respectively equal to

$$\text{Ge:}\quad \omega_\infty/\omega_c \approx 3.6, \qquad m_\infty^*/m_0 \approx 0{,}28;$$

$$\text{Si:}\quad \omega_\infty/\omega_c \approx 2{,}16, \qquad m_\infty^*/m_0 \approx 0{,}46. \tag{2.19}$$

For type III hodographs the integration of (2.14) leads to the following final expression

$$\frac{\omega_c}{\omega} = -\left\{\frac{4(A - x)}{\pi\sqrt{\gamma_4}}\,K(k) - \frac{A}{\sqrt{(A^2 - B^2 - C^2/8)^2 - (C^2/8)^2}} + \frac{2A(-\gamma_2)}{\pi\sqrt{\gamma_4}}\,\frac{1}{A^2 - B^2 - C^2/4}\,\Pi_1(\vartheta, k)\right\}. \tag{2.20}$$

Here ϑ and k are defined according to (2.16).

The expression within the curly brackets is always positive in the range where type III hodographs occur. We are thus led to a branch of negative frequencies and, hence, of negative effective masses [defined in the sense of (2.8)]. We must note that the sign of the effective mass in (2.8) depends on the first derivative $\partial\epsilon/\partial p_\perp$ and is not directly connected with the sign of the second derivatives.

The absolute magnitude of ω increases steadily in the region considered, from zero (at $x = x_2$) to a limiting value ω_3 corresponding to the disappearance of this kind of hodograph ($x = x_3$). At $x = x_3 \equiv A - B$ the quantity k vanishes and one checks easily that

$$\Pi_1(\vartheta, 0) = \pi / 2\sqrt{1+\vartheta}. \qquad (2.21)$$

Substituting this value into (2.20) we get after some transformations the following simple formula for ω_3

$$\omega_3 / \omega_c = -(C^2 + 2B^2 - 2AB) / 2B. \qquad (2.22)$$

This expression depends only on the constants in the energy spectrum. Using the values (2.12) we find

$$\text{Ge:} \qquad \omega_3 / \omega_c \approx -4.6, \quad m_3^* / m_0 \approx -0.22;$$

$$\text{Si:} \qquad \omega_3 / \omega_c \approx -4.7, \quad m_3^* / m_0 \approx -0.21. \qquad (2.23)$$

For type IV hodographs the frequency is determined by the same expression (2.20). Now, however, $x_4 < x < \infty$, and the expression within the curly brackets is always negative. We are led to a branch of positive frequencies corresponding to the "light" hole band. Hodographs of this type appear first at $x = x_4 \equiv A + B$ with a finite frequency ω_4. When x increases further, the frequency decreases steadily to a value ω'_∞.

At $x = x_4$ the quantity k tends again to zero and Π_1 attains the value (2.21). After an appropriate transformation we are led to the expression

$$\omega_4 / \omega_c = (C^2 + 2B^2 + 2AB) / 2B. \qquad (2.24)$$

For germanium and silicon we have respectively

$$\begin{aligned} &\text{Ge:} \qquad \omega_4 / \omega_c \approx 30.8, \quad m_4^* / m_0 \approx 0.032; \\ &\text{Si:} \qquad \omega_4 / \omega_c \approx 12.7, \quad m_4^* / m_0 \approx 0.078. \end{aligned} \qquad (2.25)$$

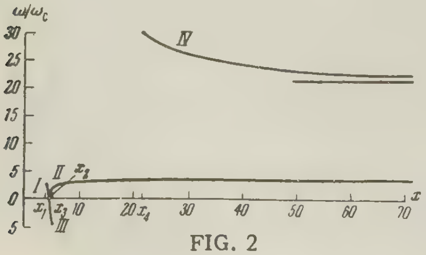

FIG. 2

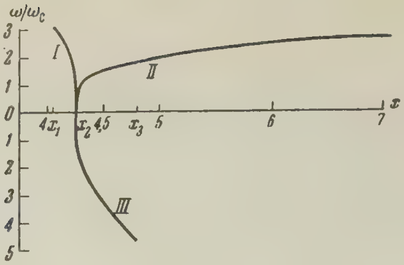

FIG. 3

As $x \to \infty$ the quantity k tends to the value (2.17) and for ω'_∞ we find from (2.20)

$$\begin{aligned} &\text{Ge:} \qquad \omega'_\infty / \omega_c \approx 22.3, \quad m^{*\prime}_\infty / m_0 \approx 0.045; \\ &\text{Si:} \qquad \omega'_\infty / \omega_c \approx 5.7, \quad m^{*\prime}_\infty / m_0 \approx 0.18. \end{aligned} \qquad (2.26)$$

In Figs. 2 and 3 we have given the whole frequency spectrum corresponding to the valence band of germanium with **H** along the [001] axis. Clearly the behavior of the cyclotron resonance depends essentially upon the form of this spectrum. In particular, the appearance in reference 1 of negative effective masses is intimately connected with the negative branch of frequencies corresponding to type III hodographs. The presence of three free ends of frequency branches, where the frequency attains a maximum absolute value, is noteworthy.

3. SOLUTION OF THE TRANSPORT EQUATION

As was noted in the preceding section, the condition for quasi-classical behavior is satisfied under the normal experimental conditions for cyclotron resonance. We restrict ourselves therefore to a consideration of the classical transport equation

$$\frac{\partial f}{\partial t} + \mathbf{v}\nabla f + \frac{\partial f}{\partial \mathbf{p}}\left(e\mathbf{E} + \frac{e}{c}[\mathbf{v}\times\mathbf{H}]\right) = L(f - f^{(0)}) + N - M,$$
$$\mathbf{v} = \partial\varepsilon / \partial\mathbf{p}. \qquad (3.1)$$

Here L is a linear operator corresponding to the collision integral, and N and M are terms describing respectively the creation and absorption of quasi-particles and referred to a unit volume (M is generally speaking a functional that depends on the distribution function of all the kinds of quasi-particles).

The need for introducing N and M into Eq. (3.1) is connected with the fact that, because of the low temperature, the cyclotron resonance experiments are performed on non-equilibrium carriers which are produced either by illumination of the semiconductor or by secondary ionization when the carriers collide with impurity atoms. In order to be specific we shall assume that the carriers are excited by illumination. We can write the solution of Eq. (3.1) in the form

$$f = f_0(\mathbf{r}, \mathbf{p}) + f_1(\mathbf{r}, \mathbf{p}, t),$$

where f_0 is the stationary solution corresponding to $\mathbf{E} = 0$. Assuming that the diffusion length is large compared to the mean free path and that the electrical field is sufficiently small, we can use the fact that the operator L is linear to write down the following set of equations

$$\mathbf{v}\nabla f_0 + \frac{e}{c}[\mathbf{v}\times\mathbf{H}]\frac{\partial f_0}{\partial \mathbf{p}} = L(f_0 - f^{(0)}) + N - M, \qquad (3.2)$$

$$\frac{\partial f_1}{\partial t} + \frac{e}{c}[\mathbf{v}\times\mathbf{H}]\frac{\partial f_1}{\partial \mathbf{p}} + e\mathbf{E}\frac{\partial f_0}{\partial \mathbf{p}} = L(f_1). \qquad (3.3)$$

We can easily transform Eq. (3.3) into

$$\frac{\partial f_1}{\partial t} + \omega\frac{\partial f_1}{\partial \psi} + e\mathbf{E}\frac{\partial f_0}{\partial \mathbf{p}} = L(f_1), \qquad (3.4)$$

where ω is the frequency of the rotation of the quasi-particles in the azimuthal plane, which is determined from (2.6), and ψ is defined by the expression

$$\psi = \frac{m_0}{m^*}\int_0^{\varphi}\left(\frac{\partial y^2}{\partial x}\right)_{\varphi, p_z} d\varphi.$$

The solution of Eq. (3.2) when the creation and absorption terms (and the appropriate boundary conditions) are present leads to a value of f_0 which is in general a function of $\mathbf{p}$. It is therefore necessary to find the solution of (3.4) for an arbitrary dependence $f_0(\mathbf{p})$. ($\mathbf{r}$ enters into the equation purely as a parameter and will not be specially designated in the following.)

The problem of solving the transport equation for an arbitrary dispersion law $\epsilon(\mathbf{p})$ and of applying it to galvanomagnetic phenomena in metals was first considered consistently in a paper by I. M. Lifshitz, Azbel', and Kaganov[13] and also by McClure.[14] We use in the following a method for solving (3.4) which is along the same principles as the method given in these papers.

At the temperatures under consideration the carriers are scattered by impurities. We use this fact and introduce instead of $L(f_1)$ approximately $-f_1/\tau(\mathbf{p})$. Taking into consideration that $\mathbf{E} \sim e^{i\omega_0 t}$ and thus $f_1 \sim e^{i\omega_0 t}$, we change (3.4) into

$$\omega\frac{\partial f_1}{\partial \psi} + f_1\frac{1 + i\omega_0\tau}{\tau} + e\mathbf{E}\frac{\partial f_0}{\partial \mathbf{p}} = 0.$$

A solution of this equation which satisfies the obvious periodicity condition can be written in the form

$$f_1 = -\frac{e\mathbf{E}}{\omega}\int_{-\infty}^{\psi}\frac{\partial f_0}{\partial \mathbf{p}}\exp\left\{-\frac{1}{\omega}\int_{\psi'}^{\psi}\frac{d\psi}{\tau}(1 + i\omega_0\tau)\right\}d\psi'. \qquad (3.5)$$

We introduce instead of τ some value of this quantity averaged over the hodograph, according to

$$\oint d\psi/\tau(\mathbf{p}) = 1/\tau' \qquad (\tau' = \tau(p_z, \varepsilon)).$$

We expand $\partial f_0/\partial \mathbf{p}$ in a Fourier series in ψ

$$\partial f_0/\partial \mathbf{p} = \sum_{m=-\infty}^{\infty} \mathbf{F}\; e^{im\psi}. \qquad (3.6)$$

After some simple manipulations we get then

$$f_1 = -e\mathbf{E}\sum_{m=-\infty}^{\infty}\mathbf{F}_m\tau' e^{im\psi}/(1 + i\omega_0\tau' + im\omega\tau').$$

We can write the corresponding expression for the current in the form

$$\mathbf{j} = -2\frac{e^2E_\alpha}{(2\pi\hbar^{3}}\sum_{m=-\infty}^{\infty}\int d^3p\tau'\mathbf{v}F_{m\alpha}e^{im\psi}/(1 + i\omega_0\tau' + im\omega\tau'). \qquad (3.7)$$

(Summation over repeated Greek indices is implied throughout.)

We expand $\mathbf{v}$ in a Fourier series in ψ and perform in (3.7) the integration over ψ. Returning again to the integration over the whole phase volume, we get

$$\mathbf{j} = -2\frac{e^2E_\alpha}{(2\pi\hbar)^3}\sum_{m=-\infty}^{\infty}\int d^3p\tau'\mathbf{v}^*_m F_{m\alpha}/(1 + i\omega_0\tau' + im\omega\tau'). \qquad (3.7')$$

Let us determine the power absorbed per unit volume of the semiconductor. We consider the case of circular polarization of the electrical field in a plane perpendicular to the magnetic field, i.e., $\mathbf{E}_y = i\mathbf{E}_x$. Omitting the intermediate steps, we can then write the final expression in the form

$$\begin{aligned} P = \tfrac{1}{2}\,\mathrm{Re}(\mathbf{j}\mathbf{E}^*) = \\ = -2\frac{e^2E_0^2}{(2\pi\hbar)^3}\sum_{m=1}^{\infty}\int d^3p\tau'\{[1 + (m\omega\tau')^2 - (\omega_0\tau')^2]^2 \\ + 4(\omega_0\tau')^2\}^{-1}\times\{(v_{mx}F_{mx} + v^*_{my}F_{my})[1 + (m\omega\tau')^2 + (\omega_0\tau')^2] \\ + 2m\omega_0\omega\tau'^2\,\mathrm{Im}(v_{mx}F_{my} - v^*_{my}F_{mx})\} \qquad (3.8) \end{aligned}$$

Equation (3.8) enables us to analyze the problem for any type of $\mathbf{p}$-dependence of f_0.

We restrict ourselves to the case where the light is incident along the direction of the magnetic field (as was the case in the experiment by Dousmanis and co-workers[1]). Taking into account that $\omega_0\tau' \gg 1$ and that in (3.8) the main contribution comes from carriers with ω near to ω_0, we can assume then that

$$f_0 = f_0(\varepsilon, p_z). \qquad (3.9)$$

Equation (3.8) simplifies then and becomes equal to

$$\begin{aligned} P = -2\frac{e^2E_0^2}{(2\pi\hbar)^3}\sum_{m=1}^{\infty}\int d^3p\left(\frac{\partial f_0}{\partial \varepsilon}\right)_{p_z}\frac{\tau'}{[1 + (m\omega\tau')^2 - (\omega_0\tau')^2]^2 + 4(\omega_0\tau')^2} \\ \times\{(|v_{mx}|^2 + |v_{my}|^2)[1 + (m\omega'\tau')^2 + (\omega_0\tau')^2] \\ + 4m\omega_0\omega\tau'^2\,\mathrm{Im}(v_{mx}v_{my})\}. \qquad (3.10) \end{aligned}$$

When the hodographs possess a symmetry axis of the fourth order, one can transform the expression obtained into the form

$$P = -4\frac{e^2E_0^2}{(2\pi\hbar)^3}\sum_{m=0}^{\infty}\int d^3p v^2_{2m+1,x}L_{2m+1}\left(\frac{\partial f_0}{\partial \varepsilon}\right)_{p_z}, \qquad (3.11)$$

$$L_{2m+1} = \tau' \frac{1+[\omega_0+(-1)^m(2m+1)\,\omega]^2\tau'^2}{[1+(2m+1)^2(\omega\tau')^2-(\omega_0\tau')^2]^2+4(\omega_0\tau')^2}. \qquad (3.12)$$

We use the expressions for the velocity components, which can easily be found from the equations of motion

$$v_x = (1/m^*)(\partial p_y/\partial\psi)_{p_z,\varepsilon}, \quad v_y = -(1/m^*)(\partial p_x/\partial\psi)_{p_z,\varepsilon}.$$

Taking into account that all types of hodographs possess mirror symmetry, we find

$$v_{nx}\Big/\left[\frac{|p_z|}{m_0}\right] = \frac{n}{2\pi}\,\frac{\omega}{\omega_c}\int_0^{2\pi}\frac{p_y}{|p_z|}\sin n\psi d\psi \equiv f(x),$$

$$v_{ny}\Big/\left[\frac{|p_z|}{m_0}\right] = -\frac{in}{2\pi}\,\frac{\omega}{\omega_c}\int_0^{2\pi}\frac{p_x}{|p_z|}\cos n\psi d\psi \equiv f'(x). \qquad (3.13)$$

Let us expand $y = p_\perp/|p_z|$ in a cosine Fourier series (when considering type I hodographs we assume that the origin is chosen on the bisectors in the points where the hodographs start)

$$y = \sum_{m=0}^{\infty} y_m(x)\cos m\varphi. \qquad (3.14)$$

One shows easily that the Fourier components of the velocity are determined by the quantities $y_n(x)$.

We change in (3.10) and (3.11) to the integration variables ϵ, p_z, and ψ. Taking into account the fact that $\omega(x)$ is not single-valued for the "heavy" hole band we have

$$\int d^3p \ldots = 2\pi\int_{-\infty}^{\infty} dp_z \Big\{4\int_{x_1p_z^2/2m_0}^{x_2p_z^2/2m_0} m^* d\varepsilon \ldots + \int_{x_2p_z^2/2m_0}^{\infty} m^* d\varepsilon \ldots$$
$$+ \int_{x_2p_z^2/2m_0}^{x_3p_z^2/2m_0} (-m^*)\,d\varepsilon \ldots\Big\}; \qquad (3.15)$$

and for the "light" hole band

$$\int d^3p \ldots = 2\pi\int_{-\infty}^{\infty} dp_z \int_{x_4p_z^2/2m_0}^{\infty} m^* d\varepsilon \ldots \qquad (3.15')$$

[In (3.15) the m^*'s are in the sequence of integrals over $d\epsilon$ determined with respect to the first, second, and third branch of the frequency spectrum.] The infinite upper limit was chosen in the conventional way: we assume that the distribution function vanishes with increasing $p_z(\epsilon)$ before any deviations from (2.1) in the dispersion law become apparent.

We substitute (3.13) into (3.10) and (3.11) and use (3.15). One sees easily that the integrand turns then out to be proportional to the frequency. As a result, singularities occur sometimes in the resonance spectrum curve, not only at extrema of the frequency, but also near maximum values at the limits of the frequency-spectrum branches. To be sure, the realization of such a possibility, together with the shape of the singularity, depends essentially on the steepness of the change in frequency and on the character of the behavior of the complete integrand near these points. In particular, the position is alleviated when the second end point of the branch corresponds to zero frequency.

We have shown in the preceding section that for the dispersion law (2.1) there are three such points in the frequency spectrum. If we turn to the cyclotron resonance spectrum in germanium, which was obtained in reference 1, it turns out that ω_3 is the same as the observed resonance frequency for negative effective masses, and that ω_4 lies near the frequency of the second new resonance, which corresponded to holes with m^* lower than the effective mass of the "light" holes. [We are dealing here with the normally determined values — they are the same as the m'_∞ in (2.26)].

The frequency ω_1 is near ω_∞, the frequency of the usual "heavy" holes [compare (2.13) and (2.19)]. Since the latter corresponds on the spectral curve to a wide resonance with a large intensity, the resonance at frequencies near ω_1 cannot appear explicitly. It is, however, possible that there are some singularities in the resonance curve near ω_∞ which are connected just with the first frequency branch.

We note that since the hodographs connected with the first frequency branch do not possess a symmetry axis, even harmonic frequencies may occur under well defined conditions near the frequency of the "heavy" holes.

4. CHARACTER OF THE CYCLOTRON SPECTRUM

Let us briefly analyze the conditions under which the usual increase in absorption near a resonance can be replaced by a decrease (with respect to the level of absorption for $H = 0$) or even change over to an emission spectrum. It can be seen explicitly from (3.10) and (3.11) that P is always positive if $\partial f_0/\partial\epsilon < 0$. In order that the sign of P change it is thus at any rate necessary that there be in p space a region with the opposite character of level population. This condition is, however, not sufficient. The fact is that the inevitable decrease of f_0 at sufficiently large energies leads in the most favorable case to the simultaneous occurrence of regions with $\partial f_0/\partial\epsilon > 0$ and $\partial f_0/\partial\epsilon < 0$. Larger values of the energy correspond, however, to a larger phase volume. In the case under consideration this leads, in particular, to $P > 0$ for any form of the function $f_0(\epsilon)$* (see below), if f_0 is a function of the energy only.

For the sake of simplicity we shall consider only the first harmonic. Using (3.10), (3.11), (3.12), and (3.15) we can write the expression for the "heavy" hole band in the form

$$P_1 = -\frac{4\pi e^2 E_0^2}{m_0 (2\pi\hbar)^3} \int\limits_0^\infty dp_z p_z^2 \left\{ 4 \int\limits_{x_1 p_z^2/2m_0}^{x_2 p_z^2/2m_0} \left(\frac{\partial f_0}{\partial \varepsilon}\right)_{p_z} \frac{\omega}{\omega_c}\ y_0^2 L_1' d\varepsilon \right.$$

$$+ \int\limits_{x_2 p_z^2/2m_0}^{\infty} \left(\frac{\partial f_0}{\partial \varepsilon}\right)_{p_z} \frac{\omega}{\omega_c}\ y_0^2 L_1' d\varepsilon$$

$$\left. + \int\limits_{x_2 p_z^2/2m_0}^{x_3 p_z^2/2m_0} \left(\frac{\partial f_0}{\partial \varepsilon}\right)_{p_z} \left(-\frac{\omega}{\omega_c}\right) y_0^2 L_1' d\varepsilon \right\}. \tag{4.1}$$

[The expression for L_1' can be obtained by comparing (4.1) with (3.10) and taking (3.13) into account.] If f_0 is not an even function of p_z (in the given point in the volume of the semiconductor) we must understand by f_0 in (4.1) (and in the following) the quantity $\frac{1}{2}[f_0(-p_z) + f_0(p_z)]$.

We integrate by parts (with respect to ϵ) in the expression obtained. One sees easily that the integrands tend to zero for all finite limits of integration. Changing from ϵ to the variable x [see (2.2)] we get then

$$P_1 = \frac{4\pi e^2 E_0^2}{m_0 (2\pi\hbar)^3} \int\limits_0^\infty dp_z p_z^2 \left\{ 4 \int\limits_{x_1}^{x_2} f_0 \frac{\partial}{\partial x}\left[\frac{\omega}{\omega_c}\ y_0^2 L_1'\right] dx \right.\cdot$$

$$\left. + \int\limits_{x_2}^{\infty} f_0 \frac{\partial}{\partial x}\left[\frac{\omega}{\omega_c}\ y_0^2 L_1'\right] dx + \int\limits_{x_2}^{x_3} f_0 \frac{\partial}{\partial x}\left[\left(-\frac{\omega}{\omega_c}\right) y_0^2 L_1'\right] dx \right\}. \tag{4.2}$$

Since f_0 is essentially positive, the negative contribution to p_1 can only be connected with regions where the derivative

$$\frac{\partial}{\partial x}\left[\left|\frac{\omega}{\omega_c}\right| y_0^2 L_1'\right] = \left|\frac{\omega}{\omega_c}\right| L_1' \frac{dy_0^2}{dx} + y_0^2 \frac{\partial}{\partial x}\left[\left|\frac{\omega}{\omega_c}\right| L_1'\right] \tag{4.3}$$

becomes negative.

Let us consider the region of negative frequencies ($x_2 < x < x_3$). In that region (and only in that region) $\partial^2 y_0^2/\partial x < 0$. If we take into account that $y_0(x) \rightarrow 0$ as $x \rightarrow x_3$, it follows from (4.3) that the integrand in the last integral in (4.2) becomes negative near x_3. When ω_3 approaches ω_0 this can, for a well defined form of the function f_0, correspond to a decrease in p_1 or even to a negative value of that quantity.

We give here an approximate discussion that enables us to make some observations about the corresponding form of the function f_0. To do this we consider a value of the magnetic field which selects an interval of negative frequencies far from the end point of the branch. Let $\omega_0 \tau' \gg 1$ and let the integrand in (4.1) change sufficiently smoothly in the range of x defined by the resonance denominator in L_1'. Neglecting the first two integrals and changing first the order of integration in (4.1), we find after some manipulations

$$P_1 \approx \text{const} \cdot \frac{y_0^2(x_0)}{x_0^{5/2}} \left|\frac{\omega(x_0)}{\omega_c}\right| \cdot \left|\frac{d\omega}{dx}\right|^{-1} \int\limits_0^\infty d\varepsilon\, \varepsilon^{3/2} \left(-\frac{\partial f_0}{\partial \varepsilon}\right)_{p_z} \Bigg|_{p_z^2 = 2m_0\varepsilon/x_0}. \tag{4.4}$$

Here x_0 is the value of x for which the frequency ω is equal to ω_0.

One can consider f_0 in (4.1) to be a function of p_z^2. Taking this into account, we have

$$\left(-\frac{\partial f_0}{\partial \varepsilon}\right)_{p_z}\Bigg|_{p_z^2 = 2m_0\varepsilon/x_0} = -\frac{df_0}{d\varepsilon} + \frac{2m_0}{x_0}\left(\frac{\partial f_0}{\partial p_z^2}\right)_\varepsilon \Bigg|_{p_z^2 = 2m_0\varepsilon/x_0}.$$

We substitute this expression into (4.4) and integrate the first term by parts

$$P_1 \sim \int\limits_0^\infty d\varepsilon \left\{\frac{3}{2}\varepsilon^{1/2} f_0 + \frac{2m_0 \varepsilon^{3/2}}{x_0}\left(\frac{\partial f_0}{\partial p_z^2}\right)_\varepsilon\right\}\Bigg|_{p_z^2 = 2m_0\varepsilon/x_0}.$$

It can be clearly seen from this expression that if f_0 depends on the energy only, p_1 will always be positive. For an emission spectrum to occur in the frequency interval considered, it is thus at any rate necessary, that, together with the regions where $(\partial f_0/\partial\epsilon)_{p_z} > 0$, there exist a region where $(\partial f_0/\partial p_z^2)_\epsilon < 0$, or more precisely where

$$\frac{4}{3}\frac{m_0\varepsilon}{x_0}\left(\frac{\partial \ln f_0}{\partial p_z^2}\right)_\varepsilon \Bigg|_{p_z^2 = 2m_0\varepsilon/x_0} < -1. \tag{4.5}$$

We note that, other things being equal, inequality (4.5) is best satisfied for the minimum values of x_0.

The condition obtained here is physically connected with the necessity of a steep decrease in the number of particles which give a contribution to p_1 in that energy range where $(\partial f_0/\partial\epsilon)_{p_z} < 0$. (It is clear that an equivalent result might be obtained if the dispersion law (2.1) were changed in that energy range in such a way that the given interval in the frequency spectrum would vanish. Compare a similar remark in reference 4.)

We must note that the ability to emit rather than absorb energy in cyclotron resonance experiments for an arbitrary initial non-equilibrium distribution is, apparently, not an exclusive privilege of the negative frequency range. In particular, an approximate analysis similar to the one given in the foregoing might also be used for the first frequency branch. (Although the first term in (4.3) is positive, the second term, which can change sign, will lead to a negative value of the integrand when the distribution has an inverse character.) We require here, to be sure, additional limitations on the function f_0, which are connected, moreover, with the fact that the second branch possesses also the same frequency interval.

---

*We assume all the time that f_0 vanishes with increasing energy before the dispersion law changes appreciably.

The author uses this occasion to express his sincere gratitude to L. D. Landau and M. I. Kaganov for valuable discussions of the results of this paper.

---

[1] Dousmanis, Duncan, Thomas, and Williams, Phys. Rev. Letters **1**, 404 (1958); G. C. Dousmanis, Phys. Rev. Letters **1**, 55 (1958).

[2] H. Krömer, Phys. Rev. **109**, 1856 (1958).

[3] P. Kaus, Phys. Rev. Letters **3**, 20 (1959).

[4] D. C. Mattis and M. J. Stevenson, Phys. Rev. Letters **3**, 18 (1959).

[5] Dresselhaus, Kip, and Kittel, Phys. Rev. **98**, 368 (1955).

[6] Dexter, Zeiger, and Lax, Phys. Rev. **104**, 637 (1956).

[7] Zeiger, Lax, and Dexter, Phys. Rev. **105**, 495 (1957).

[8] B. Lax, Rev. Mod. Phys. **30**, 122 (1958).

[9] I. M. Lifshitz and M. I. Kaganov, Usp. Fiz. Nauk **69**, 419 (1959), Soviet Phys. Uspekhi **2**, 831 (1960).

[10] W. Shockley, Phys. Rev. **79**, 191 (1950)

[11] W. Magnus and F. Oberhettinger, Formeln und Sätze für die speziellen Funktionen der mathematischen Physik, Springer, Berlin, 1948, p. 138.

[12] E. Jahnke and F. Emde, Tables of Functions, Teubner, Leipzig, 1933.

[13] Lifshitz, Azbel', and Kaganov, JETP **31**, 63 (1956), Soviet Phys. JETP **4**, 41 (1957).

[14] J. W. McClure, Phys. Rev. **101**, 1642 (1956).

Translated by D. ter Haar
354

SOVIET PHYSICS JETP VOLUME 11, NUMBER 6 DECEMBER, 1960

BREMSSTRAHLUNG AT THE BOUNDARY OF A MEDIUM WITH ACCOUNT OF MULTIPLE SCATTERING

I. I. GOL'DMAN

Physical Institute, Academy of Sciences, Armenian S.S.R.

Submitted to JETP editor January 16, 1960

J. Exptl. Theoret. Phys. (U.S.S.R.) 38, 1866-1869 (June, 1960)

An investigation is carried out of the composition of bremsstrahlung appearing at the boundary of a medium with account of the Landau-Pomeranchuk-Migdal effect.

As is well known,[1,2] multiple scattering leads to the suppression of bremsstrahlung of extremely relativistic electrons in a dense medium. Quantitative calculation of this effect was given by Migdal[3,4] for an unbounded medium. In the present paper, the effect of the boundary of the medium on this phenomenon is investigated.

1. Let a relativistic electron move with velocity $\mathbf{v}_0$ and enter normally on the surface of a semi-infinite medium at the time $t = 0$. The intensity of the radiation with frequency ω in the direction $\mathbf{n}$ is given by the expression:

$$E_{\mathbf{n}\omega} = \frac{e^2\omega^2}{4\pi^2c^3}\int_{-\infty}^{\infty} dt_1 \int_{-\infty}^{\infty} dt_2 \mathbf{A}^*(1)\mathbf{A}(2), \qquad \mathbf{A} = [\mathbf{n}\times\mathbf{v}]\,e^{i(\mathbf{kr}-\omega t)}, \tag{1}$$

$\mathbf{r}$ and $\mathbf{v}$ are the coordinate and velocity of the particle at the time t, $\mathbf{k} = \mathbf{n}\omega/c$ is the wave vector of the photon. If we divide the linear portions of the path into integrals over t_1 and t_2, then $E_{\mathbf{n}\omega}$ is divided into three components:

$$E_{\mathbf{n}\omega} = E'_{\mathbf{n}\omega} + E''_{\mathbf{n}\omega} + E'''_{\mathbf{n}\omega}.$$

$$E'_{\mathbf{n}\omega} = \frac{e^2\omega^2}{4\pi^2c^3}\int_{-\infty}^{0} dt_1 \int_{-\infty}^{0} dt_2 \mathbf{A}^*(1)\mathbf{A}(2) = \frac{e^2}{4\pi^2c^3}\frac{[\mathbf{n}\times\mathbf{v}_0]^2}{(1-\mathbf{nv}_0/c)^2}, \tag{2}$$

$$E'''_{\mathbf{n}\omega} = \frac{e^2\omega^2}{2\pi^2c^3}\operatorname{Re}\int_0^{\infty} dt_1 \int_{t_1}^{\infty} dt_2 \mathbf{A}^*(1)\mathbf{A}(2) \tag{3}$$

refer to $t < 0$ and $t > 0$, respectively, and

$$E''_{\mathbf{n}\omega} = \frac{e^2\omega^2}{2\pi^2c^3}\operatorname{Re}\int_{-\infty}^{0} dt_1 \int_0^{\infty} dt_2 \mathbf{A}^*(1)\mathbf{A}(2)$$

$$= -\frac{\epsilon^2\omega}{2\pi^2c^3}\operatorname{Im}\int_0^{\infty} dt_2 \frac{\mathbf{A}(2)[\mathbf{n}\times\mathbf{v}_0]}{1-\mathbf{nv}_0/c} \tag{4}$$

is the interference term.

The term $E'_{\mathbf{n}\omega}$ contains only the linear portions of the path, while the other two terms depend on the motion of the particle in the medium, and must be averaged over all possible trajectories. Following Migdal,[3] we consider a distribution function $w(t, \mathbf{r}, \mathbf{v}; \mathbf{v}_0)$ which satisfies the kinetic equation

$$\frac{\partial w}{\partial t} + \mathbf{v}\frac{\partial w}{\partial \mathbf{r}} = nv\int \sigma(\mathbf{v}, \mathbf{v}')[w(\mathbf{v}') - w(\mathbf{v})]\,d\mathbf{v}' \tag{5}$$

(n is the number of atoms per unit volume, σ is the elastic scattering cross section), with the initial condition

$$w(0, \mathbf{r}, \mathbf{v}; \mathbf{v}_0) = \delta(\mathbf{r})\,\delta(\mathbf{v}-\mathbf{v}_0). \tag{6}$$

Averaging of (3) and (4) yields

$$E''_{\mathbf{n}\omega} = -\frac{e^2\omega}{2\pi^2c^3}\operatorname{Im}\int_0^{\infty}\int d\mathbf{r}d\mathbf{v}dt\,w(t, \mathbf{r}, \mathbf{v}; \mathbf{v}_0)\frac{[\mathbf{n}\times\mathbf{v}_0][\mathbf{n}\times\mathbf{v}]}{1-\mathbf{nv}_0/c}, \tag{7}$$

$$E'''_{\mathbf{n}\omega} = \frac{e^2\omega^2}{2\pi^2c^3}\operatorname{Re}\int_0^{T}\int d\mathbf{r}d\mathbf{v}dt\,w(t, \mathbf{r}, \mathbf{v}; \mathbf{v}_0)\int_0^{\infty}\int d\tau d\boldsymbol{\rho} d\mathbf{v}'w$$

$$\times(\tau, \boldsymbol{\rho}, \mathbf{v}'; \mathbf{v})[\mathbf{n}\times\mathbf{v}][\mathbf{n}\times\mathbf{v}']\,e^{i(\mathbf{k}\boldsymbol{\rho}-\omega\tau)}. \tag{8}$$

The latter expression leads to Migdal's result for radiation in a homogeneous medium after a time T; it may seem necessary to use the sum of the remaining terms E' and E'' in the calculation of the boundary effect. One can verify that this is not so, however, by considering the limiting case of a low-density medium, $n \to 0$. The radiation at the boundary should vanish, while $E' + E''$ approaches a finite limit. This paradox is resolved if we note that the formally infinite (for $T \to \infty$) quantity E''' contains a finite part which pertains to radiation at the boundary. In order to separate it, we make use of the following procedure: we introduce damping, assuming that the radiating charge falls off for $t > 0$: $e = e_0\exp(-\delta t)$. Then E''' can be represented for small δ in the form $E''' = A\delta^{-1} + B$. The first term gives the radiation in the unbounded medium; the second component represents the desired contribution to the radiation due to the boundary:

$$\Delta E''' = B = -\frac{e^2\omega^2}{2\pi^2c^3}\lim_{\delta\to 0}\operatorname{Re}\int_0^\infty \delta e^{-2\delta t}dt\int d\mathbf{r}d\mathbf{v}w(t,\ \mathbf{r},\ \mathbf{v};\ \mathbf{v}_0)$$

$$\times\int_0^\infty \tau d\tau\int d\boldsymbol{\rho}d\mathbf{v}'w(\tau,\ \boldsymbol{\rho},\ \mathbf{v}';\ \mathbf{v})[\mathbf{n}\times\mathbf{v}][\mathbf{n}\times\mathbf{v}']e^{i(\mathbf{k}\boldsymbol{\rho}-\omega\tau)}. \quad (9)$$

2. In the kinetic Eq. (5) we change to the small angle approximation,[3] setting

$$\mathbf{v} = v\mathbf{n}(1-\theta^2/2)+v\boldsymbol{\theta} \qquad (\mathbf{n}\boldsymbol{\theta}=0). \quad (10)$$

For the function

$$u(t,\ \boldsymbol{\theta};\ \boldsymbol{\theta}_0) = v^2\int w(t,\ \mathbf{r},\ \mathbf{v};\ \mathbf{v}_0)e^{i(\mathbf{kr}-\omega t)}d\mathbf{r} \quad (11)$$

we get from (5) the equation

$$\frac{\partial u(\boldsymbol{\theta})}{\partial t}+\frac{i\omega}{2}(\lambda^2+\theta^2)u(\boldsymbol{\theta}) = nv\int\sigma(\boldsymbol{\theta}-\boldsymbol{\theta}')[u(\boldsymbol{\theta}')-u(\boldsymbol{\theta})]d\boldsymbol{\theta}'$$

[for brevity, we write $u(\theta)$ for $u(t,\ \theta;\ \theta_0)$; $\lambda = mc^2/E$] with the initial condition

$$u(0,\ \boldsymbol{\theta};\ \boldsymbol{\theta}_0) = \delta(\boldsymbol{\theta}-\boldsymbol{\theta}_0). \quad (13)$$

We proceed in (12) to the Fokker-Planck approximation*

$$\frac{\partial u}{\partial t}+\frac{i\omega}{2}(\lambda^2+\theta^2)u = q\Delta_\theta u. \quad (14)$$

We seek the solution of this equation in the form

$$u = \exp[\alpha(t)\theta^2+\beta(t)\boldsymbol{\theta}\boldsymbol{\theta}_0+\gamma(t)]. \quad (15)$$

The system of equations obtained for α, β, γ

$$\dot{\alpha}+\frac{i\omega}{2} = 4q\alpha^2, \qquad \dot{\beta} = 4q\alpha\beta^2,$$
$$\dot{\gamma} = q(\theta_0^2\beta^2+4\alpha)-\frac{1}{2}i\omega\lambda^2 \quad (16)$$

has the following solution, which satisfies the initial condition (13):

$$\alpha = \sqrt{i\omega/2q}\coth\sqrt{2i\omega q}\,t, \quad \beta = \sqrt{i\omega/2q}\sinh^{-1}\sqrt{2i\omega q}\,t,$$

$$\gamma = -i\omega\lambda^2 t/2-\ln\sinh\sqrt{2i\omega q}t+\theta_0^2\sqrt{i\omega/8q}\coth\sqrt{2i\omega q}\,t$$

$$+\ln\sqrt{i\omega/8\pi^2 q}. \quad (17)$$

If we substitute this solution of the kinetic equation in Eqs. (7) and (8), we get

$$E''_{\mathbf{n}\omega} = -\frac{e^2\omega^2}{\pi^2 c}\frac{1}{\lambda^2+\theta_0^2}\operatorname{Im}\int_0^\infty d\tau f(\tau,\ \theta_0), \quad (18)$$

$$E'''_{\mathbf{n}\omega} = \frac{e^2\omega^2}{2\pi^2 c}\int dtd\boldsymbol{\rho}d\mathbf{v}w(t,\ \boldsymbol{\rho},\ \mathbf{v};\ \mathbf{v}_0)\operatorname{Re}\int_0^\infty d\tau f(\tau,\ \theta), \quad (19)$$

where the following notation has been introduced:

$$\int d\boldsymbol{\theta}'(\boldsymbol{\theta}\boldsymbol{\theta}')u(\tau,\ \boldsymbol{\theta}';\ \boldsymbol{\theta}) \equiv f(\tau,\ \theta)$$
$$= \frac{2i}{\omega}e^{-i\omega\lambda^2\tau/2}\frac{d}{d\tau}\exp\left(-\theta^2\sqrt{\frac{i\omega}{8q}}\tanh\sqrt{2i\omega q}\tau\right). \quad (20)$$

3. Equation (19), integrated over $\mathbf{n}$, gives Migdal's result:

$$E_\omega = \int E'''_{\mathbf{n}\omega}d\mathbf{n} = \int dt\ \frac{8e^2 q}{3\pi c\lambda^2}\Phi(s), \quad (21)$$

$$\Phi(s) = 12s^2\int_0^\infty\left(\coth x-\frac{1}{x}\right)e^{-2sx}\sin 2sxdx, \qquad s = \frac{\lambda^2}{8}\sqrt{\frac{\omega}{q}}.$$

The radiation connected with the boundary is the sum of three terms which, after transformation to dimensionless variables

$$\tau = x/\sqrt{2\omega qi}, \qquad \theta_0^2/\lambda^2 = z, \qquad \sigma = 2(1+i)s$$

have the following form:

$$E'_{\mathbf{n}\omega} = \frac{e^2}{\pi^2 c\lambda^2}\frac{z}{(1+z)^2}, \quad (22)$$

$$E''_{\mathbf{n}\omega} = \frac{2e^2}{\pi^2 c\lambda^2}\frac{1}{1+z}\operatorname{Re}\int_0^\infty dxe^{-\sigma x}\frac{d}{dx}e^{-\sigma z\tanh x}, \quad (23)$$

$$\Delta E'''_{\mathbf{n}\omega} = -\frac{e^2}{\pi^2 c\lambda^2}\operatorname{Re}\int_0^\infty dx\sigma xe^{-\sigma x}\frac{d}{dx}e^{-\sigma z\tanh x}. \quad (24)$$

If we integrate these expressions over the angles of the photons ($d\theta_0 \to \pi\lambda^2 dz$), we obtain (after some simple transformations) the following for the radiation due to the boundary:

$$E = \frac{e^2}{\pi c}\operatorname{Re}\left\{2\int_0^\infty\frac{dz}{1+z}\int_0^\infty\sigma e^{-\sigma x-\sigma z\tanh x}dx\right.$$

$$\left.+\int_0^\infty\left(\coth x-\frac{1}{x}\right)(1-\sigma x)e^{-\sigma x}dx-2\right\}. \quad (25)$$

In the limiting case of small s,

$$E = \frac{e^2}{\pi c}\ln\frac{1}{s}, \quad (26)$$

i.e., the radiation differs from the radiation involved in stopping $E_{st} = (e^2/\pi c)\ln(E/mc^2)$ only in the factor under the logarithm. If the energy of the electron $E > E_0$ (for lead, $E_0 \sim 3\times 10^{12}$ ev), then $s > 1$ in all frequency regions and the approximating formula (26) is thus valid. The total energy loss at the boundary in this case increases linearly with the energy and exceeds the so-called transition radiation (see references 6 and 7) by six orders of magnitude. In the case $E < E_0$, Eq. (26) is valid in the region of not too hard quanta $\hbar\omega < E^2/E_0$. For the calculation of the energy lost by the particle at the boundary, quantum considerations are necessary.

I take this opportunity to express my gratitude to A. B. Migdal and G. M. Garibyan for discussion of the results.

---

*An investigation of the integral equation (12) was carried out earlier by the authors[5] and confirmed the results obtained by the method of Fokker-Planck with the expression under the logarithm sign as corrected by Migdal.[4]

[1] L. D. Landau and I. Ya. Pomeranchuk, Dokl. Akad. Nauk SSSR **92**, 535 (1953).

[2] L. D. Landau and I. Ya. Pomeranchuk, Dokl. Akad. Nauk SSSR **92**, 735 (1953).

[3] A. B. Migdal, Dokl. Akad. Nauk SSSR **96**, 49 (1954).

[4] A. B. Migdal, JETP **32**, 633 (1957), Soviet Phys. JETP **5**, 527 (1957).

[5] I. I. Gol'dman, Izv. Akad. Nauk Arm. S.S.R. **12**, 230 (1960).

[6] V. L. Ginzburg and I. M. Frank, JETP **16**, 15 (1946).

[7] G. M. Garibyan, JETP **37**, 527 (1959), Soviet Phys. JETP **10**, 372 (1960).

Translated by R. T. Beyer
355

SOVIET PHYSICS JETP VOLUME 11, NUMBER 6 DECEMBER, 1960

POLARIZATION OF NUCLEONS SCATTERED FROM NUCLEI WITH NON-ZERO SPIN

YU. P. ELAGIN

Submitted to JETP editor January 14, 1960

J. Exptl. Theoret. Phys. (U.S.S.R.) **38**, 1870-1871 (June, 1960)

The optical model is used for an analysis of the polarization of nucleons scattered from nuclei with non-zero spin. It is shown that, in general, such nuclei lead to an additional polarization as compared to nuclei with the same optical parameters and zero spin.

THE introduction of a spin-orbit interaction in the optical model of nuclear reactions allows us to compute the polarization of the nucleon as a result of the interaction with the nucleus.

The polarization P, as all quantities predicted by this model, is the result of an averaging over many resonances. The transition from the unaveraged quantities to the averaged quantities is conveniently made by averaging the phases of the scattered waves.[1] The relative amplitudes $\tilde{\eta}$ of the divergent waves are averaged.

Eder at al.[2] also considered the polarization in the scattering of nucleons from nuclei with zero spin. The polarization was found here to be completely determined by the elastic potential scattering. The expression for the polarization has the form

$$\mathbf{P} = (A^*\sigma A)/(d\sigma/d\Omega), \tag{1}$$

where A is the amplitude of the elastic potential scattering. The resonance part of the scattering does not give a contribution to the polarization; the corresponding terms drop out after the averaging.[2]

This is the situation in the case of spherical even-even nuclei.

It is of interest to generalize these considerations to the nuclei with spin I ≠ 0. The corresponding phase analysis shows that for an unpolarized incident beam and unpolarized target the final state is described by the function

$$\psi_f = \frac{1}{\sqrt{2(2I+1)}} \times \sum \varepsilon_{m_s}\varepsilon_{m_I} f(m_s m_I l0 \,|\, m_{s'} m_{I'} l' m)\, \chi_{I'}^{m_{I'}} \chi_{s'}^{m_{s'}} Y_{l'}^{m}(\theta, \varphi), \tag{2}$$

where $\chi_s^{m_s}$ is the spin function, f(... | ...) is the amplitude for scattering from a state characterized by the first set of quantum numbers to a state defined by the second set; the summation goes over all quantum numbers. The ϵ are analogous to those introduced by Blin-Stoyle.[3] The polarization of the particles after the scattering is defined by

$$\mathbf{P} = (\psi_f^* \sigma \psi_f)/(\psi_f^* \psi_f), \tag{3}$$

where σ is a vector whose components are the Pauli matrices for the particles s (nucleons). Substituting (2) in (3), we obtain

$$\frac{d\sigma}{d\Omega}(P_x + iP\ ) = \frac{e^{i\varphi}}{2I+1} \sum_{m_s m_I m_{I'}} \Big\{ \sum_{LL'} f\Big(m_s m_I L0 \,\Big|\, \frac{1}{2} m_{I'} l' m\Big)^* \times f\Big(m_s m_I L'0 \,\Big|\, -\frac{1}{2} m_{I'} l'' m'\Big)\Big\} P_{l'}^{m}(\cos\theta)\, P_{l''}^{m'}(\cos\theta). \tag{4}$$

If the expression (4) written in terms of the unaveraged quantities $\tilde{\eta}$, is then averaged over the resonances, we obtain an expression different from (1). This procedure was used in the specific case I = I′ = ½. We restrict ourselves to the consideration of the s and p phases ($l \leq 1$) and obtain after averaging (η, as opposed to $\tilde{\eta}$, is averaged over the resonances)

$$\begin{aligned} \frac{d\sigma}{d\Omega} P &= \text{const}\, e^{i\varphi}\, \mathrm{Im} \Big\{ \frac{\sqrt{2}}{3} (\eta_{22} - \eta_{11})^* (1 - \eta_{00})\, P_0 P_1^1 \\ &+ \frac{2\sqrt{2}}{3} [2|\eta_{11}|^2 - |\eta_{22}|^2 - \eta_{11}\overset{*}{\eta}_{22} + 3(\eta_{22} - \eta_{11})]\, P_1^0 P_1^1 \Big\} \\ &- \text{const}\, e^{i\varphi}\, \mathrm{Im}\, \{\overline{4\tilde{\eta}_{11}^{1}\, \eta_{12}^{1*}} - 3\eta_{11}\overset{*}{\eta}_{12} + 3\sqrt{2}\, |\eta_{21}|^2 \\ &- 6\sqrt{2}\, |\eta_{12}|^2 - 2\sqrt{2}\, \eta_{12}\overset{*}{\eta}_{21}\} \frac{P_1^0 P_1^1}{36} = P_{\mathbf{pot}} + P_{\mathbf{add}}, \end{aligned} \tag{5}$$

where $\eta_{jj'}^{J}$ is the coefficient of the outgoing wave with angular momentum j′ generated by the incoming wave with angular momentum j, both waves corresponding to an intermediate state of the system with total angular momentum J. The systems of levels corresponding to different J are assumed to be uncorrelated. The index 1 of the phases corresponds to the state $p_{3/2}$, the index 2 to the state $p_{1/2}$, and the index 0 to the s state.

Expression (5) is made up of two terms. The first term is the polarization of the particles corresponding to a nucleus with zero spin, and coincides with (1). The second term corresponds to the additional effect due to the fact that the nucleus has nonvanishing spin. In a transition to $I = 0$ P_{add} vanishes, since in this case all η_{12} and η_{21} vanish. We also note that in (5) the terms that correspond to transitions with $\Delta l = 2$ are neglected; they also enter in the quantity P_{add}. This may be regarded as the result of the correlation of the systems of resonance levels over which the phases are averaged. In the case of non-overlapping levels these correlations can be quite important, since they receive a contribution of the same sign in the averaging over the levels from all resonances.

Thus, of the two nuclei with approximately the same optical properties (lying close to each other in the periodic table), one even-even (spin $I = 0$) and the other odd ($I \neq 0$), the latter will lead to an additional polarization. This difference should be observable in experiment. The nuclei Pb^{207} and Pb^{208} are convenient for this purpose. These nuclei are spherical, and the term P_{pot} will be very nearly the same for both of them, since it is determined mainly by the nuclear radius. The additional term appears in the case of Pb^{207}, where the polarization should differ by P_{add} from the polarization caused by the neighboring even-even nuclei. This type of experiment would be helpful in estimating this quantity, which cannot be calculated from the optical model.

During the course of this work the author had frequent discussions with P. É. Nemirovskiĭ, to whom he expresses his sincere gratitude.

---

[1] P. É. Nemirovskiĭ, Doctoral Dissertation, Institute of Physics, Acad. Sci., 1958.

[2] Adair, Darden, and Fields, Phys. Rev. **96**, 503 (1954). P. É. Nemirovskiĭ and Yu. P. Elagin, JETP **32**, 1583 (1957), Soviet Phys. JETP **5**, 1293 (1957).

[3] R. J. Blin-Stoyle, Proc. Phys. Soc. **A64**, 700 (1951).

Translated by R. Lipperheide
356

SOME CONSEQUENCES OF THE SYMMETRY OF THE UNIVERSAL FERMI WEAK INTERACTION

HO TSO-HSIU and CHU HUNG-YÜAN

Joint Institute for Nuclear Research

Submitted to JETP editor January 15, 1960

J. Exptl. Theoret. Phys. (U.S.S.R.) 38, 1872-1878 (June, 1960)

It is shown that the invariance of the universal V − A Fermi weak interaction with respect to the Fierz transformation forbids the capture of a μ meson by a proton in the triplet S state. The capture of a μ meson by a proton in the singlet S state with the emission of one photon is also forbidden. It is shown further that the state of two fermions, or that of two antifermions, produced in any weak-interaction process, can be described by one wave function if we neglect the effects of other interactions of these particles; functions describing the correlation of the polarizations are given. The asymmetry of the angular distribution of the neutron emitted by a nucleus after capture of a μ meson is discussed.

1. Zel'dovich and Gershteĭn,[1] and also Chou Kuang-Chao and Maevskiĭ,[2] have shown that the capture of a μ meson by a proton in the triplet S state is forbidden within the framework of the universal Fermi weak interaction proposed by Feynman and Gell-Mann[3] and by Sudarshan and Marshak.[4] Later Dye and others[5] remarked that radiative capture of a μ meson by a proton is also forbidden in the singlet S state with emission of one photon. It is interesting to see whether the vanishing of the matrix elements that describe these processes is due to the existence of some symmetry law. Since the consequences that come from symmetry properties are usually of quite general validity, their study can be useful in testing the universality of the V − A Fermi weak interaction. On the other hand, since the presence of strong interactions usually leads to the disappearance of certain symmetry properties of weak interactions, such a study could also be useful in finding out the effects of the renormalization of the strong interactions on the weak interaction.

In the following section it is shown that the state of two fermions or of two antifermions produced in any weak interaction can be described by one wave function, if we neglect the effects of other interactions of these two particles. In their center-of-mass system these two particles have zero total angular momentum. We shall give a rigorous proof of the results of Zel'dovich and Gershteĭn[1] and of Dye and others,[2] which were previously obtained by the use of the nonrelativistic approximation and by taking into account only the first nonvanishing approximation of perturbation theory.

In the third section we present a function that describes the correlation of the polarizations of two fermions or two antifermions produced in any process described by the universal Fermi weak interaction, when other interactions are neglected; we consider the various possible forms of the Fermi interaction proposed by Gell-Mann and Feynman.[3] Measurements of the correlation of the polarizations can be used for testing the universality of the V − A Fermi weak interaction, and can also give information about the effects of the renormalization of the strong interaction. In connection with the two-component spinor theory[3] we also consider the polarization of a photon emitted in a weak-interaction process.

In the last section it is pointed out that the presence of relativistic effects can cause an asymmetry in the angular distribution of the neutrons emitted by nuclei after the capture of μ mesons, even if we neglect the influence of renormalization and the effect of interaction in the final state.

2. It is well known that the universal Fermi weak interaction

$$H_i = (A, B)(C, D) \equiv (G/\sqrt{2})\,\bar{\psi}_A \gamma_\alpha (1+\gamma_5)\psi_B \bar{\psi}_C \gamma_\alpha (1+\gamma_5)\psi_D, \tag{1}$$

where ψ_A, ψ_B, ψ_C, and ψ_D are the fields that describe four types of particles A, B, C, and D with half-integral spins, has a number of interesting symmetry properties. For example, under the transformation studied by Fierz:[6]

$$\psi_B \rightleftarrows \psi_D, \tag{2}$$

we have

$$(A, B)(C, D) \rightleftarrows (A, D)(C, B). \qquad (3)$$

For convenience in our further arguments it is helpful to subject the operator (1) to the transformation of charge conjugation:

$$H_i = -(G/\sqrt{2})\,\bar{\psi}_{\bar{B}}\gamma_\mu(1-\gamma_5)\psi_{\bar{A}}\bar{\psi}_C\gamma_\mu(1+\gamma_5)\psi_D. \qquad (4)$$

Here $\bar{A}$ and $\bar{B}$ denote the respective antiparticles; thus $\psi_{\bar{A}}$ is the operator that annihilates the antiparticle $\bar{A}$ or produces the particle A. After the Fierz transformation the operator (4) takes the form

$$H_i = \sqrt{2}\,G\bar{\psi}_C(1-\gamma_5)\psi_{\bar{A}}\psi_{\bar{B}}(1+\gamma_5)\psi_D. \qquad (5)$$

Let us study a process in which two fermions A and C are emitted as a result of the interaction (5). If we neglect other interactions of the particles A and C, the Feynman diagram can be represented schematically by Fig. 1. The corresponding element of the S matrix in the momentum representation is of the form

$$\langle \mathbf{p}_A, s_A; \mathbf{p}_C, s_C; r \,|\, S \,|\, i\rangle = \bar{u}(\mathbf{p}_C, s_C)(1-\gamma_5)v(-\mathbf{p}_A, -s_A)R, \qquad (6)$$

where p_A, s_A, and p_C, s_C are respectively the momentum and spin of particle A and the momentum and spin of particle C; r denotes all other quantum numbers of the final state; $|i\rangle$ is the wave function of the initial state; the factors u, v, and $(1-\gamma_5)$ represent respectively the external lines and part of the vertex shown in Fig. 1, u being the wave function of a state with positive energy and v that of a state with negative energy; and, finally, R represents all the other parts of the diagram, which are represented in the drawing by a block. The final state of the system can be represented in the form

$$|f\rangle = |\mathbf{p}_A, s_A; \mathbf{p}_C, s_C; r\rangle\langle \mathbf{p}_A, s_A; \mathbf{p}_C, s_C; r \,|\, S \,|\, i\rangle. \qquad (7)$$

In particular, when the energy and momentum $p_A + p_C$ imparted to the system consisting of particles A and C are prescribed, the wave function W of this system is

$$W(\mathbf{p}_A, s_A; \mathbf{p}_C, s_C) = \{\bar{u}(\mathbf{p}_C, s_C)(1-\gamma_5)v(-\mathbf{p}_A, -s_A)\} \times u(\mathbf{p}_A, s_A)u(\mathbf{p}_C, s_C) \qquad (8)$$

and does not depend on R. Thus the wave function of the partial system consisting of particles A and C does not depend on what has happened in the intermediate state, if the energy and momentum imparted to this system are prescribed and if we neglect the other interactions of the particles A and C.

It is easy to calculate the wave function W. In the center-of-mass system of particles A and C

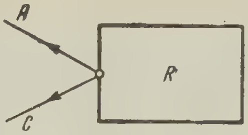

FIG. 1

their total internal angular momentum is zero. Thus W is a superposition of ${}^1S_0$ and ${}^3P_0$ states. If one of the particles is a neutrino, the ${}^1S_0$ and ${}^3P_0$ states have equal weights. If, however, the velocities of A and C are small, then the contribution of the ${}^3P_0$ state is small – of the order of v (v is the speed of particle A or particle C, with the speed of light taken as unity). This result is easy to understand directly from the expression (5).

It is convenient to regard particles A and C as a single system. If we denote $\bar{\psi}_C(1-\gamma_5)\psi_{\bar{A}}$ by Φ, then Eq. (5) takes the form

$$H_i = \sqrt{2}\,G\Phi\bar{\psi}_{\bar{B}}(1+\gamma_5)\psi_D. \qquad (9)$$

Φ behaves like a scalar under proper Lorentz transformations. Thus the intrinsic angular momentum of the system consisting of the particles A and C emitted as a result of the interaction (5) must be zero.

The results obtained earlier[1,2,5] are now easily understood. Capture of a μ meson by a proton is rigorously forbidden in the ${}^3S$ state because of the law of conservation of angular momentum. Since a radiative transition from a state with J = 0 to another state with J = 0 with the emission of one photon is impossible, radiative capture of a μ meson by a proton in the ${}^1S$ state with emission of one photon is also rigorously forbidden.

3. Since the wave function W does not depend on what happens in the intermediate state, it is very convenient for applications. As an illustration let us consider the correlation of the polarizations of particles A and C. The table shows the relative probabilities of the various combinations of polarization states; these probabilities are easily obtained by the use of the function W. (In this table v_A and v_C are the speeds of particles A and C, and θ_{AC} is the angle between p_A and p_C). The functions in the third column of the table give the amounts of correlation of the polari-

s_A, p_A	s_C, p_C	Relative probability
parallel	parallel	$\frac{1}{2}(1-v_A)(1-v_C)(1-\cos\theta_{AC})$
parallel	antiparallel	$\frac{1}{2}(1-v_A)(1+v_C)(1+\cos\theta_{AC})$
antiparallel	parallel	$\frac{1}{2}(1+v_A)(1-v_C)(1+\cos\theta_{AC})$
antiparallel	antiparallel	$\frac{1}{2}(1+v_A)(1+v_C)(1-\cos\theta_{AC})$

zations of fermions emitted in any weak interaction, under the condition that we can neglect the other interactions of these fermions. Let us investigate, for example, the correlation of the polarizations of the neutrino and neutron in the radiative capture of a μ meson by a proton. Let A denote the neutrino and C the neutron; then it can be seen from the table that the neutrino must be a left-hand screw particle, and the degree of longitudinal polarization of the neutrino is

$$(\cos\theta - v)/(1 - v\cos\theta), \tag{10}$$

where v is the speed of the neutron and θ is the angle between the momenta of the neutrino and the neutron. The table can also be applied to the decay of the μ meson, to β decays of nucleons and hyperons, and so on.

Since the theory is invariant with respect to time reversal, the correlation functions given in the table can be used to describe the dependence of the transition probability on the polarization states of the fermions in the initial state, and in particular the dependence of the rate of capture of μ mesons on the hyperfine structure of the μ-mesic atom. In this last case we can assume as a first approximation that only the ${}^1S_0$ state of the μ meson and proton contributes to the capture. For a more accurate treatment, one must take into account the contribution of the ${}^3P_0$ state.

Since the V — A Fermi interaction is invariant with respect to combined inversion, the functions that describe the correlation of the polarizations of antifermions can be obtained from the table by the replacements

$$A \to \bar{A}, \qquad C \to \bar{C} \tag{11}$$

together with change of sign of the spins of particles $\bar{A}$ and $\bar{C}$ (the operation "parallel ⇄ antiparallel"). Lack of agreement between the conclusions obtained by using these functions and experimental results would either cast doubt on the universality of the V — A theory of the Fermi weak interaction or indicate an influence of other interactions, for example, a renormalization effect.

As Feynman and Gell-Mann have remarked,[3] one could equally suitably take as the Hamiltonian of the universal weak interaction either the expression

$$H_i = (G/\sqrt{2})\,\bar{\psi}_A\gamma_\alpha(1-\gamma_5)\psi_B\bar{\psi}_C\gamma_\alpha(1-\gamma_5)\psi_D, \tag{12}$$

or the expression

$$H_i = (G/\sqrt{2})\,\bar{\psi}_A\gamma_\alpha(1-\gamma_5)\psi_B\bar{\psi}_C\gamma_\alpha(1+\gamma_5)\psi_D. \tag{13}$$

To settle which of the Hamiltonians (1), (12), or (13) is the correct one, it is necessary to find out whether they lead to different physical consequences. Therefore it is useful to note that Eqs. (1), (12), and (13) give different correlations of the polarizations.

The expression (12) can be obtained from (1) by space inversion, and consequently all formulas obtained from Eq. (1) are converted by space inversion into formulas that follow from Eq. (12). In particular, scalar quantities will remain unchanged, whereas pseudoscalar quantities will be changed in sign; thus to distinguish between Eqs. (1) and (12) one must measure pseudoscalar quantities. The correlation of the polarizations of the fermions in the process described by the Hamiltonian (12) can be obtained from the table by the interchange "parallel ⇄ antiparallel" mentioned earlier. The correlation for antifermions can be obtained in a similar way.

After a charge-conjugation transformation the expression (13) can be written in the form

$$-(G/\sqrt{2})\,\bar{\psi}_{\bar{B}}\gamma_\alpha(1+\gamma_5)\psi_{\bar{A}}\bar{\psi}_C\gamma_\alpha(1+\gamma_5)\psi_D. \tag{14}$$

Thus the correlation of the polarizations given by the Hamiltonian (13) can be obtained from the table by the replacement

$$A \to \bar{B}. \tag{15}$$

Accordingly Eq. (13) leads to a universal correlation of polarizations between fermion and antifermion.

The expression for the interaction Hamiltonian composed of two-component spinors, as proposed by Feynman and Gell-Mann,[3] leads to interesting consequences regarding the polarization state of a photon emitted by a fermion in a weak-interaction process, if the fermion is initially at rest. Let us take as an example the process described by the diagram of Fig. 2. The vertex represents the V — A Fermi interaction, and the photon is emitted by particle B. The corresponding element of the S matrix is of the form

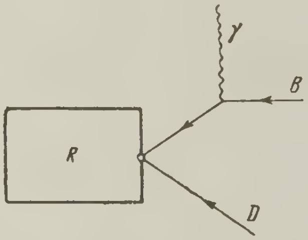

FIG. 2

$$R\gamma_\alpha(1+\gamma_5)\frac{i(\hat{p}_B-\hat{k})-m_B}{(p_B-k)^2+m_B^2}\frac{\hat{e}^*}{\sqrt{2\omega}}u(\mathbf{s}_B,\mathbf{p}_B). \tag{16}$$

R represents the rest of the diagram, excluding the part that begins with the external line B and ends at the weak-interaction vertex. The rest of the notation is obvious. We have (particle B is initially at rest)

$$\{i(\hat{p}_B - \hat{k}) - m_B\}\hat{e}^* = \hat{e}^*\{i\hat{k} - i\hat{p}_B - m_B\}. \qquad (17)$$

Since

$$\{i\hat{p}_B + m_B\}u(\mathbf{s}_B, \mathbf{p}_B) = 0, \qquad (18)$$

the expression (16) takes the form

$$iR\gamma_\alpha(1+\gamma_5)\hat{e}^*\hat{k}u(s_B, p_B)/\{(p_B - k)^2 + m_B^2\}\sqrt{2\omega}. \qquad (19)$$

We note that for a left-circularly polarized photon

$$\hat{e}^*\hat{k} = -2^{-1/2}(1-\gamma_5)\mathbf{e}^*\sigma\omega. \qquad (20)$$

If follows from Eqs. (19) and (20) that the emission of a left-circularly polarized photon by particle B is forbidden — a result first pointed out by Dye and others[5] and by Manacher and Wolfenstein.[7] It is easy to see that if the weak interaction is described by the expression (12) the emission of a right-circularly polarized photon by a particle at rest is forbidden. Therefore measurement of the polarization of a photon emitted by a particle at rest offers a possible way to settle the question as to whether the interaction Hamiltonian is of the form (1) or (12).

4. As an example of the application of the results of the preceding sections let us consider the angular distribution of neutrons emitted by nuclei that have captured μ mesons. Dolinskiĭ and Blokhintsev[8] have shown that both the neutrons emitted by polarized nuclei that have captured unpolarized mesons and the neutrons emitted by unpolarized nuclei that have captured polarized mesons have isotropic distributions if the weak interaction that leads to the capture is of the V − A type and if there are no effects of renormalization and of interaction in the final state. The nonrelativistic approximation was used in their calculations. In particular, they assumed that the speed of the proton is very small and dropped the small components of the proton wave function. The results of Dolinskiĭ and Blokhintsev can now be understood without any calculations. In the center-of-mass system of the meson and proton a μ meson can be captured by a proton only if these two particles are in a state with $J = 0$. Therefore it is obvious that the angular distribution of the emitted neutron must be isotropic, regardless of whether the nucleus and μ meson are polarized or unpolarized, provided that the μ meson and the proton in the nucleus are regarded as being at rest before the capture.

The results presented above can be affected by two things, namely: 1) the presence of strong interaction, in particular, renormalization effects and interactions in the final state, and 2) relativistic effects associated with the motion of the proton. Dolinskiĭ and Blokhintsev[8] have shown that if one takes into account effects of strong interaction, a sizable anisotropy would be observed. The main terms in their expression for the asymmetry parameter are proportional to:

$$E_\nu/m_N \approx m_\mu/m_N, \qquad (21)$$

where E_ν is the energy of the emitted neutrino, and m_μ and m_N are the masses of the μ meson and the nucleon. Because of interference between the weak-magnetism term and the pseudoscalar term the numerical coefficient of the factor (21) has the large value 4.

By using the table one can show easily that relativistic effects can also lead to an asymmetry in the angular distribution, which is proportional to m_π/m_N (m_π is the mass of the π meson). This expression is of the order of magnitude of the momentum of a nucleon in a nucleus. As has already been established above, the neutron is emitted isotropically in the system in which the center of mass of the μ meson and the proton is at rest. In a system in which the center of mass is in motion the neutron is emitted mainly in the forward direction. Let us consider the case in which the proton that captures the μ meson is in an $s_{1/2}$ state. We assume that the μ meson is at rest and is completely polarized in the direction of the z axis. The velocity of the proton, and therefore also that of the center of mass of the proton and the meson, is distributed isotropically in all directions. Since, as can be seen from the table, the capture probability depends on the spin and the velocity, relativistic effects easily lead to an asymmetry in the angular distribution of the neutron.

As illustrations let us consider two cases in detail: 1) the proton is moving in the direction of the z axis; 2) the proton is moving in the opposite direction. The particles A and C in the table must now be taken to be the proton and the μ meson, respectively. If the spin of the proton is parallel to that of the μ meson, the capture probability must be zero, according to the table. If the spin of the proton is antiparallel to that of the μ meson, the capture probability is proportional to $1 + v$ in case 1, whereas in case 2 the capture probability is proportional to $1 - v$ (v is the speed of the proton). The proton has a large probability for capturing the μ meson if its velocity is parallel to the spin of the μ meson, and thus more neutrons are emitted along the direction of polarization of the μ mesons. The asymmetry is obviously proportional to $v \approx m_\pi/m_N$. This result is confirmed by calculations, if as the proton wave function we take the wave function for a particle in a spherical region, and for the neutron wave function we take a plane wave.

The argument that has been given shows that here, as is indeed usual, the influence of renormalization is weakened by the relativistic effects. In an accidental way the effects of renormalization and the relativistic effect work against each other in this case (the effect of renormalization causes the emission of a larger number of neutrons in the direction opposite to that of the spin of the μ meson[8]). Inclusion of interactions in the final state, such as the spin-orbit interaction, complicates the situation still more. It is interesting to note that experiments by Astbury and others[9] with the isotope S^{32} have given a negative asymmetry parameter, whereas experiments of Baker and Rubbia[10] with magnesium have given a positive parameter. It would be useful to make experiments with a nucleus of simple structure, such as Ne^{20}. Since in this case the nucleons of the outer shell are in the 2s state, there is no difficulty with inclusion of the spin-orbit interaction in the final state.

It has been shown experimentally[11] that the β-decay interaction is mainly of the V—A type. It is interesting to see whether the weak interaction that leads to μ capture is also an interaction of the V—A type. Telegdi[12] has shown that the μ-capture interaction cannot be of the form (13). The experiment he uses does not, however, show that the μ-capture interaction must necessarily be of the V—A type, namely, of the form (1). Since the quantity measured in the experiment is a scalar, the experiment can also be explained by an interaction of the type (12). In order to assign the μ-capture interaction to the type V—A it is necessary to measure a pseudoscalar quantity, such as the longitudinal polarization of the neutron emitted in the capture.

---

[1] Ya. B. Zel'dovich and S. S. Gershteĭn, JETP **35**, 821 (1958), Soviet Phys. JETP **8**, 570 (1959).

[2] Chou Kuang-Chao and V. Maevsky, Acta Phys. Sinica **15**, 377 (1959).

[3] R. P. Feynman and M. Gell-Mann, Phys. Rev. **109**, 193 (1958).

[4] E. C. G. Sudarshan and R. E. Marshak, Phys. Rev. **109**, 1860 (1958).

[5] Dye, Sen, Ho, and Tzu, Scientia Sinica **8**, 423 (1959).

[6] M. Fierz, Z. Physik **104**, 553 (1937).

[7] G. K. Manacher and L. Wolfenstein, preprint.

[8] É. I. Dolinskiĭ and L. D. Blokhintsev, JETP **34**, 759 (1958) and **35**, 1488 (1958), Soviet Phys. JETP **7**, 521 (1958) and **8**, 1040 (1959).

[9] Astbury, Blair, Kemp, Muirhead, and Voss, Phys. Rev. Letters **3**, 476 (1959).

[10] W. F. Baker and C. Rubbia, Phys. Rev. Letters **3**, 179 (1959).

[11] M. Goldhaber, Proc. of Int. Conf. on High-Energy Phys, at CERN, 1958, page 233.

[12] V. L. Telegdi, Phys. Rev. Letters **3**, 59 (1959).

Translated by W. H. Furry
357

SOVIET PHYSICS JETP VOLUME 11, NUMBER 6 DECEMBER, 1960

VARIATIONAL PRINCIPLES FOR NONSTATIONARY QUANTUM MECHANICAL PROBLEMS AND PERTURBATION THEORY

Yu. N. DEMKOV

Leningrad State University

Submitted to JETP editor January 19, 1960

J. Exptl. Theoret. Phys. (U.S.S.R.) 38, 1879-1886 (June, 1960)

A variational principle is formulated which is invariant with respect to the normalization of the wave functions and which can be used in the case when the wave functions of the initial and final states are not orthogonal. The problem of the uniqueness of perturbation theory in this case is considered. The possibility of employing the variational principle for the solution of problems concerning the decay of stationary states and charge exchange is discussed. The basic equations for charge exchange at large impact parameters are derived from the variational principle.

1. INTRODUCTION

IT occurs frequently in the solution of nonstationary problems in quantum mechanics that the wave functions of the initial and final states are not orthogonal, becoming orthogonal only in the limit $t \to \pm\infty$. Processes of this kind are, for example, all collisions involving a redistribution and, in particular, the simplest of these collisions, the charge-exchange collision. If these problems are solved by perturbation theory, assuming that the transition probability is small, we are faced with the non-uniqueness of the basic formulas of perturbation theory. Indeed, adding an arbitrary function of time to the perturbation changes the transition probability calculated by perturbation theory. On the other hand, this addition can be eliminated from the energy operator by an elementary unitary transformation and, evidently, cannot affect the true transition probability. This fact was noted in a number of papers[1] and ways of removing this non-uniqueness were proposed.[2]

It is well known that the basic formulas of perturbation theory can be derived from a variational principle. It is therefore natural to investigate this non-uniqueness by variational methods. The usual formulation of the variational principle for nonstationary problems (see, for example, reference 3, Sec. 25) does not immediately lead to a solution of this problem. It turns out, however, that one can formulate a new variational principle, using a stationary expression for the transition probability which is invariant with respect to multiplications of the trial functions by arbitrary functions of time. This makes it possible to avoid the above-mentioned non-uniqueness.

The new variational principle is very convenient for the investigation of the decay of nonstationary states. Using it for processes of the charge exchange type, we are able to explain why the usual formulas of perturbation theory are unsatisfactory in this case and to establish which properties of the trial functions are essential for the correct formulation of the problem. By taking account of these properties we can give a more consistent derivation of Bates'[2] basic equations for charge exchange for large impact parameters from the variational principle.

2. FORMULATION OF THE PROBLEM AND THE VARIATIONAL PRINCIPLE

Consider the problem of finding that solution Ψ_1 of the Schrödinger equation

$$H\Psi = i\hbar\,\partial\Psi/\partial t, \tag{1}$$

which satisfies the initial condition

$$\Psi_1(t_1) = \varphi_1. \tag{2}$$

The quantity

$$a_{12} = \int \varphi_2^* \Psi_1(t_2)\,d\tau, \tag{3}$$

which is usually the unknown, determines the probability for the transition of the system from the state φ_1 at time t_1 to the state φ_2 at time t_2. We assume that the operator H is self-conjugate and can depend on the time. The functions φ_1 and φ_2 are in general nonorthogonal.

For the formulation of the variational principle we consider the functional

$$J(\Phi_2, \Phi_1) = \int_{t_1}^{t_2} dt \int \Phi_2^*(t)\,(H - ih\,\partial/\partial t)\,\Phi_1(t)\,d\tau, \qquad (4)$$

where the functions Φ_1 and Φ_2 satisfy the conditions

$$\Phi_1(t_1) = \varphi_1, \quad \Phi_2(t_2) = \varphi_2, \qquad (5)$$

and make a variation of this functional in the neighborhood of the exact solutions Ψ_1 and Ψ_2 of the Schrödinger equation (1) satisfying the condition (2) and the condition

$$\Psi_2(t_2) = \varphi_2, \qquad (6)$$

respectively. Using the hermiticity of the operator H, integrating by parts, and imposing the conditions $\delta\Psi_1(t_1) = \delta\Psi_2(t_2) = 0$, we obtain

$$J(\Psi_2 + \delta\Psi_2, \Psi_1 + \delta\Psi_1) = -ih \int \Psi_2^*(t_2)\,\delta\Psi_1(t_2)\,d\tau + \int_{t_1}^{t_2} dt \int \delta\Psi_2^* \left(H - ih\frac{\partial}{\partial t}\right) \delta\Psi_1\,d\tau. \qquad (7)$$

From this we immediately find the stationary expression for a_{12}:

$$a_{12} = \mathrm{St}\left\{\int \Phi_2(t_2)\,\Phi_1(t_2)\,d\tau + \frac{1}{ih}\int_{t_1}^{t_2} dt \int \Phi_2^* \left(H - ih\frac{\partial}{\partial t}\right)\Phi_1\,d\tau\right\}. \qquad (8)$$

Substituting in this formula functions Φ_1 and Φ_2 which are close to the exact wave functions Ψ_1 and Ψ_2, we obtain an approximate value for a_{12}, which differs from the exact value only in second order of smallness.

The first term on the right hand side of (8) represents the value of a_{12} as computed directly by (3) with the help of the approximate function Φ_1. In cases when the second term does not vanish we can improve the value of a_{12} by using (8); this improvement is often quite essential.

It is seen from (7) that (8) gives the exact value for a_{12} also if only one of the functions Φ_1, Φ_2 is replaced by the exact wave function, assuming that the other is arbitrary, satisfying only condition (5).

The asymmetry of (8) with respect to t_1 and t_2 is only seeming, for the same formula can be written in the form

$$a_{12} = \mathrm{St}\left\{\int \Phi_2^*(t_1)\,\Phi_1(t_1)\,d\tau + \frac{1}{ih}\int_{t_1}^{t_2} dt \int \left[\left(H - ih\frac{\partial}{\partial t}\right)\Phi_2\right]^* \Phi_1\,d\tau\right\}. \qquad (9)$$

By going to the limit of the stationary problem we can obtain the usual formulation of the variational principle[3] for the scattering phases and amplitudes in perturbation theory.

3. PERTURBATION THEORY. NON-UNIQUENESS OF THE BASIC FORMULAS

Let us now consider the case when the energy operator can be split up into a perturbation and an unperturbed part in two ways:

$$H = H_1 + V_1 = H_2 + V_2. \qquad (10)$$

We assume that the solutions of the Schrödinger equations for the unperturbed operators are known:

$$H_1\psi_1 = ih\,\partial\psi_1/\partial t, \quad \psi_1(t_1) = \varphi_1, \qquad (11)$$

$$H_2\psi_2 = ih\,\partial\psi_2/\partial t, \quad \psi_2(t_2) = \varphi_2. \qquad (12)$$

Regarding the perturbation as small, we can then assume that the functions ψ_1 and ψ_2 are close to the corresponding solutions Ψ_1 and Ψ_2 of equation (1). Substituting the functions ψ_1 and ψ_2 in the functional (8), we obtain an expression for a_{12} in the first order of perturbation theory:*

$$a_{12} = \int \varphi_2^*\,\psi_1(t_2)\,d\tau + \frac{1}{ih}\int_{t_1}^{t_2} dt \int \psi_2^* V_1 \psi_1\,d\tau. \qquad (13)$$

In order that this expression be invariant with respect to the addition of an arbitrary function of time to the perturbation V_1, it is necessary that the functions ψ_1 and ψ_2 are orthogonal for all times between t_1 and t_2. This condition is satisfied in the usual case, when $V_1 = V_2$, and ψ_1 and ψ_2 are functions corresponding to different stationary states of a system with the energy operator $H_1 = H_2$. However, this orthogonality requirement is evidently not fulfilled in this case if $\varphi_1 = \varphi_2$, i.e., if we ask for the probability that the system remains in its previous state. It is true that the quantity a_{12} is then not necessarily small, but in contrast to the usual formulation of perturbation theory, the use of the variational principle is not based on the assumption that a_{12} is small.

An example of the type of problem that can be treated in this way is the charge exchange problem, i.e., the transition of an electron from one atomic system to another in the collision of the two. In the simplest approximation we can assume that the atomic systems move along classical trajectories (for sufficiently large impact parameters, simply along a straight line) and describe the interaction with the electron by the effective potentials U_1 and U_2. Then the energy operator has the form

$$H = -\tfrac{1}{2}\nabla^2 + U_1(\mathbf{r} - \mathbf{R}/2) + U_2(\mathbf{r} + \mathbf{R}/2), \qquad (14)$$

---

*If the wave functions ψ_1 and ψ_2 are substituted in the functional (9), this quantity will be expressed in terms of the matrix element of the operator V_2.

$$\mathbf{R} = \boldsymbol{\rho} + \mathbf{v}t, \quad \boldsymbol{\rho}\mathbf{v} = 0. \tag{15}$$

The potentials U_1 and U_2 play the role of the perturbations V_1 and V_2, and the functions ψ_1 and ψ_2 have the form

$$\psi_1 = \chi_1(\mathbf{r} + \mathbf{R}/2)\exp\{-\tfrac{1}{2}i\mathbf{v}\mathbf{r} - i(E_1 + v^2/8)t\},$$

$$\psi_2 = \chi_2(\mathbf{r} - \mathbf{R}/2)\exp\{\tfrac{1}{2}i\mathbf{v}\mathbf{r} - i(E_2 + v^2/8)t\}, \tag{16}$$

where χ_1 and χ_2 satisfy the equations

$$[-\tfrac{1}{2}\nabla^2 + U_2(\mathbf{r})]\chi_1(\mathbf{r}) = E_1\chi_1(\mathbf{r}),$$

$$[-\tfrac{1}{2}\nabla^2 + U_1(\mathbf{r})]\chi_2(\mathbf{r}) = E_2\chi_2(\mathbf{r}). \tag{17}$$

Then the coefficient a_{12} which determines the probability for charge exchange in a transition from the state χ_1 to the state χ_2 has in first order perturbation theory the form

$$a_{12} = \frac{1}{ih}\int_{-\infty}^{+\infty} dt e^{i(E_2-E_1)t}\int \chi_2^*\left(\mathbf{r} - \frac{\mathbf{R}}{2}\right)U_1\left(\mathbf{r} - \frac{\mathbf{R}}{2}\right)\chi_1\left(\mathbf{r} + \frac{\mathbf{R}}{2}\right)e^{-i\mathbf{v}\mathbf{r}}\,d\tau. \tag{18}$$

Since the functions χ_1 and χ_2 are nonorthogonal for finite t, this expression changes if a function of time is added to U_1. The problem of how to choose this function has been discussed by Bates.[2]

4. INVARIANT VARIATIONAL PRINCIPLE

We now discuss how the formulation of the variational principle must be modified in order that the substitution of arbitrary trial functions should not lead to the above-mentioned non-uniqueness and that the expression for the transition probability be automatically invariant with respect to addition of an arbitrary function of time to the energy operator.

Let us assume that we know functions Φ_1 and Φ_2 which are close to the exact wave functions Ψ_1 and Ψ_2. Substituting these functions in (8) we obtain an approximate value for a_{12}. Then we multiply the function Φ_1 by f_1 and Φ_2 by f_2, where f_1 and f_2 are some functions of time which satisfy the conditions

$$f_1(t_1) = f_2(t_2) = 1. \tag{19}$$

We require that the functional be stationary with respect to arbitrary variations δf_1 and δf_2 with the condition

$$\delta f_1(t_1) = \delta f_2(t_2) = 0. \tag{20}$$

Using the expressions (8) and (9) for the functional we then obtain equations for the functions f_1 and f_2:

$$ih\dot{f}_1\int \Phi_2^*\Phi_1\,d\tau = f_1\int \Phi_2^*(H - ih\,\partial/\partial t)\,\Phi_1\,d\tau, \tag{21}$$

$$ih\dot{f}_2^*\int \Phi_2^*\Phi_1\,d\tau = f_2^*\int [(H - ih\,\partial/\partial t)\,\Phi_2]^*\,\Phi_1\,d\tau. \tag{22}$$

Solving these equations with the initial conditions (19), we find

$$f_1 = \exp\left\{-\frac{i}{h}\int_{t_1}^{t} Ldt\right\}, \tag{23}$$

$$L = \int \Phi_2^*(H - ih\,\partial/\partial t)\,\Phi_1 d\tau \Big/ \int \Phi_2^*\,\Phi_1\,d\tau;$$

$$f_2^* = \exp\left\{-\frac{i}{h}\int_{t}^{t_2} L\,dt\right\}\int \Phi_2^*(t_2)\,\Phi_1(t_2)\,d\tau \Big/ \int \Phi_2^*(t)\,\Phi_1(t)\,d\tau. \tag{24}$$

Let us now substitute the "improved" functions $f_1\Phi_1$ and $f_2\Phi_2$ in the functional (8). We see immediately that the function under the time integral from t_1 to t_2 vanishes; only the first term remains, and we obtain

$$a_{12} = \mathrm{St}\left\{\int \Phi_2^*(t_2)\,\Phi_1(t_2)\ \exp\left[-\frac{i}{h}\int_{t_1}^{t_2} L\,dt\right]d\tau\right\}. \tag{25}$$

This variational principle has all the required properties. Indeed, it is easily seen that the multiplication of the functions Φ_1 and Φ_2 by the arbitrary functions f_1 and f_2, which are subject only to the conditions (19), does not alter the value of the functional. Moreover, it is apparent at once that the addition of a real function of time to the operator H changes a_{12} only by a phase factor.

In contrast to the usual variational principle, the functional takes on its stationary value not only for the exact functions Ψ_1 and Ψ_2, but also for any other functions which differ from the exact functions by a time factor. In the solution of the problem by direct methods both variational principles lead, of course, to the same results if the time factor is regarded as one of the parameters to be varied. If this condition is not satisfied, the variational principle (25) guarantees the stationary property of the functional for a wider class of functions and gives, in this sense, a more exact expression for a_{12} than the functional (8). It must be borne in mind, however, that the functional (8) does not have the extremal property, so that the agreement between the approximate and exact values of a_{12} can only be accidental; in this case the extension of the class of functions to be varied leads sometimes (as we shall see later) to a poorer approximate value for a_{12}.

The remarks made in connection with the variational principle (8) at the end of Sec. 2 also apply to the new variational principle. Thus, for example, we obtain the exact value of a_{12} if we substitute $\Phi_2 = \Psi_2$ and an arbitrary Φ_1 in the functional (25). Dividing the interval $t_1 \le t \le t_2$ into the two intervals $t_1 \le t \le t_0$ and $t_0 \le t \le t_2$, we can easily rewrite the expression (25) in a symmetric form with respect to t_1 and t_2. For the transition probability we obtain

$$w_{12} = \mathrm{St}\left\{\left|\int \Phi_2^*(t_0)\,\Phi_1(t_0)\,d\tau\right|^2 \exp\left[\frac{2}{h}\,\mathrm{Im}\int_{t_1}^{t_0} L\,dt + \frac{2}{h}\,\mathrm{Im}\int_{t_0}^{t_2} L'\,dt\right]\right\},$$

$$L' = \int\left(\left(H - ih\frac{\partial}{\partial t}\right)\Phi_2\right)^* \Phi_1\,d\tau \Big/ \int \Phi_2^*\,\Phi_1\,d\tau, \qquad (26)$$

where the dependence on the intermediate time instant must disappear from the final result.

We note in conclusion that formula (25) leads immediately to an exponential law for the decay of a quasi-stationary state, if Φ_1 is replaced, as usual, by an approximate function which satisfies the equation

$$H\Phi_1 = (E_0 - i\Gamma)\,\Phi_1. \qquad (27)$$

In this case the functions of the initial and final states coincide, which is especially convenient for the application of the variational principle.

5. CHOICE OF TRIAL FUNCTIONS FOR CHARGE EXCHANGE TYPE PROBLEMS

In the calculation of the charge exchange by perturbation theory it would be natural to substitute $\Phi_1 = \psi_1$ and $\Phi_2 = \psi_2$ in the functional (25), setting $t_1 = -\infty$ and $t_2 = +\infty$. The functions ψ_1 and ψ_2 become orthogonal for $t \to \pm\infty$ and in order to avoid ambiguities it is more convenient to use the equivalent formula (26), setting in it $t_0 = 0$, for example.

In order to investigate the legitimacy of such a procedure, we return to the initial formulation of the variational principle (8). We do not impose any further restrictions on the functions Φ_1 and Φ_2 except the conditions (5) for $t = t_1$ and $t = t_2$. In particular, the normalization condition and the condition $\int \Phi_2^* \Phi_1\,d\tau = \mathrm{const}$, which hold only for the exact functions Ψ_1 and Ψ_2, may not be satisfied. If we now turn to the "corrected" functions $\Phi_1 f_1$ and $\Phi_2 f_2$ and use the explicit forms of f_1 and f_2 [formulas (23) and (24)], we see that

$$\int \Phi_2^* f_2^* \Phi_1 f_1\,d\tau = \mathrm{const}$$

and, hence, the normalizing functions f_1 and f_2 are determined by the variational principle in such a way as to make the overlap integral a constant. This implies that, if ψ_1 and ψ_2 are chosen as trial functions, the normalizing functions f_1 and f_2 will increase exponentially with time and the functions Ψ_1 and Ψ_2 will cease completely to be close to the exact Ψ_1 and Ψ_2. Indeed, the corresponding calculations for the charge exchange of protons with hydrogen atoms indicate that the integrals in the denominator of formula (26) diverge in this case and that, therefore, this choice of trial functions is unsatisfactory.

We therefore require that the class of functions to be substituted in the functional is consistent with the condition that the overlap integral $\int \Phi_2^* \Phi_1\,d\tau$ be constant without any appreciable distortion of the wave functions. The simplest choice that can be made in this case is the superposition of the functions ψ_1 and ψ_2:

$$\Phi_1 = f_1^1\psi_1 + f_1^2\psi_2, \quad \Phi_2 = f_2^1\psi_1 + f_2^2\psi_2; \qquad (28)$$

$$|f_1^1(-\infty)| = 1, \quad f_1^2(-\infty) = 0,$$

$$f_2^1(\infty) = 0, \quad |f_2^2(\infty)| = 1; \qquad (29)$$

$$w_{12} = |f_1^2(\infty)|^2. \qquad (30)$$

In this case the normalizing factor is one of the parameters to be varied, and we can require that the functional (8) or even the functional (4) be stationary in the derivation of the equations for the functions f, assuming that the variations are zero at the ends of the interval. We obtain the following equations for f_1 and f_2:

$$ih\,(\dot{f}^1 + S\dot{f}^2) = V_{11}f^1 + V_{12}f^2,$$
$$ih\,(\dot{f}^2 + S^*\dot{f}^1) = V_{21}f^1 + V_{22}f^2, \qquad (31)$$

where

$$S = \int \psi_1^*\psi_2\,d\tau, \quad V_{ij} = \int \psi_i^* U_j \psi_j\,d\tau \qquad (i, j = 1, 2). \quad (32)$$

These equations were obtained directly from the Schrödinger equation by Bates.[2] Their derivation from a variational principle is more consistent and unique (see reference 3, Sec. 13). Solving these equations with the boundary conditions (29), we can determine the probability for charge exchange for different impact parameters.

It was shown in the paper of Bates[2] that this approximation is useful for fast collisions. However, the most important criterion for the applicability of this method is provided by the value of the impact parameter ρ. For sufficiently large impact parameters (in practice, at distances of the order of two to three atomic radii) the wave functions are given with sufficient accuracy by (28), so that the approximation is adequate. Arguments can also be given in favor of the assertion that the polarization has a small effect on the probability for charge exchange.[4]

It follows immediately from the variational principle that all integrals

$$\int \Phi_i^*\left(H - ih\frac{\partial}{\partial t}\right)\Phi_j\,d\tau \qquad (33)$$

vanish. From this we obtain at once the normalization conditions and the condition that the overlap integral is constant, i.e., the condition of conservation of particles and the principle of detailed balancing:

$$|f_1^1(\infty)|^2+|f_1^2(\infty)|^2=1, \quad |f_2^1(-\infty)|^2+|f_2^2(-\infty)|^2=1, \tag{34}$$

$$f_1^2(\infty)=f_2^{1*}(-\infty). \tag{35}$$

In studying the question of the applicability of perturbation theory to the solution of the system (31) we must ascertain which parameters must be considered small in the problem. There are two such parameters: the values of $\psi_1(R)$ and $\psi_2(R)$, which determine the smallness of the coefficients V_{12}, V_{21}, and S, and the values of $U_1(R)$ and $U_2(R)$, which determine the smallness of the coefficients V_{11} and V_{22}. However, if the potentials U_1 and U_2 have Coulomb character, the second set of parameters cannot possibly be regarded as small for large R; moreover, the integrals

$$\frac{1}{h}\int_{-\infty}^{+\infty} V_{11}\,dt, \quad \frac{1}{h}\int_{-\infty}^{+\infty} V_{22}\,dt,$$

which occur in the solution of the system (31) by the method of successive approximations, are divergent. All coefficients of the system can be reduced to the same order of smallness either with the help of the transformation

$$f_1=g_1\exp\left(-\frac{i}{h}\int V_{11}\,dt\right),$$
$$f_2=g_2\exp\left(-\frac{i}{h}\int V_{22}\,dt\right), \tag{36}$$

or by preliminary orthogonalization of the functions ψ_1 and ψ_2. Thereafter the usual perturbation theory can be applied, and both methods lead to Bates' expression[2] for the transition probability

$$w=\left|\frac{1}{h^2}\int_{-\infty}^{+\infty}(V_{12}-V_{22}S)\,dt\right|^2. \tag{37}$$

We thus obtain the result that the appearance of additional terms in the formulas of perturbation theory is due to the simultaneous effects of two factors: the nonorthogonality of the zeroth order wave functions at intermediate times and the fact that the interaction has Coulomb character and cannot be regarded as small.

For the calculation of the charge exchange in slow collisions we may take recourse to the adiabatic approximation,[4,5] using as approximate wave functions the molecular wave functions with the time factor $\exp[-(i/h)\int E(R)\,dt]$. Substituting these functions in the stationary functionals, we can also consider the adiabatic approximation from the point of view of the variational principle.

6. CONCLUSION

Our formulation of the variational principle for nonstationary problems of quantum mechanics is more general than the old formulation (8). In particular, it is easily seen that, if the overlap integral for the trial functions is independent of the time, the old variational principle can be obtained from the new one by expanding the exponential in a series and keeping only the first two terms.

The use of this variational principle for direct calculations is apparently somewhat hampered by the fact that the dependence of the functional on the parameters of the trial function may be rather complicated. However, this variational principle may be useful in the most diverse problems for the investigation of various general questions and also in those cases where the approximate wave functions are already known.

In conclusion the author thanks V. A. Fock and G. F. Drukarev for a detailed discussion of this work and for valuable advice.

---

[1] D. R. Bates and A. Dalgarna, Proc. Phys. Soc. **A65**, 919 (1952) and **A66**, 971 (1953). J. D. Jackson and H. Schiff, Phys. Rev. **89**, 359 (1953).

[2] D. R. Bates, Proc. Roy. Soc. **A247**, 294 (1958).

[3] Yu. N. Demkov, Вариационные принципы в теории столкновений (Variational Principles in the Theory of Collisions) GITTL, M., 1958.

[4] Yu. N. Demkov, Уч. зап. ЛГУ, (Scientific Notes, Leningrad State U.) No. 146, 80 (1952).

[5] O. B. Firsov, JETP **21**, 1001 (1951). D. R. Bates and R. McCarroll, Proc. Roy. Soc. **A245**, 175 (1958).

Translated by R. Lipperheide
358

SOVIET PHYSICS JETP VOLUME 11, NUMBER 6 DECEMBER, 1960

SOLUTION OF EQUATION FOR THE MESON-MESON SCATTERING AMPLITUDE IN THE ASYMPTOTIC REGION

A. A. ANSEL'M

Leningrad Physico-Technical Institute, Academy of Sciences, U.S.S.R.

Submitted to JETP editor February 2, 1960

J. Exptl. Theoret. Phys. (U.S.S.R.) 38, 1887-1890 (June, 1960)

The set of integral equations deduced in references 1 and 2 for the meson-meson scattering amplitude is solved exactly. An integral equation for the amplitude which depends only on one variable is obtained as a direct mathematical corollary of this set.

THE asymptote of the meson-meson scattering amplitude was studied in references 1 and 2 by means of the summation of the "parquet" sequence of Feynman diagrams. A set of integral equations was obtained which determine the amplitude as a function of two variables (actually, the transferred momentum and the energy) and, in independent fashion, the equation for the amplitude which depends on a single variable, corresponding to the case in which all the invariants of the problem are quantities of the same order. However, it was not possible for the authors to obtain the latter equation as a direct mathematical corollary of their system of equations; moreover, the given system was solved only in certain limiting cases. In the present work, the equation for the amplitude which depends on a single variable was derived directly from the set of integral equations, and an exact solution of this system was obtained. In limiting cases the resultant solution coincides with the solution given in references 1 and 2, if we correct the computational error made in these papers.

As was shown in references 1 and 2, the amplitude P in the case of neutral pseudoscalar theory consists of three terms which can be conveniently chosen as functions of the variables x and y:

$$P(x, y) = R_0(x) + 2\Phi(x) + \Phi(x, y), \quad R_0(x) = 24(1 - x),$$
$$\Phi(x) = \Phi(x, x), \quad x = \left[1 + \frac{5g_0^2}{4\pi}\ln\frac{\Lambda^2}{t}\right]^{-1/5},$$
$$y = \left[1 + \frac{5g_0^2}{4\pi}\ln\frac{\Lambda^2}{s}\right]^{-1/5}. \tag{1}$$

Here Λ^2, s, and t are squares of the cutoff momentum, energy, and transferred momentum, and g_0 is the unrenormalized coupling constant. The quantity $R_0(x)$ is the contribution to the amplitude of the simplest diagram, while $\Phi(x)$ and $\Phi(x, y)$ are the contributions of the most important ("contractible") diagrams. The quantity P (x, y) satisfies the integral equation

$$P(x, y) = s(x) - \frac{1}{2}\int_y^x s(x) P(t, y)\frac{dt}{t^2} - \frac{1}{2}\int_x^1 s(t) P(t, y)\frac{dt}{t^2},$$
$$s(x) = R_0(x) + 2\Phi(x) = P(x) - \Phi(x), \quad P(x) = P(x, x). \tag{2}$$

It is most important for the following that the variables in (2) are separable. In fact, if we set $P(x, y) = P_1(x) P_2(y)$, divide both parts of (2) by $P_2(y)$, and differentiate with respect to y, we easily obtain

$$P_2'(y)/P_2^2(y) = P_1(y)/2y^2, \tag{3}$$

so that x-dependent terms drop out of the equation for $P_2(y)$. It follows from (3) that

$$\frac{1}{2}\int_y^x \frac{P_1(t)}{t^2}\,dt = \frac{1}{P_2(y)} - \frac{1}{P_2(x)}. \tag{4}$$

The same integral enters into (2) also, upon substituting $P(t, y) = P_1(t) P_2(y)$. If, in accord with Eq. (4), we replace it by the difference $P_2^{-1}(y) - P_2^{-1}(x)$, an integral equation is obtained which does not contain y, and which, together with (4), comprises a system equivalent to (2). The relations that follow can be obtained by starting out from this pair of equations, but we shall set them up in a somewhat simpler fashion. Differentiating (2) with respect to x and setting x = y, we get

$$P_1'(x) P_2(x) = s'(x). \tag{5}$$

It follows from (3) and (5) that

$$P'(x) = s'(x) + P^2(x)/2x^2. \tag{6}$$

It is easy to see from the definitions (1) and (2) that $s(x) = \frac{1}{3}R_0(x) + \frac{2}{3}P(x)$, which gives the following final integral equation for an amplitude dependent on one variable:

$$P(x) = R_0(x) + \frac{3}{2}\int_1^x \frac{P^2(t)}{t^2}\,dt. \tag{7}$$

This result coincides with the equation for P (x) obtained in references 1 and 2 by a special consideration of the graphs. The solution of (7) is found in references 1 and 2 in the form

$$P(x) = \frac{\alpha+1}{3}\,x(1-x^\alpha)\left[1+\frac{\alpha+1}{\alpha-1}x^\alpha\right]^{-1}, \qquad \alpha = \sqrt{145}. \tag{8}$$

The fact that P (x, y) = P_1(x) P_2(y) makes it possible to find P (x, y). It is easy to see from (3) that

$$P_2(y) = \exp\left[\frac{1}{2}\int^y \frac{P(t)}{t^2}\,dt\right] = \mathrm{const}\cdot y^{(\alpha+1)/6}\left(1+\frac{\alpha+1}{\alpha-1}y^\alpha\right)^{-1/3}. \tag{9}$$

Hence:

$$P(x,y) = \frac{\alpha+1}{3}\,x\left(\frac{y}{x}\right)^{(\alpha+1)/6}(1-x^\alpha)$$
$$\times\left[1+\frac{\alpha+1}{\alpha-1}x^\alpha\right]^{-2/3}\left[1+\frac{\alpha+1}{\alpha-1}y^\alpha\right]^{-1/3}. \tag{10}$$

The situation is somewhat more complicated in the case of symmetric pseudoscalar theory. Here the following relations hold by reason of the presence of isotopic variables[1,2]

$$P_{\xi_1\xi_2\xi_3\xi_4}(x,y) = P(x,y)\,\delta_s + P_1(x,y)\,\delta_{\xi_1\xi_2}\delta_{\xi_3\xi_4},$$
$$\Phi_{\xi_1\xi_2\xi_3\xi_4}(x,y) = \Phi(x,y)\,\delta_s + \Phi_1(x,y)\,\delta_{\xi_1\xi_2}\delta_{\xi_3\xi_4},$$
$$P(x,y) = \rho_0(x) + 2\Phi(x) + \Phi(x,y) + \Phi_1(x),$$
$$P_1(x,y) = \Phi_1(x,y) - \Phi_1(x),$$
$$\rho_0(x) = \frac{16}{3}(1-x), \quad x = \left[1+\frac{5g_0^2}{4\pi}\ln\frac{\Lambda^2}{t}\right]^{3/5},$$
$$y = \left[1+\frac{5g_0^2}{4\pi}\ln\frac{\Lambda^2}{s}\right]^{3/5}, \quad \delta_s = \delta_{\xi_1\xi_2}\delta_{\xi_3\xi_4} + \delta_{\xi_1\xi_3}\delta_{\xi_2\xi_4} + \delta_{\xi_1\xi_4}\delta_{\xi_2\xi_3}, \tag{11}$$

ξ_i is the isotopic variable of the i-th meson.

If we introduce the notation

$$L(s(x), P(x,y)) \equiv \frac{1}{3}\int_y^x s(x)\,P(t,y)\frac{dt}{t^2}$$
$$+\frac{1}{3}\int_x^1 s(t)\,P(t,y)\frac{dt}{t^2}, \tag{12}$$

then the corresponding set of integral equations can be written in the form

$$P(x,y) = s(x) + L(s(x), P(x,y)),$$
$$P_1(x,y) = -\Phi_1(x) + L[\tfrac{5}{2}(s(x)-\Phi_1(x)),$$
$$P(x,y) + P_1(x,y)] + L(\Phi_1(x), P_1(x,y)),$$
$$s(x) = \rho_0(x) + 2\Phi(x) + \Phi_1(x)$$
$$= \tfrac{2}{3}P(x) + \tfrac{1}{3}\rho_0(x) + \tfrac{1}{3}\Phi_1(x). \tag{13}$$

The first of these equations has the same structure as Eq. (2). Again setting P(x, y) = P_1(x) P_2(y), and repeating the calculations, we obtain from the first equation of (13)

$$\frac{P_2'(y)}{P_2(y)} = -\frac{P(y)}{3y^2}, \qquad P_1'(x)\,P_2(x) = s'(x),$$
$$P(x) = s(x) - \frac{1}{3}\int_1^x \frac{P^2(t)}{t^2}\,dt. \tag{14}$$

Or, taking into account Eq. (13) for s (x),

$$P(x) = \rho_0(x) + \Phi_1(x) - \int_1^x \frac{P^2(t)}{t^2}\,dt. \tag{15}$$

Using the first equation of (13), we can transform the second equation into a form coinciding with (2):

$$G(x,y) = \lambda(x) + L[\tfrac{3}{2}\lambda(x), G(x,y)],$$
$$G(x,y) = \tfrac{5}{3}P(x,y) + P_1(x,y), \qquad \lambda(x) = \tfrac{5}{3}s(x) - \Phi_1(x). \tag{16}$$

It is then clear that G(x, y) = G_1(x) G_2(y), whence

$$\frac{G_2'(y)}{G_2(y)} = -\frac{G(y)}{2y^2}, \qquad G_1'(x)\,G_2(x) = \lambda'(x),$$
$$G(x) = \lambda(x) - \frac{1}{2}\int_1^x \frac{G^2(t)}{t^2}\,dt. \tag{17}$$

Since P_1(x, x) = 0, then, in accord with (16), G (x) differs from P (x) by only the factor 5/3. Eliminating Φ_1(x) from (17) and (15), we easily obtain

$$P(x) = \rho_0(x) - \frac{11}{6}\int_1^x \frac{P^2(t)}{t^2}\,dt, \tag{18}$$

which again is identical with the result of references 1 and 2. The solution of this equation is

$$P(x) = \tfrac{16}{11}x(1-x^{-19/3})/(1+\tfrac{8}{11}x^{-19/3}), \tag{19}$$

whence, by the method given above, we can easily obtain P (x, y):

$$P(x,y) = \tfrac{16}{11}x\,(x/y)^{16/33}(1-x^{-19/3})$$
$$\times(1+\tfrac{8}{11}x^{-19/3})^{-9/11}(1+\tfrac{8}{11}y^{-19/3})^{-2/11}. \tag{20}$$

In order to find P_1(x, y), we can use the relation (17) and the first equation of (14). Since G (x) = 5/3 P (x), we obtain

$$G_2'/G_2 = 5P_2'/2P_2,$$
$$\text{i. e. } G_2 = P_2^{5/2}, \qquad G_1 = \tfrac{5}{3}P_1P_2^{-3/2}, \tag{21}$$

whence

$$P_1(x,y) = \tfrac{5}{3}(\tfrac{16}{11}x)\,x^{16/33}y^{-16/33}(1-x^{-19/3})(1+\tfrac{8}{11}x^{-19/3})^{-9/11}$$
$$\times(1+\tfrac{8}{11}y^{-19/3})^{-2/11}[(x/y)^{8/11}(1+\tfrac{8}{11}x^{-19/3})^{3/11}$$
$$\times(1+\tfrac{8}{11}y^{-19/3})^{-3/11} - 1]. \tag{22}$$

In references 1 and 2, P (x, y) and P_1(x, y) were obtained in the limiting cases $x-1 \ll 1$,

$y-1 \ll 1$ (perturbation theory) and $x \gg 1$, $y \gg 1$. If we correct the computational error contained in these papers, then the corresponding equations have the form

$$P(x, y) = \begin{cases} \frac{16}{3}(x-1)\{1-\frac{88}{27}(x-1)^2-\frac{8}{9}[(y-1)^2-(x-1)^2]+\cdots\}, & x-1 \ll 1,\ y-1 \ll 1 \\ \left(\frac{16}{11}x\right)x^{16/33}y^{-16/33}+\cdots, & x \gg 1, \quad y \gg 1, \end{cases}$$

$$P_1(x, y) = \begin{cases} -\frac{5}{12}\left(\frac{16}{3}\right)^2(x-1)[(y-1)^2-(x-1)^2]+\cdots & x-1 \ll 1,\ y-1 \ll 1 \\ \left(\frac{16}{11}x\right)\frac{5}{3}\left(x^{40/33}y^{-40/33}-x^{16/33}y^{-16/33}\right)+\cdots, & x \gg 1, \quad y \gg 1, \end{cases}$$

which is identical to the expansion obtained directly from (20) and (22).

The most curious fact is that the scattering amplitude in the asymptotic region is a product of functions each of which depends only on the transferred momentum and the energy. It is not clear, however, to what degree this property is preserved if we do not limit ourselves to a consideration of "parquet" diagrams only.

The author is grateful to V. V. Anisovich for a number of useful remarks.

---

[1] Dyatlov, Sudakov, and Ter-Martirosyan, JETP **32**, 767 (1957), Soviet Phys. JETP **5**, 631 (1957).

[2] Pomeranchuk, Sudakov, and Ter-Martirosyan, Phys. Rev. **103**, 784 (1956).

Translated by R. T. Beyer
359

SOVIET PHYSICS JETP VOLUME 11, NUMBER 6 DECEMBER, 1960

SOME EXPERIMENTAL POSSIBILTIES FOR VERIFICATION OF THE MODEL OF NONAXIAL NUCLEI ROTATIONAL SPECTRUM

D. P. GRECHUKHIN

Submitted to JETP editor February 6, 1960

J. Exptl. Theoret. Phys. (U.S.S.R.) 38, 1891-1893 (June, 1960)

It is shown that detection of E0 transitions of the $I^+ \to I^+$ type (I is the nuclear spin) in even-even nuclei is a crucial test of the model of nonaxial nuclei with a rotational spectrum. The isotopic shift predicted by the model is considered.

THE energy spectrum of individual even-even nuclei in the ranges $60 \lesssim A \lesssim 160$ and $180 \lesssim A \lesssim 240$ is interpreted by Davydov and Filippov[1] as the rotational spectrum of a nonaxial deformed nucleus whose surface is determined by two deformation parameters β and γ. In what follows we shall call this model the DF model.

The comparison with experimental data of the results of calculations in the DF model of the level spectrum and of the probabilities of the M1 and E2 transitions, carried out by Davydov and his coworkers,[1-4] shows that some even-even nuclei are accurately described by the DF model.

The DF model embraces the regions in the neighborhood of the magic nuclei and also the regions in which the nuclei have an equidistant level spectrum which was interpreted earlier as the spectrum of vibrational excitations of the nucleus.[5,6] The fundamental laws of M1 and E2 transitions are also sufficiently well described (qualitatively) in this region by the vibration model of the nucleus. In near magic regions of atomic weights, it appears that good agreement with experiment can be obtained in the shell model with residual interaction between the nucleons. We note that in our view there is at the present time no completely convincing theoretical foundation for the DF model of a nonaxial nucleus with a rotation interaction spectrum. Therefore, the problem of a model which most adequately describes the nuclear spectrum remains open, and more experimental data are necessary for its solution by means of any sort of model.

In particular, it will be shown below that the detection of E0 transitions of the type $I^+ \to I^+$ ($I \neq 0$; I is the nuclear spin) is a crucial test for the DF model in which these transitions are strictly forbidden.*

The additional data make possible a study of the isotopic shifts of the levels of the atomic electrons.

1. E0 Transitions in the DF Model

In the DF model, the wave function of the n-th rotational state with spin I and projection M is the product of the functions of the rotational motion of the nucleus $\Psi_{nIM}(\theta_i)$, where θ_i are the Euler angles, by the function of the state of the core, which depends on the deformation parameters, $\varphi_{\beta\gamma}(r'_k)$. It is assumed that in the different rotational states of the nucleus the internal state of the core remains unchanged:[1]

$$\Psi_{nIM}(\beta, \gamma, \theta_i) = \Psi_{nIM}(\theta_i)\,\varphi_{\beta\gamma}(r'_k). \tag{1}$$

Inasmuch as the operator of the E0 transition

$$\widehat{E0} = \sum_{i=1}^{Z} r_i^2 \tag{1a}$$

is a scalar, on going to a system of coordinates rotating with the nucleus, we obtain for the matrix element of the E0 transition ($n_1IM \to n_2IM$)

$$\langle n_2IM|\widehat{E0}|n_1IM\rangle = \left\langle \varphi^*_{\beta\gamma}\left|\sum_{i=1}^{Z}(r'_i)^2\right|\varphi_{\beta\gamma}\right\rangle \int \Psi^*_{n_2IM}(\theta_i)\,\Psi_{n_1IM}(\theta_i)\,d\tau. \tag{2}$$

Since the functions of the rotational motion of the nucleus for different states are orthogonal

$$\int \Psi^*_{n_2IM}(\theta_i)\,\Psi_{n_1IM}(\theta_i)\,d\tau = \delta_{n_2n_1}, \tag{2a}$$

the matrix element of the E0 transition in the DF model is exactly equal to zero.

We note that in a model of the nucleus with a vibrational spectrum of excitation E0 transitions of the $I^+ \to I^+$ type ($I \neq 0$) are not forbidden. In particular, for E0 transitions ($2^+ \to 2^+$) between the second and third excited levels of the nucleus, the following has been obtained:[7]

---

*The necessity for investigating E0 transitions in even-even nuclei with equally spaced levels was noted earlier by the author.[7] We again turn to this problem in connection with the appearance of new experimental data on E0 transitions.[8] The author is grateful to I. S. Shapiro who directed his attention to this research of Gerholm and Petterson.

$$\langle \chi_{2\mu}^{2+} | \widehat{E0} | \chi_{2\mu}^{1} \rangle = \frac{3}{4\pi} ZR_0^2 \cdot 5 \sqrt{\frac{10}{4\pi}} C_{2020}^{20} \left(\frac{\hbar\omega}{2C_2}\right)^{3/2}, \qquad (3)$$

where $\hbar\omega$ is the energy of the photon (the energy of the first excited level of the nucleus); C_2 is the stiffness of the nucleus relative to quadrupole deformations of the surface. For example, it is assumed in reference 4 that the nucleus Pt^{196} is nonaxial ($\gamma \approx 30°$) and has a rotational spectrum of levels. But is was established by Gerholm,[8] by observation of the angular correlation of the conversion electron with the γ quantum, that an E0 transition takes place between the levels $2^+ \rightarrow 2^+$, where the matrix element of the E0 transition

$$\rho = \left\langle 2.2 \left| \sum_{i=1}^{Z} (r_i / R_0)^2 \right| 1.2 \right\rangle \qquad (3a)$$

has the order of magnitude $0.017 \leq |\rho| \leq 0.05$. This value of $|\rho|$ is comparable with $|\rho| = 0.09$ for Ge^{70} and $|\rho| = 0.06$ for Zr^{90}.[9] Consequently, there is no basis for assuming the nucleus Pt^{196} to fit the DF model.

2. The Isotopic Shift of Electron Levels According to the DF Model

The isotopic displacement of the levels of atomic electrons in heavy elements is determined by the change in the mean square radius of the proton distribution in the ground state of the nucleus

$$\langle r^2 \rangle = \left\langle 0 \left| \sum_{i=1}^{Z} r_i^2 \right| 0 \right\rangle. \qquad (3b)$$

In the DF model[1] it is assumed that the protons are uniformly distributed over the volume of the deformed nucleus. Taking this into account, we obtain for $\langle r^2 \rangle_{DF}$:

$$\langle r^2 \rangle_{\mathbf{DF}} = \frac{3}{5} ZR_0^2 \left\{1 + \frac{5}{4\pi}\beta^2 + \frac{15}{8\pi}\beta^3 \cos\gamma \left[1 - 4\sin^2\gamma\right]\right\}. \qquad (4)$$

For comparison we write down $\langle r^2 \rangle_{vibr}$, obtained in the drop model with vibration spectrum:

$$\langle r^2 \rangle_{\mathbf{vibr}} = \frac{3}{5} ZR_0^2 \left\{1 + \frac{5}{4\pi}\beta_{\mathbf{vibr}}^2\right\}, \qquad (5)$$

where

$$\beta_{\mathbf{vibr}} = 5\hbar\omega/2C_2. \qquad (6)$$

The quantities β^2 and β_{vibr}^2 are determined from the given probability of E2 transitions from the first excited level of the nucleus to the ground state:

$$B(E2; 21 \rightarrow 0) \approx 9Z^2e^2R_0^4\beta^2/80\pi^2 \qquad (7)$$

and similarly for β_{vibr}^2.

As is seen from (4), we have for nuclei with equally spaced spectrum ($\gamma = 30°$)

$$\langle r^2 \rangle_{\mathbf{DF}} = \frac{3}{5} ZR_0^2 \{1 + 5\beta^2/4\pi\}, \qquad (7a)$$

which coincides with $\langle r^2 \rangle_{vibr}$.

The change in $\langle r^2 \rangle_{DF}$ on going from one isotope to another is determined by the change in the parameters β and γ. As is seen from (4), the change of γ no longer contributes to the shift for nuclei with an equally spaced spectrum, but in the regions of transitions to magic nuclei and to axially symmetric nuclei with a rotational level spectrum the parameter γ changes abruptly. For example, if we consider the isotopes Gd^{152}, Gd^{154} and Gd^{156} within the framework of a DF model, then we have here for γ the values 30, 13.7 and 0°, respectively. A similar situation holds for the isotopes Sm^{150}, Sm^{152}, Sm^{154} and, apparently, for Dy^{160}, Dy^{162} and Dy^{164}. The study of the isotopic mixture for these nuclei is important for verification of the DF model.

In conclusion, the author expresses his gratitude to I. S. Shapiro for his interest in the work.

---

[1] A. S. Davydov and G. F. Filippov, JETP **35**, 440 (1958), Soviet Phys. JETP **8**, 303 (1959).

[2] A. S. Davydov and G. F. Filippov, JETP **35**, 703 (1958), Soviet Phys. JETP **8**, 488 (1959).

[3] A. S. Davydov and V. C. Rostovskii, JETP **36**, 1788 (1959), Soviet Phys. JETP **9**, 1275 (1959).

[4] A. S. Davydov and G. F. Filippov, Nucl. Phys. **8**, 237 (1958).

[5] G. Scharf-Goldhaber and J. Weneser, Phys. Rev. **98**, 212 (1955).

[6] Alder, Bohr, Huus, Mottelson, and Winther, Revs. Modern Phys. **28**, 432 (1956).

[7] D. P. Grechukhin, JETP **32**, 1036 (1957); Soviet Phys. JETP **5**, 866 (1957).

[8] T. R. Gerholm and V. G. Petterson, Phys. Rev. **110**, 1119 (1958).

[9] D. E. Alburger, Phys. Rev. **109**, 1222 (1958).

Translated by R. T. Beyer

CONNECTION BETWEEN THE POLARIZATION OF β ELECTRONS AND THE SHAPE OF THE β SPECTRUM

B. V. GESHKENBEĬN and A. P. RUDIK

Submitted to JETP editor February 15, 1960

J. Exptl. Theoret. Phys. (U.S.S.R.) 38, 1894-1895 (June, 1960)

The connection between the longitudinal polarization of the β electrons and the shape of the β spectrum is established.

As is known,[1] the shape factor of the β spectrum C(W) and the longitudinal polarization of the β electrons $\langle\sigma\rangle$ are given by the following expressions:

$$C(W) = \sum_i M_i(Z, W) f_i(W, X), \qquad (1)$$

$$\langle\sigma\rangle = \frac{v}{c} \sum_i M_i(Z, W) f_i(W, X) a_i(Z, W) \Big/ \sum_i M_i(Z, W) \times f_i(W, X). \qquad (2)$$

Here Z is the charge of the nucleus, W and v are the energy and the velocity of the β electrons, respectively, X are the nuclear matrix elements, M_i and a_i are certain complicated functions which take account of the motion of the electron in the Coulomb field of the daughter nucleus, and the functions f_i depend on the energy of the electron and on the matrix elements.

From formulas (1) and (2) we can obtain the qualitative dependence of the polarization of the β electrons on the shape of the β spectrum for first-forbidden transitions in heavy nuclei. It appears, firstly, that, if there are no accidental relations between the matrix elements (due to some particular feature in the structure of the given nucleus), the Coulomb terms play the most important role in the expression (1) for C(W), and C(W) is constant, i.e., we have a pure Fermi spectrum. Secondly, the function $a_i(Z, W)$ is always very close to unity, deviating only by 2 to 4%. For a spectrum with Fermi shape the polarization of the β electrons therefore practically coincides with $-v/c$. This last result is well known from experiment.[2]

However, cases of first-forbidden decay are known for which the longitudinal polarization of the β electrons differs appreciably from the value $-v/c$. Here the β spectrum is not of the Fermi type.

The classic example of this type is the β decay of RaE (transition $1^- \rightarrow 0^+$). In this transition the polarization of the β electrons is appreciably different from the value $-v/c$,[3] and C(W) is definitely not a constant.[4] Both these experimental facts can be explained by assuming that the relation between the matrix elements is such that the main, energy independent terms cancel each other for the most part, so that energy dependent terms start to play the most important role.[5]

An interesting example is also the β decay of Au^{198} (transition $2^- \rightarrow 2^+$). According to the data of the group of Alikhanov et al. (private communication and reference 6) the longitudinal polarization of the β electrons is appreciably different from $-v/c$ in the region of small energies [$\langle\sigma\rangle = (-0.83 \pm 0.05)\, v/c$ for W = 100 kev] and is equal to $-v/c$ in the region of large energies [$\langle\sigma\rangle = (-0.97 \pm 0.06)\, v/c$ for W = 400 kev]. The work of reference 7 contains similar data on the polarization of the β electrons of Au^{198} in the region of small energies.

It is interesting to compare these data with the data on the shape of the β spectrum of Au^{198}. It appears[8] that C(W) is constant for $W > 300$ kev and increases sharply with decreasing energy in the region $W < 300$ kev. Thus we see again that the deviation of the polarization from $-v/c$ is intimately related to the deviation of the shape of the spectrum from the Fermi shape. In the case of unique transitions, $\Delta_j = 2$ (yes), the polarization is equal to $-v/c$, since there is only one matrix element and a cancelling out is impossible. Quantitative calculations for the case of the β decay of Au^{198} are of little interest, since the number of unknown matrix elements (six) is too large.

We note finally that the deviation of the polarization from the value $-v/c$ is due to the deviation of the shape of the spectrum from the Fermi shape also in the case of P^{32} and In^{114} (the data on the polarization are taken from Mikaélyan and Spivak,[10] the data on the spectra from reference 9).

The authors express their deep appreciation to Acad. A. I. Alikhanov and V. A. Lyubimov, who directed their attention to the anomalies in the polarization of the β electrons of Au^{198}, for their interest in this work.

[1] G. E. Lee-Whiting, Canad. J. Phys. **36**, 252 (1958).

[2] A. I. Alikhanov, Report at the International Conference on High Energy Particles at Kiev, 1959.

[3] Alikhanov, Eliseev, and Lyubimov, JETP **35**, 1061 (1958), Soviet Phys. JETP **8**, 740 (1959). Geiger, Ewan, Graham, and Mackenzie, Phys. Rev. **112**, 1684 (1958). W. Bühring and J. Heintze, Phys. Rev. Lett. **1**, 176 (1958). Wegener, Bienlein, and v. Issendorf, Phys. Rev. Lett. **1**, 460 (1958).

[4] E. A. Plassman and L. M. Langer, Phys. Rev. **96**, 1593 (1954).

[5] Geshkenbeĭn, Nemirovskaya, and Rudik, JETP **36**, 517 (1959), Soviet Phys. JETP **9**, 360 (1959); Nucl. Phys. **13**, 60 (1959). E. Wegener, Z. Phys. **154**, 553 (1959).

[6] Alikhanov, Eliseev, and Lyubimov, JETP **34**, 1045 (1958), Soviet Phys. JETP **7**, 723 (1958).

[7] Vishnevskiĭ, Grigor'ev, Ergakov, Nikitin, Pushkin, and Trebukhovskiĭ, in the volume Ядерные реакции при малых и средних энергиях, (Nuclear Reactions at Small and Intermediate Energies), 1958, p. 336.

[8] R. M. Steffen, Proc. of the Rehovoth Conference on Nuclear Structure, September 1957, New York, 1958.

[9] Johnson, Johnson, and Langer, Phys. Rev. **112**, 2004 (1958).

[10] L. A. Mikaélyan and P. E. Spivak, JETP **37**, 1168 (1959), Soviet Phys. JETP **10**, 831 (1960).

Translated by R. Lipperheide
361

SOVIET PHYSICS JETP VOLUME 11, NUMBER 6 DECEMBER, 1960

THERMODYNAMIC FUNCTIONS OF A LOW-TEMPERATURE PLASMA

A. I. LARKIN

Submitted to JETP editor February 15, 1960

J. Exptl. Theoret. Phys. (U.S.S.R.) **38**, 1896-1898 (June, 1960)

We have evaluated the thermodynamic functions of a plasma at temperatures below the ionization temperature. We have shown that if the interaction of the ions with the electrons of the continuous spectrum is properly taken into account, this will partially compensate the contribution from the excited states of the atoms and the complex ions.

THE thermodynamic potential of an electron-ion plasma is usually defined by the formula

$$-\beta\Omega = \sum_i \zeta_i, \tag{1}$$

where $\beta = 1/kT$ and where the summation is over all the types of particles, while the quantities ζ_i are expressed in terms of the corresponding chemical potentials

$$\zeta_i = (m_i / 2\pi\hbar^2\beta)^{3/2} \exp[\beta(\mu_i + I_i)]. \tag{2}$$

Here I_i is the energy for the complete ionization of the i-th ion. The conditions for equilibrium and neutrality lead to the following relations between the chemical potentials

$$\mu_z + \mu_e = \mu_{z-1}, \qquad \sum Q_i\, \partial\Omega_i / \partial\mu_i = 0. \tag{3}$$

Equation (1) is the first term in an expansion of the thermodynamic potential in powers of ζ. One must in the next approximation add to expression (1) the Debye term $\kappa^3/12\pi$, where

$$\varkappa^2 = 4\pi\beta \sum Q_i^2 \zeta_i. \tag{4}$$

Moreover, one must replace in Eq. (2) the last factor by a sum $\Sigma_m \exp(\beta I_{im})$ over all excited states of the i-th ion. This sum is formally equal to infinity. If we restrict the summation, as is done in the papers by Fermi and others,[1] only to those states where the ionic dimensions are less than the interparticle distance, we get the result that the contribution from the excited ions to the thermodynamic potential is proportional to $\zeta^{3/2}$ and is of the same order of magnitude as the Debye term.

If one, however, takes the interaction between an ion with charge Q_i and the electrons of the continuous spectrum properly into account, one is led to an expression which compensates the divergence of the sum over the bound states of the ion with charge $Q_i - e$. After separating the Debye term, there remains thus an expression which is proportional to $\zeta^2 \ln \zeta$, ζ^2, and higher powers of ζ.

Let us consider the interaction between an ion with charge Q_i and an electron. The correct magnitude of the term of order ζ^2 (see reference 2) is obtained by subtracting from the quantum mechanical expression for the virial coefficient the infinite terms: the term

$$\zeta_i\zeta_e \int \frac{\beta Q_i Q_e}{r}\, dV,$$

leading to the neutrality of the plasma, and the term

$$\frac{1}{2}\zeta_i\zeta_e \int \left(\frac{\beta Q_i Q_e}{r}\right)^2 dV,$$

were already taken into account when the Debye term was evaluated. The remaining expression

$$\zeta_i\zeta_e \left\{ \left(\frac{2\pi\hbar^2\beta}{m}\right)^{3/2} \sum_k \exp(-\beta E_k) - \int \left[1 + \frac{\beta Q_i Q_e}{r} + \frac{1}{2}\left(\frac{\beta Q_i Q_e}{r}\right)^2\right] dV \right\} \tag{5}$$

diverges logarithmically, and to remove this divergence one must replace at large distances from the ion its Coulomb potential by the Debye potential $(Q_i/r)\exp(-\kappa r)$, where κ is defined by Eq. (4). The sum in the first term of Eq. (5) is taken over all states of both the continuous and the discrete spectrum. The contribution from the largest term in that sum, which corresponds to the ground state of the ion (or atom) with charge $Q_i - e$, is equal to ζ_{i-1} and was already taken into account in Eq. (1), so that we shall assume that the summation is only over the excited states. If the ion is not a nucleus, we must take for the energies of the first levels experimental or approximately evaluated values, but at higher excitation energies the spectrum is a Coulomb one, i.e., the levels are n^2-fold degenerate and have an energy $E_n = -\frac{1}{2} m (Q_i Q_e/\hbar n)^2$. Let the condition for quasi-classical behavior $\beta m (Q_i Q_e/\hbar)^2 \gg 1$ be fulfilled; only in that case will there be an appreciable contribution from the bound states. The opposite limiting case was considered in the paper by Vedenov and Larkin.[2] We take for n_0 such a quantum number that $\beta |E_n| \ll 1$; we can then replace the sum over the bound states with $n > n_0$ and over the states of the continuous spectrum by an integral, using for the density of states the quasi-classical expression $dn = (2\pi)^{-3} dp\, dr$. For large n_0 the remaining sum is proportional to n_0^3, but the integral term contains a compensating term. In the calculation it is convenient to differentiate twice with respect to β the expression within the braces in (5), after which one can put $n_0 = \infty$ and evaluate separately the sum and the integral.

As a result we get

$$-\beta\Omega_{ie} = \zeta_i \zeta_e \left\{ \left(\frac{2\pi\hbar^2\beta}{m}\right)^{3/2} \sum_m [\exp(\beta E_m) - 1 - \beta E_m] + \frac{2\pi}{3} (\beta Q_i Q_e)^3 \left(\ln \frac{1}{3\beta Q_i Q_e \varkappa} - 2C + \frac{11}{6} \right) \right\}. \qquad (6)$$

Here C is Euler's constant, which is equal to 0.577; the sum is over all bound states and converges.

The contribution to the thermodynamical potential from the interactions between ions with charge Q_i and Q_j is evaluated from the classical formula for the second virial coefficient

$$-\beta\Omega = \zeta_i \zeta_j \int (e^{-\beta u} - 1)\, dV.$$

As the ions repel one another, there is no divergence at small distances apart and the divergence at large distances is removed in the way described above. When one evaluates this integral, as in the evaluation of the term with the integral in Eq. (6), the important distances are of the order $\beta Q_i Q_j$; at these distances the interaction even between complex ions can be assumed to be a Coulomb one. As a result we get

$$-\beta\Omega_{ij} = -\frac{2\pi}{3} (\beta Q_i Q_j)^3 \left(\ln \frac{1}{3\beta Q_i Q_j \varkappa} - 2C + \frac{11}{6} \right). \qquad (7)$$

The interaction between electrons and between ions of the same kind leads to an expression which differs from Eq. (7) only by a factor $\frac{1}{2}$.

To evaluate the Debye term we must bear in mind that the screening occurs not for free particles but for particles in the field of other particles. Using the diagram technique, described in the paper by Vedenov and the author,[2] to evaluate the correction term, we find a contribution to $-\beta\Omega$ equal to

$$\frac{\pi}{2} \beta^3 \left(\sum Q_i^4 \zeta_i\right) \left(\sum Q_i^2 \zeta_i\right).$$

If the plasma is weakly ionized, we must take into account the interaction between the atoms. If, however, the number of atoms is of the same order of magnitude as the number of ions the interaction between the atoms is less important and we shall not take it into account here. We have thus

$$-\beta\Omega = \sum \zeta_i + \frac{\varkappa^3}{12\pi} + \left(\frac{2\pi\hbar^2\beta}{m}\right)^{3/2} \zeta_e \sum_i \zeta_i \sum_m [\exp(\beta E_m) - 1 - \beta E_m] - \frac{\pi}{3} \beta^3 \sum_{ij} (Q_i Q_j)^3 \zeta_i \zeta_j \left(\ln \frac{1}{3\beta Q_i Q_j \varkappa} - 2C + \frac{11}{6} \right) + \frac{\pi}{2} \beta^3 \left(\sum Q_i^4 \zeta_i\right) \left(\sum Q_i^2 \zeta_i\right).$$

If the interelectronic interaction is not quasi-classical but must be described in the Born approximation, we must substitute for the corresponding term the analogous expression from a previous paper.[2] The interaction between the electrons and the ions can be treated in the Born approximation only when the plasma is fully ionized and in that case we must use the equations of reference 2.

In a recently published paper by Abe[3] only the interactions between the electrons were taken into account. The expression obtained there was the same as Eq. (7). The classical method used in that paper made it impossible to consider the interaction between the electrons and the ions.

---

[1] H. C. Urey, Astrophys. J. **59**, 1 (1924); E. Fermi, Z. Physik **26**, 54 (1924); R. H. Fowler, Phil. Mag. **1**, 845 (1926).

[2] A. A. Vedenov and A. I. Larkin, JETP **36**, 1133 (1959), Soviet Phys. JETP **9**, 806 (1959).

[3] R. Abe, Progr. Theoret. Phys. (Kyoto) **22**, 213 (1959).

Translated by D. ter Haar

SOVIET PHYSICS JETP VOLUME 11, NUMBER 6 DECEMBER, 1960

NEGATIVE AND LIMITING TEMPERATURES

Yu. B. RUMER

Institute of Radio Physics and Electronics, Siberian Section, Academy of Sciences, U.S.S.R.

Submitted to JETP editor February 16, 1960

J. Exptl. Theoret. Phys. (U.S.S.R.) 38, 1899-1902 (June, 1960)

It is shown that in the mathematical apparatus of statistical physics the possibility of the existence of negative and limiting positive temperatures in a thermodynamic system is connected with the analyticity of the sum of states as a function of the reciprocal of the temperature.

A number of papers in recent years have explained the usefulness of considering the "partition function" $Z(\lambda)$ for a thermodynamic system not only for real positive values of the temperature variable $\beta = 1/kT$ Re λ, but also in the entire complex plane. In fact, if we write $Z(\lambda)$ as a Laplace integral

$$Z(\lambda) = \int_0^\infty \rho(E) e^{-\lambda E} dE, \tag{1}$$

where $\rho(E)$ is the spectral density for the energy of the system, then on inverting the transformation (1) we get

$$\rho(E) = \frac{1}{2\pi i} \int_{\sigma - i\infty}^{\sigma + i\infty} Z(\lambda) e^{\lambda E} d\lambda, \tag{2}$$

where the integral is taken along a straight line Re $\lambda = \sigma$ which lies entirely in the region of analyticity of the function $Z(\lambda)$.

If the energy spectrum is bounded below, then, without loss of generality, we can take the lower limit of the spectrum to be zero. If the energy spectrum of the system is bounded above, i. e., if $\rho(E) = 0$ for $E > E_{\max}$, then the function $Z(\lambda)$ is analytic in the entire plane of the variable λ.

If the energy spectrum is not bounded above, then the region of analyticity of the function $Z(\lambda)$ depends on the degree of increase of the function $\rho(E)$. If

$$\log \rho(E)/E \rightarrow a \quad \text{as } E \rightarrow \infty, \tag{3}$$

then the function $Z(\lambda)$ is analytic in the entire region Re $\lambda > a$.

From Eq. (1) we obtain in the usual way

$$-\frac{d}{d\lambda} \ln Z(\lambda) = \frac{1}{Z(\lambda)} \int_0^\infty E\rho(E) e^{-\lambda E} dE = \bar{E}(\lambda),$$

$$\frac{d^2}{d\lambda^2} \ln Z(\lambda) = \overline{(E - \bar{E}(\lambda))^2} = \overline{(\Delta E)^2} = -\frac{d\bar{E}(\lambda)}{d\lambda}, \tag{4}$$

where $\bar{E}(\lambda)$ and $\overline{(\Delta E)^2}$ are the mean energy and the dispersion of the energy according to the complex distribution $\rho(E)e^{-E\lambda}$. On the real axis of the plane of $\lambda = \sigma + i\tau$ these quantities take the real and positive values

$$\bar{E}(\sigma) > 0, \qquad -d\bar{E}(\sigma)/d\sigma > 0. \tag{5}$$

For large values of the energy E the integral (1) can be calculated approximately by the method of steepest descent. With logarithmic accuracy we have

$$\ln \rho(E) = \ln Z(\beta) + \beta E, \tag{6}$$

where the saddle point β is a root of the equation

$$Z'(\beta) + Z(\beta) E = 0, \tag{7}$$

or, when we take the definition (4) into account, a root of the equation

$$\bar{E}(\beta) = E. \tag{7'}$$

We shall prove that the saddle point lies on the real axis. Differentiating Eq. (6) with respect to E and regarding β as a function of E defined by the equation (7), we get

$$\frac{d \ln \rho(E)}{dE} = \left(\frac{Z'(\beta)}{Z(\beta)} + E\right) \frac{d\beta}{dE} + \beta = \beta. \tag{8}$$

Since the left member of Eq. (8) is real, we must have Im $\beta = 0$.

We shall prove that the saddle point is unique. If the energy spectrum is not bounded above, then from the definition (4) it follows that

$$\bar{E}(a) = \infty, \qquad \bar{E}(\infty) = 0.$$

Since in virtue of Eq. (5) the function $\bar{E}(\sigma)$ decreases monotonically in the range $a < \sigma < \infty$, taking all values from ∞ to 0, the equation (7) has one and only one root.

If the energy spectrum is bounded above, the function $\bar{E}(\sigma)$ falls off monotonically in the interval

$$\bar{E}(-\infty) = E_{max} < E(\sigma) < E(\infty) = 0$$

and (7) has one solution in the interval $-\infty < \beta < \infty$.

We see from (4), (6), and (8) that

$$F(\beta) = -\beta^{-1}\ln Z(\beta), \qquad S(E) = \ln\rho(E), \qquad kT = 1/\beta \quad (9)$$

are the free energy, entropy, and temperature of the system. One usually considers thermodynamic systems in which $\rho(E)$ does not increase with the energy faster than algebraically, i. e., $\ln\rho(E)/E \rightarrow 0$ as $E \rightarrow \infty$, and consequently $Z(\lambda)$ is an analytic function of the complex variable λ in the entire right-hand half-plane.

We shall study here two examples of "unusual" thermodynamic systems for which negative and limiting temperatures exist.

THE ISING MODEL

As is well known (cf., e. g., reference 1) for large n the sum of states $Z(\lambda)$ of a linear Ising chain consisting of n sites has the form

$$Z(\lambda) = (2\cosh J\lambda)^n, \tag{10}$$

where J is the interaction energy between similarly directed adjacent spins. In the derivation of Eq. (11) it is assumed that the interaction energies of similarly and oppositely directed spins have opposite signs. If we take the interaction energy of similarly directed spins to be zero, and that of oppositely directed spins to be 2J, Eq. (10) takes the form

$$Z(\lambda) = (2\cosh J\lambda e^{-J\lambda})^n. \tag{11}$$

Calculating $\rho(E)$ according to Eq. (2) by the method of steepest descents on the assumption $E/n = \epsilon$ (with the ratio ϵ finite for large n), we get

$$\ln\rho(E) = n[\ln(2\cosh J\beta) + \beta\varepsilon - J\beta], \tag{12}$$

where β is the root of the equation

$$\bar{\varepsilon}(\beta) = J(1 - \tanh J\beta) = \varepsilon. \tag{13}$$

Since the energy spectrum of the lattice is bounded above, arbitrary values of β are possible. It is not hard to show that the value $\beta = 0$ ($T = \infty$, $\bar{\epsilon} = J$) corresponds to complete absence of short-range order; $\beta = +\infty$ ($T = 0$, $\bar{\epsilon} = 0$) corresponds to the establishment of complete short-range order, with adjacent spins parallel; for $\beta = -\infty$ the spins are antiparallel. It is known, however, that in the linear Ising lattice there is no temperature whatever at which long-range order is established.

The situation is different for the plane Ising lattice. Here, as in the case of the one-dimensional chain, arbitrary values of β are possible. The formula found by Onsager[2] for the free energy $f(\beta)$ per site of the lattice

$$f(\beta) = \frac{1}{\beta}\left[\frac{1}{2}\ln 2 + \frac{1}{2\pi^2}\int_0^\pi\int_0^\pi \ln[\cosh^2 2J\beta - \sinh 2J\beta(\cos\omega + \cos\omega')]\,d\omega d\omega'\right] \tag{14}$$

(as before, J is the coupling constant between adjacent spins) is invariant with respect to the interchange $\beta \rightarrow -\beta$. It is well known that the plane Ising lattice has the property of ferromagnetism and makes a phase transition of the second kind with a logarithmic discontinuity of the specific heat at $\beta = \beta_c$, where β_c is given by the equation

$$\sinh 2J\beta_c = 1. \tag{15}$$

From what has been said it follows that the plane lattice also makes one other phase transition, at the negative temperature given by the equation

$$\sinh 2J\beta_c = -1. \tag{16}$$

If for $\beta_c = 0$ the contribution to the singular part of the integral (14) is given by $\omega, \omega' = 0$, which corresponds to ferromagnetic ordering, then for $\beta_c < 0$ the main contribution to the singularity comes from $\omega, \omega' = \pi$, i. e., the transition point is antiferromagnetic.

Obviously the presence of positive and negative Curie points, corresponding to transitions to ferromagnetic and antiferromagnetic states, is also characteristic of the Heisenberg model (provided, of course, that it leads to any phase transition at all).

GAS OF NONINTERACTING PARTICLES IN AN EXTERNAL FIELD WITH AN ASYMPTOTICALLY LOGARITHMIC POTENTIAL

In the space between the planes $z = 0$ and $z = H$ let there be an ideal gas consisting of N particles of mass m, which are in an axially symmetrical field (z, r, φ are cylindrical coordinates):

$$U(r) = \begin{cases} 0 & r < a \\ 2U_0\ln(r/a) & r > a. \end{cases} \tag{17}$$

It is not hard to see that in this case the statistical weight $\rho(E)$ increases exponentially with increase of $E[\rho(E) \sim \exp(E/U_0)]$. Therefore it is to be expected that such a system possesses a limiting temperature. We shall confirm this supposition by an exact calculation.

We have for the sum of states per particle

$$Z(\lambda) = \left(\frac{2\pi m}{\lambda}\right)^{3/2} 2\pi H \int_0^\infty e^{-\lambda U(r)} r dr = \frac{\pi H (2\pi m)^{3/2} a^2}{\lambda^{1/2}(\lambda U_0 - 1)}. \qquad (18)$$

This formula is true for $\lambda U_0 > 1$. For $\lambda U_0 < 1$ the integral diverges. Thus these exists a limiting temperature $T^* = U_0$, above which the system cannot be heated.

The physical cause of the phenomenon is that because of the slowness of the increase of the potential the particles spread very far apart as their energy increases, and their kinetic energy is small in comparison with their potential energy.

---

[1] T. L. Hill, Statistical Mechanics, Chapter 7 (McGraw-Hill Book Company, 1956).

[2] Yu. B. Rumer, Usp. Fiz. Nauk 53, 245 (1954).

Translated by W. H. Furry
363

SOVIET PHYSICS JETP VOLUME 11, NUMBER 6 DECEMBER, 1960

DISPERSION FORMULAE FOR OVERLAPPING LEVELS

V. I. SERDOBOL'SKIĬ

P. N. Lebedev Physics Institute, Academy of Sciences, U.S.S.R.

Submitted to JETP editor February 18, 1960

J. Exptl. Theoret. Phys. (U.S.S.R.) **38**, 1903-1906 (June, 1960)

Dispersion formulas are deduced in a theory in which the S matrix is assumed to be linear with respect to resonances. The indefinite phase shifts of the complex reduced half-widths are calculated in a general form on the basis of the S matrix unitarity condition. Cases are considered when an isolated level corresponding to compound nucleus formation lies in the optical resonance region or when two levels of the compound nucleus overlap or a set of weakly overlapping levels exist in the optical resonance region. In all calculations the assumption is made that the levels of the compound nucleus do not overlap the nuclear reaction thresholds.

It is known that the separate resonances in the scattering cross sections and nuclear reactions are described quite well by the Breit-Wigner formula. For overlapping levels the dispersion formula may, in principle, be obtained by using Wigner's R-matrix technique.[1,2] However, the calculation of the corresponding matrix expressions involves algebraic difficulties and the final formulae are cumbersome. Clearly, it is more natural to derive the dispersion formulae on the basis of a variant of a theory proposed earlier by the author.[3] In this variant the resonance part of the S matrices is introduced in the form of a simple sum of the resonance levels, which are responsible for the formation of the compound nucleus. The remaining uniform part of the S matrix changes slightly over energy levels of the order of the width of the resonance curves, if $\Gamma \ll |E - E_t|$ where E_t is the threshold energy closest to E. The dispersion formula for these energies has the following form

$$S^J_{c'c} = (S^J_{c'c})_{\text{uniform}} + 2i \sum_\lambda \frac{u_{\lambda c'} u_{\lambda c}}{E_\lambda - E}. \tag{1}$$

Here the indices c′ and c define the totality of quantum numbers $\alpha s l J M$. The quantities $u_{\lambda c}$ in the customary notation, (see, e.g., reference 2) are

$$u_{\lambda c} = \Omega_c P_c^{1/2} \gamma_{\lambda c}. \tag{2}$$

Here both $u_{\lambda c}$ and $\gamma_{\lambda c}$ are, generally speaking, complex. Assuming the approximation $\Gamma_\lambda / |E - E_t| \ll 1$,

$$\Gamma_\lambda = 2 \sum_c |u_{\lambda c}|^2 = -2N_\lambda \operatorname{Im} E_\lambda. \tag{3}$$

The summation over c includes only the open channels. The parameter N_λ is found to be greater than or equal to unity.

We note that the dispersion expansion (1) with characteristics (2) and (3) can be deduced from the formal Kapur-Peierls' theory.[4] It is known that the fundamental deficiency of this theory is the dependence of the resonance parameters E_λ and $\gamma_{\lambda c}$ on the energy of the incident particles. However, in the energy range Δ far from the threshold, the relative change in these values does not exceed the order of magnitude $\Delta/|E - E_t|$. In order to obtain the formula (1) and relation (3) from the theory,[4] it is sufficient to change the normalization of the basic function Ψ_λ in such a way that

$$\int \tilde{\Psi}^*_\lambda \Psi_\lambda d\tau = 1 \text{ and } \int |\Psi_\lambda|^2 d\tau = N_\lambda \geqslant 1. \tag{4}$$

Here $\tilde{\Psi}_\lambda$ is the solution satisfying the complex conjugate boundary conditions.

The amplitudes of the derived half-widths $\nu_{\lambda c}$ in (1) are complex. This doubles the number of undetermined parameters in the dispersion formula and at a first glance detracts from the value of formula (1). However, the phase of $\gamma_{\lambda c}$ can be determined from the unitary condition for the S matrix. In the expansion (1) the summation over λ applies to all the quasi-stationary states, lying in the given energy range, with lifetimes significantly larger than the time of flight of the particles past the nucleus. If there is an isolated group of levels, separated from the others, then the sum over λ averaged over a sufficiently large interval of energy does not give a contribution, and the mean $\bar{S}$ coincides with the uniform part of (1).

The matrix $\overline{S}$ describes a non-compound process, weakly dependent on the energy; for energies which are not too large this matrix has only diagonal elements, corresponding to scattering by the optical potential.

ISOLATED RESONANCE LEVEL AND SCATTERING BY THE OPTICAL POTENTIAL

The uniform part of (1) is equal to the diagonal matrix of the optical scattering $\delta_{c'c}S_c^{\mathrm{opt}}$. It is convenient to introduce the logarithmic derivative of the optical wave functions

$$L_c^0 = R\left[\frac{1}{ru_c}\,\frac{\partial (ru_c)}{\partial r}\right]_R. \tag{5}$$

S_c^{opt} then has the following form

$$S_c^{\mathrm{opt}} = \Omega_c^2 (L_c^0 - L_c^*)/(L_c^0 - L_c) = \Omega_c^2 \exp(2i\delta_c^0). \tag{6}$$

Here Ω_c and L_c are as in the work of Lane and Thomas.[2] We retain in the expansion (1) the summation over λ. Over all the energy levels we must have:

$$\sum_{c''} S_{c''c'}^{J*}(E)\, S_{c''c}^{J}(E) = \delta_{c'c}. \tag{7}$$

For simplicity we consider (7) near $E \approx E_\lambda$. Using (2) and (3), we obtain

$$u_{\lambda c}/u_{\lambda c}^* = N_\lambda S_c^{\mathrm{opt}}. \tag{8}$$

It is evident that $N_\lambda = 1$, and $\gamma_{\lambda c}$ is complex. The argument of $\gamma_{\lambda c}$ equals, to within π, the optical phase δ_c^0, which is determined by (6). The fact that the $\gamma_{\lambda c}$ are complex in no way affects the nuclear-reaction cross sections, for when $c' \neq c$ only the moduli of $\gamma_{\lambda c}$ occur in the cross section.

The elastic scattering cross section is proportional to

$$|S_{cc}^J - 1|^2 = \left|1 - (S_c^{\mathrm{opt}})^{-1} + 2i\,\frac{P_c\,|\gamma_{\lambda c}|^2}{E_\lambda^r - E + i\Gamma_\lambda/2}\right|^2, \tag{9}$$

where $E_\lambda^r = \operatorname{Re} E_\lambda$. In this way we have obtained the rather obvious result that the scattering potential in the dispersion formula reduces to the optical potential; the exponent in the second term on the right-hand side of (9) comprises, for small energies, not the nuclear radius but the amplitude of scattering by the optical potential.

TWO OVERLAPPING LEVELS AND SCATTERING BY THE OPTICAL POTENTIAL

The uniform part of the S matrix in this case is equal to (6). The unitary condition (7) is considered near the poles of E_λ, $\lambda = 1$ and 2. The simple equations below are obtained,

$$\gamma_{1c}\exp(-2i\delta_c^0) = a_{11}\gamma_{1c}^* + a_{21}\gamma_{2c}^*,$$
$$\gamma_{2c}\exp(-2i\delta_c^0) = a_{21}\gamma_{1c}^* + a_{22}\gamma_{2c}^* \tag{10}$$

with coefficients

$$a_{\mu\lambda} = a_{\lambda\mu}^* = 2i\sum_c P_c\gamma_{\mu c}^*\gamma_{\lambda c}/(E_\mu^* - E_\lambda). \tag{11}$$

From these it is evident that a_{11} equals N_1 and a_{22} equals N_2. The equations (10) lead to the conclusion that

$$\sum_\lambda a_{\mu\lambda}a_{\nu\lambda} = \delta_{\mu\nu}. \tag{12}$$

From this it follows that a_{12} is purely imaginary, and the parameters N_1 and N_2 are equal,

$$N_1^2 = N_2^2 = N^2 = 1 + |a_{12}|^2. \tag{13}$$

The phase $(\arg\gamma_{\lambda c} - \delta_c^0)$, which we designate $\varphi_{\lambda c}$, arises as a consequence of the overlapping levels. From (10) it will be easily found that

$$\left|\frac{\gamma_{1c}}{\gamma_{2c}}\right| = \left(\frac{N^2 + 1 - 2N\cos 2\varphi_{2c}}{N^2 - 1}\right)^{1/2} = \left(\frac{N^2 - 1}{N^2 + 1 - 2N\cos 2\varphi_{1c}}\right)^{1/2}, \tag{14}$$

$$-\tan\varphi_{1c}\tan\varphi_{2c} = (N - 1)/(N + 1). \tag{15}$$

Together with (3), these equations determine the phases of the derived half widths and the normalizing parameters N. It is evident that the deviation of N from unity characterizes the degree of interaction between the dissociated states with $\lambda = 1$ and $\lambda = 2$. For $\Gamma \ll D$ the difference $N - 1$ is, to an order of magnitude, equal to $(\Gamma/D)^2$. The formulae obtained give new, rather more graphic parameters of the resonance curves. Furthermore they remain valid in the energy range close to optical resonance.

A GROUP OF OVERLAPPING LEVELS WITH THE APPROXIMATION $\Gamma/D \ll 1$

In this case the phases $\gamma_{\gamma c}$ and the parameter N_λ are determined to an equal degree by the two neighboring levels, and the previous formula is rendered useless. Let us assume that $\Gamma \ll D$ for all the levels from the group under consideration. The unitary condition for $E \approx E_\lambda$ gives

$$\gamma_{\lambda c}\exp(-2i\delta_c^0) = \sum_\mu a_{\mu\lambda}\gamma_{\mu c}^*. \tag{16}$$

With an accuracy to higher-order terms

$$\gamma_{\lambda c} = \gamma_{\lambda c}^r(1 + i\varphi_{\lambda c})\exp(i\delta_c^0). \tag{17}$$

Here $\gamma_{\lambda c}^r$ are real positive or negative quantities. The phases $\varphi_{\lambda c}$ to an accuracy π equal $(\arg\gamma_{\lambda c} - \delta_c^0)$. Equation (16) shows that $\varphi_{\lambda c} \sim \Gamma/D$ and to a first approximation

$$\varphi_{\lambda c} = (2i\gamma^{r}_{\lambda c})^{-1} \sum_{\mu}{}' a_{\mu\lambda}\gamma^{r}_{\mu c}. \tag{18}$$

Here the summation applies to the indices μ not equal to λ. The parameter N_λ differs from unity by a quantity of order $(\Gamma/D)^2$. Equation (12) with $\mu = \nu$ gives

$$N_\lambda - 1 = -\frac{1}{2}\sum_{\mu}{}' a^2_{\mu\lambda}. \tag{19}$$

Formulae (1) — (3), (18), and (19) enable us to calculate the cross section with an accuracy up to magnitudes of a higher order of smallness compared with $(\Gamma/D)^2$. For $c' \neq c$, the order of the terms that are linear with the phase rises. The result is that the overlapping of the levels changes the cross section of the reaction only by a magnitude of the order of $(\Gamma/D)^2$. The addition to the cross section of elastic scattering and the total cross section, however, turns out to be of first order in Γ/D.

As a special case let us examine a group of levels which lie in a range of small energies, $(kR \ll 1)$. The total cross section of a weak beam of particles incident along the channel c is

$$\sigma_c \sim 2\,(1 - \mathrm{Re}\, S^{J}_{cc}). \tag{20}$$

When $(kR) \ll \Gamma/D$ we have $\Omega_c \approx 1$ and $\delta^0_c \approx 0$. By means of (17) we find that

$$\sigma_c \sim \sum_{\lambda} \frac{\Gamma_{\lambda c}\Gamma_\lambda}{(E - E^{r}_{\lambda})^2 + \Gamma^2_\lambda/4}\left(1 - \frac{4\varphi_{\lambda c}(E - E^{r}_{\lambda})}{\Gamma_\lambda}\right),$$

$$\Gamma_{\lambda c} = 2\sum_{c} P_c\,(\gamma^{r}_{\lambda c})^2. \tag{21}$$

The formula (21) shows that overlapping levels lead to the appearance of terms, which destroy the symmetry of the curves with respect to the resonances E^{r}_{λ}. In order of magnitude, these terms are equal to Γ/D.

In conclusion I wish to thank Professor A. S. Davydov for his consideration and valuable advice.

---

[1] E. P. Wigner and L. Eisenbud, Phys. Rev. **72**, 29 (1947).

[2] A. M. Lane and R. G. Thomas, Revs. Modern Phys. **30**, 257 (1958).

[3] V. I. Serdobol'skiĭ, JETP **36**, 1903 (1959), Soviet Phys. JETP **9**, 1354 (1959); Nuclear Phys. (in Press).

[4] P. L. Kapur and R. E. Peierls, Proc. Roy. Soc. (London) **A166**, 277 (1938).

Translated by K. J. S. Cave
364

Letters to the Editor

POSSIBILITY OF USING NUCLEAR REACTIONS TO OBTAIN INFORMATION ABOUT THE $\pi\pi$ INTERACTION

Yu. D. BAYUKOV and G. A. LEKSIN

Submitted to JETP editor February 23, 1960

J. Exptl. Theoret. Phys. (U.S.S.R.) 38, 1907-1908 (June, 1960)

HIGH energy processes with small momentum transfers are now attracting much attention in nuclear physics. This interest is caused by the apparent possibility of a theoretical interpretation of these processes which yields some information on the $\pi\pi$, πK, and KK interactions. This information concerns the corresponding vertices in the Feynman graphs

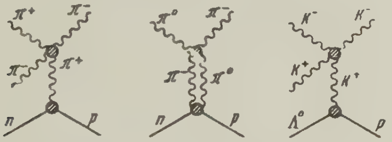

etc.

We consider specifically the process of the creation of a π meson by a π meson. Chew and Low[1] have shown that for small momentum transfers the cross section for this process is related to the cross section for the $\pi\pi$ interaction ($\sigma_{\pi\pi}$) by the formula

$$d^2\sigma / dp^2\, d\omega^2 = (f^2/2\pi)\, p^2 (p^2+1)^{-2}\, \omega \sqrt{\omega^2/4 - 1}\, q^{-2} \sigma_{\pi\pi} + B(\omega p), \quad (1)$$

where f^2 is the meson-nucleon coupling constant, p is the momentum transferred to the nucleon, ω is the total energy of the mesons in their center-of-mass system, and q is the momentum of the incoming meson in the laboratory system. The quantities p, ω, and q are expressed in units of the meson mass. The term $B(\omega p)$ takes account of the contribution of the processes described by diagrams with three, five, etc. virtual mesons. There is reason to think — and this is indeed our assumption — that $B(\omega p)$ makes only a small contribution to the cross section in the region of small momentum transfers ($p \sim 1$ to 2) of interest to us. We can then integrate (1) over p and ω up to these values of p, and estimate the value of $\sigma_{\pi\pi}$ from the total cross section for the process of creation of one meson by another.

The interaction of the π meson with the nucleus can be regarded as the sum of the interactions with the separate nucleons of the nucleus. For light nuclei this reduces in most cases to the interaction with only one nucleon. The binding energy of the nucleon in the nucleus is much smaller than the binding energy of the π meson in the nucleon. We can therefore use (1) for the creation of a meson by a meson in the nucleus without making a large error. Since the nucleus almost always carries away (without splitting up) only a small momentum, the total cross section for nuclear reactions of the type

$$\pi + A \rightarrow \pi + \pi + B \quad (2)$$

contains information about the $\pi\pi$ interaction. Indeed, in the impulse approximation, (1) must be multiplied before integration by the quantity

$$S^2 = \left\{ \int_0^\infty \psi^*(r)\, e^{ipr}\, \psi(r)\, dr \right\}^2, \quad (3)$$

the probability that the nucleus with the ground state wave function $\psi(r)$ remains in the ground state when the momentum p is transferred to it. The function S^2 decreases sharply with increasing p. This can be verified by computing it under various assumptions for the wave function $\psi(r)$ or by estimating it directly from the experimental data on those processes (for example, on the elastic scattering of nucleons by nuclei[2]) in the description of which S^2 plays an important role. As we go from one nucleus to the next, S^2 changes in such a way that the admissible region of momenta p becomes smaller as the atomic number of the nucleus increases. In the region of light nuclei it is bounded by the value $p \sim 2$.

A convenient nuclear reaction in the region of light nuclei is

$$\pi^- + C^{12} \rightarrow \pi^- + \pi^- + N^{12}. \quad (4)$$

The initial nucleus C^{12} is contained in the material of the scintillators and in some liquids used in bubble chambers, so that the target and detector can be combined, which leads to a setup in which the 4π geometry is guaranteed. The presence of the β^+ active N^{12} nucleus with the β^+ end point energy 16.6 Mev and the life time 0.012 sec permits us to detect the reaction (4) and to separate it clearly from the background. For this purpose one can use discrimination by energy or amplitude analysis, registration of the decays in the absence of a pulse from the accelerator, or coincidence measurements of the two γ quanta from the annihilation of the β^+ in the target-detector. It is important that the N^{12} nucleus has no excited levels, and formula (3) is valid. The function S^2, as ob-

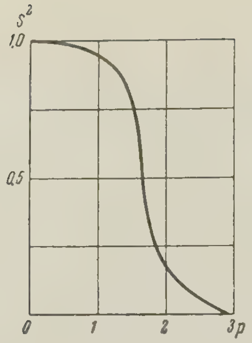

tained from the experimental data on the elastic scattering of nucleons by C^{12}, is shown in the figure.

In conclusion we express our deep gratitude to K. A. Ter-Martirosyan for valuable advice and constant assistance.

---

[1] G. F. Chew and F. E. Low, Phys. Rev. **113**, 1640 (1959).

[2] G. A. Leksin, On the Elastic Scattering of Nucleons by Nuclei, Preprint, Joint Inst. Nuc. Res., 1957.

Translated by R. Lipperheide
365

SINGLE CRYSTALS OF MAGNESIUM-MANGANESE FERRITES WITH A NARROW FERROMAGNETIC RESONANCE ABSORPTION CURVE

K. P. BELOV, V. F. BELOV, and A. A. POPOVA

Institute of Crystallography, Academy of Sciences, U.S.S.R.

Submitted to JETP editor March 18, 1960

J. Exptl. Theoret. Phys. (U.S.S.R.) **38**, 1908-1910 (June, 1960)

A considerable interest has been noted recently in investigations of ferrites with narrow ferromagnetic resonance-absorption lines.[1-4] This interest is caused by the fact that the ferrite crystals can be used in nonlinear microwave apparatus. Particular attention is paid here to the investigation of single crystals of yttrium ferrite with garnet structure.[1-3] It appears to us, however, that not all the possibilities of the spinel class of ferrites have been disclosed in this respect.

Our experiments have shown that in some ferrite systems with spinel structure one can encounter compositions with single crystals that have a sufficiently narrow ferromagnetic resonance absorption line. We have measured the width of the line ΔH in single crystals of magnesium-manganese ferrites for different ratios of the manganese and magnesium oxides. The single crystals were grown by the Verneil method and machined into spheres 0.8 — 1 mm in diameter. The surfaces of the spheres were polished by running in with air on emery cloth with 20.15 μ and 10 μ grains. The measurements were made in a short-circuited waveguide section at 9470 Mcs. The width of the line was determined from the resonance curve at the 0.5 level. In the single crystals of magnesium-manganese ferrites which we investigated, ΔH = 12 to 18 oe (see Table I).

The narrowest absorption line at the surface finish employed by us (which obviously is not the ultimate one) was observed in a single crystal of the ferrite 8.4 MgO, 23.9 MnO, 67.5 Fe_2O_3. This sample had ΔH = 12 oe and $4\pi I_s$ = 2950 gauss.

Figure 1 (solid curve) shows the results of measurements of the anisotropy of the width of the line for the single crystal of 6.9 MgO, 37.3 MnO, 55.9 Fe_2O_3 in the (110) plane at room temperature. It is seen that ΔH reaches a minimum along [100] (axis of difficult magnetization) and a maximum in the direction [$1\dot{1}1$] (axis of easy magnetization). The amplitude of the anisotropy ΔH at room temperature amounts to (3.5 to 0.5) oe. The dotted curve in Fig. 1 shows the anisotropy of the resonant field H_r.

The character of the anisotropy of ΔH, established in our experiments, corresponds to the phenomenological calculation of Skrotskiĭ and Kurba-

TABLE I. Width of resonant absorption line ΔH, saturation magnetization $4\pi I_s$, and electric resistivity ρ in magnesium-manganese ferrites

Composition in percent by weight (calculated)	ΔH, oe	$4\pi I_s$, gauss	ρ, Ω·cm
9.4 MgO; 16,5 MnO; 74.1 Fe_2O_3	18	3320	800
8.4 MgO; 23.9 MnO; 67.5 Fe_2O_3	12	2950	$1.6 \cdot 10^5$
8.0 MgO; 28,3 MnO; 63.7 Fe_2O_3	16	2740	10^6
6,9 MgO; 37.3 MnO; 55,9 Fe_2O_3	18	2480	$4.6 \cdot 10^6$

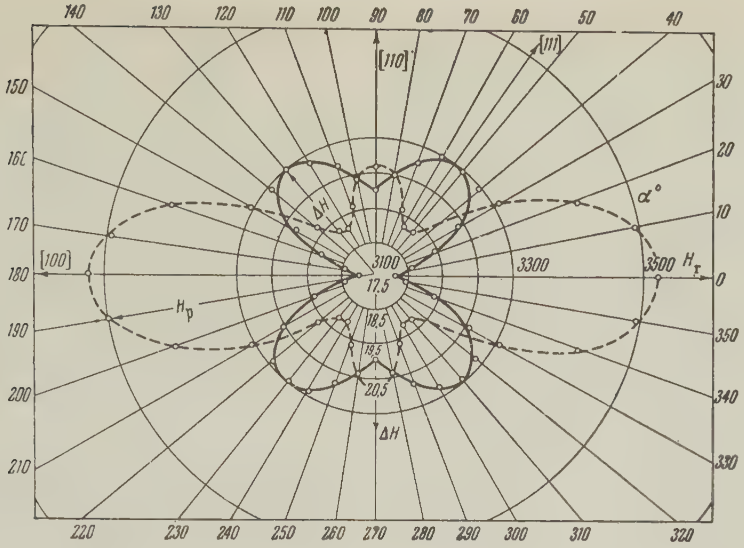

FIG. 1

tov.[5] It must be noted that in the interval from room temperature to +200° C the width of the resonance absorption line depends little on the temperature (see Fig. 2), whereas the constant of the magnetic crystallographic anisotropy, determined by the resonance method, is reduced by a factor of almost 20 in the same temperature interval.

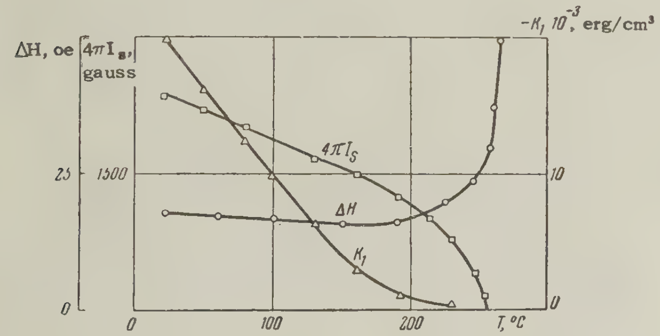

FIG. 2. Temperature dependence of the width ΔH of the line of ferromagnetic resonance absorption in the [100] direction, of the saturation magnetization $4\pi I_s$, and of the constant of magnetic anisotropy K_1, for the ferrite 6.9 MgO, 37.3 MnO, 55.9 Fe_2O_3.

The increase in ΔH in the region of the Curie point (Fig. 2) is apparently connected with the fluctuations of magnetization at the Curie point.

---

[1] J. F. Dillon, Phys. Rev. **111**, 6 (1958).

[2] Spencer, LeCraw, and Porter, J. Appl. Phys. **30**, 3 (1959).

[3] A. G. Gurevich and I. E. Gubler, Физика твердого тела, **1**, 1847 (1959), Soviet Phys.-Solid State Physics **1**, 1693 (1959).

[4] Fabrikov, Kudryavtsev, and Gushchina, Izv. Akad. Nauk SSSR Ser. Fiz. **23**, 372 (1959), Columbia Tech. Transl. p. 359.

[5] G. V. Skrotskiĭ and L. V. Kurbatov, JETP **35**, 216 (1958), Soviet Phys. JETP **8**, 148 (1959).

Translated by J. G. Adashko
366

ADDITIONAL ANOMALOUS LIGHT WAVES IN ANTHRACENE IN THE EXCITON ABSORPTION REGION

M. S. BRODIN and S. I. PEKAR

Institute of Physics, Academy of Sciences, Ukrainian S.S.R.

Submitted to JETP editor March 19, 1959

J. Exptl. Theoret. Phys. (U.S.S.R.) **38**, 1910-1912 (June, 1960)

ONE of the authors[1-3] predicted theoretically the existence of additional anomalous light waves in crystals in the region of exciton absorption. In our earlier paper[4] we proposed a method of experimentally proving the existence of these waves. The method reduces to a measurement of the intensity of monochromatic light, passing through a plane-parallel slab of crystal as a function of the thickness of the slab. The existence of two waves in a crystal is manifest in the interference of these waves as they leave the crystal. This interference leads to distinctive intensity oscillations that depend on the thickness of the slab. It is necessary here to prevent the two waves connected with the usual double refraction from occuring in the slab. This is accomplished by so polarizing the incident light wave, that the electric vector is strictly parallel to the principal direction of polarization of the crystal. It is also necessary that the absorption of the light in the slab be so great, that the multiple reflection of the light from the surfaces of the slab can be neglected.

In an earlier paper[4] we processed previously obtained experimental data[5] on the absorption of light in slabs of anthracene of different thickness (at $T = 20°$K) within the intrinsic band absorption with a maximum at 25,200 cm^{-1}. The intensity of the transmitted light was indeed found to oscillate with the thickness in approximately the manner predicted by the theory of anomalous waves.

Taking into consideration the importance of the conclusions that must be drawn from experiments of this kind, we decided to repeat the measurements in anthracene more carefully. Thus, it was noted in reference 4 that the data used there on the optical density of the crystals were taken in arbitrary units. In the present work, however, absolute measurements were made of the intensity of light by photographic photometry (using an eight-step attenuator, the intensity reference of which was chosen at the frequency 24,720 cm^{-1}). The high-dispersion DFS-3 spectrograph was used. A three-lens system was used to illuminate the slit of the spectrograph.

Furthermore, the earlier measurements,[5] as was noted by I. V. Obreimov, in discussions with the authors, are of doubtful accuracy as regards the polarization of the light along the monoclinic crystal axis chosen for the investigation. Such an inaccuracy would produce in the crystal a second wave of usual double refraction. To dispel this doubt, we made our measurements with two parallel polarizers, located before (Glan prism) and after (spar) the crystal (only one polarizer was used in reference 5). The use of a second polarizer decreases the intensity of the second beam of ordinary double refraction at least by two orders of magnitude (compared with reference 5), i.e., it makes this beam negligible.

With the spar fixed and the crystal removed, the Glan prism was first rotated until one of the beams emerging from the spar was completely extinguished. Insertion of the approximately oriented crystal restored this beam, which was then again extinguished by slightly rotating the crystal. The monoclinic axis of the crystal was thus set parallel to the vector of the electric field intensity of the light wave. The described adjustment was carried out in white light, since the direction of the investigated principal axis of crystal polarization (monoclinic axis) is independent of the frequency.

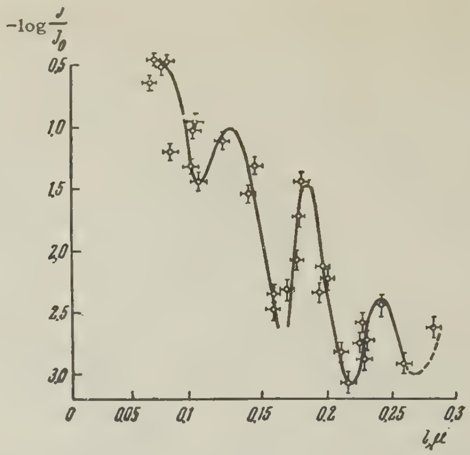

Finally, in the present investigation we studied 30 crystal thicknesses, i.e., we obtained twice as many points as in reference 4.

The diagram shows the experimentally obtained dependence of the optical density of the crystal on its thickness, for a frequency 25,108 cm^{-1}. The experimental points are plotted with their probable errors in the abscissas and ordinates. The measurements were made at $T = 20°$K (an estimate of the errors in the mounting of the crystals, in the measurement of their thickness, and in the method of cooling is given in reference 4). It seems to us that the figure indicates a considerably more pronounced oscillating character than in reference 4. It is important to emphasize the almost identical interval Δl between the extrema, something which is not at all inherent in a simple straggle of points. Actually, the abscissas of the maxima are: $l = \sim 0.072$, 0.128, 0.188, and 0.245 μ. The differences Δl are ~ 0.056, 0.060, and 0.057 μ. The minima are at $l = 0.105$, 0.168, and 0.233 μ. The corresponding differences are $\Delta l = 0.063$ and 0.055 μ. The average period of oscillation is 0.058 μ and the corresponding difference in the indices of refraction of the two interfering waves is 6.9.

We note that if we attempt to ascribe the observed oscillation, on the basis of the usual theory, to interference between beams that have passed once and three time, respectively, through the slab, it would be necessary to assume for the anthracene an index of refraction 3.45, whereas it actually exceeds 5 at the same frequency and temperature.[6] At the frequency investigated, the intensity of the thrice-passing beam is two or three orders of magnitude smaller than the intensity of the singly-passing beam, i.e., the former can be neglected.

The curve shown in the figure is similar in character to the theoretical curve, corresponding to the interference of two parallel polarized anomalous waves (see reference 4). Thus, our earlier qualitative conclusions are confirmed by the present more accurate results. The latter, it appears to us, represent a weighty experimental proof of the existence of additional anomalous waves in the anthracene crystal, as predicted by the theory.

It is quite desirable that similar investigations be carried out by others, both in anthracene and in other crystals. It is necessary to bear in mind here that, depending on the frequency, the difference in the indices of refraction of the two waves may prove to be considerably greater than in the case described above (see Figs. 1 and 2 of reference 2). Accordingly, the frequency of oscillation of the curve such as shown in the figure, will be much greater, and this will require a greater accuracy in the measurement of l. Otherwise the experimental points will be merely disordered.

The authors express their gratitude to A. F. Prikhot'ko for continuous interest in this work and for a discussion of the results, and also to S. V. Marisova for help with the measurements.

---

[1] S. I. Pekar, JETP **33**, 1022 (1957), Soviet Phys. JETP **6**, 785 (1958).

[2] S. I. Pekar, JETP **34**, 1176 (1958), Soviet Phys. JETP **7**, 813 (1958).

[3] S. I. Pekar, JETP **36**, 451 (1959), Soviet Phys. **9**, 314 (1959).

[4] M. S. Brodin and S. I. Pekar, JETP **38**, 74 (1960), Soviet Phys. JETP **11**, 55 (1960).

[5] M. S. Brodin and A. F. Prikhot'ko, Оптика и спектроскопия (Optics and Spectroscopy) **7**, 132 (1959).

[6] M. S. Brodin and A. F. Prikhot'ko, ibid. **2**, 448 (1957).

Translated by J. G. Adashko
367

INFLUENCE OF MAGNETIC FIELDS ON RESONANT ABSORPTION OF GAMMA RAYS

V. A. LYUBIMOV and A. I. ALIKHANOV

Institute of Experimental and Theoretical Physics, Academy of Sciences, U.S.S.R.

Submitted to JETP editor April 25, 1960

J. Exptl. Theoret. Phys. (U.S.S.R.) **38**, 1912-1914 (June, 1960)

THE discovery by Mössbauer[1] of the emission and resonance absorption of γ rays without loss of energy due to nuclear recoil opened the possibility of directly detecting the Zeeman splitting of excited nuclear states and of measuring their magnetic moments. This possibility was pointed out independently by several people,[2] in particular by one of the authors (A.I.A.).

To observe the Zeeman effect, we chose the γ transition in Sn^{119m} with an energy of 23.8 kev and a lifetime of 2.67×10^{-8} sec, i.e., with a level width of 2.5×10^{-8} ev.

However, in the mixture of isotopes of Sn there is a very strong source of x rays with an energy near to this (around 24 kev) in the form of In^{113} formed from Sn^{112} with a high cross section after neutron capture. For this reason we used a sample of tin enriched in the Sn^{118} isotope (96%) in which the impurity of Sn^{112} was less than 0.05%.

The apparatus for the measurements with a magnetic field consisted of an electromagnet with poles of pyramidal shape. The separation of the poles was 6 mm and the field could reach 20,000 gauss. The γ-ray source was 20×4 mm and 5 mg/cm^2 in thickness, and was fixed tight to one side of a Plexiglas plate 2 cm thick, while absorbers of natural tin of various thicknesses were attached to the other side of the plate. The absorption length of 23.8 kev γ rays due to the photoeffect in tin is 70 mg/cm^2, i.e., exceeds by far the resonance absorption lengths both in the source and in the absorber. The end of the plate holding the source was placed between the poles of the magnet. The source and absorber were immersed in liquid nitrogen. At the position of the absorber, there was a fringing magnetic field whose magnitude at high fields reached around 24% of the value of the magnetic field at the position of the source.

The experiment consisted in the following: Using a proportional counter filled with a mixture of krypton, argon and propane, we measured the intensity of the soft radiation from the source passing through the absorber after filtering by a plate of Plexiglas 2 cm thick and a palladium plate 60 mg/cm^2 thick for absorption of the x-ray

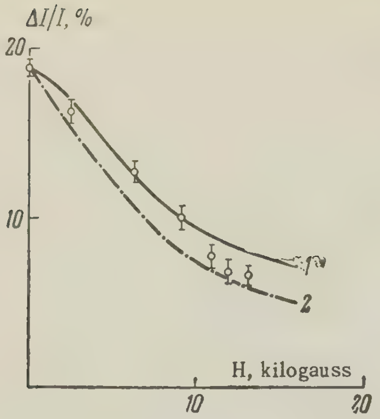

Dependence of intensity difference on magnetic field, for temperatures of source and absorber equal to 90 and 293°K. 1 – theoretical curve for a Debye temperature $\Theta = 170°K$ and a magnetic moment of the excited state of Sn^{119m} equal to $\mu = 1.5\,\mu_0$, where μ_0 is the magnetic moment of the ground state of Sn^{119}; 2 – similar curve for $\mu = 2.0\,\mu_0$.

radiation of tin with energy ~ 25 kev. When the source was cooled to 90° K, the intensity of the soft radiation recorded by the counter dropped by 12%. When the magnetic field was turned on with source and absorber cooled, the intensity of the soft radiation began to increase with increasing magnetic field. The magnetic field splits the 23.8-kev level and shifts the energy of the recoilless radiation from its resonant energy by an amount of the order of 10^{-7} ev, while the 23.8-kev level in the absorber, which is in a much weaker field, is shifted much less. As a result of this detuning of the energy, the absorption in the absorber decreases and the intensity increases.

The measurements were carried out for three thicknesses of the absorber of natural white tin: 36, 11, and 5 mg/cm^2. In the figure we show the data of the experiment for the thinnest absorber. From all the data we determine with good internal consistency a value for the magnetic moment of the excited state of Sn^{119m} equal to $\mu = -(1.1 \pm 0.1)\mu_0$ or $\mu = (1.72 \pm 0.06)\mu_0$ with a value of the Debye temperature Θ equal to 170° K, which follows from our experiments. The value $\mu = -(1.1 \pm 0.1)\mu_0$ is to be preferred since it is in good agreement with the established level scheme for Sn^{119m}. The value of the magnetic moment calculated from our experiments was only slightly dependent on the value chosen for the Debye temperature of white tin: for $\Theta = 200°K$ we have $\mu = -1.15\mu_0$, while for $\Theta = 140°K$, we get $\mu = -1.05\mu_0$, where μ_0 is the value of the magnetic moment of the ground state of Sn^{119} which is equal to −1.046 nuclear magnetons.

We express our profound gratitude to L. A. Artsimovich for preparing the samples of enriched tin, to G. M. Kukavadze for the mass spectrographic analysis of the samples, and to V. I. Anan'ev for help in the measurements.

---

[1] R. L. Mössbauer, Z. Naturforsch. **14a**, 211 (1959).

[2] R. L. Mössbauer, M. Hamermesh. Cf. L. L. Lee et al., Phys. Rev. Letters **3**, 223 (1959); Barit, Podgoretskiĭ, and Shapiro, JETP **38**, 301 (1960), Soviet Phys. JETP **11**, 218 (1960).

Translated by M. Hamermesh
368

ELECTRICAL AND GALVANOMAGNETIC PROPERTIES OF LITHIUM FERRITE-CHROMITE NEAR THE COMPENSATION POINT

K. P. BELOV, A. N. GORYAGA, and LIN CHANG-TA

Moscow State University

Submitted to JETP editor March 29, 1960

J. Exptl. Theoret. Phys. (U.S.S.R.) **38**, 1914-1915 (June, 1960)

In certain ferrites one observes a highly anomalous temperature dependence of the spontaneous magnetization, with a so-called compensation point Θ_c at which a "balancing" of the magnetic moments of the sublattices occurs.$^{1-3}$ The study of such ferrites is of interest from the point of view of explaining the extent to which one or another sublattice "shares" in the ferrimagnetism, and could contribute to a deeper understanding of the nature of the physical properties of crystalline materials of the ferrite type.

In reference 4 it was established that in gadolinium ferrite-garnet the magnetostriction properties are markedly different in character above and below Θ_c. Below Θ_c they are chiefly due to the "gadolinium" sublattice, and above Θ_c to the "iron" sublattices. With the aim of further studying the role of the sublattices in ferrimagnetism and the physical phenomena which accompany it in ferrites, we undertook the measurement of the electrical and galvanomagnetic properties of

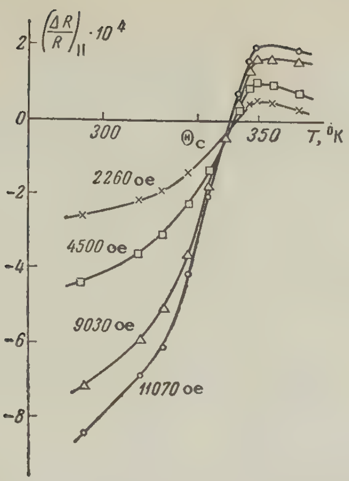

FIG. 1

lithium ferrite-chromite, which has a compensation point. In Fig. 1 are shown the curves of temperature dependence of the longitudinal galvanomagnetic effect $(\Delta R/R)_{\parallel}$ at various magnetic fields for the ferrite $Li_2O \cdot 2\frac{1}{2}Fe_2O_3 \cdot 2\frac{1}{2}Cr_2O_3$ prepared by the usual ceramic techniques. It is evident that after Θ_C has been passed (some 10° to 20° above Θ_C) a change of sign occurs in the longitudinal galvanomagnetic effect. At first sight one would say that, since $(\Delta R/R)_{\parallel}$ is an even-order effect, it should not change its sign upon passing through Θ_C (where the direction of the resultant spontaneous magnetization is reversed). The change in sign of the effect can be understood if it is assumed that the sublattices of the lithium ferrite-chromite under study have different electrical properties, determined obviously by the nature of the ions located on the corresponding sublattices. As a result, the character of the galvanomagnetic effect below Θ_C, where the magnetization of the ions in the octahedral locations is "predominant," differs from its character above Θ_C, where the magnetization of the ions in the tetrahedral locations is "predominant."

At each given temperature the "resultant" galvanomagnetic properties of the ferrite as a whole will be determined by the magnitudes and signs of the galvanomagnetic effects of the corresponding sublattices. Hence the experimentally observed dependence of the galvanomagnetic effect on the temperature and field must be of a very complicated nature. From this point of view, the shift (shown in Fig. 1) of the temperature of the null of the galvanomagnetic effect (the compensation point of the galvanomagnetic effect) relative to Θ_C becomes understandable.

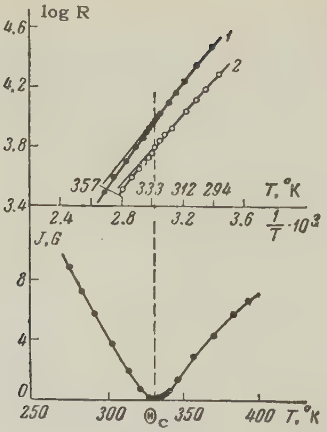

FIG. 2

We have also measured the temperature dependence of the electrical resistivity of our ferrite. In Fig. 2 are shown the curves of log R(1/T) for the ferrite $Li_2O \cdot 2\frac{1}{2}Fe_2O_3 \cdot 2\frac{1}{2}Cr_2O_3$, measured with direct current (curve 1) and with alternating current (200 kcs, curve 2). The same figure shows the curve of temperature dependence of the magnetization at H = 250 oe. It is apparent that a noticeable kink in the log R(1/T) curve occurs in the region of Θ_C. Measurements of log R(1/T) curves have been carried out on several samples with the composition indicated above, prepared by the ceramic method under differing conditions. In all cases a kink was observed in the curves, with both direct and alternating current. From Fig. 2 it is evident that the kinks in the curves near Θ_C are similar in nature to the kinks in the curves observed in ferrites at the Curie temperature. It should be observed, however, that the electrical resistance anomalies in the region of the compensation point are due to other causes. The presence of a kink in the log R(1/T) curve at the point Θ_C is explained not by the collapse of spontaneous magnetization, such as occurs at the Curie point, but is connected, according to the theoretical assumptions of Turov and Irkhin,[5] with the compensation of the exchange fields of the magnetic sublattices at Θ_C. It is also possible to explain the appearance of these kinks if the ferrite sublattices have different electrical properties, and if this difference appears somehow near the compensation point. The latter assumption, in our view, is confirmed by the behavior of the galvanomagnetic effect in the region of the compensation point. We are continuing with further studies of the above effects.

---

[1] L. Neel, Ann. de Phys. **3**, 137 (1948).

[2] E. W. Gorter, Phillips Res. Reports **9**, 295 (1954).

[3] R. Pauthenet, Compt. rend. **242**, 1859 (1956);

243, 1499 (1956).

[4] Belov, Zaĭtseva, and Ped'ko, JETP **36**, 1672 (1959), Soviet Phys. JETP **9**, 1191 (1959).

[5] E. A. Turov and Yu. P. Irkhin, Материалы конференции по ферритам, (Proceedings of the Conference on Ferrites), Minsk, June 1959.

Translated by D. C. West
369

LIFETIME OF THE 321-kev LEVEL IN Hf^{177}

G. A. VARTAPETYAN

Physics Institute, Academy of Sciences, Armenian S.S.R.

Submitted to JETP editor April 4, 1960

J. Exptl. Theoret. Phys. (U.S.S.R.) **38**, 1916-1917 (June, 1960)

SOME properties of the levels in deformed odd nuclei may be explained within the framework of the model of Bohr-Mottelson and Nilsson.[1] But the intensity rule is not always satisfied; in particular, for Hf^{177} the ratios obtained for the probability of 208- and 321-kev E1 transitions considerably differ from the theoretically calculated values.[2]

It is of interest to find the absolute values of the probabilities of the transitions for γ radiation with $h\nu = 208$ and 321 kev. These E1 transitions are forbidden by the asymptotic selection rules.[1] M2 transitions may occur if they are not forbidden by the above-mentioned rules. As regards the allowed M2 transitions, in the case of the neighboring deformed nuclei, the experimental values for the transition probabilities coincide with the theoretical values.[2] Knowing the value of the M2 mixture in the 208-kev transition, obtained[3] from the measurement of the 208 — 113 kev angular correlation $[(M2/E1)_{208} = 10^{-3}]$ and the intensity ratio[2] $L_{\gamma_{208}}/L_{\gamma_{321}} = 20$, we can calculate the amount of M2 mixture in the 321-kev transition and the period of the 321-kev level. We find

$$(M2/E1)_{321} \approx 0.35, \quad T_{1/2} \approx 4 \cdot 10^{-10}\ \text{sec}.$$

The measurement of the 321-kev level transition was carried out by the method of delayed coincidences with the use of a fast-slow coincidence circuit[2] (resolving time 7×10^{-9} sec). The γ quanta were recorded by a NaI(Tl) crystal, and the β electrons were recorded by an anthracene crystal 2 mm thick. In the latter case, there was a certain difficulty in the measurements, since some of the conversion electrons from the 113 kev γ transition were detected apart from the β radiation with $E_{max} = 176$ kev. (The period of the 113-kev level is 4.2×10^{-10} sec.[4]) Then the experimental curve of the coincidences $\beta + e^-_{113} - \gamma_{208}$ (curve 1 in the figure) is the sum of the coincidences $\beta - \gamma_{208}$ and $e^-_{113} - \gamma_{208}$. In order to obtain the $\beta - \gamma_{208}$ curve (curve 2), a third channel, which detected the 113-kev γ quanta (curves 1 and 2 were measured simultaneously), was connected in coincidence. The $\beta - \gamma_{208}$ curve was compared with the delayed coincidences curve $\beta - \gamma_{208\,(\text{comp. from } 495)}$ for Ru^{103} (curve 3), which was obtained under the same conditions. (The period of the 495-kev transition is less than 10^{-10} sec.)

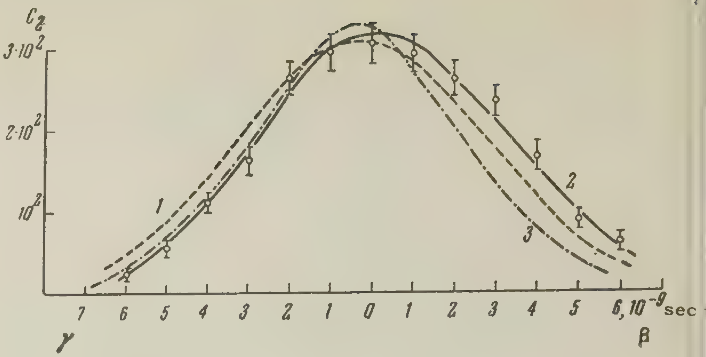

Delayed coincidences: curve 1 – Lu^{177}, $\beta + e^-_{113} - \gamma_{208}$; 2 – Lu^{177}, $\beta - \gamma_{208}$; 3 – Ru^{103}, $\beta - \gamma_{208\,(\text{comp. 495})}$.

Hence, by determining the shift in the centers of gravity of curves 2 and 3, we found the mean lifetime of the 321-kev level [which was equal to $(7 \pm 2) \times 10^{-10}$ sec] and the half-life $T_{1/2} = (5 \pm 1.5) \times 10^{10}$ sec. This value is in good agreement with that obtained from the measurement of the intensities[2] and angular correlation,[3] if one takes into account here the formula of Weisskopf and Alaga, which is valid for the allowed M2 transitions. The probabilities for the 321- and 208-kev transitions may be calculated:

$$P_{\gamma 321}(E1) = 5.5 \cdot 10^7\,\text{sec}^{-1}, \quad P_{\gamma 208}(E1) = 1.4 \cdot 10^9\,\text{sec}^{-1}.$$

From comparison with the theoretical values we find the degree to which the transitions are forbidden: $f_{B_{321}} = 4 \times 10^6$ and $f_{B_{208}} = 3.5 \times 10^4$ from the formula of Weisskopf and $f_{H_{321}} = 4 \times 10^2$ and $f_{H_{208}} = 0.6$ from the formula of Nilsson.[5]

The fact that the 321-kev E1 transition is forbidden is comparable to the fact that the 396- and 282-kev E1 transitions[6] in Lu^{175} and the 147-kev transition[1] in Lu^{177} are forbidden. If it is assumed that these transitions are accounted for by a simple collective model (in this case, the formula of Nilsson is approximate), we find that the 208-kev transition is considerably accelerated (by a factor of 800) in comparison with the transition which would take place between the single-particle level (321 kev) and the pure rotational level (113 kev). This difference can be the result of the interaction between the individual and collective motions in the nucleus.

On the other hand, if we assume that the 208-kev transition is in agreement with the simple collective model and with Nilsson's formula ($f_{H_{298}} = 0.6$), then the 396- (Lu^{175}), 321- (Hf^{177}), and 147-kev (Lu^{177}) E1 transitions are retarded by secondary effects.

In conclusion, I wish to express my gratitude to A. I. Alikhanyan for his interest in this work.

---

[1] B. Mottelson and S. Nilsson, Mat.-fys Skr. Danske Videnskab. Selskb. **1**, No. 8 (1959).

[2] H. Vartapetian, Ann. phys. **3**, 569 (1958).

[3] E. Klema, Phys. Rev. **109**, 1652 (1958).

[4] É. Berlovich, Izv. Akad. Nauk SSSR, Ser. Fiz. **20**, 1438 (1956), Columbia Tech. Transl. p. 1315.

[5] S. Nilsson, Kgl. Danske Videnskab. Selskab. Mat.-fys. Medd. **29**, 16 (1955).

[6] H. Vartapetian, Compt. rend. **244**, 65 (1957).

Translated by E. Marquit
370

MEASUREMENT OF THE RELATIVE NUCLEAR ACTIVITY OF π MESONS NEAR THEIR PLACE OF GENERATION

B. S. NEGANOV, L. B. PARFENOV, and A. A. TYAPKIN

Joint Institute for Nuclear Research

Submitted to JETP editor April 19, 1960

J. Exptl. Theoret. Phys. (U.S.S.R.) **38**, 1917-1918 (June, 1960)

In the work of the Irish group[1] on π mesons produced in $K_{\pi 2}$ decay, an anomalously large inelastic interaction cross section was observed, equal approximately to 2 or 3 times the geometric cross section. For ordinary π mesons of the same energy, this cross section is close to geometric.

As possible causes for the obtained discrepancy, the authors indicated two possibilities: either particles different from the ordinary π mesons are produced in the K decay there, or the difference is connected with the fact that the nuclear activity of the π mesons in the given work was studied close to the place of their generation, at distances of up to 4 cm.

Analyzing these possibilities, we found that the first cause can account for the discrepancy only if there is an unknown particle among the products of the inelastic interaction of these mesons with emulsion nuclei. In the opposite case, it follows from the principle of detailed balance that, in nuclear collisions, there should be generated mainly mesons which interact just as strongly as those produced in the K decay.

Contradicting the possibility of the second explanation of the observed discrepancy are the experiments on the comparison of the cross sections for the direct and inverse reactions $p + p \rightleftarrows \pi^+ + d$. If the anomalously nuclear-active mesons of mass close to the mass of the π meson were then to decay into the less active ordinary π mesons, then the results obtained in the above experiment would contradict the assumption that the same reaction was investigated in the direct and inverse directions.

It is desirable that the question on the production of mesons having an anomalously large nuclear activity close to the point of generation be elucidated in the general case of nucleon collisions, and not only in the case of the emission of mesons along with the production of a deuteron in the final state.

In this connection, we carried out measurements to compare the nuclear activity of mesons produced at an angle of 90° on carbon nuclei by 660-Mev protons at distances of 2 — 4, 10 — 20, 21 — 23, and 105 — 115 cm from the place of generation. The measurements were made by an electronic method with the aid of scintillation counters. The usual methods of measurement were not used for this purpose, since a beam of mesons cannot be formed at a distance of several centimeters from the target. This difficulty was overcome by the employment of the method of similar geometry. In the measurements we used telescopes consisting of three scintillation counters, the dimensions of which differed exactly by a factor of five. Brass filters in the telescopes contained uniform quantities of matter per cm^2, but differed in geometrical size also by a factor of five.

In the experiment we determined the relative change in counts of both telescopes due to the addition of brass filters 17 g/cm^2 thick. The filters were placed either in front of the first counters or behind the second counters of the telescopes. Aside from these filters, brass filters of thickness 8.5 g/cm^2 were permanently installed in front of the last counters.

Thus, we investigated in this experiment the nuclear absorption of mesons, the mean energy of which changed from 100 to 70 Mev as they passed through the filters. (This energy interval corresponds to the energy of mesons emitted in $K_{\pi 2}$ decay.)

These experiments showed only a slight change in the nuclear activity of the mesons, which could be explained by the decay of π mesons into μ mesons at a distance of one meter. Apart from the decrease in the nuclear activity, the errors of measurement allow a change of not more than 15% of the geometric cross section in the cross section for the nuclear absorption of mesons at a distance of 3 to 110 cm.

Hence, it should be assumed that the results obtained in the study of the nuclear activity of π mesons from the $K_{\pi 2}$ decay are apparently due to errors in measurements.

---

[1] Alexander, Johnston, and O'Ceallaigh, Nuovo cimento **6**, 478 (1957).

Translated by E. Marquit
371

MEASURING OF THE CHIRALITY OF THE MU MESON

A. I. ALIKHANOV, Yu. V. GALAKTIONOV, Yu. V. GORODKOV, G. P. ELISEEV, and V. A. LYUBIMOV

Institute of Theoretical and Experimental Physics, Academy of Sciences, U.S.S.R.

Submitted to JETP editor April 25, 1960

J. Exptl. Theoret. Phys. (U.S.S.R.) **38**, 1918-1920 (June, 1960)

IT is known that the decay of the μ meson is characterized, in particular, by the chirality of the μ meson, i.e., by the direction of the spin of the μ meson relative to its momentum. In the universal (V-A) theory of weak interaction, the direction of the spin of the μ meson is opposite to its momentum, and in the STP interaction the reverse is true.

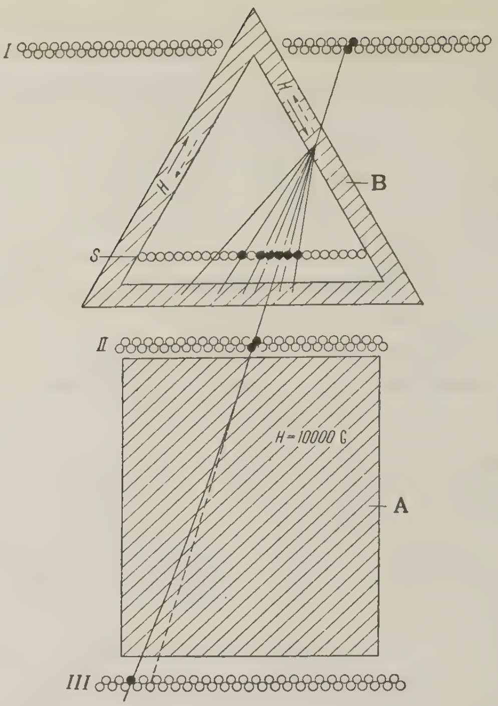

I, II, and III are rows of hodoscopic counters for the determination of the trajectory of the μ meson. S is a row of counters for the registration of the showers. A is the iron yoke of a permanent magnet for the determination of the sign of the μ mesons from the deflection in a magnetic field. B is the iron core of an electromagnet with a triangular cross-section, in which the μ mesons produced showers, including some on electrons polarized by the magnetic field.

In the present work we measured the chirality of the μ meson by a method proposed earlier,[1] based on measuring the cross section of the scattering of polarized μ mesons by polarized electrons, since this cross section depends on the relative orientation of the colliding particles.

The quantity measured directly in the test was the number of δ showers produced by μ mesons in magnetized iron and having not less than two particles ($n \geq 2$). Formulas and tentative estimates on the magnitude of this effect for cosmic-ray μ mesons are given in reference 1. The drawing shows the experimental setup. I, II, and III are arrays of hodoscopic counters, which allow to plot the trajectory of the particle from three points and to determine its sign from the deflection in a magnetic field of ~ 10,000 gauss in the iron yoke of the permanent closed magnet A. The μ meson was deflected in the iron core by the effect of the magnetic field (Δ_H) and by repeated scattering (Δ_S). Under our conditions $\Delta_H/\Delta_S = 6.7$. The δ showers occurred in the iron core of the closed electromagnet B, which had a triangular cross section.

The magnetic field had an induction of 14,400 gauss. The row of counters S registered the showers produced in the lateral sides of the "triangle." The direction of the magnetic field in the "triangle" was reversed after the registration of each shower.

The cases of interest to us were registered by a coincidence circuit I, II, III, and S, whenever not less than three counters ($m \geq 3$) operated in the array S. The number of μ mesons passing through the setup was 500 per minute, of which one or two gave rise to showers with $m \geq 3$. To date, 116,000 showers have been registered in which not less then three counters in an array were operated. The energies of the μ mesons that produced these showers ranged from 3 to 6.5 Bev. The upper limit of the μ-meson energy, 6.5 Bev, corresponded to a deflection in the magnetic field ($\Delta \approx 0.5$ cm) such that the signs of the particles were still distinguishable. The lower limit of the μ-meson energy was determined by the requirement $n \geq 2$ in the given thickness of the iron of the "triangle." μ mesons with an energy less than 3 Bev are unable to produce a δ electron that can satisfy the requirement $n \geq 2$.

The results of the test were the following: for μ^+ mesons the difference in the number of showers for two different directions of the current in the winding of the "triangle" yields

$$s_+ = -0.37 \pm 0.41 \qquad (s = (N_+ - N_-)/(N_+ + N_-)),$$

for μ^- mesons

$$s_- = +0.82 \pm 0.42$$

and, finally, for both signs of the μ-meson charge the effect is

$$s_\pm = 0.58 \pm 0.29$$

with an expected value $s_{\text{theor}} = 0.6$, corresponding to a 50% of polarization of the μ mesons.[2] The sign of the effect is in accord with the predictions of the V-A theory of interaction, i.e., left-handed chirality of the μ^+ meson.

The probability that the effect is zero or less is 2×10^{-2}. The measurements are being continued, and a further increase in the statistics will reduce this probability.

---

[1] A. I. Alikhanov and V. A. Lyubimov, JETP **36**, 1334 (1959), Soviet Phys. JETP **9**, 946 (1959).

[2] A. I. Alikhanyan, Trans. of the Conference on Cosmic Rays, Moscow, 1959 (in press).

Translated by I. Schroer
372

Author Index to Volume 11

References with L are Letters to the Editor

Abelishvili, T. L., T. G. Gachechiladze, and O. M. Mdivani. Angular Distribution of Neutrons in the Reaction C^{13}(d, n)N^{14} — 453L.

Abramenkov, A. D. (see Grizhko, V. M.) — 987.

Abrosimov, A. T., G. A. Bazilevskaya, V. I. Solov'eva, and G. B. Khristiansen. Ultra-High-Energy Extensive Air Showers — 74.

Adamovich, M. I., E. G. Gorzhevskaya, V. G. Larionova, V. M. Popova, S. P. Kharlamov, and F. R. Yagudina. Photoproduction of Charged Pions near Threshold — 779.

Akhiezer, I. A., and R. V. Polovin. The Motion of a Conducting Piston in a Magnetohydrodynamic Medium — 383.

— and S. V. Peletminskiĭ. Use of the Methods of Quantum Field Theory for the Investigation of the Thermodynamical Properties of a Gas of Electrons and Photons — 1316.

Akimov, Yu. K., O. V. Savchenko, and L. M. Soroko. The $d + d \to \pi^0 + He^4$ Reaction at 400 Mev Deuteron Energy — 221L.

—, O. V. Savchenko, and L. M. Soroko. The Reaction $p + d \to t + \pi^+$ at Proton Energy 670 Mev — 462L.

Akimova, M. K. (see Strutinskiĭ, V. M.) — 430.

Akindinov, V. V. (see Lin'kova, N. V.) — 566.

Aleksandrov, A. P., Ya. I. Khanin, and É. G. Yashchin. Observation of Spontaneous Coherent Radiation of a Ferrite in a Resonator — 960L.

Alekseevskiĭ, N. E. and M. N. Mikheeva. Critical Currents in Superconducting Tin Films — 211L.

—, V. V. Bondar', and Yu. M. Polukarov. The Superconductivity of Electrolytically Deposited Copper-Bismuth Alloys — 213L.

— and Yu. P. Gaĭdukov. Anisotropy of the Electrical Resistance of Mg and Pt Single Crystals in a Magnetic Field at 4.2°K — 1242.

Alikhanov, A. I. (see Lyubimov, V. A.) — 1375L.

—, Yu. V. Galaktionov, Yu. V. Gorodkov, G. P. Eliseev, and V. A. Lyubimov. Measuring of the Chirality of the μ Meson — 1380L.

Alikhanov, R. A. A Cryostat for Neutron Diffraction Studies — 585.

Alikhanyan, A. I., V. G. Kirillov-Ugryumov, L. P. Kotenko, E. P. Kuznetsov, and A. V. Samoĭlov. Single Scattering of 10-30 Mev Negative Muons on Carbon — 282.

Al'tshuler, L. V., S. B. Kormer, A. A. Bakanova, and R. F. Trunin. Equation of State for Aluminum, Copper, and Lead in the High-Pressure Region — 573.

—, S. B. Kormer, M. I. Brazhnik, L. A. Vladimirov, M. P. Speranskaya, and A. I. Funtikov. The Isentropic Compressibility of Aluminum, Copper, Lead, and Iron at High Pressures — 766.

Amaglobeli, N. S., B. M. Golovin, Yu. M. Kazarinov, S. V. Medved', and N. M. Polev. Determination of the Coupling Constant for the Pion-Nucleon Interaction from Cross Sections for the Elastic Scattering of 630-Mev Neutrons by Protons — 474L.

Amirov, R. Sh. (see Lin'kova, N. V.) — 566.

Amus'ya, M. Ya. Dependence of the Parameters of the Nuclear Potential on the Number of Particles — 604.

Andreev, V. V. (see Kosevich, A. M.) — 637.

Andronikashvili, E. L. and R. E. Kazarov. Experimental Investigation of the Energy Spectrum of the Penetrating Component of Extensive Air Showers — 507.

Ankudinov, V. A. (see Fogel', Ya. M.) — 18.

Ansel'm, A. A. On Certain General Properties of the Photon Propagation Function in Quantum Electrodynamics — 929.

— Solution of Equations for Meson-Meson Scattering Amplitude in the Asymptotic Region — 1356.

Antonova, S. F., S. S. Vasilenko, M. G. Kaganskiĭ, and D. L. Kaminskiĭ. Positron Decay of Ir^{192} — 276.

—, S. S. Vasilenko, M. G. Kaganskiĭ, and D. L. Kaminskiĭ. Investigation of the Gamma Spectrum of Ce^{140} — 554.

Arifkhanov, U. R., M. M. Makarov, N. A. Perfilov, and V. P. Shamov. Fragment Production by 100-Mev Protons — 806.

Arutyunyan, V. M. (see Kerimov, B. K.) — 1294.

Astaf'ev, V. A. On the Momentum Spectrum of π^+ Mesons from the Interaction $\pi^+ + p \to 2\pi^+ + n$ — 709L.

Astrov, D. N. The Magnetoelectric Effect in Antiferromagnetics — 708L.

Azbel', M. Ya. (see Gurzhi, R. N.) — 379.

— (see Rozentsveĭg, L. N.) — 1121.

Azimov, S. A., U. G. Gulyamov, R. Karimova, and B. G. Rakhimbaev. Anomalous Decays of Hyperfragments — 502.

Babayan, Kh. P., M. G. Sarinyan, and É. R. Tumanyan. Investigation of a High-Energy Interaction Event in Photographic Emulsion — 227.

Babikov, V. V. On the Cross Section for Compound Nucleus Formation in the Interaction of Atomic Nuclei — 198L.

Badalyan, A. M., and Chou Kuang-Chao. On the Production of an Electron-Positron Pair by a Neutrino in the Field of a Nucleus — 477L.

Bakanova, A. A. (see Al'tshuler, L. V.) — 573.

Balatz, M. Ya., L. N. Kondrat'ev, L. G. Landsberg, P. I. Lebedev, Yu. V. Obukhov, and B. Pontevorvo. Nonradiative Transitions in Heavy μ-Mesic Atoms — 1239.

Baldin, A. M. Analysis Based on Dispersion Relations of Data on Pion Photoproduction Near Threshold — 416.

Bally, D. and L. Müller. Investigation of the Main K X-ray Absorption Edge in Selenium — 995.

Barabanenkov, Yu. N. Possible Mode of Oscillation for a Charge in Crossed Fields — 190L.

— Coulomb Scattering of Charges in a Strong Magnetic Field — 1091.

Barashenkov, V. S., Wang Pei, and V. M. Mal'tsev. Momentum Distribution of Particles Produced in Inelastic N-N Collisions at E = 9 Bev — 467L.

Barbashov, B. M. and G. V. Efimov. Green's Function in the Fixed-Source Model of Charged Scalar Mesons — 145.

Barit, I. Ya, M. I. Podgoretskiĭ, and F. L. Shapiro. Several Possible Applications for the Resonant Scattering of Gamma Rays — 218L.

Bar'yakhtar, V. G. and G. I. Urushadze. On the Theory of Relaxation Processes in Ferrodielectrics with Weak Magnetic Anisotropy at Low Temperatures — 905.

Basov, N. G., O. N. Krokhin, and Yu. M. Popov. Semiconductor Amplifiers and Generators with Carriers Having Negative Effective Mass — 720L.

Bayukov, Yu. D. and G. A. Leksin. On the Possibility of Using Nuclear Reactions to Obtain Information about the $\pi\pi$ Interaction — 1371.

Bazhanov, E. B. Curves for the Photoproton Yield from the C^{12} Nucleus — 193L.

— and L. A. Kul'chitskiĭ. Investigation of High-Energy Protons Emitted in the Photodisintegration of Li^9 — 1215.

Bazilevskaya, G. A. (see Abrosimov, A. T.) — 74.

Begiashvili, G. A. and E. V. Gedalin. Cerenkov Radiation of Dipoles in a Medium with Spatial Dispersion — 1254.

Belov, K. P., B. S. Mingalev, and V. M. Shekhter. Possibility of Determining the Form Factors in Leptonic Decay of Hyperons — 392.

—, A. N. Goryaga, and Lin Chang-Ta. Electrical and Galvanomagnetic Properties of Lithium Ferrite-Chromite Near the Compensation Point — 1376L.

—, V. F. Belov, and A. A. Popova. Magnesium-Manganese Ferrite Single Crystals with Narrow Ferromagnetic-Absorption Resonance Curve — 1372L.

Belov, V. F. (see Belov, K. P.) — 1372L.

Belovitskiĭ, G. E. On the Applicability of the Fermi-Teller "Z-Law" to a Photoemulsion Containing Uranium — 473L.

—, N. T. Kashchukeev, A. Mikhul, M. G. Petrashku, T. A. Romanova, and F. A. Tikhomirov. On the Mechanism of Uranium Fission Induced by Slow Negative Muons — 296.

Belyaev, V. B., B. N. Zakhar'ev, and V. G. Solov'ev. Superfluidity of Light Nuclei — 686.

Berdyshev, A. A. (see Karpenko, B. V.) — 666.

Berkovich, I. B., A. P. Zhdanov, F. G. Lepekhin, and Z. S. Khokhlova. Non-Mesonic Decays of Hyperfragments — 311.

Bilen'kiĭ, S. M. Concerning the Article by S. M. Bilen'kiĭ, R. M. Ryndin, Ya. A. Smorodinskiĭ, and Ho Tso-Hsiu, "On the Theory of Neutron Beta Decay" — 729L.

Bliodze, Yu. A. (see Selinov, I. P.) — 1191L.

Bogachev, N. P., S. A. Bunyatov, T. Vishki, Yu. P. Merekov, V. M. Sidorov, and V. A. Yarba. Charged Pion Production in Interactions of 9-Bev Protons with Emulsion Nuclei — 317.

—, S. A. Bunyatov, Yu. P. Merekov, V. M. Sidorov, and V. A. Yarba. Inelastic Interactions of 9-Bev Protons with Free and Bound Nucleons in Emulsion — 968L.

Bogachov, B. A., A. P. Komar, and G. E. Solyakin. Kinetic Energy of Fragments from the Photofission of U^{238} — 990.

Bondar', V. V. (see Alekseevskiĭ, N. E.) — 213L.

Boos, É. G. and Zh. S. Takibaev. Distribution of the Transverse Momentum of Shower Particles in Jets — 920.

Borisoglebskiĭ, V. P. (see Timrot, D. L.) — 1248.

Borovik, E. S. and V. G. Volotskaya. Galvanomagnetic Phenomena in Indium and Aluminum — 189L.

Borovik-Romanov, A. S. Piezomagnetism in the Antiferromagnetic Fluorides of Cobalt and Manganese — 786.

Borovskiĭ, I. B., A. N. Kabanov, Yu. M. Kushnir, and V. V. Schmidt. Effect of Temperature on Characteristic Energy Losses of Electrons in Iron — 997.

Braginskiĭ, V. B., D. D. Ivanenko, and G. I. Rukman. On the Possibility of Measuring in the Laboratory the Speed of Propagation of Gravitational Waves — 723L.

Brandt, N. B. On the Hole Component of the Fermi Surface in Bismuth — 975L.

Brazhnik, M. I. (see Al'tshuler, L. V.) — 766.

Brish, A. A., M. S. Tarasov, and V. A. Tsukerman. Electrical Conductivity of Dielectrics in Strong Shock Waves — 15.

Brodin, M. S. and S. I. Pekar. On an Experimental Demonstration of the Existence of Additional Anomalous Light Waves in a Crystal in the Exciton Absorption Region — 55.

— and S. I. Pekar. Additional Anomalous Light Waves in Anthracene in the Exciton-Absorption Region — 1372L.

Budagov, Yu. A., S. Wiktor, V. P. Dzhelepov, P. F. Ermolov, and V. I. Moskalev. Elastic Scattering of 128- and 162-Mev Negative Pions by Protons — 531.

—, S. Wiktor, V. P. Dzhelepov, P. F. Ermolov, and V. I. Moskalev. Internal Conversion Pairs in the Decay of Neutral π Mesons — 755.

Budyanskiĭ, G. M. Polarization of Deuterons Elastically Scattered on Zero-Spin Nuclei — 847.

Bulyanitsa, D. S. The Effect of an External Electric Field on the Shape of the Intrinsic Absorption Edge in Non-Conducting Crystals — 868.

Bunyatov, S. A. (see Bogachev, N. P.) — 317.

— (see Bogachev, N. P.) — 968L.

Cerenkov, P. A. (see Gorbunov, A. N.) — 51.

Chaban, A. A. Collective Excitations of Non-Axial Even-Even Nuclei — 1174.

— (see Davydov, A. S.) — 946.

Chandra, G. (see Klimentovskaya, M. V.) — 210L.

Charakhch'yan, A. N., V. F. Tulinov, and T. N. Charakhch'yan. Large Cosmic-Ray Intensity Fluctuations in the Stratosphere — 742.

Charakhch'yan, T. N. (see Charakhch'yan, A. N.) — 742.

Cheng P'u-Ying. (see Dzhanelidze, L. P.) — 722L.

Chernavskiĭ, D. S. (see Dremin, I. M.) — 167.

— (see Romanov, Yu. A.) — 819.

Chernikova, L. A. (see Galkina, O. S.) — 1.

— (see Kondorskiĭ, E. I.) — 464L.

Chetkin, M. V. (see Krinchik, G. S.) — 1184L.

Chikhladze, V. L., D. E. Khulelidze, and I. P. Selinov. Beta and Gamma Spectra of the Sb^{113} and Sb^{115} Isotopes — 974L.

— (see Selinov, I. P.) — 728L.

Chilashvili, G. A. (see Vashakidze, I. Sh.) — 675.

— (see Kopaleĭshvili, T. I.) — 1267.

Ch'ing Ch'en-Jui and F. Yanoukh. Internal Bremsstrahlung in the β Decay of Polarized Nuclei — 683.

Chirko, V. I. (see Val'ter, A. K.) — 1025.

Chasov, V. P. High Energy Photonuclear Deuterons and Tritons — 587.
Chikhladze, I. M. (See Usatadze, D. S.) — 457L.
Chou Kuang-Chao. Possible Symmetry Properties for the Σ-Λ System — 750L.
— On the Decay of Σ Hyperons — 836L.
— (See Baldin, A. M.) — 477L.
— (See Zastavenko, L. G.) — 97.
— (See Lapidus, L. I.) — 147.
Chu Hung-Yuan (See Ho Tso-Hsiu) — 1346.
Chudakov, Yu. V. (See Polikanov, S. M.) — 214L.
Chuev, V. I. (See Vlasov, N. A.) — 205L.
Chueva, S. A. (See Varfolomeev, A. A.) — 23.
Chuvilo, I. V. On Possible Properties of ρ^0 Mesons — 721L.
— (See Vlyasov, N. M.) — 327.
Ciulli, S. (See Fischer, J.) — 1256.
Daion, M. I. Energy Losses of Fast μ-Mesons in Thick Layers of Matter — 1206.
Darovskikh, V. F. (See Perfilov, N. A.) — 527.
Davydov, A. S., N. S. Rabotnov, and A. A. Chaban. Rotational Energy and Moments of Inertia of Non-axial Nuclei — 946.
Deigen, M. F. and V. Ya. Zevin. The Shape and Temperature Dependence of the Electron-Spin Resonance Lines of Localized Electron Centers in Crystals — [illegible].
Delyagin, N. N. Resonance Scattering of Gamma Rays by Sn^{119} — [illegible].
— and V. S. Shpinel'. Investigation of the Decay Scheme of Sn^{117} by the γ-γ Coincidence Method — [illegible].
Demidov, A. M. (See Groshev, L. V.) — [illegible].
Demkov, Yu. N. Variational Principles for Nonstationary Quantum Mechanical Problems and Perturbation Theory — [illegible].
Denisenko, G. F. (See Perfilov, N. A.) — 527.
Denisov, F. P. (See [illegible]) — [illegible].
[illegible] (See [illegible]) — [illegible].
[illegible] (See [illegible]) — [illegible].
[illegible] (See [illegible]) — [illegible].
[illegible] Comparison of the [illegible] C^{12}, O^{16} and N^{14} — [illegible].
[illegible] and V. P. [illegible]. The [illegible] Back-Ray Electrons from [illegible] — 1098.
Dolgov-Savel'ev, G. G., V. S. Mukhovatov, V. S. Strelkov, M. N. Shepelev, and N. A. Yavlinskii. Toroidal Discharge in a Strong Magnetic Field — 287.
Dovzhenko, O. I., S. I. Nikol'skii, and I. V. Rakobol'skaya. Energy Spectra of the Electron-Photon Component in Extensive Atmospheric Showers Near the Shower Axis — 552.
Dremin, I. M. and D. S. Chernavskii. Production of "Superfast" [illegible] — [illegible].
[illegible] (See [illegible]) — [illegible].
[illegible] and D. S. [illegible] — [illegible].
Drozdov, S. I. Excitation of Nuclear Collective States in Charged Particle Scattering — [illegible].
— (See Grin', Yu. T.) — [illegible].
— (See Grin', Yu. T.) — 336.
Druin, V. A. (See Flerov, G. N.) — 61.
Dunaitsev, A. F. and Yu. D. Prokoshkin. The $\pi^- \to \pi^0$ Reaction in the Energy Range [illegible] — [illegible].
Dykhne, A. M. Quantum Transitions in the Adiabatic Approximation — 411.
Dzhelepov, B. S., [illegible], and [illegible]. The Gamma Spectrum of [illegible] in the Energy Range [illegible] kev — [illegible].
[illegible] (See [illegible]) — [illegible].
— (See [illegible]) — [illegible].
[illegible] Angular Distribution of [illegible] of C^{12} [illegible] Protons in Photoemulsion — [illegible].
Efremov, V. A., V. S. Nekrasov, and E. A. [illegible]. Possible Occurrence of a Second-Order Process in Inelastic Scattering of Deuterons by Nuclei — 1301.
Efimov, G. V. (See Barbashov, B. M.) — 345.
[illegible], K. and L. [illegible]. On Elastic Scattering of Photons by the Nuclear Coulomb Field — 971L.
[illegible] (See [illegible]) — [illegible].
[illegible] — [illegible].
[illegible] Interaction between Electrons and Lattice Vibrations of a Semiconductor — [illegible].
[illegible] (See [illegible]) — [illegible].
[illegible] The Two-Center Problem and [illegible] Theory of [illegible] of Particles — [illegible].
Emel'yanov, B. A. (See Dmitriev, E. S.) — [illegible].
[illegible] (See Balagin, Yu. A.) — 521.
— (See Balagin, Yu. A.) — 785.
[illegible] (See [illegible]) — [illegible].
Fainberg, V. Ya. (See Kirzhnits, D. A.) — [illegible].
— (See [illegible]) — [illegible].
Fainberg, Ya. B. (See [illegible]) — [illegible].
— (See [illegible]) — [illegible].
[illegible] and L. S. [illegible] — [illegible].
[illegible] (See [illegible]) — [illegible].
[illegible] (See [illegible]) — [illegible].
[illegible] (See [illegible]) — [illegible].
— (See [illegible]) — [illegible].
Filippov, A. T. On the Equilibrium Shape of Atomic Nuclei — [illegible].
Fischer, J. and S. Ciulli. Dispersion [illegible] — 1256.
[illegible] (See [illegible]) — [illegible].
[illegible] (See [illegible]) — [illegible].
[illegible] (See [illegible]) — [illegible].
Flerov, G. N., S. M. Polikanov, A. S. Karamyan, A. S. Pasyuk, D. M. Parfanovich, N. I. Tarantin, V. A. Karnaukhov, V. A. Druin, V. V. Volkov, A. M. Semchinova, Yu. Ts. Oganesyan, V. I. Khalizev, G. I. Khlebnikov, B. F. Myasoedov, and K. A. Gavrilov. The Production of Element 102 — 61.
Fock, V. A. Comparison of Different Coordinate Conditions in Einstein's Gravitation Theory — [illegible].
— The Einstein Spaces in Conformal Space — [illegible].
Fogel', Ya. M., A. G. Koval', and Yu. Z. Levchenko.

mental Determination of the Polaron Mass in Cuprous Oxide — 247.
Gulyamov, U. G. (see Azimov, S. A.) — 502.
Gurevich, A. V. Certain Special Features of Ohmic Heating of Electron Gas in a Plasma — 85.
— On the Amount of Accelerated Particles in an Ionized Gas Under Various Accelerating Mechanisms — 1150.
Gurevich, I. I. (see Varfolomeev, A. A.) — 23.
Gurzhi, R. N. and M. Ya. Azbel'. Electron Relaxation Time in a High-Frequency Electromagnetic Field and the Surface Impedance of a Metal — 379.
Guseĭnov, N. G. (see Turov, E. A.) — 955.
Guzhavin, V. V. and I. P. Ivanenko. Dependence of Three-Dimensional Development of a Cascade Shower on the Energy of the Primary Particle — 476L.
Guzenko, S. Ya. and P. I. Fomin. Radiative Corrections to Photoproduction and Single-Photon Annihilation of Pairs — 372.
Gvaladze, Yu. S. (see Kvartzkhava, I. F.) — 1182L.
Ho Tso-Hsiu. Possibility of an Experimental Test for Form Factors in the Theory of the Universal Fermi Interaction — 466L.
— The Form Factor and the μ Capture by Light Nuclei with Spin $\frac{1}{2}$ — 1167.
— and Chu Hung-Yuan. Some Consequences of the Symmetry of the Universal Fermi Weak Interaction — 1346.
— (see Bilen'kiĭ, S. M.) — 729L.
— (see Smorodinskiĭ, Ya. A.) — 724L.
Hsien Ting-Ch'ang. Cross Section for the Formation of Ω^- Particles in the Reactions $\pi^- + p \rightarrow \Omega^- + 3K$ at 8 Bev and $p + \bar{p} \rightarrow \Omega + \bar{\Omega}$ at 4 Bev — 209L.
— On the D Meson — 1172.
Ignatenko, A. E. On Transitions Between Hyperfine Structure Levels in μ-Mesic Atoms — 1093.
Il'in, Yu. I. (see Vasil'ev, Yu. A.) — 483.
Inopin, E. V. Structure of the Giant Resonance in Photonuclear Reactions — 714L.
— and B. I. Tishchenko. Scattering of Electrons by Nuclei according to the α-Particle Model — 840.
— (see Volkov, D. V.) — 1273.
Iodko, M. G., V. V. Tuchkevich, V. A. Romanov, and O. M. Kresin. Investigation of the Relative Intensities of Some Conversion Lines of the Spectrum of Neutron-Deficient Lutetium Isotopes — 739.
— (see Romanov, V. A.) — 733.
Ioffe, B. L. Renormalization in Parity-Nonconservation Theory — 911.
— Limits of Applicability of the Weak Interaction Theory — 1158.
— (see Galanin, A. D.) — 347.
Iogansen, L. V. (see Rabinovich, M. S.) — 856.
Ionov, I. I. and M. A. Mittsev. Determination of the First Ionization Potentials of Neodymium and Praseodymium by the Surface Ionization Method — 972L.
Isakov, A. I., Yu. P. Popov, and F. L. Shapiro. Measurements of the Energy Dependence of Radiative Neutron Capture in Iron, Silver, and Gold at Energies up to 30 kev — 712L.
Itskevich, E. S. The Heat Capacity of Bismuth Telluride at Low Temperatures — 255.
Iusim, Ch. (see Weiner, R.) — 629.
Ivanenko, D. D. (see Braginskiĭ, V. B.) — 723L.
Ivanenko, I. P. (see Guzhavin, V. V.) — 476L.
Ivanov, V. G. (see Wang Kang-Ch'ang) — 313.
— (see Wang Kang-Ch'ang) — 726L.
Ivanova, N. S. (see Perfilov, N. A.) — 250.
Kabanov, A. N. (see Borovskiĭ, I. B.) — 997.
Kagan, Yu. Cyclotron Resonance in Germanium and Silicon and the Effect of Negative Effective Masses — 1333.
Kaganov, M. I. and V. M. Tsukernik. Nonresonance Absorption of Oscillating Magnetic Field Energy by a Ferromagnetic Dielectric. II — 952.
Kaganskiĭ, M. G. (see Antonova, S. F.) — 276.
— (see Antonova, S. F.) — 554.
Kalinin, S. P. (see Vlasov, N. A.) — 203L.
— (see Vlasov, N. A.) — 1251.
Kalinkin, B. N. Heavy Ion Excitation of Nuclei Accompanied by Radiation of γ Quanta — 1111.
Kalinkin, D. F. (see Melioranskiĭ, A. C.) — 548.
Kalitkin, N. N. The Thomas - Fermi Model of the Atom with Quantum and Exchange Corrections — 1106.
Kaminskiĭ, D. L. (see Antonova, S. F.) — 276.
— (see Antonova, S. F.) — 554.
Kaminskiĭ, V. A. (see Timashev, S. F.) — 206L.
Kandaurova, G. S., Ya. S. Shur, and F. V. Maslennikova. Dependence of the Magnetic Structure of a Cobalt Crystal on its Size — 45.
Kaner, É. A. On the Theory of Ultrasonic Absorption by Metals in a Strong Magnetic Field — 154.
Kaplan, S. A. Effect of Conductivity Anisotropy in a Magnetic Field on the Structure of a Shock Wave in Magnetogasdynamics — 183L.
Karamyan, A. S. (see Flerov, G. N.) — 61.
Karimova, R. (see Azimov, S. A.) — 502.
Karnaukhov, V. A. and Yu. Ts. Oganesyan. Gamma Radiation Produced in the Interaction between Accelerated C^{12} Ions and Tin Nuclei — 964L.
— (see Flerov, G. N.) — 61.
Karpenko, B. V. and A. A. Berdyshev. The Indirect Interaction of d Electrons in Transition Metals. II. Antiferromagnetism — 666.
Karpukhin, O. A. (see Gol'danskiĭ, V. I.) — 1223.
Kashchukeev, N. T. (see Belovitskiĭ, G. E.) — 296.
Kataev, G. I. and Z. D. Sirota. Anomalies in the Modulus of Elasticity and in Internal Friction in the Alloy Fe_3Pt — 747.
Katyshev, Yu. V. (see Wang Kang-Chang) — 313.
Kazarinov, Yu. M. (see Amaglobeli, N. S.) — 474L.
Kazarnovskiĭ, M. V. Theory of Resonant Interaction of Gamma Rays with Crystals — 1191L.
Kazarov, R. E. (see Andronikashvili, É. L.) — 507.
Kerimov, B. K. and V. M. Arutyunyan. Polarization of Electrons in Elastic Scattering with Account of the Finite Size of the Nucleus — 1294.
Kervalidze, K. N. (see Kvartzkhava, I. F.) — 1182L.
Khalizev, V. I. (see Flerov, G. N.) — 61.
Khalkin, V. A. (see Selinov, I. P.) — 1191L.
Khanin, Ya. I. (see Aleksandrov, A. P.) — 960L.
Kharlamov, S. P. (see Adamovich, M. I.) — 779.
Kharchenko, I. F., Ya. B. Faĭnberg, R. M. Nikolaev, E. A. Kornilov, E. A. Lutsenko, and N. S. Pedenko. Interaction of an Electron Beam with a Plasma — 493.
Khlebnikov, G. I. (see Flerov, G. N.) — 61.
Khokhlova, Z. S. (see Berkovich, I. B.) — 311.

Khristiansen, G. B. (see Abrosimov, A. T.) — 74.
— (see Vernov, S. N.) — 215L.
Khulelidze, D. E. (see Selinov, I. P.) — 1191L.
— (see Chikhladze, V. L.) — 974L.
Khutsishvili, G. R. On the Nuclear Orientation Associated with a Saturated Forbidden Resonance and with Double Resonance — 679.
— The Polarization of Nuclei in Nonmetallic Ferromagnetic Substances — 1187L.
Kim Hu In (see Wang Kang-Ch'ang) — 976L.
— (see Viryasov, N. M.) — 327.
Kirakosyan, Z. A. (see Kocharyan, N. M.) — 12.
Kirillov, A. D. (see Viryasov, N. M.) — 327.
Kirillov-Ugryumov, V. G. (see Alikhanyan, A. I.) — 282.
Kirzhnits, D. A., V. Ya. Faĭnberg, and E. S. Fradkin. On the Structure of the Photon Green's Function — 174.
— Internal Structure of Super-Dense Stars — 365.
— (see Vagradov, G. M.) — 1082.
Kitzenko, A. B. and K. N. Stepanov. Instability of a Plasma with Anisotropic Distribution of Ion and Electron Velocities — 1324.
Kladnitskaya, E. N. (see Wang Kang-Ch'ang) — 313.
— (see Wang Kang-Ch'ang) — 726L.
— (see Wang Kang-Ch'ang) — 976L.
Klimentovskaya, M. V. and G. Chandra. Measurement of the Angular Correlations of 298-880 kev and 298-966 kev Gamma Cascades of Dy^{160} — 210L.
Klimontovich, Yu. L. A Relativistic Transport Equation for a Plasma. II — 876.
Klyucharev, A. P. and N. Ya. Rutkevich. Elastic Scattering of Protons by Chromium Isotopes at 5.40 Mev — 207L.
— (see Val'ter, A. K.) — 1025.
Kobzarev, I. Yu., L. B. Okun', and A. P. Rudik. Remark on the Decay of the Cascade Hyperon — 728L.
— (see Grashin, A. F.) — 624.
Kocharov, G. E. (see Komar, A. P.) — 1038.
Kocharyan, N. M., Z. A. Kirakosyan, E. G. Sharoyan, and A. P. Pikalov. Polarization of High-Energy μ^+ Mesons in Cosmic Rays — 12.
Kochelaev, B. I. Longitudinal Relaxation of Nuclear Spins in a Paramagnetic Crystal at Very Low Temperatures — 719L.
Kol'chuzhkin, A. M. and N. N. Kolesnikov. Scattering and Radiative Capture of Λ Particles — 716L.
Kolesnikov, N. N. (see Kol'chuzhkin, A. M.) — 716L.
Kolesnikova, M. M. (see Sokolov, A. A.) — 120.
— (see Sokolov, A. A.) — 1281.
Kolkunov, V. A., L. B. Okun', and A. P. Rudik. The Singular Points of Some Feynman Diagrams — 634.
Koloskova, N. G. and U. Kh. Kopvillem. The Line Shape of the Nuclear Acoustic Resonance — 973L.
Kolotukhin, V. A. (see Gorbunov, A. N.) — 783.
Komar, A. P., G. A. Korolev, and G. E. Kocharov. Investigation of the α Decay of U^{236} — 1038.
— (see Bogachov, B. A.) — 990.
Komarov, V. V. and A. M. Popova. Energy Distributions of Products of Reactions in which Several Particles are Emitted — 184L.
—, A. B. Kurepin, and A. M. Popova. Possibility of Application of the (n, 2n) Reaction in Nuclear Spectroscopy — 1312.
— and A. M. Popova. Investigation of the Spectra of Neutrons Emitted in the Disintegration of Deuterons by Protons — 1123.
Kondorskiĭ, E. I., O. S. Galkina, and L. A. Chernikova. Electrical Resistance Maximum for Ferromagnets at their Curie Points at Low Temperatures — 464L.
— and V. L. Sedov. The Change of Atomic Magnetic Moments in Ferromagnetic Metals under Hydrostatic Compression — 561.
Kondrat'ev, L. I. (see Balatz, M. Ya.) — 1239.
Konin, A. D. (see Zinov, V. G.) — 1223.
Konstantinov, O. V. and V. I. Perel'. Possible Transmission of Electromagnetic Waves through a Metal in a Strong Magnetic Field — 117.
Kopaleĭshvili, T. I., I. Sh. Vashakidze, V. I. Mamasakhlisov, G. A. Chilashvili. Alpha-Deuteron Model of the Li^6 Nucleus — 1268.
— (see Vashakidze, I. Sh.) — 675.
Koprov, V. M. The Schwinger Effect with Account of the Screening of the Nucleus by the Atomic Electrons — 459L.
Kopvillem, U. Kh. The Second Moment of a Paramagnetic Absorption Line, Including the Effect of Fine and Hyperfine Structure — 109.
— (see Koloskova, N. G.) — 973L.
Kopylov, G. I. and Z. D. Lomakina. On the Problem of the Direct Reconstruction of the Elastic-Scattering Amplitude — 1188L.
Kopylova, D. K. (see Dzhanelidze, L. P.) — 722L.
Korenchenko, S. M. (see Zinov, V. G.) — 794.
— (see Zinov, V. G.) — 1010.
— (see Zinov, V. G.) — 1017.
— (see Zinov, V. G.) — 1223.
Kormer, S. B. (see Al'tshuler, L. V.) — 573.
— (see Al'tshuler, L. V.) — 766.
Kornienko, L. C. and A. M. Prokhorov. Electronic Paramagnetic Resonance of the Ion Ti^{3+} in Corundum — 1189L.
Kornilov, E. A. (see Kharchenko, I. F.) — 493.
Korolev, G. A. (see Komar, A. P.) — 1038.
Korolevich, Yu. B. (see Dzhanelidze, L. P.) — 722L.
Korolyuk, A. P. (see Galkin, A. A.) — 1218.
Kosevich, A. M. and V. V. Andreev. On the Quantum Analog of the Collision Integral for Electrons in Magnetic and Electric Fields — 637.
Kostanashvili, N. I. (see Dzhanelidze, L. P.) — 722L.
Kotenko, L. P. (see Alikhanyan, A. I.) — 282.
Koval', A. G. (see Fogel', Ya. M.) — 760.
Koval'skiĭ, N. G., I. M. Podgornyĭ, and M. M. Stepanenko. Investigation of Fast Electrons in Powerful Pulsed Discharges — 1040.
Kovrizhnykh, L. M. and A. A. Rukhadze. Instability of Longitudinal Oscillations of an Electron-Ion Plasma — 615.
Kozodaev, M. S., M. M. Kulyukin, R. M. Sulyaev, A. I. Filippov, and Yu. A. Shcherbakov. Inelastic Interaction of Pions with Helium Nuclei at Approximately 300 Mev — 300.
—, M. M. Kulyukin, R. M. Sulyaev, A. I. Filippov, and Yu. A. Shcherbakov. Interaction between 630-Mev Protons and He^4 Nuclei — 511.
Kresin, O. M. (see Iodko, M. G.) — 739.

Krinchik, G. S. and M. V. Chetkin. Farady Effect in Ittrium Garnet at Infrared Frequencies — 1184L.
Krivko, N. I. (see Gubanov, A. I.) — 247.
Krokhin, O. N. and Yu. M. Popov. Slowing-Down Time of Nonequilibrium Current Carriers in Semiconductors — 1144.
— (see Basov, N. G.) — 720L.
Kryukova, L. N. (see Gnedich, A. V.) — 524.
Kudinov, B. S. (see Melioranskiĭ, A. S.) — 548.
Kulakov, B. A. (see Viryasov, N. M.) — 327.
Kul'chitskiĭ, L. A. (see Bazhanov, E. B.) — 1215.
Kulik, I. O. (see Zil'berman, G. E.) — 859.
Kulikov, G. V. (see Vernov, S. N.) — 215L.
Kulyukin, M. M. (see Kozodaev, M. S.) — 300.
— (see Kozodaev, M. S.) — 511.
Kulyukina, L. A. (see Wang Kang-Ch'ang) — 313.
Kumekin, Yu. P., M. G. Meshcheryakov, S. B. Nurushev, and G. D. Stoletov. Triple Scattering of 660 Mev Protons II. Angular Dependence of Depolarization — 1049.
Kupriyanova, K. P. (see Dzhelepov, B. S.) — 205L.
Kurdgelaidze, D. F. On the Nonlinear Theory of Elementary Particles — 339.
Kurepin, A. B. (see Komarov, V. V.) — 1312.
Kutsenko, A. V. (see Gol'danskiĭ, V. I.) — 1223.
Kushnir, Yu. M. (see Borovskiĭ, I. B.) — 997.
Kuznetsov, A. A. (see Wang Kang-Ch'ang) — 726L.
— (see Wang Kang-Ch'ang) — 976L.
Kuznetsov, E. P. (see Alikhanyan, A. I.) — 282.
Kuznetsov, M. I. (see Protopopov, A. N.) — 279.
Kvartskhava, I. F., K. N. Kervalidze, and Yu. S. Gvaladze. Instability of the Induction Pinch — 1182L.
Landsberg, L. G. (see Balatz, M. Ya.) — 1239.
Lapidus, L. I. and Chou Kuang-Chao. Scattering of Gamma-Ray Quanta by Nucleons near the Threshold for Meson Production — 147.
Larionova, V. G. (see Adamovich, M. I.) — 779.
Larkin, A. N. Thermodynamic Functions of a Low-temperature Plasma — 1363.
Lavrukhina, A. K., L. P. Moskaleva, V. A. Malyshev, L. M. Satarova, and Su Hung-Kuei. Angular Distribution of Na^{24} Nuclei and Fission Fragments Produced by Interactions between High-Energy Protons and Au and U Nuclei — 715L.
Lebedev, A. I. and V. A. Petrun'kin. Formation of Pions in πN Collisions — 962L.
Lebedev, P. I. (see Balatz, M. Ya.) — 1239.
Leĭpunskiĭ, O. I. Possible Magnetic Effects from High-Altitude Explosions of Atomic Bombs — 219L.
Leksin, G. A. (see Bayukov, Yu. D.) — 1371L.
Lepekhin, F. G. (see Berkovich, I. B.) — 311.
Levchenko, Yu. Z. (see Fogel', Ya. M.) — 760.
Li Meng-Ha. Cerenkov Radiation from a Charged Particle with Intrinsic Magnetic Moment — 673.
Lifshitz, I. M. Anomalies of Electron Characteristics in the High Pressure Region — 1130.
— and V. G. Peschanskiĭ. Galvanomagnetic Characteristics of Metals with Open Fermi Surfaces. II — 137.
Lin Chag-Ta. (see Belov, K. P.) — 1376L.
Lin'kova, N. V., R. M. Osokina, B. S. Ratner, R. Sh. Amirov, and V. V. Akindinov. Photoprotons from Cu^{65} — 566.
Lipmanov, É. M. On the Analogy between the Weak and Electromagnetic Interactions — 891.
Lomakina, Z. D. (see Kopylov, G. I.) — 1188L.
Lomkatsi, G. S. Polarization of Hydrogen Nuclei in a Free Radical — 455L.
Lovchikova, G. N. Angular Distribution of Elastically Scattered Neutrons — 1036.
Lozhkin, O. V., N. A. Perfilov, A. A. Rimskiĭ-Korsakov, and J. Fremlin. Disintegration of Emulsion Nuclei by 930 Mev Protons — 1001.
— (see Perfilov, N. A.) — 250.
Lukin, Yu. T., Zh. S. Takibaev, and E. V. Shalagina. Energy Spectrum of Mesons from Nuclear Disintegrations Produced by 9-Bev Protons — 776.
Lutsenko, E. A. (see Kharchenko, I. F.) — 493.
Lyubimov, A. L. (see Viryasov, N. M.) — 327.
Lyubimov, V. A. and A. I. Alikhanov. Influence of Magnetic Fields on Resonant Absorption of γ rays — 1376L.
— (see Alikhanov, A. I.) — 1380L.
— (see Vishnevskiĭ, M. E.) — 1029.
Makar'ina, L. A. (see Varfolomeev, A. A.) — 23.
Makarov, M. M. (see Arifkhanov, U. R.) — 806.
— (see Perfilov, N. A.) — 250.
Makaryunas, K. V. and S. V. Starodubtsev. Investigation of the Reactions (α, α'), (α, p), and (α, t) on Lithium Nuclei — 271.
Makhnovskiĭ, E. D. (γ, p) Reaction on Au^{197} — 70.
Maksimenko, V. M. On the Problem of Peripheral Collisions of Nucleons with High Energies — 222L.
— On the Question of a Resonant π-π Interaction — 469L.
Malakhov, V. V., E. P. Rashevskaya, and V. Ya. Faĭnberg. Application of Dispersion Relation Techniques to a Study of the Simplest Green's Functions in Mesodynamics — 1298.
Mal'tsev, V. M. (see Barashenkov, V. S.) — 467L.
Malyshev, V. A. (see Lavrukhina, A. K.) — 715L.
Mamaladze, Yu. G. and S. G. Matinyan. Damping of Oscillations of a Disc in Rotating Helium II — 134.
— and S. G. Matinyan. Damping of the Oscillations of a Cylinder in Rotating Helium II — 471L.
Mamasakhlisov, V. I. (see Vashakidze, I. Sh.) — 675.
— (see Kopaleĭshvili, T. I.) — 1268.
Mandritskaya, K. V. (see Dzhanalidze, L. P.) — 722L.
Manenkov, A. A. and A. M. Prokhorov. Spin-Lattice Relaxation in Chromium Corundum — 527.
— and V. B. Fedorov. Investigation of the Line Width and Shape in the Paramagnetic Resonance Spectrum of the Cr^{+++} Ion in Corundum Single Crystals — 751.
Margolina, V. I. (see Shur, Ya. S.) — 33.
Markov, P. K., E. N. Tsyganov, M. G. Shafranova, and B. A. Shakhbazyan. Elastic Scattering of 8.5-Bev Protons on Protons — 1063.
Mashkevich, V. S. Electromagnetic Waves in a Medium with a Continuous Energy Spectrum — 653.
Maslennikova, F. V. (see Kandaurova, G. S.) — 45.
Matinyan, S. G. (see Mamaladze, Yu. G.) — 134.
— (see Mamaladze, Yu. G.) — 471L.
Matulenko, Yu. A. (see Viryasov, N. M.) — 327.
Matyash, I. V. (see Galkin, A. A.) — 959L.
Mdivani, O. M. (see Abelishvili, T. L.) — 453L.
Medved', S. V. (see Amaglobeli, N. S.) — 474L.

Melioranskiĭ, A. S., I. V. Éstulin, L. F. Kalinkin, and B. S. Kudinov. Excited States of Cs^{134} — 548.
Merekov, Yu. P. (see Bogachev, N. P.) — 317.
— (see Bogachev, N. P.) — 968L.
Meshcheryakov, M. G. (see Kumekin, Yu. P.) — 1049.
Mikheeva, M. N. (see Alekseevskiĭ, N. E.) — 211L.
Mikhul, A. (see Belovitskiĭ, G. E.) — 296.
— (see Wang Kang-Ch'ang) — 976L.
Mingalov, B. S. (see Belov, V. P.) — 392.
Mishakova, A. P. (see Nikol'skiĭ, B. A.) — 1087.
Mishnev, S. I. and S. I. Nikol'skiĭ. Number of Extensive Atmospheric Showers of Cosmic Rays near Sea Level — 186L.
Mitsek, A. I. (see Turov, E. A.) — 1328.
Mittsev, M. A. (see Ionov, N. I.) — 972L.
Moskalev, V. I. (see Bugadov, Yu. A.) — 531.
— (see Bugadov, Yu. A.) — 755.
Moskaleva, L. P. (see Lavrukhina, A. I.) — 715L.
Motulevich, G. P. (see Golovashkin, A. I.) — 38.
Mukhovatov, V. S. (see Dolgov-Savel'ev, G. G.) — 287.
Müller, L. (see Bally, D.) — 995.
Mur, V. D. and V. D. Skarzhinskiĭ. Application of the Dispersion Method for Investigation of the Simplest Green's Functions in Quantum Electrodynamics — 1298.
Murav'eva, V. V. (see Gnedich, A. V.) — 524.
Myasoedov, B. F. (see Flerov, G. N.) — 61.
Nechin, Yu. A. (see Vernov, S. N.) — 215L.
Nefedov, V. N. On the Mechanism of Emission of Prompt Fission Neutrons — 1195.
Neganov, B. S., L. B. Parfenov, and A. A. Tyapkin. Measurement of the Relative Nuclear Activity of π Mesons Near Their Place of Generation — 0000L.
Nekrasov, F. M. On the Nonlinear Theory of Stationary Processes in an Electron Plasma — 170.
Nelipa, N. F. and V. A. Tsarev. Inverse Dispersion Relations for Photoproduction of Pions on Nucleons — 187L.
Nemets, O. F., L. S. Saltykov, and M. V. Sokolov. The (p, d) Reaction and Inelastic Scattering of Protons on Be^{9} — 1199.
— and G. A. Prokopets. The Inelastic Scattering of Protons and Deuterons from Mg^{24} — 499.
— (see Zaika, N. I.) — 208L.
Nemirovskiĭ, P. É. and Yu. D. Fiveĭskiĭ. Influence of Coulomb Attraction on the Cross Section for Absorption of Antiprotons by Nuclei — 1073.
Neudachin, V. G. (see Edakova, V. A.) — 180L.
Nguyen, Dinh Ty (see Wang Kang-Ch'ang) — 313.
— (see Wang Kang-Ch'ang) — 726L.
— (see Wang Kang-Ch'ang) — 976L.
Nikishov, A. I. Statistical Theory of Multiple Particle Production — 369.
Nikitin, A. V. (see Wang Kang-Ch'ang) — 313.
— (see Wang Kang-Ch'ang) — 726L.
— (see Wang Kang-Ch'ang) — 976L.
Nikolaev, R. M. (see Kharchenko, I. F.) — 493.
Nikol'skiĭ, B. A. and A. P. Mishakova. Fluctuations in the Angular Distribution of Secondary Particles of Explosive Showers — 1087.
Nikol'skiĭ, S. I. (see Dovzhenko, O. I.) — 981.
— (see Mishnev, S. I.) — 186L.
Nurushev, S. B. (see Kumekin, Yu. P.) — 1049.
Obukhov, A. I. Asymmetry of Uranium Fission at High Proton Energies — 196L.
— (see Perfilov, N. A.) — 517.
Obukhov, Yu. V. (see Balatz, M. Ya.) — 1239.
Oganesyan, Yu. Ts. (see Karnaukhov, V. A.) — 964L.
— (see Flerov, G. N.) — 61.
Ogievetskiĭ, V. I. (see Grishin, V. G.) — 725L.
Ogloblin, A. A. (see Vlasov, N. A.) — 203L.
Okun', L. B. (see Kobzarev, I. Yu.) — 728L.
— (see Kolkunov, V. A.) — 634.
Osipov, B. D. On the Possibility of Measuring a Gravitational Frequency Shift in the Sun's Field — 472L.
Osokina, R. M. (see Lin'kova, N. V.) — 566.
Ostroumov, V. I. (see Perfilov, N. A.) — 250.
Otvinovskiĭ, S. Z. (see Wang Kang-Ch'ang) — 313.
Otvinovskiĭ, S. Z. (see Wang Kang-Ch'ang) — 726L.
Pakhomov, V. I. (see Stepanov, K. N.) — 1126.
Palev, Ch. D. (see Patera, I.) — 710L.
Parfanovich, D. M. (see Flerov, G. N.) — 61.
Parfenov, L. B. (see Neganov, B. S.) — 1379L.
Parfenova, V. P. Circular Polarization of Internal Bremsstrahlung Accompanying K-Capture in Fe^{55} — 42.
Pasechnik, L. L. (see Gabovich, M. D.) — 1033.
Pasechnik, M. V. (see Val'ter, A. K.) — 1025.
Pasyuk, A. S. (see Flerov, G. N.) — 61.
Patera, I. and Ch. D. Palev. Theoretical Interpretation of Elastic π^--p Scattering Experiments on the Proton Synchrotron of the Joint Institute for Nuclear Research — 710L.
Pavlovskaya, V. V. (see Gol'danskiĭ, V. I.) — 1223.
Pavlovskiĭ, E. S. (see Gandel'man, G. M) — 851.
Pedenko, N. S. (see Kharchenko, I. F.) — 493.
Pekar, S. I. Identification of Excitons with Light Waves in a Crystal and the Macroscopic Theory of Excitons with and without Account of Retardation — 1286.
— (see Brodin, M. S.) — 55.
— (see Brodin, M. S.) — 1373L.
Peletminskiĭ, S. V. (see Akhiezer, I. A.) — 1317.
Pelkhov, V. I. (see Groshev, L. V.) — 423.
Perasada, V. I. The Thermodynamic Average of Functions of the Displacement of Atoms in a Non-Ideal Crystalline Lattice — 825.
Perel', V. I. (see Konstantinov, O. V.) — 117.
Perfilov, N. A., N. S. Ivanova, O. V. Lozhkin, M. M. Makarov, V. I. Ostroumov, Z. I. Solov'eva, and V. P. Shamov. Fragmentation of Ag and Br Nuclei by 9-Bev Protons — 250.
—, V. F. Darovskikh, G. F. Denisenko, and A. I. Obukhov. Fission of Uranium Nuclei Induced by 9-Bev Protons — 517.
— (see Arifkhanov, U. R.) — 806.
— (see Lozhkin, O. V.) — 1001.
Peschanskiĭ, V. G. (see Lifshitz, I. M.) — 137.
Peshkov, V. P. Second Sound in Helium II — 580.
Peterson, V. K. On the Calculation of Scattering Phase Shifts — 1100.
Petrashku, M. G. (see Belovitskiĭ, G. E.) — 296.
Petrov, Yu. G. (see Petrzhak, K. A.) — 1244.
Petrukhova, N. I. (see Dzhanelidze, L. P.) — 722L.
Petrunkin, V. A. (see Lebedev, A. I.) — 962L.
Petrzhak, K. A., Yu. G. Petrov, and E. A. Shlyamin.

Range and Energy Dispersion of U^{233} Fission Fragments — 1244.
— (see Dmitriev, V. N.) — 718L.
Pik-Pichak, G. A. Nucleon Emission by a Rotating Nucleus — 557.
Pikalov, A. P. (see Kocharyan, N. M.) — 12.
Pilipenko, D. V. (see Fogel', Ya. M.) — 18.
Podgoretskiĭ, M. I. (see Barit, I. Ya.) — 218L.
Podgornyĭ, I. M. (see Koval'skiĭ, N. G.) — 1040.
Podkopaev, Yu. N. (see Dzhelepov, B. S.) — 205L.
Pokatilov, E. P. Resonance Absorption of High-Frequency Sound Energy by Semiconductor Current Carriers in a Magnetic Field — 835.
Polev, N. M. (see Amaglobeli, N. S.) — 474L.
Polikanov, S. M. and Yu. T. Chuburkov. Formation of the Isomer Cd^{115m} by the Fission of Gold under the Action of Heavy Ions — 214L.
— (see Flerov, G. N.) — 61.
Polovin, R. V. The Motion of a Piston in a Conducting Medium — 1113.
— (see Akhiezer, I. A.) — 383.
Polukarov, Yu. M. (see Alekseevskiĭ, N. E.) — 213L.
Polumordvinova, N. I. (see Zinov, V. G.) — 1016.
Pomeranchuk, I. Ya. (see Galanin, A. D.) — 347.
Pontecorvo, B. On New Strange Particles — 1192L.
— (see Balatz, M. Ya.) — 1239.
— (see Zinov, V. G.) — 1233.
Popov, N. P. (see Dolginov, A. Z.) — 1095.
Popov, V. S. Rotation of the Spin of a Relativistic Particle with a Magnetic Moment Moving in an External Field — 1141.
Popov, Yu. M. (see Basov, N. G.) — 720L.
— (see Krokhin, O. N.) — 1144.
Popov, Yu. P. (see Isakov, A. I.) — 712L.
Popova, A. A. (see Belov, K. P.) — 1376L.
Popova, A. M. (see Komarov, V. V.) — 184L.
— (see Komarov, V. V.) — 1123.
— (see Komarov, V. V.) — 1312.
Popova, V. M. (see Adamovich, M. I.) — 779.
— (see Gorzhevskaya, É. G.) — 200L.
Prokhorov, A. M. (see Zverev, G. M.) — 330.
— (see Kornienko, L. S.) — 1189L.
— (see Manenkov, A. A.) — 527.
Prokopenko, V. S. (see Zaika, N. I.) — 208L.
Prokopets, G. A. (see Nemets, O. F.) — 499.
Prokoshkin, Yu. D. Production of Pions in p-d Collisions and Motion of Nucleons Inside the Nucleus — 334.
— (see Dunaĭtsev, A. F.) — 540.
Protopopov, A. N., M. I. Kuznetsov, and É. G. Dermendzhiev. Fission of Th^{232} by 14.9-Mev Neutrons — 279.
Pucherov, N. N. (see Val'ter, A. K.) — 1025.
Rabinovich, M. S. and L. V. Iogansen. Coherent Electron Radiation in a Synchrotron. III — 856.
Rabotnov, N. S. (see Davydov, A. S.) — 946.
Raĭzer, M. D. (see Grebenshchikov, S. E.) — 1201.
Rakhimbaev, B. G. (see Azimov, S. A.) — 502.
Rakobol'skaya, I. V. (see Dovzhenko, O. I.) — 981.
Rapoport, V. O. (see Getmantsev, G. G.) — 871.
Rashevskaya, E. P. (see Malakhov, V. V.) — 1298.
Ratner, B. S. (see Lin'kova, N. V.) — 566.
Rebane, T. K. A Variational Principle for the Calculation of a Correction, Quadratic with Respect to the Magnetic Field Intensity, to the Electron Energy in a Molecule — 694.
Reĭnov, N. M. (see Gubanov, A. I.) — 247.
Rimskiĭ-Korsakov, A. A. (see Lozhkin, O. V.) — 1001.
Ritus, V. I. The Relativistically Covariant Spin Structure of the S Matrix — 1075.
Roĭtsin, A. B. (see Deĭgen, M. F.) — 356.
Romanov, V. A., M. G. Iodko, and V. V. Tuchkevich. Long-lived Lutetium Isotopes — 733.
— (see Iodko, M. G.) — 739.
Romanov, Yu. A. and D. S. Chernavskiĭ. Multiple Production of Jet Particles in Peripheral Collisions — 819.
Romanov, Yu. F. (see Dmitriev, V. N.) — 718L.
Romanova, T. A. (see Belovitskiĭ, G. E.) — 296.
Romanovskiĭ, E. A. (see Edakova, V. A.) — 180L.
Romantseva, A. S. (see Varfolomeev, A. A.) — 23.
Rozenfel'd, L. A. (see Tsvetaeva, N. E.) — 460L.
Rozental', I. L. (see Emel'yanov, A. A.) — 142.
Rozentzveĭg, L. N. and M. Ya. Azbel'. On the Preparation of Polarized Hydrogen Targets — 1121.
Rudik, A. P. (see Geshkenbeĭn, B. V.) — 1361.
— (see Kobzaev, I. Yu.) — 728L.
— (see Kolkunov, V. A.) — 634.
Rukhadze, A. A. and V. P. Silin. On the Magnetic Susceptibility of a Relativistic Electron Gas — 463L.
— (see Kovrizhnykh, L. M.) — 615.
Rukman, G. I. (see Braginskiĭ, V. B.) — 723L.
Rumer, Yu. B. Negative and Limiting Temperatures — 1365.
Rus'kin, V. I. and P. A. Usik. The Significance of Strange Particles in Fermi's Statistical Theory — 669.
Rutkevich, N. Ya. (see Klyucharev, A. P.) — 207L.
Ryazanov, M. I. On the Processes Involving Transfer of Momentum to the Medium — 617.
Rybakov, B. V. (see Vlasov, N. A.) — 1251.
Ryndin, R. M. (see Vilen'skiĭ, S. M.) — 729L.
Saakyan, G. S. Dispersion in High-Density, High-Temperature Media — 610.
— Single-photon Annihilation and Electron-pair Creation in Medium — 1147.
Saltykov, L. S. (see Nemets, O. F.) — 1199.
Samoĭlov, B. N., V. V. Sklyarevskiĭ, and E. P. Stepanov. The Polarization of Nuclei of Diamagnetic Elements Dissolved in Iron — 261.
Samoĭlov, A. V. (see Alikhanyan, A. I.) — 282.
Sarinyan, M. G. (see Babayan, Kh. P.) — 227.
Satarova, L. M. (see Lavrukhina, A. K.) — 715L.
Savchenko, O. V. (see Akimov, Yu. K.) — 221L.
— (see Akimov, Yu. K.) — 462L.
Savin, I. A. (see Viryasov, N. M.) — 327.
Schmidt, V. V. (see Borovskiĭ, I. B.) — 997.
Sedov, V. L. (see Kodorskiĭ, E. I.) — 561.
Selinov, I. P. and V. L. Chikhladze. New Isomer Sn^{113m} — 728L.
—, N. A. Vartanov, D. E. Khulelidze, Yu. A. Bliodze, N. G. Zaitseva, and V. A. Khalkin. New Isotope Te^{115} — 1191L.
— (see Chikhladze, V. L.) — 974L.
Semchinova, A. M. (see Flerov, G. N.) — 61.
Serdobol'skiĭ, V. I. Dispersion Formulae for Overlapping Levels — 1368.
Shafranov, M. D. (see Wang Kang-Ch'ang) — 313.

Shafranova, M. G. (see Markov, P. K.) — 1063.
Shakhbazyan, B. A. (see Markov, P. K.) — 1063.
Shakhulashvili, O. A. (see Dzhanelidze, L. P.) — 722L.
Shalagina, E. V. (see Lukin, Yu. T.) — 776.
Shamov, V. P. (see Arifkhanov, U. R.) — 806.
— (see Perfilov, N. A.) — 250.
Shapiro, F. L. (see Barit, I. Ya.) — 218L.
— (see Isakov, A. I.) — 712L.
Shapiro, I. S. On the Non-Radiative Transformation of the μ Meson into an Electron — 1186L.
Sharoyan, É. G. (see Kocharyan, N. M.) — 12.
Sharvin, Yu. V. A Measurement of the Surface Tension at the Boundary between the Superconducting and Normal Phases of Indium — 216L.
— and V. F. Gantmakher. Anisotropy of Surface Tension at the Boundary between the Superconducting and Normal Phases of Tin — 1052.
Shcherbakov, Yu. A. (see Kozodaev, M. S.) — 300.
— (see Kozodaev, M. S.) — 511.
Shekhter, V. M. Interference of Form Factors in Leptonic Decay of Hyperons — 387.
— On the Process $e^- + p \rightarrow \Lambda + \nu$ — 967L.
— (see Belov, V. P.) — 392.
Shepelev, M. N. (see Dolgov-Savel'ev, G. G.) — 287.
Shirokov, Yu. M. Space and Time Reflections in Relativistic Theory — 101.
Shkoda-Ul'yanov (see Grizhko, V. M.) — 987.
Shlyamin, É. A. (see Petrzhak, K. A.) — 1244.
Shmelev, V. P. Polarization of the Hydrogen Atom in the Ground State by the Field of a Point Charge — 1102.
Shramenko, B. I. (see Grizhko, V. M.) — 987.
Shtol'ts, E. V. (see Shur, Ya. S.) — 33.
Shubin, A. A. (see Golovashkin, A. I.) — 38.
Shur, Ya. S., E. V. Shtol'ts, and V. I. Margolina. Magnetic Structure of Small Monocrystalline Particles of MnBi Alloy — 33.
— (see Kandaurova, G. S.) — 45.
Shvartsman, B. F. (see Galanina, N. D.) — 1045.
Sidorov, V. A. (see Vlasov, N. A.) — 0000.
Sidorov, V. M. (see Bogachev, N. P.) — 317.
— (see Bogachev, N. P.) — 968L.
Sikora, D. I. (see Grizhko, V. M.) — 987.
Silin, V. P. Contribution to the Theory of Absorption of Ultrasound in Metals — 703.
— Kinetic Equation for Rapidly Varying Processes — 1277.
— On the Electromagnetic Properties of a Relativistic Plasma — 1136.
— (see Rukhadze, A. A.) — 463L.
Sirota, Z. D. (see Kataev, G. I.) — 747.
Sirotinin, E. I. (see Vasil'ev, Yu. A.) — 483.
Skarzhinskiĭ, V. D. (see Mur, V. D.) — 1308.
Sklyarevskiĭ, V. V. (see Samoĭlov, B. N.) — 261.
Skobov, V. G. Contribution to the Theory of Electron-Gas Conductivity in a Strong Magnetic Field — 941.
Smirnov, E. V. (see Viryasov, N. M.) — 327.
Smorodinskiĭ, Ya. A. and Ho Tso-Hsiu. On the Radiative Correction in Weak-Interaction Processes — 724L.
— (see Bilen'kiĭ, S. M.) — 729L.
Sokolov, A. A. and M. M. Kolesnikova. The Behavior of Fermion Spin in Elastic Scattering — 120.
— and M. M. Kolesnikova. On the Scattering of Transversely Polarized Fermions — 1281.
Sokolov, M. V. (see Nemets, O. F.) — 1199.
Solov'ev, M. I. (see Wang Kang-Ch'ang) — 313.
— (see Wang Kang-Ch'ang) — 726L.
— (see Wang Kang-Ch'ang) — 976L.
Solov'ev, V. G. (see Belyaev, V. B.) — 686.
Solov'eva, V. I. (see Abrosimov, A. T.) — 74.
Solov'eva, Z. I. (see Perfilov, N. A.) — 250.
Solyakin, G. E. (see Bogachov, B. A.) — 990.
Sorokin, A. A. (see Delyagin, N. N.) — 799.
Sorokin, V. S. and I. V. Sushkin. Stability of Equilibrium of a Conducting Liquid Heated from Below in a Magnetic Field — 440.
Soroko, L. M. (see Akimov, Yu. K.) — 221L.
— (see Akimov, Yu. K.) — 462L.
Sosnovskiĭ, R. (see Wang Kang-Ch'ang) — 313.
Speranskaya, M. P. (see Al'tshuler, L. V.) — 766.
Spiridonov, V. M. (see Gorbunov, A. N.) — 51.
Starodubtsev, S. V. (see Makaryunas, K. V.) — 271.
Stepanenko, M. M. (see Koval'skiĭ, N. G.) — 1040.
Stepanov, E. P. (see Samoĭlov, B. N.) — 261.
Stepanov, K. N. Cyclotron Absorption of Electromagnetic Waves in a Plasma — 192L.
— and V. I. Pakhomov. Magnetic Bremsstrahlung of a Confined Plasma — 1126.
— (see Kitsenko, A. B.) — 1323.
Stoletov, G. D. (see Kumekin, Yu. P.) — 1049.
Stratonovich, R. L. On the Theory of Non-Equilibrium Statistical Processes — 598.
Strelkov, V. S. (see Dolgov-Savel'ev, G. G.) — 287.
Strunov, L. N. (see Viryasov, N. M.) — 327
Strutinskiĭ, V. M. Excitation of Vibrational Levels and Coulomb Excitation in Alpha Decay — 89.
—, L. V. Groshev, and M. K. Akimova. Spectra of Gamma Rays Produced in the Capture of Thermal Neutrons by Heavy Nuclei. II — 430.
Su Hung-Kuei (see Lavrukhina, A. K.) — 715L.
Sukharevskiĭ, V. G. Collective Properties of Si^{30}, Si^{31}, and Ne^{23}, and Reduced Widths in Stripping Reactions — 159.
Sulyaev, R. M. (see Kozodaev, M. S.) — 300.
— (see Kozodaev, M. S.) — 511.
Sushkin, I. V. (see Sorokin, V. S.) — 440.
Takibaev, Zh. S. Possible Influence of Nucleon Structure in High-Energy Interactions — 454L.
— (see Boos, É. G.) — 920.
— (see Lukin, Yu. T.) — 776.
Tarantin, N. I. Competition between Neutron Evaporation and Fission in the Reactions of Multiply Charged Ions with Heavy Nuclei — 181L.
— (see Flerov, G. N.) — 61.
Tarasov, M. S. (see Brish, A. A.) — 15.
Tentyukova, G. N. (see Zinov, V. G.) — 1016.
Ter-Mikaelyan, M. L. A Study of the Limits of Applicability of the Theory of Ionization Losses — 646.
— Allowance for the Medium in Radiation Corrections to Coulomb Scattering — 845.
Tikhomirov, F. A. (see Belovitskiĭ, G. E.) — 296.
Timashev, S. F. and V. A. Kaminskiĭ. Anisotropic Distribution of Internal Bremsstrahlung in K Capture by Polarized Nuclei — 206L.
Timrot, D. L. and V. P. Borisoglebskiĭ. The Density of

Liquid Oxygen on the Saturation Curve — 1248.
Ting Ta-Ts'ao (see Wang Kang-Ch'ang) — 313.
— (see Wang Kang-Ch'ang) — 726L.
Ting Ta-Chao (see Wang Kang-Ch'ang) — 976L.
Tishchenko, B. I. (see Inopin, E. V.) — 840.
Tishkov, P. G. and G. P. Vishnevskaya. Paramagnetic Relaxation in Manganese Salt Solutions — 243.
Toropov, P. V. (see Vasil'ev, Yu. A.) — 483.
Tret'yakov, E. F. (see Vishnevskiĭ, M. E.) — 1029.
Troĭnar, E. Destruction of Superconductivity by a Current — 470L.
Trunin, R. F. (see Al'tshuler, L. V.) — 573.
Tsakadze, D. S. and I. M. Chkheidze. Measurement of the Logarithmic Damping Decrement of a Hollow Cylinder in Rotating Helium II — 457L.
Tsarev, V. A. (see Nelipa, N. F.) — 187L.
Tsekhmistrenko, Yu. V. On the Structure of the S Matrix in the Theory of Elastic and Inelastic Scattering of Nonrelativistic Particles — 894.
Tseplyaev, V. I. Isothermal Discontinuities in Magnetohydrodynamics — 185L.
Tsukerman, I. S. Leptonic Decays of Hyperons with Emission of Pions — 927.
Tsukerman, V. A. (see Brish, A. A.) — 15.
Tsukernik, V. M. (see Kaganov, M. I.) — 952.
Tsvetaeva, N. E. and I. A. Rozenfel'd. Investigation of Beta Radiation of Nb^{95} and Ce^{144} by the Method of Absorption in Air — 460L.
Tsvirko, Yu. A. On the Connection between the Exciton Band Structure and the Natural Optical Activity of Crystals — 1163.
Tsyganov, É. N. (see Markov, P. K.) — 1063.
Tuchkevich, V. V. (see Iodko, M. G.) — 739.
— (see Romanov, V. A.) — 733.
Tulinov, V. F. (see Charakhch'yan, A. N.) — 742.
Tumanyan, É. R. (see Babayan, Kh. P.) — 227.
Tumanyan, V. A. Direct Electron-Positron Pair Production by Electrons — 191L.
Turchinskaya, M. I. (see Volkenshteĭn, N. V.) — 195L.
Turov, E. A. and N. G. Guseĭnov. Magnetic Resonance in Rhombohedral Weak Ferromagnetics — 955.
— and A. I. Mitsek. Temperature Dependence of Magnetostriction — 1327.
Tuvdendorzh, D. (see Dzhanelidze, L. P.) — 722L.
Tyapkin, A. A. (see Neganov, B. S.) — 1379L.
Urazakov, É. I. (see Granovskiĭ, V. L.) — 974L.
Urin, M. G. Effect of Superfluidity of Heavy Nuclei on Single-Particle Electromagnetic Transitions and Beta Decay — 1331.
Urushadze, G. I. (see Bar'yakhtar, V. G.) — 905.
Usik, P. A. (see Rus'kin, V. I.) — 669.
Vagradov, G. M. and D. A. Kirzhnits. On the Theory of Nuclear Matter — 1082.
Valiev, K. A. On the Theory of Quadrupole Relaxation of Nuclear Spins in Liquids — 883.
Val'ter, A. K., I. I. Zalyubovskiĭ, A. P. Klyucharev, M. V. Pasechnik, N. N. Pucherov, and V. I. Chirko. Angular Distributions of 6.8-Mev Protons Elastically Scattered by Chromium, Nickel, and Copper Isotopes — 1025.
Varfolomeev, A. A., R. I. Gerasimova, I. I. Gurevich, L. A. Makar'ina, A. S. Romantseva, and S. A. Chueva. Influence of the Medium Density on Bremsstrahlung in Electron-Photon Showers in the Energy Range 10^{11} — 10^{13} ev — 23.
Varshalovich, D. A. Electromagnetic Transition Probabilities and Static Moments of Odd-Odd Atomic Nuclei — 125.
Varsimashvili, T. V. Transition Effect of Stars Produced by Cosmic Rays in Lead and Graphite Absorbers — 231.
Vartanov, N. A. (see Selinov, I. P.) — 1191L.
Vartapetyan, G. A. Lifetime of the 321-kev Level in Hf^{177} — 1378L.
Vashakidze, I. Sh., T. I. Kopaleĭshvili, V. I. Mamasakhlisov, and G. A. Chilashvili. On the Structure of the Be^9 Nucleus — 675.
— (see Kopaleĭshvili, T. I.) — 1268.
Vasilenko, S. S. (see Antonova, S. F.) — 276.
— (see Antonova, S. F.) — 554.
Vasil'ev, Yu. A., Yu. S. Zamyatnin, Yu. I. Il'in, E. I. Sirotinin, P. V. Toropov, and É. F. Fomushkin. Measurements of the Spectra and Average Number of Neutrons Emitted in the Fission of U^{235} and U^{238} Induced by 14.3-Mev Neutrons — 483.
Vasil'eva, M. Ya. (see Zaĭtzev, A. A.) — 1180L.
Vasilevskiĭ, I. M. and V. V. Vishnyakov. Elastic Scattering of 300-Mev Negative Pions by Hydrogen — 323.
— and V. V. Vishnayakov. Polarization of Recoil Protons From the Scattering of 300 Mev π^- Mesons on Hydrogen — 1185L.
Veksler, V. I. Energy Distribution of Sputtered and Scattered Ions in the Bombardment of Tantalum and Molybdenum by Positive Cesium Ions — 235.
— (see Wang Kang-Ch'ang) — 976L.
Vernov, S. N., N. N. Goryunov, V. A. Dmitriev, G. V. Kulikov, Yu. A. Nechin, and G. B. Khristiansen. Lateral Distribution Function of the Flux of Charged Particles in an Individual Extensive Atmospheric Shower — 215L.
Viryasov, N. M., A. S. Vovenko, G. G. Vorob'ev, A. D. Kirillov, Kim Hu In, B. A. Kulakov, A. L. Lyubimov, Yu. A. Matulenko, I. A. Savin, E. V. Smirnov, L. N. Strunov, and I. V. Chuvilo. Antiproton Channel with 2.8 Bec/c Momentum — 327.
— (see Wang Kang-Ch'ang) — 976L.
Vishki, T. (see Bogachev, N. P.) — 317.
Vishnevskaya, G. P. (see Tishkov, P. G.) — 243.
Vishnevskiĭ, M. E., V. A. Lyubimov, E. F. Tretyakov, and G. I. Grishuk. Investigation of Polarization of Internal Conversion Electrons in Transitions Following Decay of Heavy Elements — 1029.
Vishnyakov, V. V. (see Vasilevskiĭ, I. M.) — 323.
— (see Vasilevskiĭ, I. M.) — 1185L.
Vladimirov, L. A. (see Al'tshuler, L. V.) — 766.
Vlasov, K. B. Equations of State Determining the Magnetoelastic Properties of Ferromagnetic Monocrystals — 642.
Vlasov, N. A., S. P. Kalinin, A. A. Ogloblin, and V. I. Chuev. (d, t) Reactions on Medium and Heavy Nuclei 203L.
—, S. P. Kalinin, B. V. Rybakov, and V. A. Sidorov.

Neutron Spectra From the d + p Reaction — 1251.
Volkenshteĭn, N. V. and G. V. Fedorov. Temperature Dependence of the Hall Effect of Pure Ferromagnets — 48.
— and M. I. Turchinskaya. Magnetic Anisotropy of the Disordered Alloy Ni$_3$Mn at Helium Temperatures — 195L.
Volkov, V. V. (see Flerov, G. N.) — 61.
Volkov, D. V. S Matrix in the Generalized Quantization Method — 375.
— and E. V. Inopin. Motion of Nucleons in an Anisotropic Oscillator Potential with Allowance for Spin-Orbit Interaction — 1273.
Volotskaya, V. G. (see Borovik, E. S.) — 189L.
Vorob'ev, G. G. (see Viryasov, N. M.) — 327.
Vovenko, A. S. (see Viryasov, I. M.) — 327.
Vrana, I. (see Wang Kang-Ch'ang) — 976L.
Vrejoiu, C. (see Eftimiu, C.) — 971L.
Vul, B. M. and É. I. Zavaritskaya. The Capacitance of p-n Junctions at Low Temperatures — 6.
Wang Kang-Ch'ang, Wang Ts'u-Chieng, Ting Ta-Ts'ao, V. G. Ivanov, Yu. V. Katyshev, E. N. Kladnitskaya, L. A. Kulyukina, Nguyen Dinh Ty, A. V. Nikitin, S. Z. Otvinovskiĭ, M. I. Solov'ev, R. Sosnovskiĭ, and M. D. Shafranov. Investigation of the Elastic Scattering of π Mesons with Momenta 6.8 Bev/c from Protons in a Propane Bubble Chamber — 313.
—, Wang Ts'u-Chieng, Ting Ta Ts'ao, V. G. Ivanov, E. N. Kladnitskaya, A. A. Kuznetsov, Nguyen Din-Ty, A. V. Nikitin, S. Z. Otvinovskii, and M. I. Solov'ev. Creation of Antiprotons in Interaction of Negative Pions with Nucleons — 726L.
—, Wang Ts'u-Chieng, V. I. Veksler, N. M. Viryasov, I. Vrana, Ting Ta-Ts'ao, Kim Hu In, E. N. Kladnitskaya, A. A. Kuznetsov, A. Mikhul, Nguyen Din Ty, A. V. Nikitin, and M. I. Solov'ev. Production of a Σ Hyperon by 8.3-Bev/c Negative π Mesons — 976L.
Wang Pei (see Barashenkov, V. S.) — 467L.
Wang Ts'u-Chieng (see Wang Kang-Ch'ang) — 313.
— (see Wang Kang-Ch'ang) — 726L.
— (see Wang Kang-Ch'ang) — 976L.
Weiner, R. and Ch. Iusim. Effect of Deformation of the Nucleus on the Electronic Wave Functions. Application to Beta Decay — 629.
Wiktor, S. (see Budagov, Yu. A.) — 531.
— (see Budagov, Yu. A.) — 755.
Yagudina, F. R. (see Adamovich, M. I.) — 779.
— (see Gorzhevskaya, É. G.) — 200L.
Yanoukh, F. Polarization of Gamma-Ray Quanta from the Internal Compton Effect — 131.
— (see Ch'ing Ch'en-Jui) — 683.
Yarba, V. A. (see Bogachev, N. P.) — 317.
— (see Bogachev, N. P.) — 968L.
Yashchin, É. G. (see Aleksandrov, A. P.) — 960L.
Yavlinskiĭ, N. A. (see Dolgov-Savel'ev, G. G.) — 287.
Yazeva, V. G. (see Gabovich, M. D.) — 1033.
Zagorodnov, O. G., Ya. B. Faĭnberg, and A. M. Egorov. Reflection of Electromagnetic Waves from a Plasma Moving in Slow-Wave Guides — 4.
Zaika, N. I., O. F. Nemets, and V. S. Prokopenko. Angular Distribution of Protons from the Reaction Ca^{40} (d, p) Ca^{41} — 208L.
Zaĭtzev, A. A. and M. Ya. Vasil'eva. Connection Between Oscillation and Rate of Loss Of Charged Particles in a Cylindrical Plasma of Low Pressure in a Longitudinal Magnetic Field — 1180L.
Zaĭtzeva, N. G. (see Selinov, I. P.) — 1191L.
Zakhar'ev, B. N. (see Belyaev, V. B.) — 686.
Zakharov, A. L. Instability in a Semiconductor Amplifier with Negative Effective Carrier Mass — 478L.
Zalyubovskiĭ, I. I. (see Val'ter, A. K.) — 1025.
Zamyatnin, Yu. S. (see Vasil'ev, Yu. A.) — 483.
Zaretskiĭ, D. F. (see Grin', Yu. T.) — 162.
— (see Grin', Yu. T.) — 936.
Zastavenko, L. G. and Chou Kuang-Chao. Integral Transformations of the I. S. Shapiro Type for Particles of Zero Mass — 97.
Zatsepin, G. T. (see Gerasimova, N. M.) — 899.
Zavaritzkaya, É. I. (see Vul, B. M.) — 6.
Zavaritzkiĭ, N. V. The Thermal Conductivity of Superconductors in the Intermediate State — 1207.
Zel'dovich, Ya. B. Quasistable States with Large Isotopic Spin in Light Nuclei — 202L.
— Scattering by a Singular Potential in Perturbation Theory and in the Momentum Representation — 594.
— The Existence of New Isotopes of Light Nuclei and the Equation of State of Neutrons — 812.
Zhdanov, A. P. (see Berkovich, I. B.) — 311.
Zhirnov, N. I. On the Energy Levels of μ-Mesic Atoms — 691.
Zhitnikov, R. A. (see Drabkin, G. M.) — 729L.
Zil'berman, G. E. and I. O. Kulik. Quantum Oscillations of the Photoelectric Yield of Metals in a Magnetic Field — 859.
Zinov, V. G. and S. M. Korenchenko. Elastic Scattering of 240-330 Mev π^- Mesons by Hydrogen — 794.
—, A. D. Konin, S. M. Korenchenko, and B. Pontecorvo. A Search For the ρ^0 Meson and a Check of the Dispersion Relations in TFN Scattering — 1223.
— and S. M. Korenchenko. Charge-Exchange Scattering of 240-330 Mev π^- Mesons on Hydrogen — 1010.
—, S. M. Korenchenko, N. I. Polumordvinova, and G. N. Tentyukova. Phase Shift Analysis of Scattering of 240-330 Mev Pions by Hydrogen — 1016.
Zverev, G. M. and A. M. Prokhorov. Electron Paramagnetic Resonance Spectrum of V^{3+} in Corundum — 330.

SOVIET PHYSICS JETP VOLUME 11, NUMBER 6 DECEMBER, 1960

Analytic Subject Index to Volume 11

References with L are Letters to the Editor. Items are listed under the following categories:

Astrophysics
Atomic Explosions
Cosmic Rays
Crystalline State (Optical Properties, Structure)
Elementary Particle Interactions (Experiment)
Gravitation
Helium, Liquid
Ions, Ionization
Isotopes
Magnetic Properties of Matter (Antiferromagnetism, Ferromagnetism)
Magnetic Resonance, Magnetic Relaxation
Magnetohydrodynamics
Metals (Electric Properties, Elastic Properties)
Methods and Instruments
Multiple Production of Particles
Muons
Nuclear Fission
Nuclear Polarization
Nuclear Reactions, Disintegrations, Scattering (Theory)
Nuclear Reactions and Scattering at High Energy (Experiment)
Nuclear Reactions and Scattering at Medium and Low Energies (Experiment)
Nuclear Reactions on Multiply Charged Ions
Nuclear Spectra (α, β, γ) (Experiment)
Nuclear Structure (Theory)
Photonuclear Reactions
Plasma (Theory)
Plasma, Gas-discharge (Experiment)
Pressure, High
Quantum Electrodynamics
Quantum Mechanics (Various Problems)
Radiation
Scattering (General Theory)
Scattering of Electrons and Photons
Semiconductors
Statistical Physics (General Problems)
Strange Particles
Strong Interactions (Theory)
Superconductivity
Thermal Properties
Weak Interactions
X Rays

Astrophysics
- Dispersion in High-Density, High-Temperature Media. G. S. Saakyan — 610.
- Internal Structure of Super-Dense Stars. D. A. Kirzhnits — 365.

Atomic Explosions
- Possible Magnetic Effects from High-Altitude Explosions of Atomic Bombs. O. I. Leĭpunskiĭ — 219L.

Cosmic Rays
- Dependence of Three-Dimensional Development of a Cascade Shower on the Energy of the Primary Particle. V. V. Guzhavin and I. P. Ivanenko — 476L.
- Disintegration of Cosmic-Ray Nuclei by Solar Photons. N. M. Gerasimova and G. T. Zatsepin — 899.
- Energy Spectra of the Electron-Proton Component in Extensive Atmospheric Showers Near the Shower Axis. O. I. Dovzhenko, S. I. Nikol'skiĭ, and I. V. Rakobol'skaya — 981.
- Experimental Investigation of the Energy Spectrum of the Penetrating Component of Extensive Air Showers. É. L. Andronikashvili and R. E. Kazarov — 507.
- Fluctuations in the Angular Distribution of Secondary Particles of Explosive Showers. B. A. Nikol'skiĭ and A. P. Mishakova — 1087.
- Influence of the Medium Density on Bremsstrahlung in Electron-Photon Showers in the Energy Range 10^{11} - 10^{13} ev. A. A. Varfolomeev, R. I. Gerasimova, I. I. Gurevich, L. A. Makar'ina, A. S. Romantseva, and S. A. Chueva — 23.
- Investigation of a High-Energy Interaction Event in Photographic Emulsion. Kh. P. Babayan, M. G. Sarinyan, and É. R. Tumanyan — 227.
- Large Cosmic-Ray Intensity Fluctuations in the Stratosphere. A. N. Charakhch'yan, V. F. Tulinov, and T. N. Charakhch'yan — 742.
- Lateral Distribution Function of the Flux of Charged Particles in an Individual Extensive Atmospheric Shower. S. N. Vernov, N. N. Goryunov, V. A. Dmitriev, G. V. Kulikov, Yu. A. Nechin, and G. B. Khristiansen — 215L.
- Number of Extensive Atmospheric Showers of Cosmic Rays near Sea Level. S. I. Mishnev and S. I. Nikol'skiĭ — 186L.
- Polarization of High-Energy μ^+ Mesons in Cosmic Rays. N. M. Kocharyan, Z. A. Kirakosyan, É. G. Sharoyan, and A. P. Pikalov — 12.
- Transition Effect of Stars Produced by Cosmic Rays in Lead and Graphite Absorbers. T. V. Varsimashvili — 231.
- Ultra-High-Energy Extensive Air Showers. A. T. Abrosimov, G. A. Bazilevskaya, V. I. Solov'eva, and G. B. Khristiansen — 74.

Crystalline State (Optical Properties, Structure)
- Additional Anomalous Light Waves in Anthracene in the Exciton-Absorption Region. M. S. Brodin and S. I. Pekar — 1373L.
- Electromagnetic Waves in a Medium with a Continuous Energy Spectrum. I. V. S. Mashkevich — 653.
- Identification of Excitons with Light Waves in a Crystal and the Macroscopic Theory of Excitons with and

without Account of Retardation. S. I. Pekar — 1286.
On an Experimental Demonstration of the Existence of Additional Anomalous Light Waves in a Crystal in the Exciton Absorption Region. M. S. Brodin and S. I. Pekar — 55.
On the Connection between the Exciton Band Structure and the Natural Optical Activity of Crystals. Yu. A. Tsvirko — 1163.
The Effect of an External Electric Field on the Shape of the Intrinsic Absorption Edge in Non-Conducting Crystals. D. S. Bulyanitsa — 868.
The Thermodynamic Average of Functions of the Displacement of Atoms in a Non-Ideal Crystalline Lattice. V. I. Peresada — 825.

Elementary Particle Interactions (Experiment)
A Search For the ρ^0 Meson and a Check of the Dispersion Relations in π-N Scattering. V. G. Zinov, A. D. Konin, S. M. Korenchenko, and B. Pontecorvo — 1233.
Antiproton Channel with 2.8 Bev/c Momentum. N. M. Viryasov, A. S. Vovenko, G. G. Vorob'ev, A. D. Kirillov, Kim Hi In, B. A. Kulakov, A. L. Lyubimov, Yu. A. Matulenko, I. A. Savin, E. V. Smirnov, L. N. Strunov, and I. V. Chuvilo — 327.
Charge-Exchange Scattering of 240-330 Mev π^- Mesons on Hydrogen. V. G. Zinov and S. M. Korenchenko — 1010.
Creation of Antiprotons in Interaction of Negative Pions with Nucleons. Wang Kang-Ch'ang, Wang Ts'u-Tseng, Ting Ta Ts'ao, V. G. Ivanov, E. N. Kladnitskaya, A. A. Kuznetsov, Nguyen Din-Ty, A. V. Nikitin, S. Z. Otvinovskiĭ, and M. I. Solov'ev — 726L.
Elastic Scattering of 8.5-Bev Protons on Protons. P. K. Markov, E. N. Tsyganov, M. G. Shafranova, and B. A. Shakhbazyan — 1063.
Elastic Scattering of 128- and 162-Mev Negative Pions by Protons. Yu. A. Budagov, S. Wiktor, V. P. Dzelepov, P. F. Ermolov, and V. I. Moskalev — 531.
Elastic Scattering of 240-330 Mev π^- Mesons by Hydrogen. V. G. Zinov and S. M. Korenchenko — 794.
Elastic Scattering of 300-Mev Negative Pions by Hydrogen. I. M. Vasilevskiĭ and V. V. Vishnyakov — 323.
Internal Conversion Pairs in the Decay of Neutral π Mesons. Yu. A. Budagov, S. Viktor, V. P. Dzelepov, P. F. Ermolov, and V. I. Moskalev — 755.
Investigation of the Elastic Scattering of π^- Mesons with Momenta 6.8 Bev/c from Protons in a Propane Bubble Chamber. Wang Kang-Ch'ang, Wang Ts'u-Chieng, Ting Ta-Ts'ao, V. G. Ivanov, Yu. V. Katyshev, E. N. Kladnitskaya, I. A. Kulyukina, Nguyen Dinh Ty, A. V. Nikitin, S. Z. Otvinovskiĭ, M. I. Solov'ev, R. Sosnovskiĭ, and M. D. Shafranov — 313.
Measurement of the Relative Nuclear Activity of π Mesons Near Their Place of Generation. B. S. Neganov, L. B. Parfenov, and A. A. Tyapkin — 1375L.
On the Existence of Particles of Mass $2m_e \leq \mu \leq 25m_e$. A. N. Gorbunov, V. M. Spiridonov, and P. A. Cerenkov — 51.
Phase Shift Analysis of Scattering of 240 — 330 Mev Pions by Hydrogen. V. G. Zinov, S. M. Korenchenko, N. I. Polumordvinova, and G. N. Tentyukova — 1016.
Polarization of Recoil Protons From the Scattering of 300 Mev π^- Mesons on Hydrogen. I. M. Vasilevskiĭ and V. V. Vishnayakov — 1185L.
The $pn \rightarrow pn\pi^0$ Reaction in the Energy Range from Threshold to 665 Mev. A. F. Dunaĭtsev and Yu. D. Prokoshkin — 540.
Triple Scattering of 660-Mev Protons. II. Angular Dependence of Depolarization. Yu. P. Kumekin, M. G. Meshcheryakov, S. B. Nurushev, and G. D. Stoletov — 1049.

Gravitation
Comparison of Different Coordinate Conditions in Einstein's Gravitation Theory. V. A. Fock — 80.
On the Possibility of Measuring a Gravitational Frequency Shift in the Sun's Field. B. D. Osipov — 472L.
On the Possibility of Measuring in the Laboratory the Speed of Propagation of Gravitational Waves. V. B. Braginskiĭ, D. D. Ivanenko, and G. I. Rukman — 723L.
The Einstein Statics in Conformal Space. V. A. Fock — 1067.

Helium, Liquid
Damping of Oscillations of a Disc in Rotating Helium II. Yu. G. Mamaladze and S. G. Matinyan — 134.
Damping of the Oscillations of a Cylinder in Rotating Helium II. Yu. G. Mamaladze and S. G. Matinyan — 471L.
Measurement of the Logarithmic Damping Decrement of a Hollow Cylinder in Rotating Helium II. D. S. Tsakadze and I. M. Chkheidze — 457L.
Second Sound in Helium II. V. P. Peshkov — 580.

Ions, Ionization
A Study of the Limits of Applicability of the Theory of Ionization Losses. M. L. Ter-Mikaelyan — 646.
Determination of the First Ionization Potentials of Neodymium and Praseodymium by the Surface Ionization Method. N. I. Ionov and M. A. Mittsev — 972L.
Electron Capture and Detachment in Collisions of Fast Helium, Boron, and Fluorine Atoms with Gas Molecules. Ya. M. Fogel', V. A. Ankudinov, and D. V. Pilipenko — 18.
Energy Distribution of Sputtered and Scattered Ions in the Bombardment of Tantalum and Molybdenum by Positive Cesium Ions. V. I. Veksler — 235.
Ionization of Gases by Negative Ions. Ya. M. Fogel', A. G. Koval', and Yu. Z. Levchenko — 760.
Ionization of Inert Gases by Multiply Charged Ions. N. V. Fedorenko, I. P. Flaks, and L. G. Filippenko — 519.

Isotopes
Long-lived Lutetium Isotopes. V. A. Romanov, M. G. Iodko, and V. V. Tuchkevich — 733.
New Isotope Te^{115}. I. P. Selinov, N. A. Vartanov, D. E. Khulelidze, Yu. A. Bliodze, N. G. Zaitseva, and V. A. Khalkin — 1191L.
Super-Heavy Isotopes of Hydrogen and Helium. V. I. Gol'danskiĭ — 1179L.
The Existence of New Isotopes of Light Nuclei and the Equation of State of Neutrons. Ya. B. Zel'dovich — 812.
The Production of Element 102. G. N. Flerov, S. M. Polikanov, A. S. Karamyan, A. S. Pasyuk, D. M. Parfanovich, N. I. Tarantin, V. A. Karnaukhov, V. A. Druin, V. V. Volkov, A. M. Semchinova, Yu. Ts. Oganesyan, V. I. Khalizev, G. I. Khlebnikov, B. F. Myasoedov, and K. A. Gavrilov — 61.

Magnetic Properties of Matter (Antiferromagnetism, Ferromagnetism)
Dependence of the Magnetic Structure of a Cobalt Crystal on its Size. G. S. Kandaurova, Ya. S. Shur, and F. V. Maslennikova — 45.
Electrical and Galvanomagnetic Properties of Lithium Ferrite-Chromite Near the Compensation Point. K. P. Belov, A. N. Goryaga, and Lin Chang-Ta — 1376L.
Equations of State Determining the Magnetoelastic Properties of Ferromagnetic Monocrystals. K. B. Vlasov — 642.
Faraday Effect in Ittrium Garnet at Infrared Frequencies. G. S. Krinchik and M. V. Chetkin — 1184L.
Magnesium-Manganese Ferrite Single Crystals with Narrow Ferromagnetic-Absorption Resonance Curve. K. P. Belov, V. F. Belov, and A. A. Popova — 1372L.
Magnetic Anisotropy of the Disordered Alloy Ni$_3$Mn at Helium Temperatures. N. V. Volkenshteĭn and M. I. Turchinskaya — 195L.
Magnetic Structure of Small Monocrystalline Particles of MnBi Alloy. Ya. S. Shur, E. V. Shtol'ts, and V. I. Margolina — 33.
Nonresonance Absorption of Oscillating Magnetic Field Energy by a Ferromagnetic Dielectric. II. M. I. Kaganov and V. M. Tsukernik — 952.
Piezomagnetism in the Antiferromagnetic Fluorides of Cobalt and Manganese. A. S. Borovik-Romanov — 786.
Temperature Dependence of Magnetostriction. E. A. Turov and A. I. Mitsek — 1327.
The Change of Atomic Magnetic Moments in Ferromagnetic Metals under Hydrostatic Compression. E. I. Kondorskiĭ and V. L. Sedov — 561.
The Indirect Interaction of d Electrons in Transition Metals. II. Antiferromagnetism. B. V. Karpenko and A. A. Berdyshev — 666.
The Magnetoelectric Effect in Antiferromagnetics. D. N. Astrov — 708L.

Magnetic Resonance, Magnetic Relaxation (see also Polarization of Nucleus)
Electron Paramagnetic Resonance Spectrum of V^{3+} in Corundum. G. M. Zverev and A. M. Prokhorov — 330.
Electronic Paramagnetic Resonance of the Ion Ti^{3+} in Corundum. L. S. Kornienko and A. M. Prokhorov — 1189L.
Investigation of the Line Width and Shape in the Paramagnetic Resonance Spectrum of the Cr^{+++} Ion in Corundum Single Crystals. A. A. Manenkov and V. B. Fedorov — 751.
Magnetic Resonance in Rhombohedral Weak Ferromagnetics. E. A. Turov and N. G. Guseĭnov — 955.
Observation of Spontaneous Coherent Radiation of a Ferrite in a Resonator. A. P. Aleksandrov, Ya. I. Khanin, and É. G. Yashchin — 960L.
On the Theory of Relaxation Processes in Ferrodielectrics with Weak Magnetic Anisotropy at Low Temperatures. V. G. Bar'yakhtar and G. I. Urushadze — 905.
Paramagnetic Relaxation in Manganese Salt Solutions. P. G. Tishkov and G. P. Vishnevskaya — 243.
Spin-Lattice Relaxation in Chromium Corundum. A. A. Manenkov and A. M. Prokhorov — 527.
The Second Moment of a Paramagnetic Absorption Line, Including the Effect of Fine and Hyperfine Structure. U. Kh. Kopvillem — 109.
The Shape and Temperature Dependence of the Electron-Spin Resonance Lines of Localized Electron Centers in Crystals. M. F. Deĭgen and A. B. Roĭtsin — 356.

Magnetohydrodynamics
Effect of Conductivity Anisotropy in a Magnetic Field on the Structure of a Shock Wave in Magnetogasdynamics. S. A. Kaplan — 183L.
Isothermal Discontinuities in Magnetohydrodynamics. V. I. Tseplyaev — 185L.
Stability of Equilibrium of a Conducting Liquid Heated from Below in a Magnetic Field. V. S. Sorokin and I. V. Sushkin — 440.
The Motion of a Conducting Piston in a Magnetohydrodynamic Medium. I. A. Akhiezer and R. V. Polovin — 383.
The Motion of a Piston in a Conducting Medium. R. V. Polovin — 1113.

Metals (Electric Properties, Elastic Properties) (See also Pressure, High)
Absorption of Ultrasound in Zinc at Low Temperatures. A. A. Galkin and A. P. Korolyuk — 1218.
Anisotropy of the Electrical Resistance of Mg and Pt Single Crystals in a Magnetic Field at 4.2°K. N. E. Alekseevskiĭ and Yu. P. Gaĭdukov — 1242.
Anomalies in the Modulus of Elasticity and in Internal Friction in the Alloy Fe$_3$Pt. G. I. Kataev and Z. D. Sirota — 747.
Anomalies of Electron Characteristics in the High Pressure Region. I. M. Lifshitz — 1130.
Contribution to the Theory of Absorption of Ultrasound in Metals. V. P. Silin — 703.
Contribution to the Theory of Electron-Gas Conductivity in a Strong Magnetic Field. V. G. Skobov — 941.
Determination of Microscopic Parameters of Aluminum from its Optical Constants and Electric Conductivity. A. I. Golovashkin, G. P. Motulevich, and A. A. Shubin — 38.
Effect of Temperature on Characteristic Energy Losses of Electrons in Iron. I. B. Borovskiĭ, A. N. Kabanov, Yu. M. Kushnir, and V. V. Schmidt — 997.
Electrical Resistance Maximum for Ferromagnets at their Curie Points at Low Temperatures. E. I. Kondorskiĭ, O. S. Galkina, and L. A. Chernikova — 464L.
Electron Relaxation Time in a High-Frequency Electro-Magnetic Field and the Surface Impedance of a Metal. R. N. Gurzhi and M. Ya. Azbel' — 379.
Galvanomagnetic Characteristics of Metals with Open Fermi Surfaces. II. I. M. Lifshitz and V. G. Peschanskiĭ — 137.
Galvanomagnetic Phenomena in Indium and Aluminum. E. S. Borovik and G. V. Volotskaya — 189L.
On Certain General Properties of the Photon Propagation Function in Quantum Electrodynamics. A. A. Ansel'm — 929.
On the Hole Component of the Fermi Surface in Bismuth. N. B. Brandt — 975L.
On the Quantum Analog of the Collision Integral for Electrons in Magnetic and Electric Fields. A. M. Kosevich and V. V. Andreev — 637.

- On the Theory of Ultrasonic Absorption by Metals in a Strong Magnetic Field. É. A. Kaner — 154.
- Possible Transmission of Electromagnetic Waves through a Metal in a Strong Magnetic Field. O. V. Konstantinov and V. I. Perel' — 117.
- Temperature Dependence of the Hall Effect of Pure Ferromagnets. N. V. Volkenshteĭn and G. V. Fedorov — 48.
- The Relation between the Temperature Dependence of Electrical Resistance at Low Temperatures and the Galvanomagnetic Effect in Strong Magnetic Fields. O. S. Galkina and L. A. Chernikova — 1.

Methods and Instruments
- A Cryostat for Neutron Diffraction Studies. R. A. Alikhanov — 585.

Multiple Production of Particles (see also Cosmic Rays)
- Distribution of the Transverse Momentum of Shower Particles in Jets. É. G. Boos and Zh. S. Takibaev — 920.
- Momentum Distribution of Particles Produced in Inelastic N-N Collisions at E=9 Bev. V. S. Barashenkov, Wang Pei, and V. M. Mal'tsev — 467L.
- Multiple Production of Jet Particles in Peripheral Collisions. Yu. A. Romanov and D. S. Chernavskiĭ — 819.
- On the Problem of Peripheral Collisions of Nucleons with High Energies. V. M. Maksimenko — 222L.
- Peripheral Interaction of 9-Bev Nucleons. L. M. Dremin and D. S. Chernavskiĭ — 167.
- Possible Influence of Nucleon Structure in High-Energy Interactions. Zh. S. Takibaev — 454L.
- Statistical Theory of Multiple Particle Production. A. I. Nikishov — 369.
- The Significance of Strange Particles in Fermi's Statistical Theory. V. I. Rus'kin and P. A. Usik — 669.
- The Two-Center Model and the Hydrodynamical Theory of the Multiple Production of Particles. A. A. Emel'yanov and I. L. Rozental' — 142.

Muons (see also Weak Interactions)
- Energy Losses of Fast μ Mesons in Thick Layers of Matter. M. I. Daĭon — 1203.
- Measuring of the Chirality of the μ Meson. A. I. Alikhanov, Yu. V. Galaktionov, Yu. V. Gorodkov, G. P. Eliseev, and V. A. Lyubimov — 1380L.
- Nonradiative Transitions in Heavy μ-Mesic Atoms. M. Ya. Balatz, L. N. Kondrat'ev, L. G. Landsberg, P. I. Lebedev, Yu. V. Obukhov, and B. Pontecorvo — 1715,
- On the Energy Levels of μ-Mesic Atoms. N. I. Zhirnov — 691.
- On the Non-Radiative Transformation of the μ Meson into an Electron. I. S. Shapiro — 1186L.
- On Transitions Between Hyperfine Structure Levels in μ-Mesic Atoms. A. E. Ignatenko — 1093.
- Single Scattering of 10-30 Mev Negative Muons on Carbon. A. I. Alikhanyan, V. G. Kirillov-Ugryumov, L. P. Kotenko, E. P. Kuznetsov, and A. V. Samoĭlov — 282.

Nuclear Fission
- Angular Distribution of Na^{24} Nuclei and Fission Fragments Produced by Interactions between High-Energy Protons and Au and U Nuclei. A. K. Lavrukhina, L. P. Moskaleva, V. A. Malyshev, L. M. Satarova, and Su Hung-Kuei — 715L.
- Asymmetry of Uranium Fission at High Proton Energies. A. I. Obukhov — 196L.
- Comparison of the Probabilities of the Triple Fission of U^{233}, U^{235}, and Pu^{239}. V. N. Dmitriev, L. V. Drapchinskiĭ, K. A. Petrzhak, and Yu. F. Romanov — 718L.
- Competition between Neutron Evaporation and Fission in the Reactions of Multiply Charged Ions with Heavy Nuclei. N. I. Tarantin — 181L.
- Excitation of Fission Fragments and Their Mass Distribution. B. T. Geĭlikman — 688.
- Fission of Th^{232} by 14.9-Mev Neutrons. A. N. Protopopov, M. I. Kuznetsov, and É. G. Dermendzhiev — 279.
- Fission of Uranium Nuclei Induced by 9-Bev Protons. N. A. Perfilov, V. F. Darovskikh, G. F. Denisenko, and A. I. Obukhov — 517.
- Measurements of the Spectra and Average Number of Neutrons Emitted in the Fission of U^{235} and U^{238} Induced by 14.3-Mev Neutrons. Yu. A. Vasil'ev, Yu. S. Zamyatnin, Yu. I. Il'in, E. I. Sirotinin, P. V. Toropov, and É. F. Fomushkin — 483.
- On the Applicability of the Fermi-Teller "Z-Law" to a Photoemulsion Containing Uranium. G. E. Belovitskiĭ — 473L.
- On the Mechanism of Emission of Prompt Fission Neutrons. V. N. Nefedov — 1195.
- On the Mechanism of Uranium Fission Induced by Slow Negative Muons. G. E. Belovitskiĭ, N. T. Kashchukeev, A. Mikhul, M. G. Petrashku, I. A. Romanova, and F. A. Tikhomirov — 296.
- Range and Energy Dispersion of U^{233} Fission Fragments. K. A. Petrzhak and E. A. Shlyamin — 1244.

Nuclear Polarization
- Investigation of Nuclear Magnetic Resonance in Adsorbed Gas. A. A. Galkin and I. V. Matyash — 959L.
- Longitudinal Relaxation of Nuclear Spins in a Paramagnetic Crystal at Very Low Temperatures. B. I. Kochelaev — 719L.
- On the Nuclear Orientation Associated with a Saturated Forbidden Resonance and with Double Resonance. G. R. Khutsishvili — 679.
- On the Preparation of Polarized Hydrogen Targets. L. N. Rozentsveĭg and M. Ya. Azbel' — 1121.
- On the Theory of Quadrupole Relaxation of Nuclear Spins in Liquids. K. A. Valiev — 883.
- Polarization of Hydrogen Nuclei in a Free Radical. G. S. Lomkatsi — 455L.
- Production of "Supercold" Polarized Neutrons. G. M. Drabkin and R. A. Zhitnikov — 729L.
- The Line Shape of the Nuclear Acoustic Resonance. N. G. Koloskova and U. Kh. Kopvillem — 973L.
- The Polarization of Nuclei in Nonmetallic Ferromagnetic Substances. G. R. Khutsishvili — 1187L.
- The Polarization of Nuclei of Diamagnetic Elements Dissolved in Iron. B. N. Samoĭlov, V. V. Sklyarevskiĭ, and E. P. Stepanov — 261.

Nuclear Reactions, Disintegrations, Scattering (Theory)
- Angular Distribution of Neutrons in the Reaction $C^{13}(d, n)N^{14}$. T. L. Abelishvili, T. G. Gachechiladze, and O. M. Mdivani — 453L.

Circular Polarization of Gamma Quanta Accompanying Nuclear Capture of Slow Neutrons. D. P. Grechukhin — 446.

Collective Properties of Si^{30}, Si^{31}, and Ne^{23}, and Reduced Widths in Stripping Reactions. V. G. Sukharevskiĭ — 159.

Dispersion Formulae for Overlapping Levels. V. I. Serdobol'skiĭ — 1368.

Effect of Deformation of the Nucleus on the Electronic Wave Functions. Application to Beta Decay. R. Weiner and Ch. Iusim — 629.

Effect of Superfluidity of Heavy Nuclei on Single-Particle Electromagnetic Transitions and Beta Decay. M. G. Urin — 1331.

Energy Distributions of Products of Reactions in which Several Particles are Emitted. V. V. Komarov and A. M. Popova — 184L.

Excitation of Nuclear Collective States in Charged Particle Scattering. S. I. Drozdov — 362.

Excitation of Vibrational Levels and Coulomb Excitation in Alpha Decay. V. M. Strutinskiĭ — 89.

Influence of Coulomb Attraction on the Cross Section for Absorption of Antiprotons by Nuclei. P. É. Nemirovskiĭ and Yu. D. Fiveĭskiĭ — 1073.

Investigation of the Spectra of Neutrons Emitted in the Disintegration of Deuterons by Protons. V. V. Komarov and A. M. Popova — 1123.

Nucleon Emission by a Rotating Nucleus. G. A. Pik-Pichak — 557.

Polarization of Nucleons Scattered from Nuclei with Non-Zero Spin. Yu. P. Elagin — 1343.

Possible Occurrence of a Second-Order Process in Inelastic Scattering of Deuterons by Nuclei. V. A. Edakova, V. G. Neudachin, and E. A. Romanovskiĭ — 180L.

Production of Pions in p-d Collisions and Motion of Nucleons Inside the Nucleus. Yu. D. Prokoshkin — 334.

The Schwinger Effect with Account of the Screening of the Nucleus by the Atomic Electrons. V. M. Koprov — 459L.

Nuclear Reactions and Scattering at High Energy (Experiment)

Angular Distributions of 6.8-Mev Protons Elastically Scattered by Chromium, Nickel, and Copper Isotopes. A. K. Val'ter, I. I. Zalyubovskiĭ, A. P. Klyucharev, M. V. Pasechnik, N. N. Pucherov, and V. I. Chirko — 1025.

Charged Pion Production in Interactions of 9-Bev Protons with Emulsion Nuclei. N. P. Bogachev, S. A. Bunyatov, T. Vishki, Yu. P. Merekov, V. M. Sidorov, and V. A. Yarba — 317.

Determination of the Coupling Constant for the Pion-Nucleon Interaction from Cross Sections for the Elastic Scattering of 630-Mev Neutrons by Protons. N. S. Amaglobeli, B. M. Golovin, Yu. M. Kazarinov, S. V. Medved', and N. M. Polev — 474L.

Disintegration of Emulsion Nuclei by 930-Mev Protons. O. V. Lozhkin, N. A. Perfilov, A. A. Rimskiĭ-Korsakov, and J. Fremlin — 1001.

Energy Spectrum of Mesons from Nuclear Disintegrations Produced by 9-Bev Protons. Yu. T. Lukin, Zh. S. Takibaev, and E. V. Shalagina — 776.

Fragment Production by 100-Mev Protons. U. R. Arifkhanov, M. M. Makarov, N. A. Perfilov, and V. P. Shamov — 806.

Fragmentation of Ag and Br Nuclei by 9-Bev Protons. N. A. Perfilov, N. S. Ivanova, O. V. Lozhkin, M. M. Makarov, V. I. Ostroumov, Z. I. Solov'eva, and V. P. Shamov — 250.

Inelastic Interactions of 9-Bev Protons with Free and Bound Nucleons in Emulsion. N. P. Bogachev, S. A. Bunyatov, Yu. P. Merekov, V. M. Sidorov, and V. A. Yarba — 968L.

Inelastic Interaction of Pions with Helium Nuclei at Approximately 300 Mev. M. S. Kozodaev, M. M. Kulyukin, R. M. Sulyaev, A. I. Filippov, and Yu. A. Shcherbakov — 300.

Interaction between 630-Mev Protons and He^4 Nuclei. M. S. Kozodaev, M. M. Kulyukin, R. M. Sulyaev, A. I. Filippov, and Yu. A. Shcherbakov — 511.

Neutron Spectra From the d + p Reaction. N. A. Vlasov, S. P. Kalinin, B. V. Rybakov, and V. A. Sidorov — 1251.

The $d + d \rightarrow \pi^0 + He^4$ Reaction at 400 Mev Deuteron Energy. Yu. K. Akimov, O. V. Savchenko, and L. M. Soroko — 221L.

The (p, d) Reaction and Inelastic Scattering of Protons on Be^9. O. P. Nemets, L. S. Saltykov, and M. V. Sokolov — 1199.

The Reaction $p + d \rightarrow t + \pi^+$ at Proton Energy 670 Mev. Yu. K. Akimov, O. V. Savchenko, and L. M. Soroko — 462L.

Theoretical Interpretation of Elastic π^--p Scattering Experiments on the Proton Synchrotron of the Joint Institute for Nuclear Research. I. Patera and Ch. D. Palev — 710L.

Nuclear Reactions and Scattering at Medium and Low Energies (Experiment)

Angular Distribution of Elastically Scattered Neutrons. G. N. Lovchikova — 1036.

Angular Distribution of Protons from the Reaction $Ca^{48}(d, p)Ca^{41}$. N. I. Zaika, O. F. Nemets, and V. S. Prokopenko — 208L.

(d, t) Reactions on Medium and Heavy Nuclei. N. A. Vlasov, S. P. Kalinin, A. A. Ogloblin, and V. I. Chuev — 203L.

Elastic Scattering of Protons by Chromium Isotopes at 5.40 Mev. A. P. Klyucharev and N. Ya. Rutkevich — 207L.

Investigation of the Reactions (α, α'), (α, p), and (α, t) on Lithium Nuclei. K. V. Makaryunas and S. V. Starodubtsev — 271.

Measurements of the Energy Dependence of Radiative Neutron Capture in Iron, Silver, and Gold at Energies up to 30 kev. A. I. Isakov, Yu. P. Popov, and F. L. Shapiro — 712L.

The Inelastic Scattering of Protons and Deuterons from Mg^{24}. O. F. Nemets and G. A. Prokopets — 499.

Nuclear Reactions on Multiply Charged Ions

Formation of the Isomer Cd^{115m} by the Fission of Gold under the Action of Heavy Ions. S. M. Polikanov and Yu. T. Chuburkov — 214L.

Gamma Radiation Produced in the Interaction between

Accelerated C^{12} Ions and Tin Nuclei. V. A. Karnaukhov and Yu. Ts. Oganesyan — 964L.
Heavy Ion Excitation of Nuclei Accompanied by Radiation of γ Quanta. B. N. Kalinkin — 1111.
On the Cross Section for Compound Nucleus Formation in the Interaction of Atomic Nuclei. V. V. Babikov — 198L.

Nuclear Spectra (α, β, γ) (Experiment)
Beta and Gamma Spectra of the Sb^{113} and Sb^{115} Isotopes. V. L. Chukhladze, D. E. Khulelidze, and I. P. Selinov — 974L.
Beta Decay of P^{32}. B. V. Geshkenbeĭn — 965L.
Circular Polarization of Internal Bremsstrahlung Accompanying K-Capture in Fe^{55}. V. P. Parfenova — 42.
Determination of the Spins of Pt^{196} Nuclear Levels on the Basis of γ Rays Emitted in the Capture of Resonance Neutrons. N. D. Galanina, B. F. Shvartsman, and A. Ya. Diament — 1045.
Excited States of Cs^{134}. A. S. Melioranskiĭ, I. V. Éstulin, L. F. Kalinkin, and B. S. Kudinov — 548.
Influence of Magnetic Fields on Resonant Absorption of γ rays. V. A. Lyubimov and A. I. Alikhanov — 1375L.
Investigation of Beta Radiation of Nb^{95} and Ce^{144} by the Method of Absorption in Air. N. E. Tsvetaeva and I. A. Rozenfel'd — 460L.
Investigation of the α Decay of U^{236}. A. P. Komar, G. A. Korolev, and G. E. Kocharov — 1038.
Investigation of the Decay Scheme of As^{76} by the γ-γ Coincidence Method. N. N. Delyagin and A. A. Sorokin — 799.
Investigation of the Gamma Spectrum of Ce^{140}. S. F. Antonova, S. S. Vasilenko, M. G. Kaganskiĭ, and D. L. Kaminskiĭ — 554.
Investigation of the Relative Intensities of Some Conversion Lines of the Spectrum of Neutron-Deficient Lutetium Isotopes. M. G. Iodko, V. V. Tuchkevich, V. A. Romanov, and O. M. Kresin — 739.
Lifetime of the 321 Kev Level in Hf^{177}. G. A. Vartapetyan — 1378L.
Measurement of the Angular Correlations of 298-880 kev and 298-966 kev Gamma Cascades of Dy^{160}. M. V. Klimentovskaya and G. Chandra — 210L.
New Isomer Sn^{113m}. I. P. Selinov and V. L. Chikhladze — 728L.
Positron Decay of Ir^{192}. S. F. Antonova, S. S. Vasilenko, M. G. Kaganskiĭ, and D. L. Kaminskiĭ — 276.
Possibility of Application of the (n, 2n) Reaction in Nuclear Spectroscopy. V. V. Komarov, A. B. Kurepin, and A. M. Popova — 1312.
Spectra of Gamma Rays Produced in the Capture of Thermal Neutrons by Heavy Nuclei. I. L. V. Groshev, A. M. Demidov, and V. I. Pelekhov — 423.
Spectra of Gamma Rays Produced in the Capture of Thermal Neutrons by Heavy Nuclei. II. V. M. Strutinskiĭ, L. V. Groshev, and M. K. Akimova — 430.
The Gamma Spectrum of La^{140} in the Energy Range 2300-3900 kev. B. S. Dzhelepov, B. A. Emel'yanov, K. P. Kupriyanova, and Yu. N. Podkopaev — 205L.

Nuclear Structure (Theory)
Alpha-Deuteron Model of the Li^{6} Nucleus. T. I. Kopaleĭshvili, I. Sh. Vashakidze, V. I. Mamasakhlisov, and G. A. Chilashvili — 1268.
Collective Excitations of Non-Axial Even-Even Nuclei. A. A. Chaban — 1174.
Dependence of the Parameters of the Nuclear Potential on the Number of Particles. M. Ya. Amus'ya — 604.
Electromagnetic Transition Probabilities and Static Moments of Odd-Odd Atomic Nuclei. D. A. Varshalovich — 125.
Experimental Possibilities of Verifying the Model of Nonaxial Nuclei with a Rotational Spectrum. D. P. Grechukhin — 1359.
Green's Function for Odd Nuclei. Yu. T. Grin', S. I. Drozdov, and D. F. Zaretskiĭ — 162.
Moments of Inertia of Odd Atomic Nuclei. Yu. T. Grin', S. I. Drozdov, and D. F. Zaretskiĭ — 936.
Motion of Nucleons in an Anisotropic Oscillator Potential with Allowance for Spin-Orbit Interaction. D. V. Volkov and E. V. Inopin — 1765.
On the Equilibrium Shape of Atomic Nuclei. G. F. Filippov — 949.
On the Structure of the Be^{9} Nucleus. I. Sh. Vashakidze, T. I. Kopaleĭshvili, V. I. Mamasakhlisov, and G. A. Chilashvili — 675.
On the Theory of Nuclear Matter. G. M. Vagradov and D. A. Kirzhnits — 1082.
Quasistable States with Large Isotopic Spin in Light Nuclei. Ya. B. Zel'dovich — 202L.
Relative γ-Transition Probabilities in Strongly Deformed Nuclei. A. V. Gnedich, L. N. Kryukova, and V. V. Murav'eva — 524.
Rotational Energy and Moments of Inertia of Non-Axial Nuclei. A. S. Davydov, N. S. Rabotnov, and A. A. Chaban — 946.
Superfluidity of Light Nuclei. V. B. Belyaev, B. N. Zakhar'ev, and V. G. Solov'ev — 686.

Photonuclear Reactions
Curves for the Photoproton Yield from the C^{12} Nucleus. E. B. Bazhanov — 193L.
(γ, p) Reaction on Au^{197}. E. D. Makhnovskiĭ — 70.
High-Energy Photonuclear Deuterons and Tritons. V. P. Chizhov — 587.
Investigation of High-Energy Protons Emitted in the Photodisintegration of Li^{6}. E. B. Bazhanov and L. A. Kul'chitskiĭ — 1215.
Kinetic Energy of Fragments from the Photofission of U^{238}. B. A. Bochagov, A. P. Komar, and G. E. Solyakin — 990.
Photoproduction of Charged Pions near Threshold. M. I. Adamovich, E. G. Gorzhevskaya, V. G. Larionova, V. M. Popova, S. P. Kharlamov, and F. R. Yagudina. — 779.
Photoproduction of Positive Pions in Hydrogen near Threshold. É. G. Gorzhevskaya, V. M. Popova, and F. R. Yagudina — 200L.
Photoprotons from Cu^{65}. N. V. Lin'kova, R. M. Osokina, B. S. Ratner, R. Sh. Amirov, and V. V. Akindinov — 566.
Structure of the Giant Resonance in Photonuclear Reactions. E. V. Inopin — 714L.
The $Al^{27} \to Na^{24}$, $Co^{59} \to Mn^{56}$, and $P^{31} \to Na^{24}$ Reactions in the 260-Mev Gamma-Ray Energy Range. A. N. Gorbunov, F. P. Denisov, and V. A. Kolotukhin — 783.
Yield of Photoneutrons Emitted from Lead Under the

Action of 10.5 — 20.5 Mev Electrons (Thick Absorber Method). V. M. Grizhko, D. I. Sikora, V. A. Shkoda-Ulyanov, A. D. Abramenkov, B. I. Shramenko, and A. N. Fisun — 987.

Plasma (Theory)
- A Relativistic Transport Equation for a Plasma. II. Yu. L. Klimontovich — 876.
- Certain Special Features of Ohmic Heating of Electron Gas in a Plasma. A. V. Gurevich — 85.
- Connection Between Oscillation and Rate of Loss Of Charged Particles in a Cylindrical Plasma of Low Pressure in a Longitudinal Magnetic Field. A. A. Zaĭtsev and M. Ya. Vasil'eva — 1180L.
- Cyclotron Absorption of Electromagnetic Waves in a Plasma. K. N. Stepanov — 192L.
- Gyromagnetic Resonance Absorption of Electromagnetic Waves in a Plasma. B. N. Gershman — 657.
- Instability of a Plasma with Anisotropic Distribution of Ion and Electron Velocities. A. E. Kitsenko and K. N. Stepanov — 1323.
- Instability of Longitudinal Oscillations of an Electron-Ion Plasma. L. M. Kovrizhnykh and A. A. Rukhadze — 615.
- Kinetic Equation for Rapidly Varying Processes. V. P. Silin — 1771.
- Magnetic Bremsstrahlung of a Confined Plasma. K. N. Stepanov and V. I. Pakhomov — 1126.
- On the Amount of Accelerated Particles in an Ionized Gas Under Various Accelerating Mechanisms. A. V. Gurevich — 1150.
- On the Build-up of Electromagnetic Waves in a Plasma Moving in a Non-Dispersive Dielectric in the Presence of a Constant Magnetic Field. G. G. Getmantsev and V. O. Rapoport — 871.
- On the Electromagnetic Properties of a Relativistic Plasma. V. P. Silin — 1136.
- On the Magnetic Susceptibility of a Relativistic Electron Gas. A. A. Rukhadze and V. P. Silin — 463L.
- On the Nonlinear Theory of Stationary Processes in an Electron Plasma. F. M. Nekrasov — 170.
- Possible Mode of Oscillation for a Charge in Crossed Fields. Yu. N. Barabanenkov — 190L.
- Thermodynamic Functions of a Low-temperature Plasma. A. I. Larkin — 1363.

Plasma, Gas-Discharge (Experiment)
- A Rotatory Magneto-Mechanical Effect in a Low-Pressure Plasma. V. L. Granovskiĭ and E. I. Urazakov — 974L.
- Instability of the Induction Pinch. I. F. Kvartskhava, K. N. Kervalidze, and Yu. S. Gvaladze — 1182L.
- Interaction of an Electron Beam with a Plasma. I. F. Kharchenko, Ya. B. Faĭnberg, R. M. Nikolaev, E. A. Kornilov, E. A. Lutsenko, and N. S. Pedenko — 493.
- Investigation of Fast Electrons in Powerful Pulsed Discharges. N. G. Kovalskiĭ, I. M. Podgornyĭ, and M. M. Stepanenko — 1040.
- Observation of Ion Oscillations in a Plasma. M. D. Gabovich, L. L. Pasechnik, and V. G. Yazeva — 1033.
- Reflection of Electromagnetic Waves from a Plasma Moving in Slow-Wave Guides. O. G. Zagorodnov, Ya. B. Faĭnberg, and A. M. Egorov — 4.
- Skin Effect and Shock Waves in an Induction Gas Discharge. S. E. Gerebenshchikov and M. D. Raĭzer — 1201.
- Toroidal Discharge in a Strong Magnetic Field. G. G. Dolgov-Savel'ev, V. S. Mukhovatov, V. S. Strelkov, M. N. Shepelev, and N. A. Yavlinskiĭ — 287.

Pressure, High
- Electrical Conductivity of Dielectrics in Strong Shock Waves. A. A. Brish, M. S. Tarasov, and V. A. Tsukerman — 15.
- Equation of State for Aluminum, Copper, and Lead in the High-Pressure Region. L. V. Al'tshuler, S. B. Kormer, A. A. Bakanova, and R. F. Trunin — 573.
- The Isentropic Compressibility of Aluminum, Copper, Lead, and Iron at High Pressures. L. V. Al'tshuler, S. B. Kormer, M. I. Brazhnik, L. A. Vladimirov, M. P. Speranskaya, and A. I. Funtikov — 766.

Quantum Electrodynamics
- Application of the Dispersion Method for Investigation of the Simplest Green's Functions in Quantum Electrodynamics. V. D. Mur and V. D. Skarzhinskiĭ — 1817.
- Direct Electron-Positron Pair Production by Electrons. V. A. Tumanyan — 191L.
- Leptonic Decays of Hyperons with Emission of Pions. I. S. Tsukerman — 927.
- On Gauge Transformations in Quantum Electrodynamics. Yu. A. Gol'fand — 223L.
- On the Structure of the Photon Green's Function. D. A. Kirzhnits, V. Ya. Faĭnberg, and E. S. Fradkin — 174.
- Polarization of Gamma-Ray Quanta from the Internal Compton Effect. F. Yanoukh — 131.
- Radiative Corrections to Photoproduction and Single-Photon Annihilation of Pairs. S. Ya. Guzenko and P. I. Fomin — 372.
- Single-photon Annihilation and Electron-pair Creation in Medium. G. S. Saakyan — 1147.
- Some General Relations in Statistical Quantum Electrodynamics. E. S. Fradkin — 114.
- The Relativistic Photoeffect in the L Shell. M. Gavrila — 224L.

Quantum Mechanics (Various Problems)
- A Variational Principle for the Calculation of a Correction, Quadratic with Respect to the Magnetic Field Intensity, to the Electron Energy in a Molecule. T. K. Rebane — 694.
- Integral Transformations of the I. S. Shapiro Type for Particles of Zero Mass. L. G. Zastavenko and Chou Kuang-Chao — 97.
- Polarization of the Hydrogen Atom in the Ground State by the Field of a Point Charge. V. P. Shmelev — 1102.
- Quantum Transitions in the Adiabatic Approximation. A. M. Dykhne — 411.
- Rotation of the Spin of a Relativistic Particle with a Magnetic Moment Moving in An External Field. V. S. Popov — 1141.
- S Matrix in the Generalized Quantization Method. D. V. Volkov — 375.
- Scattering by a Singular Potential in Perturbation Theory and in the Momentum Representation. Ya. B. Zel'dovich — 594.
- Space and Time Reflections in Relativistic Theory. Yu. M. Shirokov — 101.
- The Thomas - Fermi Model of the Atom with Quantum

and Exchange Corrections. N. N. Kalitkin — 1106.
- Variational Principles for Nonstationary Quantum Mechanical Problems and Perturbation Theory. Yu. N. Demkov — 1351.

Radiation
- Bremsstrahlung at the Boundary of a Medium with Account of Multiple Scattering. I. I. Gol'dman — 1341.
- Cerenkov Radiation from a Charged Particle with Intrinsic Magnetic Moment. Li Meng-Ha — 673.
- Cerenkov Radiation of Dipoles in a Medium with Spatial Dispersion. G. A. Begiashvili and E. V. Gedalin — 1254.
- Coherent Electron Radiation in a Synchrotron. III. M. S. Rabinovich and L. V. Iogansen — 856.
- Critical Velocity for Radiation of Light in Optically Anisotropic Media. I. M. Frank — 1263.

Scattering (General Theory)
- Allowance for the Medium in Radiation Corrections to Coulomb Scattering. M. L. Ter-Mikaelyan — 845.
- Coulomb Scattering of Charges in a Strong Magnetic Field. Yu. N. Barabanenkov — 1091.
- On the Calculation of Scattering Phase Shifts. V. K. Peterson — 1100.
- On the Problem of the Direct Reconstruction of the Elastic-Scattering Amplitude. G. I. Kopylov and Z. D. Lomakina — 1188L.
- On the Processes Involving Transfer of Momentum to the Medium. M. I. Ryazanov — 617.
- On the Scattering of Transversely Polarized Fermions. A. A. Sokolov and M. M. Kolesnikova — 1281.
- On the Structure of the S Matrix in the Theory of Elastic and Inelastic Scattering of Non-relativistic Particles. Yu. V. Tsekhmistrenko — 894.
- Polarization of Deuterons Elastically Scattered on Zero-Spin Nuclei. G. M. Budyanskiĭ — 847.
- Recurrent Construction of Angular Operators. J. Fischer and S. Ciulli — 1256.
- The Behavior of Fermion Spin in Elastic Scattering. A. A. Sokolov and M. M. Kolesnikova — 120.
- The Possibility of the Determination of the Scattering Amplitudes of Unstable Particles at Zero Energy. V. N. Gribov — 400.
- The Relativistically Covariant Spin Structure of the S Matrix. V.I. Ritus — 1075.

Scattering of Electrons and Photons
- Elastic γp Scattering at 40 — 70 Mev and the Polarizability of the Proton. V. I. Gol'danskiĭ, O. A. Karpukhin, A. V. Kutsenko, and V. V. Pavlovskaya — 1223.
- On Elastic Scattering of Photons by the Nuclear Coulomb Field. C. Eftimiu and C. Vrejoiu — 971L.
- Polarization Effects in the Scattering of Electrons by Deuterons. G. V. Frolov — 831.
- Polarization of Electrons in Elastic Scattering with Account of the Finite Size of the Nucleus. B. K. Kerimov and V. M. Arutyunyan — 1294
- Resonance Scattering of Gamma Rays by Se^{76}. N. N. Delyagin — 803.
- Scattering of Electrons by Nuclei according to the α-Particle Model. E. V. Inopin and B. I. Tishchenko — 840.
- Scattering of Gamma-Ray Quanta by Nucleons near the Threshold for Meson Production. L. I. Lapidus and Chou Kuang-Chao — 147.
- Several Possible Applications for the Resonant Scattering of Gamma Rays. I. Ya. Barit, M. I. Podgoretskiĭ, and F. L. Shapiro — 218L.
- Theory of Resonant Interaction of Gamma Rays with Crystals. M. V. Kazarnovskiĭ — 1191.

Semiconductors
- Cyclotron Resonance in Germanium and Silicon and the Effect of Negative Effective Masses. Yu. Kagan — 1333.
- Experimental Determination of the Polaron Mass in Cuprous Oxide. A. I. Gubanov, N. I. Krivko, and N. M. Reĭnov — 247.
- Instability in a Semiconductor Amplifier with Negative Effective Carrier Mass. A. L. Zakharov — 478L.
- Resonance Absorption of High-Frequency Sound Energy by Semiconductor Current Carriers in a Magnetic Field. E. P. Pokatilov — 835.
- Semiconductor Amplifiers and Generators with Carriers Having Negative Effective Mass. N. G. Basov, O. N. Krokhin, and Yu. M. Popov — 720L.
- Slowing-Down Time of Nonequilibrium Current Carriers in Semiconductors. O. N. Krokhin and Yu. M. Popov — 1144.
- The Capacitance of p-n Junctions at Low Temperatures. B. M. Vul and E. I. Zavaritskaya — 6.

Statistical Physics (General Problems)
- Negative and Limiting Temperatures. Yu. B. Rumer — 1365.
- On the Theory of Non-Equilibrium Statistical Processes. R. L. Stratonovich — 598.
- Use of the Methods of Quantum Field Theory for the Investigation of the Thermodynamical Properties of a Gas of Electrons and Photons. I. A. Akhiezer and S. V. Peletminskiĭ — 1316.

Strange Particles
- Angular Distribution of Decay Products of $\Sigma^{\pm}$ Hyperons Produced by Protons in Photoemulsions. L. P. Dzhanelidze, K. V. Mandritskaya, O. A. Shakhulashvili, D. K. Kopylova, Yu. B. Korelevich, N. I. Petukhova, D. Tuvdendorzh, Cheng P'u-Ying, and N. I. Kostanashvili — 722L.
- Anomalous Decays of Hyperfragments. S. A. Azimov, U. G. Gulyamov, R. Karimova, and B. G. Rakhimbaev — 502.
- Cross Section for the Formation of Ω^- Particles in the Reactions $\pi^- + p \rightarrow \Omega^- + 3K$ at 8 Bev and $p + \overline{p} \rightarrow \Omega + \overline{\Omega}$ at 4 Bev. Hsien Ting-Ch'ang — 209L.
- Interference of Form Factors in Leptonic Decay of Hyperons. V. M. Shekhter — 387.
- Leptonic Decays of Hyperons with Emission of Pions. I. S. Tsukerman — 927.
- Non-Mesonic Decays of Hyperfragments. I. B. Berkovich, A. P. Zhdanov, F. G. Lepekhin, and Z. S. Khokhlova — 311.
- On New Strange Particles. B. Pontecorvo — 1192L.
- On Possible Properties of D^0 Mesons. I. V. Chuvilo — 721L.
- On the $\underline{D}$ Meson. Hsien Ting-Ch'ang — 1172.
- On the Decay of Σ Hyperons. Chou Kuang-Chao — 966L.
- On the Process $e^- + p \rightarrow \Lambda + \nu$. V. M. Shekhter — 967L.
- Possible Symmetry Properties for the π-K System. Chou Kuang-Chao — 730L.
- Possibility of Determining the Form Factors in Leptonic

Decay of Hyperons. V. P. Belov, B. S. Mingalev, and V. M. Shekhter — 392.

Production of a Σ Hyperon by 8.3-Bev/c Negative π Mesons. Wang Kang-Chang, Wang Chu-Chien, V. I. Veksler, N. M. Viryasov, I. Vrana, Ting Ta-Chao, Kim Hu In, E. N. Kladnitskaya, A. A. Kuznetsov, A. Mikhul, Nguyen Din Tu, A. V. Nikitin, and M. I. Solov'ev — 976L.

Remark on the Decay of the Cascade Hyperon. I. Yu. Kobzarev, L. B. Okun', and A. P. Rudik — 728L.

Scattering and Radiative Capture of Λ Particles. A. M. Kol'chuzhkin and N. N. Kolesnikov — 716L.

Strong Interactions (Theory)

Analysis Based on Dispersion Relations of Data on Pion Photoproduction Near Threshold. A. M. Baldin — 416.

Formation of Pions in πN Collisions. A. I. Lebedev and V. A. Petrun'kin — 962L.

Green's Function in the Fixed-Source Model of Charged Scalar Mesons. B. M. Barbashov and G. V. Efimov — 145.

Inverse Dispersion Relations for Photoproduction of Pions on Nucleons. N. F. Nelipa and V. A. Tsarev — 187L.

Nucleon-Nucleon Scattering in the Two-Meson Approximation for Large Orbital Angular Momenta. A. D. Galanin, A. F. Grashin, B. L. Ioffe, and I. Ya. Pomeranchuk — 347.

On an Estimate of the Minimum Radius of Two-Particle Interactions at High Energies. V. G. Grishin and V. I. Ogievetskiĭ — 725L.

On Meson-Nucleon Scattering in Large Orbital Angular Momentum States. A. D. Galanin — 177.

On the Momentum Spectrum of π^+ Mesons from the Interaction $\pi^+ + p \rightarrow 2\pi^+ + n$. V. A. Astaf'ev — 709L.

On the Nonlinear Theory of Elementary Particles. D. F. Kurdgelaidze — 339.

On the Question of a Resonant π-π Interaction. V. M. Maksimenko — 469L.

On the Possibility of Using Nuclear Reactions to Obtain Information about the π-π Interaction. Yu. D. Bayukov and G. A. Leksin — 1371L.

Peripheral Nucleon Interaction in the Two-Meson Approximation. A. F. Grashin and I. Yu. Kobzarev — 624.

Solution of Equations for Meson-Meson Scattering Amplitude in the Asymptotic Region. A. A. Ansel'm — 1356.

The Singular Points of Some Feynman Diagrams. V. A. Kolkunov, L. B. Okun', and A. P. Rudik — 634.

Transition Radiation for a Charged Particle at Oblique Incidence. G. M. Garibyan — 1306.

Superconductivity

A Measurement of the Surface Tension at the Boundary between the Superconducting and Normal Phases of Indium. Yu. V. Sharvin — 216L.

Anisotropy of Surface Tension at the Boundary between the Superconducting and Normal Phases of Tin. Yu. V. Sharvin and V. F. Gantmakher — 1052.

Critical Currents in Superconducting Tin Films. N. E. Alekseevskiĭ and M. N. Mikheeva — 211L.

Destruction of Superconductivity by a Current. E. Troĭnar — 470L.

Interactions between Electrons and Lattice Vibrations in a Superconductor. G. M. Éliashberg — 696.

The Superconductivity of Electrolytically Deposited Copper-Bismuth Alloys. N. E. Alekseevskiĭ, V. V. Bondar', and Yu. M. Polukarov — 213L.

The Thermal Conductivity of Superconductors in the Intermediate State. N. V. Zavaritskiĭ — 1207.

Thermal Properties

On the Quantum-Mechanical Calculations of the Pressure in Solids. G. M. Gandel'man and E. S. Pavlovskiĭ — 851.

The Density of Liquid Oxygen on the Saturation Curve. D. L. Timrot and V. P. Borisoglebskiĭ — 1297.

The Heat Capacity of Bismuth Telluride at Low Temperatures. E. S. Itskevich — 255.

Weak Interactions

Anisotropic Distribution of Internal Bremsstrahlung in K Capture by Polarized Nuclei. S. F. Timashev and V. A. Kaminskiĭ — 206L.

Concerning the Article by S. M. Bilen'kiĭ, R. M. Ryndin, Ya. A. Smorodinskiĭ, and Ho Tso-Hsiu, "On the Theory of Neutron Beta Decay" — 729L.

Internal Bremsstrahlung in the β Decay of Polarized Nuclei. Ch'ing Ch'en-Jui and F. Yanoukh — 683.

Investigation of Polarization of Internal Conversion Electrons in Transitions Following Decay of Heavy Elements. M. E. Vishnevskiĭ, V. A. Lyubimov, E. F. Tretyakov, and G. I. Grishuk — 1029.

Limits of Applicability of the Weak Interaction Theory. B. L. Ioffe — 1158.

On the Analogy between the Weak and Electromagnetic Interactions. É. M. Lipmanov — 891.

On the Connection Between the Polarization of β Electrons and the Shape of the β Spectrum. B. V. Geshkenbeĭn and A. P. Rudik — 1361.

On the Production of an Electron-Positron Pair by a Neutrino in the Field of a Nucleus. A. M. Badalyan and Chou Kuang-Chao — 477L.

On the Radiative Correction in Weak-Interaction Processes. Ya. A. Smorodinskiĭ and Ho Tso-Hsiu — 724L.

Possibility of an Experimental Test for Form Factors in the Theory of the Universal Fermi Interaction. Ho Tso-Hsiu — 466L.

Renormalization in Parity-Nonconservation Theory. B. L. Ioffe — 911.

Some Consequences of the Symmetry of the Universal Fermi Weak Interaction. Ho Tso-Hsiu and Chu Hung-Yuan — 1346.

The Form Factor and the μ Capture by Light Nuclei with Spin $\frac{1}{2}$. Ho Tso-Hsiu — 1167.

The Polarization of the Beta-Ray Electrons from Oriented RaE. A. Z. Dolginov and N. P. Popov — 1095.

X-Rays

Investigation of the Main K X-ray Absorption Edge in Selenium. D. Bally and L. Müller — 995.

ERRATA TO VOLUME 10

page	reads	should read
Article by A. S. Khaĭkin		
1044, title	. . . resonance in lead	. . . resonance in tin
6th line of article	~ 1000 oe	~ 1 oe
Article by V. L. Lyuboshitz		
1223, Eq. (13), second line	$\ldots-\mathrm{Sp}_{1,2}\mathscr{E}(\mathbf{e}_1)$	$\ldots-\mathrm{Sp}_{1,2}\mathscr{E}(\mathbf{e}_2)\ldots$
1226, Eq. (26), 12th line	$\cdots\{(\mathbf{p}+\mathbf{q},\ \mathbf{p}$	$\cdots\{(\mathbf{p}+\mathbf{q},\mathbf{p})-(\mathbf{p}+\mathbf{q},\mathbf{n})\cdot$ $\cdot(\mathbf{pn})\}$
1227, Eqs. (38), (41), (41a) numerators and denominators	$(\mathbf{p}^2-\mathbf{q})$	$(\mathbf{p}^2-\mathbf{q}^2)^2$
1228, top line	$\mathbf{m}_2=\begin{matrix}\mathbf{q}_1-\mathbf{p}_1\\ \mathbf{q}_1-\mathbf{p}_1\end{matrix}$	$\mathbf{m}_2=[\mathbf{m}_3\ \mathbf{m}_1]$

ERRATA TO VOLUME 12

Article by Dzhelepov et al.		
205, figure caption	54	5.4
Article by M. Gavrila		
225, Eq. (2), last line	$-2\gamma\Theta^{-4}\,{}^1\!/_8$	$-2\gamma\Theta^{-4}-{}^1\!/_8$
Article by Dolgov-Savel'ev et al.		
291, caption of Fig. 5, 4th line	$p_0 = 50 \times 10^{-4}$ mm Hg	$p_0 = 5 \times 10^{-4}$ mm Hg.
Article by Belov et al.		
396, Eq. (24) second line	$\ldots-(4-2\eta)\sigma_1+\ldots$	$\ldots+(4-2\eta)\sigma_1+\ldots$
396, 17th line (r) from top	. . less than 0.7	. . less than 0.07
Article by Kovrizhnykh and Rukhadze		
615, 1st line after Eq. (1)	$\omega_{0e}^2 = 2\pi e^2 n_e/m_e,$	$\omega_{0e}^2 = 4\pi e^2 n_e/m_e,$
Article by Belyaev et al.		
686, Eq. (1), 4th line	$\ldots b_{\rho_2 m_2}{}_{,\,,}(s_2')+\cdots$	$\ldots b_{\rho_1 m_1}{}_{,\,,}(s_1')+\cdots$
Article by Zinov and Korenchenko		
798, Table X, heading of last column	$\sigma_{\pi^-\to\pi^+}=$	$\sigma_{\pi^-\to\pi^-}=$
Article by V. M. Shekhter		
967, 3d line after Eq. (3)	$s\equiv 2m_pE+m_p^2$	$s\equiv(2m_pE+m_p^2)^{1/2}$
967, Eq. (5), line 2	$+(B_V^2+B_A^2)\ldots$	$+(B_V^2+B_A^2)\,Q\ldots$
968, Eq. (7)	$\ldots(C_V^2+C_A^2).$	$\ldots C_V^2+C_A^2-Q^2(B_V^2+B_A^2).$
968, line after Eq. (7)	for $C_V^2+C_A^2\equiv\ldots$	for $C_V^2+C_A^2$ $-Q^2(B_V^2+B_A^2)\equiv\ldots$
Article by Dovzhenko et al.		
983, 11th line (r)	$\gamma=1{,}8\pm$	$\gamma=1{,}8\pm0{,}2$
Article by Zinov et al.		
1021, Table XI, col. 4	$-1{,}22$	$1{,}22$
Article by V. I. Ritus		
1079, line 27 (1)	$-\Lambda_{\pm}(t),$	$\Lambda_{\pm}(t),$
1079, first line after Eq. (33)	$\frac{1}{2}(1+\beta).$	$\frac{1}{2}(1\pm\beta).$
1079, 3d line (1) from bottom	$\ldots\mathfrak{N}(q'p;\ pq')\ldots$	$\ldots\mathfrak{N}(p'q;\ pq')\ldots$
Article by R. V. Polovin		
1119, Eq. (8.2), fourth line	$U_{0x}u_xg(\gamma)-[\gamma\cdots$	$-U_{0x}u_xg(\gamma)\,[\gamma\ldots$
1119, Eq. (8.3)	$\cdots$sign $u.$	$\cdots$sign $u_g.$
Article by V. P. Silin		
1138, Eq. (18)	$\cdots+\frac{4}{5}c^2k^2$	$\cdots+\frac{6}{5}c^2k^2.$